

**TECHNICAL
TRANSACTIONS**

**CIVIL
ENGINEERING**

**ISSUE
3-B (8)**

**YEAR
2014 (111)**

**CZASOPISMO
TECHNICZNE**

BUDOWNICTWO

**ZESZYT
3-B (8)**

**ROK
2014 (111)**



**WYDAWNICTWO
POLITECHNIKI
KRAKOWSKIEJ**

**TECHNICAL
TRANSACTIONS**
CIVIL ENGINEERING

**CZASOPISMO
TECHNICZNE**
BUDOWNICTWO

ISSUE 3-B (8)
YEAR 2014 (111)

ZESZYT 3-B (8)
ROK 2014 (111)

Chairman of the Cracow University
of Technology Press Editorial Board

Jan Kazior

Przewodniczący Kolegium
Redakcyjnego Wydawnictwa
Politechniki Krakowskiej

Chairman of the Editorial Board

Józef Gawlik

Przewodniczący Kolegium
Redakcyjnego Wydawnictw
Naukowych

Scientific Council

**Jan Błachut
Tadeusz Burczyński
Leszek Demkowicz
Joseph El Hayek
Zbigniew Florjańczyk
Józef Gawlik
Marian Giżejowski
Sławomir Gzell
Allan N. Hayhurst
Maria Kuśnierova
Krzysztof Magnucki
Herbert Mang
Arthur E. McGarity
Antonio Monestiroli
Günter Wozny
Roman Zarzycki**

Rada Naukowa

Civil Engineering Series Editor

Marek Piekarczyk

Redaktor Serii Budownictwo

Section Editor
Editorial Compilation
Typesetting

**Dorota Sapek
Aleksandra Urzędowska
Anna Pawlik**

Sekretarz Sekcji
Opracowanie redakcyjne
Skład i łamanie

Native Speakers

**Tim Churcher
Cathal Gantley
Bart Kukula
Anna Miodus
Ron Mukerji
Richard Orange
Joel Paisley
Ian Transue**

Weryfikacja językowa

Cover Design
Cover Photo

**Michał Graffstein
Jan Zych**

Projekt okładki
Zdjęcie na okładce

Pierwotną wersją każdego Czasopisma Technicznego jest wersja on-line
www.czasopismotechniczne.pl www.technicaltransactions.com

© Politechnika Krakowska
Kraków 2014

Civil Engineering series

Editorial Board

Editor-in-Chief:

Marek Piekarczyk, Cracow University of Technology, Poland

Editorial Board:

Andrzej Cholewicki, Building Research Institute, Poland
Wit Derkowski, Cracow University of Technology, Poland
Jean-François Destrebecq, French Institute for Advanced Mechanics, France
Dariusz Gawin, Lodz University of Technology, Poland
Jacek Gołaszewski, Silesian University of Technology, Poland
Bożena Hoła, Wrocław University of Technology, Poland
Maria E. Kamińska, Lodz University of Technology, Poland
Oleg Kapliński, Poznan University of Technology, Poland
Tadeusz Kasprócz, Military University of Technology, Poland
Renata Kotynia, Lodz University of Technology, Poland
Robert Kowalski, Warsaw University of Technology, Poland
Mária Kozlovská, Technical University of Košice, Slovakia
Andrzej Łapko, Białystok University of Technology, Poland
Marco Menegotto, Sapienza University of Rome, Italy
Peter Mesároš, Technical University of Košice, Slovakia
Piotr Noakowski, TU Dortmund University, Germany
Andrzej Nowak, University of Michigan, United States
Zygmunt Orłowski, AGH University of Science and Technology, Poland
Hartmut Pasternak, Brandenburg University of Technology Cottbus–Senftenberg, Germany
Edyta Plebankiewicz, Cracow University of Technology, Poland
Maria Polak, University of Waterloo, Canada
Charles Rodrigues, Universidade Nova de Lisboa, Portugal
Tomasz Siwowski, Rzeszow University of Technology, Poland
Marcela Spišáková, Technical University of Košice, Slovakia
Zuzana Struková, Technical University of Košice, Slovakia
Maria Szerszeń, University of Nebraska – Lincoln, United States
Jolanta Tamošaitienė, Vilnius Gediminas Technical University, Lithuania
Alena Tažiková, Technical University of Košice, Slovakia
Martins Vilnītis, Riga Technical University, Latvia
Szczepan Woliński, Rzeszow University of Technology, Poland

Executive Editor:

Tomasz Kisilewicz, Cracow University of Technology, Poland

MARIUSZ ADAMSKI*, JUSTYNA SIERGIEJUK*, GRZEGORZ OJCZYK**

HEAT PUMP INSTALLATION (JOHN PAUL II CENTRE, KRAKOW)

INSTALACJA POMP CIEPŁA (BUDYNEK CENTRUM JANA PAWŁA II W KRAKOWIE)

Abstract

In the paper energy balances for heating and cooling of buildings are presented. Heat pump diagrams are discussed and original solutions are presented. There are related drawings, tables and photographs in the paper.

Keywords: heat pump, heating system

Streszczenie

W artykule przedstawiono krótką charakterystykę obiektu, w tym bilanse energii do celów ogrzewania i chłodzenia. Omówiono zastosowane schematy instalacji pompy ciepła, instalacji grzewczych oraz chłodniczych. Szczególną uwagę zwrócono na zastosowane oryginalne rozwiązania. Artykuł uzupełniono rysunkami, tabelami oraz zdjęciami.

Słowa kluczowe: pompa ciepła, instalacja ogrzewania

* Ph.D. Eng. Mariusz Adamski, M.Sc. Eng. Justyna Siergiejuk, Cathedral of District Heating, Faculty of Civil and Environmental Engineering, Białystok University of Technology.

** M.Sc. Eng. Grzegorz Ojczyk, Herz Valves UK LTD.

1. Introduction

Heat pumps are part of the environmentally friendly technologies using renewable energy. They are quoted in the European Directives on the use of Renewable Energy (RES), on the Energy Performance of Buildings (EPBD) and on Energy related products (ErP). In addition, heat pumps are also referenced in the Directive on the promotion of the use of energy from renewable sources (2009/28/EC, RES Directive, §2). The Directive recognizes the technology as using renewable energy sources from air, water and ground. Heat pumps are seen as a great opportunity to reach the EU target for a reliable, affordable and sustainable energy supply.

2. Heat pump system description

The heat pump installation system consists of heat pump units and lower and upper heat sources. Heat pump installation is constructed with three circuits: lower and upper heat source and heat pump. Operation of heat pump begins with the acquisition of heat from heat source (land) by glycol solution. A simplified diagram of the heat pump system is presented in Fig. 1. In reality, four heat pump units of type Vatra GIGA 160B are installed; each is connected to the lower heat source independently. Node points numbered. Nos. 1–5 are related to the lower heat source, 7–13 to the heating system and 14–17 to the hot water system. Vertical ground heat exchangers are designed as the lower heat source for each of the four heat pumps. Each vertical ground heat exchanger has 14 holes with a depth of up to 170 m.

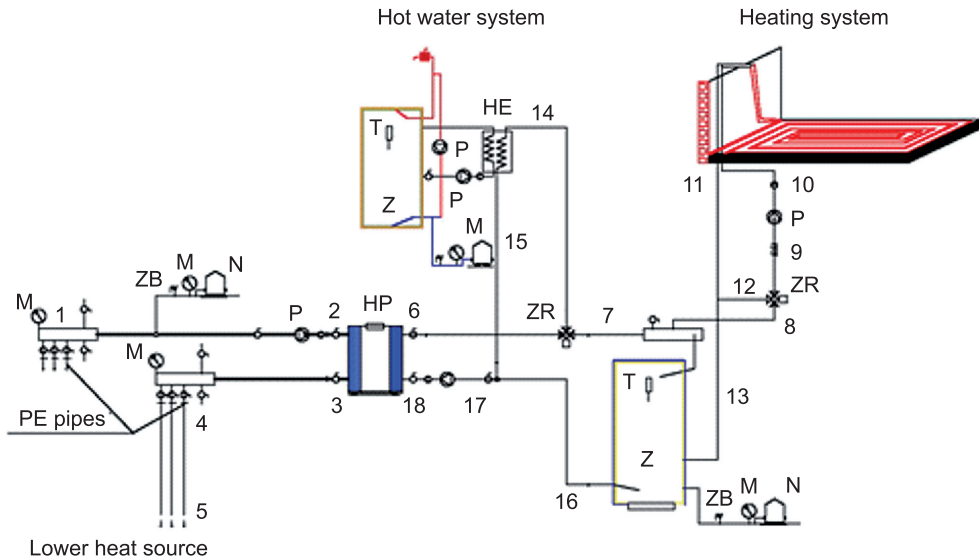


Fig. 1. Simplified diagram of the heat pump system: HP – heat pump, HE – heat exchanger, M – manometer, T – thermometer, N – expansion tank, ZR – regulating valve, ZB – security valve

The distance between the wells ranges from 12 m to 15 m. The wells are connected in series in the loop. Vertical ground collectors are made of polyethylene pipes placed in boreholes connected at the bottom with an u-shaped moulder.

A 33% aqueous solution of propylene glycol is provided as the heat transfer medium. In the wells two pipes with a diameter of 40 mm are used. Heat pumps work with heat buffers, consolidating additional heat source and heat consumers. It is expected that excess heat will be discharged into the ground heat exchanger and atmosphere.

The installation enables production of cold chill, which is accumulated in the ground after the heating season. This is called passive cooling. After the initial regeneration of the lower source, a cold solution of propylene glycol will be produced using the heat pumps. This is so called active cooling. Further regeneration of the lower source is exploited by the refrigerant condensation heat. This heat pump system provides heat in the heating period and cooling during the summer. The designed and installed system allows for the simultaneous generation of heat and cold. A combustion engine OTTO – the CHP system produces electricity to drive heat pumps and heat to power the heating system. CHP is powered by a fuel gas GZ50.

3. Heat pump specifications

Technical details of the used heat pumps type Vatra GIGA 160B are presented in Table 1.

Table 1

Technical details of the heat pump type Vatra GIGA 160B [5]

Dimensions <i>W./H./D.</i> :	880/1310/1850 [mm]
Net weight:	965 [kg]
Lower heat source temperature:	-5 to +25 [°C]
Central heating maximum temperature:	55 [°C]
Preparation of hot water:	through an external water tank
Medium:	R 407c
Application:	for central heating for installation of hot water
Nominal output:	158.3 [kW]
Cooling power:	122.4 [kW]
Input power:	38.65 [kW]
COP:	4.15 assuming at 0/35 [°C]
Noise level:	66 [dB]
Country of production	Poland

4. Heat pump circuit

Thermodynamic cycle is carried out using R407C refrigerant. The evaporator and condenser are constructed of plate heat exchangers, brazed copper plates of stainless steel AISI 316. The parameters given in the characteristics (Fig. 2) are in accordance with the following data [5]:

– cooling side – medium: 33% aqueous solution of propylene glycol and:

$$\Delta T_E = t_2 - t_3 = 4K \quad (1)$$

– heating side – medium: water, and:

$$\Delta T_C = t_6 - t_{18} = 8K. \quad (2)$$

The thermal power P_c of the evaporator in steady state conditions is described by the following equation:

$$P_C = c_{pg} m_{lhs} (t_2 - t_3) = m_R \Delta i_E \quad (3)$$

where:

- c_{pg} – specific heat of the 33% solution of propylene glycol,
- m_{lhs} , m_R – mass flow rates, in lower heat source and refrigerant respectively,
- Δi_E – refrigerant enthalpy increase in the evaporator.

The electric power P_e of the compressor is described by the following equation:

$$P_e = m_R \Delta i_C \quad (4)$$

- Δi_C – refrigerant enthalpy increase in the compressor.

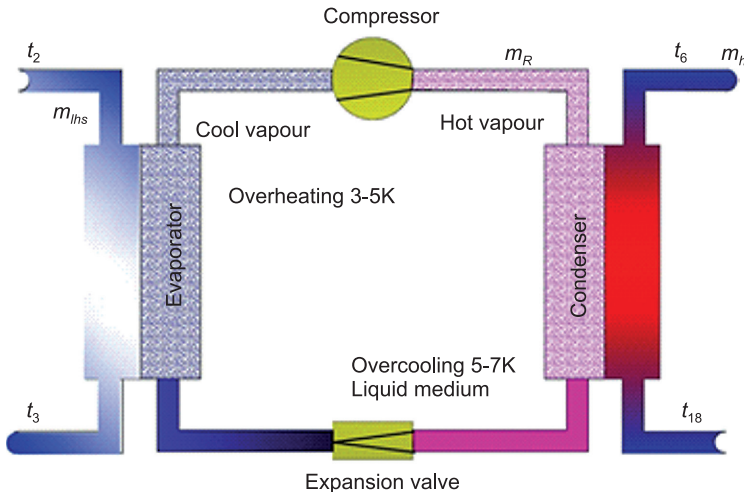


Fig. 2. Diagram of the heat pump with marked symbols

The thermal power P_h of the condenser in steady state conditions is described by the following equation:

$$P_h = c_w m_h (t_6 - t_{18}) = m_R \Delta i_h \quad (5)$$

where:

- c_w – specific heat of the water in heating system,
- m_h, m_R – mass flow rates, for operating medium in the upper heat source and refrigerant mass flow rate respectively,
- Δi_h – refrigerant enthalpy decrease in the condenser.

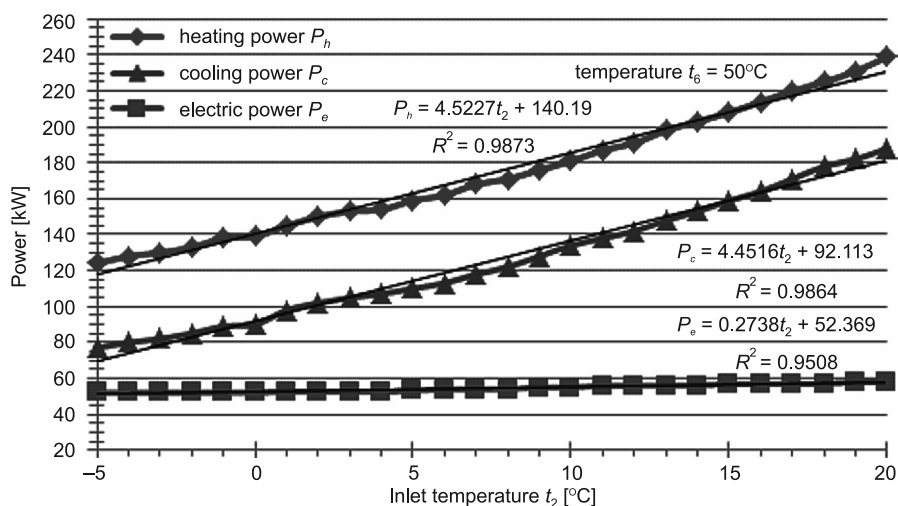


Fig. 3. Heating power P_h , cooling power P_c and electric power P_e versus inlet temperature t_2 to the evaporator, $t_6 = 50^\circ\text{C}$

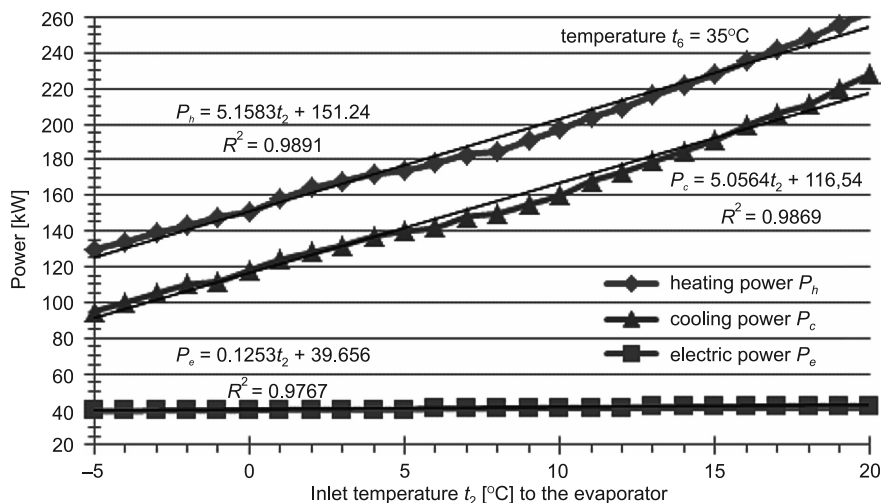


Fig. 4. Heating power P_h , cooling power P_c and electric power P_e versus inlet temperature t_2 to the evaporator, $t_6 = 35^\circ\text{C}$

In theoretical considerations, neglecting energy losses to the environment and assuming isentropic expansion process in valve, it is assumed that:

$$P_h = P_c + P_e, \quad (6)$$

This is equivalent to that:

$$\Delta i_h = \Delta i_c + \Delta i_e. \quad (7)$$

Approximations P_h , P_c and P_e versus inlet temperature t_2 to the evaporator are presented in Fig. 3, t_6 is assumed 50°C. Hence the COP installed heat pumps for heating could be calculated from formula:

$$\text{COP}_{\text{heating}} = \frac{P_h}{P_e} = \frac{4.5227t_2 + 140.19}{0.2738t_2 + 52.369}. \quad (8)$$

Approximations for $t_6 = 35^\circ\text{C}$ are given in Fig. 4. In this case, for temperature $t_6 = 35^\circ\text{C}$, COP for heating is represented by the equation:

$$\text{COP}_{\text{heating}} = \frac{P_h}{P_e} = \frac{5.1583t_2 + 151.24}{0.1253t_2 + 39.656}. \quad (9)$$

Obtained functions can be used to assessment of economic and energy efficiency heat pump installations in varying outside temperatures.

5. Economical considerations

Price c_h per unit of heat energy gained from the heat pump is calculated from equation:

$$c_h = \frac{1 + \psi}{\text{COP}_{\text{heating}}} c_e. \quad (10)$$

where:

- c_h – electrical energy price,
- ψ – factor related to the energy dissipation.

Table 2

The prices of energy carriers

Energy carriers	Cost of energy (in Poland, May 2014) [€/kWh]*
Electrical energy, rate I	0.133
Propane	0.111
Fuel oil	0.089
Electrical energy, rate II	0.081
Natural gas	0.074
Thermal network	0.051
Hard coal mill	0.033
Wood, biomass (pellets)	0.019

* It was taken 1€ = 4,2 zł

The prices of energy carriers are shown in Table 2. The value of the parameter ψ is assumed 0.1. Calculated values of the heat energy prices are presented in Figs 5 and 6.

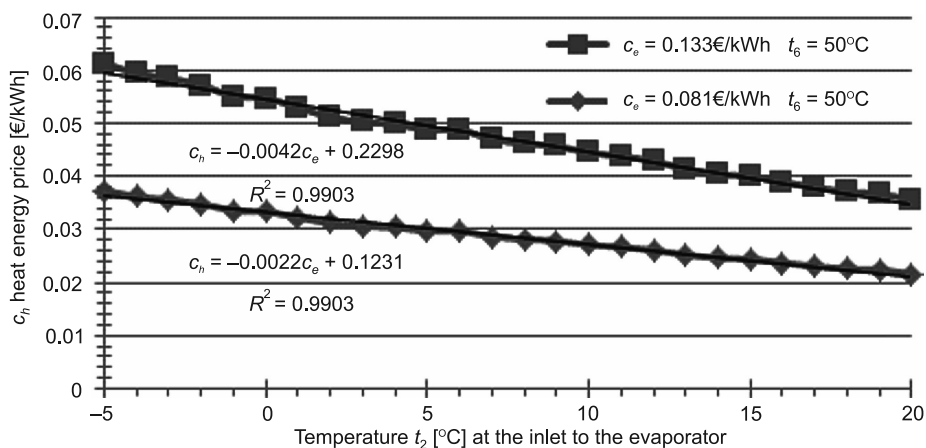


Fig. 5. Heat energy price c_h for heating ($t_6 = 50^\circ\text{C}$) versus inlet temperature t_2 to the evaporator

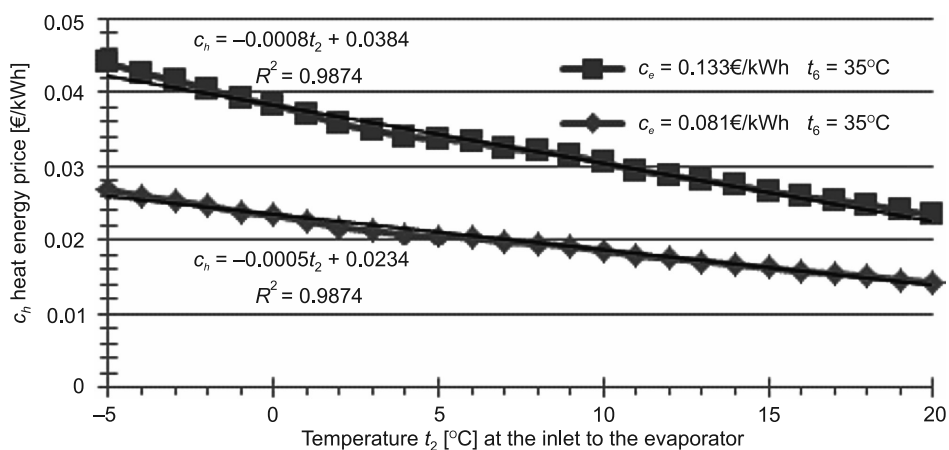


Fig. 6. Heat energy price c_h for heating ($t_6 = 35^\circ\text{C}$) versus inlet temperature t_2 to the evaporator

6. Conclusions

This paper presents heat pumps installation in John Paul II Centre in Krakow. The new installation presented here is an important element in the development of heat pump installations. Start-up phase was successful and the installation is working properly.

If the second electricity tariff is used properly then the operating costs of heating are less than the heat from the thermal network.

The experience in the installation and startup of the heat pumps are important in the subsequent heat pump systems with significant capacities.

This study has been made within the frame of the Project No. S/WBiŚ/4/2014.

References

- [1] <http://www.janpawel2.pl/budowa-centrum/galeriab/category/51-opis-koncepcji-centrum>
- [2] Borre A.V., *Definition of heat pumps and their use of renewable energy sources*, REHVA Journal – August 2011, 38-39.
- [3] Knaga J., *Changeability of heat output of heat pump with scroll type compressor*, TEKA Kom. Mot. Energ. Roln. – OL PAN, 2007, 7A, 41-45.
- [4] Adamski M., *Obliczanie płytowych wymienników ciepła zastosowanych jako skraplacze albo parowniki*, Współczesne problemy techniki chłodniczej: Konferencja Naukowo-Techniczna, [org.] Stowarzyszenie Inżynierów i Techników Mechaników Polskich, Stowarzyszenie Producentów i Użytkowników Urządzeń Chłodniczych, Centralny Ośrodek Chłodnictwa, Kraków, 21–22 października 1999, 95-101.
- [5] Dane techniczne pompy ciepła VATRA GIGA (www.vatra.pl).

KAROL BANDURSKI*, TOMASZ MIELCZYŃSKI**, HALINA KOCZYK*

THERMAL COMFORT AND ENERGY CONSUMPTION OF THE ECOLOGICAL HOUSE – SIMULATION ANALYSIS OF *DOMTRZON*

KOMFORT TERMICZNY I ZUŻYCIE ENERGII DOMU EKOLOGICZNEGO – ANALIZA SYMULACYJNA *DOMTRZON*

Abstract

The paper describes the concept of *DomTrzon* which means 'ecological house'. Measurements carried out in the existing building are presented. Based on this data the building envelope model assumptions are verified. A simplified model of a wood-lag accumulation stove (NunnaUuni) is proposed. The indoor thermal comfort and the building's *final energy* consumption are investigated using TRNSYS simulation software. During periods when the building is occupied, most zones fulfill thermal comfort requirements. The final energy consumption of *DomTrzon*, for heating purposes, is equal to 66 kWh/m²/year.

Keywords: ecological, wooden building, accumulation stove, energy efficiency, simulation

Streszczenie

Artykuł opisuje koncepcję ekologicznego domu – *DomTrzon*. Zaprezentowano pomiary przeprowadzone w istniejącym obiekcie. W oparciu o pomiary zweryfikowano założenia dotyczące modelu konstrukcji budynku. Zaproponowano uproszczony model pieca akumulacyjnego na drewno (NunnaUuni). Wewnętrzny komfort termiczny i energię końcową budynku zbadano przy użyciu programu symulacyjnego TRNSYS. W trakcie użytkowania większość pomieszczeń spełniała wymagania komfortu termicznego. Energia końcowa *DomTrzon* na cele grzewcze jest równa 66 kWh/m²/rok.

Słowa kluczowe: budynek drewniany, ekologiczny, piec akumulacyjny, efektywność energetyczna, symulacja

* M.Sc. Eng. Karol Bandurski, Prof. D.Sc. Ph.D. Eng. Halina Koczyk, Institute of Indoor Environmental Engineering, Faculty of Civil and Environmental Engineering, Poznan University of Technology.

** M.Sc. Eng. Arch. Tomasz Mielczyński – BUILDgreen Design.

1. Introduction

The concept of ecological buildings, according to the authors, has two purposes. Firstly, ecological buildings are energy efficient and provide high indoor air quality. Secondly, they are constructed and operated in a way that ensures low input of additional energy used in the process of production and distribution. In other words ecological houses are characterized by low **energy demand** and low **final energy** consumption, but simultaneously **primary energy** consumption should be lower than **final energy** consumption [4].

DomTrzon is an innovative and multi-option project of a single family house that meets the requirements of an ecological building concept. The project is based on the idea of a wooden family house that supports residents' integration and thermal comfort but is dedicated for people who prefer to stay close to nature and lifestyle in harmony within weather cycle. The main heat source in *DomTrzon* is a wood-lag accumulation stove that is used as a heating unit and kitchen appliance [2]. The first *DomTrzon* has been built in the countryside, in the north part of Greater Poland.

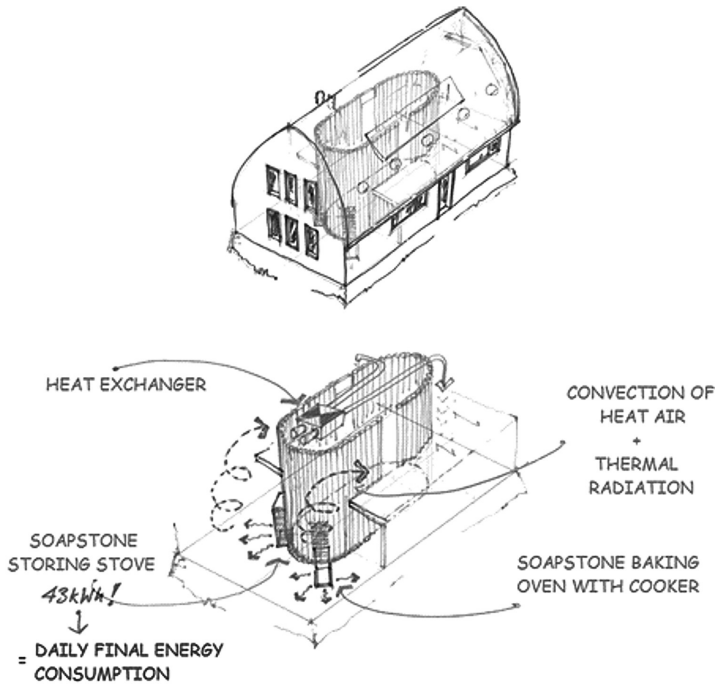


Fig. 1. *DomTrzon* – sketch of concept [2].

The aim of this paper is to analyze the concept of *DomTrzon* in the context of thermal comfort and energy consumption. The analysis is based on measurements carried out in the existing building (unoccupied) and by TRNSYS simulation. Measurement data are used to check the assumption of the building envelope model. Indoor temperature data are obtained based on TRNSYS simulation.

2. Analyzed option of *DomTrzon*

The investigated building has an area of about 150 m². The orientation and functional division of the house is shown in Fig. 2, but in reality, all zones of the building are open (without doors), the only partition wall is the central palisade. The first floor is 2.82 m high, the second floor is an attic and the highest vertical dimension is 2.86 m. The living room is two floors high, so the second floor is entresol. Daylight is supplied to the entresol by four skylights: two in the technical room and two on both sides of the entresol.

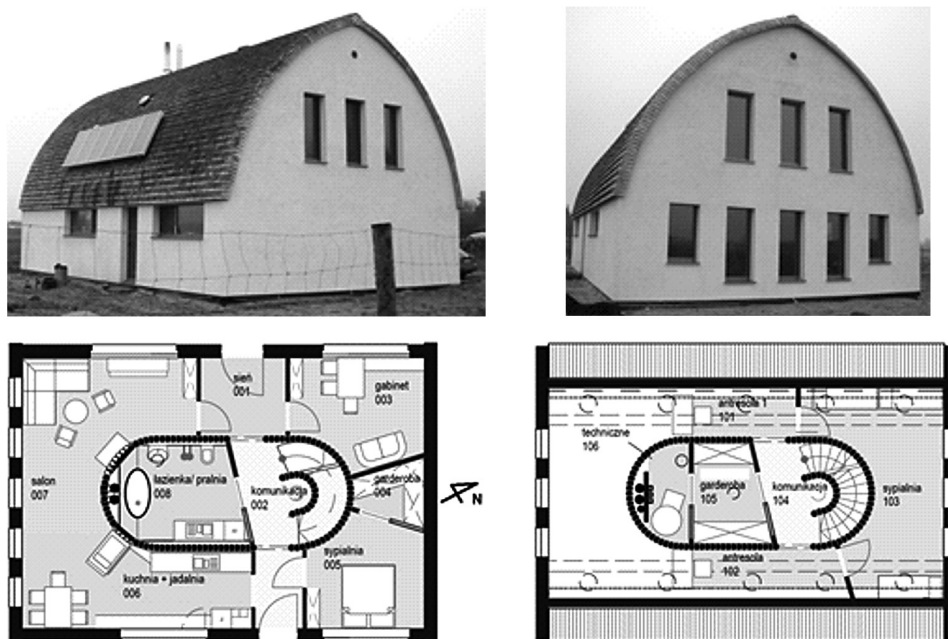


Fig. 2. *DomTrzon* – analyzed variant. Living room (two floors high) with kitchen on south side, two bedrooms: 1st floor (east side) and 2nd floor (entresol), study room is on west side on the 1st floor, in the center: bathroom (1st floor) and technical room (2nd floor) [2]

The construction is heavy and wooden. The thermal properties of the external envelope are presented in Table 1.

The building is occupied by a family of five (parents and three children). The parents sleep in the bedroom and the children sleep in the entresol. The family wakes up at 7:30 AM and goes to bed at 10:00 PM. Four persons spent most of the time in living room and one person works for 7 hours in the study room every day. Four people leave the house for 1.25 hours at noon. There are three kinds of heat gain taken into account: occupant (according to ISO 7730); bathwater/shower (138 W, 0.5 h every evening and morning); equipment in the technical room (20 W, all the time). Moisture gains are assumed in the bathroom (1.8 kg/h, 0.5 h every evening and morning) and in the living-kitchen zone from cooking (proportional to cooking intensity max 1.8 kg/h, 2h, three times per day).

External envelope construction (capital letters indicates PAVATEX products)

Wall	Layers (from inside)	thickness [m]	conductivity [W/(mK)]	heat capacity [kJ/(kgK)]	density [kg/m ³]
External wall $d = 0.41$ [m] $U = 0.115$ [W/(m ² K)]	wood	0.1	0.13	2.51	550
	PAVAFLEX	0.24	0.038	2.1	55
	DIFFUTHERM	0.06	0.043	2.1	250
	plaster	0.01	0.82	0.84	1850
Roof $d = 0.59$ [m] $U = 0.086$ [W/(m ² K)]	wood fibers (with rafter)	0.45	0.043	2.1	60
	ISOLAIR	0.022	0.047	2.1	240
	air gap (battens)	$R = 0.2$ [m ² K/W]			
	aspen chips	0.019	0.14	0.9	530
Windows					
$U = 0.73 - 0.84$ [W/(m ² K)], $g = 0.45 - 0.58$					

The analyzed option of *DomTrzon* is equipped with one source heating system – an accumulation wood-lag stove with a baking oven and cooker – Eva 1 [3]. The stove is used above all as kitchen equipment: three times per day with different batch of wood to fireplace. Although the stove is placed in the living-kitchen zone, the back wall is part of the bathroom wall. A more detailed description of stove is given in the next section.

Fresh air is supplied to zones by a balanced mechanical ventilation system with recuperation. Heat exchanger is supported by an auxiliary heater (800 W).

3. Model verification

The investigated building is modeled in TRNSYS software. There are three sub models: envelope model (using type 56); model of stove (type 963); ventilation system model (TRNSFLOW). The first two of these sub models are verified based on measurement data (envelope) and the manufacturer's technical specifications (stove).

3.1. Envelope model

The measurement of indoor and outdoor temperature was carried out in the building for one week: 25th–31st December 2013. The house was unoccupied and not operated, so its cooling process could be observed. The same process is simulated using the envelope model. The assumed boundary conditions (weather data) are from a meteorological station situated about 30 km from the building. Outdoor temperature on site is compared with the ambient temperature for the meteorological station in Fig. 3. It could be seen that values were very close and therefore the assumed boundary condition was reasonable.

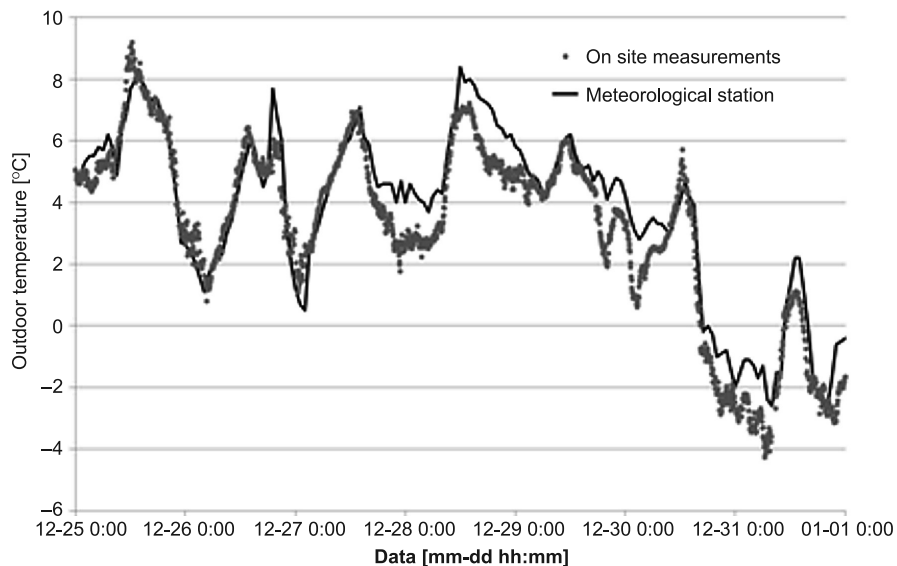


Fig. 3. Comparison of outdoor temperature collected by meteorological station (about 30 km away) and during onsite measurements

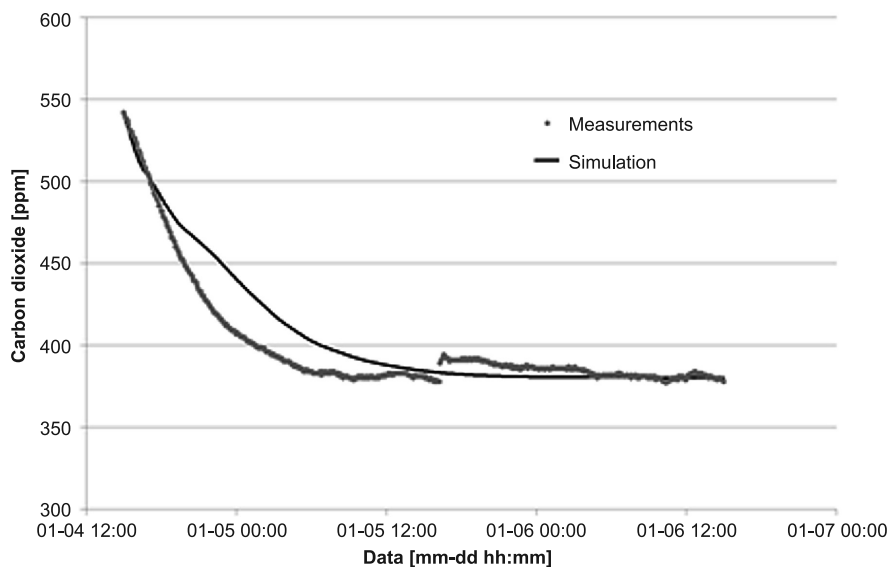


Fig. 4. Comparison measured data and simulated results. Decrease in CO₂ concentration in living-kitchen zone, after leaving house by occupant

Fig. 5 shows comparison of measured data and the data generated during simulation. It was observed that data suggests a higher increase of indoor temperature caused by direct sunlight. Explanation of this difference is that sensors were placed in specific locations

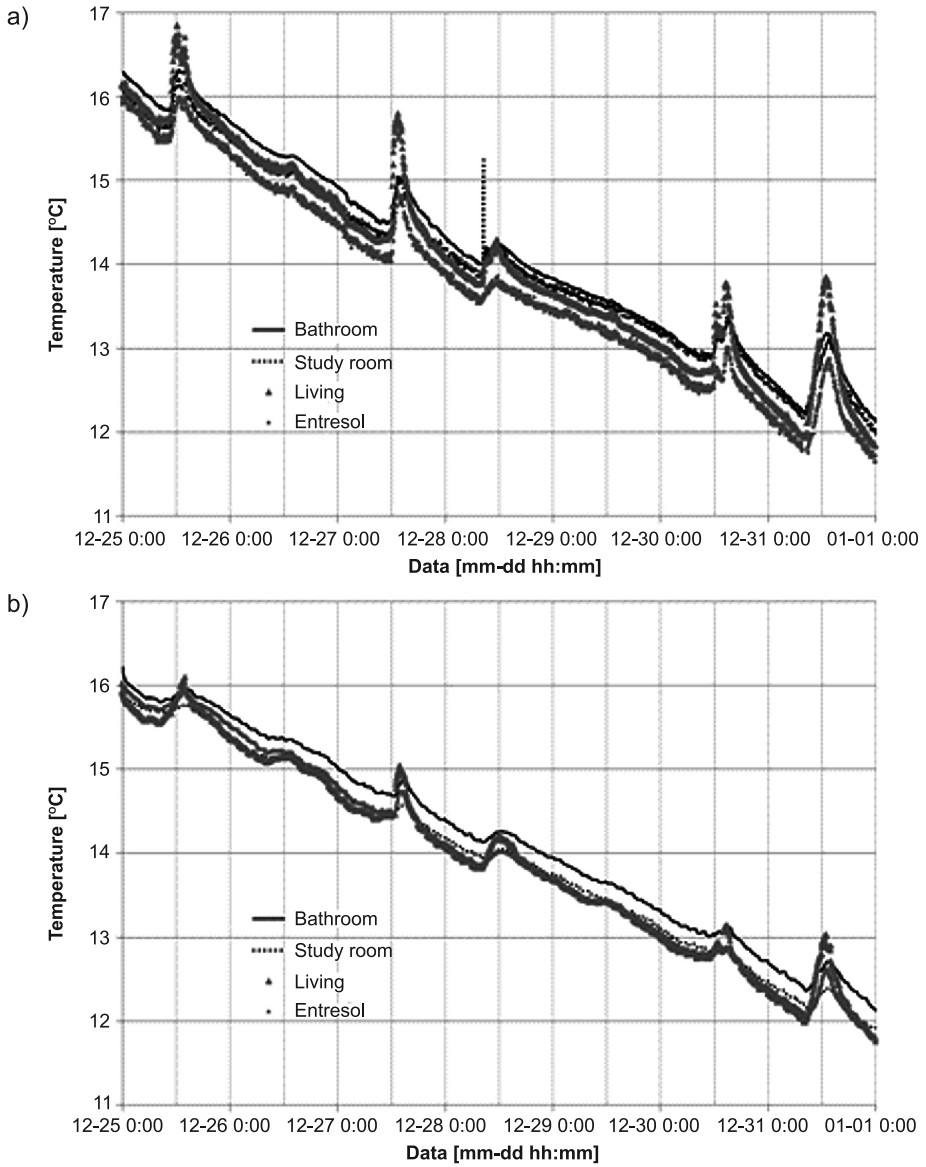


Fig. 5. Comparison of (a) measured and (b) simulated indoor temperatures of investigated building during cooling process

(e.g. close to windows) whereas the simulation calculates the mean temperature of the whole zone.

Monitoring of CO_2 concentration has also been carried out. These data are used to check assumptions regarding building airtightness. A comparison of the simulated

and measured decrease in CO₂ concentration (in the unoccupied building) proves the accuracy of the envelope model (Fig. 4).

3.2. Accumulation stove model

The model of the stove is based on the manufacturer's technical specifications [3]. Because there is no detailed information about product Eva 1 that is being used in the investigated option of *DomTrzon*, approximations of stove parameters are deduced from the technical specifications of similar stoves. The operation of these stoves can be divided in three phases. The first phase lasts 2 hours, during this time single bath is burned and stoves warms up. Then, the accumulated energy released with almost constant (nominal) power over 6–8 hours. The power decreases during the last phase. All three phases together last about 48 h. Based on manufacturer specifications it is assumed that max. batch for the stove is 10 kg. Nominal power of the stove is maintained for 7 h and is equal 2.03 kW. The stove heat capacity stove is about 1500 kJ/K (Fig. 6).

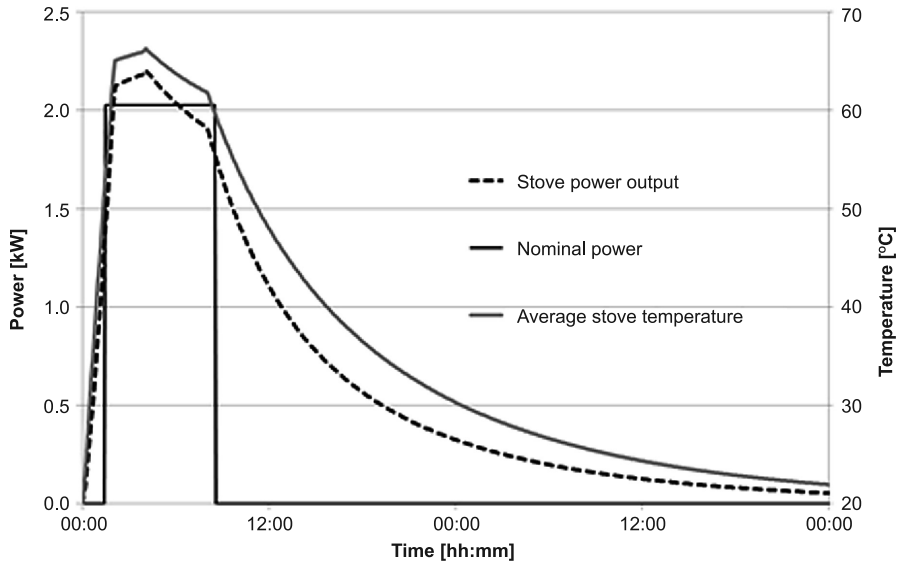


Fig. 6. Power and temperature output of accumulation stove installed in the investigated building

Heat transfer between stove and zones is realized by convection and radiation. Based on simplified calculation, two correlations have been identified:

$$h_{c+r} = f(t_{\text{stove}}) \quad (1)$$

$$\frac{Q_r}{Q} = f(\Delta t) \quad (2)$$

where

- h_{c+r} – the total (radiation and convection) heat transfer coefficient,
- Q_r – the radiation power released by stove to zone,

- Q – the total power released by stove to zone,
 t_{stove} – the average temperature of the stove,
 Δt – the temperature difference between average stove temperature and mean temperature of zone.

The above correlation is used to calculate heat transfer between stove and zone. The heat from the stove emitted to the living-kitchen zone and bathroom is proportional to the stove's surface area turned towards the specified zone. These simplifications are based on the model presented by Georges and Novakovic, but their method is more detailed and verified [1].

4. Simulation

Poland is in the climatic zone where energy consumption by residential buildings is higher during the heating season, therefore, the analysis below takes into account the period from the 1st of November to 31st of March. Weather data are generated by Meteonorm as TMY2 data set for Poznań–Ławica meteorological station.

4.1. Ventilation system and stove operation

A ventilation system is two-mode. Both modes have a balanced supply/return airflow of 200 m³/h. The first one uses a heat exchanger to restore heat from exhaust air. Heat exchanger efficiency is 82%, it is constant because airflow is also constant. Fresh air flows into the auxiliary heater before the heat exchanger. The heater ensures that the temperature of the air flowing into the heat exchanger is not lower than -5°C. If the indoor temperature is too high, then fresh air is supplied to the house through heat exchanger bypass. The second mode is turned on if the temperature of the exhausted air is higher than 22°C. The ventilation system returns to the first mode if the exhausted air temperature falls to 21°C.

The stove is used three times per day, at: 8AM, 1 PM and 8PM, for cooking purposes. The lower calorific value of burned wood is equal to 15.1 kJ/kg. The mass of batches depends on the time of day and indoor temperatures. If the exhausted air temperature falls below 19°C, the stove is fed according to the extreme mode until the temperature increases to 21°C, batches are then supplied again according to the standard mode.

Table 2

Mass of batches to the accumulation stove

Hour of day	Mass of batch [kg]	
	standard mode	extreme mode
8 AM	3	10
1 PM	8	10
8 PM	3	10

The efficiency of the combustion process depends on many factors, among others on the amount and temperature of air supplied to the fireplace. In reality, air to the fireplace

is supplied from the living-kitchen zone. Because of the complexity of this solution and the lack of sufficient data (problem with modeling), it is assumed that air for combustion is supplied directly from outside and the efficiency of the combustion process is constant and equal to 75%.

4.2. Results

A simulation was carried out to analyze the thermal comfort and energy consumption of the chosen variant of *DomTrzon*. Peeters et al. propose comfort temperature ranges for residential buildings that could easily be used in building energy simulation programs, they prove their approach based on literature and data review [5]. This approach is used to assess thermal comfort in the investigated house. Thermal comfort ranges are defined separately for bathrooms, bedrooms and other rooms – therefore, results are presented in three graphs (Fig. 7–9).

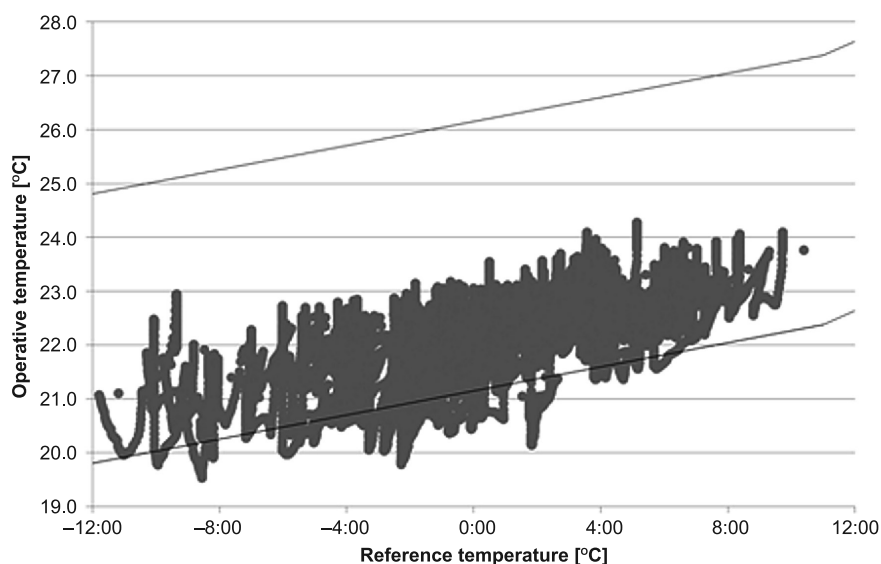


Fig. 7. Operative temperature in bathroom and thermal comfort range [5] during simulation period (November–March)

DomTrzon consumes energy in three ways: burning wood in the stove, running the ventilation system fans and heating fresh air in the auxiliary heater. The most energy is consumed by stove. **Final energy** (for heating and ventilation purposes) consumed by the building is compared with **energy demand** of the building and **primary energy** consumption of the heating and ventilation system (Fig. 10). **Energy demand** is calculated for buildings with indoor air temperature higher or equal to 24°C in the bathroom and 20°C in other rooms, the outside air flow rate into the building is equal to the ventilation air flow (200 m³/h) and the heat exchanger efficiency is 82%. Internal heat gains are the same for **energy demand** and **final energy** (as described in section 2). Calculation of **primary energy** consumption is based on Polish methodology for building energy performance calculation [4].

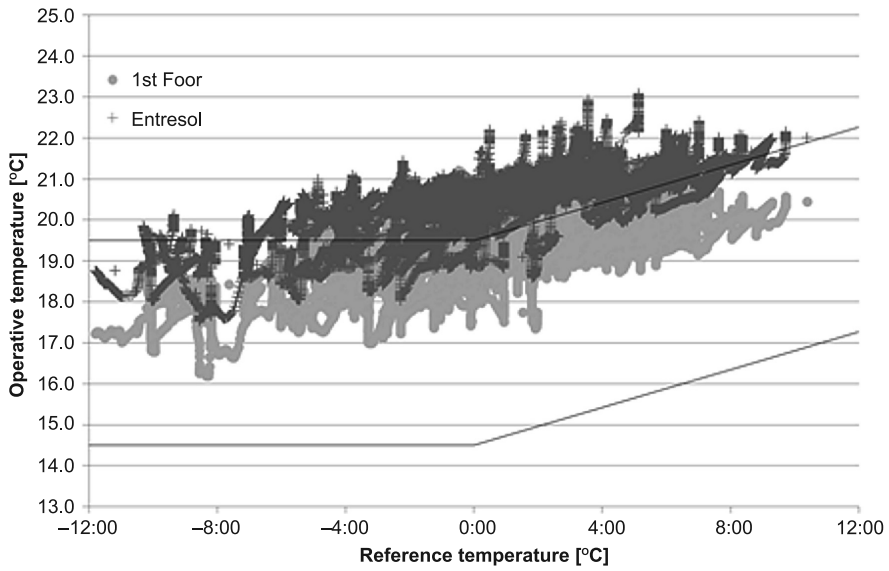


Fig. 8. Operative temperature in bedrooms and thermal comfort range [5] during simulation period (November–March)

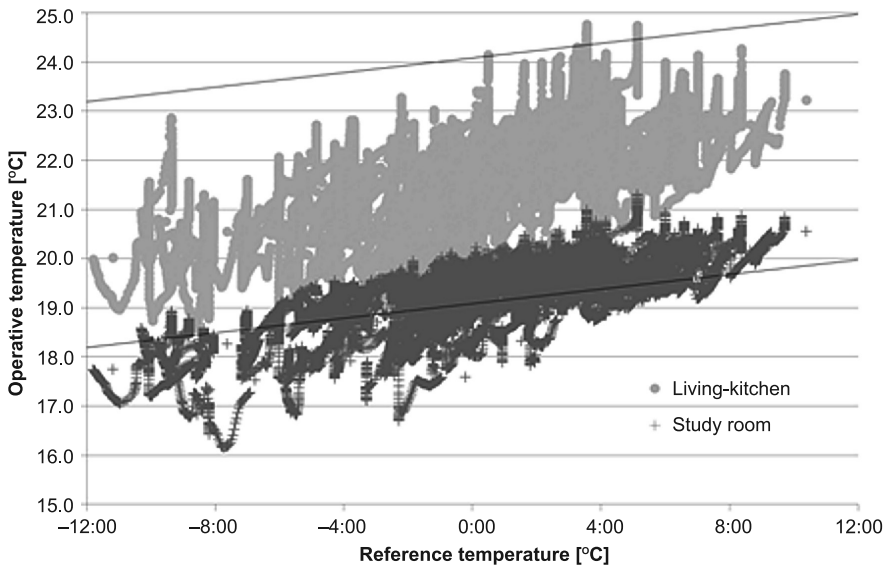


Fig. 9. Operative temperature in living zones (living kitchen and study room) and thermal comfort range [5] during simulation period (November–March)

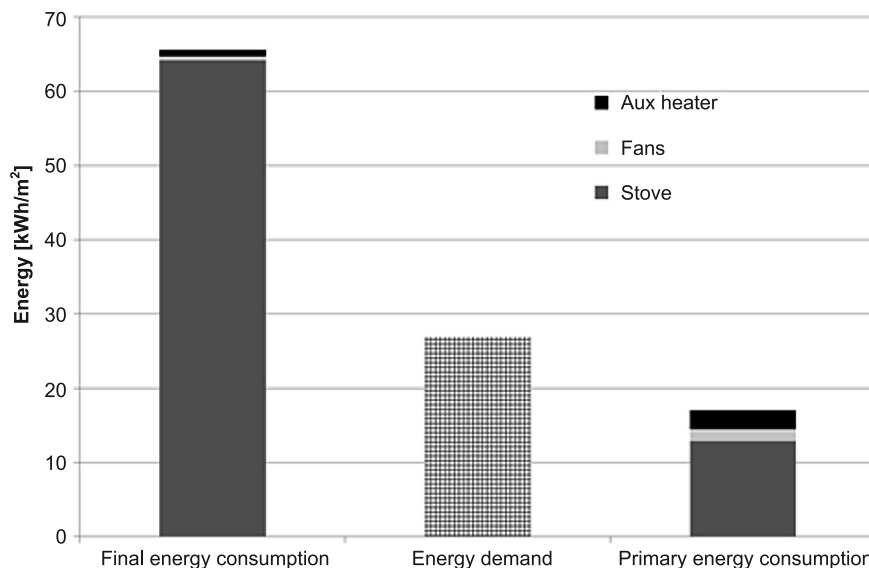


Fig. 10. **Final energy** consumption, **energy demand** and **primary energy** consumption (for heating and ventilation purposes) of investigated variant of *DomTrzon*

4.3. Discussion

It can be seen that high temperature differences occur in the building. The difference between the bathroom and the study room is about 3 K. The coldest zones are placed in the north side of the first floor because of a lack of solar radiation and the heat buoyancy effect. The highest temperatures occur in the center of the house and in zones close to the stove. The bathroom operative temperature is partially outside the thermal comfort range, but the coldest periods occur during the night-time, when zones are unoccupied. In the case of the bedroom zones, the situation is similar – comfortable temperatures are during the night time, when rooms are used. The entresol could also be used as a living room, because its operative temperature is in the comfortable range during the day-time. The worst situation is in the study room. Some days during winter are completely off the scale in this zone. On the other hand, it is stated by occupants that wooden walls cause the perceived temperature to be a bit higher than the measured one. Nonetheless, comfort in the study room is a serious problem especially if the activity of the occupants is very low.

Final energy consumption of the building is more than two times higher than **energy demand**. This is because the accumulation stove is used mainly for cooking purposes and therefore, a high temperature heat source is needed (which causes greater fuel consumption). It can be seen that on the one hand, an excess of heat causes high temperatures in zones close to the stove. On the other hand, there are some zones that, despite the energy excess, remain under-heated. Some of under-heated zones are ‘cold’ zones, as bedrooms, where lower temperatures are desired (Fig. 8). However, the indoor condition in the study room (Fig. 9) could be very uncomfortable if desk work is performed. It seems that better

management or utilization of the occurring energy excess (e.g. by ventilation system modification) could improve the building's performance. The issue could be even more important during summer time because the energy excess is higher and stays in the living-kitchen zone and could become uncomfortable, especially in the middle of day.

Although the final energy consumption should be improved, the primary energy consumption (Fig. 10) is even lower than the energy demand, which proves that *DomTrzon* is a solution with highly sustainable energy efficiency potential.

5. Conclusions

Energy demand of the investigated *DomTrzon* is higher than in passive houses (15 kWh/m²), but is still low. Moreover, its **primary energy** is lower than its **final energy** consumption. Therefore *DomTrzon* could be titled an ecological house. It can also be stated that *DomTrzon* ensures thermal comfort. However, there are a few issues that should be considered to develop the concept. The main ones are the management and utilization of excess energy from the stove and the low operative temperatures in the study room. Natural demand controlled ventilation should also be investigated as a solution to reduce investment costs. Any used and proposed solution should be also analyzed in summer and transitional seasons.

Proposed models are useful, but can also be developed. The combustion process should especially be considered in a more detailed way to take into account the amount and temperature of air and stack effect. Thereby, a real case could be investigated. More detailed calculations of heat exchange between zones and stove worth carrying out.

The weather data was donated by Joe Huang from www.whiteboxtechnologies.com. These data support is highly appreciated.

References

- [1] Georges L., Novakovic V., *On the integration of wood stoves for the space-heating of passive houses: assesment using dynamic simulation*, 1st Building Simulation and Optimization Conference, Loughborough UK, 10–11 September 2012, 157-164.
- [2] <http://domtrzon.buildgreen.pl>
- [3] <http://nunnauni.com.pl>
- [4] Rozporządzenie Ministra Infrastruktury z dnia 6.11.2008 w sprawie metodologii obliczania charakterystyki energetycznej budynku i lokalu mieszkalnego lub części budynku stanowiącej samodzielną całość techniczno-użytkową oraz sposobu sporządzania i wzorów świadectw ich charakterystyki energetycznej. (Dziennik Ustaw nr 201, poz. 1240).
- [5] Peeters L., de Dear R., Hensen J., D'haeseleer W., *Thermal comfort in residential buildings: Comfort values and scales for building energy simulation*, Applied Energy, vol. 86, 2009, 772-780.

JANUSZ BELOK*, BEATA WILK-SŁOMKA*

ENERGETIC EFFECTIVENESS OF A BUILDING WITH A SURFACE HEATING SYSTEM

EFEKTYWNOŚĆ ENERGETYCZNA BUDYNKU Z SYSTEMEM OGRZEWANIA PŁASZCZYZNOWEGO

Abstract

In the paper authors have undertaken a trial to present energetic effect developed by cooperation of a surface heating system and a building construction on the basis of object modeling using ESP-r software. Performed analyses concern impact of heat capacity of the building construction and different heating panels on final energetic effectiveness taking into consideration the algorithm of heating system operation control. The article is an example of a changing approach to building facilities designing – in case of integrated method of design it allows for obtaining considerable improvement of energetic quality.

Keywords: panel heating foundation, air floor heating system

Streszczenie

W artykule autorzy podjęli próbę przedstawienia efektu energetycznego wywołanego współpracą pomiędzy systemem ogrzewania płaszczyznowego a konstrukcją budynku na bazie modelowania obiektu w programie ESP-r. Przeprowadzone analizy dotyczą wpływu pojemności cieplnej struktury budynku i rozwiązań płyt grzewczych na końcową efektywność energetyczną w powiązaniu z algorytmem sterowania pracą systemu grzewczego.

Słowa kluczowe: płytowy fundament grzewczy, powietrzny system ogrzewania podłogowego

* Ph.D. Jan Belok, Ph.D. Beata Wilk-Słomka, Chair of Building Engineering and Buildings Physics, Faculty of Civil Engineering, The Silesian University of Technology.

1. Introduction

In every room temperature differences exist in a vertical and horizontal direction. Vertical distribution, the closest to the optimal temperature, is achieved in the case of a floor heating system [1]. Amongst many technical implementations of such a heating system – it is possible to find a solution connecting into a whole a heating system and a building foundation. A heating foundation panel [5] connects features of a construction element and a floor heating panel. Each foundation is designed individually. Foundations are insulated from the ground using foamed polystyrene plates of total thickness $d = 16.0$ cm and heat transfer coefficient $U = 0.16$ [W/m² K]. The heating system consists of distribution of heated air in channels placed inside a foundation panel. Hot air is distributed using pipes of “Spiro” type of diameter $\varnothing = 100$ mm placed on covered reinforced mesh foamed polystyrene. Next, pipes are poured with concrete. The heating unit in this system is electrical or water heating set placed in metal enclosure placed in the foundation slab (covered by a masking board). Water sets may be supplied from low temperature boilers or from other sources (oil or coal boilers, combined heat and power plant, heat pump). A distance between pipes is of 0.8–1.2 m. Loop length and number of elbows in all circuits must be the same for assuring equal air flow. The system is controlled by thermostats placed in a room [5]. Figure 1 presents an exemplary heating foundation.



Fig. 1. The exemplary heating foundation [5]

2. The subject of analyses

The subject of this paper is the single floor individual building with non-usable attic (not heated), without cellars, with wooden light frame construction. The building is located near Gliwice and is assigned for four persons. It has the ridge roof with slope angle of 40°; the roof is covered by zinc-titanium plates. The building is composed of the living room connected with the kitchen, three bedrooms, two bathrooms, the study, the boiler room, the vestibule (heated part) and the garage and the maintenance room (not heated part). Fig. 2 represents

the projection and the façade of the building under consideration. Specification of individual rooms' areas: total area 165.15 m²; usable heated area 136.03 m². Calculations of final energy demand were performed in accordance with the procedure presented in [3]. Annual demand for heat for this building is of 12.280.28 [kWh]; the index of annual demand for final energy: EK = 90.28 [kWh/m²]. Table 1 represents the heat transfer coefficients of building's partition walls.

Table 1

Heat transfer coefficients of building's partition walls

Type of partition	Heat transfer coefficient U [W/m ² K]
floor on ground	0.36
external wall	0.20
ceiling over first level	0.25
roof	0.18

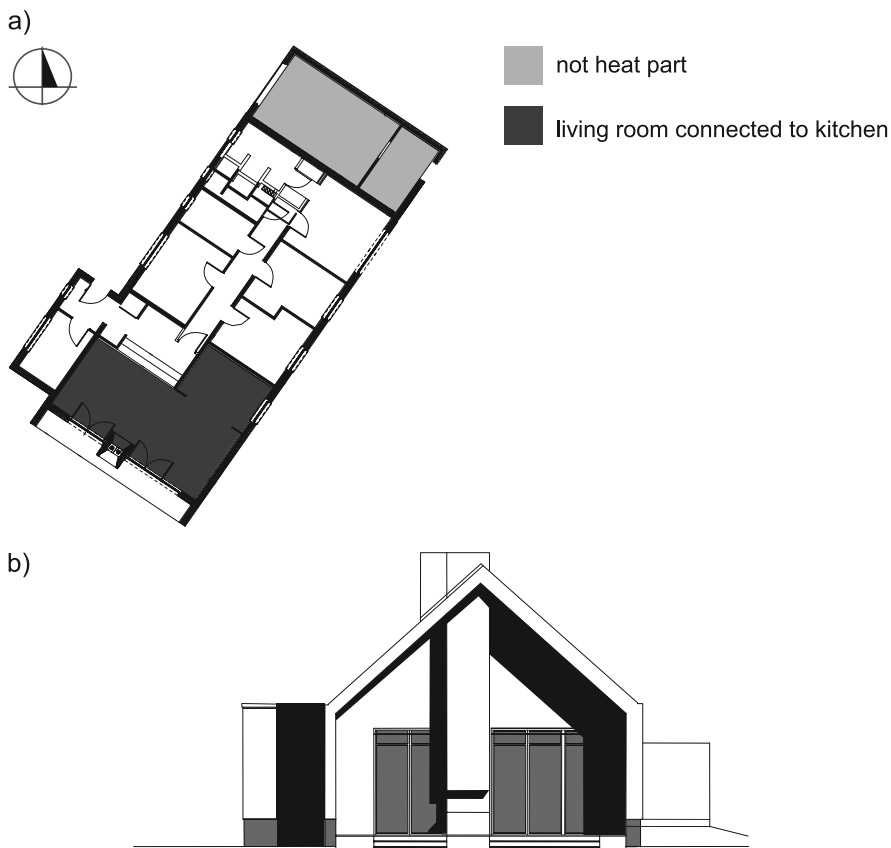


Fig. 2. Analyzed building: a) first level view; façade; b) South-West

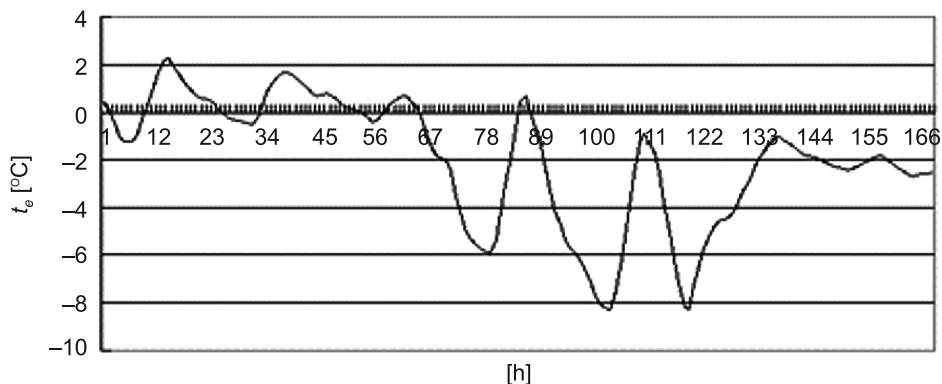


Fig. 4. Long-term values of external air temperatures for Katowice – 09.01-15.01

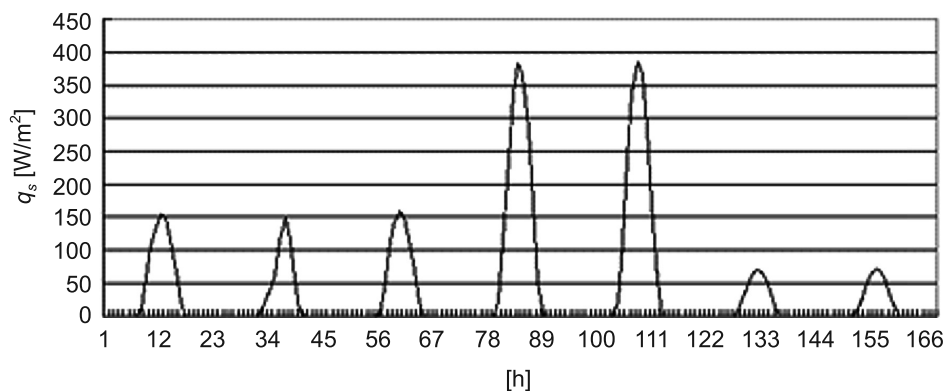


Fig. 5. Long-term average values of direct solar radiation intensity for Katowice – 09.01-15.01

4. Results of analyses

The performed analyses included the determination of the impact of building thermal capacity and breaks in heating at various thickness of slab heating foundation on thermal comfort parameters (PMV index) along with air temperature in rooms and consumption of energy required for building heating. Presented values concern the selected part of the heating season – January; in order to keep proper readability of presented results.

The simulations were performed for the entire building while part of presented results refers to the living room together with the kitchen (orientation: South-West). The living room and the kitchen make one space with greatest area of glass partitions (13.23 m²) and greatest heated area (47.77 m²). In calculations assumptions were taken described in paragraphs 2 and 3. In Figures 6–11 results for January are represented and for various thickness of the heating panel ($d = 100; 150; 200; 250; 300$ and 350 mm). Additionally some consecutive coldest days were selected (12–14 January).

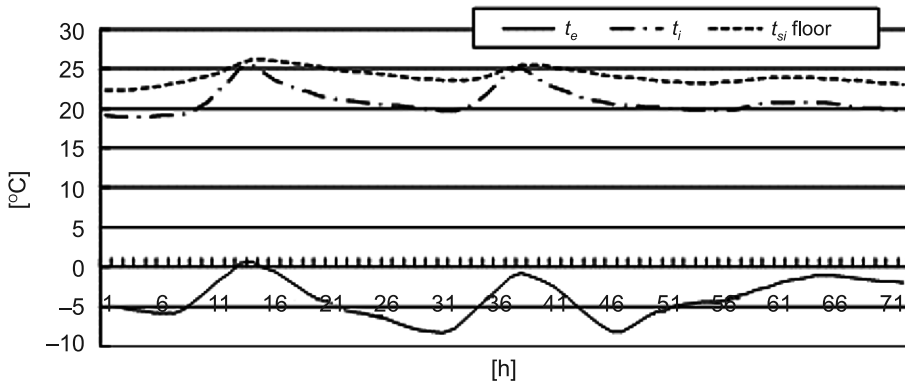


Fig. 6. Air and floor surface temperature in the living room for heavy construction and heating panel thickness $d = 300$ mm – 12–14.01

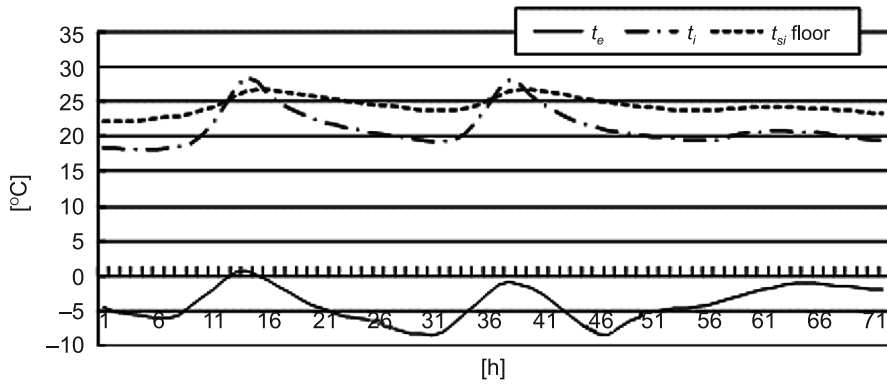


Fig. 7. Air and floor surface temperature in the living room for light construction and heating panel thickness $d = 300$ mm – 12–14.01

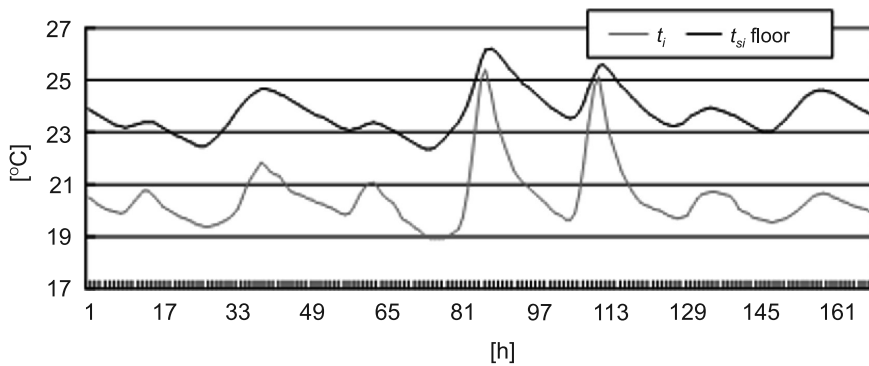


Fig. 8. Air and heating panel temperature in the living room for heavy construction and heating panel thickness $d = 300$ mm – 9–15.01

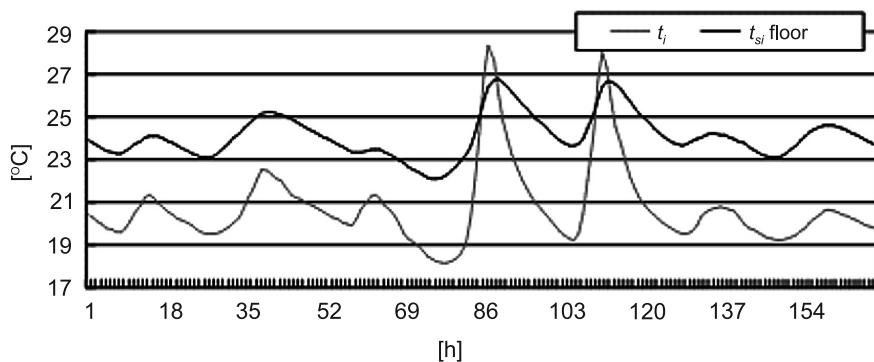


Fig. 9. Air and heating panel temperature in the living room for light construction and heating panel thickness $d = 300$ mm – 9–15.01

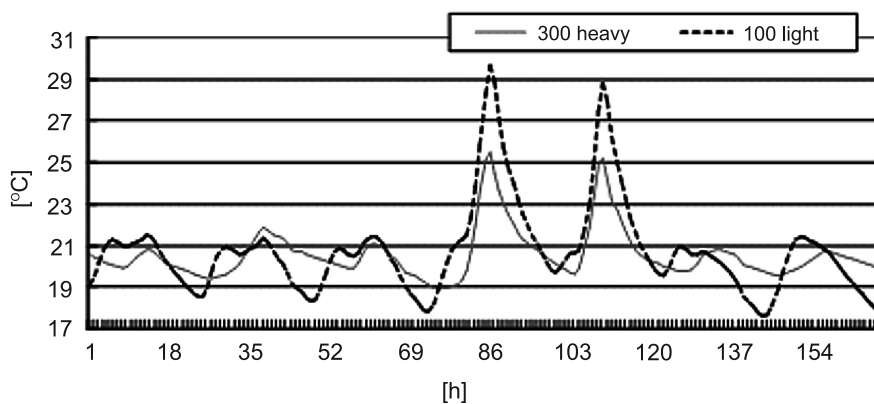


Fig. 10. Air temperature in the living room at heating panel thickness $d = 300$ mm – for heavy construction and $d = 100$ mm for light construction – 9–15.01

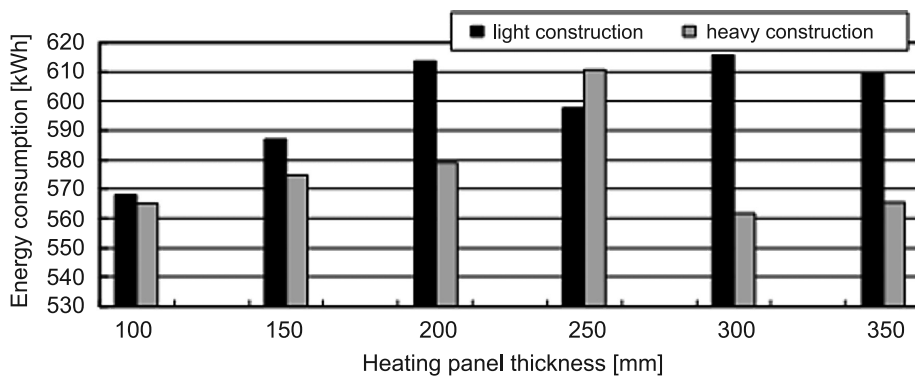


Fig. 11. Energy consumption for the building depending on partitions construction and heating panel thickness – 9–15.01

The analysis of calculations results allows for the following statements:

- air temperature in the room for the selected month (January) fluctuates between 16–28°C;
- floor surface temperature fluctuates between 21–24°C in coldest consecutive days (14–18 of February). Comparing above values with floor surface temperature in rooms like: living room, bedroom, kitchen for floor heating system that cannot exceed 29°C [1], obtained values are satisfying;
- for the coldest day (1–2 of February) air temperature in the largest room fluctuates between 19.5–21°C (the design temperature has been assured);
- appraisal of thermal comfort is more advantageous for the building in heavier version with great thermal capacity; PMV values fluctuate between –0.47 to +0.93 – see Table 2; independently of heating panel thickness;
- comparing versions with lowest energy consumption for heavy and light building in aspect of thermal comfort its clearly visible (Fig. 11) that the building with heavy construction has lower temperature fluctuations assuming the same scheme of energy supply;
- if thermal capacity of the heating panel is the same then changes of temperature are more advantageous for the heavy building (Fig. 6 and 7);
- energy consumption depends on thermal capacity of the heating panel and thermal capacity of the entire building (Fig. 11).

5. Conclusions

Performed simulations prove the necessity for making precise analyses for obtaining effective cooperation of the heating system and the building facility. It is especially important in case of low-energy housing. Annual consumption of energy assigned for heating of a heavy and light building is presented: heavy building: 13494.54 kWh; light building: 14216.24 kWh (heating capacity of the heating panel for both buildings is the same).

Analyses of obtained results proved that use of breaks in heating (heating only during time of night tariff) assured temperature above 18.5°C. Only during the period when external temperatures were lowest in the room under analysis, temperature falls to approx. 18°C. Obtained calculations results allow to state that the computer simulation method gives such heating capacity of the heating panel that in connection with the building heating capacity could assure required thermal comfort and minimize energy consumption.

References

- [1] Recknagel H. at al., *Ogrzewanie i klimatyzacja*. EWFE, Gdańsk 1994.
- [2] Decree of Infrastructure Ministry, Off. J. No 75 item 690 as amended.
- [3] Decree of Infrastructure Ministry, Off. J. No 201, item 1240 as amended.
- [4] PN-EN ISO 7730:2006. Ergonomia środowiska termicznego.
- [5] www.legalett.com.pl.
- [6] www.vatenfall.pl.
- [7] www.esru.strath.ac.uk/Programs/ESP-r.

BORIS BIELEK*

CONCEPT OF THE NEW PHYSICAL-ENERGY
QUANTIFICATION OF BUILDINGS
IN THE DEVELOPMENT OF TECHNOLOGY
IN ARCHITECTURE FOR SUSTAINABLE SOCIETY

KONCEPCJA NOWEJ FIZYKO-ENERGETYCZNEJ
OCENY BUDYNKÓW
W ROZWOJU TECHNOLOGICZNYM ARCHITEKTURY
DLA ZRÓWNOWAŻONEGO SPOŁECZEŃSTWA

Abstract

Renewable energy sources as a conditioning factor of fundamental concept changes of energy quantification of buildings. 1st generation of low energy buildings. 2nd generation of low energy buildings. Green buildings with zero heat balance of the network – buildings with nearly zero energy balance of the network. Sustainable buildings with zero energy balance of the network. Sustainable building with an active energy balance in relation to distribution networks.

Keywords: renewable energy sources, low energy buildings, green buildings, sustainable buildings

Streszczenie

Źródła energii odnawialnej jako kluczowy czynnik fundamentalnych zmian w ocenie energetycznej budynków. Pierwsza generacja budynków niskoenergetycznych. Druga generacja budynków niskoenergetycznych. Zielone budynki niskoenergetyczne – budynki niemal zero-energetyczne. Budynki zrównoważone zeroenergetyczne. Budynki zrównoważone z aktywnym bilansem energetycznym w stosunku do sieci dystrybucyjnych.

Słowa kluczowe: odnawialne źródła energii, budynki niskoenergetyczne, budynki zielone, budynki zrównoważone

* Doc. Ph.D. Eng. Boris Bielek, Faculty of Civil Engineering, Slovak University of Technology in Bratislava.

1. Introduction

Two separate but closely connected categories are expressed by the term new physical-energy quantification of buildings:

- physical quantification particularly of envelope constructions of buildings, which are in global relations expressed by the weighted average coefficient of the thermal transmittance U_m (W/(m²·K)) and
- energy quantification of a building which is expressed by the specific energy demand for heating, ventilation, cooling, (hot water preparation) Q_H (kWh/(m²·a)), (kWh/(m³·a)).

A very close connection of these two categories can be seen in existing design solutions of buildings with purposeful energy saving where the reduction of energy demand of the buildings is in principal solved by an increase of the physical quantification of their envelope constructions. The new physical-energy quantification of buildings is also about the change of relations of these two categories. It is going to be about the optimization of the physical quantification of envelope constructions of buildings in economic relations to energy of renewable sources and the technology of their conversion.

The economic costs connected with the increase of physical quantification of envelope constructions until they reach the point of economic reversal, become inefficient from the investment point of view ($U_m < 0.4$ W/(m²·K)). On the contrary, investment and operational costs into renewable energy sources with in situ conversion might be of such parameters that even higher level of energy demand for acquiring the state of zero energy demand in relation to the distribution network might be economically profitable and therefore justifiable.

It is more convenient to set an interval of specific energy demand which allows the investors to determine the optimal mix of technologies, ensuring the energy efficiency of the energy conversion and the required return on investment.

The part of the concept of a new physical-energy quantification of a building is also the principle to measure separately the energy demand in a building for:

- heating, ventilation, cooling, (preparation of domestic hot water), which is converted from the primary energy source to the heat and separately to,
- lighting, appliances, motor drives, (possibly the preparation of domestic hot water), which is optimally converted from the primary energy source to the form of electric energy.

Electric distribution network represents a strategic task for the development of the infrastructure for a transformed society based on renewable energy sources.

2. Common Characteristics of Zero Energy Buildings in Relation to the Energy Distribution Networks

It is necessary to seek a balance of a new physical-energy quantification of buildings in the applied ratio of:

- energy from ecologically clean renewable sources and ecologically clean conversion of the energy in local facilities, optimally in situ (without energy losses from the distribution) and

– energy from fossil fuels and conversion of the energy in centralized facilities which is characterized by the production of emissions of greenhouse type and is distributed by the energy networks (with energy losses from the distribution).

The ratio of these two ecologically significantly different types of energy in buildings is possible to measure quantitatively. It is therefore possible to define buildings on the physical and economic principles in the form of “Net Zero Energy Buildings” in their three basic modifications [9] (Fig. 1):

1. Nearly Net Zero Energy Buildings. These are the buildings that have practically zero energy demand (heating, ventilation, cooling (hot water preparation) from the distribution network, from which only take energy (electrical lighting, electrical appliances, electric motor drives).
2. Net Zero Energy Buildings. These are the buildings that have zero energy demand and zero electric energy demand from the distribution networks.
3. Net Plus Energy Buildings. These are the buildings that have higher energy conversion in situ than their annual demand in real time.

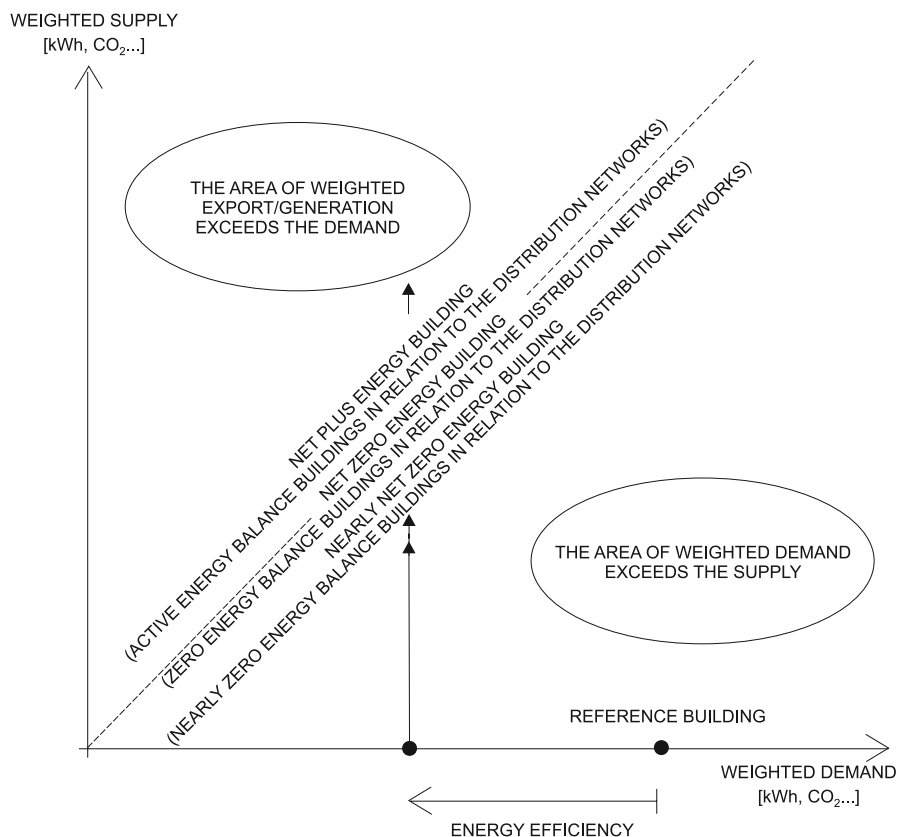


Fig. 1. Scheme of graphic dependence representing a way towards zero energy buildings in relation to the distribution network with alternatives “nearly” and “active”

Zero energy buildings are characterized by:

- the concept of application of the construction design of the theory of low energy house, based on the system relation BUILDING – CLIMATE – ENERGY [7], which defines requirements on all the elements of the building (Fig. 2), influencing its overall annual energy demand,
- the concept of application of ecologically clean local renewable energy sources which are optimally renewed by the power of nature for the economic processes of man,
- the concept of application of ecologically clean conversion of this energy in small technology devices in situ. The buildings of this concept are generally only connected to the electric distribution network (the demand of motor energy eventually the storage of energy in real time). The distribution network of electric energy represents a strategic task for the development of the infrastructure of the transformed society,

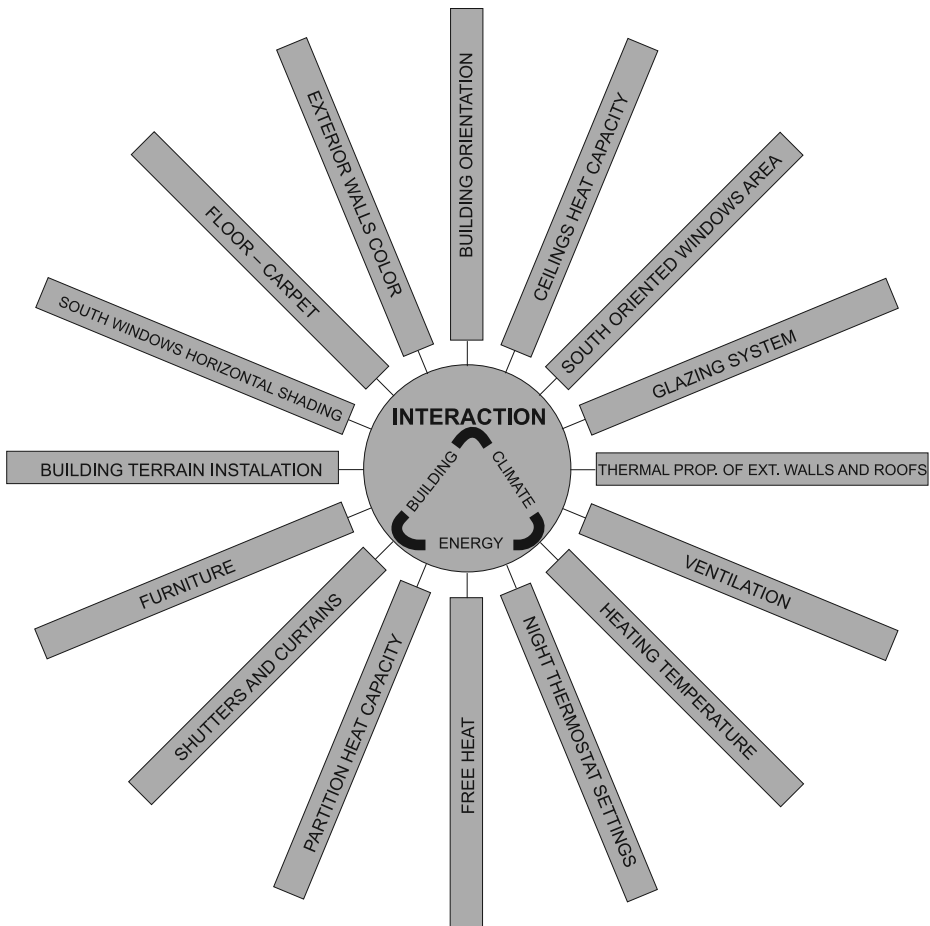


Fig. 2. Building in the system building – climate – energy is defined by the subsystem factors influencing its annual energy consumption

- the concept of a systematic decrease of production of emissions and not only by the change of energy source (from fossil to a renewable one), but also by the orientation to the application of ecologically clean building materials and their ecologically clean manufacture,
- the concept of the transformation of buildings from “a passive model of a consumer” of energy taken from the energy distribution network to “a dynamic model of collection and conversion of renewable energy and to its consumer at the same time” in situ, eventually to a supplier of energy into the distribution network.

3. New Physical-Energy Quantification of Buildings in the Development of Technology in Architecture for Sustainable Society

New physical-energy quantification of buildings must continuously build on the existing development of the energy demand of buildings. We determined its beginning by defining a building before the process of purposeful energy saving in buildings. The initial state (\approx year 1990) represents COMMON BUILDING (A) – Table 1.

3.1. 1st generation of low energy buildings

Among buildings of purposeful energy saving type belong low energy buildings of 1st generation. These include ENERGY EFFICIENT BUILDING (B) – Table 1. It is represented by a new or significantly refurbished building, designed and realized in accordance with the theory of construction design of low energy buildings in the system relation BUILDING – CLIMATE – ENERGY [7]. Energy demand of this building is in full range acquired from the distribution energy networks, i.e. the energy on the basis of fossil fuels. The only element of this building, utilizing the renewable source of solar radiation is a transparent construction (window, glass wall).

A higher level of low energy building of 1st generation represents LOW ENERGY SOLAR BUILDING (C) – Table 1. In essence, it is a building of category (B), with the additional application of renewable energy sources in the form of simple, mainly solar systems (passive solar systems, hybrid and active solar systems e.g. collectors etc.) with photothermal conversion of energy in situ. This category of buildings is also classified by the term SOLAR BUILDING with a shape-expression elements of solar architecture.

The buildings of category (A), (B), (C) – Table 1, are characterized by the fact that the physical quantification of their envelope constructions was the main criterion for reduction of their energy demand for heating, ventilation and cooling. This situation, unfortunately, in some cases, persists to this day. The increase of physical quantification of the buildings envelope for reduction of specific heat in the building, as experience has shown, is limited. The increase of physical quantification of the envelope constructions lower than the value of weighted average coefficient of the thermal transmittance $U_m < 0,4 \text{ W}/(\text{m}^2 \cdot \text{K})$ is economically inefficient, with long energy return on investment (≈ 40 years). Moreover, buildings with high physical quantification of their envelope constructions necessarily require mechanical cooling connected with an additional energy demand (high temperatures of indoor climate in summer period). These significantly reduce the energy savings from the physical quantification of their envelope constructions (in winter period).

Tabela 1

Classification and approximate new physical-energy quantification of buildings in accordance with the development of technology in architecture for a sustainable society

Categories of building: – Residential buildings	Informative weighted aver. coefficient of the thermal transmittance of the envelope constructions	Informative specific heat use for:		Informative specific energy use for: – Electric lighting – Electrical appliances – Motorized power – (DHW)		
		$\frac{Q_H}{Q_E}$				
		[kWh/(m ² · a)]	[kWh/(m ² · a)]			
Basic Classification of Buildings	U_m [W/m ² ·K]	From power distribution network based on fossil fuels	From the local renewable sources with the conversion of energy in situ	From power distribution network based on fossil fuels	From the local renewable sources with the conversion of energy in situ	
		100	0	15	0	
		70	0	15	0	
Buildings before systematic energy saving	0.80–0.85	Common building	50	5–10	15	0
Low energy buildings of 1 st generation	0.55–0.65	Energy efficient building	5–7	35–40	13	0
	0.45–0.55	Low energy building – solar	0	30–35	0	15–18
Low energy buildings of 2 nd generation	0.40–0.45	Green building, with nearly zero energy balance in relation to the distribution networks	0	30–35	0	15–18
	0.40–0.45	Sustainable building, with zero energy balance in relation to the distribution networks	0	30–35	0	15–18
	0.40–0.45	Sustainable building – Plus, with an active energy balance in relation to the distribution networks	0	30–35	0	15–18

3.2. 2nd generation of low energy buildings

The dominant production technology of the natural capital in the form of renewable energy sources fundamentally changes the point of view to the energy quantification of buildings in the development of the technology in architecture for a sustainable society. The trend of buildings with purposeful energy saving is represented here by LOW ENERGY BUILDINGS of 2nd generation (D), (E), (F) – Table 1. Essentially, it is about a building of category (C) with the optimized application of renewable energy sources in the widest sense.

Among low energy buildings of 2nd generation belongs GREEN BUILDING (D) – Table 1, with nearly zero energy balance in relation to the distribution networks (nearly Net Zero Energy Building). The energy demand for heating, ventilation, cooling and domestic hot water preparation is covered by the local renewable sources, with the conversion of energy in situ. It is thus a building, which for the creation of an artificial living – architectural environment, has nearly zero energy balance – without the requirements for energy demand from the distribution energy network – Table 1, with the exception of energy for motor drives and the energy for regulation, or a reserve (Fig. 3). Thus is defined nearly Net Zero Energy Building, characterized by the tendency to save energy and reduce production of emissions, possess system features of green architecture, product of which is GREEN BUILDING [2].

A higher level of low energy buildings of 2nd generation represents SUSTAINABLE BUILDING (E) – Table 1, with zero energy balance in relation to the distribution networks (Net Zero Energy Building). The energy demand for heating, ventilation, cooling and domestic

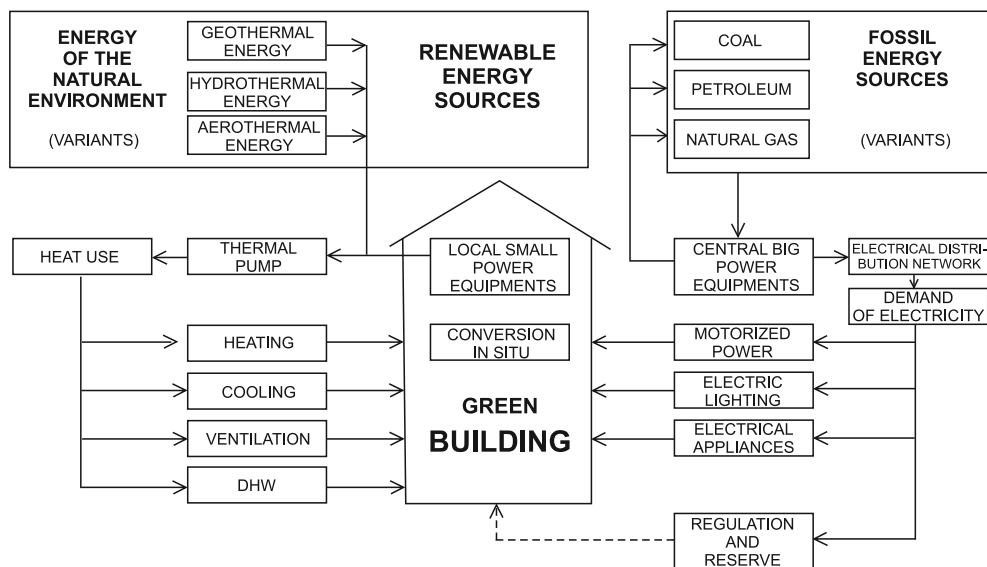


Fig. 3. Scheme of green building with nearly zero energy balance in relation to the distribution networks (nearly net zero energy green building). It has zero requirements of the energy demand for heating, cooling, ventilation and domestic hot water preparation from the distribution energy network

hot water preparation and also the energy demand for artificial electric lighting, electric appliances and motor drives are covered by the local renewable sources with the conversion of energy in situ (Table 1, Fig. 4). Nature with its processes ensures the renewal of these energy inputs, namely:

- in real time of the economic activity of man (geothermal, hydrothermal and aerothermal energy of the natural environment etc.) (Figs. 3, 4) or
- not entirely in real time of the economic activity of man (solar energy, wind energy etc.) – Fig. 4. These sources require additional technologies enabling the conversion of this energy from unpredictable form to the energy of standard quality, suitable for the economic utilization in real time (e.g. in connection with the distribution network of electric energy etc.).

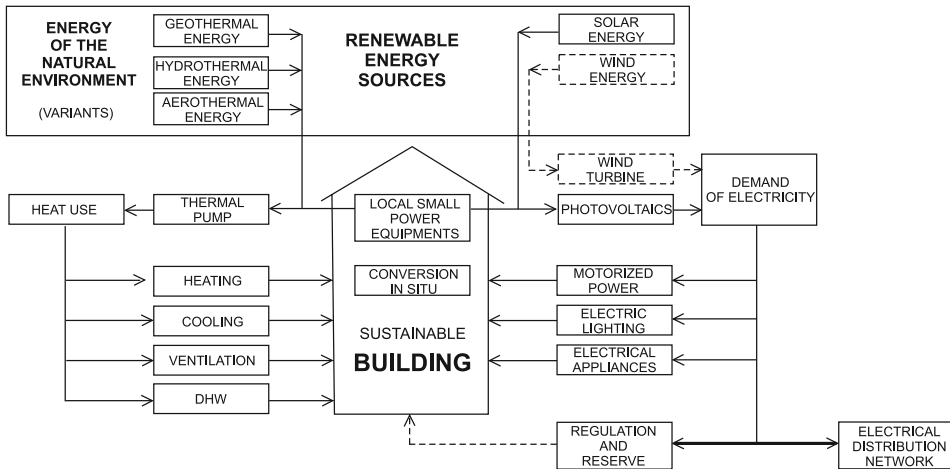


Fig. 4. Scheme of sustainable building with zero energy balance in relation to the distribution networks (net zero energy sustainable building). It has zero requirements of the energy demand for heating, cooling, ventilation and domestic hot water preparation and also zero requirements of the energy for motor drives, electric lighting and appliances. It is, in terms of the regulation and the reserve, always connected to the distribution network of electric energy

It is thus a building, which not only for the creation of the climate of artificial living – architectural environment, but also for other operation technologies has zero energy balance – has no requirements for energy from distribution energy networks, with the exception of energy for regulation or reserve (Fig. 4). Thus is defined Net Zero Energy Building, characterized by the rational utilization of energy and an optimal reduction of emissions (to the extent of the coverage by the ecosystems of the locality, region or state), possess system features of sustainable architecture, product of which is SUSTAINABLE BUILDING [2].

The highest level of low energy buildings of 2nd generation represents SUSTAINABLE BUILDING – PLUS (F) – Table 1, with an active energy balance in relation to the distribution networks (Net Plus Energy Building).

It can be seen that zero energy buildings or plus energy buildings in the final perception of sustainable buildings must also utilize the renewable energy source of solar radiation, namely at photovoltaic conversion it is a direct conversion to the electric energy (Fig. 4).

Low energy buildings of 2nd generation of type (D), (E), (F) are always connected to the distribution network of electric energy fulfilling the function of the regulation and the reserve (Figs. 3, 4). For the building of type (F) fulfills the distribution network also the function of a supplier – storage – electric energy consumer.

4. Conditioning Factors and Time Relations of Energy Transformation of the Society Towards Renewable Energy Sources

The process of the transformation towards renewable energy sources (the transformation of buildings from passive energy consumer to a dynamic system of energy collection and conversion) might be economically efficient only under the conditions of an anti discriminatory approach to all the energy sources (fossil and renewable), i.e. under the conditions of the united energy market based on the economic fundamentals [8]. Their principle comprises built-in motivation, but also repressive factors, declaring a new value system of the energy with reduced impact of emissions of greenhouse type on the atmosphere of the planet. This new economic value, which enters into the organization of the energy market, is a social value of the emissions of greenhouse type. It represents additional costs that the society must pay to prevent the creation of emissions.

Determination of the social value of CO₂ emissions in the range of ≈ 85 USD/1 tonne [6] or 65 to 75 EUR/1 tonne [8], represents a rational approach in the current period. The amount represents the costs that a company must pay additionally to produce 1 MWh of electric energy without 1 tonne of CO₂ emissions.

The transformation of the energy market thus requires transformation costs. It is possible to measure them – quantify them with the index of CO₂ emissions for each particular type of energy source and the technology of conversion of the energy. This enables the selection between the technologies or energy sources which is provided by the knowledge curve of emissions – Fig. 5. Utilizing it can optimize the order of relevant technologies, i.e. create a strategy of a logical economical allocation of the capital for investments in renewable energy sources [8].

The knowledge curve in Fig. 5 shows the fact that some technologies have not yet reached the parameters within the range of the reversal point to ensure investment returns. The necessary technological development of a new generation of photovoltaic panels and devices for storage of electricity allows us to consider such a situation of the utilization of solar energy until sometime between 2020–2025.

Therefore, in the current period, in the field of low energy buildings of 2nd generation it is realistic to have a green building with nearly zero energy balance in relation to the distribution networks, i.e. a net zero energy building. The energy is thus supplied from the renewable energy sources of natural environment (geothermal, hydrothermal and aerothermal energy) with the conversion in situ by the utilization of heat pumps according to the scheme in Fig. 3. Sustainable building according to the scheme in Fig. 4 with zero

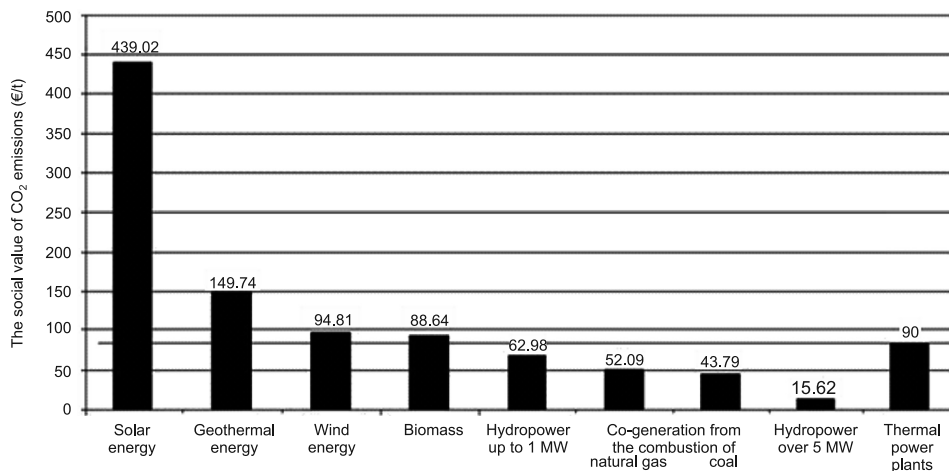


Fig. 5. Knowledge curve of CO₂ emissions in the production of electricity

energy balance in relation to the distribution networks in accordance with the development of the technology in architecture seems to be realistic after the year ≈ 2020 .

This paper was supported by the Slovak research and development agency under contract no. APVV-0624-10.

References

- [1] Syed A., *Advanced Building Technologies for Sustainability*, John Wiley & Sons, Inc., Hoboken, New Jersey 2012.
- [2] Bielek B., Híreš J., Lukášik D., Bielek M., *Development of Technology in Architecture for Sustainable Society*, Nakladateľstvo STU, Bratislava 2012.
- [3] Constanza R., Cemberland J., Darly H., Goodland R., Nogaard R., *An Introduction to Ecological Economics*, CRC Press LLC, St. Lucie Press Bold Raton, Florida 1997.
- [4] Sartori I., Napolitano A., Woss K., *Net zero energy buildings: A consistent definition framework*, Energy and Buildings, Elsevier 2012.
- [5] Marszal A.J., Heiselberg P., Bourrelle E., Mussall K., Woss K., Sartori I., Napolitano A., *Zero Energy Building – A review of definitions and calculation methodologies*, Energy and Buildings, Elsevier 2011.
- [6] Stern N., et al., *Stern Review on the Economics of Climate Change*, London 2006.
- [7] Bielek M., *Calculated Experiments of the Low Energy Buildings in the Slovak Climate*, Building Research Journal, Bratislava 1993.
- [8] Lukášik D., *Návrh riešenia princípov transformácie energetického trhu od fosilných palív smerom k obnoviteľným zdrojom energie na princípe adaptačného mechanizmu*, Centrum výskumu ekonomiky obnoviteľných zdrojov energie a distribučných sústav, Košice 2012.
- [9] Woss K., Sartori I., Lollini R., *Nearly – zero, Net zero and Plus Energy Buildings – How definitions & regulations affect the solutions*, REHVA Journal 12/2012.

BORIS BIELEK*

NEW CLASSIFICATION OF RENEWABLE ENERGY SOURCES IN THE DEVELOPMENT OF TECHNOLOGY IN ARCHITECTURE FOR A SUSTAINABLE SOCIETY

NOWA KLASYFIKACJA ODNAWIALNYCH ŹRÓDEŁ ENERGII W ROZWOJU TECHNOLOGICZNYM W ARCHITEKTURZE DLA ZRÓWNOWAŻONEGO SPOŁECZEŃSTWA

Abstract

The transformation to a sustainable society. The transformation of the energy market. The social value of CO₂ emissions. Change of the value system in society. The dominant production technology of the capital of nature with simultaneous restoration of ecosystems. Division and economic quantification of renewable energy sources as a production technology of capital provided to man by nature. Predictable and unpredictable renewable energy sources. Renewable energy sources generated in economic human activity as a secondary product. Development of technology in architecture for a sustainable society.

Keywords: renewable energy sources, sustainable society, CO₂ emissions, energy market

Streszczenie

Transformacja do społeczeństwa zrównoważonego. Transformacja rynku energii. Społeczne znaczenie emisji CO₂. Zmiana społecznego systemu wartości. Dominująca technologia produkcyjna bazująca na kapitale przyrody z jednoczesnym przywróceniem ekosystemów. Podział i ilościowa ocena ekonomiczna odnawialnych źródeł energii jako technologia produkcji kapitału dostarczanego człowiekowi przez naturę. Przewidywalne i nieprzewidywalne odnawialne źródła energii. Odnawialne źródła energii generowane w działalności gospodarczej człowieka jako produkty wtórne. Rozwój technologii w architekturze dla zrównoważonego społeczeństwa.

Słowa kluczowe: odnawialne źródła energii, społeczeństwo zrównoważone, emisja CO₂, rynek energii

* Doc. Ph.D. Eng. Bielek, Faculty of Civil Engineering, Slovak University of Technology in Bratislava.

1. Introduction

The economic activity of man leads to the creation of two fundamental economics-based utility values: energy as a product required by the market and CO₂ emissions as a parallel undesirable product.

While fossil fuels facilitated the rise of the standard of living on the planet and the biocapacity of the Earth has been able to assimilate the resulting greenhouse gases, no violation of the balance between energy sources and the economic activity of man or production of emissions from it has been recorded.

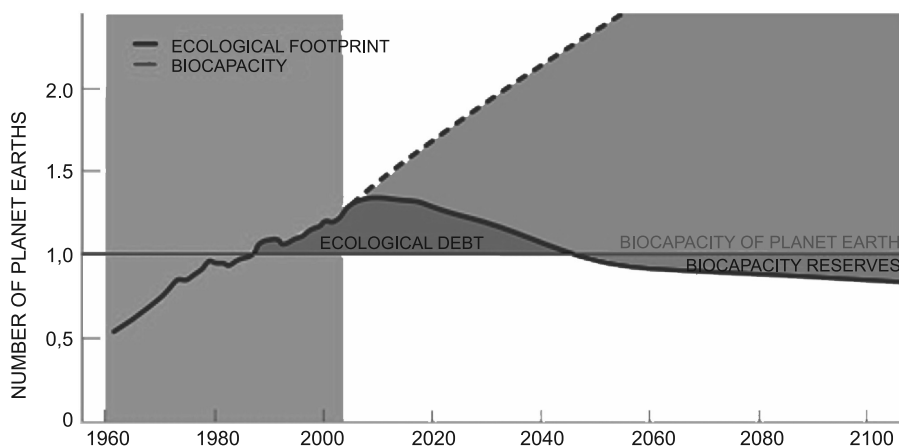


Fig. 1. Graph of renewal of function of the Earth's biocapacity [4]

Around the 1980s, the economic system representing the activities of man (industry, transportation, human dwellings) rose above the production value of the Earth's biocapacity – Fig.1. Man crossed the limit set by nature. Man has started to produce ecological debt on the planet. Currently, the ecological load exceeds the absorption ability of the planet's ecological systems approximately 30% [4].

2. Transition to Sustainability by Changing the Value System of Economic Models in Society

The crisis of fossil fuels in the 70s, related to their high level of usage; the crisis of ecological systems of nature in the second half of the 80s, resulting in the problem of climate changes; and the crisis of financial markets as a culmination of economic processes starting in early 1995 and with their peak in 2008 in the USA and in 2010 in the EU, have become the catalyst for a global social movement. This results in a long-term, irreversible transition process, accompanied by the disintegration of the old and the establishment of a new value system [3].

It is about transition to a sustainable society in terms of the reassessment of priorities in social investments, leading to the transformation of the energy sector and to the

change of the organization of the energy market from a combined market of fossil fuels and renewable energy sources to a market comprising only renewable energy sources; the transformation of the materials sector, with the focus on ecologically clean materials and their composites; and the transformation of the whole economy towards low-energy and low-emission technologies and to the manufacture of ecologically clean products [2].

Renewable energy sources (Fig. 2) perform two significant functions in a synergy effect: they represent a new capital provided to man by nature and simultaneously significantly reduce greenhouse emissions, therefore restoring the assimilation capacity of the planet [2]. In this context, the conditioning factor of the combined energy market is the social value of CO₂ emissions. This represents the additional costs which society must pay to reduce emissions.

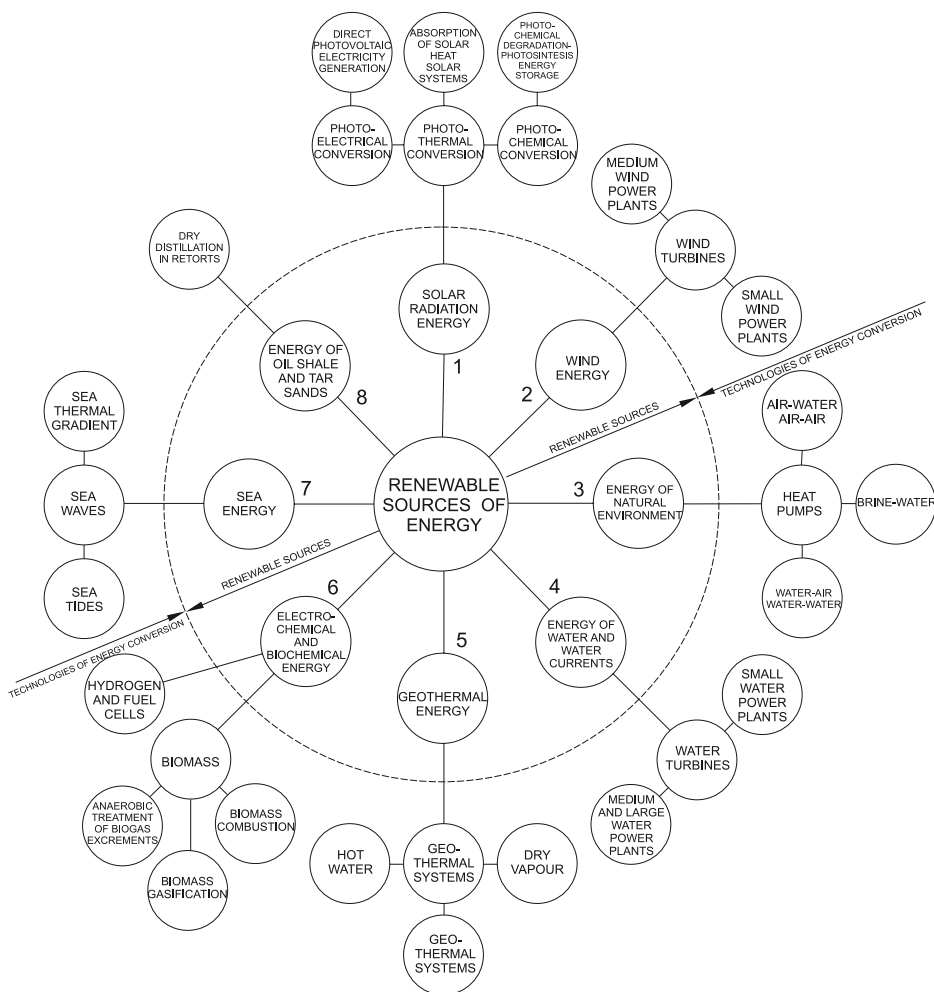


Fig. 2. Renewable energy sources – production technology of the capital provided to man by nature

Oneway to describe the acceptance of the change of value system would be to say that until now it was man who set the quantitative physical parameters e.g. in the technology of architecture for a construction or building and nature was obliged to ensure concentrated energy for these parameters. The new value system means that man must first evaluate how much energy is available in a given locality to be utilized for his economic activity, and in what form. It is only within the limits set by nature that man can subsequently define parameters, e.g. in the technology of architecture of a particular construction or building.

From the existing system, “man first and nature second”, the value system is transformed to a new one in which nature first sets the limits of individual parameters, and man then accepts these parameters in his economic activities [2]. This way, it is possible to practically illustrate the change of value system in general. If man imagined that he, with the help of modern technology, subordinates nature, nature now shows us that he was mistaken.

However, in order to change the value system it is necessary to change people’s way of thinking. It is necessary to give up the prioritization of the interests of the individual and look for a solution where the interests of society are at one with the interests of the individual. Unifying the interests of society and the individual represents one of the fundamental criteria of a proper solution to any social problem.

In the suggested transition of society and the change of value system, as has been shown, it is necessary to accept that nature sets the terms of creating and maintaining the new required balance between natural capital and the economic activity of man [5].

History has shown that in the economy of society there have always existed dominant production technologies which, in a given long-term period (on average 50 years), provided above-standard added value and facilitated the fundamental development of society (Fig. 3). It is a reasonable assumption that environmental technologies and renewable energy sources in their various forms will become the next such dominant production technology.

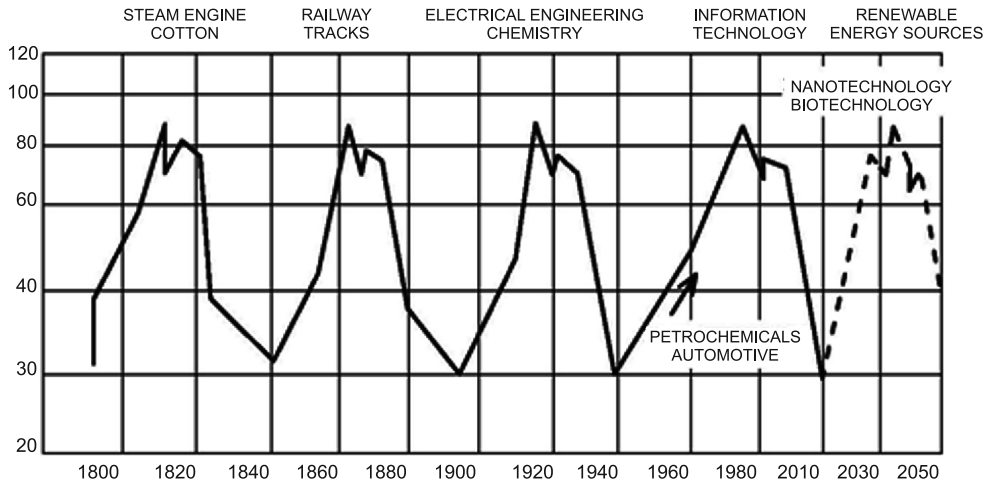


Fig. 3. Kondratiev cycles

3. Economic Quantification of Renewable Energy Sources as a Dominant Production Technology of Capital Provided to Man by Nature

Mankind faces the necessity of broadening the energy base for society on the basis of renewable energy sources. A renewable energy source is capable of renewing its energy output by natural processes in the ecosystems of nature. The renewal of the energy output of the source can take time, which is a very important consideration in relation to its utilizability in the economic activity of man in real time. If we take the term renewable energy source out of context, either in terms of the time taken for its renewal or its utilizability in real time in the economic activity of man, it is easy to come to incorrect conclusions [2].

Renewable energy sources may be divided into four groups, depending on the economic base (Fig. 4):

1. Renewable sources where natural ecosystems provide the necessary energy output continuously with a constant intensity in real time relative to the economic activity of man. We call them predictable renewable energy sources (Fig. 4). After repayment of the initial investments into the technology of energy conversion done in situ (such as a heat pump, etc.), they do not require any additional economic costs. Utilization of these energy sources is without any associated production of CO₂ emissions. These include geothermal, hydrothermal and aerothermal energy from the natural environment (ground, water and air), energy from water gradients of natural lakes and reservoirs, energy from rivers, sea gradients, geothermal hot water and dry steam, and electrochemical energy (hydrogen fuel cells) (Fig. 4).
2. Renewable sources where natural ecosystems provide energy output discontinuously, with variable intensity and not entirely in real time relative to the economic activity of man. We call them unpredictable renewable energy sources (Fig. 4). After repayment of the initial investments into the technology for energy conversion done in situ, e.g. photovoltaic cells, wind turbines etc., they require economic costs in the form of additional technologies enabling the conversion of the characteristics of this energy from unpredictable energy to that of standard quality, suitable for economic utilization in real time relative to the economic activity of man (e.g. problem of energy storage etc.). Utilization of these energy sources is without any associated production of CO₂ emissions. These include solar energy, wind energy, and energy from sea dynamics (waves and tide) (Fig. 4).
3. Renewable sources where natural ecosystems provide the energy output created as a result of a long term natural process (e.g. growth of wood) (Fig. 4).
4. Renewable energy sources created in the economic activity of man as a secondary product. These sources provide energy output with a phase delay, but effectively in real time relative to the economic activity of man, and therefore may be classified as predictable renewable energy sources (Fig. 4). They have their economic significance only the primary economic activity of man of which they are by-products is economically viable in and of itself. The change of the status of renewable energy sources created as a secondary product of the economic activity of man to a primary economic activity can cause a lot of economic losses which rise with the price of human labour and the availability of additional production technologies which cannot be expected to create above-standard

economic added value. With all of the energy sources in this group, the energy is generated by combustion, a secondary effect of which is the production of CO₂ emissions. Their production of CO₂ per unit of energy is high (e.g. biomass is comparable to black coal). These include wood mass, oil shale, tar sands, biomass, biogas, and landfill gas from sewage treatment plants (Fig. 4).

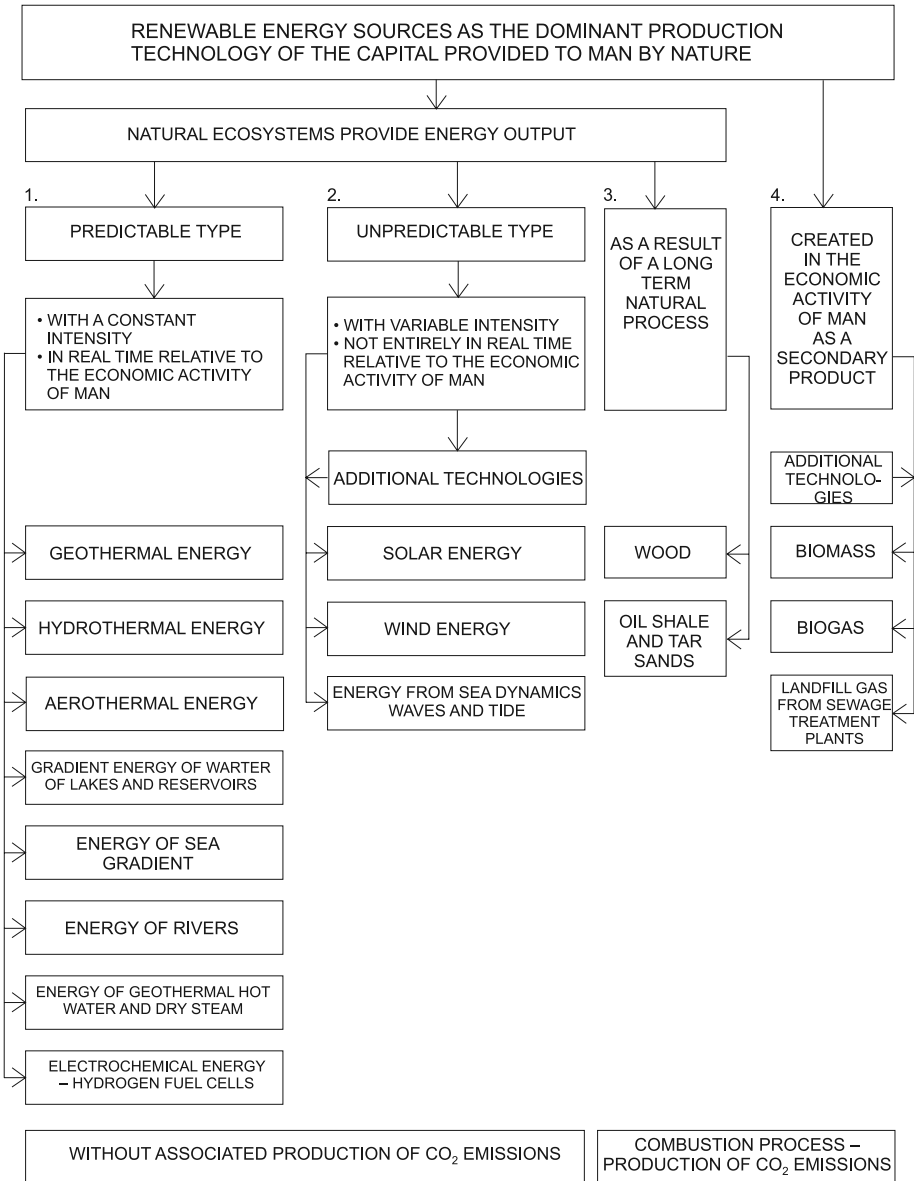


Fig. 4. Division and classification of renewable energy sources in terms of economic base

4. Development of Technology in Architecture in the Transition to Sustainability

Local renewable energy sources and the transformation of buildings in accordance with the development of technology in architecture enable us to reshape existing knowledge to incorporate new knowledge and to create new working models for the energy efficiency of human settlements on their basis. This way, renewable energy sources as the dominant production technology of natural capital with simultaneous renewal of ecosystems become the conditioning factor in changes to the principal concept of energy quantification of buildings.

A part of the transformation, as has been shown, must not only be a new arrangement of relationships in society, including the arrangement of human settlements, but also the whole range of parameters especially in the technology of architecture expressed by the technological transformation of the building itself. This becomes a place for the collection of renewable sources and conversion of energy in situ as a part of the transformation of the organization of the energy market. Buildings cease to be only consumers of energy, and are technologically transformed to become part of the complex system of conversion and distribution of energy [1]. They become a part of energy distribution networks. And just in the interaction with these distribution networks, a new quantification of the physical-energy demand of buildings is outlined, expressed by the term zero-energy building in relation to the distribution networks (Net-Zero-Energy Building), nearly-zero-energy building in relation to the distribution networks (nearly-Net-Zero-Energy Building) or plus-energy building, supplying energy to the distribution networks (Net-Plus-Energy Building) [6, 7].

This paper was supported by the Slovak research and development agency under contract no. APVV-0624-10.

References

- [1] Syed A., *Advanced Building Technologies for Sustainability*, John Wiley & Sons, Inc., Hoboken, New Jersey 2012.
- [2] Bielek B., Hřeš J., Lukášik D., Bielek M., *Development of Technology in Architecture for Sustainable Society*, Nakladateľstvo STU, Bratislava 2012.
- [3] Zelený M., *Human Systems Management Integrating Knowledge Management and Systems*, World Scientific Publishing Co. Plc. Ltd., Singapore 2008.
- [4] Cambridge University, *Global Climate Change Impacts in the United States*, Cambridge University Press, New York 2009.
- [5] Constanza R., Cemberland J., Darly H., Goodland R., Nogaard R., *An Introduction to Ecological Economics*, CRC Press LLC, St. Lucie Press Bold Raton, Florida 1997.
- [6] Sartori I., Napolitano A., Woss K., *Net Zero Energy Buildings: A Consistent Definition Framework*, Energy and Buildings, Elsevier 2012.
- [7] Marszal A.J., Heiselberg P., Bourrelle E., Mussall K., Woss K., Sartori I., Napolitano A., *Zero Energy Building – A Review of Definitions and Calculation Methodologies*, Energy and Buildings, Elsevier 2011.

ALEKSANDER BYRDY*

POINT THERMAL BRIDGES IN WALLS WITH EXTERNAL STONE LAYER

PUNKTOWE MOSTKI TERMICZNE W ŚCIANACH Z OKŁADZINĄ Z KAMIENIA NATURALNEGO

Abstract

The main aim of the following article is to define the impact of anchorage of external stone wall cladding on their thermal insulation. The results of FEM and approximate calculations of point thermal bridges at steel anchors, fixing façade boards, are compared in the following article.

Keywords: thermal bridges, stone claddings, anchors

Streszczenie

Celem artykułu jest określenie wpływu zakotwienia okładzin kamiennych ścian zewnętrznych na ich izolacyjność termiczną. W artykule przeprowadzono analizę obliczenia punktowych mostków termicznych tworzonych przez stalowe kotwie mocujące płyty elewacyjne.

Słowa kluczowe: mostki termiczne, okładziny kamienne, zakotwienia

* Ph.D. Eng. Aleksander Byrdy, Institute of Building Materials and Structures, Faculty of Civil Engineering, Cracow University of Technology.

1. Introduction

Natural stone is one of the oldest known construction materials. Historically it was used to raise buildings, nowadays, however natural stone is used as a finishing element giving the building proper architectural design. Stone boards are applied in exterior and interior modern facades and connected to the ground with stainless steel or aluminum anchors. Stone linings may be used in buildings raised in various technologies from brick constructions as well as frameworks.

Modern stone facades decorate prestigious buildings and are often used as the linings of high buildings in big metropolitan areas. Stone boards used in modern facades are fixed to the ground by means of anchor-elements made of stainless steel. Thanks to the application of ventilating gap and proper thermal insulation, stone facade constructions allow for the protection or at least limitation of bad influence of atmospheric factors having an effect on the construction. Ventilated air layer allows for diffusing of water vapor from the inside of the building and it makes it easier for stone lining to dry. Nowadays, fixing boards to the constructional ground by means of anchors made of flat stainless steel bars, is the most popular method of natural stone lining assembly [1]. The assembly comprises drilling a hole in the ground and putting an anchor in it with mortar on which lining boards are put. Each slab is supported at four points on horizontal or vertical edges of the boards. The schemes of facades with stone lining fixing on steel anchors are presented in Figs. 1, 2.

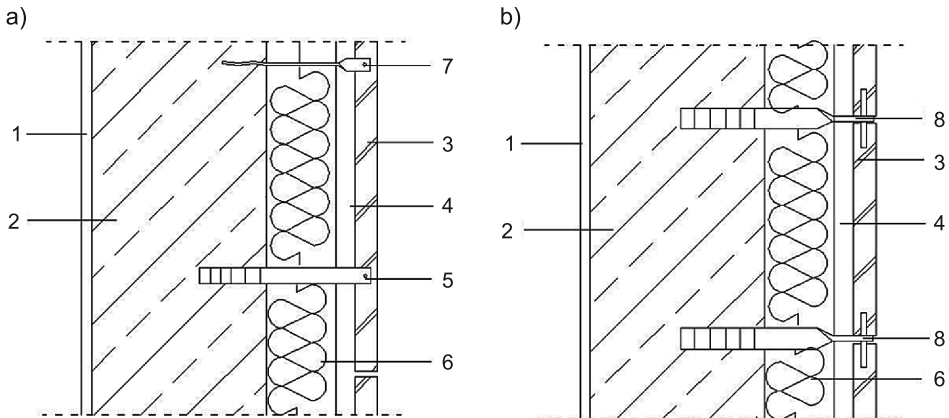


Fig. 1. Schemes of stone slabs connected with steel anchors: a) slabs fixed on the vertical edges, b) slabs fixed on the horizontal edges. Markings: 1 – interior plaster. 2 – construction layer, 3 – stone cladding, 4 – air void, 5 – bearing anchor fixed in the vertical joint, 6 – thermal insulation of the wall, 7 – stabilization anchor, 8 – bearing anchor fixed in the horizontal joint

2. Technology of thermal insulation of the walls with stone cladding

In order to provide proper thermal insulation of the walls made with stone lining, layers of mineral wool thermal insulation are applied. It is advisable to use semi-hard boards

made of rock wool with brand-made layer of wind insulation made with the veil of glass fibre on the exterior side of the board. Rock wool is fixed to the ground mechanically with 6–9 pins per square meter of the wall.

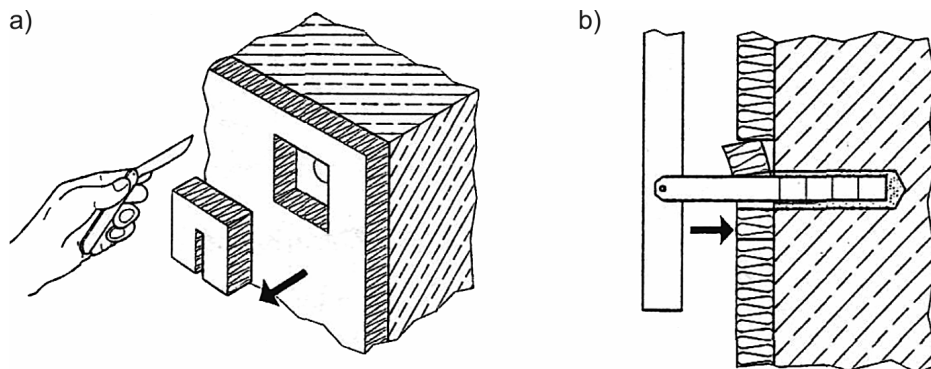


Fig. 2. The technology of areas anchoring stone board insulation: a) cutting thermal insulation, b) filling up thermal insulation [2]

The next stage is to fix stone lining anchors in the bearing ground of the wall. Steel anchors are fixed in the holes made in the rock wool in the areas of anchors. When the process of mortar setting in the anchor areas is complete, all gaps in rock wool are filled up, so that the continuity of the thermal insulation layer can be provided (refer to Fig. 2).

3. Point thermal bridges in the walls with stone cladding

It is necessary to be very careful when creating walls with stone external layers fixed on steel anchors. Knowledge of thermal physics of building is also indispensable. While fixing layers of thermal insulation, stainless steel mechanical fasteners cause point thermal bridges. According to [3] the presence of mechanical fasteners can be calculated approximately by the formula (1):

$$U_c = U + \Delta U \quad (1)$$

where:

U – thermal transmittance of the building component without point bridges [W/(m²K)],

ΔU – correction to the thermal transmittance for mechanical fasteners [W/(m²K)].

$$\Delta U_f = \alpha \cdot \frac{\lambda_f A_f n_f}{d_0} \left(\frac{R_1}{R_{T,h}} \right)^2 \quad (2)$$

where:

α – factor describing the depth of penetration of insulating layer by the fastener,

λ_f – thermal conductivity of the fastener [W/(mK)],

- A_f – the field of linking section [m²],
 n_f – the number of fasteners per square meter,
 d_0 – thickness of the insulation layer containing the fastener [m],
 R_1 – thermal resistance of the insulation layer penetrated by the fastener [m² K/W],
 $R_{T,h}$ – total thermal resistance of the component ignoring any thermal bridges [m² K/W].

The other way of taking into consideration the impact of point bridges may be the detailed numeral analysis of thermal transmittance of the component with the use of a 3D model. According to [3] the correction for the thermal transmittance with mechanical fasteners is described by the following formula (3):

$$\Delta U_f = n_f \cdot \chi \quad (3)$$

where:

- n_f – as for the formula (2),
 χ – point thermal transmittance according to the formula (4).

$$\chi = L_{3D} - U_i \cdot A_i \quad (4)$$

where:

- L_{3D} – the factor of thermal coupling gained from the calculation of component 3-D [W/K],
 U_i – thermal transmittance of component 1-D [W/(m²K)],
 A_i – the area of the component [m²].

4. An example of the analysis of point thermal bridges in walls with stone cladding

The analysis of point thermal bridges in the walls with stone lining was conducted on the basis of the office building handed over for use in 2013 in Katowice. Stratification of the walls and an example of arrangement of fasteners in the analyzed building is presented

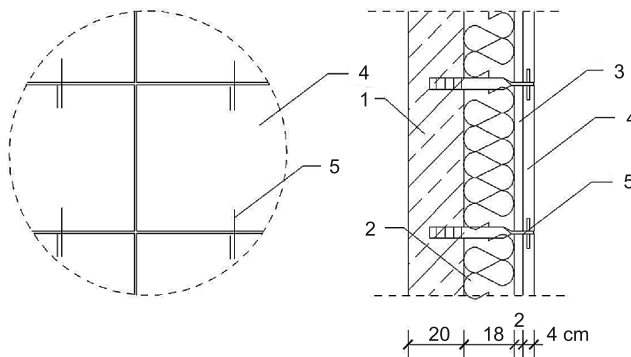


Fig. 3. Arrangement of anchors of the board and stratification of the analyzed division. Markings: 1 – reinforced concrete wall, 2 – rock wool Wentirock, 3 – ventilated air aperture, 4 – sandstone board, 5 – bearing anchor made of stainless steel with the section 6 × 35 mm

in Figure 3. The analyzed surface of the facade has regular anchorage setting, with 3.16 anchors per square meter.

Calculation analysis of the thermal transmittance of building component was conducted with Psi-therm 3D 2012 program. The thermal transmittance through 1square meter of the component was checked on the assumption that the edge conditions inside the building and in the ventilated aperture are stable. For the needs of the calculation the difference between the temperature inside and outside the building was taken into account. It is about 25 (+20 the air inside and – 5 the air in the ventilated air layer).

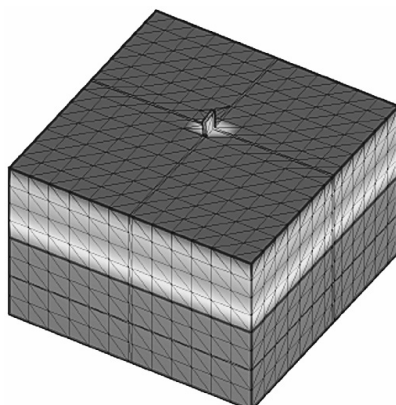


Fig. 4. The model of the component altogether with the temperature isotherms

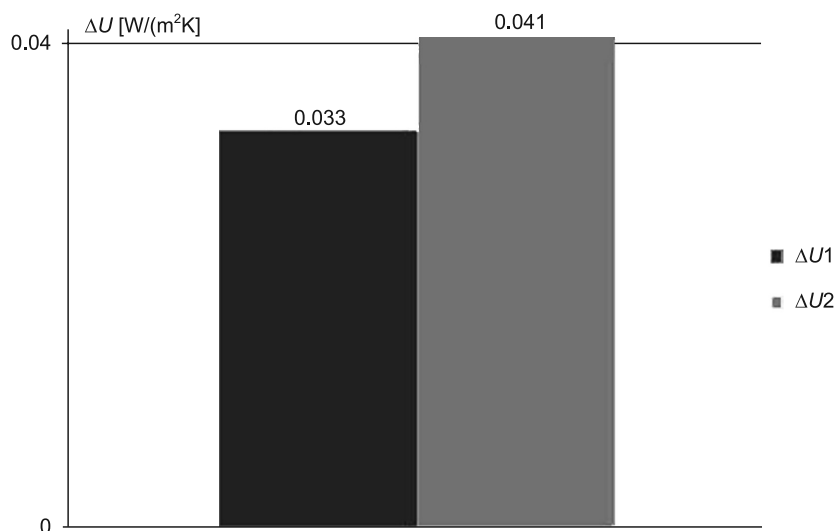


Fig. 5. Results of FEM and approximate calculations of the corrections to the thermal transmittance due to mechanical fasteners. Markings: $\Delta U1$ – correction gained as a result of FEM calculations and formula (3), $\Delta U2$ – correction gained as a result of approximate calculations according to formula (2)

The anchorage was modeled as a single flat bar with the cross section 6×35 mm for 0.316 m of the component. The thermal transmittance of the component was analyzed in the three-dimensional FEM model. The component was modeled with a regular net consisting of 9962 tetrahedral elements. The results of the conducted analysis are presented in Fig. 4.

On the basis of the formula (2) and formula (3) calculations for the correction of the thermal transmittance, including the impact of fasteners on the thermal insulation of the wall with the stone lining, were conducted. The results of the calculations are presented in Fig. 5.

5. Conclusions

The analyzed example was chosen in order to cover the largest congestion of anchorages. The cross section area of the fixing anchors was also suitable for the largest available sections used so far in the technology of fixing stone layers. That is why the results of the conducted analysis show the maximum effects of the impact of anchorages on the thermal insulation of component with external stone layer. On the basis of the conducted analysis it can be estimated that there is a 24% difference of correction value for the thermal transmittance value including mechanical fasteners described according to the formula 2 and FEM analysis (refer to Fig. 5). Approximate calculation method of the influence of point thermal bridges is sufficient to determine the total thermal transmittance of building components with stone layer. Values of the factor U_c calculated according to formula 1 and taking into consideration corrections calculated numerically and analytically differ only insignificantly (3%). The results of the FEM analysis with the usage of formula (3) are more accurate. The derived value of the correction ΔU makes it possible to define necessary thickness of additional thermal insulation, which must be applied to equalize the impact of thermal bridges created because of the boards' anchorages. For the analyzed example, recommended additional thickness of rock wool is 4 cm.

The span and section of the anchorages of stone boards is chosen according to the needs of architectural projects and construction needs individually for each façade. Due to this fact, those who are responsible for the project should check value of thermal transmittance for each project and it must be done in a detailed way after receiving information about the choice of anchorages of façade boards.

In the analyzed example, currently permissible value of the total thermal transmittance factor U_c for the external walls is met ($U_c = 0.24$ W/(m²K)). Planned further tightening of the requirements according to [7] will lead to the necessity of the application of thicker thermal insulation and anchors with larger cross section. Cross section area of anchor applied in the analyzed example is maximal considering the drilling technique of anchors with traditional methods. Any further increase of thickness of thermal insulation would result in the necessity of using drill rigs applied for making anchor areas or the change of the technique of stone claddings fixing by the application of substructure to suspend boards described in [6].

The work reported in this paper was partially funded by the project L-1/116/DS/2013 "Revitalization of existing buildings".

References

- [1] Byrdy A., *Okladziny kamienne stosowane do wykonywania zewnętrznych elewacyjnych*, Izolacje 6/2007, 68-70.
- [2] DNV 1.5 Bautechnische Information Naturwekstein. Fassadenbekleidung. Würzburg 2000.
- [3] EN ISO 6946:2007 Building components and building elements. Thermal resistance and thermal transmittance. Calculation method.
- [4] EN 12524:2000 Building materials and products – Hygrothermal properties – tabulated design.
- [5] EN ISO 10211:2007 Thermal bridges in building construction – Calculation of heat flows and surface temperatures.
- [6] Patrika R., Kalousek M., *Spidi kotvy u provětrávaných fasád XII th*, International Conference Defects and Renovation of Building Envelope Structures. Podbanske 07th.–09th March 2012, 261-268.
- [7] Rozporządzenie Ministra Transportu, Budownictwa i Gospodarki Morskiej z dnia 5.07.13 zmieniające rozporządzenie w sprawie warunków technicznych, jakim powinny odpowiadać budynki i ich usytuowanie. Dziennik Ustaw z dnia 13.08.2013, poz. 926.

DOROTA BZOWSKA*

THE EFFECT OF THERMAL RESISTANCE OF BUILDING'S OPAQUE ELEMENTS AND WINDOWS SURFACE ON AIR EXCHANGE INTENSITY DURING THE SUMMER SEASON

WPŁYW OPORU CIEPLNEGO ŚCIAN BUDYNKU ORAZ POWIERZCHNI PRZESZKLENIA NA NATURALNĄ WYMIANĘ POWIETRZA W OKRESIE LETNIM

Abstract

The purpose of this work – connected with overheating process occurring in buildings – was to investigate the intensity of natural air exchange when a value of thermal resistant for outside walls is being increased together with the increase of the window's surface. To obtain higher thermal resistant the outside partition were covered with insulating material subsequently from 3 to 30 cm. Window surface to wall surface ratio (wwr) was changing from 5% to 50%. The window's test surface was facing east, south and west in turn while the wwr of the remaining orientations was kept at a constant 1/10 of the wall. The intensity of the buoyancy flux was analyzed as well. Three forms of ventilation airflow were considered – with assisting and opposing winds and no wind appearance. The process was examined in a single zone building, naturally ventilated, fitted with heat accumulating mass.

Keywords: thermal resistance, buoyancy flux, natural air exchanger, solar heat gains

Streszczenie

Przeanalizowano wpływ sukcesywnie wzrastającego oporu cieplnego obudowy budynku oraz powierzchni okna na ilość wymienianego powietrza wentylacyjnego. Ściany zewnętrzne docieplano warstwami izolacji, począwszy od 3 cm, a kończąc na 30 cm. Dla każdej warstwy izolacji rozpatrywano przeszklenia obejmujące udział powierzchni okna w przegrodzie od 5% do 50% kolejno dla orientacji E, S, oraz W. Zbadano także zmiany strumienia wyporu termicznego powietrza. Obliczenia uwzględniały wpływ różnie ukierunkowanego wiatru.

Słowa kluczowe: opór przenikania ciepła, wypór termiczny powietrza wewnętrznego, naturalna wymiana powietrza w budynku, słoneczne zyski energetyczne

* Ph.D. D.Sc. Eng. Dorota Bzowska, Institute of Civil Engineering, Faculty of Civil Engineering, Mechanics and Petrochemistry, Warsaw University of Technology.

1. Introduction

Untill recently, when energy performance in buildings was considered, the main areas of research were concentrated on the building envelope to keep its thermal transmittance values of opaque elements as low as possible. The aim was to design low energy buildings to perform well during heating season. This approach is still present in building regulations where maximum acceptable U-values are set. The U-values order was followed by the idea, generally forced by architects, of large window area facing south. The concept focused on window size rather than on the combined effect of low-emission glass and heat accumulation. The results show that the size of the energy efficient windows did not have a substantial influence on heating demand during winters, especially if glazing choice was disregarded and the thermal mass together with the heat accumulation is not followed either [9]. Energy demand in these circumstances during heating season was not especially lower when cold conditions are investigated. Moreover architectural solutions concerning transparent elements of a building envelope, which may influence energy reduction in heating seasons are very likely to generate its growth during summer periods.

The effects of: window size and its orientation, the kinds of glazing, as well as solar transmittance on heating and cooling demands have been published in a number of papers [2–7, 9].

According to the state of the art, the energy balance of a building is directly related to much higher number of parameters and factors then it used to be. The architectural design must be now more complex, especially where the first stage of designing is concerned. This stage will usually pay a significant role in the creation of the future energy performance of building. The research being carried out on energy balance needs a deeper understanding of the heat and air exchange processes undergoing in buildings. Influence of thermal mass, thermal properties of the glazing system and natural air exchange on indoor comfort should be of careful investigation among others. Building project cannot be designed to fulfill esthetics and functional expectation only but energy requirement in all of the aspects of the issue have to be analyzed. The architectural design parameters must show the influence on energy performance during heating season as well as for the cooling demand. Energy requirements for heating and cooling purposes should be analyzed separately especially in cold climate. The aim of this work is to show some relations among: windows size, their orientation, thermal resistance of buildings opaque partitions and air exchange. These basic, but not obvious, interdependences may help to get some alternatives in choosing the appropriate design when thermal comfort and energy consumption is discussed.

2. Results of calculation

The graphs presented in this chapter are based on computer simulation for unsteady exchange of heat and ventilation flow rates. The mathematical model and methodology of numerical computation can be found in [1]. The calculations have been made for a single zone building, naturally ventilated, fitted with an internal heat accumulating mass. Nowadays one-family houses are mainly designed as open space buildings. Three modes

of airflow throughout the buildings have been simulated. The first one regards assisting wind, the second opposing one and the third simulates the process when wind does not appear. The weather parameters represent a typical July in Warsaw [1].

The thermal resistance of the whole building envelope is $0.66 \text{ m}^2\cdot\text{K}/\text{W}$. The partitions were being covered with foam polystyrene. The first thickness of the insulation layer was 3 cm, the second was 5 cm and then with the step of 5 cm obtained 30 cm layer. Thermal resistance eventually reaches $7.8 \text{ m}^2\cdot\text{K}/\text{W}$. The building is fitted with three windows facing east, south and west. The north wall has no window. Similarly to varying thickness of insulation the windows area was changed as well. Window to wall ratio (wwr) was changing from 5% to 50% with the step of 5%. The heat transmittance coefficient for a window equals $1.6 \text{ W}/(\text{m}^2\cdot\text{K})$. Heat adopted in the calculations came from solar energy that was being gained through windows, the heat generated by occupants and of the electrically supplied outfit the building is equipped in. Heat, except solar energy, had constant value and equaled 300 W. The computer simulations of ventilation air flow were carried out for numerous sets of varying parameters: the thickness of the insulation layer, wwr parameter, windows orientation and the forms of wind appearance in air exchange. For every thickness of insulation and every orientation: east, south and west the window to wall ratio was changing from 5% to 50%, while windows area of the remaining orientations were kept at constant 1/10 of the surface of the wall. The flow fluctuated due to thermal buoyancy and wind pressure. After collecting the time history of air flow for every set of parameters, minimum and maximum value can be easily obtained. The values of air change rate at different: insulation layer and window surface (wwr) at E and S orientation in July in Warsaw are presented by Fig. 3–6. Three forms of wind influence were taken in to account. Due to limited space, only selected, results have been presented. Additionally Fig. 1 shows time history of buoyancy flux for east, south and west window's orientation when surface to wall area (wwr) equals 50% and the insulation layer equals 30 cm. The algorithm to calculate buoyancy flux is enclosed in [8]. Fig. 1 shows the time history of indoor temperature as well as ambient temperature. The graphs present the calculations only when wind does not influence ventilation flows. It means that all the air flow is driven by buoyancy forces. The absence of wind can even generates a reversed flow [1]. It happens usually during hot hours and creates uncomfortable conditions. Although that may not occur very often, it may cause problems associated with overheating.

When the window is facing east (Fig.1a), the buoyancy flux reaches the highest value in the forenoon. In the afternoon the buoyancy flux is smaller because of smaller wwr parameter for the south and west windows. But it still is generated mainly by heat sources of 300 W and heat accumulated in partitions. At the window facing south (Fig. 1b), the buoyancy flux is almost symmetrical to 12 o'clock at noon and reaches the highest value of $0.805 \text{ m}^4/\text{s}^3$ at one o'clock. The maximum value is slightly lower in comparison with that created at the east oriented window when reaches $0.859 \text{ m}^4/\text{s}^3$ at nine o'clock in the morning. During the summer, solar gains gathered by the south perpendicular partitions, are lower to those being picked of the east or the west ones. The highest buoyancy flux at the west window is generated in the afternoon and is more intensive then the east one. It equals $0.834 \text{ m}^4/\text{s}^3$ at four o'clock in the afternoon (Fig. 1c). Indoor temperature has more or less the same value in all three cases and it exceeds 30°C . However the time history

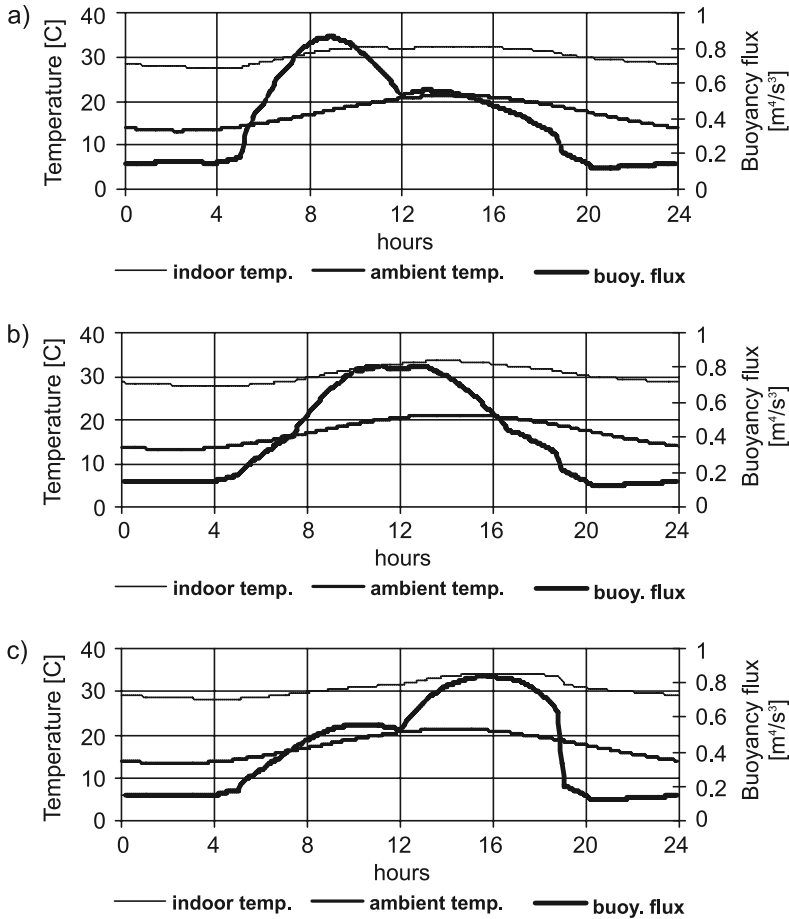


Fig. 1. Time history of indoor and outdoor temperature and buoyancy flux in July in Warsaw without influence of wind, wwr equals 50%, insulation layer equals 30 cm: a) east, b) south, c) west window

of indoor temperatures shows that their values are almost constant throughout 24 hours because of heat accumulation in partitions. Fig. 2 shows time history of air changes which reflect the intensity of buoyancy flux presented by Fig. 1. The air change rate at the West window must be higher in the afternoon because buoyancy flux is of higher value at that time. In turn at the south window more intensive air flow is observed in the early afternoon hours. But almost no differences in air exchange are observed among buildings insulated with 5, 10, 30 cm of foamed polystyrene. All the sets of the computer simulations were carried out to demonstrate the relative importance of parameters such as: outdoor temperature internal heat sources, solar gains, thermal conductance of the building envelope, windows surface and influence of wind on intensity of natural air exchange. For assisting wind the air flow is upwards. For the opposing one can be either upwards or downwards. The direction depends

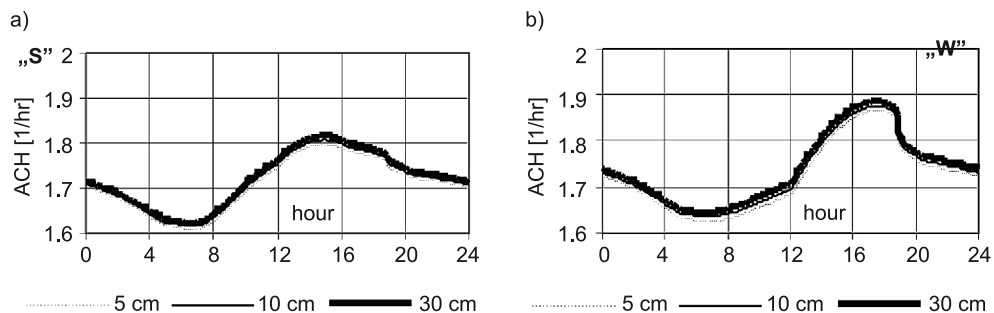


Fig. 2. Time history of air rate change rate at different insulation in July in Warsaw when wind appearances are not observed (without influence of wind), window surface to wall area (wwr) equals 50%: a) south orientation; b) west orientation

on relative strengths of wind and buoyancy forces [1, 8]. In well insulated buildings where buoyancy force substantially benefits from solar gains a reverse flow does not usually occur [1]. Sometimes the wind does not appear and the buoyancy force acts on its own. All the graphs presented by Fig. 3–6 display the highest and the lowest values of air change rates as the function of insulation thickness and window to wall rate (wwr). The layer of polystyrene is equaling 10, 20, 30 cm. The wwr parameter is varying from 5% to 50%.

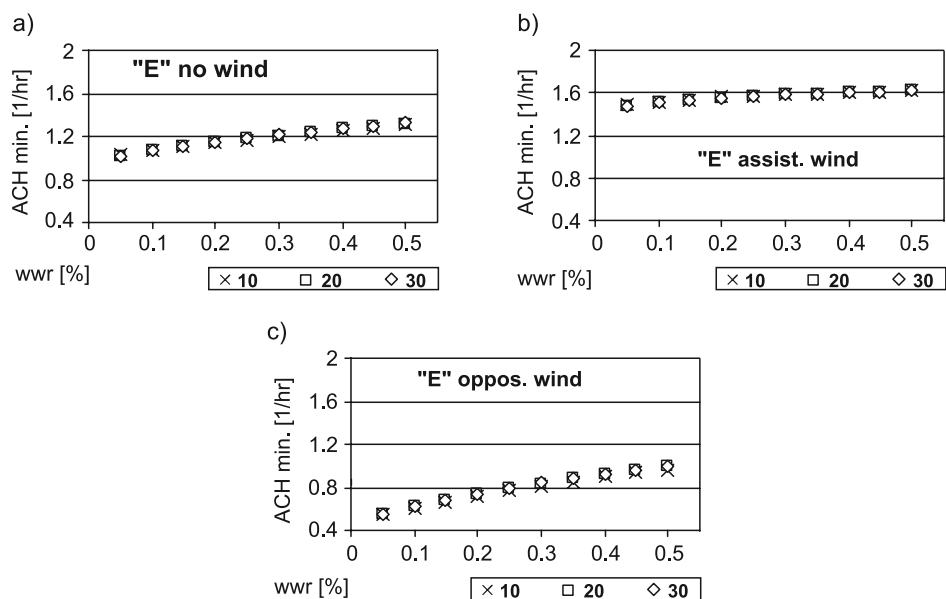


Fig. 3. Min. ACH at the east window in July in Warsaw: a) no wind, b) assisting, c) opposing wind

The common feature of all the graphs is, what is obvious, that the smallest value of air change rate is when wwr equals 5% because solar gains are the least intensive. The highest ones occur at wwr equal to 50%. At the considered thickness of layers the difference

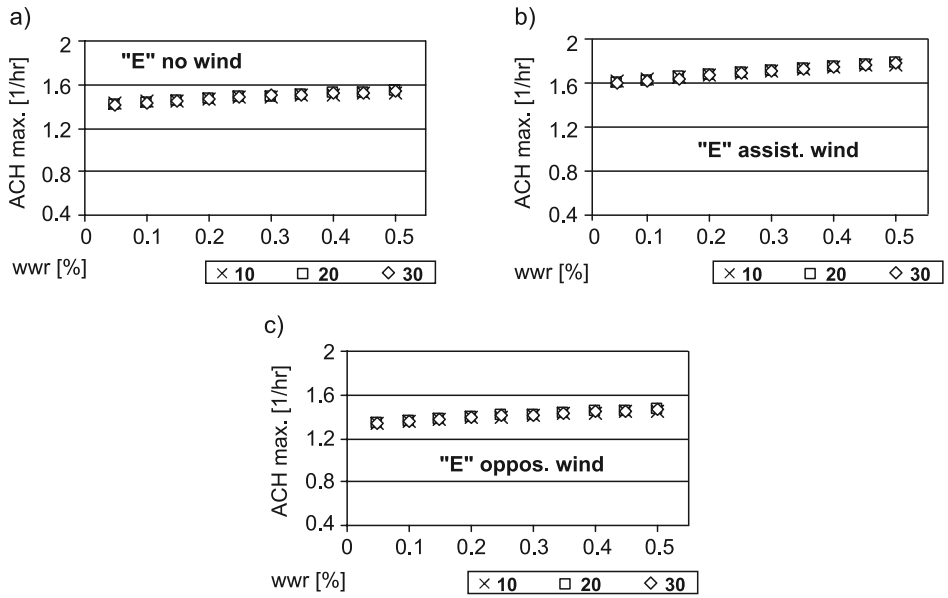


Fig. 4. Max. ACH at the east window in July in Warsaw: a) no wind, b) assisting, c) opposing wind

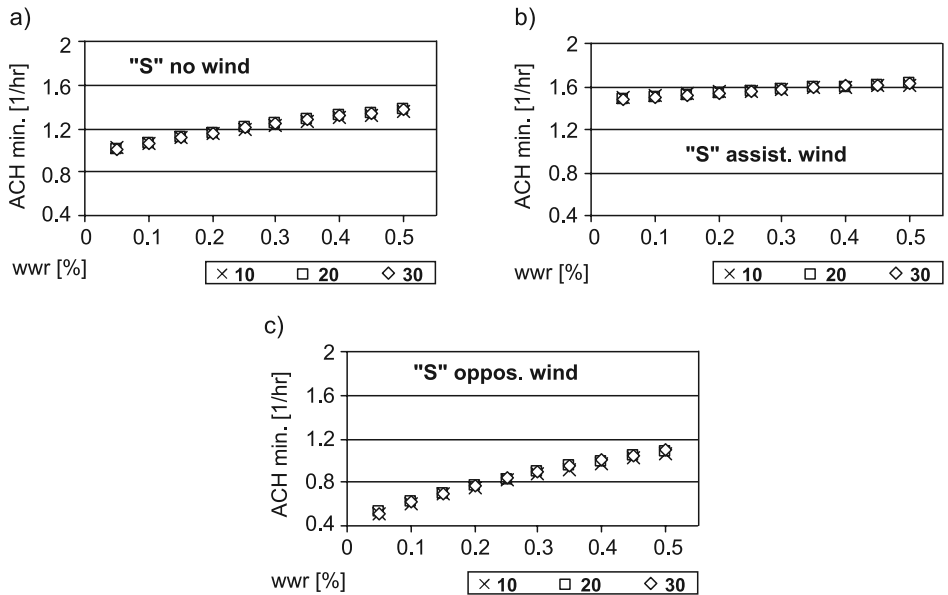


Fig. 5. Min. ACH at the south window in July in Warsaw: a) no wind, b) assisting, c) opposing wind

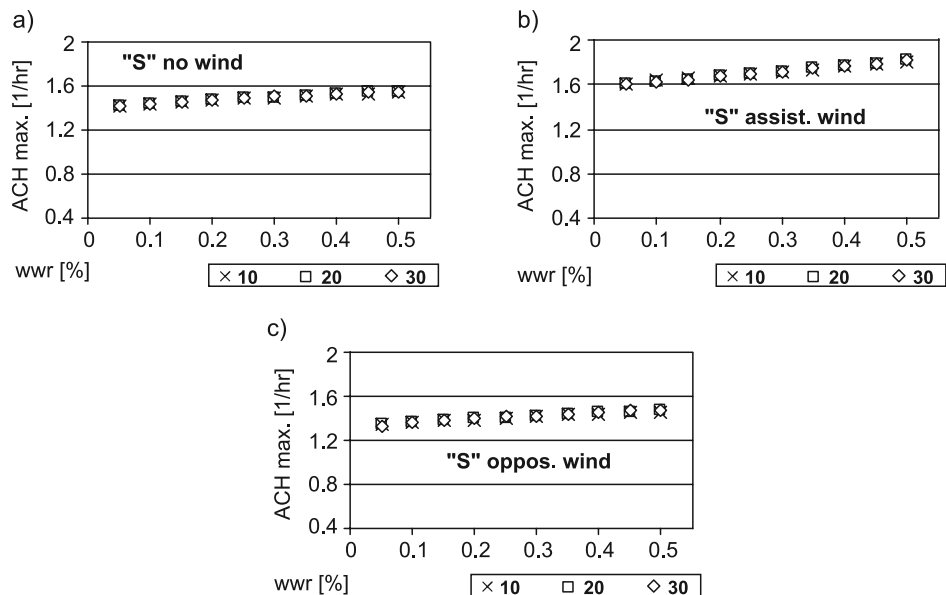


Fig. 6. Max. ACH at the south window in July in Warsaw: a) no wind, b) assisting, c) opposing wind

in intensity of air exchange is hardly visible. This is not true when the heat transmittance coefficient of the building envelope is not reduced by much, for instance between a not insulated and an insulated wall [1]. Then the wwr parameter decides about the intensity of air exchange. The results of these calculations are placed in Tab. 1. The further conclusion is then the intensity of air exchange depends mainly on the form of wind appearance. The value of buoyancy flux plays less significant role in the process [1, 8]. The lowest value is obtained at the opposing wind. No matter if the window faces east or south. Similarly the differences of the ACH rates are of less importance when orientation is concerned. The paper presents only the part of the research considering some aspects of overheating process that takes place in buildings during summer period.

Table 1

Minimum and maximum ACH values induced or not by wind at east and wouth oriented window

	no wind		assist. wind		oppos. wind	
	ACH		ACH		ACH	
	min.	max.	min.	max.	min.	max.
E min. – Fig. 3	1.02	1.33	1.47	1.62	0.54	1.0
E max. – Fig. 4	1.41	1.54	1.6	1.78	1.34	1.47
S min. – Fig.5	1.0	1.37	1.47	1.63	0.52	1.1
S max. – Fig. 6	1.41	1.55	1.6	1.8	1.33	1.48

References

- [1] Bzowska D., *Dynamika procesów wymiany ciepła i naturalnej wymiany powietrza w budynkach o różnej strukturze materiałowej przegród*, Prace IPPT 2/2007.
- [2] Gasparella A., et al., *Analysis and modelling of window and glazing systems energy performance for a well insulated residential building*, Energy & Buildings 43, 2011, 1030-1037.
- [3] Grinning S., et al., *Windows in the building of tomorrow: Energy losers or energy gainers?*, Energy & Buildings 61, 2013, 185-192.
- [4] Haim D., et al., *Optymalizacja fasad podwójnych pod kątem oszczędności energii i środowiska wewnętrznego*, Monografia, Wydawnictwo PŁ, 2013.
- [5] Kim T., Todorovic M., *Tuning control of building glazing's transmittance dependence on the solar radiation wavelength to optimize daylighting and building's energy efficiency*, Energy & Buildings 63, 2013, 108-118.
- [6] Kisilewicz T., *Wpływ izolacyjnych, dynamicznych i spektralnych właściwości przegród na bilans cieplny budynków energooszczędnych*, Monografia, Wydawnictwo PK, Kraków 2008.
- [7] Leskvar V.Z., Premrov M., *An approach in architectural of energy-efficient timber buildings with a focus on the optimal glazing size in the south-oriented façade*, Energy & Buildings 43, 2011, 3410-3418.
- [8] Li Y., Delsante A., *Natural ventilation induced by combined wind and thermal forces*, Building and Environment, 36, 2001, 59-71.
- [9] Persson M., et al., *Influence of window size on the energy balance of low energy houses*, Energy & Buildings 38, 2006, 181-188.

DOROTA CHWIEDUK*, ANDRZEJ GRZEBIELEC*, ARTUR RUSOWICZ*

SOLAR COOLING IN BUILDINGS

SŁONECZNE CHŁODZENIE W BUDOWNICTWIE

Abstract

The paper presents a kind of review of solar cooling technologies applied in construction. There are three cooling technologies: absorption, adsorption and DEC – Desiccant Evaporative Cooling – applied coupled with solar systems. What the stress is placed on are cooling systems of a high installed capacity of several hundred kW. Large scale solar cooling systems are not used in Poland. However, modern public buildings, especially offices with huge glazed facades very often require more energy for cooling than space heating. Solar cooling seems to be prospective technology to reduce energy consumption used by traditional air conditioning units.

Keywords: solar cooling, solar collectors, refrigeration systems

Streszczenie

W artykule przedstawiono przegląd instalacji chłodzenia słonecznego stosowanych w budownictwie. Są stosowane trzy technologie chłodnicze: absorpcyjne, adsorpcyjne oraz oparte na chłodzeniu przez osuszanie i odparowanie, które kojarzy się z instalacjami słonecznymi. Rozważane są systemy dużej mocy rzędu kilkuset kW i więcej. Systemy słonecznego chłodzenia dużej mocy nie są stosowane w Polsce. Jednakże nowoczesne budynki użyteczności, szczególnie biurowce o dużych przeszklonych powierzchniach fasad, wymagają coraz częściej więcej energii do chłodzenia niż do ogrzewania. Technologie słonecznego chłodzenia są perspektywnym rozwiązaniem na rzecz oszczędności zużycia energii w porównaniu z tradycyjnymi systemami klimatyzacyjnymi.

Słowa kluczowe: słoneczne instalacje chłodnicze, kolektory słoneczne, urządzenia chłodnicze

* Prof. Ph.D. D.Sc. Eng. Dorota Chwieduk, Ph.D. Eng. Andrzej Grzebielec, Ph.D. D.Sc. Eng. Artur Rusowicz, Institute of Heat Engineering, Faculty of Power and Aeronautical Engineering, Warsaw University of Technology.

1. Introduction

Nowadays, solar cooling systems are usually applied in public buildings, offices, hospitals with high cooling demand of several hundred kW. The solar cooling system is generally comprised of three sub-subsystems: the solar energy conversion system, refrigeration system, and the cooling load [10]. The appropriate cooling technology for any applications depends on cooling demand, its distribution in time, temperature levels of the refrigerated object and the heat source. A number of possible “paths” from solar energy to “cooling services” are demonstrated in Fig. 1.

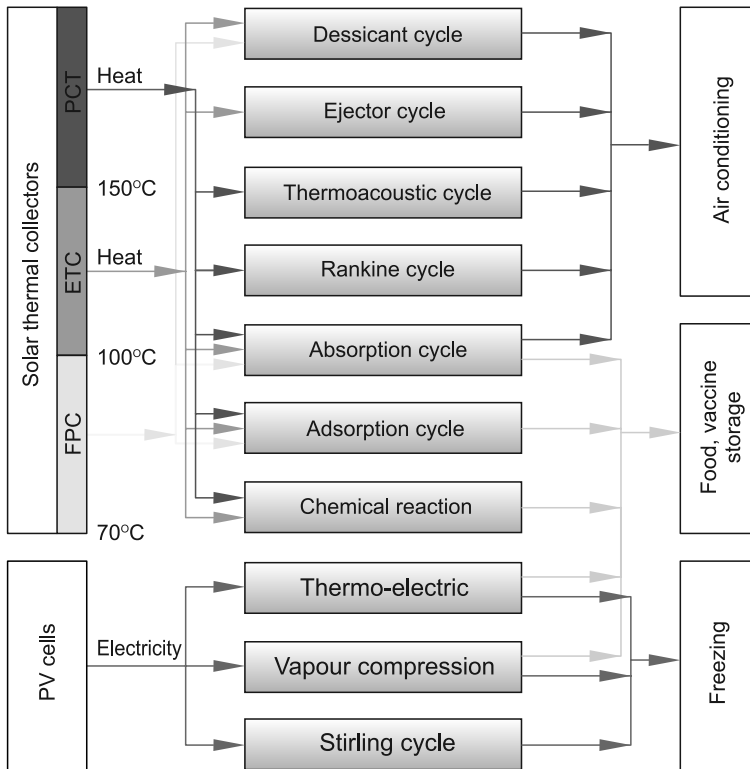


Fig. 1. Solar refrigeration cycles

Starting with the inflow of solar energy there are obviously two significant paths to follow: utilizing solar thermal collectors to convert solar radiation into heat and using PV cells to convert solar radiation directly into electricity [16]. Depending on the type of solar collectors and insolation conditions different temperature levels of solar working fluid can be achieved. This temperature level can be matched to various cycle demands. For example, the Rankine cycle (duplex type) [19] and thermoacoustic cycle [4, 5, 7] require a rather high driving temperature whereas the desiccant cycle functions at lower temperature levels of heat supply [1].

2. Large solar cooling systems

2.1. Absorption systems

Solar absorption refrigeration systems perform a typical absorption refrigeration cycle. Solar radiation is its energy source. Due to the fact that absorption systems require a minimum temperature of 80°C [11, 14, 15] evacuated tube collectors (ETC) are usually used. However, to improve the efficiency of the whole system solar concentrating collectors can be applied.

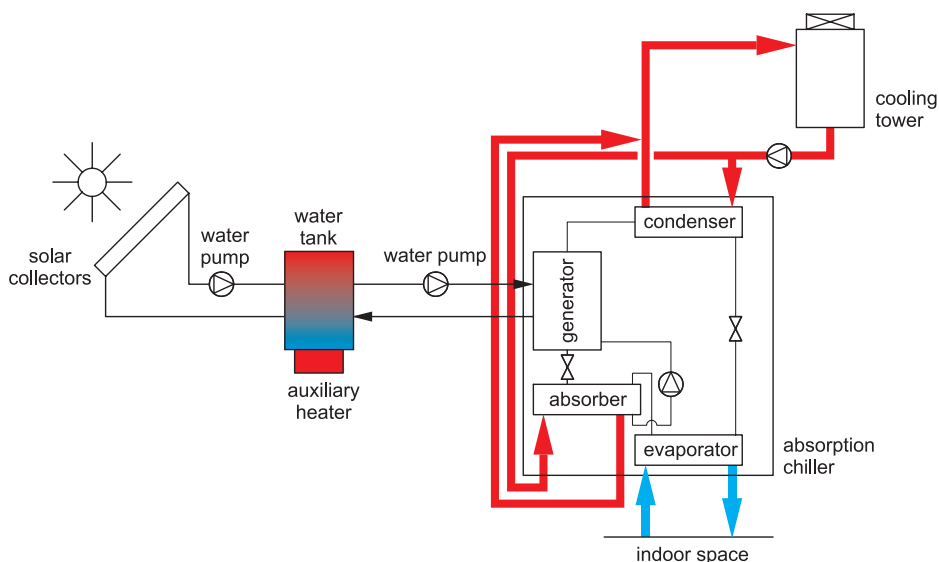


Fig. 2. Solar absorption refrigeration

A relevant application for solar cooling is occurs in buildings which exhibit a high energy demand through air conditioning. Every year the number of buildings that employ such technology increases. Solar cooling systems are mainly used in warm and hot climates. For example, in the year 2006 a solar cooling plant was implemented in the Surgery Hospital for children in Soba, near Khartoum in Sudan. The main aim of the plant was to supply energy for air conditioning throughout the year. Vacuum tube CPC collectors covering an area of $12\,000\text{ m}^2$ were installed to supply heat to the 50 m^3 water store at approximately 100°C . Hot water is used to feed 2 Li-Br absorbers, each of 615 kW . The cooling of the building is accomplished via fan-coil systems. Another example of a great solar absorption cooling technology is the installation at United World College in Singapore with a cooling capacity of 1470 kW and 3900 m^2 of solar collectors [18]. In Europe, the largest absorption solar cooling system is in Rome, Italy (METRO Cash & Carry) with a cooling capacity of 700 kW .

2.2. Adsorption systems

Adsorption refrigeration systems powered by solar energy operate in such a way that the secondary fluid supplies energy alternately to one adsorber, then to another [2, 6, 8]

(see Fig. 3). The refrigerant released from the bed during this process flows through a condenser, expansion valve and evaporator generating cooling power. Heat from the condenser is transferred to the cooling tower. Depending on the type of working pairs (solid and fluid) a different temperature of solar working fluid is required to thermally drive the adsorption cycle. If solar irradiation is high, it is possible to use even flat plate solar collectors working at a temperature of 80–90°C.

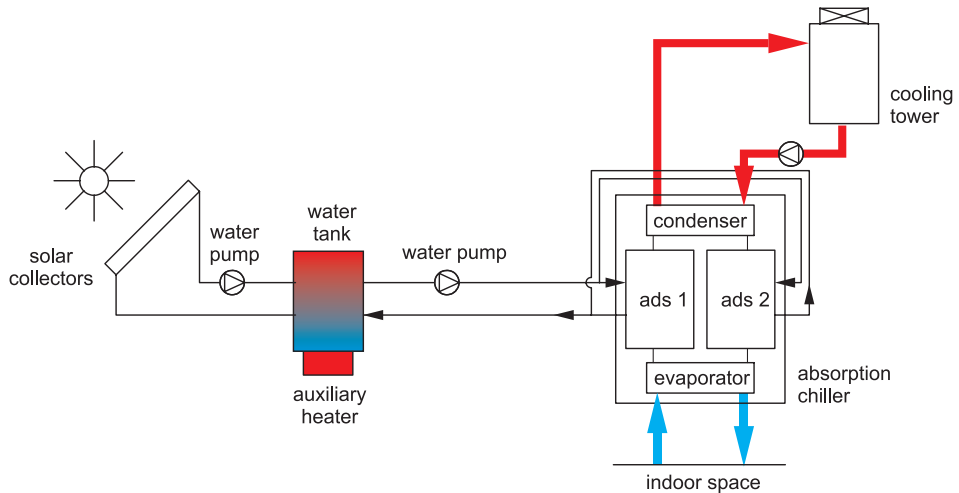


Fig. 3. Solar adsorption refrigeration

Festo in Esslingen-Berkheim (Germany) is currently running the largest adsorption cooling system in the world. Three MYCOM ADR-100 cooling machines produce a nominal output of 353 kW each. The generated cooling energy cools a 26 760 m² area of office buildings as well as three atriums with an area of 2790 m². The cooling machines were driven by heat from gas boilers and waste heat of compressors. What was introduced as a third source of heat was the solar system with vacuum tube collectors of the absorber surface of 1218 m². Thus, gas consumption was significantly decreased. The vacuum tube CPC collectors have been installed on a shed roof of a 30° slope and with an azimuth angle of +17°. The solar collectors covering a surface area of 1330 m² consist of 58 collectors of 3.29 m² each (CPC30) and 232 collectors of 4.91 m² (CPC45). One CPC30 and four CPC45 are respectively connected into series. Water heated in the solar collectors is transported to the two solar buffer storage tanks (of 8500 liters each) [18].

The next large solar cooling plant is located in Viota (Greece). It has been constructed for a cosmetic factory and it is made of 2 adsorption chillers (350 kW each). There are 2700 m² of flat plate collectors delivering heat to the adsorption chillers as well as to the factory as process heat. It is evident that the installed capacity of adsorption solar systems is usually significantly lower than that of absorption systems.

2.3. Desiccant Evaporative Cooling (DEC)

An example of solar solid desiccant cooling system shown in Fig. 4 consists of the following elements: two air ducts, two fans, a heat wheel, a desiccant wheel, two evaporative coolers (humidifiers) and a heater. The heater is driven by solar energy. The principle of work lies in the fact that fresh air is dried by removing the heat from this fresh air to heat up the air going out of a building [9]. Subsequently, the fresh air is cooled in the rotary heat exchanger and then cooled by humidification. The drier the inlet air becomes, the more cooled down this air can become during the humidification process.

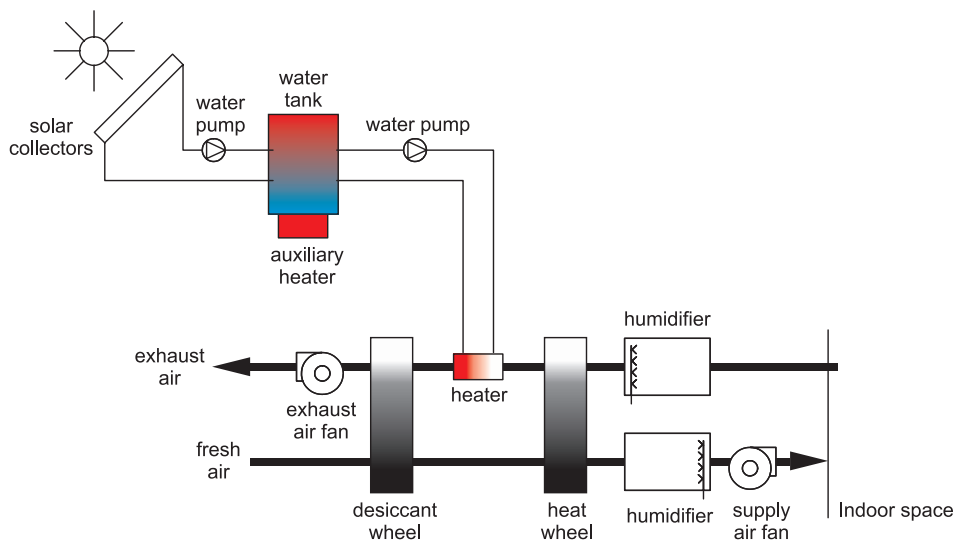


Fig. 4. Solar solid desiccant cooling

The total number of large solar DEC installations in the world is 22 (19 of which are in Europe). Among these DEC installations only 7 systems use a liquid regenerator (DEC liquid) [3, 17, 18]. These DEC systems are predominantly operational in hot humid countries. Their cooling capacity is usually much lower than in the case of adsorption and especially absorption technologies.

3. Present state of solar cooling systems application

In 2011, about 750 solar cooling systems of different capacities were installed worldwide, including small capacity systems (< 20 kW). In 2012, 159 new solar cooling systems were installed around the world [3]. In last six years the number of large solar cooling systems has doubled. At the same time, the total capacity of cooling systems has increased from 9.3 MW to 17.6 MW. In terms of systems with a cooling capacity above 20 kW there are three dominating technologies: absorption, adsorption and DEC. Table 1 presents the different categories of sorption processes (columns: “Abs”, “Ads”, “DECs” and “DECI” refer to given

technologies) with the nominal thermal cooling capacities of the installations in different world regions in 2012. Closed cycles using absorption or adsorption are indicated by “Abs” or “Ads”, whereas desiccant evaporative cooling systems with an open cycle are indicated by “DECs” when a solid sorption material, for example, in a sorption rotor is used. When a liquid sorption material is applied the system is referred to as “DECI”.

Table 1

Worldwide solar cooling systems in 2012

Continent	Abs [kW]	Ads [kW]	DECs [kW]	DECI [kW]
Australia	300	0	0	0
Asia	976	0	43	350
Europe	10314	2932	703	195
Africa	1265	0	0	0
North America	245	290	0	0
Total:	13100	3222	746	545

The list counts 159 installed large-scale solar cooling systems, where 128 installations are located in Europe, 9 in Asia (China, Japan, Singapore, Israel, Armenia), and 10 in America (USA, Mexico), 2 in Africa and 1 Australia. Countries having the largest cooling capacity in solar cooling systems worldwide are presented in Fig. 5.

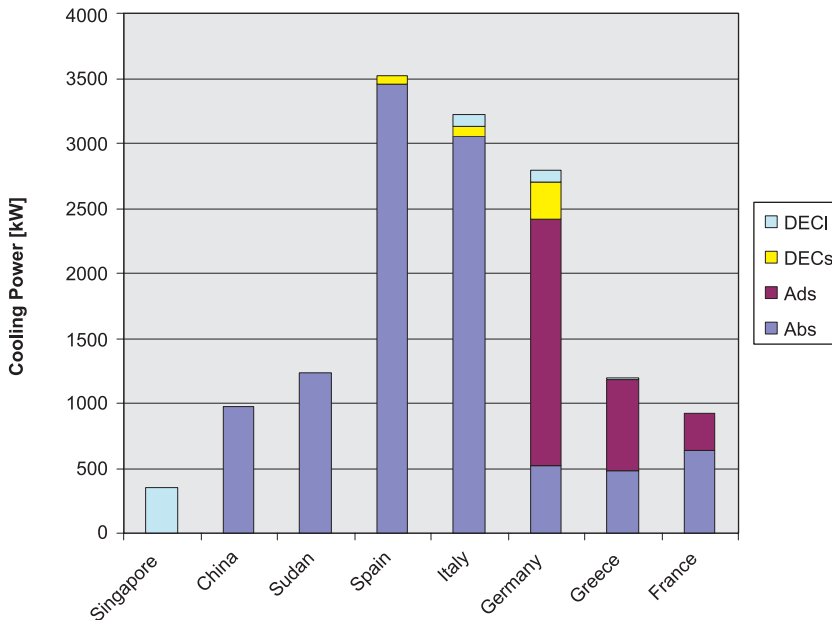


Fig. 5. Worldwide distribution of the cooling power assisted by solar energy. The types of thermally driven chillers applied in the different countries are also listed

In Europe, there are 94 absorption chiller installations, 15 adsorption chillers and 19 DEC (Desiccant Evaporative Cooling) systems. Among the DEC installations, only 5 systems use a liquid regenerator (DEC liquid). The overall cooling capacity of the solar thermally driven chillers amounts to 13.25 MW, with 26% installed in Spain, 23.1% in Italy, 18.2% in Germany and 9% in Greece (Fig. 6).

In Europe, 60% of these installations are dedicated to office buildings, 15% to laboratories and education centers, 7% to factories, 6% to hotels and hospitals and the rest to buildings with different uses (such as, canteens, sport centers, etc).

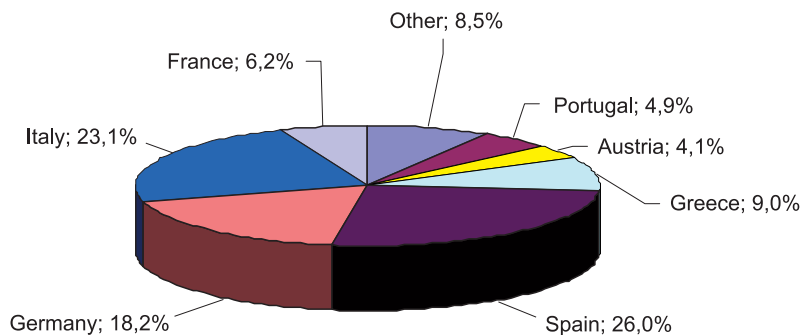


Fig. 6. Percentage of cooling capacity solar cooling systems in European countries

The overall solar cooling capacity is assisted by about 50000 m² of solar thermal collectors [17]. About 50% of the total gross area is made up of FPCs (Flat Plate Collectors), about 40% of VTCs (Vacuum Tube Collectors), about 10% of CPCs (Compound Parabolic Collectors).

In Poland, there is no solar cooling plant with a cooling capacity above 20 kW.

4. Conclusions

According to the National Renewable Energy Laboratory (NREL) (in USA) twenty years ago, most solar cooling systems, of the absorption or desiccant types, were designed to handle 30–60% of all cooling requirements, with the remainder supplied by a backup heat source such as natural gas. Currently, most of the new systems are designed to meet the cooling demand for the entire building, although in many cases backup heat sources do exist [12]. Most applications of this type are located in Europe and the Far East and are mainly used to cool the air in the air-conditioning systems of office buildings.

As mentioned earlier, solar cooling is not being implemented in Poland. However, modern public buildings, especially offices with huge glazed facades frequently require more energy for cooling than for space heating. Solar cooling seems, therefore, to be prospective technology. Its application should reduce the consumption of traditional fossil fuels as traditional air conditioning units largely use electricity produced by coal fired plants.

Furthermore, the solar cooling system does not involve a simple traditional installation located in the HVAC center or boiler room inside a building. The implementation of this

technology entails the installation of its component parts, i.e. the solar collectors, to be incorporated into building envelope. It must be emphasized that building-related solar energy issues are not limited to the installation itself, but also to the architectural and civil engineering aspects. Solar collectors can be placed on a special supporting structure on top of a roof, as a stand-alone solar system, or just on the ground. Solar collectors on the roof of a single family house usually look quite good. However, in the case of a big installation, the vast array of solar collectors on a special supporting structure mounted to the flat roof of a building does not look good aesthetically. In addition, such a series of collectors is very much subject to environmental factors, such as low ambient air temperature and wind. As a result, heat losses from solar collectors are great and thus reduce the thermal efficiency of the system. Therefore, it is recommended to incorporate solar collectors into the external walls of a building as their integral element. BIST – Building Integrated Solar Thermal – systems are increasingly popular in different types of modern low-energy buildings, both public and private. All aspects of BIST systems are being considered by the COST Action TU1205 “Building Integration of Solar Thermal Systems (BISTS)”.

References

- [1] Chwieduk M., Chwieduk D., *Chłodzenie słoneczne*, Zeszyty Naukowe Politechniki Rzeszowskiej, Budownictwo i Inżynieria Środowiska 57, 4, 2010, 61-70.
- [2] Cyklis P., Kantor R., *Concept of ecological hybrid compression-sorption refrigerating systems*, Czasopismo Techniczne, Mechanika 109, 2012, 31-40.
- [3] Ehrismann B., *Collated and updated list of solar cooling installations in participating countries*, Task Report 5.3.1 QAISt, Stuttgart, Germany 2012.
- [4] Grzebielec A., *Historia rozwoju termoakustycznych urządzeń chłodniczych*, Część 1, *Źródła termoakustyki*, Chłodnictwo 11, 2011, 14-16.
- [5] Grzebielec A., *Historia rozwoju termoakustycznych urządzeń chłodniczych*, Część 2, *Współczesne urządzenia termoakustyczne*, Chłodnictwo 2, 2012, 19-21.
- [6] Grzebielec A., Rusowicz A., *Analysis of the use of adsorption processes in trigeneration systems*, Archives of thermodynamics 34, 2013, 4, 35-49.
- [7] Grzebielec A., Rusowicz A., *Thermoacoustic methods for liquefaction of natural gas*, Rynek Energii 106, 2013, 87-92.
- [8] Jakob U., *Development and investigation of a compact silica gel/water adsorption chiller integrated in solar cooling systems*, VII Minsk International Seminar “Heat Pipes, Heat Pumps, Refrigerators, Power Sources”, Minsk, Belarus, 8–11 September 2008.
- [9] Jarocki P., Rusowicz A., *System DEC w klimacie umiarkowanym*, Chłodnictwo 4, 2009, 32-36.
- [10] Kalogirou S.A., *Building Integration of Solar Thermal Systems*, ICLAS3, Greece, July 2013.
- [11] Macia A., Bujdo L.A., Magraner T., Camorro C.R., *Influence parameters on the performance of an experimental solar-assisted ground-coupled absorption heat pump in cooling operation*, Energy and Buildings 66, 2013, 282-288.
- [12] Maurer C., Baumann T., Hermann M., Di Lauro P., Pavan S., Lars M., Kuhn T.E., *Heating and cooling in high-rise buildings using façade integrated transparent solar thermal collector systems*, Proceedings of Building Simulation 2011:12th Conference of International Building Performance Simulation Association, Sydney, 14–16 November.
- [13] Mu’azu M., *Novel evaporative cooling systems for building application*, Phd Thesis. Univesity of Notthingam, UK, 2008.

- [14] Rusowicz A., *Rozwój bromolitowych absorpcyjnych urządzeń chłodniczych*, Chłodnictwo 1–2, 2008, 30-33.
- [15] Rusowicz A., Ruciński A., *The mathematical modelling of the absorption refrigeration machines used in energy systems*, Proc. 8th International Conference Environmental Engineering, Vilnius, Lithuania, 19–20 May, 1–3, 2011, 343-346.
- [16] Shahat A.E., *PV Module Optimum Operation Modeling*, Journal of Power Technologies 94 (1), 2014, 50-66.
- [17] Sparber W., Napolitano A., Melograno P., *Overview on world-wide installed solar cooling systems*, 2nd International Conference Solar Air Conditioning, Tarragona–Spain, October 2007.
- [18] Thorpe D., *Energy Management in Buildings: Earthscan Expert Guide*, Routledge, New York 2014.
- [19] Vakiloroyaya V., Ha Q.P., Skibniewski M., *Modeling and experimental validation of a solar-assisted direct expansion air conditioning system*, Energy and Buildings 66, 2013, 524-536.

ANNA DUDZIŃSKA*

THE ROLE OF ANTI-SOLAR PROTECTION
IN THE REDUCTION OF SOLAR GAINS
IN THE PASSIVE SPORTS HALL

ROLA OSŁON PRZECIWSŁONECZNYCH
W OGRANICZENIU ZYSKÓW SOLARNYCH
W PASYWNEJ HALI SPORTOWEJ

Abstract

In this paper, the influence of anti-solar protection on the reduction of solar gains in a public building was analysed. Indoor thermal conditions in the building were verified by way of computer simulations for two scenarios: without any protection against solar gains and with the application of blinds and overhangs.

Keywords: passive building, anti-solar protection

Streszczenie

W artykule przeanalizowano wpływ osłon przeciwsłonecznych na ograniczenie zysków solarnych w pasywnym budynku użyteczności publicznej. Dokonano porównania warunków wewnętrznych w badanym obiekcie bez zabezpieczeń przed zyskami solarnymi oraz z zastosowaniem rolet i łamaczy światła.

Słowa kluczowe: budynek pasywny, osłony przeciwsłoneczne

* M.Sc. Eng. Anna Dudzińska, Institute of Building Materials and Structures, Faculty of Civil Engineering, Cracow University of Technology.

1. Introduction

The necessity of reducing solar gain in periods of high air temperatures in the context of passive buildings, results in the formation of special structural solutions. Technical requirements on glass partitions have been specified by the Regulation of the Ministry of Infrastructure concerning the buildings and their locations [1]. In the summer, overheated rooms may cause unreasonable economical and operating problems. Thus, anti-solar protection is used. It plays an important role in creating advantageous indoor environmental conditions as well as positively affecting the energy efficiency of the building.

Systems of anti-solar protection, as a necessary part of glazed surfaces, have to determine the amount of the sunlight getting into the building. This control over the sunlight itself, and the amount of thermal energy it introduces to the internal environment, is accomplished by way of such devices as window blinds and overhangs. They can be situated both outside and inside the building. Their location, dimensions and the slope determines the effectiveness of their ability to deal with the radiation [2].

In case of the analysed sports hall building, there were horizontal stationary large size blinds (so-called “overhangs”) mounted on the south elevation. Aluminium screens prevent sunlight penetrating into the building when the sun is high. However, stationary overhangs do not adjust to the current light needs. Thus, additional indoor blinds were used. This popular solution reduces the exposure to the sunlight and visual contact with the outside environment.

2. Input assumptions for the Design Builder software analyses

Thermal analyses were performed using the Design Builder software, which is the GUI (Graphical User Interface) of the computational software Energy Plus. The latter was created on the request of the government of the USA.

Geometry data of the analysed sports hall building was thoroughly represented in the context of its shape, dimensions and the location of the windows. A geometric model of the building created using the Design Builder software is presented in the Fig. 1.

The above mentioned model enabled an analysis of the real structure in terms of its thermal behaviour. Characteristics of both transparent and opaque walls, infiltration of the air from outside, internal heat sources' gains as well as the presence of various installations were taken into account in the utilized program.

In accordance with the design assumptions, 1m long overhangs were modelled in a program.

Simulations were performed for the time period with the highest air temperature, i.e. from the 1st of May to the 30th of August. Four simulation cases with different versions of the south elevation equipment were considered:

- Basic – with no overhangs nor window blinds,
- With overhangs but without window blinds,
- Without overhangs but with window blinds,
- With both overhangs and window blinds.

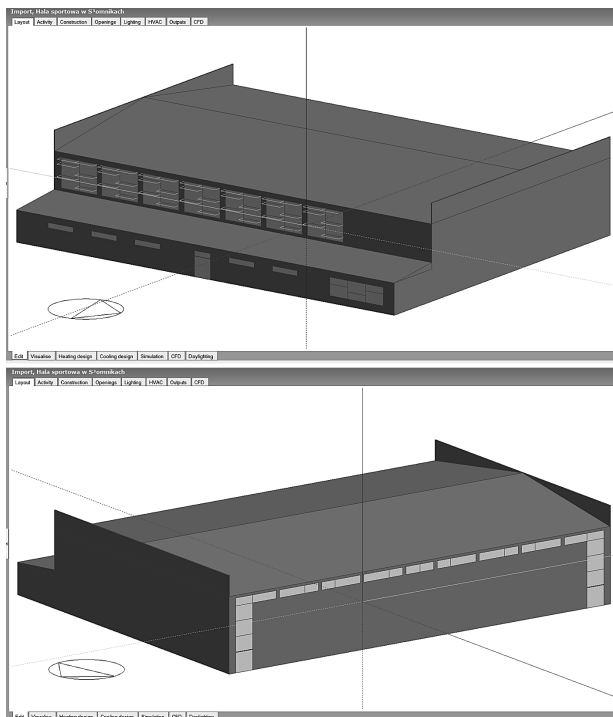


Fig. 1. South and north elevation of the sports hall building

External Windows

Glazing type Slomniki_glazing

Layout Preferred height 1.5m, 50% glazed

Dimensions

Type 3-Preferred height

Window to wall % 50,00

0 10 20 30 40 50 60 70 80 90 100

Window height (m) 1,50

Window spacing (m) 0,40

Sill height (m) 0,80

Reveal

Frame and Dividers

Shading

Window shading

Type Mid-pane blind with medium reflectivity slats

Position 1-Inside

Control type 6-Outside air temp

Outside air temperature setpoint (°C) 24,00

Operation

Operation schedule D1_Edu_DrySpt-Hall_Occ

Local shading

Type 1.0m Overhang

Internal Windows

Roof Windows/Skylights

Doors

Vents

Fig. 2. Foundations received in modelling

3. Numerical results

On the basis of the performed numerical simulations, one can formulate conclusions concerning the effectiveness of the applied anti-overheating solutions and also evaluate their impact on the microclimate conditions inside the sports hall passive building *n* the period of high outdoor air temperatures.

A building with no anti-solar protection generates approximate energy gains of 117.73 kWh per day within the whole analysis period. The maximum daily gain was equal to 187.24 kWh. The lowest values of the undesired solar energy (in summer) were calculated in case of overhangs and the application of internal window blinds. They were equal to approximately 79,25 kWh.

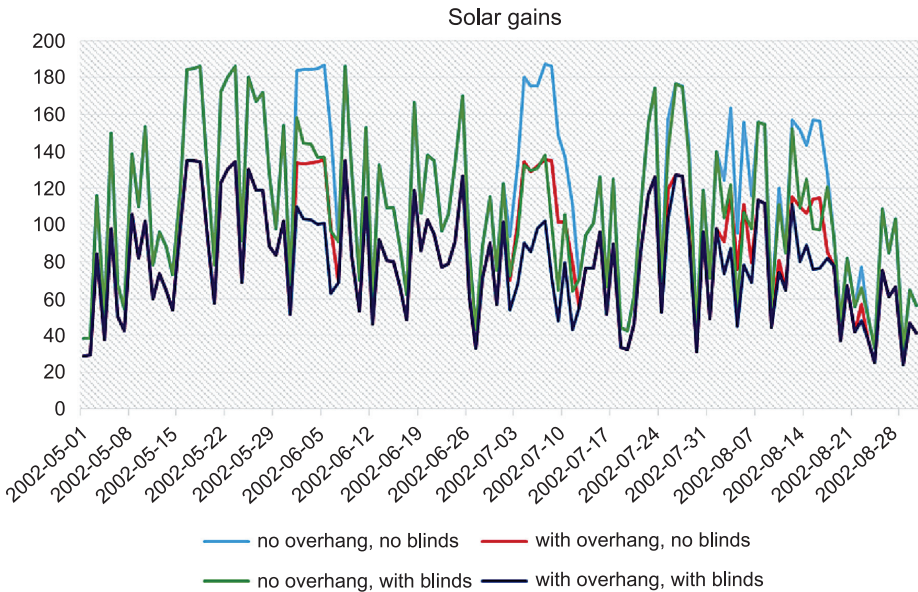


Fig. 3. Solar gains through external windows for four simulation cases

Table 1

Min, max and medium values for all simulations

[kWh]	no overhang no blind	with overhang no blind	no overhang with blind	with overhang with blind
Min	31.66	24.03	31.66	24.03
Max	187.24	135.55	186.19	135.12
Medium	117.73	108.23	108.23	79.25

The air temperature inside the building reaches the maximum (equal to 27.28°C) in the case of the application of window blinds (without external overhangs). The average air temperatures are also the highest in the above case. The lowest air temperature inside

the building was calculated in the case of the application of overhangs with no blinds. However, it should be pointed out that solar gains are larger than for the case that is marked with navy blue in Fig. 3.

Table 2

Min, max and medium air temperature

[°C]	no overhang no blind	with overhang no blind	no overhang with blind	with overhang with blind
Min	15.09	15.07	15.09	15.07
Max	26.20	25.68	27.28	26.87
Medium	20.44	20.07	20.64	20.29

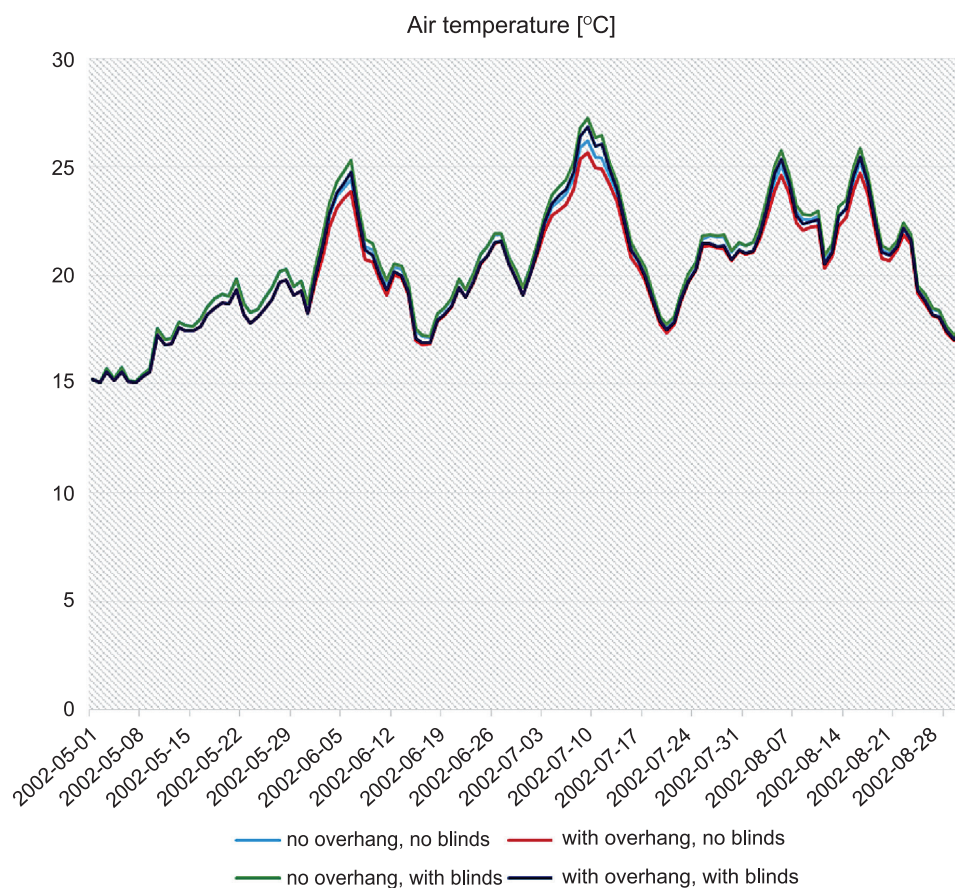


Fig. 4. Indoor air temperature for four simulation cases

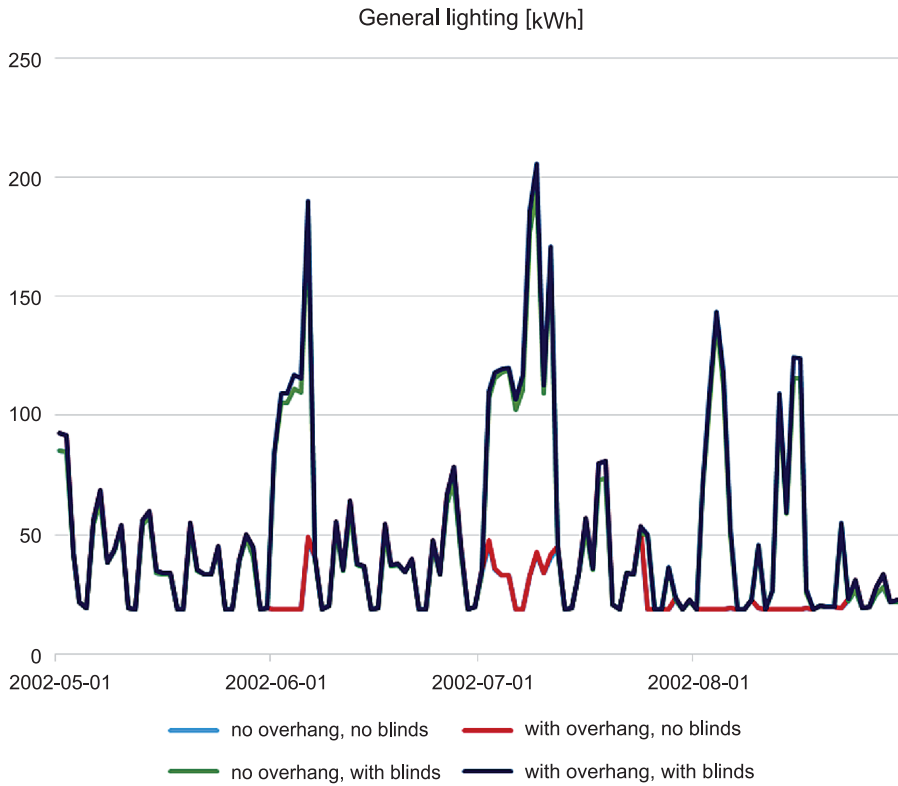


Fig. 5. General lighting for four simulation cases

Table 3

General lighting

[kWh]	no overhang no blind	with overhang no blind	no overhang with blind	with overhang with blind
Min	18.75	18.75	18.75	18.75
Max	85.47	92.78	193.74	205.72
Medium	31.32	32.28	50.69	52.60

In both cases with no internal window blinds, the energy used for lighting was the lowest. The largest lighting demand can be observed for the fourth variant (with internal window blinds and external overhangs), when the artificial lighting consumes the energy of 52.60 kWh.

4. Conclusions

Periods of high external air temperatures and strong sunlight are very difficult in the context of maintaining good conditions inside passive buildings. Exposure to sunlight of buildings with walls made mostly of glass may result into their overheating. Thus, application of anti-solar protection is necessary in order to reduce excessive solar gains.

According to the performed analyses, the most effective method of solar gain reduction is using both window blinds and overhangs during periods of the most intensive sunlight. In such a case, solar gains are approximately 30% lower compared to windows without anti-solar protection and they are equal to 79.25 kWh per day. However, it should be remarked that more energy is necessary for lighting purposes. It results in the generation of additional thermal gains inside the sports hall building. The total energy demand in this case is equal to 131.86 kWh and the maximum air temperature equals 26.87°C. The worst situation steps out in variant third (without overhangs but with internal window blinds) where solar gains are equal to 158.93 kWh and the maximum air temperature equals 27.28°C.

The most effective strategy from an economic point of view (regarding indoor environmental conditions) is the application of both overhangs and blinds. They reduce sunlight to a full extent. Internal roller blinds increase the demand on lighting by about 70%, but total gains are the lowest when he joins them with overhangs I don't know what you mean with this last phrase, it needs rewriting.

References

- [1] Rozporządzenie Ministra Infrastruktury w sprawie warunków technicznych jakim powinny odpowiadać budynki i ich usytuowanie.
- [2] Tymkiewicz J., *Systemy osłon przeciwsłonecznych – wady i zalety różnych rozwiązań*, Technical Transactions, 2-A/2/2011.

PAVOL ĎURICA*, MÁRIA JANIKOVÁ*, MAREK CANGÁR*,
DANIELA ŠTAFFENOVÁ*

LONG TIME TESTING OF THERMAL PARAMETERS IN SELECTED WINDOWS

DŁUGOFALOWE POMIARY WŁAŚCIWOŚCI TERMICZNYCH W WYBRANYCH OKNACH

Abstract

The paper presents an evaluation of the measured data of the temperatures of three window constructions made from different materials and with different glazing systems. Measurements were carried out at different points on window friezes and glazing and they underway continuously throughout the year. These windows are suitable for low-energy buildings. Window structures were placed in the pavilion type testing laboratory. The windows were installed in an outer wall of known thermal characteristics, in a room with a constant indoor climate. The windows were exposed to the real effects of external climate conditions. The article shows the results of temperature measurements and thermo-optical properties.

Keywords: windows, surface temperature, condensation of water vapor

Streszczenie

W artykule przedstawiono ocenę danych z pomiarów temperatury trzech różnych konstrukcyjnie okien zbudowanych z różnych materiałów i z różnymi układami szybowymi. Pomiaru są przeprowadzane w różnych miejscach ram i przeszkleń nieprzerwanie przez okres jednego roku. Okna te są odpowiednie dla budynków niskoenergetycznych. Okna są umieszczone w laboratorium (typ pawilonu), gdzie okna są zainstalowane w zewnętrznej ścianie pomieszczenia o znanej charakterystyce cieplnej oraz stałych warunkach wewnętrznych. Jednocześnie są wystawione na działanie rzeczywistych zewnętrznych warunków klimatycznych. W artykule przedstawiono wyniki pomiarów temperatury oraz właściwości termooptycznych.

Słowa kluczowe: okna, temperatura powierzchni, kondensacja pary wodnej

* Doc. Eng. Pavol Ďurica, C.Sc. Eng. Mária Janiková, Doc. Eng. Ján Rybárik, PhD. Eng. Daniela Štaffenová, Department of Building Engineering and Urban Planning, Faculty of Civil Engineering, University of Žilina.

1. Introduction

Window constructions are one of the most important elements of building facades. They not only constitute a significant structural element, they also contribute to the final architecture. Recently, they have become considerably involved in energy losses and in the creation of an optimal indoor environment.

The window constructions evaluated in this article were installed in the testing laboratory of the Department of Building Engineering and Urban Planning, Faculty of Civil Engineering, University of Žilina. This is so-called “pavilion type” laboratory, where the windows are fixed into an outside wall of known thermal characteristics, in a room with a constant indoor climate and they are exposed to real effects of external climate conditions.



Fig. 1. Exterior and interior of climatic chamber with integrated samples of window constructions

In the chamber, an internal environment identical to basic boundary conditions of thermal standard according to the STN 73 0450:2002 [6] is formed, i.e., the indoor air temperature θ_{ai} is maintained at 20°C and the relative humidity φ_{ai} is 50%.

1.1. Climatic chamber

The climatic chamber must be suitably calibrated so that the samples of window constructions show the correct values. This state is crucial in ensuring the correct operation of the chamber with regard to the elimination of heat losses. These could arise from heat transmission through the ceiling, because above the chamber, there is a double-coat roof construction, and through the external wall, which isolates the room from the external environment. Obviously, heat losses also arise through the window constructions themselves.

We can determine the equation of heat balance of the indoor air (in afore-mentioned climatic chamber) according to the scheme of the thermal balance of the air (Fig. 2):

$$Q_h + Q_s + c_p \cdot (Q_v + Q_t) \cdot (\theta_e - \theta_i) + \sum h_{sj} \cdot S_{jp} \cdot (\theta_{jp} - \theta_i) = 0 \quad (1)$$

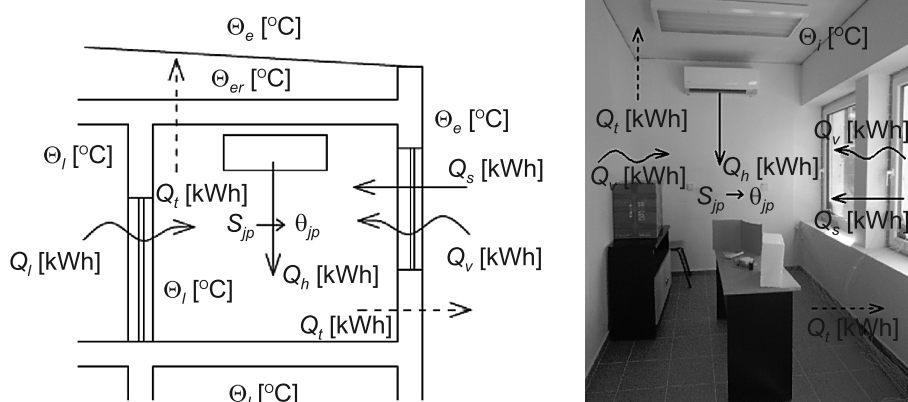


Fig. 2. The scheme of thermal balance of indoor air in the climatic chamber: Q_i – air infiltration [kWh], Q_s – solar gains [kWh], Q_h – heat gains from the air handling unit [kWh], Q_v – transmission of heat [kWh], θ_e – outdoor air temperature [°C], θ_i – indoor air temperature [°C], θ_{er} – under roof space temperature [°C], θ_{jp} – surface temperature [°C], S_{jp} – surface area [m²], c_p – specific heat capacity at constant pressure (J/kg·K), h_{sj} – convective heat transfer coefficient on the inner surface [W/m²·K]

1.2. Method of measurement of the thermal parameters of window constructions

Samples of window constructions, which were installed in the climatic chamber, are of various materials and various glazing types. Two of these constructions are plastic and one of them is wooden. The difference between the two plastic windows is in the addition of thermal modules on one of them – such window should fulfil thermal properties better. All three of the windows have different glazing systems (Fig. 3).

For purposes of this article, measurements were taken of internal and external surface temperatures in the middle of the glazing on the studied window constructions, on the frieze of the leaf, and on the glazing in the close contact with the rail frieze.

profile	color	No. of chambers	glazing	gas of glazing	embedment depth of glazing [mm]	U_w [W/(m ² ·K)]	U_f [W/(m ² ·K)]	U_g [W/(m ² ·K)]	thickness of constr. [mm]
	white	6	insulating triple glass	Ar	12	0.8	1	0.5	86
	white	6	insulating triple glass	Kr	12	0.78	0.85	0.5	86
	gray		insulating triple glass		18	0.79	0.8	0.6	

Fig. 3. The samples of window constructions and their parameters

Surface temperatures of these windows are measured through the use of thermocouples, which are protected against sunlight using the special tapes. Each data logger recorded in the long-term with the time period of 30 minutes. For purposes of this article, the relevant measurements were realized between the 27th January and the 2nd February 2012 ($\theta_{ae,min} = -18.9^{\circ}\text{C}$, $\theta_{ae,max} = +4.6^{\circ}\text{C}$) – the heating period of the year (Fig. 4).

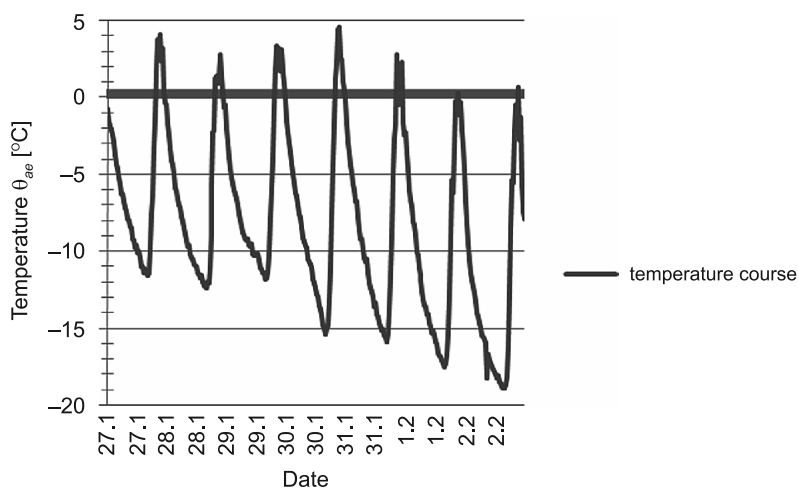


Fig. 4. The shape of external temperatures θ_{ac} [$^{\circ}\text{C}$] during the evaluated measuring period

2. Analysis of samples of window constructions

For window constructions, it is important in terms of energy savings and the prevention of thermo-humidity failures, to fulfil the requirements specified in the Slovak standard STN 73 0540-2 [6]. All fragments of window construction have to be made in the right way and are required to be of the high-quality material in order to ensure one of main functions of the window – this being the capturing of excessive heat and cold from the outside and the prevention of heat transmission from the interior during the heating period.

Figures 5–7 show the surface temperatures $\theta_{si,w}$ [$^{\circ}\text{C}$] of the external and internal sides of the considered window constructions. Comparing these figures with Fig. 4, it may be observed that the surface temperatures depend on the outside air temperature and the solar irradiation.

In pictures 5–7, the dew point temperature which corresponds to the value of $\theta_{dp} = 9.26^{\circ}\text{C}$ is highlighted. This value is specified in the Slovak standard STN 73 0540-2. It determines that the dew point occurs when the temperature of internal air is $\theta_{ai} = 20^{\circ}\text{C}$ and humidity is $\varphi_{ai} = 50\%$ for all fragments of the window i.e. for frames, and translucent and lightproof panels. Internal surface temperatures for all of the windows in the glazing (in close contact with the rail frieze) fall below this value.

During the research, some pictures using the infrared camera were taken at the end of January 2014, i.e. in the winter period. To avoid the contamination of the data by sunlight,

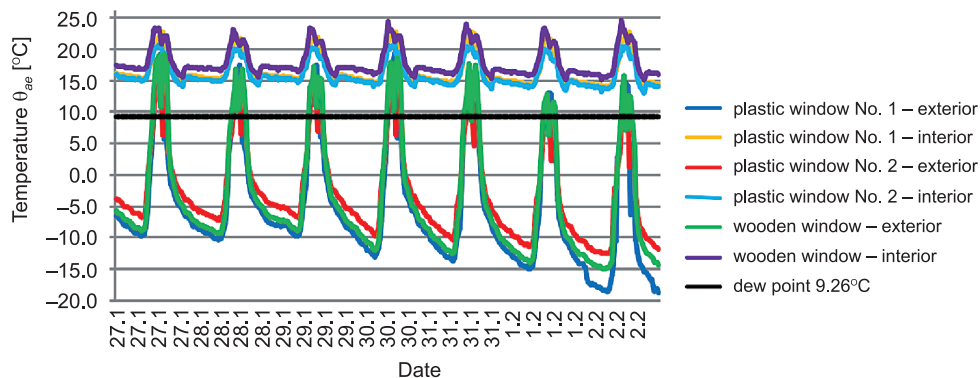


Fig. 5. The shape of the surface temperatures $\theta_{si,w}$ [°C] from the external and internal side of the window constructions, in the middle of glazing

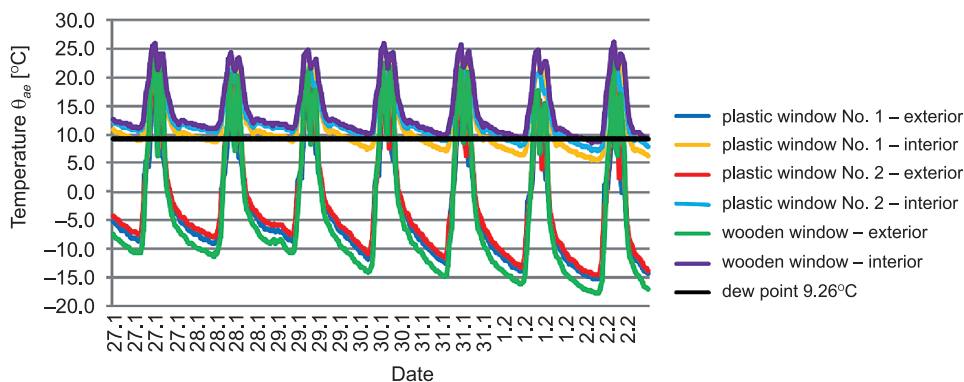


Fig. 6. Surface temperature curves $\theta_{si,w}$ [°C] from the external and internal sides of the window constructions on the glazing in close contact with the rail frieze

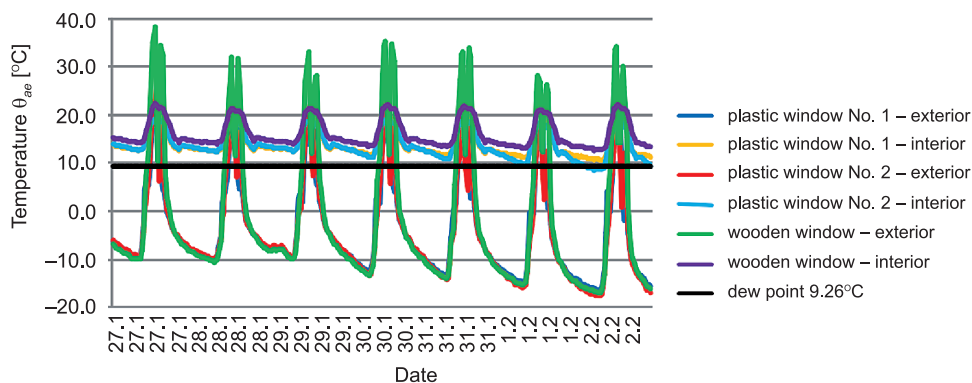


Fig. 7. Surface temperature curves $\theta_{si,w}$ [°C] from the external and internal side of the window constructions on the rail frieze

thermographic diagnostics was taken during the night. According to the pictures, it is obvious that the critical points of the windows are the points of contact between the window and the wall and also the points of contact of the glazing with the rail frieze.

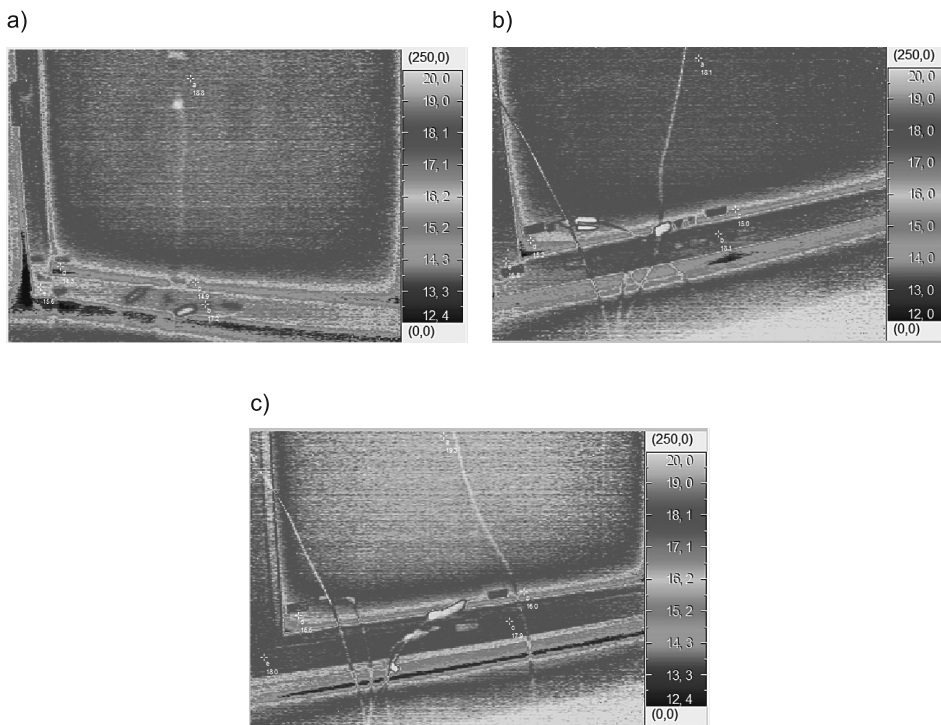


Fig. 8. Pictures of window constructions from infrared camera: a) plastic window without thermal modules; b) plastic window with thermal modules; c) wooden window

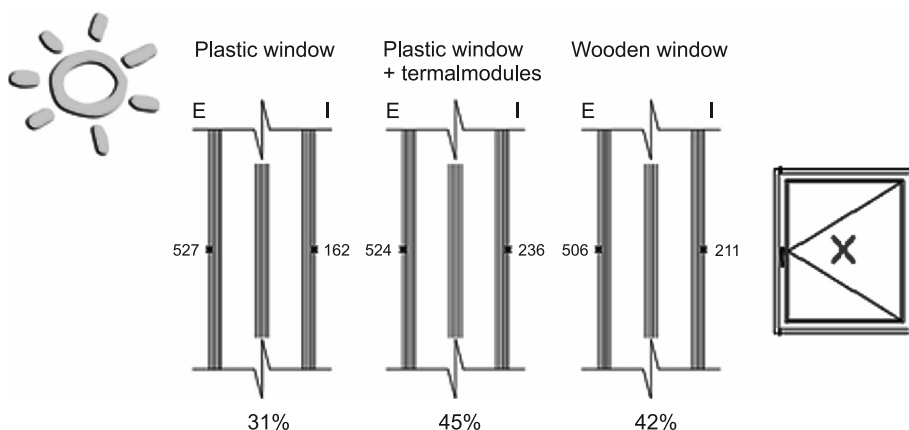


Fig. 9. Measured values of solar transmittance permeability

Solar radiation transmittance was measured on samples of window constructions through the use of a pyranometer. The measurement was taken at 12²⁰ (at the end of October 2013) under a bright sunny sky. The pyranometer was placed in the centre of each glazing sheet. From the measured values, it is obvious that a transmittance of solar radiation above 50% was not reached by any window. Comparing the declared values with the measurement shows that the measured values were lower. These values are identical with a permissible deviation of 5–10%. This deviation could be attributed to fouling of the window panes.

3. Conclusions

As a result of the evaluation of measured values, we can conclude that the internal surface temperatures depend on the outside air temperature and on solar irradiation. Decreases of internal surface temperatures in places on the lower edge of the glazing occurred in all windows during the considered period as a result of extremely low temperatures. These temperatures decreased below the dew point temperature, while in the middle of glazing there was no occurrence of temperatures below 13.5°C. The lowest average surface temperature was registered on the glazing in the immediate vicinity of contact with the lower edge of the frieze rail at each window. For these constructions it's known that the bottoms of window rails are more prone to the condensation of water vapour than the rest of the window construction and the measurements confirmed the occurrence of thermal bridges in these places, which became significantly evident by the occurrence of external temperatures below –15°C. The inner surface temperature dropped below the dew point on all of the windows. It is possible that the value of the temperature at this point is caused by the thermal bridge. Distance profiles of isolating glazing and the depth of fixing of the glazing into the frame frieze have the significant impact on genesis of such thermal bridges. It is visible, that the quality of triple glazing did not remove the problem with temperature by the extreme freeze. On the other hand, the triple glazing caused the elimination of the effects of cold radiation (average temperatures in the middle of the glazing were from 15.9 to 17.9°C) by the normal external temperatures in area of glazing. It is important that window constructions eliminate the cold radiation (especially during the heating and the transitional period) in these critical places. In conclusion, the wooden window, which is provided with the heat optimized distance frame, achieves the best values of measurement during all the measured periods. The surprising finding was the curve of internal surface temperatures compared to plastic windows in place of the lower frieze of window. The internal surfaces of windows were more undercooled at frieze of rail for window with thermal modules (in average of 0.3°C, but at maximum up to 3°C) during extreme temperatures of the external air.

Pictures taken through the infrared camera show the critical positions of window constructions. The measured values of thermographic diagnostics were few different from the values measured using thermocouples in a period. It was confirmed again that the weakest points of these constructions are the glazing margins.

The permeability of solar radiation in all of the window constructions was under 50%. These values are consistent with the deviation of 5–10% compared to the declared values from the producer. This deviation can be attributed to the pollution of windowpanes. But

when we compare particular samples together, it is visible that the highest solar gains were measured in the case of the plastic window. The filling between glasses is krypton.

Internal surface temperatures during the heating period were significantly higher than the external surface temperatures. This shows the high-quality materials used for window constructions. They are able to capture the excessive heat from solar radiation and they are able to eliminate the coldness from exterior, too. The comfort of internal environment in the most problematic point of window construction is maintained.

During measurements, the temperature and relative humidity in the chamber were at a constant level. It is to say that parameters of the internal environment were maintained with air conditioner. The hot air from air conditioner does not affect the windows. Window constructions were not influenced by the flow of hot air from the radiators.

The presented results were obtained with the support of grant project VEGA no. 1/0729/13.

References

- [1] Ďuriniková M., Ďurica P., *The evaluation of temperature parameters in selected windows during the whole year*, 17th International Conference “Thermal protection of buildings 2013”, Vysoké Tatry – Štrbské Pleso, 16–17 May 2013, 81-84.
- [2] Ďurica P., Ďuriniková M., Rybárik J., Štaffenová D., *Long time testing of temperature parameters in selected windows*, International Conference Advanced Building Construction and Materials, Kočovce, 26–27 September 2013, 81-84.
- [3] Bielek M., *Building and Energy*, Vidas, Banská Bystrica 1995.
- [4] Ballast D.K., *Architect's Handbook of Construction Detailing*, John Wiley & Sons, New Jersey 2009.
- [5] Humm O., *Niedrge Energie Häuser*, Verlag, Praha 1997.
- [6] STN 730540:2012. Thermal properties of building structures and buildings. Thermal protection of buildings. Parts 1, 2, 3, Slovak Standards Institute, Bratislava 2012.

PAVOL ĎURICA*, MARIANNA ŠUŠTIAKOVÁ*, RADOSLAV PONECHAL*,
JÁN RYBÁRIK*

MEASURED AND SIMULATED PARAMETERS OF WOODEN LIGHTWEIGHT EXTERNAL WALLS

POMIAROWE ORAZ SYMULACYJNE PARAMETRY LEKKICH DREWNIANYCH ŚCIAN ZEWNĘTRZNYCH

Abstract

The partial knowledge of the area of thermo-technical properties of wooden lightweight external walls is presented in this article. The distribution of temperatures inside the structure during a typical winter week is described as observed on samples of walls built in a chamber pavilion type. What is compared is the thermal performance variant of sandwich construction walls obtained on the basis of calculations, measurements and simulations.

Keywords: long time testing measurements, wooden lightweight external walls, temperatures, simulations

Streszczenie

W artykule przedstawiono częściowy zakres wiedzy na temat właściwości cieplno-technicznych drewnianych lekkich ścian zewnętrznych. Rozkład temperatury wewnątrz struktury podczas typowego zimowego tygodnia został opisany i obserwowany dla próbek ścian w komorze typu pawilon. Na podstawie obliczeń, pomiarów oraz symulacji dokonano porównania właściwości termicznych ściany warstwowej.

Słowa kluczowe: badania długotrwałe, drewniane lekkie ściany zewnętrzne, temperatura, symulacje

* Doc. Eng. Pavol Ďurica, C.Sc. Eng. Marianna Šuštiaková, Eng. Radoslav Ponechal, Doc. Ph.D. Eng. Ján Rybárik, Department of Building Engineering and Urban Planning, Faculty of Civil Engineering, University of Žilina.

1. Introduction

Temperature measurements were taken of the lightweight-construction of the external wall, which was made of three different material solutions and three different colored exterior side surfaces. Temperatures flow patterns were developed on the basis of temperature measurements taken of a sample of the wall built in a climate chamber in the laboratory pavilion type centre KPSU FCE ŽUŽ (KPSU – Department of Building Constructions and Urban Planning, FCE – Faculty of Civil Engineering, ŽUŽ – University of Žilina). Its facade was oriented to the south with a rotation of 17° to the west. The dimensions of the monitored experimental walls were 3670×2670 mm and they comprised five fields (Fig. 1). The walls differ in material composition and surface color. The first, second, fourth and fifth fields constituted diffusion sealed constructions while the third field represented a diffusion open construction. The composition of the wall from the interior toward the exterior was as follows: OSB, PE film (except for the third field), infill insulation, exterior Hofatex insulation, and a thin coating plaster. Temperatures were recorded at 30 minute intervals in areas: in a fragment of the external wall on the outer surface of the structure, under the plaster, under an additional thermal insulation, and under the infill thermal insulation (Fig. 2). Indoor air temperature was kept 20°C and the chamber's relative humidity was kept at 50%. The sample was being exposed to actual external climate conditions from the outside. Indoor climate parameters, relative humidity and indoor air temperature were maintained by an air handling unit.

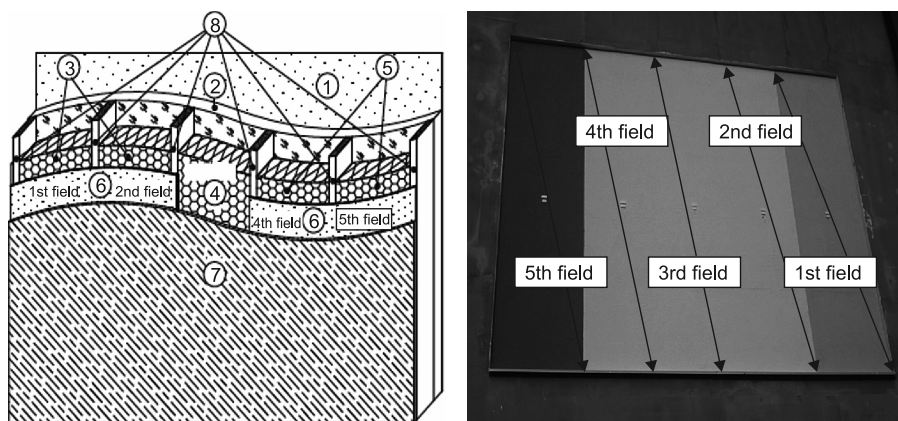


Fig. 1. Left: external plaster/4 mm; 2– woodfiber board/100 mm; 3 – Stone wool insulation/220 mm; 4 – Hemp insulation/220 mm; 5 – Mineral wool insulation/220 mm; 6 – vapor layer/0,2 mm; 7 – OSB/12mm; 8 – wood column/60×220 mm, from left to right 1st, 2nd, 3rd, 4th, 5th field, right external view of climate chamber in the laboratory center pavilion type

The sensors were placed in the middle of the field. The temperature flow pattern in the lightweight-construction of the external wall were observed for one week of the cold period between January 27th and February 2nd 2012 ($\theta_{ae, \min} = -18.9^\circ\text{C}$, $\theta_{ae, \max} = 4.6^\circ\text{C}$).

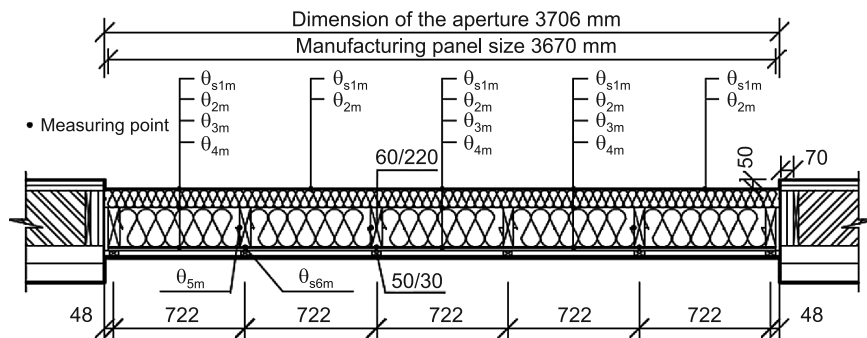


Fig. 2. Diagram of the observed temperatures: θ – temperature ($^{\circ}\text{C}$), s – surface, m – measured temperature, 1 – external plaster, 2 – lower plaster, 3 – lower thermal insulation, 4 – lower infill thermal insulation, 5 – middle of column, 6 – inner surface column 2

Different temperature patterns in the construction (Figs. 4–6) were not only influenced by its different material compositions, but also by the natural effects of its environment and the different light absorption and reflectance attributable to surface treatment. The highest temperatures were measured, as expected, on the grey-colored surface finish exhibiting the lowest (34%) reflectance of solar radiation that absorbs most light radiation, while examining the temperature on the surface of the structure. The third field with a diffusion open structure has the lowest surface temperature at the time of exposure to the sun when compared to the white-finish fields. This had been caused by the diffusion flux of water vapor, which increases the specific heat of layers and, therefore, necessitated the addition of more heat to raise the temperature of the material. The surface temperature of the wall dropped below the ambient temperature in all the fields at night during the period. At that time, minimum temperatures were recorded mostly in the fourth white-finish field (which had the reflectance of solar radiation of almost 100%), and the first yellow-finish field (at 61% reflectance of solar radiation).

2. Thermal simulations

ESP-R software was used for thermal simulation. The simulated model reproduces reality in a research lab. Its facade is oriented to the south with a rotation of 17° to the west. The internal temperature was set according to the measured temperature values of the interior. A test reference year from the IWEC (International Weather for Energy Calculations) Ostrava database was used to simulate the thermo physical processes present in construction. A day with nearly the same conditions as those measured had been chosen from the IWEC database because of the possibility for comparing the simulated temperature patterns in the winter with the experimental measurements. Measured outside air temperatures were used in the simulations instead of those from the database.

The temperatures inside the layers of each field have been documented as the results. On the basis of the simulation results of the heat flux, the heat flow path coefficients

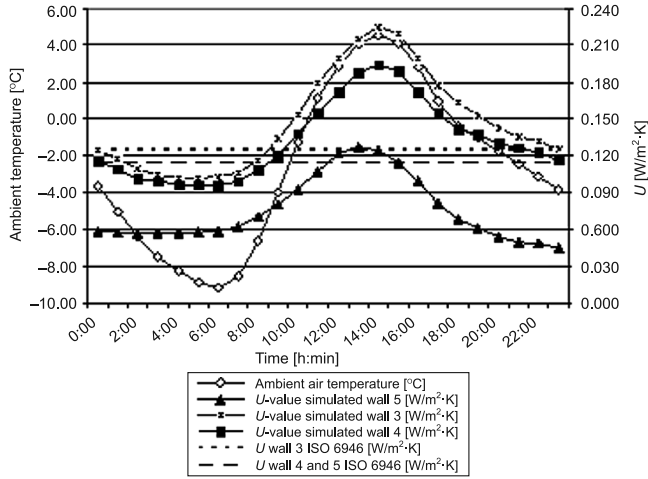


Fig. 3. Ambient temperature and U -value patterns obtained from simulation

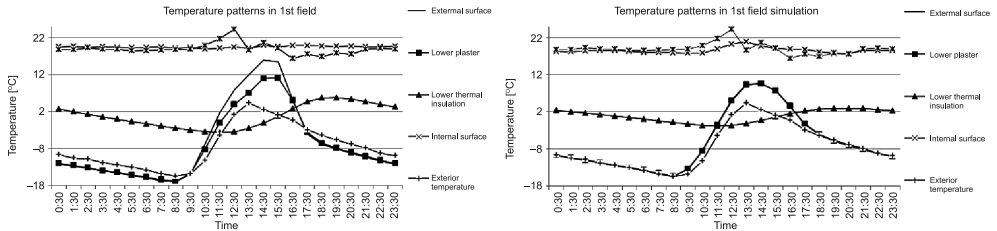


Fig. 4. Temperatures of the construction measured (on the left) and simulated (on the right) on 30th January, 2012

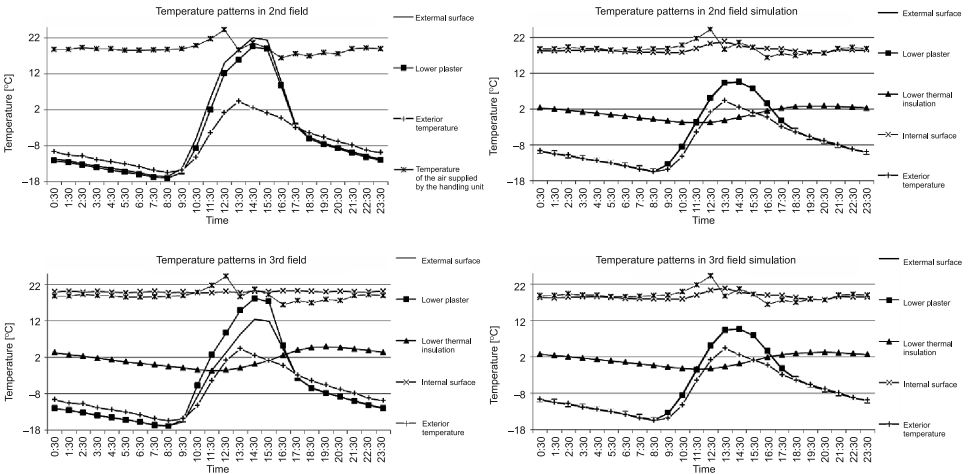


Fig. 5. Temperatures of the construction measured (on the left) and simulated (on the right) on 30th January, 2012

were determined for the different fields of the outer wall (Fig. 3). U -value patterns of the temperature cross-sectional structures (Fig. 4–6) display a significant effect of solar radiation absorption relative to heat flow and temperature in the reported structure.

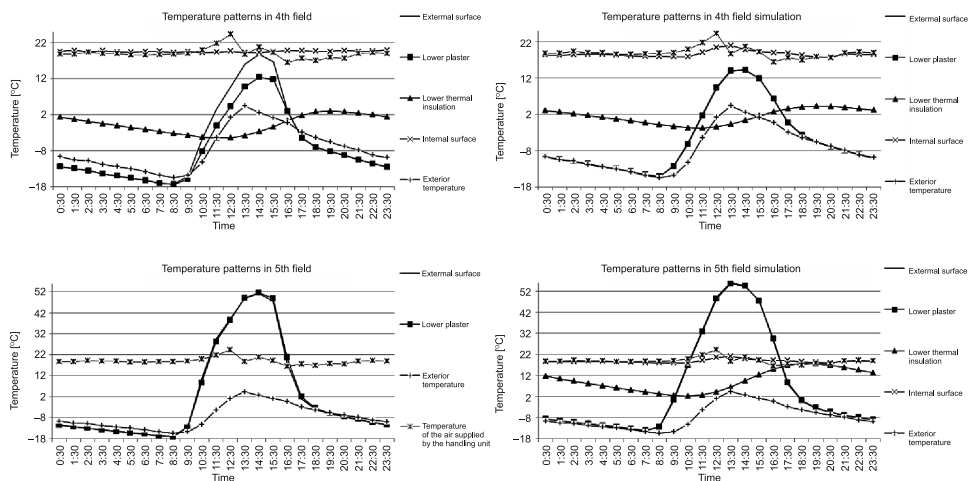


Fig. 6. Temperatures of the construction measured (on the left) and simulated (on the right) on 30th January, 2012

3. Conclusions

The difference between outside temperature and that under the plaster was higher in reality than in the simulation. Surface temperatures were, with the exception of the third field, higher than outside temperatures. The path of temperatures in the layers of the third field is affected by the diffusion of water vapor, which increases the thermal conductivity of the material. The energy of sunlight is, therefore, passed on to the construction faster. The measured temperature of external surfaces fell below the outside air temperature at night, unlike in the simulation, which had not taken into account the impact of negative radiation of the night sky. Temperatures of the inner surface of the structure per measurements were more stable as shown by the calculations in the simulation. The calculation of heat transfer coefficients showed highly variable non-stationary progressions, which were significantly different from the stationary standard values (Fig. 3, Table 1). Surprisingly, apparent opposite progressions of U -values are recorded at midday which confirms the findings in [4], and [5] as listed in the reference section of this paper.

Table 1

The material characteristic and U-values of each field in stationary conditions

Material (1st and 2nd fields)	Description	d	λ	ρ	c	μ	R	
		[m]	[W/ (m×K)]	[kg/m ³]	[J/(kg×K)]	[-]	[m ² ×K/W]	
External plaster	StoSilco	0.004	0.7	1900	720	40	0.01	
Woodfiber board	HofaTexSysThem	0.1	0.045	210	2100	5	2.22	
Stone wool insulation	Rockwool MWW	0.22	0.037	40	840	1	5.95	
Vapor layer	Isover Vario KM Duplex	4.00E-05	1	2000	–	90000	0.00	
							$U = 0.120$ [W/(m ² ×K)]	
Material (3rd field)	Description	d	λ	ρ	c	μ	R	
		[m]	[W/ (m×K)]	[kg/m ³]	[J/(kg×K)]	[-]	[m ² ×K/W]	
External plaster	StoSilco	0.004	0.7	1900	720	40	0.01	
Woodfiber board	HofaTexSysThem	0.1	0.045	210	2100	5	2.22	
Hemp insulation	Cannabest Plus	0.22	0.04	36	1200	1.9	5.50	
							$U = 0.127$ [W/(m ² ×K)]	
Material (4th and 5th fields)	Description	d	λ	ρ	c	μ	R	
		[m]	[W/ (m×K)]	[kg/m ³]	[J/(kg×K)]	[-]	[m ² ×K/W]	
External plaster	StoSilco	0.004	0.7	1900	720	40	0.01	
Woodfiber board	HofaTexSysThem	0.1	0.045	210	2100	5	2.22	
Mineral wool insulation	Isover ENV	0.22	0.035	24	840	1	6.29	
Vapor layer	Isover Vario KM Duplex	4.00E-05	1	2000	–	90000	0.00	
							$U = 0.115$ [W/(m ² ×K)]	

The presented results were obtained with the support of European Regional Development Fund grant projects and the “Research Centre of the University of Žilina” Slovak state budget projects, ITMS 26220220183 and VEGA no. 1/0729/13.

References

- [1] Chmúrny I., *Teplná ochrana budov*, Jaga Group, Bratislava 2003.
- [2] Amandine Piot and col., *Experimental wooden frame house for the validation of whole building heat and moisture transfer numerical models*, Energy and Buildings, Vol. 43(6), 2011, 1322-1328, <http://www.sciencedirect.com/science/article/pii/S037877881100017X> – 3.02.2014.
- [3] Asan H., *Numerical computation of time lags and decrement factor for different building materials*, <http://amet-me.mnsu.edu/userfiles/shared/solarwall/Solar%20Passive%20%28Trombe%29%20Wall%20Documents/Technical%20Publications/Numerical%20computation%20of%20time%20lags%20and%20decrement%20factors%20for%20different%20building%20materials.pdf> – 4.11.2013.
- [4] Anderson B.R., *Conventions for U-Value Calculations*, IHS – BRE Press, 2006, 2 edition.
- [5] Anderson B.R., *The measurement of U-values on site*, <http://web.ornl.gov/sci/buildings/2012/1985%20B3%20papers/001.pdf> – 4.11.2013.
- [6] Štúňová M., Ďurica P., *The course of temperatures in construction of lightweight external wall in stationary conditions of the internal environment and the actual conditions of outdoor climate*, Conference TRANSCOM Žilina, Slovak Republic, 2013.
- [7] STN 730540:2012 Thermal properties of building structures and buildings, Thermal protection of buildings, Parts 1, 2, 3, Slovak Standards Institute, Bratislava 2012.

JOLANTA FIEDUCIK*, JAN GODLEWSKI**

THE LOW ENERGY HOUSE USING AN AIR SOLAR COLLECTOR – A CASE STUDY

DOM ENERGOOSZCZĘDNY WYKORZYSTUJĄCY SŁONECZNE KOLEKTORY POWIETRZNE – STUDIUM PRZYPADKU

Abstract

The main aim of this paper is to present the prospect of heating and cooling a house using solar air collectors. An analysis made of an energy-efficient house, for which the energy requirements for heating shall not exceed 40 kWh/m²/a. The calculations used air collectors with an area of 60 m² and performance efficiency of 70%, which are available commercially. In the analyzed building the solar heating system provides almost full coverage of energy needs throughout the year, with a small shortfall occurring in December and January. The above-mentioned deficits at the beginning and end of the year can be supplemented with other alternative energy sources.

Keywords: low energy house, solar air collector, heating and cooling system in buildings

Streszczenie

Celem tego artykułu jest przedstawienie możliwości ogrzewania i chłodzenia domu jednorodzinnego przy wykorzystaniu słonecznych kolektorów powietrznych. W analizie uwzględniono dom energooszczędny, którego wskaźnik sezonowego zapotrzebowania na ciepło wynosi 40 kWh/m²/a. Do obliczeń przyjęto kolektory powietrzne dostępne na rynku o powierzchni 60 m² i wydajności wynoszącej 70%. W analizowanym budynku występuje prawie pełne pokrycie potrzeb na energię grzewczą w ciągu roku z powietrznych kolektorów słonecznych, oprócz niewielkich braków w tym względzie występujących w grudniu i styczniu. Wspomniane w tym przypadku pewne braki ciepła w końcu i na początku roku można uzupełnić z innych alternatywnych źródeł ciepła.

Słowa kluczowe: dom energooszczędny, słoneczne kolektory powietrzne, system grzania i chłodzenia w budynkach

* Ph.D. Jolanta Fieducik, Faculty of Technical Sciences, University of Warmia and Mazury in Olsztyn.

** Ph.D. Jan Godlewski, Faculty of Applied Physics and Mathematics, Gdańsk University of Technology.

1. Introduction

The use of solar energy for heating and other energy-producing purposes is becoming more and more of a topical issue as the supply of fossil fuels diminishes [3, 4]. This is especially important for small buildings which take up enough space, that the solar energy that reaches them would, in theory, be sufficient to cover the building's full energy needs. A single family house is such an example. The aim of providing the energy from solar supplies can be realized in various ways [1–4]. The goal of this article is to analyze the possibility of using solar collectors to obtain the thermal energy to heat a low energy house throughout the whole year. Additionally, an analysis regarding using the collectors to cool the building is included in the article. The analysis is carried out using the climatic conditions of the city of Olsztyn and commercially available air collectors as an example. As part of the evaluation the energy balancing task is to be carried out without giving any particulars of the control systems used during the utilization of the building.

2. The construction and parameters of air collectors

In air collectors, the solar energy passes into the absorber, in which the air is heated. Solar collectors can be uncovered, in which the solar energy hits the absorber directly, or covered, in which the absorber is covered by a transparent screen. Depending on the construction of the collector, the air stream can either flow over or under the absorber, and in more advanced constructions, over and under or through the absorber. In the collector, the air stream flows

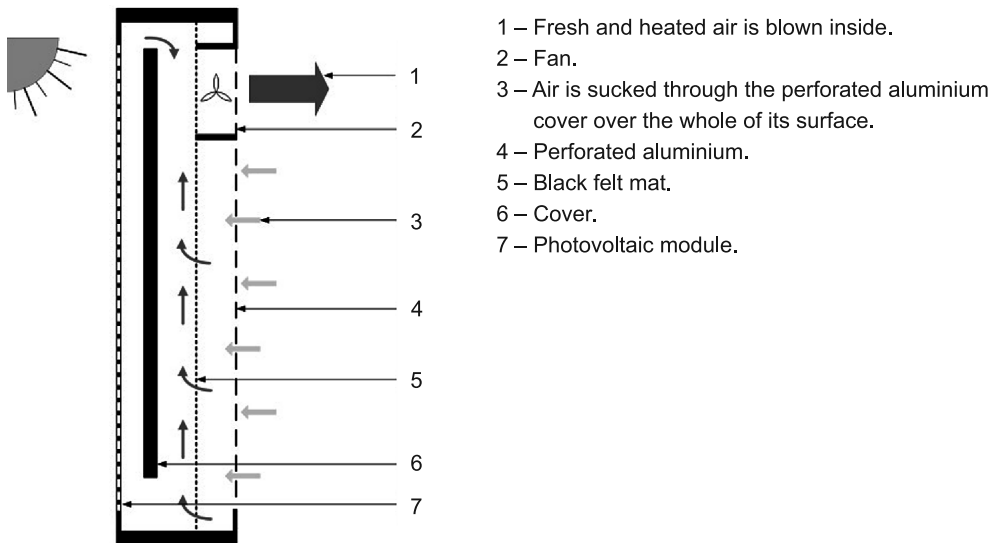


Fig. 1. A diagram and the working principles of an air collector

through specially shaped channels. The channels can have a rectangular, triangular or oval cross-section. The absorber can be flat, or it can be bumpy or porous, which highly increases the surface area and efficiency of the heat exchange between the absorber and the passing air. A diagram of an air collector is shown in Fig. 1.

Air collectors are characterized by both a very efficient rate of exchange from solar to thermal energy [1–5], and the fact that the working element is air. In temperatures typical for the Earth's climate, air does not undergo changes of state, so the use of air collectors is not hindered by difficulties related to temperature changes. Additionally, air heated in collectors can be used directly to heat the building, without the use of any intermediary systems. The use of the air flowing through the collector can also provide very good ventilation of the heated space. An undeniable advantage of air collectors is the ease with which the air stream can be controlled and the thermodynamic space monitored, and also the speed with which the temperature can be changed. A diagram of a collector produced by SolarVenti is shown in Fig. 2.

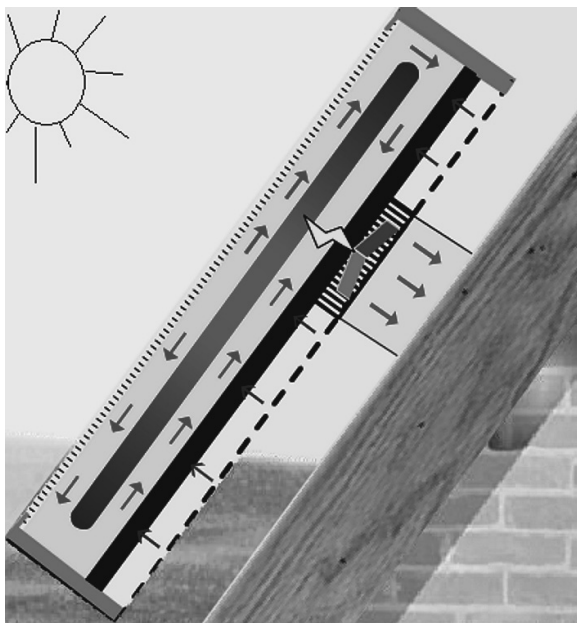


Fig. 2. A working diagram of a SolarVenti air collector during a heating cycle [7]

One disadvantage of air collectors is that, if changing the working element from air to any liquid, to heat a house or any other building, the heat exchanger needs to be more complicated than in the case of a liquid-liquid exchange [2]. There is a variety of manufacturers of air collectors of various types and purposes. Table 1 below presents the technical parameters of a typical air collector produced by SolarVenti.

Specifications of the SolarVenti SV30X [6] air collector

Air manifold surface area	3 [m ²]
Maximum air flow	200 [m ³]
Total time to exchange all air in the room	2 [hours]
Efficiency	70 [%]
Average energy production	2100 [kWh/year*]
Increase in temperature in the intake manifold, in relation to the outside temperature	c. 40 [°C] (eg. from 10 [°C] to 50 [°C])
Manifold dimensions in mm: length x width x depth	3000 × 1020 × 75 [mm]
Solar PV power	38 [Watt]
Fan power	5.1 [Watt]
Weight (panel)	22.5 [kg]
Maintenance-free period	Up to 15 [years]
Product warranty	5 [years]
Collector housing	Aluminum
Cover (transparent)	Polycarbonate
Can also be used as a cooling system	Yes

* the value given is for Danish atmospheric conditions

3. Energy conditions

As indicated in the subject of this thesis, there will be an analysis of the energy conditions related to the demand for thermal energy for heating purposes in a single family house, under the assumption that the area of the house is 150 m², while the dimensions of the house at its base are 10x10m. The demand for heat in the house is 40 kWh/m²/a in accordance with the NF40 standard. For the purpose of this analysis it has been assumed that the roof is at a 45 degree slope, and that one side of the roof has an area of 60 m² and is completely covered in solar collectors. Based on the meteorological data for the city of Olsztyn, using the program GetSolar Professional [5], for each month the following values of solar energy per square metre of the collector are obtained (labelled radiation – column 2, Table 2). Other figures are also given in Table 2 which are necessary for the calculations.

As has been assumed previously, the radiation energy hits an array of collectors with a surface area of 60 m². For the calculations the demand for thermal energy for a 150 m² house has been set at the rate of 6000 kWh/year, in accordance with regulations for a low

energy house. From Table 2 and Fig. 3 it can be seen that for the house parameters specified above and a collector array of 60 m², there is a surplus of heat, especially during the summer. Heat deficits only exist for two months in winter, specifically November and January. During the months in which there is an explicit energy surplus, the total value of this surplus is approximately 40 000 kWh. Relatively speaking, the deficit during the winter months is small – 771 kWh. The energy missing during the winter months could be covered by other sources of energy, if energy is not stored. In [8] it has been shown that the energy necessary to heat the house during the winter can easily be stored during the summer.

Table 2

The energy balance for solar energy obtained from the sun and energy necessary for heating purposes for a single family house on a month-by-month basis

Month	Radiation per [m ²] of the collector	Energy necessary to heat a 150 [m ²] NF 40 standard house	Total radiation on a 60 [m ²] collector	Solar gain from a 60 [m ²] collector – efficiency 70%	Surplus or deficit of energy from a 60 [m ²] collector
1	2	3	4	5	6
	[kWh/m ²]	[kWh]	[kWh]	[kWh]	[kWh]
January	24.4	1310	1464	1025	-285
February	37.2	886	2232	1562	+677
March	77.9	700	4674	3272	+2572
April	119	379	7140	4998	+4619
May	152	184	9120	6384	+6200
June	165	45	9900	6930	+6885
July	168	0	10080	7056	+7056
August	144	13	8640	6048	+6035
September	100	160	6000	4200	+4040
October	61.6	532	3696	2587	+2055
November	25.6	575	1536	1075	+500
December	17.4	1217	1044	731	-486
Total	1092	6000	65526	45868	39868

The table has been created using data from the program GetSolar, for Olsztyn – latitude 53.5 and longitude 20.3. The results are presented in graphical form in Fig. 3.

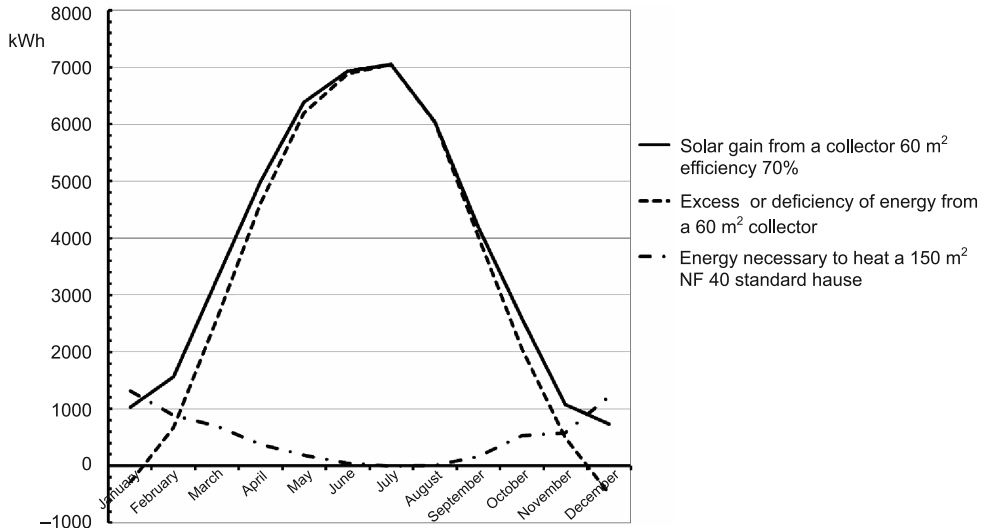


Fig. 3. Energy balance obtained from collectors and the energy necessary to heat the house

4. Using sun collectors for cooling purposes

Sun collectors also have, if in a limited scope, the ability to cool buildings. Certain types of collectors have specially adapted streaming systems that can be used for a cooling effect. Obtaining a cooling effect, however, requires that the whole building has been specially

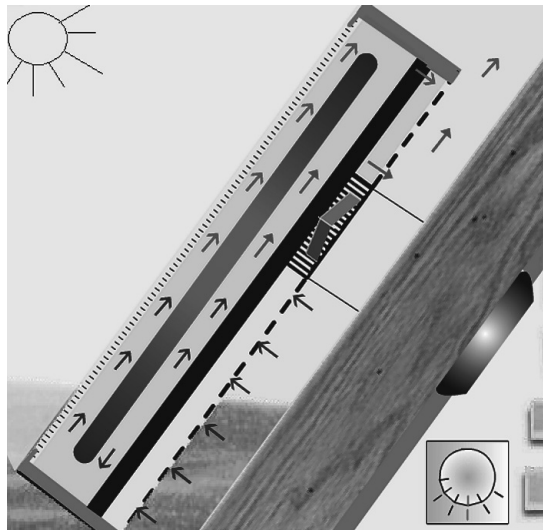


Fig. 4. A working diagram of a SolarVenti sun collector during a cooling cycle [7]

adapted for that purpose. In the case of a single family house, the part of the building that is exposed to sunlight should be covered in air collectors, and the rest of the building's surface should be made of a material that significantly reflects electromagnetic radiation of different wavelengths (for example metal foil). The heated air should be sucked away from the part of the building exposed to sunlight, or else kept for storing heat. This would result in a temperature only a couple of degrees higher than that of the ground – approximately 20 Celsius degrees. Cooling with the use of a collector is a relatively cheap method, though, this cooling system would not be sufficient in hot climates. In such conditions, a more sophisticated cooling system based on sun collectors should be used. Such systems have been described in [2]. A diagram of a SolarVenti collector is presented in Fig. 4.

5. Conclusions

New potential uses of solar air collectors have been introduced. Due to the simple construction, relative cheapness and the fact that the working element is air, these collectors are excellent for heating and cooling houses in temperate climates. Air collectors can also be used for the ventilation of buildings, which is an important consideration in low energy architecture. The use of sun collectors for heating, cooling and ventilation purposes should be accounted for when the building is being designed.

References

- [1] Kalogirou S.A., *Solar thermal collectors and applications*, Progress in Energy and Combustion Science 30, 2004, 231-295.
- [2] Kim D.S., Infante Ferreira C.A., *Solar refrigeration options – a state – of-the-art review*, International Journal of Refrigeration, 31, 2008, 3-15.
- [3] Smolec W., *Fototermiczna konwersja energii słonecznej*, PWN, Warszawa 2000.
- [4] Timilsina G.R., Kurdgelashvili L. Narbel P.A., *A review of solar energy; Markets, economics and policies*, Policy Research Working Paper 5845, Soc. Sci. Res. Netw., 2011, 49 pages.
- [5] GetSolar software author: Dipl.-Ing Markus Maier. version 10.1.1. 21.12.2009.
- [6] <http://www.ventilacionsolarcanarias.com>
- [7] <http://www.galileaenergy.com/kolektory-powietrzne-systemy-solar-venti.php>
- [8] Fieducik J., Godlewski J., *Storing thermal energy from solar collectors for the needs of a detached house*, Polish Journal of Environment Studies, 2014 (in print).

SZYMON FIRLAĞ*

PRE-WAR PUBLIC UTILITY BUILDINGS – RESULTS OF SURVEYS

PRZEDWOJENNE BUDYNKI UŻYTECZNOŚCI PUBLICZNEJ – WYNIKI BADAŃ

Abstract

The paper summarizes the results of surveys conducted in three pre-war public utility buildings: a children's home, a forensic medicine department and a nursing home. The study examined the indoor air quality, airtightness, ventilation efficiency and thermal insulation of building envelope. The buildings were surveyed before, during or after modernization works were undertaken.

Keywords: revitalization, public utility buildings, quality of the indoor environment

Streszczenie

W artykule przedstawiono wyniki badań przeprowadzonych w trzech przedwojennych budynkach użyteczności publicznej: domu dziecka, zakładzie medycyny sądowej i domu opieki społecznej. Przedmiotem badań były parametry powietrza wewnętrznego, szczelność powietrzna, efektywność systemu wentylacji oraz izolacyjność cieplna przegród. Badane budynki były przed, w trakcie lub po pracach modernizacyjnych.

Słowa kluczowe: rewitalizacja, budynki użyteczności publicznej, jakość środowiska wewnętrznego

* Ph.D. Eng. Szymon Firląg, Institute of Building Engineering, Faculty of Civil Engineering, Warsaw University of Technology.

1. Introduction

Many pre-war public utility buildings require modernization or renovation. These processes are complicated and expensive. They are usually performed in order to reduce energy consumption, to change the use of a building or to meet current technical and construction standards. Unfortunately, we very often omit to check the efficiency of these measures or to make a careful assessment of the benefits of the status quo. Consequently, the results of such works can prove to be worse than anticipated and internal environmental quality conditions can decrease.

2. Children's Home

The first study was conducted at a children's home located in Otwock. It is a three-storey building from 1930s with basement. The walls are of full brick construction, and the ceilings are made from reinforced concrete. In the 80s, an additional wooden storey was added with a mansard roof, covered with metal sheeting. The building was last renovated in 2005. This work saw external walls and the flat roof insulated, windows replaced and the heating and hot water system modernized. Thermographic measurements were taken to verify the quality of the works carried out. These readings were taken inside and outside the building. Measurements were also taken of indoor and outdoor air conditions – notably relative humidity and temperature. Research focussed on the following spaces: the ground floor dining room, the first floor lounge, and the second floor lounge and bathroom. The measurements were carried out between 11:00 on 02/13/2013 to 13:00 on 02/14/2013 (26 hours – at 1 minute measurement steps).

Table 1

Building envelope before and after renovation

	<i>U</i> -value before [W/m ² K]	<i>U</i> -value after [W/m ² K]
External walls	1.05	0.34
Flat roof	0.58	0.24
Windows	2.6	1.3
Doors	2.5	2.5
Floor	1.07	1.07

External wall insulation had a positive effect in terms of increasing internal surface temperatures. The lowest temperature measured in one corner on the first floor was 19.5°C (where the internal air temperature was about 23°C). Unfortunately the renovation works had no discernible effect on the second floor. Figure 1 clearly shows a significant decrease in surface temperature in the corner and also under a computer table in the computer room on the second floor. The temperatures were recorded as 11.9°C and 10.2°C respectively, with an internal air temperature of about 20°C. Such a situation presents the risk of mould growth – where the surface temperature falls below 12.7°C (at 20°C and with 50% relative air humidity).

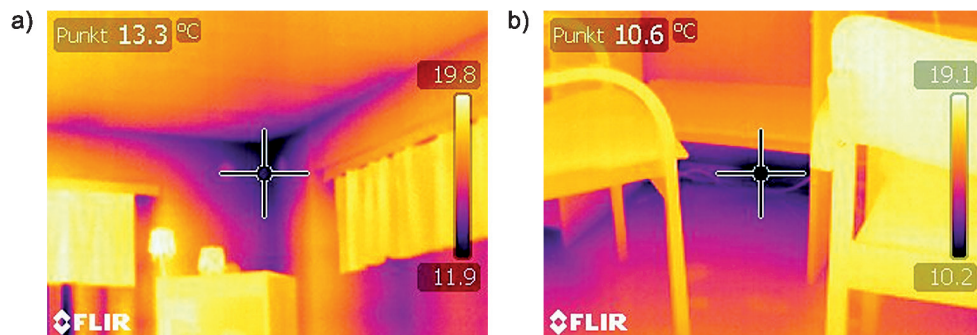


Fig. 1. The computer room on the second floor: a) the corner – at the juncture of the external wall and the second floor ceiling, b) under the computer table – at the juncture of the external wall and second level flooring

The temperature of the external wall surface was $4,5^{\circ}\text{C}$ (Fig. 2a.) when the outside air temperature was 0°C . The 4.5 K difference illustrates that the thermal insulation of the walls could be improved. The U-value following renovation was $0.34 \text{ W/m}^2\text{K}$, but according to current regulations it should be no higher than $0.25 \text{ W/m}^2\text{K}$. Figure 2a and 2b also show there to be a lack of insulation around window openings, on the basement walls and in the thermal bridge caused by the eaves. The readings have confirmed a reduction of heat loss through the building facade but at the same time have allowed for construction errors to be identified. The insulation is not contiguous which allows thermal bridges to form. The most significant error is that the second floor mansard roof is insufficiently insulated. As a result, heat loss on the second floor is much greater than elsewhere. In such a situation, the interior air and internal surface temperatures decrease. In addition, mould can grow or condensation and rising damp can occur.

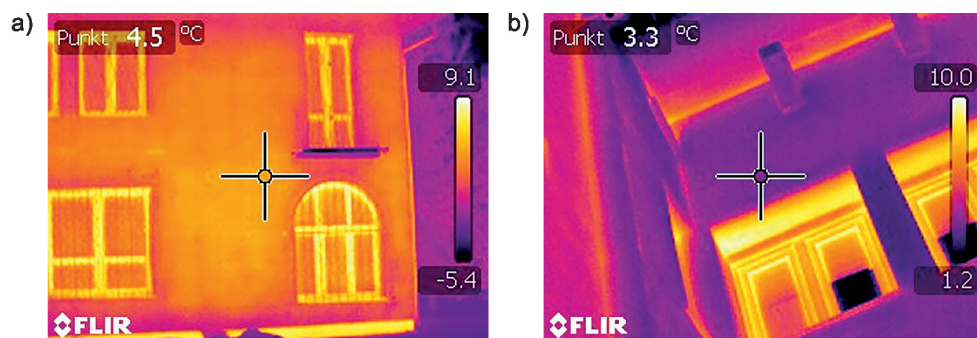


Fig. 2. Termogram of: a) external wall, b) windows openings

Indoor air parameters were checked in relation to the PN-78/B-03421 [1] requirements for winter and low-scale physical activity: namely for optimum and acceptable temperature ranges ($20,0\text{--}22,0^{\circ}\text{C}$), for optimum humidity ranges (40–60%), and for acceptable humidity ranges (30–60%). Readings taken in selected rooms were as follows:

- ground floor dining room, temperature range of 23.2–26.8°C, relative humidity range 22.2–32.7% – excessively high temperatures for 100% of the time, excessively low humidity for 81% of the time, acceptable humidity for 9% of the time;
- first floor lounge, temperature range of 23.4–25.5°C, relative humidity range 23.4–29.6% – excessively high temperatures for 100% of the time, excessively low humidity for 100% of the time;
- second floor bathroom, temperature range of 19.6–21.7°C, relative humidity range 44.5–64.8% – optimum temperatures for 91% of the time, excessively low temperatures for 9% of the time, optimum humidity for 88% of the time, excessively high humidity for 12% of the time;
- second floor lounge, temperature range of 20.2–22.9°C, relative humidity range of 39.4–43.3% – optimum temperatures for 42% of the time, excessively low temperatures for 58% of the time, optimum humidity for 88% of the time, unacceptable humidity levels for 12% of the time.

On the basis of these measurements, it is apparent that the temperatures on the ground floor and first floor are too high. Overheating at lower levels probably occurs due to the un-insulated mansard roof and the heating system failing. In order to keep the temperature on the second floor within a comfortable range, the temperature of the water supplied to radiators have to be increased. Adequate and proper temperature control is not possible because some of the radiators (on the ground and first floor levels) do not have thermostatic heads and the system was not hydraulically adjusted after the renovation works were carried out. The overheating causes a decrease in relative humidity and comfort. Higher humidity levels in the bathroom result from the failing ventilation system – the exhaust ducts are dirty and there is no ventilation grill in the bathroom door. The poor insulation of the mansard roof and the high humidity levels can result in the growth of mould or condensation and rising damp.

3. Forensic Medicine Department

The Forensic Medicine Department, at the Medical University of Warsaw, ul. Oczki 1, was constructed between 1924 and 1927. During World War II, the building was almost all but completely destroyed, and was rebuilt after the conflict. It is listed in the Ochota district municipal register of Warsaw monuments. A thorough reconstruction of the building began in June 2013, the main objectives being: modernisation and adaptation for teaching and learning for students, residential facilities, and for experiments/examinations. The building works are scheduled to be completed by 1st October 2014.

The research was concerned with assessing the interior environmental air quality (measuring temperature and relative humidity) in selected rooms, namely: a small dissection room, a genetic laboratory, a basement, a planned director's office, a large dissection room, an existing director's office, a toxicology laboratory, a histopathology laboratory, a caretaker's flat, and a library. Exterior air readings were also taken. The measurements were conducted before stage I of the construction work commenced. The stage II evaluations are scheduled to take place following completion of this modernization and renovation

work, in order to evaluate changes in the quality of the interior environment. Simultaneous readings were taken in every room over a week-long period between 15:00 on 04/16/2013 and 15:00 on 23/04/2013 – at 5 minute intervals. Readings addressed a range of parameters and absolute humidity calculations are shown in Table 2.

On the strength of these measurements, it is apparent that the following rooms are subject to overheating: the genetic laboratory, the toxicology laboratory, the histopathology laboratory, the caretaker's flat and the library. This effect can be attributed to heat generated by people and equipment. The highest relative humidity levels were recorded in the small dissection room, the basement and in the large dissection room. However, the absolute humidity was noticeably higher only in the large dissection room and library in comparison with the outdoor air conditions. This increase was probably caused by high moisture gains, e.g. from medical students participating in classes and medical experiments, and by fluids used to clean spaces. A second explanation for the humidity levels in the dissection rooms is likely to be a lack of sufficient ventilation and the presence of new airtight windows. Unlike other rooms inspected, the dissection rooms have a mechanical ventilation system in place. Unfortunately, it is very rarely used because of a high level of noise emission. During the earlier modernization works, old wooden windows were changed for new plastic-framed ones, which caused a reduction in the rate of air filtration from outdoors. In other rooms, the absolute humidity was at very similar levels to that of the outdoor air, which indicates high ventilation. In reality, the fresh air is infiltrating into the building in an uncontrolled manner through the old and poorly-fitting windows. This situation should be remedied as part of the on-going modernization, because the old windows will be changed for new airtight units.

Table 2

Indoor and outdoor air parameters

Room/place	Temperature range [°C]	Relative humidity range [%]	Absolute humidity range [g/kg]
Outdoor air conditions	6.1–22.3	15.4–81.9	2.8–7.7
Small dissection room	17.0–19.6	31.0–66.6	4.1–8.8
Genetic lab	22.1–24.7	21.3–38.5	4.0–7.2
Basement	14.8–16.1	51.1–66.4	5.7–7.4
Planned director's office	19.8–22.0	28.4–45.3	4.2–7.0
Large dissection room	20.2–22.9	26.3–67.8	4.1–11.1
Existing director's office	21.3–22.9	30.9–45.8	5.0–7.7
Toxicology lab	24.5–28.3	20.6–35.6	4.2–7.8
Histopathology lab	23.4–25.3	24.1–37.3	4.5–7.3
Caretaker's flat	22.4–24.0	29.7–40.9	5.4–7.1
Library	20.6–25.9	27.4–46.0	4.1–9.2

4. The Nursing Home

The final subject of the research is a care facility in Otwock, built in 1927. It is a two-storey building, with a partial basement, and is used as a nursing home for the elderly and disabled. The building has a wooden construction with walls built of solid brick. The floors, stairs and the gable roof sections are wooden. The roof is covered with metal tiles. The survey was designed to check the quality of the indoor environment and the efficiency of the ventilation system. Measurements were taken in the dining room and the director's office.

Readings were taken between 11:25 and 14:00 on 13/02/2013 – before, during and after the midday meal. Measurements were taken for the relative humidity, temperature, circulation of air in the rooms and carbon dioxide concentrations (in ppm). The outdoor CO₂ levels were measured at around 460 ppm. The readings were in the following ranges:

- air temperature: 20.3–22.1°C,
- relative humidity: 38.2–53.0%,
- absolute humidity: 5.8–8.2 g/kg,
- air circulation: 0.0–0.03 m/s (max 0,09 m/s),
- CO₂ concentration: 865–1707 ppm.

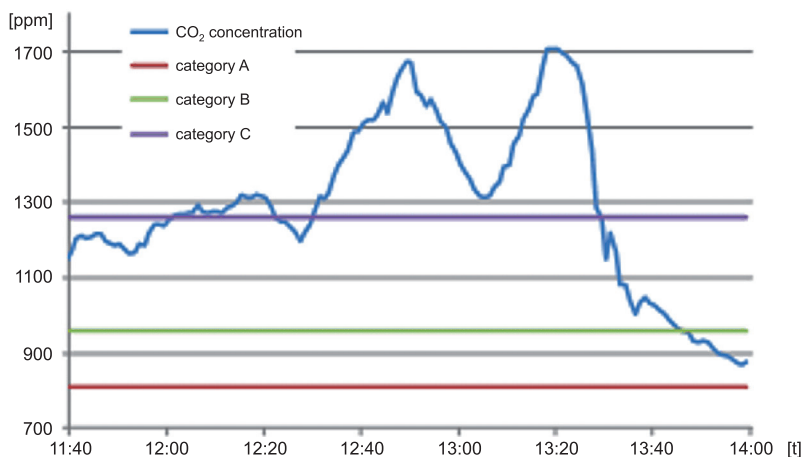


Fig. 3. Change of CO₂ concentration levels in the dining room with PN-EN 15251 categories A, B & C marked

Indoor air quality was assessed on the basis of CO₂ concentration levels, in relation to the PN-EN 15251 [2] categories (A, B & C). The highest concentrations in each category are shown in the graph: 810 ppm for A, 960 ppm for B and 1260 ppm for C. Air quality readings exceeded all categories for a significant period of time. CO₂ concentration levels decreased only after the residents had left the dining room, firstly dropping below the category C threshold and then the category B limit.

These measurements show that indoor air quality (CO₂ concentration) levels are unsatisfactory, despite optimal measures to control indoor air parameters in regard to

temperature and relative humidity. A further indication that the ventilation system is failing is that the relative humidity levels in wintertime are at the 50% level, when humidification does not occur.

The decline of CO₂ concentration levels (as recorded in Fig. 3.) was used to determine the rate of air exchange in the dining room. Calculations were based on the following formula:

$$N = \frac{\ln\left(\frac{C_o - C_i(\tau)}{C_o - C_{io}}\right)}{-\tau} = \frac{\ln\left(\frac{460 - 868}{460 - 1707}\right)}{-0.633} = 1.76 \text{ 1/h} \quad (1)$$

The outdoor CO₂ concentration level (C_o) was 460 ppm. The maximum indoor concentration level (C_{io}) was 1707 ppm. The decline rate (τ) was 38 min. The lowest indoor concentration level ($C_{i(\tau)}$) was 868 ppm. The estimated air exchange rate (n) was 1.76 h⁻¹. The ventilation rate in the dining room is below adequate standards. Accordingly, it is recommended [3] that the air exchange rate should be between 5–10 h⁻¹.

In light of the wooden construction of the nursing home, it is likely that the building envelope is prone to airleaks. The director's office was tested because it has a corner location, lacks ventilation ducts and can be taken out of service on a temporary basis. The tests were designed to determine the n_{50} coefficient values, to locate air leaks and to estimate the approximate rate of air exchange under normal conditions. In a preliminary examination, (where air pressure was about 80 Pa) leaks and cracks were identified using an infra-red camera. It was possible to do so due to a high temperature difference inside and outside the building. Cold air seeping into the rooms showed up well on the thermographic pictures, as shown below.

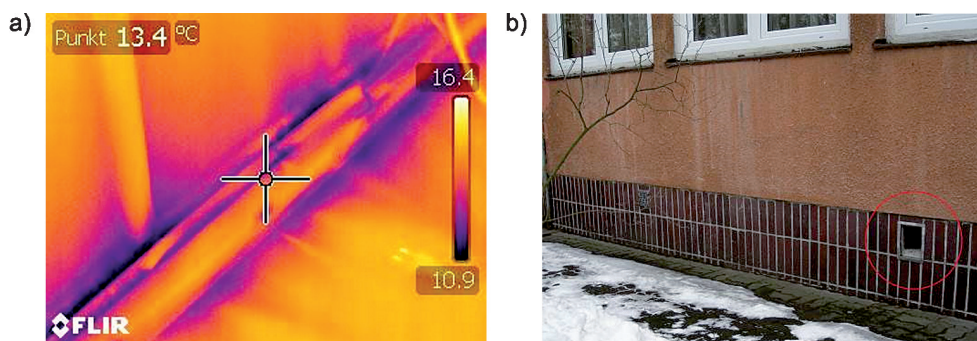


Fig. 4. Leaks: a) at connection of external wall with floor and their source, b) ventilation space under the floor – marked the vent in the socle

Air leaks (Fig. 4a.) were detected around the perimeter of the room and were caused by poor flushing between the floor and the external wall. The air penetrated into the room from ventilated spaces under the floor (Fig. 4b.). Carpeting provided the only sealing layer, which had been taken up for the test. Other leaks were also detected in gaps between the old wooden window frame and the external wall (Fig. 5a.). New plastic windows were installed in old

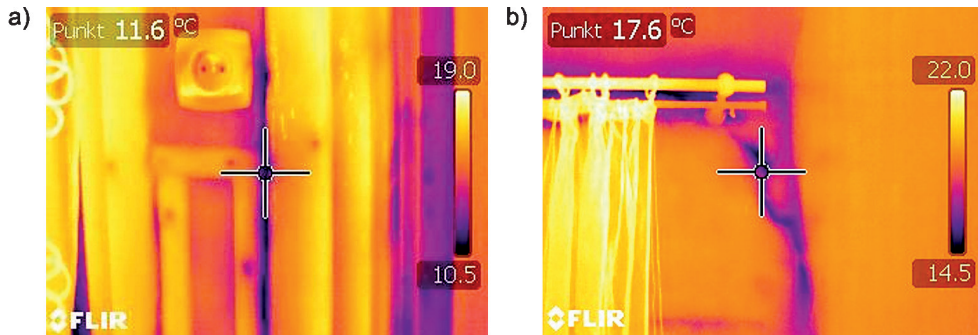


Fig. 5. Leaks: a) in a gap between the old wooden window frame and the external wall, b) in a crack in the external wall in a corner of the room

wooden frames. A crack in the external wall in a corner (Fig. 5b) also enabled air to leak into the room.

A full test was undertaken after all leaks were identified. Automatic measurements were carried out using a Minneapolis Bower Door 4 at under and over pressures. The test results gave the following mean values:

- $V_{50} = 1048 \text{ m}^3/\text{h}$ – air flow rate at a pressure difference of 50 Pa,
- $n_{50} = 11.69 \text{ h}^{-1}$ – air exchange rate at pressure difference of 50 Pa.

The results obtained show that the room has a very low score in terms of its airtightness. According to the WT2014 requirements, n_{50} should be lower than 3.0 h^{-1} in a building with natural ventilation. The test result was almost four times higher. The estimated exchange rate resulting from air infiltration can be calculated using the following formula: $n = n_{50}/20 = 0,58 \text{ h}^{-1}$. The air flow rate attributable to air infiltration is about $52,6 \text{ m}^3/\text{h}$. Two people occupy the director's office so the air flow rate should be about $40 \text{ m}^3/\text{h}$ ($20 \text{ m}^3/\text{h}$ per person). The tests show that in spite of the lack of ventilation ducts, excessive infiltration of air occurs in the room. This is an undesirable situation, because ventilation should be controlled. Moreover, air entering the room through the cracks and gaps lead to a decrease in thermal comfort levels. Measurements show that measures to make the Nursing Home more airtight need to be taken before the ventilation system is modernized. Only if that is done can there be any improvement in the effectiveness of the ventilation in the building.

5. Conclusions

In the light of the research carried out in these pre-war public utility buildings, the following conclusions have been drawn:

- the rooms often overheat because the heating system does not comply with the relevant regulations. There is a significant potential for energy savings, by modernizing and adjusting the heating systems;
- the building lacks an efficient ventilation system, suited to the activities carried out in the rooms – much of the fresh air enters the rooms in an uncontrolled manner through gaps and cracks;

- modernization works often result in a deterioration of indoor air quality, e.g. by installing new bathroom doors without ventilation grills;
- plans for modernization works are not always as comprehensive as they should be, and do not address the requirements of the building,
- research to measure the quality of the internal environment and the efficiency of the installations should be conducted before modernization and/or renovation works are planned and undertaken;
- in too many instances, building managers lack the necessary knowledge about the maintenance and general usage needs of the ventilation systems and installations/controls.

References

- [1] PN-78/B-03421 Wentylacja i klimatyzacja. Parametry obliczeniowe powietrza wewnętrznego w pomieszczeniach przeznaczonych do stałego przebywania ludzi.
- [2] PN-EN 15251 Kryteria środowiska wewnętrznego, obejmujące warunki cieplne, jakość powietrza wewnętrznego, oświetlenie i hałas.
- [3] Nowakowski E., *Wentylacja w salach konsumpcyjnych zakładów żywienia*, Polski Instalator 3/2001.

PAWEŁ GAŁEK*

OPTIMISING ENERGY PRODUCED BY PHOTOVOLTAIC CELLS

OPTIMALIZACJA POZYSKIWANIA ENERGII Z OGNIW FOTOWOLTAICZNYCH

Abstract

This paper presents a comparative analysis of energy produced by photovoltaic (PV) panels installed on fixed structures and on solar trackers. Measurements were taken continuously over a period of one year. Performance results for both one year and 24 hours are presented. Attention is also paid to current Polish and European legislation promoting the installation of systems that use energy from renewable sources.

Keywords: photovoltaic, solar energy, PV modules, tracker, renewable energy

Streszczenie

A artykule przedstawiono analizę porównawczą zysków energii z paneli fotowoltaicznych zamontowanych na konstrukcji stacjonarnej oraz na konstrukcji nadążnej, kierującej się w stronę słońca. Pomiarzy prowadzone były przez okres roku w trybie ciągłym. Przedstawiono analizę roczną oraz dobową. Zwrócono również uwagę na aktualne polskie i europejskie ustawodawstwo promujące budowę instalacji pozyskujących energię ze źródeł odnawialnych.

Słowa kluczowe: fotowoltaika, energia słoneczna, ogniwa PV, system nadążny, energia odnawialna

* Ph.D. Eng. Paweł Gałek, Institute of Building Materials and Structures, Faculty of Civil Engineering, Cracow University of Technology.

1. Introduction

Directive 2009/28/EC [1] of the European Parliament and Council was passed in April 2009 and came into force on 25th June 2009. Its aim is to promote the use of energy from renewable sources and the target set out by the European Union is for renewable energy to make up 20% of total energy consumption by the year 2020. This target was translated into individual goals for the Member States, in Poland's case this has been set at 15.48%. According to Eurostat [2], the average EU consumption of renewable energy in 2012 was 14.1%, while in Poland it was 11% (Table 1).

Table 1

Share of renewable energy in gross final energy consumption [%]

	2005	2009	2010	2011	2012	Target
European Union (28 countries)	8.7	11.9	12.5	13.0	14.1	20
Poland	7.0	8.8	9.3	10.4	11.0	15.48

The support system for renewable energy production in Poland is included in the draft law on renewable energy sources. The recently published revision 6.2 of 4th February 2004 [7] contains provisions that regulate the connection of micro and small installations (up to 40 kW) to the national power grid. The user of such an installation will pay for the energy difference between the energy consumed from the grid and the energy transmitted into the grid, and the excess energy will be paid to the user at 80% of the energy price on the competitive market.

The European Commission Report of March 2013 [9] provides progress assessments of the Directive's [1] targets and performance forecast, with division into individual sources of renewable energy. The most promising development is seen in the solar energy sector. This is due to dynamic developments in technology, especially in photovoltaics. PV systems are easy to install, long-lasting and scalable, which allows their use both in household systems and in the construction of high power plants. The solutions proposed in the draft law on renewable energy sources allow the simplification of PV systems by eliminating the need for expensive batteries to store surplus energy.

Compared to southern European countries, Poland has nearly two times less solar radiation intensity, falling to three times lower when compared to areas on Earth that are most exposed to solar radiation (Fig. 1). It is therefore especially important that PV systems are designed to optimise any energy gain. The amount of solar energy absorbed is affected by the location of the system, inclination, possibly obstacles that shade the solar radiation, weather conditions and the solar cell temperature. Not all of these conditions are within our control. However, what we can control is the solar panel inclination angle, which can follow the movement of the sun (solar tracking system). The use of a solar tracking system provides significant improvements in energy efficiency, but also limits the number of locations where such systems can be installed. In a later part of the paper, analysis and results of measurements of energy produced by PV panels installed on a tracking system of the author's own design is presented (Fig. 4).

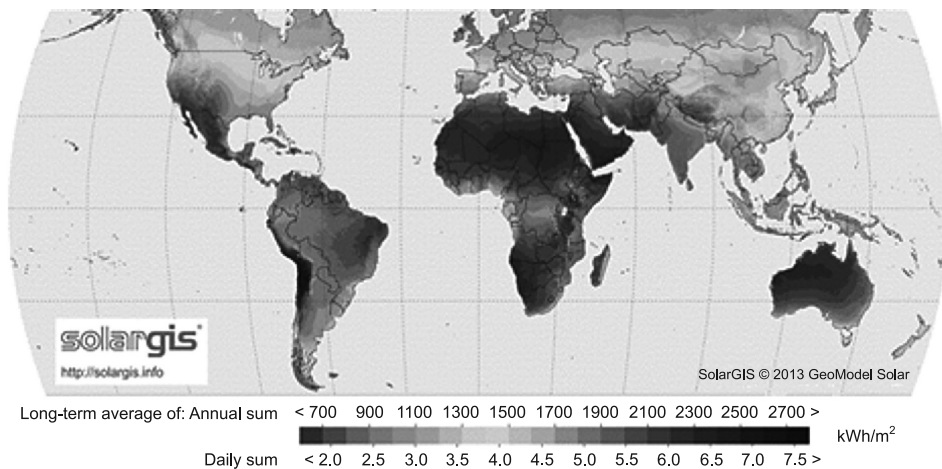


Fig. 1. World map of global horizontal irradiation [3]

2. Photovoltaic (PV)

The total solar energy reaching the Earth has a power of ca. 8×10^{10} MW. Average power consumption needs are estimated to be ca. 0.001×10^{10} MW. Solar energy is potentially an unlimited and an environmentally-friendly source of energy. The simplest way of producing solar energy is the use of photovoltaic (PV) panels. There has been very strong growth in this sector of the economy over the last dozen years or so. The European Photovoltaic Industry Association (EPIA) states that at least 37 GW of new PV systems [6] were installed in 2013. At the end of 2013, the world's power from installed PV systems was 136.7 GW [6], which gives about 0.4% of the world's total energy demand.

2.1. Photovoltaic effect

A solar cell operates according to the photovoltaic effect principle, which produces electromotive force as a result of radiation falling onto a photovoltaic semiconductor cell (Fig. 2). This effect was observed as early as the year 1839. The voltage and power produced by a single PV cell is low (about 0.5 V), therefore the cells are combined into modules, and these into panels.

With regard to the design of PV cells, several generations can be distinguished. Currently, the most popular are still the 1st generation cells based on crystalline silicon (mono or polycrystalline). The second generation cells (CdTe, CIGS) that are now being mass-produced are increasing their market share year on year. However, the biggest hope for the future is brought by the third generation cells (organic and Dye Sensitized Solar Cells – DSCC). DSCC solar cells generate electricity via the phenomenon of photosynthesis. Their design uses platinum, which makes production significantly more expensive. However, developments in recent years have allowed platinum to be replaced with cheap 3D structure graphene components [5].

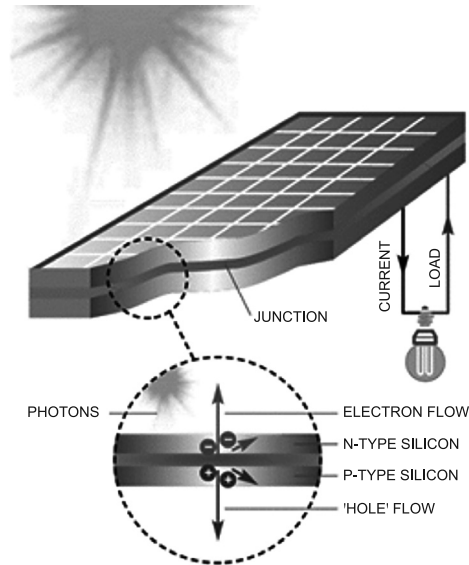


Fig. 2. Example of the photovoltaic effect [8]

2.2. PV Systems

PV systems can be divided according to location into free-standing, Building Adapted PV Systems (Building Adapted PV Systems – BAPV) and Building Integrated PV Systems (Building Integrated PV Systems – BIPV). In terms of connection with the power grid, PV systems are divided into those connected to the grid (on-grid systems) and those not connected to the grid (off-grid systems). The latter type is used in areas where the power grid is not available, and in Europe, these are rare. A typical on-grid system diagram is shown in Fig. 3. The PV panels generate direct current (DC). The direct current (DC) is converted into alternating current (AC) using inverters, which allows the power to be used to supply

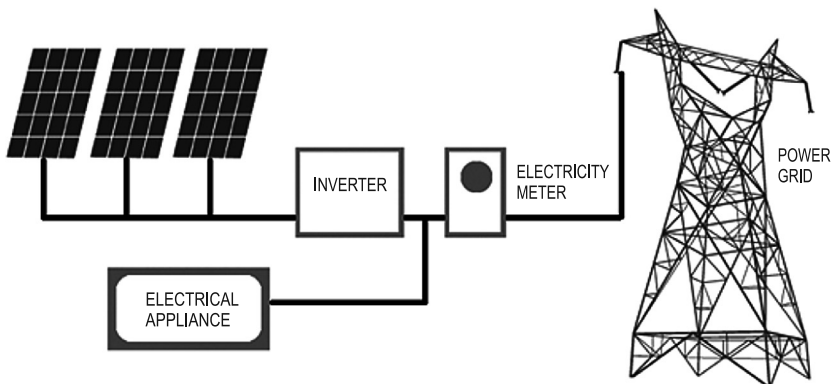


Fig. 3. Grid-connected (on-grid) PV system configuration

the site loads. When there is a surplus of energy, it can be transferred to the power grid through a bi-directional power meter. In the case of insufficient power produced by the PV panels, power is taken from the grid. The solar energy producer pays or receives payment, according to the balance of energy consumed and supplied to the grid.

2.3. PV panel support structures

The PV panels are installed on support structures. In Poland, all panels should be directed south. The inclination angle should be about 25 degrees in summer and about 60 degrees in winter. The universal angle used in fixed installations (without inclination angle adjustment) is assumed at 33-38 degrees. A free standing PV installation can use a solar tracker system, which follows the movement of sun to keep the panel perpendicular to the sun's rays. The best performance is achieved using double axis tracking systems. Such systems can be controlled based on the calculated position of the sun or on measurement of radiation.

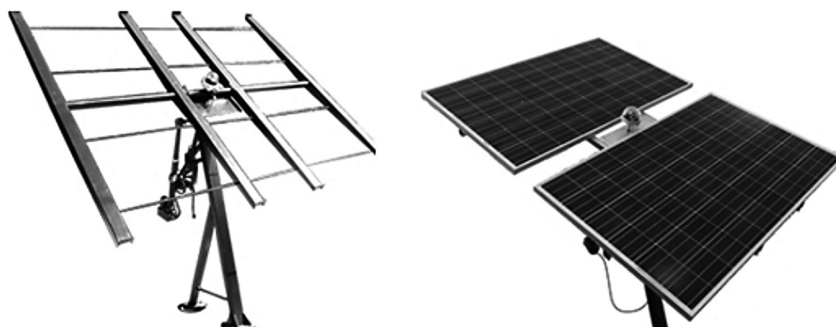


Fig. 4. Double axis solar tracking systems

The proprietary solution uses a double axis system (Fig. 4) with an infrared sensor. The IR sensor allows the system to operate even on cloudy days. The system features a very wide range of movement. In the east-west line, the maximum angle of movement is 238 degrees, while in the north-south line, it is 85 degrees.

3. Optimising the PV cell output

The amount of energy produced by the photovoltaic cell depends on the efficiency of the cell and the intensity of radiation. The efficiency of solar cells currently manufactured by industry is 15–18%. This solar cell efficiency is also affected by its operating temperature – the higher the temperature, the lower the efficiency. At a temperature of 80 degrees, which can be achieved in summer, the efficiency drop is about 25%. To eliminate the reduction of cell efficiency in summer, it should be provided with appropriate ventilation or cooling. Also, the PV surface should be kept clean, especially in dry seasons. Even a small stain caused by bird droppings, can lower the PV efficiency by as much as 33% [10]. The highest intensity of solar radiation is when the sunrays' incidence is perpendicular to the PV surface. Only the use of solar tracking systems ensures optimum energy output.

3.1. The intensity of the solar radiation

The intensity of the solar radiation reaching the upper limit of the Earth's atmosphere is described by the solar constant. This value is defined for the average Earth-Sun distance and it is about 1366.1 W/m^2 . About 50% of this radiation reaches the Earth's surface, and the remaining part is reflected or absorbed by the atmosphere. The actual intensity of solar radiation depends on the geographical position of the measurement point and the transparency of the atmosphere. The highest intensity occurs within the equatorial zone, and decreases



Fig. 5. Global horizontal irradiation. Poland [4]

with the distance from the equator. Poland is located within the moderate radiation zone with solar radiation intensity nearly 3 times lower than in the most insolated regions of the Earth (Fig. 1). In Poland (Fig. 5), the assumed yearly energy gain from a horizontal plane is from 900 to 1200 kWh/m^2 , depending on location. The solar radiation that reaches the Earth's surface can be divided into direct and dispersed. Poland is characterised by a high portion of dispersed radiation, which is estimated at 47% in summer, and up to 77% in winter. About 80% of the yearly total radiation occurs during the six months of the spring and summer seasons.

3.2. Analysis of energy gains using the solar tracking system

The installed proprietary solar tracking system allows tracking of the solar rays within the full range of angles. The system is controlled using infrared sensor measurement. This allows the system to be directed towards the sun even during cloudy weather.

Measurements were carried out during the period from March 2013 to February 2014 to determine the power output from PV panels installed in a solar tracker and in a fixed system directed to the south at an angle of 36 degrees. Each system contained two PV panels

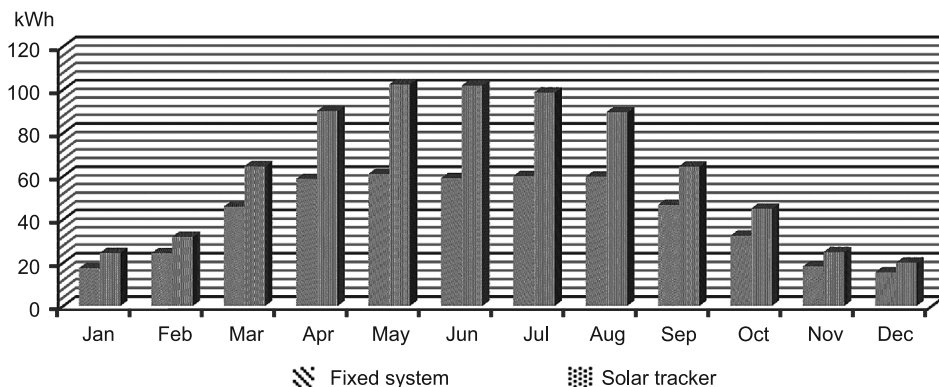


Fig. 6. Average monthly electricity production from the given system (kWh)

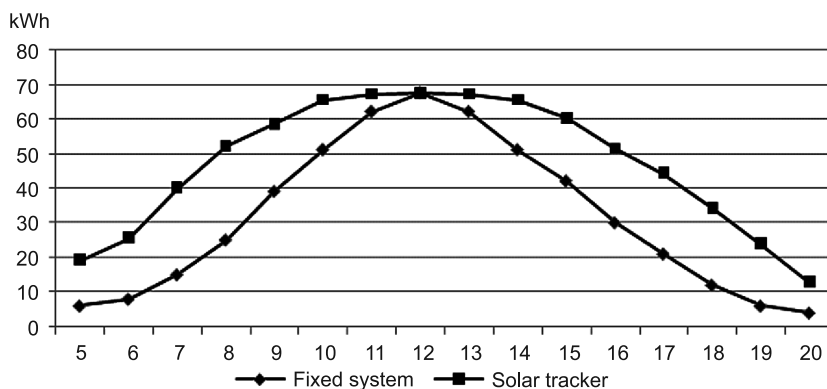


Fig. 7. Average daily electricity production from the given system (kWh)

of total power 510W, according to the manufacturer's specification. Measurements were carried out continuously, from sunrise to sunset. The goal of the analysis was to determine the difference between the energy outputs of the solar tracking system and the fixed system. Results of the analysis for periods of 24h (Fig. 7) and the entire year (Fig. 6), are given in the attached charts.

4. Conclusions

The study shows that the monthly average energy output improvement achieved by the use of the solar tracker compared to the fixed system ranges from 28% in winter to 72% in summer. During the morning and evening hours, the fixed system operates at a very

unfavorable angle. Such a high difference during the summer season is a result of the increased amount of daylight – when the daylight period is longer, the solar tracker operates more efficiently than the fixed system. The difference over the whole year is 52% more energy obtained from the solar tracker. If you add the benefits of proper system maintenance (good ventilation, surface cleaning, clearing of snow) the system efficiency can be up to two times higher. This shortens the time required for return on investment.

Solar tracking system design idea: Paweł Galek, Gwalbert Stefański

System implementation: F.H.U. Bartek

References

- [1] Dyrektywa Parlamentu Europejskiego i Rady 2009/28/WE z dnia 23 kwietnia 2009 r. w sprawie promowania stosowania energii ze źródeł odnawialnych, uchylająca dyrektywy 2001/77/WE oraz 2003/30/WE.
- [2] Eurostat, Headline indicators, <http://epp.eurostat.ec.europa.eu> – 2014.03.15.
- [3] http://solargis.info/doc/_pics/freemaps/1000px/ghi/SolarGIS-Solar-map-World-map-en.png – 2014.03.15.
- [4] http://solargis.info/doc/_pics/freemaps/1000px/ghi/SolarGIS-Solar-map-Poland-en.png – 2014.03.15.
- [5] Hui Wang, Kai Sun, Franklin Tao, Dario J. Stacchiola, Yun Hang Hu, *3D Honeycomb-Like Structured Graphene and Its High Efficiency as a Counter-Electrode Catalyst for Dye-Sensitized Solar Cells*, *Angewandte Chemie*, 2013; DOI:10.1002/ange.201303497.
- [6] Masson G., 2013, *A qualified record-year for photovoltaics*, European Photovoltaic Industry Association, march 2014, <http://www.epia.org/news/news> – 2014.03.15.
- [7] Projekt ustawy o odnawialnych źródłach energii, wersja 6.2 z dnia 4.02.2014 r.
- [8] *Solar Generation 6*, European Photovoltaic Industry Association, February 2011, <http://www.epia.org/news/publications> – 2014.03.15.
- [9] Sprawozdanie Komisji dla Parlamentu Europejskiego, Rady, Europejskiego Komitetu Ekonomiczno-Społecznego i Komitetu Regionów, *Sprawozdanie na temat postępów w dziedzinie energii odnawialnej*, Komisja Europejska, Bruksela, 27.3.2013 COM(2013) 175 final.
- [10] Szymański B., *Myć czy nie myć?*, *GLOBEnergia*, Vol. 12, 2012, 26-27.

MARTIN GAVLÍK*, LADISLAV BÖSZÖRMÉNYI*

DETERMINE THE OPTIMAL SYSTEM STRUCTURE OF THE COMBINED PRODUCTION OF ELECTRICITY AND HEAT

WYZNACZANIE OPTYMALNEJ STRUKTURY SYSTEMU KOGENERACJI CIEPŁA I ELEKTRYCZNOŚCI

Abstract

For most of the EU, final energy is consumed in buildings as low-temperature heat for space heating and hot water. This is mostly produced by burning fuels that are linked to adequate environmental load environment, regardless of whether it is a fossil or bio-fuel. It is therefore high efficiency fuel which is a natural requirement in designing, implementation and operation of heat sources for the supply of buildings. For this reason, before commonly used conventional mono-production of heat a more efficient technology should be preferred, combining heat and power. This technology is, however, much more difficult as far as investments are concerned. Accordingly, its share in total production of heat needs to be set so that the operation of the heat source was also economy effective. This paper presents a simple method to solve this problem.

Keywords: biomass, renewable energy sources, cogeneration

Streszczenie

W większości krajów Unii Europejskiej energia końcowa jest używana w formie ciepła niskotemperaturowego do ogrzewania i ciepłej wody użytkowej. Jest ono głównie wytwarzane przez spalanie paliwa, co związane jest z obciążeniem środowiska, niezależnie od tego, czy jest to paliwo kopalne czy biopaliwo. Potrzebne jest zatem wysoko wydajne paliwo, jako oczywisty wymóg w zakresie projektowania, realizacji i eksploatacji źródeł ciepła dla budynków. Z tego powodu, zamiast powszechnie stosowanych konwencjonalnych monoźródeł wytwarzania energii cieplnej należy preferować bardziej efektywne techniki łącznego wytwarzania ciepła i energii elektrycznej. Ta technologia jest jednak znacznie trudniejsza, w szczególności ze względów inwestycyjnych. W związku z powyższym jej udział w całkowitej produkcji ciepła musi być ustawiony tak, żeby działanie takiego źródła ciepła było również efektywne ekonomicznie. W artykule przedstawiono prostą metodę rozwiązania tego problemu.

Słowa kluczowe: biomasa, odnawialne źródła energii, kogeneracja

* Doc. Eng. Martin Gavlik, Ph.D. Ladislav Böszörményi, Institute of Architectural Engineering, Faculty of Civil Engineering, Technical University of Košice.

1. Introduction

In the EU the proportion of the energy supply in buildings is the biggest with 45% (Fig. 1). The energy demand of buildings means the use of end-energy in the complex system of energy supply. The electrical energy demand of lighting, household appliances etc. can be often neglected compared to the summarised yearly heat demand of heating and DHW supply and of the HVAC, but in households or in exceptional cases, like in shopping centres, this proportion can be inverted.

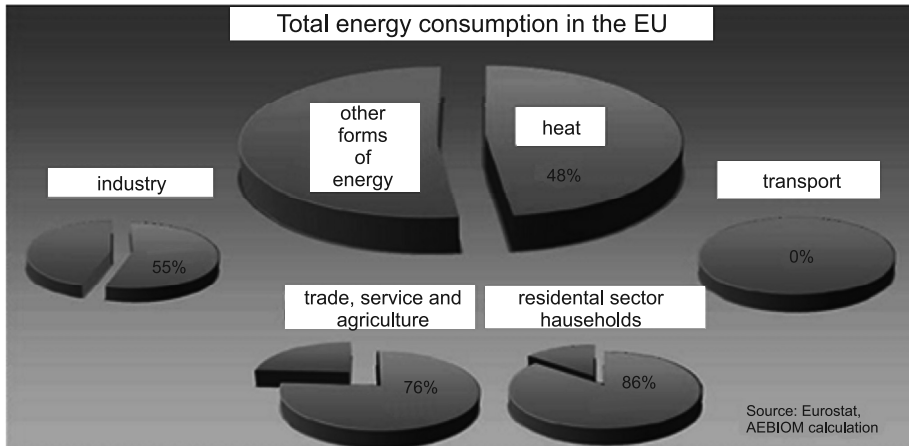


Fig. 1. Proportion of energy consumption of building

Figure 1. shows that the heat supply in residential buildings, like the heat demand of the heating and DHW is more than 80%. This heat demand can be covered from low temperature heat sources (renewable energies, waste heat). In Slovakia the most expensive fossil energy (natural gas) is used in ca. 70% with low effective direct heat production. This fact is even more worrying because in Slovakia almost 100% of natural gas demand is covered by importing from Russia. The last Russian-Ukraine gas conflict caused a big drop in Slovakian industrial production and this shows that high import dependency presents a reasonable risk parameter for a national economy.

Energy and environmental viability of production of electricity and heat in cogeneration production in condensing power sources compared with separate and conventional heat sources is beyond doubt. To ensure the competitiveness of this technology is, however, crucial to higher economic efficiency. In the area of decentralized heat-supply systems this is, difficult to achieve. Specific investment costs are substantially higher than for cogeneration technologies for conventional heat sources. The incorrect choice of the parameters of the source, e.g. the cogeneration. The resizing, therefore has a much less favourable impact on economic results, rather than in the case of conventional heat sources.

Therefore, it is necessary in the preparation of projects to analyse and take into account all the factors of cogeneration sources which are particularly sensitive, the resulting effect in a positive or negative sense. Conceptual weaknesses of the project of a particular system

as well as the weaknesses of the technical performance of its individual components and incorrect conception of operation may spoil the “image” of this very progressive energy technology.

2. Distribution of the peak power source of cogeneration

According to cybernetic model of cogeneration source is generally made up of cogeneration and conventional subsystems. Cogeneration of heat and electricity generated in the production of storage subsystems. It consists of one or more according to the size of cogeneration units. Conventional systems produce heat output only, which is also often divided into two, or even more boilers.

The resulting economic efficiency crucially depends on the peak distribution source of the cogeneration of heat and power necessary for the supply of cogeneration systems on conventional consumers and subsystems. The use of cogeneration units of smaller performance allow flexibility of the heat output to adapt the total piston gas engines or micro-turbine to the requirements of consumers. Determination of thermal performance of cogeneration in the subsystem often solves the problem as the number of election of cogeneration units. In the manufacture of the same quantity of heat (cogeneration production of heat) while saving primary energy by any unit causes, compared with mono-production heat, but by far not certain that this is sufficient to compensate for higher investment in more sophisticated systems. From the perspective of competitiveness of cogeneration it is necessary that such distribution of peak power sources, where high energy efficiency is achieved at the maximum economic efficiency. The target function can be the maximum value of profits caused by cogeneration production. Condition may be the choice of a number of smaller cogeneration units at which the unit with the smallest annual gain.

In the elaboration of the methodology, we relied on the results of the energy and economic analysis of the combined production of heat and electricity published in (1).

The most important result of the energy analysis is the expression of the primary energy savings related to the heat Q_{KJ} produced by the cogeneration unit.

$$\alpha_{Q,KJ} = \frac{G_U}{Q_{KJ}} \quad (1)$$

where:

G_U – the saving of primary energy caused by the operation of a cogeneration unit.

From energy analysis: primary energy savings on the quantity of heat produced by the cogeneration subsystem.

$$\alpha_{Q,KJ} = \sigma_{KJ} \left(\frac{1}{\eta_{KE}} - \frac{1}{\eta_{G,KJ}} \right) \quad (2)$$

where:

$\sigma_{KJ} = \frac{E_{KJ}}{Q_{KJ}}$ – modul of electricity production,

η_{KE} – efficiency of electricity production,
 $\eta_{G,KJ} = \frac{E_{KJ} + Q_{KJ}}{G_{KJ}}$ – total efficiency of the cogeneration unit.

Saving primary energy caused by the cogeneration unit can be expressed by:

$$G_U = Q_{KJ} \alpha_{G,KJ} \text{ [MWh/year]} \quad (3)$$

The most valuable result of economic analysis is the expression of specific cost savings to the heat produced by the cogeneration unit:

$$k_{G,U,KJ} = \frac{C_U}{Q_{KJ}} \quad (4)$$

$$k_{G,U,KJ} = \sigma_{KJ} \left(k_{KE} - \frac{P_{G,KJ}}{\eta_{G,KJ}} \right) \text{ [-/MWh]} \quad (5)$$

where:

k_{KE} – the cost of separate production of electricity [€/MWh].

Cost saving can be expressed by relationship:

$$C_U = Q_{KJ} \cdot k_{G,U,KJ} \text{ [-/year]} \quad (6)$$

Cost saving allows you to express the profit due to a cogeneration unit:

$$\Delta Z = C_U - \alpha \Delta B \text{ [-/rok]} \quad (7)$$

where:

$\Delta B = Q_{KJ} \cdot \Delta b$ – the excess of investment costs,

Δb [€/GJ] – specific investment costs and α is annual annuity.

Previous relations allow us to express gain related to surplus investment cost $\Delta Z/\Delta B$. The relations can be used to determine the optimal proportion of heat and power in a cogeneration subsystem. In particular cases, they can often be used as to determine the optimal number of cogeneration units in which the maximum gain for smaller performances is obtained.

3. Application of the methodology for determining the optimal heat-power cogeneration subsystem

We have applied the methodology for determining the optimal number of cogeneration units to the case in which the source designed for cogeneration was one KJ with microturbine (IR Energy Systems 70LM), with an electric power of 70 kW, and a heat output of 108 kW for the annual preparation of the determination of the optimal number of cogeneration units. Such a proposal may cause primary energy savings, while the simplified and costs and ultimately profit, but from the optimal alternatives may be quite far away.

Theoretically in this case it would be possible to operate 6 such cogeneration units with annual use as in Fig. 2. By means of input data specified by table 1 we have received

the above relations results, which are summarised in Table 2 for the autonomous operation of the individual cogeneration unit, and in Table 3 for the operation of the current cogeneration unit.

Table 1

Assessment of energy performance			
INPUT DATA			
Heat output of the cogeneration unit	Q_{KJ}	0.108	[MW]
Electric power cogeneration unit	P_{KJ}	0.07	[MW]
Modul of heat plant production	Θ_{KJ}	0.65	
The overall efficiency of the cogeneration unit	$\eta_{G,KJ}$	0.6	
Efficiency of separate heat production	η_K	0.85	
Efficiency of separate electricity production	η_{KE}	0.37	
Specific costs of separate production of electricity	K_{KE}	82	[€/MWh]
Overlap specific investment costs	Δb_{KJ}	750000	[€/MWh]
Average annual annuity	a	0.16	[1/year]
Price of fuel in the source	p_G	21.6	[€/MWh]

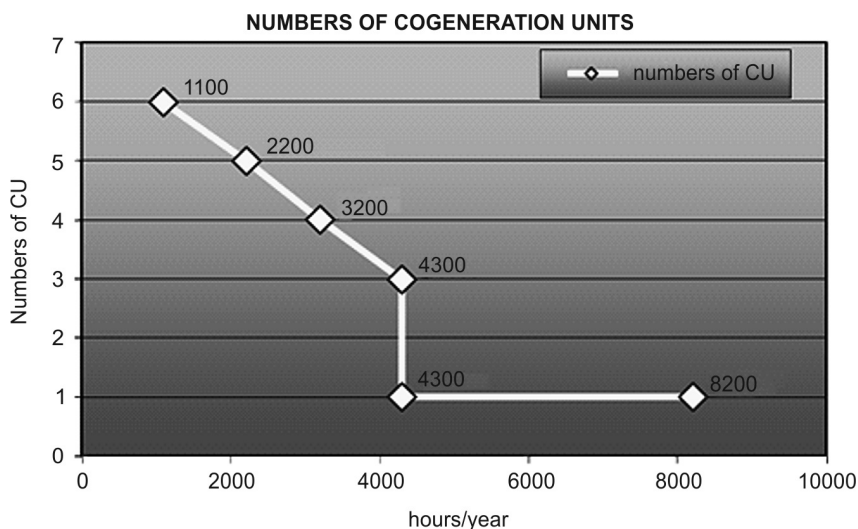


Fig. 2. Technically adequate structure of the cogeneration subsystem

The number of cogeneration units is determined from the condition that in the last one cogeneration unit must be involved in generating profit. After determining the number of cogeneration units, we can take stock of the impact of increasing the number of cogeneration units to save energy, costs and profit. Based on the input data which was evaluated by software, the numerical values of the parameters and their graphical representation.

Table 2

Parameter of the autonomous service of individual cogeneration unit

Number	Q_{KJ}	G_U	C_U	ΔZ	ΔB	$\Delta Z/\Delta B$	
CU	[h/year]	[MWh/year]	[MWh/year]	[€/year]	[€/year]	[%/year]	
1	8200	885,6	594.685	26404.000	18004.000	52500	34.293
1-2	6250	1350.000	906.532	40250.000	23450.000	105000	22.333
1-3	5600	1814.400	1218.378	54096.258	28896.258	157500	18.347
1-4	5000	2160.000	1450,450	64399.098	30799.098	210000	14.666
1-5	4440	2397.600	1610.000	71483.292	29483.292	262500	11.232
1-6	3883.333	2516.400	1689.775	75024.068	24624.068	315000	7.817

Table 3

Parameter of the autonomous service of individual cogeneration unit

τ	Q_{KJ}	G_U	C_U	ΔZ	ΔB	$\Delta Z/\Delta B$	
CU	[h/year]	[MWh/year]	[MWh/year]	[€/year]	[€/year]	[%/year]	
1	8200	885.6	594.685	26404.000	18004.000	52500	34,293
2	4300	464.400	311.847	13846.000	5446.000	52500	10,373
3	4300	464.400	311.847	13846.258	5446.258	52500	10,374
4	3200	345.600	232.072	10302.841	1902.841	52500	3,624
5	2200	237.600	159.550	7084.193	-1315.807	52500	-2.506
6	1100	118.800	79.775	3540.776	-4859.224	52500	-9.256

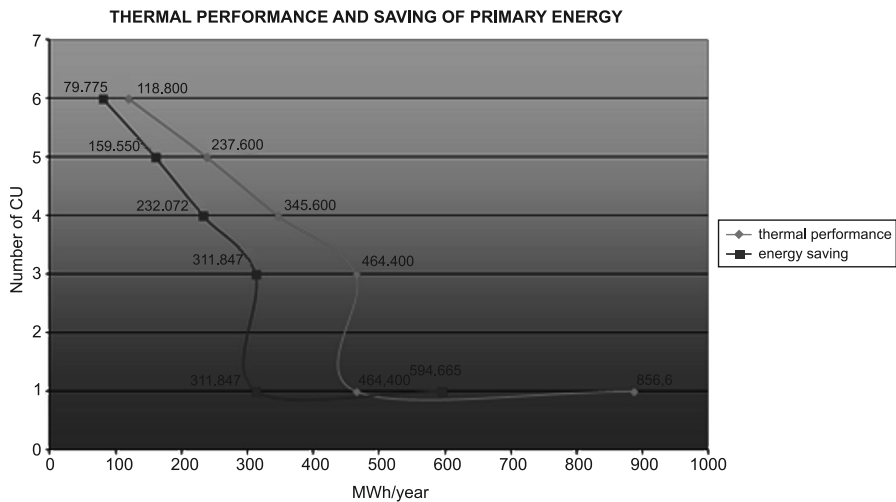


Fig. 3. Thermal performance and saving of primary energy

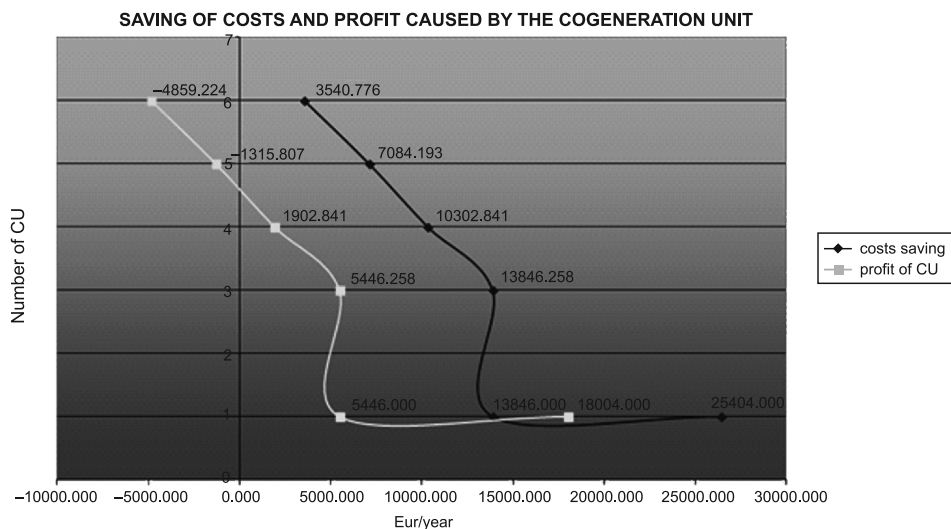


Fig. 4. Saving of costs and profit caused by the cogeneration unit

The number of cogeneration units is determined from the conditions that, in order to produce profit for the latest cogeneration unit shall $\Delta Z_n > 0$. It follows that the optimal number of cogeneration units in this case would be $n = 4$, which should reach almost twice the profit compared with the original proposal with one cogeneration unit.

4. Conclusions

In professional circles it is considered that when designing cogeneration subsystems of electricity need, in the current economic environment it is necessary to achieve the desired economic efficiency. Thermal performance of cogeneration and, consequently, also the share of annual consumption of cogeneration heat tends to be relatively small. However, the point of view of energy efficiency and the environment tends to be less favourable than the design of the heat needed as necessary.

The original philosophy of cogeneration is based on an effort to utilize waste heat released when electricity is produced. However, the concept is based on an effort to produce electricity more effectively in cases when it is necessary to produce a relatively large amount of heat. It follows that cogeneration source should be scaled according to the heat needed, but with a certain compromise as to the share of the thermal performance of cogeneration in the overall heat performance of the source. Increasing fuel prices used in the cogeneration sources and electricity energy pushes this proportion to be higher.

References

- [1] Buki G., *Kapcsolt energiatermelés*, Műegyetemi Kiadó, Budapest 2007.
- [2] Dvorský E., Hejtmánková P., *Kombinovaná výroba elektrické a tepelné energie*, Vydavatel'stvo Technická literatura BEN, Praha 2005.
- [3] Faninger G., *Thermal Energy Storage*, IEA SHC Task 28, Subtask 28.2.4 (www.iea.shc.org).
- [4] Böszörményi L., Böszörményi G., *The Barriers and Possibilities of Heat Supply Sustainability*, [In:] ASHREA Transaction, Volume 114, Part 2.
- [5] Eurostat, AEBIOM calculation (www.enef.eu).

STANISŁAW GUMUŁA*, KATARZYNA STANISZ**

AN EXPERIMENTAL EVALUATION OF RESOURCES AND THE POTENTIAL FOR USING THE KINETIC ENERGY OF WIND TO PRODUCE ELECTRICITY

EKSPERYMENTALNA OCENA ZASOBÓW I MOŻLIWOŚCI WYKORZYSTANIA ENERGII KINETYCZNEJ WIATRU DO PRODUKCJI ENERGII ELEKTRYCZNEJ

Abstract

This article presents the results of a three-year study of local wind energy resources. The results were analyzed in respect to their compliance with the Weibull distribution model. The objective was to determine whether the actual distributions differ from the theoretical ones which are available in the IMG P studies. The potential for meeting electricity needs was determined on the basis of an assessment of local kinetic energy wind resources. This was based on producing wind energy for buildings that have no possibility of connecting to the grid. Several variants were considered in terms of demand for electricity at different buildings.

Keywords: kinetic energy of wind, conversion of the kinetic energy of wind into electrical energy, the potential for meeting the electricity needs of a building

Streszczenie

W artykule przedstawiono wyniki trzyletnich badań lokalnych zasobów energii wiatru. Wyniki badań poddano analizie z punktu widzenia ich zgodności z rozkładem Weibulla. Analiza miała na celu określenie o ile rozkłady rzeczywiste różnią się od rozkładów teoretycznych dostępnych w opracowaniach IMG P. Na podstawie oceny lokalnych zasobów energii kinetycznej wiatru wskazano możliwości zaspakajania potrzeb na energię elektryczną w oparciu o energię wiatru w budynkach nie mających możliwości przyłączenia do sieci elektrycznej. Rozważono kilka wariantów budynku różniących się zapotrzebowaniem na energię elektryczną.

Słowa kluczowe: energia kinetyczna wiatru, konwersja energii kinetycznej wiatru na energię elektryczną, możliwości zaspokojenia potrzeb budynku na energię elektryczną

* Prof. Stanisław Gumuła, Faculty of Energy and Fuels, AGH, University of Science and Technology in Cracow.

** Ph.D. Katarzyna Stanisiz, Polytechnic Institute, Department of Building, State Higher Vocational School Stanislaus Pigoń in Krosno.

1. Introduction

Estimating the potential for electricity generation from wind energy is a fundamental issue of today but any decision relating to the level of investment in wind energy is fraught with difficulty. Assessing wind energy resources is a complicated task due to its stochastic nature.

A preliminary assessment of wind energy resources may be based on meteorological data. Meteorological stations are mainly located at large distances from one another, are often sited in the vicinity of trees and tall aerodynamic buildings, and do not have measuring equipment working continuously. This means that the average wind speed reported in the literature (climate maps) can significantly differ from the average velocity defined more precisely for energy purposes. Furthermore, the climatic zone in which Poland resides can see significant changes in meteorological conditions in consecutive years. Therefore, any analysis of results of observations should be based on long-term studies, the standard period being for three-years. A series of annual measurements are the minimum required. The most favourable elevation for measurements is taken at the height of the projected axis of the wind turbine rotor above ground level. However, measurements conducted in meteorological stations are usually carried out at a lower height, as wind measurements at high altitudes are costlier due to the fact that they require a high mast with a complex construction. Therefore, wind speed recordings taken at much lower elevations than the actual or intended height of the nacelle of the wind turbine have to be extrapolated for higher altitudes. It is a very difficult task and feasible only in approximate terms. This is due to the fact that, in changing the wind profile in relation to height, it is also necessary to take into account the formation and development of the land and the atmospheric stratification conditions [1].

This article explores the issue in the light of experimental studies.

2. Studies of the kinetic energy of wind

Studies of the kinetic energy of wind were made in the Subcarpathian province at location 304 m above sea level. According to the six-class roughness model by Żmuda [2], the area on which the measurements were undertaken correspond to the roughness class 2 scale. An anemometer LB-747 was used to measure the wind speed. The measurements were sent from the device in a digital format to the data collection master system of an LB-486 converter. The measurements were undertaken over a three-years period from the beginning of 2007 to the end of 2009.

The average monthly wind speed was calculated as an arithmetic average of the daily average, while the daily average was calculated as an arithmetic average of the measurements taken every 10 minutes throughout the day and night.

According to the Institute's data readings, it is necessary to interpolate an average wind speed in the measurements. For this region, the measurements should be about 4 m/s [3].

Wind power depends on the wind speed to the third power [4]. In accordance with this and assuming the same air density, the following ratio occurs:

$$\frac{\text{energy}_{V=4.0 \text{ m/s}}}{\text{energy}_{V=5.03 \text{ m/s}}} = \frac{4^3}{5.03^3} = \frac{64}{127.3} = \frac{1}{2} \tag{1}$$

$$\text{energy}_{V=4.0} = \frac{1}{2} \text{energy}_{V=5.3} \tag{2}$$

Therefore, the increase of wind speed by a factor of 25.75% from 4 m/s to 5.03 m/s will result in a two-fold increase in wind energy.

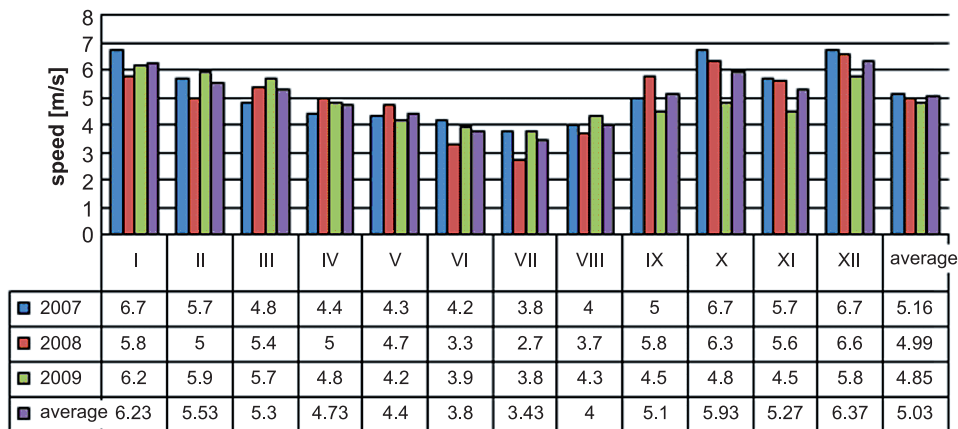


Fig. 1. Distribution of monthly average wind speed measurements for three consecutive years, and the three-year average

The expected number of hours of wind activity at a certain speed at a given average wind speed can be determined by the Weibull distribution model in graphical or tabular format [5].

As can be seen in Figure 2a, the actual distribution of wind speed in a given area and in a given year may significantly differ from one calculated by the Weibull distribution graph

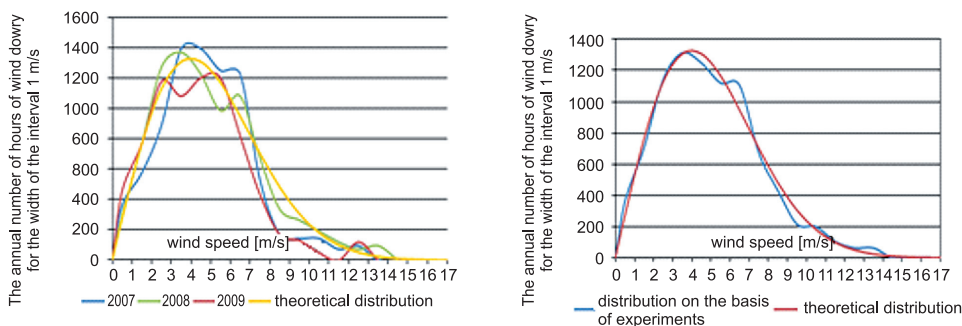


Fig. 2. a) Distributions recorded on the basis of actual measurements for three consecutive years of readings; b) The annual number of hours of wind activity for three years as averaged measurements (blue curve), together with the theoretical Weibulla distribution (red curve)

(yellow curve). However, measurements taken and then averaged out over a longer period of years bring the results of the experiment closer to a theoretical Weibull distribution curve – as shown in Figure 2b.

In relation to the three-year average wind speeds, it is important to ascertain what kind of fluctuations occur in individual months and in different years (Table 1).

Table 1

Fluctuations in wind speed in different months of the year compared to the three-year average

Three-year average	Monthly wind speed											
	I	II	III	IV	V	VI	VII	VIII	IX	X	XI	XII
	6.2	5.5	5.3	4.8	4.4	3.8	3.4	4	5.1	5.9	5.6	6.4
	%											
2007	+1.5	+3.6	-9.5	-8.4	-2.3	+10.5	+11.7	0	-3.9	+11.6	+5.5	+3
2008	-12.2	-9.1	+1.8	+4.1	+6.8	-13.2	-20.6	+7.7	+11.5	+5	+3.7	+1.5
2009	-6.1	+7.2	+7.5	0	-4.6	+2.6	+11.7	+7.5	-11.8	-18.6	-19.6	-9.4

As can be seen, the deviation from the three-year average (about 94%) does not exceed +/-15% most of the time. The displacement values in the remaining period of time does not exceed 21%. These deviation rates show what to expect in terms of variations in practice.

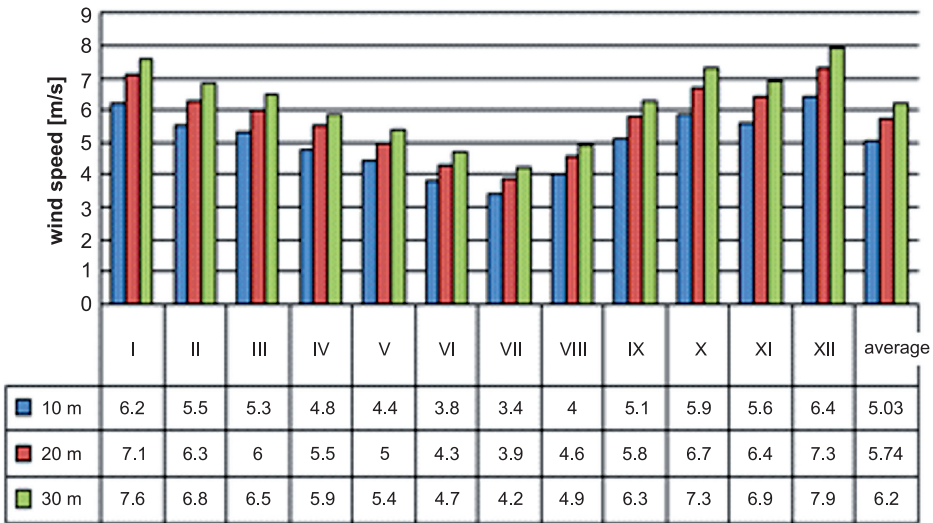


Fig. 3. Extrapolation for the area of roughness class 2 and averaging time 1 h

Wind speed measurements are usually conducted at a lower altitude than the anticipated/ planned height of a wind turbine nacelle of. However, the approximate wind speed at a height above or below the height at which measurements were conducted for this study can be calculated from Sutton’s power-law formula [4, 5].

Figure 3 shows the approximate wind speed at a height of 20 and 30 m above ground level, as calculated by Sutton’s power-law formula.

3. The concept of using wind power plant

Furnished with the average annual wind speeds and applying the Weibull distribution formula, we can determine the production output of electricity by a wind power plant and then identify the most suitable location to meet the required electricity energy needs of the building in question.

Figure 4 shows the power generation characteristics of commercial, catalogue standard power wind turbines with respective outputs of 1 kW; 2 kW; 3 kW; 1.8 kW; 1 kW; 3.2 kW.

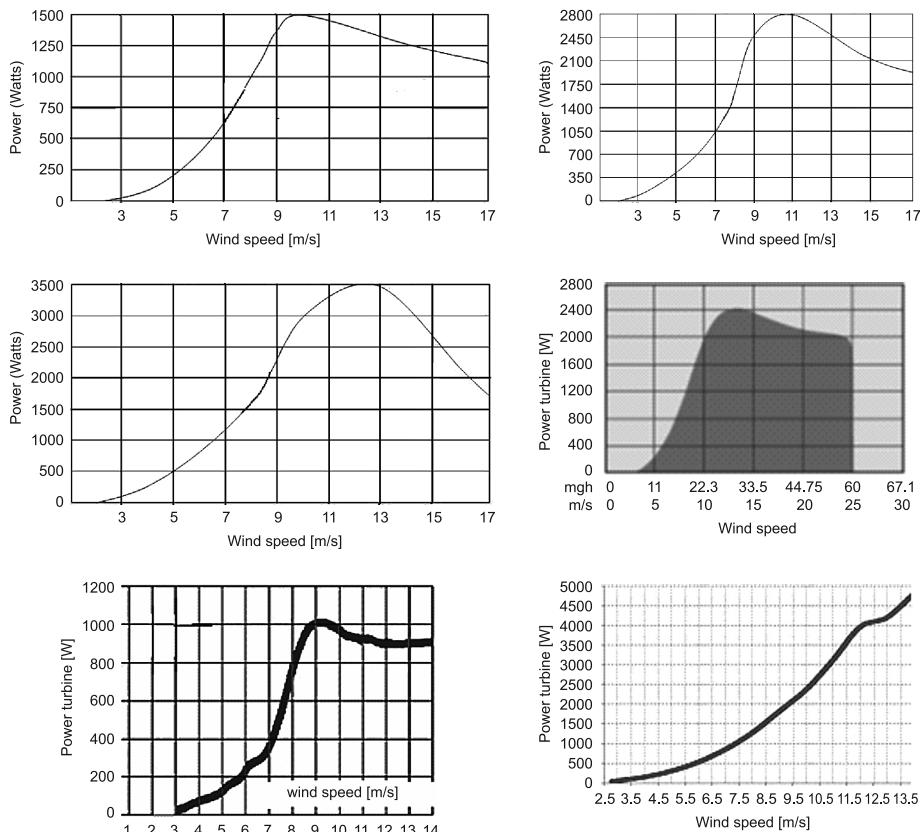


Fig. 4. Power characteristics of a wind turbine with a power output of 1 kW; 2 kW; 3 kW; 1.8 kW; 1 kW; 3.2 kW [6, 7]

Figure 5 shows the energy production levels of electricity, depending on the elevation of the wind turbines nacelle with the power characteristics as shown in Fig. 4, at a wind speed of 5 m/s at 10 m above ground level.

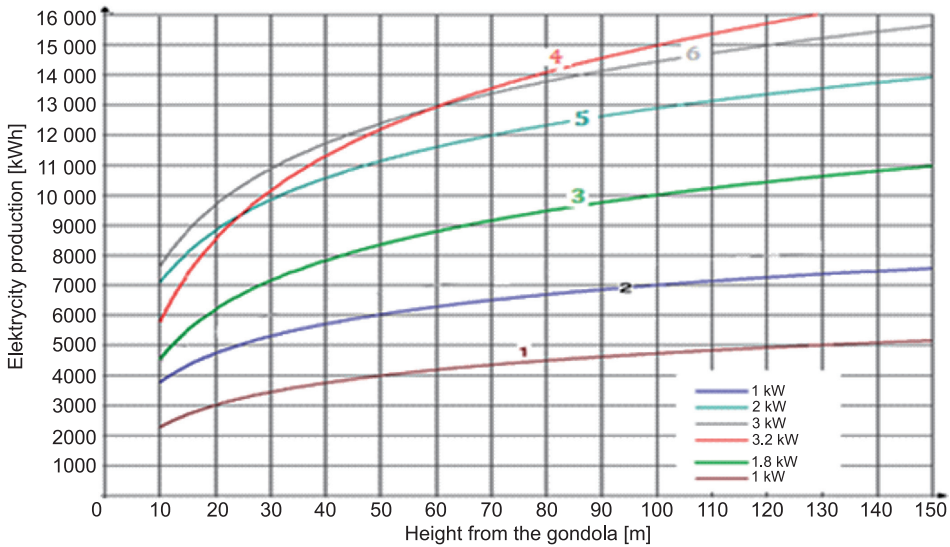


Fig. 5. Wind power plant electricity generation with the nacelle at different elevations

Curves 2, 5, 6 show production levels of electricity for a wind power plant from the same manufacturer, with the same startup speed and respective capacity – 2 m/s of 1, 2, 3 kW. Graph 1 shows the production of energy by another manufacturer’s wind turbine, albeit, similar to Graph 2 with a power of 1 kW, but a take-off speed of 3 m/s. Graph 4 shows the production of electricity with a capacity of 3.2 kW and a starting speed of 3 m/s. As can be seen from Fig. 7, it is not always the case that the greater the power of a wind turbine, the greater is the production of electricity.

Table 2

Production of electricity in thousands of kWh per year, depending on the average wind speed and plant power

Wind speed [m/s]	Power wind power plant					
	1 [kW]	2 [kW]	3 [kW]	5 [kW]	10 [kW]	20 [kW]
4	1–1.5	2–3	2–4	4–7	5–9	6–10
4,5	1.5–2	3–4	3–5	5–9	7–13	9–14
5	2–2.5	4–5	4–6	7–12	10–16	13–17
5,5	2–3	5–6	5–7	8–13	14–20	15–20
6	2.5–4	6–7	6–8	10–14	18–26	18–22
6,5	3–5	7–8	7–9	12–16	23–29	21–26
7	4–6	8–9	8–10	14–17	26–32	28–34

4. The accumulation of electrical energy

In the case of an independent (autonomous) power system in a detached house, electricity demand throughout the year can only be met by using batteries of a sufficiently large capacity – preferably located in the building. This is because, in winter, low temperatures cause a deterioration in energy recovery efficiency levels.

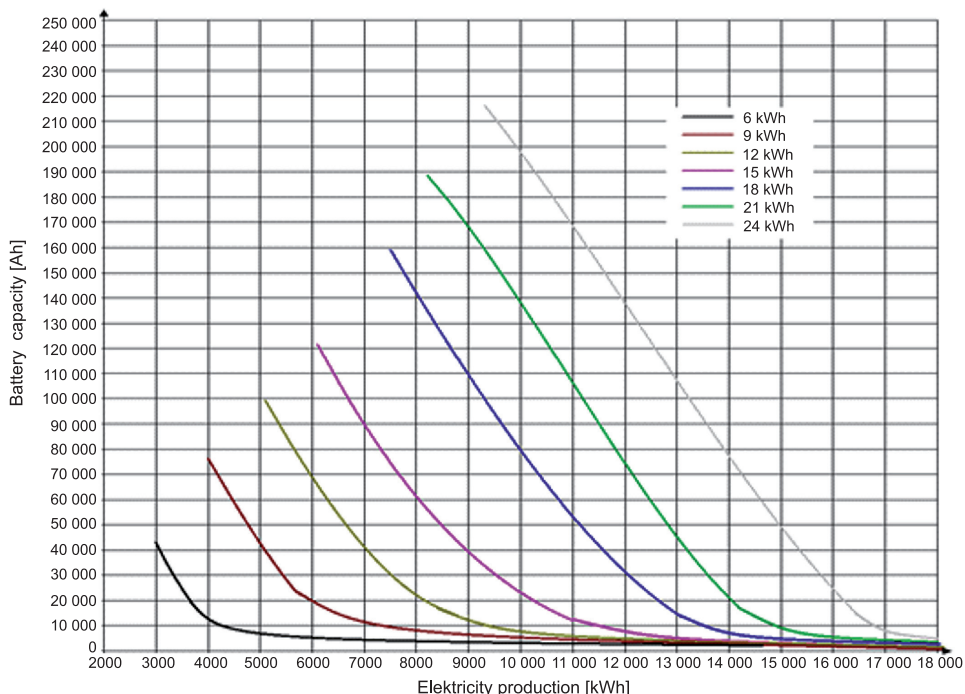


Fig. 6. The battery's running-time capacity measured against electricity production by the wind power plant, comparing results for varying daily energy demand (nominal voltage of a 12 V battery)

Figure 6 shows battery capacity dependence from electricity production of a wind power plant providing for a variety of daily energy needs.

5. The demand for electricity in a building

The electrical energy demand for detached houses (low energy buildings) varies depending on the cladding and the types of electrical appliances in the building. Examples of the levels of electricity demand are shown in Table 3.

As can be seen from the data in Table 3 and in Fig. 4, there is potential for an autonomous power system based on small wind turbines. However, due to the stochastic nature of wind

energy, it is necessary to supplement production, accumulation and storage of energy using batteries on a periodic basis.

Table 3

Building demand for electricity and the battery capacity of electricity

Lp.	Demand for electricity	The wind turbine should produce	The amount of chemical batteries 230 [Ah], 12 [V]
1.	3 500	4 900	230
2.	4 000	5 530	270
3.	4 300	6 100	250
4.	4 500	6 300	300
5.	5 000	7 000	330
6.	6 300	8 820	410

6. Conclusions

There is potential for operating a stand-alone power system derived from wind energy for single-family dwellings. The stochastic nature of wind energy requires periodic storage of and access to the energy produced.

Wind speed measurements obtained at selected measuring points, averaged out over three years, differed by 25.75% from the results detailed in the corresponding IMiGW published studies. Variations, in wind jet power show a discrepancy rate of up to 100% in some cases, because the power of the wind stream is proportional to the cube of wind speed movement in the airstream. These discrepancies can be explained because average speeds often vary to a significant degree at two distant points in a given area. It follows that the selection of locations for wind power plants requires an assessment of wind energy resources as near to the intended site as possible.

The biggest difference between the average wind speeds, averaged out for the same monthly period each year, occurred in October (almost 29%).

In contrast, the largest deviation of the average monthly wind speed for the three-year average period occurred in July 2008, when the wind speed reached 2.7 m/s and the three-year average for the month was 3.4 m/s. The wind speed difference was nearly 21%, and this difference (expressed in terms of the wind power plane) was about 80%.

It should be emphasized that a statistical distributions of wind speeds for a three-years period ought to provide a good statistical match with the theoretical Weibull distribution formula.

References

- [1] Gumuła S., Stanisław K., Ważniak A., *Influence of selected factors on the capacity utilization nominal power of the wind and the economic indicators of energy production*, Systems Journal of Transdisciplinary Systems Science, Vol. 13, 2008.

- [2] Lorenz H., *Structure and wind energy resources in Poland*, Materials Research, Series: Meteorology, 25.
- [3] <http://ww.imgw.pl>
- [4] Gumuła S., Knap T., Strzelczyk P., Szczerba Z., *Energetics wind*, Uczelniane Wydawnictwo Naukowo-Techniczne, AGH, Kraków 2006.
- [5] Soliński J., *Energy and economic aspects of wind energy*, GSMiE, PAN, Kraków 1999.
- [6] <http://www.xenergy.pl>
- [7] <http://www.windpower.com.pl>

DARIUSZ HEIM*, MARCIN JANICKI*, EWELINA KUBACKA*

A MODEL OF INFILTRATING AIR FLOW AND ITS DISTRIBUTION IN A ROOM WITH A DOUBLE SKIN FAÇADE

MODEL DYSTRYBUCJI POWIETRZA INFILTRUJĄCEGO DO BUDYNKU PRZEZ FASADĘ DWUPOWŁOKOWĄ

Abstract

In the paper, the authors analyzed the impact of space and time discretization on the simulation results of air flow through the double skin façade and its distribution in the adjacent zone. Temperature and air flow in the different parts of the room were considered, taking into account the influence of changeable solar irradiation and wind speed. The calculations additionally took into account: geometry of the zone and its position in the building; weather conditions; façade orientation relative to the cardinal directions; size and types of ventilation components in the network flow.

Keywords: double skin façades, air flow, natural ventilation, solar energy conversion, simulation

Streszczenie

W artykule przeanalizowano wpływ dyskretyzacji w przestrzeni i czasie na wyniki obliczeń przepływu powietrza przez fasadę budynku i jego dystrybucji w pomieszczeniu. Rozważano parametry termiczne w poszczególnych fragmentach pomieszczenia z uwzględnieniem oddziaływania promieniowania słonecznego i przepływu powietrza o różnych stopniach intensywności. W obliczeniach uwzględniono dodatkowo: geometrię pomieszczenia oraz jego umiejscowienie w budynku, warunki pogodowe, orientację elewacji względem głównych kierunków geograficznych, a także wielkość i metodę definiowania otworów wentylacyjnych w sieci przepływów.

Słowa kluczowe: fasady podwójne, przepływ powietrza, wentylacja naturalna, konwersja fototermiczna, symulacja

* Ph.D. D.Sc. Eng. Dariusz Heim, M.Sc. Eng. Marcin Janicki, M.Sc. Eng. Ewelina Kubacka, Department of Environmental Engineering, Faculty of Process and Environmental Engineering, Lodz University of Technology.

1. Introduction

In engineering practice, there are many cases in which the complexity of the physical phenomena of construction and their thermal inertia have a significant impact on building assessment methods, which requires the use of advanced computational techniques. Methods based on numerical solutions of physical processes occurring at the boundary of the building and the external environment, generate results burdened with relatively low errors when the problem is properly defined with regard to both space and time. For building components exposed to the intense impact of the external environment, with no doubt, all the elements exposed to solar radiation and wind pressure can be included, in particular, highly glazed and ventilated building envelopes. One of the practical solutions of this type of components are Double Skin Façade systems (DSF). Those are the systems in which the specificity of transient phenomena is just as important as the long-term effects.

The paper presents a short description of the different approaches to space discretization by the Air-Flow Network (AFN) method in space and time. AFN was applied for simulations of heat and mass transfer in the naturally ventilated office room with Double Skin Façade (DSF) applied on the certain percentage of external envelope. For the purpose of research, the computational system ESP-r was employed. It is an integrated energy modelling tool for the simulation of thermal and visual performance of buildings and energy use. The system is equipped to model heat, air and electrical power flows at a user determined resolution. Systematics of selected types of models is outlined in the next section of the paper together with a brief explanation of air-flow network modelling techniques. All simulations were performed using a Polish weather data set prepared for the city of Lodz [1]. The total value of flow rate and air velocity between components was calculated with the time step amounting to 5 or 60 minutes.

Finally, sample results representing the effect of natural ventilation, with the air stream passing through the buffer zone of the façade, during the selected one-month period is discussed. Based on the obtained results, it was found that variation in the vertical/horizontal cross-section of the zone does not generate measurable differences in the context of the volume flow rate counted for comparable connections in the AFN. However, the division of the zone allows for the estimation of the gradation of the internal zone temperature. These results show potential for the further use of AFN in the thermophysical analysis without the necessity for the implementation of time consuming CFD techniques. What should be emphasized and was revealed in the results is that the simulation of air-flow through large openings between thermal zones can act as an oscillating flow. This situation is caused by a simulation engine which re-evaluates conditions at fixed intervals, while in the real world, the flow continually adapts in the whole zone and endeavors to self-balance under changing conditions.

2. Methods

A lot of experimental and numerical analysis has been conducted up til now for the DFS system. Air flow through the façade was analyzed numerically by both: Manz & Frank [2] and Safer et al [3] to investigate strategies leading to a reduction of the overheating

during summer and winter. Additionally, combining DSF with HVAC systems was assessed numerically and experimentally by Stec & Paassen [4]. All the main strategies to optimize the energy efficiency of DSF were summarized by Saelens et al. [5].

According to the commonly accepted classification [6], DSFs may be divided into different categories. For the purpose of analysis, a single-storey and partially glazed type of façade was applied. The proposed air curtain system with operable openings improves the thermal insulation of the transparent part of building envelope during the absence of sunlight, especially in the heating season – when the openings tend to be closed for most of the time (Fig. 1a–c). During exposition of the intense solar irradiation in the cooling season (Fig. 1d–f) the DSF is considered as a ‘solar chimney’, extracting air from the cavity through openings in the skins (inlets and outlets tend to be opened at that time) [7]. The driving force of air movement in the cavity is natural ventilation induced by a combination of the stack effect and the wind pressure distribution at the external skin. The intensity of the air flow in the cavity increases when ventilation in the façade is combined with natural or mechanical ventilation in the zone.

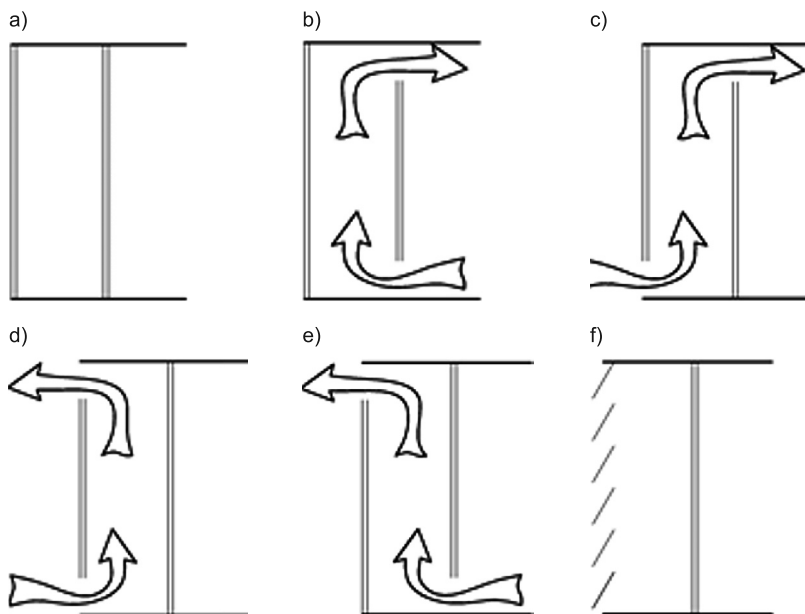


Fig. 1. Distinguish between DSFs due to method of air exchanged between the zone, the adjacent facade and the external environment

Modelling of thermal phenomena for the dynamic simulation of buildings requires the proper numerical description of the particular partitions and of the fluid flow. In the presented approach, all of the components are defined by the nodes representing the volume of solids or the volume of air and the associated heat capacities [8]. The thermal model is based on the finite-volume discretization heat balance method, in which elements of the building structure, zones and associated systems are represented via nodes. Energy

balance calculations are made individually for each node. Exchange of heat flux between the nodes, including conduction, convection and radiation (short and long term) is determined on the basis of the solutions of differential equations in space and time. Effects of solar radiation are taken into account in the analysis by the use of instantaneous distribution of the direct radiation, associated to scattered radiation distribution. The system of equations is solved simultaneously to keep the transient thermal equilibrium at each node, including the exchange of energy between them.

In order to determine appropriate coupling phenomena regarding heat and mass transfer, the Air Flow Network method was used. In the AFN method, zones are represented by the patterns of nodal network flow, wherein zones (nodes) with different physical parameters are linked by a flow path and remain in thermodynamic equilibrium. The network connection is described by a number of simultaneously solved nonlinear differential equations that represent the characteristics and form of the flow. Zone models vary in complexity ranging from single zone approximations of entire objects, to complex multi-zone models. Regardless of the model complexity, the flow rate through each connection proceeds with the following assumption: the amount of air flowing in and out of each zone remains at equilibrium (in accordance with the principle of mass conservation).

3. Case study

The first part of analysis was devoted to the sensitivity studies of the model under weather data set, type WYEC2 (Weather Year for Energy Calculation, Version 2) developed for the city of Lodz [1]. The same weather data set was used for the remaining simulations. The preliminary study was carried out for the whole calendar year, with a 1 hour time step, to search for appropriate volume flow rate. This volume should provide healthy indoor parameters for a 3 office user. Minimal flow rate was set to 20 m³/h per person. The sensitivity studies were performed for case the described in Fig. 2a). The system for heating and cooling was set to maintain indoor temperature in range of 20°C–26°C. 3 persons were assumed to occupy zone from Monday to Friday during office hours (8:00–16:00). According to the number of occupants, the total heat gains were specified to 220 W per person, where 120 W was delivered by the equipment. It was assumed that solar radiation would be a sufficient source of the daylight, therefore, heat gains from artificial lighting were set to zero. Network flow assumes the occurrence of 5 nodes (2 internal and 3 external – boundary with wind induced pressure). The coefficient of pressure distribution was determined for the 2 external nodes located on the façade as well as for semi-exposed walls and for one node representing air outlet (located in the zone) and for a semi-exposed roof with a slope of less than 10 [8]. The flows at nodes are a function of nodal pressures and the connected components' characteristics. Thus, two main features of components were the object of the first part of analysis – the area of opening and discharge coefficient. This two characteristics (yearly and monthly) were set-up in the number of simulations to assure an average volume flow rate at a value of 60 m³/h for the office zone.

Additionally, it was established that for certain months and air-flow controlling functions, the energy loads for cooling were nearly equal to zero. The heating season persisted from

the beginning of October till the end of April. Two months, May and September, were considered as transitional and the month of May was later considered in final analyses with two time steps – 5 or 60 minutes. The month of May was selected due to the fact that in this period, the heating and cooling energy demands are equal to zero (for a well-insulated and properly ventilated zone). The following statement was also proved by the authors in the previous publications [9] – zero energy loads leads to the switching off of the system which maintains assumed minimal and maximal temperatures and further allows air flow to function without disruptions.

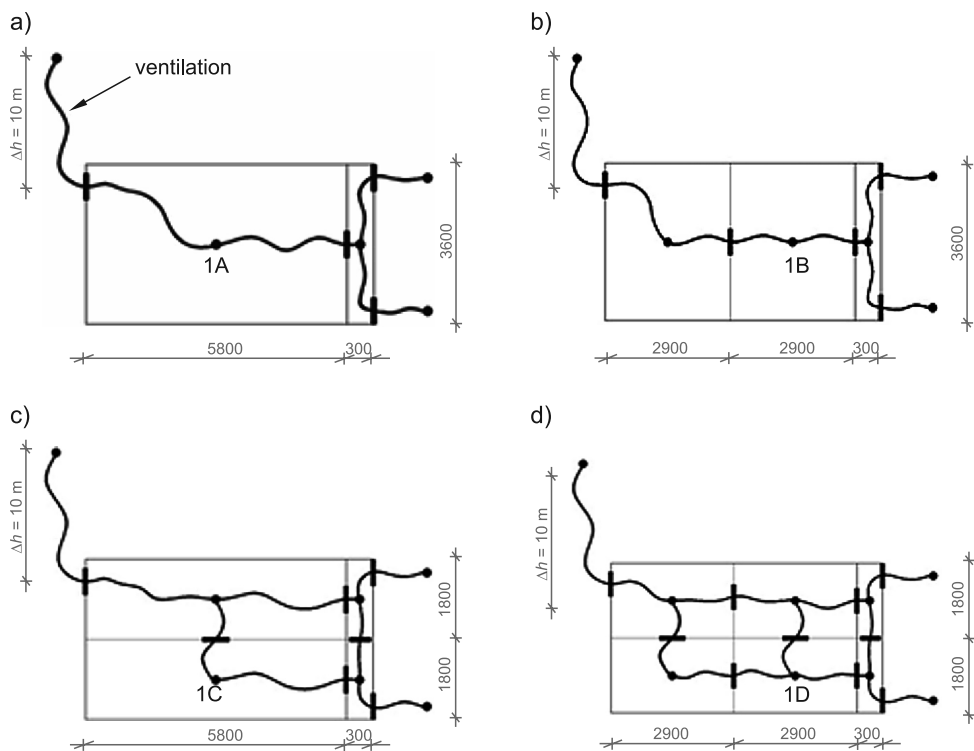


Fig. 2. Overview of analyzed cases: a) two zones Model A, b) three zones Model B with vertical division, c) four zones Model C with horizontal division, d) six zones Model D with mixed horizontal and vertical division

The main part of the analysis was devoted to the assessment of the total value of volume flow rate and air velocity through the ventilation openings extracting the air from the zone (due to impact of different zones' discretization). First, the air-flow was evaluated for the zone and façade without sub-division (Fig. 2a – Model A). In the next step, the internal zone was sub-divided into 2 (Fig. 2b – model B and 2c – Model C) and 4 sub-zones (Fig. 2d – model D) by use of horizontal and vertical partitions. In other words, the number of external nodes remained constant (3 nodes) while the number of internal nodes was set to 2, 3, 4 and 6 (Fig. 2, cases: a, b, c, d).

The influence for heat and mass transfer of internal partitions, located between sub-zones, was neglected due to the special physical properties assigned to these partitions. These partitions were prescribed using a so-called 'fictitious material', with the following assumptions: near-zero thermal mass; solar radiation and absorptivity; close unity emissivity; solar radiation penetrates the fictitious surface without major obstacles and changes in intensity of the component factors.

The area of the façade was either modelled as a single zone or divided into two zones and connected via components to create a set of flow paths. Two external nodes were assigned to the inlet and outlet. A single office area was created based on a real zone with dimensions of (depth \times width \times height) 5.8 m \times 3 m \times 3.6 m with additionally vertically added façade – given its dimensions of (depth \times width \times height) 0.3 m \times 0.6 m \times 3.6 m. The basic material structure of the initial zone was developed based on the assumption of high thermal insulation and a constant heat capacity of the compartments. As the insulating material, rock wool was applied on the internal part of the partition with the thickness equals to 200 mm, regardless of the vertical or horizontal partitions.

Due to the investigated problems of the air flow, a standardized construction of glazing was defined. From the available database of materials, clear float glass was chosen with a thickness of 2 \times 6 mm for the internal double glazed unit and 10 mm for the external single glazed unit. Air gap in the double glazed unit was filled with 12 mm of pure air. As was previous mentioned, all condition controlling systems were switched off.

4. Results

The results presented below relate to the month of May and were obtained with 5 or 60 minutes lasting time steps. Figures 3 and 4 show the Volume Flow Rates (VFR) through the zone by ventilation connections (Fig. 2a). Figures 5 and 6 show velocities recorded for the connections between nodes 1A, 1B, 1C and 1D (Fig. 2 a–d) and the nearest nodes located in the cavity of the double skin facade. Additionally, the temperatures of 1A, 1B, 1C and 1D nodes were considered to evaluate potential gradations of this parameter, these are presented on Figs. 7 and 8.

Figs. 3 and 4 show that the differences in the office zone discretization did not generate noticeable errors in the total VFRs for office zone ventilation purposes for each of the analyzed cases. The average VFR value is in each case equal to 0.02 m³/s. The highest noted value of the volume flow rate reached approx. 0.11 m³/s. Periodically 'reverse' flow was also noted (reverse in relation to the direction of flow, which for natural ventilation means suction of air by the ventilation opening), with the minimal value equal to -0.02 m³/s. Comparison of Fig. 3 and 4 indicates a lack of significant difference in the results of VFRs recorded for time step of 5 or 60 minutes.

In the future analyses of the office zone, one of the criteria of assessment could be occupant's comfort. For this reason, the temperature and velocity of air movement in the area of glazing and at the bottom area of the office zone (where users' desks are usually located) will play an important role. On that basis, nodes 1A, 1B, 1C and 1D were considered for the estimated air velocity and temperature on the nodes. A synthetic glance at Fig. 5 and 6

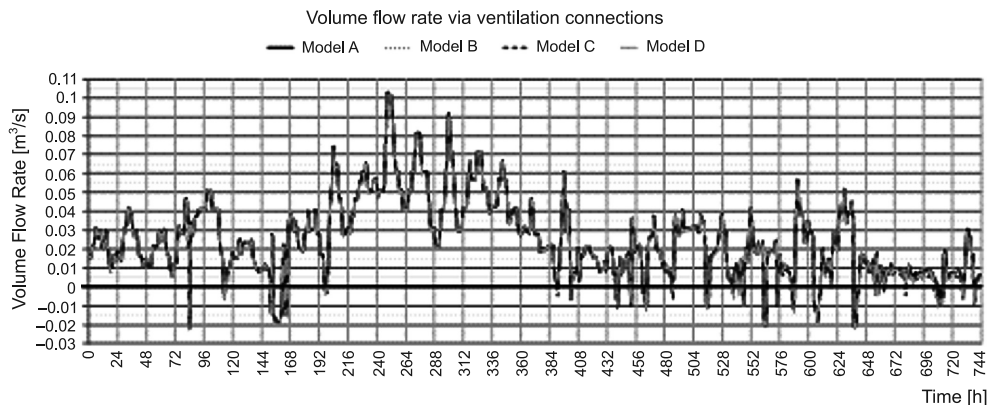


Fig. 3. Volume flow rates through the zone ventilation connections recorded with 60 min. time step

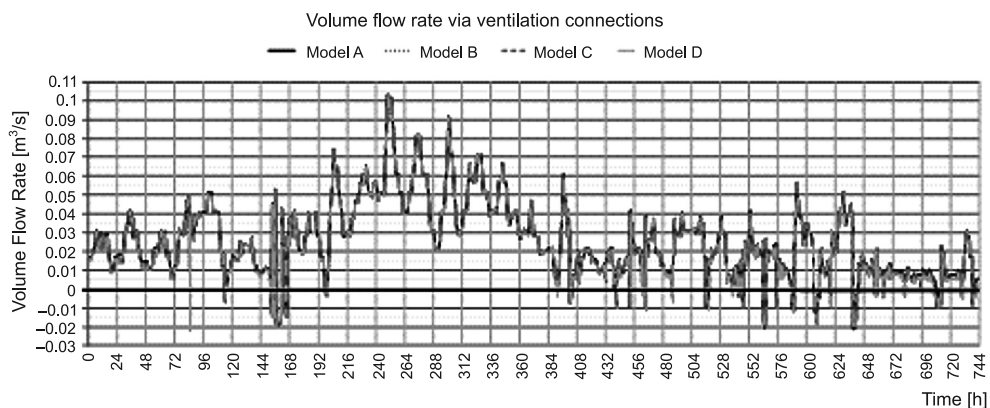


Fig. 4. Volume flow rates through the zone ventilation connections recorded with 5 min. time step

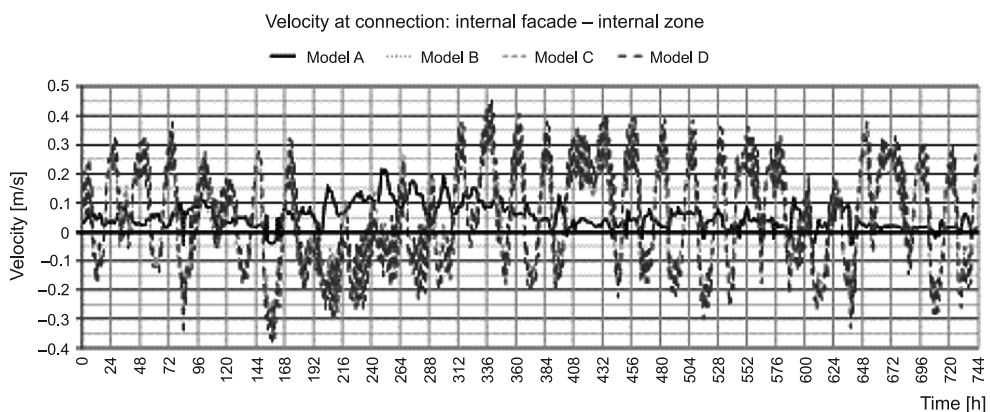


Fig. 5. Velocities at the connections between nodes 1A, 1B, 1C and 1D (see Fig. 1 a-d) and the corresponding façade nodes recorded with 60 min. time step

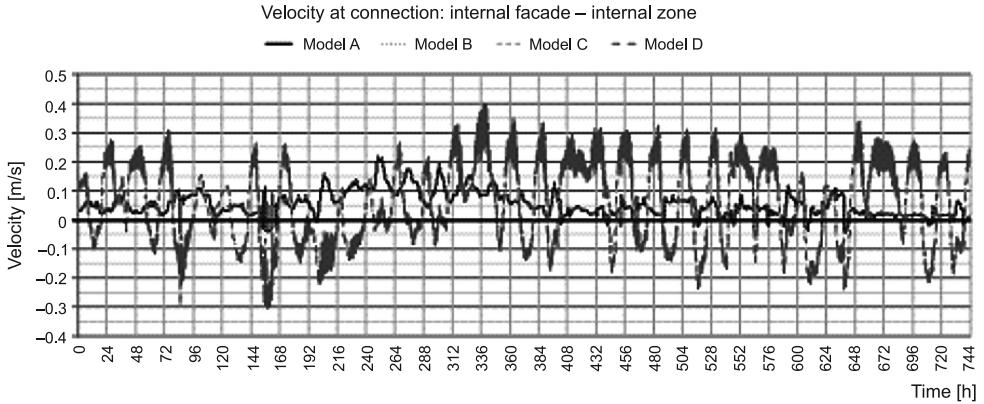


Fig. 6. Velocities at the connections between nodes 1A, 1B, 1C and 1D (see Fig. 2 a–d) and the corresponding façade nodes recorded with 5 min. time step

allows for a quick description of the results which is as follows. Between velocities recorded for model A and B, there are no divergences in the value. However, due to the fact of the zone division, velocities recorded in the results for Model C and D have greater values than in models A or B. This is the result of separation of the air flow flux from one to two channels. What is also very important, in the results for model C and D, some oscillations at the peaks in the velocities can be observed for both time steps – 5 and 60 minutes.

The velocities in models A and B usually have values greater than 0 m/s (which means that flow is consistent with ‘typical’ functioning of natural ventilation) while the values of velocities in the models C and D relatively often drops below 0 m/s (which means that flow is contrary to ‘typical’ functioning of natural ventilation). While in all 4 cases, the average velocity remains at a level of 0.05m/s, the maximum values differ significantly comparing cases A & B to the cases C & D. In models A & B, the max. value of air movement is 0.2 m/s. In models C & D, the maximum value of air movement is 0.4 m/s.

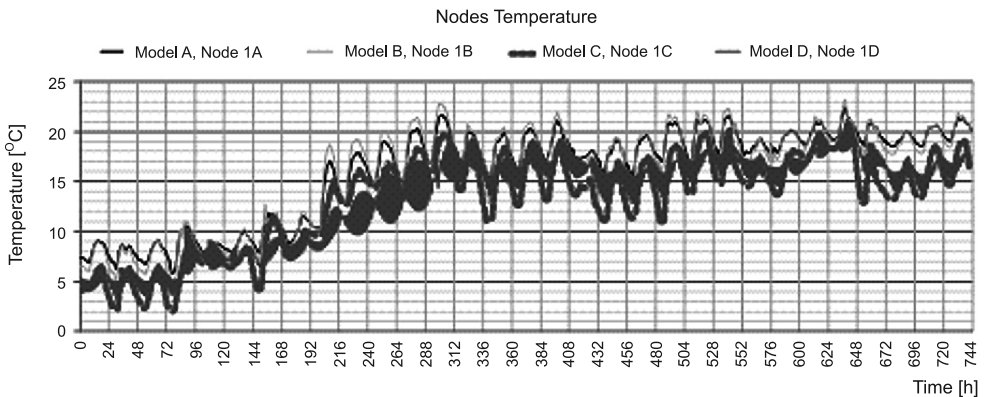


Fig. 7. Temperature of 1A, 1B, 1C and 1D nodes recorded with 60 min. time step

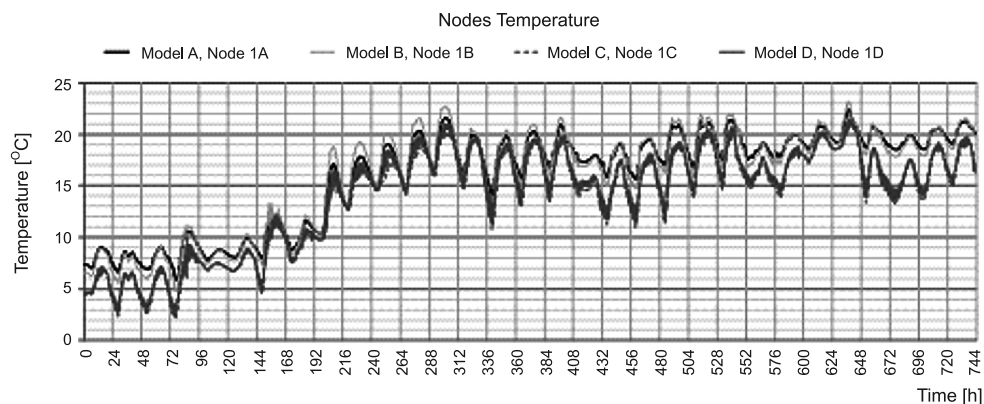


Fig. 8. Temperature of 1A, 1B, 1C and 1D nodes recorded with 5 min. time step

Similarly, in relation to the oscillations in the velocities considered above, the situation is observed for the temperatures of nodes 1A, 1B, 1C and 1D, presented in Figures 7 and 8. In the case of temperatures however, much higher oscillations occurred for the 60 minutes time step results. The greatest oscillations were noticed for the fluctuation of the temperature for node 1D, in model D, computed with a 60 minutes time step. For the 5 minutes time step, these oscillations were significantly lower for the same case. Also, noticeable differences are recorded due to the different locations of the considered nodes. The highest temperature was recorded for node 1B in Model B, and the lowest temperatures for node 1D, in model D.

5. Result analyses and discussion

On the basis of the presented results, the following conclusions can be drawn. The method of discretization of office zone in time and space does not significantly affect the volume of air flow through the ventilation. For all four models, the average value of the flow rate through the zone was approximately $0.02 \text{ m}^3/\text{s}$, which corresponds to $72 \text{ m}^3/\text{h}$. This value satisfies the requirements to ensure hygienic conditions for the office users. However, it is also highly variable and depends on the boundary conditions, namely wind speed pressure distribution at the external nodes. In extreme cases, the flow rate can reach values of up to $0.1 \text{ m}^3/\text{s}$, which corresponds to approx. $360 \text{ m}^3/\text{h}$ and far exceeds the expected value. In the other recorded cases, natural ventilation performs as air supply instead of air exhaust, what is not a preferred phenomenon because of accumulated in chimneys dirt and sediments.

Due to the assessment of user comfort and, associated with these analyses, the air flow velocities and temperature of the selected nodes, the results prompt caution. An obvious phenomenon is the appearance of a different distribution of air flow velocities and temperature of the nodes – the authors raised no less concern towards the revealed oscillations observed for certain parameters of selected nodes. It turns out that the errors of numerical solutions grow dramatically when the network flow goes through the large openings, leading to oscillation in the range of 8%–15% for the 5 and 60 minutes time step respectively. It is therefore

recommended in the literature [9], and was confirmed by the results presented on the Figures 7 and 8, that the simulation of the network flow through the large openings should be done using a time step no longer than one minute. This will allow for the estimation of results with an error decrease within the range of 1%–2%.

The conducted simulations lead to the conclusion that in order to obtain the most reliable and accurate results, simulation models should be designed accurately. Formation of the proper air flow network, constructed from the optimal number of nodes and their correct distribution, has the most significant influence on the results.

References

- [1] Narowski P., Janicki M., Heim D., *Comparison of Untypical Meteorological Years (UMY) and their influence on building energy performance simulations*, Proc. of Conference “Building Simulation – BS2013”, Le Bourget-du-Lac, 2013, 1414-1421.
- [2] Manz H., Frank Th., *Thermal simulation of buildings with double-skin façades*, Energy and Buildings, Issue 37, 2005, 1114-1121.
- [3] Safer N., Woloszyn M., Rusaouen G., Roux J.-J., *Numerical studies with CFD approach of the heat and air flow transfers combined with solar radiation in double-skin façades*, The 21th conference on passive and low energy architecture (PLEA 2004), Eindhoven 2004.
- [4] Stec W.J., van Paassen A.H.C., *Symbiosis of the double skin façade with the HVAC system*, Energy and Buildings Issue 37, 2005, 461-469.
- [5] Loncour X., Deneyer A., Blasco M., Flamant G., Wouters P., *Ventilated Double Façades – Classification & illustration of façade concepts*, Belgian Building Research Institute 2004, Department of Building Physics, Indoor Climate and Building Services, BBRI, 2004, 8-17.
- [6] Saelens D., Roels S., Hens H., *Strategies to improve the energy performance of multiple-skin façades*, Building and Environment, Issue 43 (4), 2008, 638-650.
- [7] Saelens D., *Energy performance assessment of single storey multiple-skin façades*, PhD Thesis, Katholieke Universiteit Leuven, Leuven, Belgium 2002, 107-108.
- [8] Clarke J.A., *Energy simulation in building design*, 2nd-edition, Butterworth-Heineman, Oxford 2001
- [9] Samuel A., Hand J., *CFD assessments within strongly transient domains*, Proc. of X IBPSA Conference BS 2007, Beijing, 2007, 945-951.
- [10] Heim D. et al., *Optymalizacja fasad podwójnych pod kątem oszczędności energii i jakości środowiska wewnętrznego*, Wyd. Politechnika Łódzka, Łódź 2013.

IRENA ICKIEWICZ*

WHITE CERTIFICATES – LEGAL, TECHNICAL AND ECONOMIC ASPECTS

BIAŁE CERTYFIKATY – UWARUNKOWANIA PRAWNE, TECHNICZNE I EKONOMICZNE

Abstract

The present article describes the basic legal, technical, and economic aspects of the functioning of the White Certificate Scheme in Poland. A method of performing the energy audit process (a basic element of the tender procedure) in a simplified way is presented. Essential conditions which guarantee participating in tender procedures as a necessary condition for getting bonuses for the implementation of investments resulting in reducing the primary energy consumption are also listed in this paper.

Keywords: White Certificates, energy audit, invitations to tender

Streszczenie

W artykule zamieszczono podstawowe uwarunkowania prawne, techniczne i ekonomiczne funkcjonowania BC w Polsce. Przedstawiono sposób sporządzenia audytu efektywności energetycznej (podstawowego elementu w procedurze przetargowej), wykonanego w sposób „uproszczony”. Zwrócono również uwagę na istotne warunki gwarantujące przystąpienie do przetargu jako niezbędnego działania do uzyskania premii za realizację inwestycji generujących efekt w postaci zmniejszenia zużycia energii pierwotnej.

Słowa kluczowe: Białe certyfikaty, audyt efektywności energetycznej, przetargi

* D.Sc. Ph.D. Eng. Irena Ickiewicz, Associate Prof., Faculty of Civil and Environmental Engineering at Białystok University of Technology.



1. Introduction

The Directive of the European Parliament and of the Council 2012/27/EU of 25 October 2012 on energy efficiency (amending Directives 2009/125/EC and 2010/30/EU and repealing Directives of 2004/8/EC and 2006/32/EC) obliges the European Union Member States to develop National Energy Efficiency Action Plans every three years [1]. In order to meet these requirements, Poland created its first National Energy Efficiency Action Plan (1st NEEAP). The purpose of the first NEEAP was to save final energy in an amount which is equivalent to **no less than 9%** of the annual average amount of the final energy consumption from the period 2001–2005 (i.e. 53 452 GWh) by the year 2016. The subsequent second National Energy Efficiency Action Plan (2nd NEEAP) was adopted by the Polish government in April 2012. In the 2nd NEEAP, the effectualness of applying the energy efficiency means suggested in the 1st NEEAP, i.e. in the period 2008–2009, and of the forecast energy savings by the year 2016, was analysed.

As the results of these analyses and computations conducted by experts showed, the energy savings in the years 2008–2009, mainly resulting from a ‘motivating’ increase in energy prices, proved to be unsatisfactory (the energy prices in Poland have increased threefold during the last few years and they are currently among the highest prices in Europe, but this fact has not caused any noticeable reduction in energy consumption). This situation leads to the conclusion that it would not be very possible to achieve an increase in energy efficiency exceeding **1%** per year (according to the EU recommendations) in subsequent years. To meet these requirements, it was assumed in the 2nd Polish National Energy Efficiency Action Plan that the amount of energy saved in Poland in 2016 should be equal to 4.5 Mtoe (million tonnes of oil equivalent).

To that end, the following 4 main mechanisms of action were suggested:

- projects concerning energy efficiency, financed by the National Fund of Environmental Protection and Water Management (NFEP&WM) (0.7 Mtoe),
- the Thermomodernisation and Repairs Fund (0.7 Mtoe),
- information campaigns and the so-called ‘soft’ actions (0.9 Mtoe),
- White Certificates (2.2 Mtoe).

It has to be emphasised that almost a half of the planned 4.5 Mtoe of energy savings, i.e. 2.2 Mtoe, should come from the White Certificate Scheme.

2. White Certificate Scheme in Poland

White Certificates are documents certifying energy efficiency, which can be obtained for implementing measures aiming at increasing the energy efficiency of buildings. The White Certificate Scheme (WCS) has been functioning in the European Union for over 10 years now, e.g. since 2001 in Italy, since 2002 in Great Britain, and since 2006 in France.

In Poland, the WCS was implemented pursuant to the Act on energy efficiency of 15.04.2011. The Act imposes an obligation to obtain White Certificates and submit them for redemption to the President of the Energy Regulatory Office (ERO) on the following groups of entities:

- energy sector companies which sell energy to final users,
- final users connected to the power grid within the territory of the Republic of Poland, who are trading members as provided for in Art. 2 (5) of the Act of 26.10.2000 on commodity exchanges,
- commodity brokerage houses which enter into transactions commissioned by final users connected to the power grid within the territory of the Republic of Poland.

The introduced White Certificate Scheme assumes generating measurable energy savings in three areas:

- by final users,
- in own equipment,
- reducing power, heat, and natural gas loss during their transmission and distribution.

Invitations to tender for White Certificates are issued by the ERO President in the above three areas (categories) of undertakings aiming at improving energy efficiency. The tender procedures adopted for the White Certificate Scheme are aimed at stimulating energy-efficient behaviour in the form of selecting projects including the most effective solutions, i.e. solutions **which ensure the highest energy savings at the lowest level of direct support**. The ERO President is authorised to issue and redeem the Certificates. Property rights resulting from White Certificates are transferable and constitute goods traded on the power exchange.

The first invitation to tender for WCs in Poland was issued on 31.12.2012, and the winning tender was selected as late as on 13.09.2013. Approximately 100 tenderers submitted 212 tenders (it was possible for one bidder to submit more than 1 certificate). Unfortunately, as many as 107 out of the 212 certificates submitted for the tender were rejected because they contained mistakes. The basis for rejecting all these 107 offers was Section 10 (3) (1) of the Regulation on tender offers, which says, ‘the offer does not include an appropriately filled in tender declaration or energy audit form’.

The second invitation to tender was announced on 27.12.2013, with one month for potential contractors to submit their proposals, i.e. until 27.01.2014. Certain amounts of energy efficiency certificate values were allocated to each of the 3 categories of undertakings, and acceptance percentages (ts) were established. For the 1st invitation to tender, this percentage amounted to $t = 0.5$, and for the 2nd invitation to tender $t = 0.4$. It needs to be emphasised that the acceptance percentages adopted in both of these invitations to tender were very low (0.5 and 0.4, respectively). The Certificate values for the particular categories, as determined by the ERO President, are listed in Table 3 in Section 3 of this article.

The certification process was previously applied in Poland in the fields of renewable energy (the so-called green certificates) and of generating combined heat and power (the so-called red certificates).

2.1. Conditions and procedures

It is possible to obtain a White Certificate for a pro-efficiency project which has already been implemented (but which was not completed prior to 1 January 2011) or for a project which is planned to be implemented, provided that the amount of energy saved as a result of such project is not less than **10 tonnes** of oil equivalent (toe) per year. A White Certificate can also be issued collectively for multiple projects of the same kind, for which the total

amount of energy saved exceeds 10 toe (10 tonnes of oil equivalent correspond to the energy produced by the combustion of e.g. 15.6 tonnes of hard coal or 11800 litres of fuel oil).

Conditions for obtaining a **White Certificate**:

- a) an energy efficiency audit including the suggested technical solutions must be carried out for a selected pro-efficiency project,
- b) the optimal solution in terms of technical and economic aspects must be selected,
- c) an offer must be submitted as a response to an invitation to tender,
- d) after an energy performance certificate is received, the pro-efficiency project has to be implemented according to the guidelines from the preliminary audit. After the modernisation works have been completed, an energy efficiency audit confirming the declared energy savings (the confirming audit is performed for the declared energy savings exceeding 100 toe as the annual average value) must be conducted,
- e) after the confirming audit is conducted (or, if it is not required, after the modernisation is finished), the entity which received the certificate must notify the ERO President within the statutory period of completing the undertaking. This constitutes the grounds for conferring the property rights arising from the certificate.

These rights constitute goods traded on the power exchange and are transferable. In practice, it means obtaining funds which will improve the economic indicators of the implemented pro-efficiency project. Pursuant to the Act on energy efficiency, entities which are obliged to receive White Certificates and which do not receive them and do not submit them for redemption, shall pay a substitution or penalty fee whose amount is determined by the said Act (PLN 1000/toe, 1 toe = 11.63 MWh) [2, 4].

2.2. Probability of obtaining White Certificates

In order for an offer to win an invitation to tender, the value of the energy performance coefficient must be between ω_{av} and ω_{max} . Certificates are issued to entities which successfully undergo tender procedures, that is, are classified within the following range:

$$t \cdot \omega_{av} \quad \text{and} \quad \omega_{max} \quad (1)$$

where:

- t – the acceptance percentage announced by the ERO President,
- ω_{av} – the average energy performance value – the average value of all the undertakings aiming at improving the energy efficiency, declared in a given tender
- ω_{max} – the highest value of energy performance declared in a given tender.

The energy performance is the relationship between the amount of energy saved on average per year as a result of the implementation of an energy efficiency improvement project (or energy efficiency improvement projects) and the value of the energy savings certificate. The ω_{av} and ω_{max} values are determined by the market [8].

While selecting the winning tender, the tender committee chooses tenders in which the declared energy performance is within the range of between $t \cdot \omega_{av}$ and ω_{max} for each category of undertakings. Table 1 presents an example of the results of a small invitation to tender and the criteria (values) which were taken into consideration when accepting and rejecting tenders.

It is assumed that 10 entities applying for certificates whose values ranged from several to a dozen tonnes of oil equivalent took part in the invitation to tender. The maximum value declared by one of the tenderers amounted to $\omega_{\max} = 3.5$, the weighed average was $\omega_{av} = 2.68$, the total amount of toe to be awarded was 160, and the acceptance percentage for the tenders was 0.9.

Table 1

Results of invitation to tender

Tenderer	Energy performance value (ω)	$t \cdot \omega_{av}$	selected offers [condition]	Entities receiving WCs	Aspects
1	3.50	2.41	within the range of between $t \cdot \omega_{av}$ and ω_{\max} ; $0.9 \cdot 2.68 = 2.41$; $\omega_{\max} = 3.5$	1	Total of 160 toe
2	3.40	2.41		2	
3	3.12	2.41		3	
4	3.00	2.41		4	
5	2.95	2.41		5	
6*	2.8	2.41		6	There were not enough WCs allocated by the ERO
7*	2.47	2.41		7	
8	2.1	2.41	Not qualified for the invitation to tender	8	Not in the range of 2.41–3.50
9	1.9	2.41		9	
10	1.6	2.41		10	

* There were 'not enough' White Certificates allocated for the given tender for the tenderers No. 6 and 7, despite the fact that their declared energy performance was within the range required by the applicable law. If this happens, these entities can offer the same undertakings in other invitations for tender, and they are not (as for now) obliged to implement the undertaking described in their tenders.

3. Energy audit

The most important part of a tender declaration in an invitation to tender for WCs is an energy audit including an energy consumption profile, information on the technical condition of a structure (or of a device or system), and a list of undertakings aimed at the improvement of its energy efficiency. Evaluating the economic feasibility and the possible energy savings is also important here.

Any pro-efficiency project implemented under any energy efficiency obligation scheme must be **appropriately documented** (in the form of an energy audit).

A detailed description of the procedure for preparing energy audits is provided in the Regulation of the Minister of Economy of the Republic of Poland of 10.08.2012 [3]. Pursuant to the Regulation, audits can be carried out using one of the following two methods:

- the balance method,
- the simplified method.

Simplified audits are conducted for **small projects**, while **balance audits** (calculations taking into account engineering estimates and the scale of the project under concern) are performed for more complex projects.

A list of undertakings aimed at energy efficiency improvement, for which simplified audits can be carried out, is provided in Appendix 1 to the Regulation [6]. These undertakings mainly concern adding thermal insulation to building envelopes, woodwork and joinery, modernisation of light fixtures or light sources, and replacement of household appliances (washing machines, refrigerators, etc.).

Energy audits with the use of the balance method include performing a full energy balance of the building (or technical device or system) under the given project. The scope of a balance audit is very much wider. In this type of audit, data and different methods concerning determining the amount of energy saved are used. This requires applying the documented method of engineering calculations, often described in other documents.

Apart from in-depth engineering analyses, balance audits of this type require measurements to be performed, and the results of the measurements need to be analysed with the use of specialist equipment as well as measuring and research methods in most cases [6, 8].

3.1. Determining amount of final energy saved as a result of introducing means aiming at energy efficiency improvement – simplified audit of energy efficiency

Determining the amount of final energy saved as a result of introducing means aiming at the energy efficiency improvement is the main purpose of the performed audit of final energy, thus checking whether the scope of the thermomodernization works is sufficient for applying for White Certificates. An example of calculating how much final energy was saved for heating purposes (as a result of thermomodernization works aimed at the energy efficiency improvement) in the case of a residential building, using the simplified method, is presented below.

3.1.1. General details concerning the building under study

The building under study is a 3-storey multi-family residential building located in the Podlaskie Voivodship, with the basement built with the use of the traditional method, with a total usable area of 1728 m², and a volume of 5184 m³. The exterior walls of the building are made from cellular brick of 38 cm thickness, $U = 1.28 \text{ W}/(\text{m}^2 \cdot \text{K})$, the roof is a full flat roof, $U = 1.64 \text{ W}/(\text{m}^2 \cdot \text{K})$. For the ceiling above the unheated basement (Ackerman), $U = 2.45 \text{ W}/(\text{m}^2 \cdot \text{K})$ and for the double-glazed window frames $U = 2.6 \text{ W}/(\text{m}^2 \cdot \text{K})$.

In the building described above, the following thermomodernization works were conducted: the exterior walls; the flat roof; the ceiling above the unheated basement was thermally insulated; the windows were replaced with new ones. The total area of the insulated exterior walls was 980 m², the area of the insulated flat roof was 576 m², and the total surface of the replaced windows amounted to 190 m². The average temperature of heated rooms was 19°C (including the staircase). The heating system of the building obtains hot water from a heat transfer station of a municipal heat distribution network.

The results of the calculations are listed in Table 2.

3.1.2. Calculations

The savings resulting from insulating the exterior walls and the flat roof were calculated from the following formula (2)

$$\Delta Q_o = \frac{0.3356 \cdot k_1 \cdot k_2 \cdot k_3 \cdot A_p \left(U_o - \frac{1}{\frac{1}{U_o} + \frac{d}{\lambda}} \right)}{\eta_i} \quad (2)$$

where:

- ΔQ_o – amount of final energy saved [GJ/year],
- k_1 – climate zone coefficient,
- k_2 – correction factor depending on the average value of the temperature in the heated room,
- k_3 – reducing factor due to the correction of the actual climatic conditions
 $k_3 = 0.90$,
- A_p – area of the insulated wall [m²],
- U_o – heat transfer coefficient for the barrier [W/(m²·K)],
- d – thickness of the insulation layer [m],
- λ – thermal conductivity of the insulating material [W/(m·K)],
- η_i – total efficiency of the heating system.

It is also possible to use the formula (2) to compute the savings resulting from insulating the basement ceiling; however, the value of 0.3356 has to be replaced with 0.1426 [3].

Savings on account of the window replacement were set from the formula (3)

$$\Delta Q_o = \frac{0.3356 \cdot k_1 \cdot k_2 \cdot k_3 \cdot A_{ok} [0.336(U_{ook} - U_{1ok}) + 0.57]}{\eta_i} \quad (3)$$

where:

- A_{ok} – surface of the replaced windows [m²],
- U_{ook} – heat transfer coefficient for the windows before the exchange [W/(m²·K)],
- U_{1ok} – heat transfer coefficient for the windows after the exchange [W/(m²·K)].

The other symbols are the same as in the formula (2).

The calculation results.

The energy savings brought about by insulating the exterior walls with a 15 cm thick layer of extruded polystyrene foam:

$$\Delta Q_o = [0.3356 \cdot 1.124 \cdot 0.942 \cdot 0.9 \cdot 890 \cdot (1.28 - 1/(0.78 + 3.75))] : 0.9 = 333.18 \text{ GJ/year}$$

The energy savings caused by insulating the flat roof with a 20 cm thick layer of extruded polyurethane foam:

$$\Delta Q_o = [0.3356 \cdot 1.124 \cdot 0.942 \cdot 0.9 \cdot 576 \cdot (1.64 - 1/(0.61 + 5.555))] : 0.9 = 336.12 \text{ GJ/year}$$

The energy savings as a result of replacing the windows with windows for which $U = 1.5 \text{ W/(m}^2 \cdot \text{K)}$:

$$\Delta Q_o = [0.3356 \cdot 1.124 \cdot 0.942 \cdot 0.9 \cdot 190 \cdot (0.336 (2.6 - 1.5) + 0.57)] : 0.9 = 189.67 \text{ GJ/year}$$

The energy savings resulting from insulating the basement ceiling with an 8 cm thick layer of extruded polystyrene foam:

$$\Delta Q_o = [0.1426 \cdot 1.124 \cdot 0.942 \cdot 0.9 \cdot 576 \cdot (2.45 - 1/(0.408 + 2.0))] : 0.9 = 177.41 \text{ GJ/year}$$

Table 2

Amounts of energy saved as a result of conducted thermomodernization works

Thermomodernization works	Area [m ²]	U coefficient [W/(m ² · K)]		Demand reduction (ΔQ_o)	
		before thermo-modernization	after thermo-modernization	GJ/year	toe
Wall insulation	890	1.28	0.220	333.18	7.958
Flat roof insulation	576	1.64	0.162	336.12	8.028
Insulation of ceiling above unheated basement	576	2.45	0.415	177.41	4.230
Window replacement	190	2.60	1.5	189.67	4.530
Total				1036.38	23.746*

* They constitute a group of works of the same kind, for which the total savings resulting from the implementation of thermomodernization works exceeded the amount of 10 toe, and are therefore the basis for applying for White Certificates.

4. Recommended undertakings aiming at energy efficiency improvement

In Art. 17 of the act on energy efficiency [2], and then in the Announcement of the Minister of Economy of the Republic of Poland [6], a detailed list of undertakings aiming at improving energy efficiency, was published. The undertakings were divided into 8 groups. In the 2 announced invitations to tender, these undertakings were classified into 3 categories; 1 – final recipients, 2 – own devices, 3 – power, heat, or natural gas loss in transmission or distribution. Some specified amounts of energy efficiency certificate values were allocated to each of these three categories. The recommended groups of undertakings as well as the certificate values allotted to them in the 1st and 2nd invitations to tender, provided for in the Announcement of the Minister of Economy, are listed in Table 3.

An analysis of the values of the energy efficiency certificates planned to be issued under the 1st and 2nd invitation to tender, presented in Table 3, shows that the vast majority of the certificate values (80%) was allocated to projects aiming at improving the energy efficiency through energy savings classified under the first category, that is, by final recipients.

Table 3

List of recommended undertakings improving energy efficiency and amounts of energy efficiency certificate values granted in 1st and 2nd invitations to tender

Project group	Scope	Cate-gory	% of amount granted ([toe])	
			1st invitation to tender	2nd invitation to tender
1	Insulation of industrial systems	1	80% (440 000)	80% (1094638.8)
2	Alteration or modernization of buildings	1		
4	Devices and systems used in industrial processes	1		
3	Modernization or replacement of own devices	2	10% (55 000)	10% (136 829.6)
6	Heat recovery in industrial processes	2		
5	Local heat distribution networks and local sources of heat	3	10% (55 000)	10% (136 829.6)
7	Reducing loss (including transmission loss)	3		
8	Replacing low-effective local and individual sources of heat with sources of higher efficiency	3		
Total [toe]			550 000	1 368 296

5. Conclusions

Pursuant to the Act on energy efficiency [2], the obligation of obtaining and cancelling WCs was imposed in Poland with the effect from the beginning of 2013, and it will continue until the first quarter of 2016. So far, 2 invitations to tender have been announced, the first one on 31.12.2012, for the total value of the certificates of 550 000 toe, and the other was published on 31.12.2013 with the total certificate value of 1 368 296 toe, which, added together, is 1 918 296 toe. Assuming that 100% of the certificate values are used, only 282 000 toe will be left for the last year, i.e. 2015 (the amount estimated in the 2nd NEEAP is 2.2 Mtoe).

By 30 October 2013, the ERO had issued only 7 energy efficiency certificates for the total amount of 1 901.00 toe. The total amount of the final energy savings declared in these certificates in the period of generating energy saving is 24 666.40 toe (which is as little as 1.12% of the established target). The total amount of the reduction in CO₂ emission, resulting from the implementation of improvements, is estimated at 212 482.100 tonnes [7]. The number of certificates issued increased to 24 in mid-November 2013.

Enterprises which received the certificates are mainly heating companies and Polskie Sieci Elektroenergetyczne S.A. Very few entities which have submitted their offers so far represented housing cooperatives, public utilities owned by local public administrative bodies (possible thermomodernization works), energy-intensive companies, or other enterprises.

Entities which fail to comply with the obligation imposed on them (of obtaining WCs) (will) have to pay a substitution or penalty fee proportional to the amount of savings below the level needed by these entities to fulfil the obligation (usually determined in Euros per unit of energy), up to the amount which does not exceed 10% of their gross revenue. In cases where an enterprise has not implemented the undertakings described in their tender declaration, or in cases where the savings generated by any enterprise prove to be lower than in the declaration, the amount of such a penalty fee might even be as much as 2 m Euros, and additionally, such an entity is excluded from procedures of awarding contracts for a period of 5 years. The proceeds from the penalty fee collection go to the NFEP&WM.

Any property rights resulting from the energy efficiency certificates are listed from the moment they are marketed until they are blocked with the intention of cancelling the energy efficiency certificate which they result from. Any certificate cancelled on or before 31 March each year is taken into account in calculating the amounts resulting from the duty of cancelling the certificates for the previous calendar year. According to the Art. of 27 (7) of the act on energy efficiency, **any property rights which are not cancelled on or before 31 March 2016, expire by virtue of law on 1 April 2016** [2].

If the experience gained during the functioning of the WC Scheme in Poland (2013–2015) proves to be effective in obtaining the planned result of increasing energy savings, and the costs of the suggested mechanism of financial support are optimal (and the energy efficiency improvement proves to be economically profitable), they can be used as valuable instructions for supporting the energy efficiency policy in Poland in the years of 2016–2020.

References

- [1] Dyrektywy 2012/27/UE z 25.10.2012 dot. efektywności energetycznej.
- [2] Ustawa z 15.04.2011 o efektywności energetycznej (Dz.U. 94, poz. 551).
- [3] Rozporządzenia Ministra Gospodarki z 10.08.2012 w sprawie szczegółowego zakresu i sposobu sporządzenia audytu efektywności energetycznej, wzoru karty audytu efektywności energetycznej oraz metod obliczania oszczędności energii (Dz.U. poz. 962).
- [4] Rozporządzenia Ministra Gospodarki z 4.09.2012 (Dz.U. poz. 1039) w sprawie sposobu obliczania ilości energii pierwotnej odpowiadającej wartości świadectwa efektywności energetycznej oraz wysokości jednostkowej opłaty zastępczej.
- [5] Rozporządzenia Ministra Gospodarki z 23.10.2012 (Dz.U. poz. 1227) w sprawie przetargu na wybór przedsięwzięć służących poprawie efektywności energetycznej.
- [6] Obwieszczenie Ministra Gospodarki z 21.12.2012 w sprawie szczegółowego wykazu przedsięwzięć służących poprawie efektywności energetycznej.
- [7] Rozporządzenie Ministra Środowiska z dnia 12 września 2008 r. w sprawie sposobu monitorowania wielkości emisji substancji objętych wspólnotowym systemem handlu uprawnieniami do emisji (szacowaniu wielkości redukcji emisji CO₂).
- [8] KAPE – System Białych certyfikatów w Polsce, MG, Warszawa 2012.

GABRIELA JAGLARZ*, FILIP CIESIELSKI*

FEASIBILITY ANALYSIS OF UPGADING AN OLD BUILDING TO THE STANDARD REQUIREMENT OF A LOW ENERGY REQUIREMENT BUILDING

ANALIZA MOŻLIWOŚCI PRZYSTOSOWANIA BUDYNKU W STARYM BUDOWNICTWIE DO STANDARDÓW BUDYNKU NISKOENERGETYCZNEGO

Abstract

The paper presents a case study analysis of the energy demand for an old building located in Cracow. Some improvements in construction of the building envelope, especially in thermal insulation and in the heating system, have been analyzed. Reduction of the energy demand index has been shown in the three variants that were considered. The goal of this study was to assess the possibility of obtaining low energy demand in a typical old poorly insulated building.

Keywords: energy demand, modernization, low energy requirements building

Streszczenie

Artykuł stanowi analizę przypadku zapotrzebowania na energię dla budynku w starym budownictwie. Wprowadzono ulepszenia w konstrukcji budynku, głównie poprawiając izolację, a także w instalacji ogrzewania. Wykazano redukcję wskaźnika zapotrzebowania na energię dla trzech rozważanych wariantów. Celem analizy było sprawdzenie możliwości przystosowania budynku w starym budownictwie do standardów budynku o niskim zapotrzebowaniu na energię.

Słowa kluczowe: zapotrzebowanie na energię, modernizacja, budynki o niskim zapotrzebowaniu na energię

* M.Sc. Eng. Gabriela Jaglarz, M.Sc. Eng. Filip Ciesielski, Institute of Thermal Eng. and Air Protection, Faculty of Environmental Engineering, Cracow University of Technology.

1. Introduction

In recent times, energy saving has become an important topic of discussion at the scientific fields of energetic and environmental engineering. The global economy is mostly based on fossil fuels such as gas, petroleum and coal. The main issues are the limited amounts of conventional fuels and the pollution caused by using them in every area of human life. In Poland, more than 90% of energy comes from fossil fuels [1] and the structure of energy consumption is equal to that of other Western European countries [2].

Table 1

The structure of the energy demand in Poland [3]

Direct Consumption	Total energy [TJ]	Percentage [%]
Mining and quarrying	56129	1.8
Manufacturing	905346	28.7
Electricity supply	110976	3.5
Water supply; waste management	23276	0.7
Construction	67552	2.1
Transport	704082	22.3
Household	821257	26
Agriculture	153895	4.9
Other	315288	10

Table 1 shows that in Poland, 26% of final energy consumption is derived from households. The EC Directive 2002/91/EC on the energy performance of buildings [4] also presents that in the European Union, more than 40% of energy consumption comes from the residential and tertiary sector. Therefore, the residential buildings are the target area to reduce energy consumption and related greenhouse emissions through improvements to the energy efficiency of these buildings [4]. Literature points out that coupling energy efficiency measures with increased renewable energy production techniques enables the generation of some or all of a building's energy consumption, thus reducing dependence on fossil fuels [5, 6]. The undertaken action should focus both on the demand and supply side of energy as is indicated in, for example, Demand – Side Management.

2. Purpose and scope

The paper presents a case study of energy performance enhancement methods in a residential building constructed in the 1980's. The subject of the study was built in the north part of Cracow. The main goal of the analysis was to check the feasibility of transforming a typical old, residential, multi-family building into a low energy requirement building by upgrading heating and ventilation installations. The National Fund for Environmental

Protection (Narodowy Fundusz Ochrony Środowiska i Gospodarki Wodnej NFOŚiGW) defined that 40 kWh/m²,year is the usable energy demand index in single and multi-family building with low energy requirement standard [7].

The presented assessment includes the calculation of energy demand for the purposes of heating and ventilation in existing state (variant 0) and also after two modifications (variant 1 and variant 2). Variant 1 is based on the improved thermal insulation of the building envelope to achieve significant reduction of heat losses. Variant 2 includes all solutions from variant 1 and also few more improvements, for example, a thicker insulation layer, a reduction of thermal bridges and the appliance of an energy efficient heat distribution system with high heat recovery.

3. Methodology

All calculations presented in this paper were done with the Audytor OZC 6.1 Pro computer program. The calculations are based on:

- A Standard PN-EN ISO 13790 [8],
- The ordinance from the Polish Ministry of Infrastructure from 6 November 2008 on the methodology of calculating the energy performance of buildings [9].

The assessment of the energy standard of a building requires the calculation of usable energy demands based on standard PN-EN ISO 13790 [8]. In order to make the analysis more accurate, the subroutine ‘Energy performance of the building’ was used. The second method enables the estimation of the energy demand for domestic hot water (DHW) and operation of auxiliary devices (pumps or fans). Moreover, with the option ‘Energy performance of the building’ it is possible to evaluate the amount of non-renewable primary energy consumption. Calculations done with both methods enable the examination of whether or not it is possible to reach the standard of a low energy requirement building.

3.1. Description of building

The examined building consists of a cellar, 50 dwellings and 4 shop premises, which are located in one underground and four above-ground floors having a total surface area of 3527 m². The estimated number of users is about 150 (3 people per dwelling). The main construction elements are made from reinforced concrete and the rest are constructed from prefabricated components. The external walls are not thermally insulated (Table 2). Ceilings are also made from prefabricated components and insulated with 2 cm of foamed polystyrene. The roof is ventilated and insulated with 12 cm of mineral wool. In wooden windows and doors, leakages occur causing heat loss and drafts.

3.2. Variant 0 – building in existing state

The building is equipped with heating installation supplied from the district heating network (MPEC Cracow), which does not have thermostatic valves or any devices for temperature regulation. Domestic hot water is prepared individually with gas boilers. The airflow in the building is calculated according to PN-EN ISO 12831-2009 [8] and is provided by natural ventilation.

Table 2

Building envelope heat transfer coefficients – Variant 0

Name	Insulation	U [W/m ² K]
Cellar external wall	Foamed polystyrene 5 cm, $\lambda = 0.045$ W/mK	0.486
External wall	–	0.479
Ceiling	Foamed polystyrene 2 cm, $\lambda = 0.045$ W/mK	1.145
Ceiling over cellar	Foamed polystyrene 4 cm, $\lambda = 0.045$ W/mK	0.686
Ventilated roof	Mineral wool 12 cm, $\lambda = 0.050$ W/mK	0.322
External window	–	2.60
External door	–	3.50

3.3. Variant 1 – first modification

The first modification in the building serves to reduce the energy consumption for the purposes of heating and ventilation and is based on improvements only in the building envelope thermal insulation. The building heating and ventilation systems are not changed in this variant.

In this variant, the insulated building envelope meets the regulations of Ordinance of Ministry of Transport, Building and Maritime Economy from 5 July 2013 [10]. Table 3 includes the modification with inserted layers of foamed polystyrene ($\lambda = 0.040$ W/mK) and mineral wool ($\lambda = 0.050$ W/mK) as well as the replacement of windows and doors.

Table 3

Building envelope heat transfer coefficients – Variant 1

Name	Insulation	U [W/m ² K]	U_{\max} [W/m ² K] [7]
Cellar external wall	Foamed polystyrene 5 cm	0.486	0.650
External wall	Foamed polystyrene 12 cm	0.247	0.250
Ceiling	Foamed polystyrene 7 cm	0.497	1.000
Ceiling over cellar	Foamed polystyrene 10 cm	0.358	1.000
Ventilated roof	Mineral wool 22 cm	0.196	0.200
External window	–	1.300	1.300
External door	–	1.700	1.700

3.4. Variant 2 – second modification

The second modification in the building for further reduction of the energy demand for the purposes of heating and ventilation is based on further improvements in the building envelope insulation (Table 4) in order to meet guidelines for low energy requirement buildings [7]. Natural ventilation is replaced with mechanical ventilation with heat recovery. An air handling unit equipped with a highly efficient counter-current heat exchanger with 78%

efficiency is planned to be installed on the roof. The fresh air is transported to the bedrooms and living rooms of the apartments and is exhausted by ducts in the kitchens and bathrooms.

In order to achieve optimization of energy demand, the heating installation will be modernized (hydraulic regulation, pipelines insulation). Mechanical ventilation does not allow for the installation of open furnace gas hot water boilers, so it was assumed that DHW would be heated by the standard local heating system.

Table 4

Building envelope heat transfer coefficients – Variant 2

Name	Insulation	U [W/m ² K]	U_{\max} [W/m ² K] [7]
Cellar external wall	Foamed polystyrene 20 cm	0.185	0.200
External wall	Foamed polystyrene 20 cm	0.156	0.200
Ceiling	Foamed polystyrene 7 cm	0.465	1.000 [10]
Ceiling over cellar	Foamed polystyrene 10 cm	0.358	1.000 [10]
Ventilated roof	Mineral wool 30 cm	0.146	0.150
External window	–	0.800	1.300
External door	–	0.800	1.500

4. Results of calculations

Table 5 and Table 6 present results of the calculations of the seasonal usable energy demand for heating and ventilation. The building in its existing state (variant 0) has very high energy consumption, which reaches a level of 190–200 kWh/(m²,year) depending on the calculation method.

In the variant 1, the undertaken modifications enable a significant reduction in energy demand. The usable energy index (yearly seasonal unit usable energy demand for heating and ventilation [11]) decreased from 191 to 93 kWh/(m²,year) in the method based on PN-EN ISO 13790:2009[8] (Table 5) and decreased from 202 to 99 kWh/(m²,year) in the method based on ‘Energy performance of the building’[9] (Table 6). The building in variant 1 approaches the standard required of an energy efficient building [12].

Due to further improvements in the building envelope and the installation of mechanical ventilation with heat recovery as described in variant 2, the reduction of the usable energy demand index reaches a satisfactory level of 33 kWh/(m²,year). As a result, the examined building achieved the standards of a low energy requirement building (below 40 kWh/(m²,year)) [7].

The results of the energy demand calculations for heating, ventilation, domestic hot water and supply to auxiliary devices are included in table 7. The lower value of the primary energy index (EP) relative to the final energy index (EK) results from the choice of heat source. Energy from cogeneration has a low effort indicator (w_p) at the level of 0,8. Relatively small electric energy demands do not have such an influence on the final result of primary energy at the variant 0 and 1. The situation changes in the variant 2 because of mechanical

Table 5

**Calculation of seasonal usable energy demand for heating and ventilation
in accordance with PN-EN ISO 13790:2009 [8]**

Variants	$L_{H,m}$	Q_D	Q_{iv}	Q_{ve}	$\eta_{H,gn}$	Q_{sol}	Q_{int}	$Q_{H,nd}$	$Q_{H,nd}$	EU
	[h]	[GJ/year]	[GJ/year]	[GJ/year]	[-]	[GJ/year]	[GJ/year]	[GJ/year]	[kWh/year]	[kWh/m ² year]
0	6102	1529	265	901	0.19	838	511	2431	675191	191
1	5307	628	265	901	0.45	857	511	1177	326808	93
2	4304	442	156	413	0.44	861	511	414	114973	33

Table 6

**Calculation of seasonal usable energy demand for heating and ventilation
in accordance with 'Energy performance of the building' [9]**

Variants	$L_{H,m}$	Q_D	Q_{iv}	Q_{ve}	$\eta_{H,gn}$	Q_{sol}	Q_{int}	$Q_{H,nd}$	$Q_{H,nd}$	EU
	[h]	[GJ/year]	[GJ/year]	[GJ/year]	[-]	[GJ/year]	[GJ/year]	[GJ/year]	[kWh/year]	[kWh/m ² year]
0	6399	1455	249	1029	0.19	529	383	2564	712068	202
1	5963	597	249	947	0.59	529	383	1259	349753	99
2	4596	421	147	412	0.61	529	383	425	118123	33

Abbreviation: $L_{H,m}$ – heating season length [h], Q_D – loss of heat by building envelope [GJ/year], Q_{iv} – loss of heat by internal walls and ceilings [GJ/year], Q_{ve} – loss of heat by ventilation, $\eta_{H,gn}$ – heat gain efficiency ratio [-], Q_{sol} – solar energy gain [GJ/year], Q_{int} – domestic (internal) heat gain [GJ/year], $Q_{H,nd}$ – total usable energy demand for heating and ventilation with heat gains taken into account [GJ/year], EU – usable energy demand index without auxiliary devices [kWh/m²rok]

Table 7

**Calculation of seasonal usable energy demand for heating and ventilation
in accordance with 'Energy performance of the building' [9]**

Variants	$Q_H + Q_{V,nd}$	$Q_{K,nd} + Q_{K,V}$	$Q_{W,nd}$	$Q_{K,W}$	$E_{el,pom}$	EU	EK	EP
	[kWh/year]	[kWh/year]	[kWh/year]	[kWh/year]	[kWh/year]	[kWh/m ² year]	[kWh/m ² year]	[kWh/m ² year]
0	712068 + 0	996735 + 0	98069	106597	11201	233	316	269
1	349750 + 0	489571 + 0	98069	106597	10312	130	172	153
2	80431 + +37692	88164 + +41316	98069	185170	31707	70	98	98

Abbreviation: $Q_{H,nd}$, $Q_{K,nd}$ – respectively, usable and final energy demand for heating and natural ventilation [kWh/year], $Q_{V,nd}$, $Q_{K,V}$ – respectively, usable and final energy demand for mechanical ventilation [kWh/year], $Q_{W,nd}$, $Q_{K,W}$ – respectively, usable and final energy demand for DHW, $E_{el,pom}$ – final energy demand for auxiliary devices.

Energy demand index: EU – usable energy, EK – final energy, EP – primary energy.

ventilation, which consumes more electrical energy. In variant 2, the central preparation of domestic hot water also has a negative influence due to heat losses in the pipelines. According to current regulations, the maximum value of the primary energy index for multi-family buildings is 105 kWh/(m²year) [10], which means that only the building in variant 2 meets the requirements from 'Energy performance of the building'.

5. Analysis of heat losses

Figs. 1, 2, 3 compare differences in heat losses between the three analysed variants. There are significant changes in the heat demands for ventilation, from 35.7% (Fig. 1) in variant 0 through to 50.2% (Fig. 2) in variant 1 and to 40.5% (Fig. 3) in variant 2. This inequality is caused by differences in the insulation of the building. In variant 0, where the building envelope does not consist of any foamed polystyrene layer, the percentage of heat losses for ventilation is the lowest. Due to the modernization of the thermal insulation in variant 1 and no changes in ventilation, the percentage of heat losses for ventilation is higher by about 15%. In the last case (variant 3), further improvements were taken (a thicker insulation layer and mechanical ventilation with heat recovery), which generates a decrease in heat losses for ventilation.

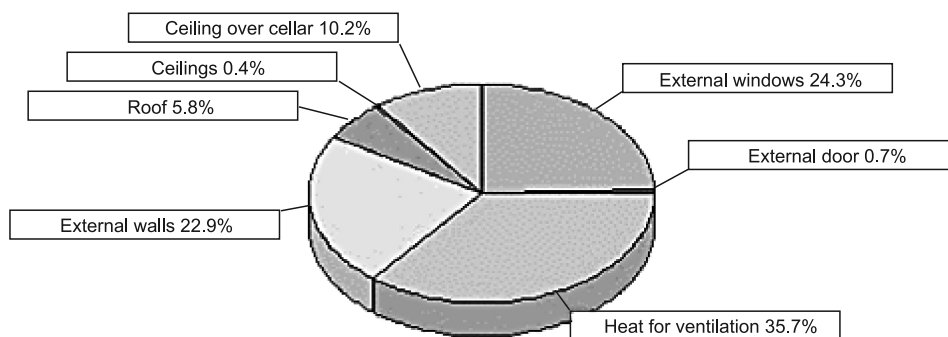


Fig. 1. Heat losses – Variant 0

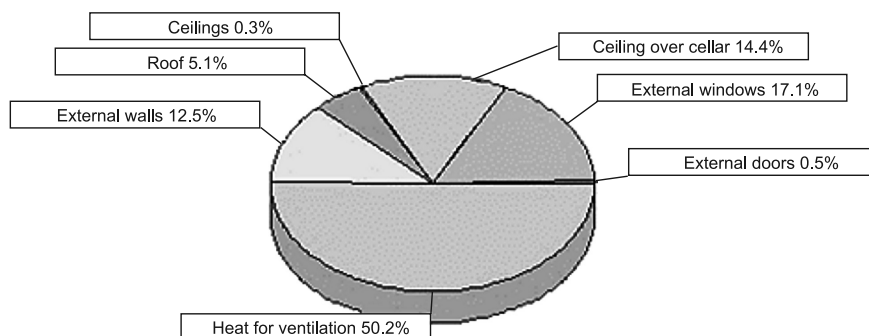


Fig. 2. Heat losses – Variant 1

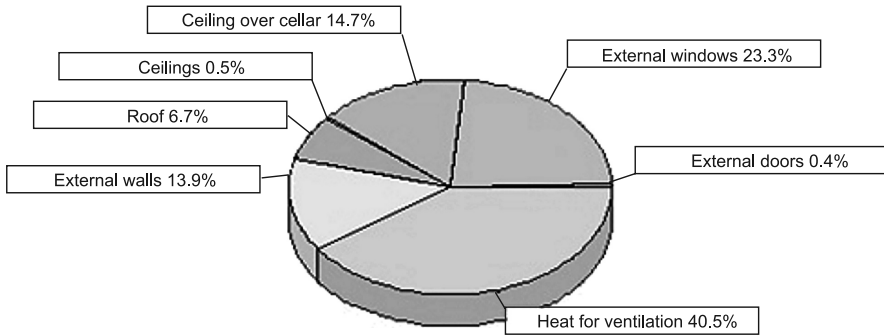


Fig. 3. Heat losses – Variant 2

6. Conclusions

Due to increasing energy consumption, comprehensive action connected with energy saving should be undertaken. The case study of building in Cracow confirms that achieving a standard of low energy requirement building is possible. The decrease in the overall energy demand is significant when reduction reaches a level of 16% of the initial value ($EU = 202 \text{ kWh/m}^2/\text{year}$). The main differences between variant 1 and variant 2 are the thickness of the insulation layer and the installation of mechanical ventilation. Achieving the standard of low energy requirement building is possible only with a mechanical ventilation system with heat recovery. As a result, final costs in variant 2 will be far greater than in variant 1. What is more, the realization of mechanical ventilation in an already inhabited building might be almost impossible. In conclusion, variant 2 is much more energy saving, but unfortunately also unprofitable. In existing buildings, variant 1 seems to be more beneficial, while the reduction of energy demand is significant, the expenditures should not be burdensome.

References

- [1] http://www.stat.gov.pl/cps/rde/xbcr/gus/ENERGIA_2013.pdf – 15.02.2014.
- [2] Perez-Lombard L., Ortiz J., Pout C., *A review on buildings energy consumption information*, Energy Build, 2008, 40:394-8.
- [3] http://www.stat.gov.pl/cps/rde/xbcr/gus/SE_gosp_paliw_energ_2011-2012.pdf – 15.02.2014.
- [4] European Parliament and the Council of the European Union. Directive 2002/91/EC of the European Parliament and the of the council of 16 December 2002 on the energy performance of buildings. Brussels: Official Journal of the European, Communities, 2002. p. 1, 7.
- [5] Hachem C., Athienitis A., Fazio P., *Energy performance enhancement in multistory residential buildings*, Applied Energy, 2014.
- [6] Stephan A., Crawford R.H., Myttenaere K., *A comprehensive assessment of the life cycle energy demand of passive houses*, Applied Energy, 2013.

- [7] Narodowy Fundusz Ochrony Środowiska i Gospodarki Wodnej, Wytoczne do weryfikacji projektów budynków mieszkalnych, zgodnych ze standardem NFOŚiGW, Warszawa 2012.
- [8] PN-EN ISO 13790:2009 Energetyczne właściwości użytkowe budynków. Obliczanie zużycia energii na potrzeby ogrzewania i chłodzenia.
- [9] Rozporządzenie Ministra Infrastruktury z dn. 6 listopada 2008 r. w sprawie metodologii obliczania charakterystyki energetycznej budynku i lokalu mieszkalnego lub części budynku stanowiącej samodzielną całość techniczno użytkową oraz sposobu sporządzania świadectw ich charakterystyki energetycznej” (Dz.U. 2008 nr 201 poz. 1240).
- [10] Rozporządzenie Ministra Transportu, Budownictwa i Gospodarki Morskiej z dnia 5 lipca 2013 r. zmieniające rozporządzenie w sprawie warunków technicznych jakim powinny budynki i ich usytuowanie (Dz.U. nr 0 poz. 926).
- [11] http://www.swiadectwo.builddesk.pl/ep_ek_eu.php – 20.02.2014.
- [12] Wnuk R., *Instalacje w Domu Pasywnym i Energooszczędnym*, Przewodnik Budowlany, 2007.

PETER KAPALO*, ANNA SEDLÁKOVÁ**, SILVIA VILČEKOVÁ***,
FLORIN DOMINTA****

ENERGY EFFICIENCY OF VENTILATION SYSTEM IN APARTMENT BUILDINGS

EFEKTYWNOŚĆ ENERGETYCZNA SYSTEMU WENTYLACJI W BUDYNKU MIESZKALNYM

Abstract

The article shows impact of the location of apartments on the heat requirement of each type of apartment as well as the possibility of different savings of heat by using ventilation equipments including recuperative devices.

Keywords: ventilation, heat, apartment, building, energy saving

Streszczenie

Artykuł przedstawia wpływ lokalizacji mieszkania na wymagania cieplne poszczególnych lokali jak również możliwości oszczędzania energii przy użyciu systemu wentylacji z rekuperacją.

Słowa kluczowe: wentylacja, ciepło, lokal mieszkalny, budynek, oszczędność energii

* Ph.D. Eng. Peter Kapalo, Department of Technical Building Equipment, Faculty of Civil Engineering, Technical University of Kosice, Slovakia.

** Doc Ph.D. Eng. Anna Sedláková, Department of Architectural Engineering, Faculty of Civil Engineering, Technical University of Kosice, Slovakia.

*** Doc Ph.D. Eng. Silvia Vilčeková, Department of Environmental Engineering, Faculty of Civil Engineering, Technical University of Kosice, Slovakia.

**** Ph.D. Eng. Florin Domnita, Faculty of Building Services Engineering, Technical University of Cluj-Napoca, Romania.

1. Introduction

In this paper, the energy performance of the ventilation system in an apartment building is documented. Twenty-one flats are in the building. Only some apartments have the same equipment. Energy consumption in the individual apartments is different, because their location within the apartment building varies.

2. Ventilation of the apartment building

The research was carried out in an apartment building with four floors above ground level. The building has a total of 21 apartments. On the first floor 6 apartments of type A-1, B-1 and C-1 are located. On the second floor 6 apartments of type A-2, B-2 and C-2 are located. On the third floor also, 6 apartments of type A-3, B-3 and C-3 are located. On the first floor, second floor and the third floor are identically located apartments. But the heat transfer through building envelope is different, because the apartment's location is different within the building. On the fourth floor there are 3 apartments of type D-4 and E-4.

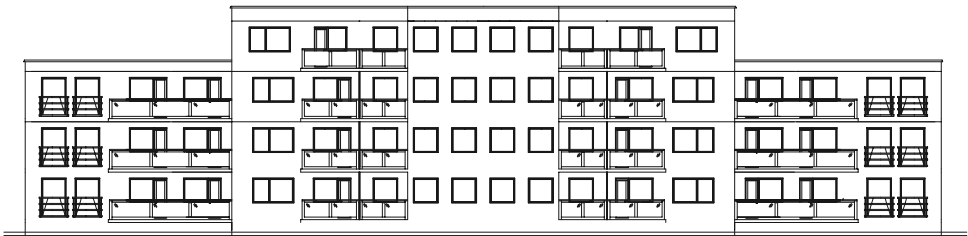


Fig. 1. View of the apartment building [3]

Table 1

The basic parameters (calculation according to STN EN 73 0540, STN EN 13 790 [4, 5])

Type of apartment	Apartment area [m ²]	Volume of apartment [m ³]	Specific thermal loss of transition (apart. 1/2/3) [W/K]	Specific thermal loss of ventilation ($n = 0.5$) (apart. 1/2/3) [W/K]	Specific thermal loss of ventilation ($n = \text{infiltration}$) (apart. 1/2/3) [W/K]
A	85	235	58/58/84	31/31/31	7/7/7
B	75	209	33/33/33	28/28/28	3/3/3
C	58	160	31/31/31	21/21/21	4/4/4
D	98	300	95/95	40/40	7/7
E	112	340	77	45	7

The external wall in the upper floors are made out of brick with thickness of 380 mm. Thermo-insulating plaster thickness is 35 mm [3].

The roof deck of the building is formed by a flat roof. The slope is on the inside of the roof. Thermal insulation is made from extruded polystyrene – thermal insulation boards of 150 and 200 mm. Windows are proposed as plastic with insulating double glazing. Heat transfer coefficient of window is $U = 1,0 \text{ W}/(\text{m}^2 \cdot \text{K})$ [2]. The annual energy demand for heating and ventilation was calculated according to methodology of STN EN 73 0540 and STN EN 13790 [4, 5].

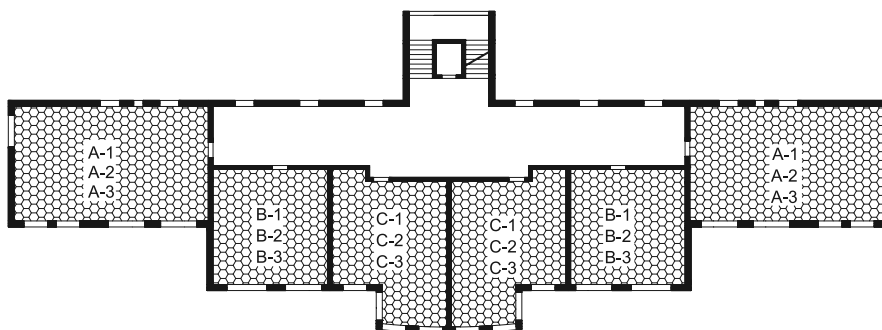


Fig. 2. Floor plan of the 1st, 2nd and 3rd floors above the ground

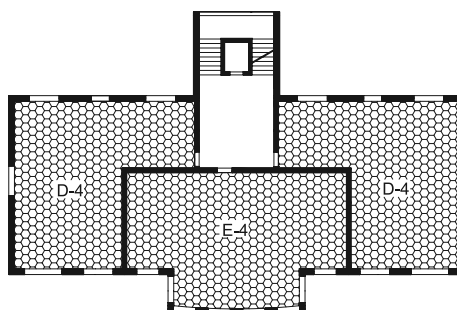


Fig. 3. Floor plan of the 4th floor above the ground

In this building a controlled air handling unit is designed to provide heat recovery by means of recovery equipment. In this study two alternatives of the ventilation system are analyzed.

The first alternative involved installing an individual air handling unit in each apartment. The task of these units will be to provide the required indoor climate for just one apartment. Each ventilation unit is in operation independently.

In the second alternative central air handling units are designed for more apartments, which are situated one above another. A central air handling unit will be installed on the roof of the apartment building. In each apartment a control element will be installed to provide the air supply required for a particular apartment. Each apartment can have a different desired microclimate and also different required flow rate, which is dependent on the size of the apartment, number of persons in the apartment and individual requirements of people in the apartment.

For each apartment equipment is designed, which provides equal pressure of ventilation. The device ensures a forced inlet of fresh air and concurrently lets out the polluted air.

Table 2

The efficiency of the heat recovery unit (example of the evaluation)

	Type of apartment	Type of the ventilation unit	Supply air [m ³ /h]		The efficiency of the heat recovery unit [%]		
			Max.	Required	Min.	Max.	Mean
1. altern.	B	DUPLEX 180 EC4	180	104	89.4	95.4	90.6
	C	DUPLEX 180 EC4	180	80	90.7	96.2	91.4
	D	DUPLEX 180 EC4	180	150	88.4	94.3	89.6
	E	DUPLEX 180 EC4	180	170	88.1	93.9	89.3
2. altern.	$3 \times (B + C) + D + E$	DUPLEX NS 1500	1500	872	74.3	79.6	74.7

In the ventilation system heat recovery is used. This will significantly reduce the heat consumption for heating of outside air. Air handling unit is used for transporting air. The unit consists of fans, filters, heat exchanger and heater. The fan has the ability to regulate the power according to required air exchange. Ventilation units are controlled according to required temperature, air humidity, concentrations of carbon dioxide etc.

3. Energetic assessment of the ventilation system

Energy requirement was calculated for each apartment. Heat consumption was calculated (Fig. 4):

- for transmission of heat across the construction of the building,
- for warming the ventilated air:
 - Energy requirement for warming the infiltrated air,
 - Heat loss of ventilation,
 - Obtained heat from heat recovery air.

While calculating energy requirements, it is also necessary to add the energy required to run the ventilation system. For simplicity, in this case, the energy required to drive the fan has not been considered.

Heat demands for individual apartments are shown in figure 4. The arrangement of individual apartments are deliberately illustrated so as to show the location of apartments within the apartment building.

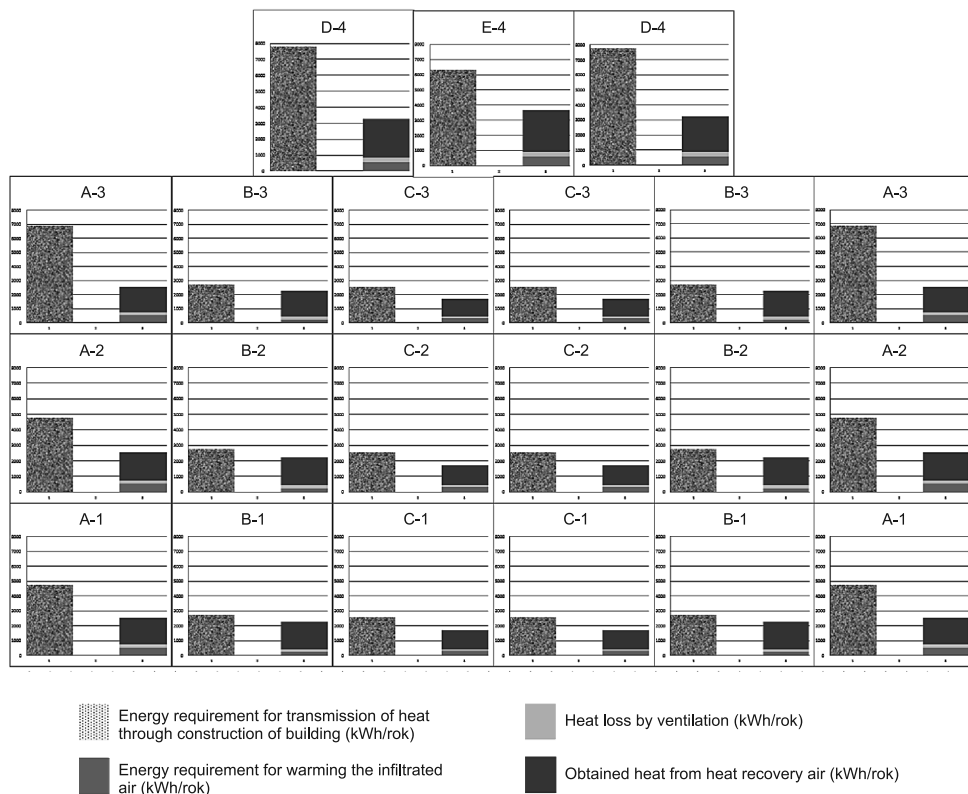


Fig. 4. The heat demand for individual apartments

4. Discussion

The aim of this paper was to analyze heat saving when using ventilation systems, whose component part is a device with heat recovery air. Advanced production technology of fans enables production of efficient electric motors with controlled rotation speed. So we can provide controlled ventilation of spaces with minimal energy consumption. Whereas the purpose of ventilation is to provide comfort while ensuring appropriate hygienic environment in the apartment, it is needed to design a device taking into account energy consumption and hygienic parameters. In addition to these parameters, it is important to take into account the environmental parameters [1].

Each mechanical ventilation system requires regular check-maintenance: change of filters, cleaning air ducts and etc. Also, this activity requires finances.

Apartment of type B (area 75 m²) has energy savings of 37% and return on investment is 18 years. Apartment of type C (area 58 m²) has energy savings of 30% and return on investment is 25 years. The central ventilation unit, which is for: three apartments of type B,

three apartments of type C, one apartments of type D and one apartment of type E, has energy savings of 26% and return on investment is 12 years.

Table 3

Obtained heat from waste air

Apartment type	A-1	A-2	A-3	B-1	B-2	B-3	C-1	C-2	C-3	D-1	E-1
Obtained heat from waste air (%)	22	22	18	37	37	37	30	30	30	22	28

5. Conclusions

From the analysis it can be concluded, that it is preferable to install individual ventilation units with heat recovery in apartments with more built-up volume. For apartments with less built-up volume it is advantageous to install a central ventilation unit with heat recovery designed for more apartments.

In this analysis an air handling unit with a constant air flow is used. For this case, the projected saving of energy will approximately of 18–37 % – see table 3. We assume that energy saving will be larger, when we use controlled ventilation system.

This article was elaborated in the framework of the project VEGA 1/0405/13 and KEGA 052TUKE-4/2013.

References

- [1] Kridlová Burdová E., *The strategy process of the integrated design of buildings*, Proceedings of peer-reviewed scientific papers UEI 2013. Košice 2013, 73-78.
- [2] Pašeň P., *Dwelling buildings*, Diploma work, Technical University of Košice, Civil Engineering, Košice 2012.
- [3] Vojtuš J., *Structural design of the roof cladding model house for the purpose of research activities integration of renewable energy sources*, [In:] 4th Cassootherm: scientific and technical conference with international Participation: 16th–18th April 2012, Vysoké Tatry, Stará Lesná. Košice 2012, 92-98.
- [4] STN EN 730540-2: 2012, Thermal performance of buildings and constructions.
- [5] STN EN 13790: 2008, Energy performance of buildings. Calculation of energy use for space heating and cooling.

DANIELA KAPOSZTASOVA*, ZUZANA VRANAYOVA*, PAVOL PURCZ*

RAINWATER HARVESTING SYSTEM AND RISK MANAGEMENT APPLICATION

ZASTOSOWANIE SYSTEMU ZARZĄDZANIA RYZYKIEM PRZY WYKORZYSTANIU WODY OPADOWEJ

Abstract

Submitted paper presents risk assessment using risk analysis of the rainwater harvesting system. The aim of this article is to present selected approach in risk factors identification within proposed RWH system evaluation for an experimental family house. In our case, we were able to collect helpful information from questionnaires that later facilitated the risk identification as well as risk assessment phase along with the aid of brainstorming activities within a team of experts. The results from the risk analysis were verified by the AHP and empirical multilevel comprehensive evaluation, which was also found to be useful.

Keywords: rainwater harvesting, risk analysis, risk assessment, questionnaire

Streszczenie

W artykule przedstawiono zastosowanie metody oceny ryzyka w odniesieniu do sytemu gromadzenia wody opadowej. Celem artykułu jest identyfikacja czynników ryzyka w proponowanym dla eksperymentalnego domu systemie RWH. W naszym przypadku udało się zebrać przydatne informacje z ankiet, które później ułatwiły identyfikację oraz ocenę ryzyka. Równolegle korzystano też z burzy mózgów. Rezultaty analizy ryzyka były weryfikowane przez AHP i doświadczalną wielopoziomową ewaluację, która okazała się także użyteczna.

Słowa kluczowe: wykorzystanie wody opadowej, analiza ryzyka, ocena ryzyka, ankieta

* Ph.D. Eng. Daniela Kaposztasova, Assoc. Prof. Ph.D. Zuzana Vranayova, RNDr. Ph.D. Pavol Purcz, Department of Building Services, Faculty of Civil Engineering, Technical University of Košice.

1. Introduction

Rainwater harvesting system, although well-known all around the world, is still not well established in our conditions of Slovak Republic. In the past, there had been no need to look for new alternative water sources for domestic or commercial use because of the availability of good water sources in Slovak Republic. Furthermore, there are still voices that support the claim that it still is unnecessary in our conditions. However, overloaded sewerage systems and water treatment plants, cases of urban floods or water scarcity make us consider the sustainable usage of water sources all around the world and about proper water quality usage for different purposes [1]. That is the reason why we are interested in this topic and why we would like to increase awareness of this topic in our conditions as well. Relevant information on the developments in the field were obtained for the purpose of this article from the following reading materials listed in the reference section of this paper: [10–15]. As with all human activities this system could potentially be risky in some cases, as well. Risk management has its place in science and our everyday life [8]. Water management in general comprises a wide range of problems – especially in recent years when we started seeing an increasing need to manage rain water in a decentralized way. This entails the use of different infiltration or percolation systems or yet other ways of reusing this water. Generally, it is called rainwater harvesting, or RWH.

Indisputably, rainwater harvesting systems bring many benefits but, as with other areas, some events can be categorized as risky according to risk management.

Risk management programs generally cover five main components:

Context – What is at risk and why?

Risk identification – What and where are the risks?

Risk analysis – What is known about them?

Risk evaluation – How important are they?

Risk treatment – What should be done about them? [2].

Effective risk management requires identification of potential risks or hazards as described in methodology below. This methodology has been designed step-by-step in accordance with Water Safety Plan and WSP Manual and comprises the following stages:

1. Formation of a team of experts.
2. Description of an RWH system.
3. Risk identification.
4. Risk assessment.
5. Determination and evaluation of control measures [2].

RWH systems and other sustainable urban drainage systems undeniably offer many benefits, but as in others areas, some events can be categorized as risky from the perspective of risk management. The objective of risk analysis is to detect these potential risks, summarize them, determine their importance and find out the solution for how to prevent or eliminate them.

1.1. Questionnaire as a tool for risk analysis

The questionnaire was completed by designers and construction companies in Slovakia and it should provide many ideas, opinions and experiences related to the design process as

well as to the construction and operation of such systems. Hopefully the questionnaire will help identify and assess risks.

The questionnaire was completed by 63 respondents. Not all of the respondents, however, felt knowledgeable enough to answer all of the questions. The last part of the questionnaire focused on the risks in RWH, as described below, and was assessed by 20 respondents. At the beginning of the questionnaire there were a few basic questions about the respondents pertaining to their experience, position and opinion about RWH. The second group of questions focused on practical experiences, such as for example: when did you produce your first design?, what problems did you face during the design process?, have you seen an increased demand for RWH in recent years?, what standards or manuals do you use for your designs?, etc. Finally, the target of the last group of questions was to obtain information about the risks involved in RWH.

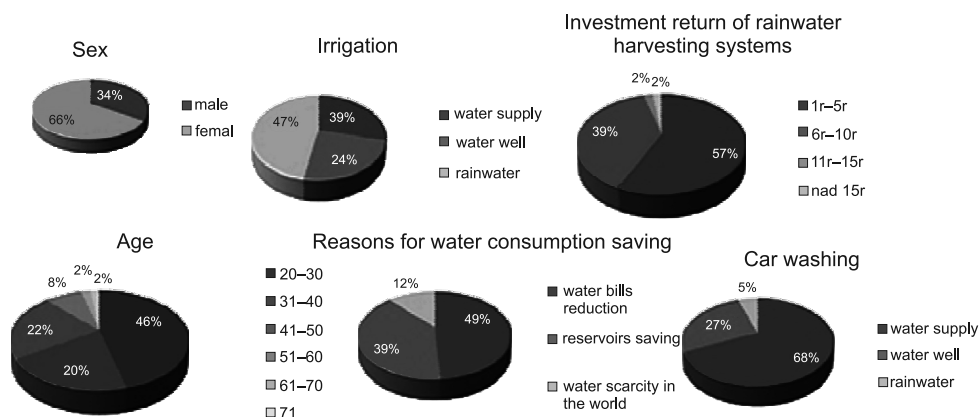


Fig. 1. Sample of results obtained from the questionnaire – according to [7]

This part is strongly subjective as it is based on a respondent's experiences and opinions. In this section we will introduce a few results obtained through the last group of questions in the questionnaire where respondents were asked to assign values ranging from 1 to 10 (1 referring to the lowest risk, 10 having the highest risk) to the main parts of the system (as shown in Fig. 2) contingent on the significance of the risk. The results show that the riskiest parts of the system according to questionnaire responses are: the pump, the filter, and the tank. Accordingly, we can say that the greatest attention should be paid to the design, installation and maintenance of these three parts of the system. Approximately half of the respondents think that there is a lack of information about system maintenance and water usage by users which pins our attention also to this kind of risk. We can say that the questionnaire is a good example of how to obtain relevant practical information about the design process, experiences and opinions on the risk analysis steps such as risk identification and risk assessment.

2. Risk analysis –aims and methods

The aim was to prepare a general risk analysis methodology for rainwater harvesting systems. This methodology can especially be applied to small scale projects such as family houses. In our case, it was applied to a newly constructed family house with a RWH system (see Fig. 1). The installed system is brand new and supplied with a 4 m³ underground water tank. Rainwater is used for flushing toilets, irrigation, property maintenance, and potentially for washing machine usage as well.

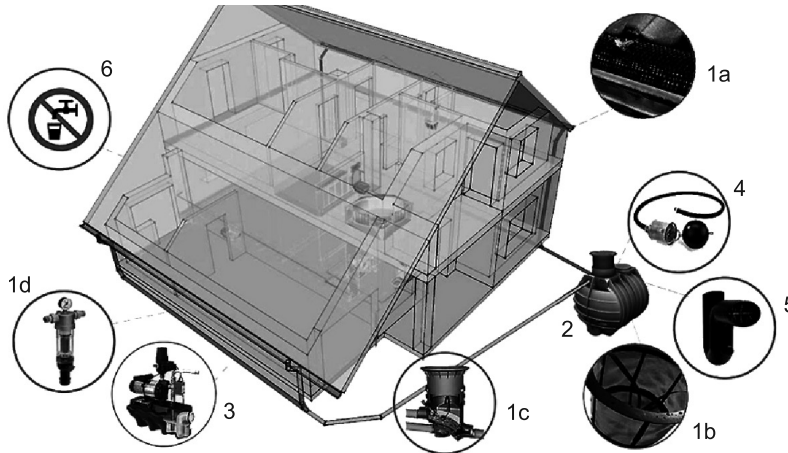


Fig. 2. Experimental family house and RWH system (1a – gutters, 1c, 1b – filters 1d water level sensors, 2 – tank, 3 – pumps, 4 – floating suction assembly, 5 – safety overflow, 6 – label –non-potable water)

One of the aims of this risk analysis is to prepare a check-list for this type of user. The check list should serve as a tool for standard system checks which can eliminate various types of events and also inform the user about the system. The methodology was designed in accordance with Water Safety protocols mentioned in section 1.

Quantitative or qualitative methods can be used for the risk evaluation. A semi-quantitative methodology was selected for the RWH evaluation of our experimental system. The semi-quantitative risk assessment is a method for differentiating risks, focusing on the big issues, and managing the entire risk portfolio better. The scoring system is inherently imperfect, but so is any other risk evaluation system [3].

By using the semi-quantitative risk assessment method, the team of experts who is performing the evaluation can calculate a priority score for each identified hazard. The objective of the prioritisation matrix is to rank hazardous events to provide a focus on the most significant hazards. The likelihood and severity of these events can be derived from the team's technical knowledge and expertise, historical data and relevant guidelines [2].

For the purposes of risk identification and assessment, the RWH system was divided into 4 parts according to Fig. 3. These four parts have thus subdivided our system into 4 main evaluation folders. Each part was then divided into sub-systems. A sub-system encompasses

main system components where all sorts of potential hazards – ranging from minor ones to those most important – can be identified. These potential hazards constitute a list which constitutes the last level of our evaluation hierarchy. This final list is not presented in this article.

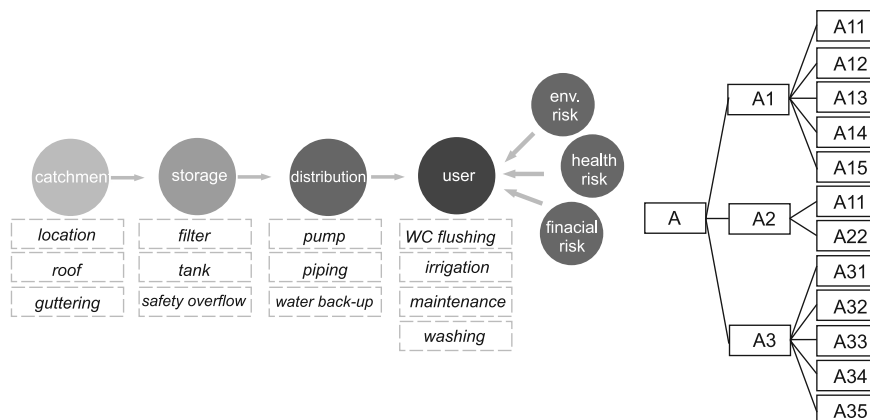


Fig. 3. Flow diagram: A – catchment, B – storage, C – distribution, D – user–each part was divided into subsections (A1, A2, A3, B1, etc.) and the last level of our system contains potential hazards (A11, A12, A13, A21, A31)

The objective of our work was to prepare risk analysis methodology for small scale RWH projects in particular. The methodology was applied on an experimental family house with an RWH system where rainwater will be used for flushing toilets, irrigation and potentially for washing machine usage as well.

The risk score consistent with semi-quantitative methodology is determined in accordance with this formula [4]:

$$\text{Risk} = \text{likelihood of occurrence} \times \text{severity of consequence}$$

The risk is determined by multiplying these two values. This approach allows us to distinguish serious risks from minor ones and to determine priorities both for their prevention and their elimination.

Table 1

Table of risk scores resulting from the semi-quantitative risk matrix

risk score	1–3	4–6	8–10	12–16	20–25
risk rating	very low	low	medium	high	very high

All potential hazards with a risk score of 9 or higher were taken into further consideration. The risk score value of 9 constitutes our point of division. This value was chosen by the team of experts based on their knowledge; it is a noticeably subjective value.

The team can choose whatever point of division or can consider all of the potential hazards. However, we have chosen this value and have taken into further consideration and evaluation only those potential hazards with the risk score of 9 or higher. These potential hazards can be found in Table 2.

Table 2

Identified potential hazards with the risk score of 9 or higher

sub-system	potential hazards
location	microbiological contamination
	dustiness
	drought
guttering	modification and maintenance
filters	upgrade and maintenance
tank	under sizing
	over sizing
	microbiological contamination
	upgrade and maintenance
pump	clogging
WC flushing	toilet lid closing
	joint bathroom and toilet
	inhalation of dangerous microbes

We have observed that the risk level of the system is not high at all. What is the most important aspect of this RWH system evaluation are thorough and regular system upgrades and maintenance and good knowledge of the system function by its users.

The results of this semi-quantitative risk analysis were verified by other mathematical methods and a questionnaire. The questionnaire facilitated the identification and assessment of risks. According to the respondents (who included construction companies' staff and other professionals) the parts of the RWH system most risk-prone include the pump, filters and the tank. We can find these parts mentioned in the results section of our risk analysis as well.

The mathematical method was also useful in this process. The most objective and appropriate method amidst mathematical methods is the AHP (which stands for Analytic Hierarchy Process). The highest significance as indicated by this method was attributed to location, pump, filter and tank. These verification methods show that the results obtained through the semi-quantitative method can be considered valid. Based on that, easy-to-use control measures for the RWH systems can be designed in order to reduce potential hazards to minimum or eliminate them even if the system is considered non-risky.

3. Discussion and conclusion

What must be indicated is that even if we focus our attention only on some parts of the system, its other component parts are equally essential due to the interconnectedness of the system. Failure to maintain one part the system can lead to potential risks in its other parts. Good knowledge of the system being used is equally imperative [5].

It must also be mentioned that even if we work with numbers and methods which are considered objective, the interpretation of given evaluations and evaluation input is subjective and based on the knowledge of a team of experts. In this kind of evaluation it is impossible to exclude a level of subjectivity [6].

The risk assessment provides a checklist for users of RWH systems, enabling them to use this list of questions to perform regular system checks, to be informed about their system and serving also as a prevention tool [7].

3.1. Conclusion

Systems using rainwater are well-known, although they are not widespread enough in our country yet. The use of this alternative water resource, as well as other resources, definitely offers many benefits, however, the risks should not be ignored. The risks are associated with any activity we do in our everyday life. Early risk identification allows us to prevent potential hazardous events, which is crucial for proper system functioning and user satisfaction. In conclusion, it can be stated that most risk event-prone parts of RWH include the pump, filter, tank and the location itself. The goal is to design an easy-to-use risk management approach in order to prevent potential hazardous events, especially for small-scale RWH projects consistent with this experimental one.

This work was supported by the VEGA 1/0450/12 Energy balance research on rainwater management in the cities of the future.

The APVV – SK-CZ-2013-0188 LetsTalk about the Water – An Essential Dimension of Sustainable Society of the 21st Century.

References

- [1] Slyš, D., Stec A., Zeleňáková M., *A LCC analysis of rainwater management variants*, [In:] *Ecological Chemistry and Engineering*, S 19(3), 2012, 359-372 (retrieved from: www.scopus.com).
- [2] Water Safety Plan Manual, *Step-by-step risk management for drinking-water suppliers*, WHO, Geneva 2009.
- [3] Water Safety Plans, *Managing drinking-water quality from catchment to consumer*, WHO, Geneva 2005 (http://www.who.int/water_sanitation_health/dwq/wsp170805.pdf).
- [4] Očipová D., *Teoretická a experimentálna analýza distribučných systémov teplej vody z hľadiska mikrobiologického znečistenia*, Dizertačná práca, TUKE, 2009.
- [5] Karellová Z., *System of RWH evaluation*, Young Scientist 2013, The 5th PhD, Student Conference of Civil Engineering and Architecture, TUKE, 2013.

- [6] Karellová at col, *Risk analysis for RWH system and its verification by mathematical methods*.
- [7] Vranayová Z., Karellová Z., Káposztásová D., *Riziková analýza a využívanie zrážkovej vody z povrchového odtoku*, [In:] *Sanhyga 2012*, 17, vedecko – odborná medzinárodná konferencia, SSTP Bratislava 2012.
- [8] Peračková J., Markovič G., *Využitie zrážkovej vody z povrchového odtoku v budovách*, [In:] TZB Haustechnik, Roč. 18, č. 5, 2010, s. 34-37.
- [9] N.F. Gray Phd.Sc.D., *Water Technology (Third edition)*, An Introduction for Environmental Scientists and Engineers, Chapter 23, IWA Publishing, 2010.
- [10] The Water Framework Directive, Directive 2000/60/EC of the European Parliament and of the Council.
- [11] Kinkade-Levario H., *Design for Water: Rainwater Harvesting, Stormwater Catchment, and Alternate Water Reuse*, New Society Publishers, 1 edition (1 June 2007).
- [12] Lancaster B., *Rainwater Harvesting for Drylands and Beyond*, Volume 1, 2nd Edition: *Guiding Principles to Welcome Rain into Your Life and Landscape*, Rainsource Press, Revised second edition edition (1 July 2013).
- [13] Minnesota Stormwater Manual (2008), Version 2, Minnesota Pollution Control Agency, online: <http://www.pca.state.mn.us/index.php/view-document.html?gid=8937> – 24.08.2010.
- [14] Semadeni-Davies A., Bengtsson L., *Theoretical Background, Chapter 1* [in:] *Urban Drainage in Specific Climates*, Vol II, Urban Drainage in Cold Climate, IHP-V Technical Documents in Hydrology, No. 40, UNESCO, Paris 2000.
- [15] Scholes L. (2007), *Stormwater reuse: why, how and where?*, SWITCH – presentation, online: http://switchurbanwater.lboro.ac.uk/outputs/pdfs/WP2-1_PRS_Stormwater_reuse.pdf – 21.09.2010.
- [16] Water cycle safety plan framework, proposal, PREPARED 7th FP, 2010.

KATARZYNA KLEMM*

AN ASSESSMENT OF CONDITIONS OF HUMAN COMFORT IN OPEN LANDSCAPED AREAS OF LODZ

OCENA KOMFORTU CZŁOWIEKA W STREFIE NIEZABUDOWANEJ ŁODZI

Abstract

The paper presents an assessment of human comfort conditions in the suburban area of Lodz. The proposed criteria for comfort were based on thermal loads on the human body. An analysis of meteorological data for a 30 year period was used to determine the probable comfort levels.

Keywords: human comfort, thermal loads, open landscape

Streszczenie

W artykule przedstawiono ocenę komfortu człowieka w środowisku niezabudowanym Łodzi. Zaproponowano kryterium komfortu oparte o progi obciążenia cieplnego organizmu. Na podstawie analizy danych meteorologicznych z okresu 30 lat określono prawdopodobieństwo wystąpienia warunków komfortu.

Słowa kluczowe: człowieka, obciążenia cieplne, teren otwarty

* Assoc Prof. Katarzyna Klemm, Associate Professor, Institute of Architecture and Urban Planning, Faculty of Civil Engineering, Architecture and Environmental Engineering, Technical University of Lodz.

1. Introduction

Anthropogenic factors such as air pollution, heat emission, the systematic limitation of green areas and urban development have a major impact on climate changes both at the global and urban level. The scale of the problem is reflected in the action taken by international organizations, the European Union and also individual countries. For example, in Poland the Ministry of Environment published the National Strategy for Adaptation to Climate Change in 2013 (SPA 2013) [1], which emphasized the need for the development of comfortable microclimatic conditions in cities. In order to foster such an environment, more information is required the criteria for human comfort and the prevailing climatic conditions.

Considering the problem of heat exchange between man and the environment, it is noted that the increase or loss of internal body heat is an essential factor. An excessive degree of heat gain and loss can be dangerous for the human body. An equilibrium can only be attained over a period of time (e.g. one day). Since the heat exchange balance is formed both as a result of physiological and meteorological factors, the balance may be an indicator of the thermal load on the body and an indicator of thermal sensations.

To determine whether the environment is comfortable for inhabitants, a simple criterion of comfort has to be established. This criterion must take into account the complex nature of heat exchange between man and the environment. Secondly, it is essential to determine the probability for comfortable and uncomfortable conditions based on long-term meteorological data. In the case of built up areas, the situation is more complicated due to the effect of the urban landscape and the arrangement of buildings on wind flow. This paper is limited to examining non-built-up suburban areas of Lodz.

2. Comfort and discomfort criteria based on heat loads on the body

The comfort sensation is associated with changes in body temperature caused by an increase or decrease in ambient temperature, the cooling effect of wind, the convective and the radiative heat loss from the body. There are a number of factors affecting the heat exchange between man and the external environment. The most important physical parameters include: air temperature, wind speed, solar radiation, relative humidity and radiation temperature. Equally important are the parameters related to the individual person, such as the activity, exposure time, clothing thermal insulation and finally the psychological factors associated with the level of adaptation, expectations or previous experiences. The inclusion of so many factors requires the application of complex models and detailed meteorological and physiological data, which in practice are difficult to obtain. As a result there is a need for a more simplified method of determining criteria for human comfort in open areas.

In the light of extensive research carried out in many countries [2] it can be demonstrated that there is a correlation between the intensity of heat fluxes with air temperature and wind speed, which allows approximations to be applied. In order to identify thermal criteria based on heat balance equations, some assumptions have been made:

- Metabolism $M = 70 \text{ W/m}^2$,
- Thermal insulation of the cloths 1 clo,

- Solar radiations absorption $R = 30 \text{ W/m}^2$
- Heat exchange through evaporation $Q_E = 8 \text{ W/m}^2$ for $T_a < +5^\circ\text{C}$, 20 W/m^2 for $T_a \geq +5^\circ\text{C}$,
- Heat exchange through conduction Q_K is not taken into account,
- Heat loss caused by respiration $Q_R = 8 \text{ W/m}^2$.

Further more heat transfer by convection and long wave radiation, based on temperature and wind speed, are specified thus:

For weather conditions where wind speed $U \leq 4 \text{ m/s}$ and temperature $T_a \geq +5^\circ\text{C}$

$$Q_C + Q_L = 3.4T_a + 0.2\bar{U} - 118.8 \quad (1)$$

Where the wind speed $U \leq 4 \text{ m/s}$ and temperature $T_a < +5^\circ\text{C}$

$$Q_C + Q_L = 1.7T_a + 6.0\bar{U} - 101.4 \quad (2)$$

Where the wind speed $U > 4 \text{ m/s}$ and temperature $T_a \geq +5^\circ\text{C}$

$$Q_C + Q_L = 3.3T_a + 0.2\bar{U} - 127.8 \quad (3)$$

Where the wind speed $U > 4 \text{ m/s}$ and temperature $T_a < +5^\circ\text{C}$

$$Q_C + Q_L = -3.31.5T_a + 0.3\bar{U} - 126 \quad (4)$$

By applying the above to the heat balance equation, thermal loads on the body were derived [3]. The parameter can be used for relative comparison of different environmental conditions.

In weather conditions where wind speed $U \leq 4 \text{ m/s}$ and temperature $T_a \geq +5^\circ\text{C}$

$$\Delta Q = 2.8T_a - 4.8\bar{U} - 29.8 \quad (5)$$

Where the wind speed $U \leq 4 \text{ m/s}$ and temperature $T_a < +5^\circ\text{C}$

$$\Delta Q = 1.7T_a - 6.0\bar{U} - 23.0 \quad (6)$$

Where the wind speed $U > 4 \text{ m/s}$ and temperature $T_a \geq +5^\circ\text{C}$

$$\Delta Q = 2.3T_a - 3.5\bar{U} - 35.4 \quad (7)$$

Where the wind speed $U > 4 \text{ m/s}$ and temperature $T_a < +5^\circ\text{C}$

$$\Delta Q = 1.5T_a - 3.0\bar{U} - 34.0 \quad (8)$$

Taking into account the efficiency ranges of the thermoregulatory systems, which are applied in thermo physiology, it is assumed that $|\Delta Q| < 20 \text{ W/m}^2$ does not trigger system loads. However, where there is deficiency and excess heat ΔQ equal to $20\text{--}40 \text{ W/m}^2$ then unfavourable loads will affect the body. Strong heat load can be observed when ΔQ is between $40\text{--}80 \text{ W/m}^2$. Higher values than the threshold value 90 W/m^2 can trigger disturbances in the proper function of the thermoregulatory system, which consequently can lead to dangerous overheating or conversely hypothermia.

Finally the criteria for thermal comfort were established based on the following thresholds for heat loads on the body ΔQ :

- $|\Delta Q| < 20 \text{ W/m}^2$ – comfortable condition,
- $|\Delta Q|$ in ranges $20\text{--}40 \text{ W/m}^2$ – unfavourable loads on the body,
- $|\Delta Q|$ in ranges $40\text{--}80 \text{ W/m}^2$ – strong unfavourable loads on the body,
- $|\Delta Q| > 80 \text{ W/m}^2$ – dangerous loads on the body.

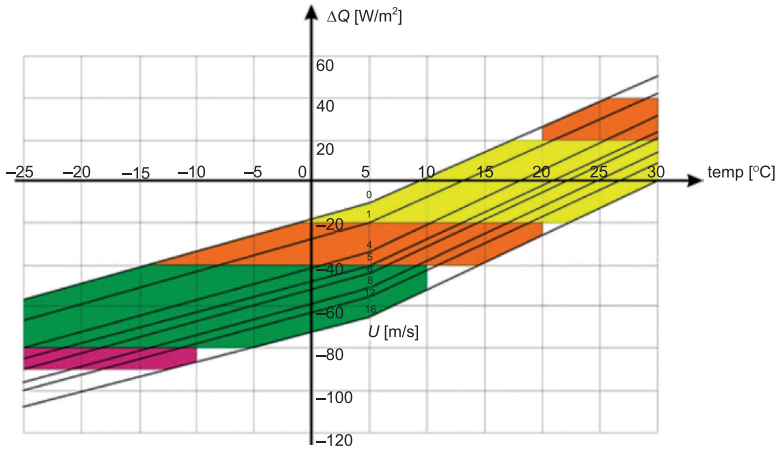


Fig. 1. Threshold values of the thermal loads on the body

Figure 1 presents the relationship between ΔQ and air temperature T_a and wind speed as well as body heat load thresholds.

The detailed analysis of body heat loads with the corresponding ranges in temperature and wind speed are presented in [3].

3. Selected meteorological data of suburban area of Lodz

In order to assess the conditions for human comfort in the selected open area of Lodz, meteorological data has been analysed based on 30 years of records and hourly mean values. As the comfort criteria relates to thermal loads on the human body, the analysis focused mainly on temperature and wind speed.

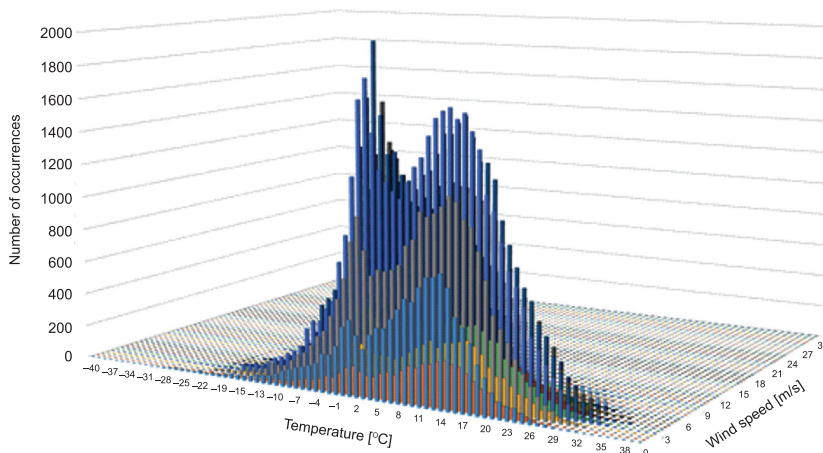


Fig. 2. Wind speed frequency and temperature in Lodz

However, other meteorological parameters such as solar radiation were also taken into account. Since the evaluation concerned comfort in non-urban developed areas, wind direction was not included in the data. Fig. 2 shows the frequency distribution of wind speed and temperature over the time period analyzed.

4. Probability of conditions of comfort and discomfort in the open landscape of Lodz

With the previously outlined assumptions taken into account, temperature and velocity combinations that satisfy the human comfort criteria can now be specified. Fig. 3 and Fig. 4 express the probability density function levels for instances of specific ranges of thermal loads, depending on wind speed and temperature respectively. In view of the fact that the velocity and temperature values which fulfill the requirement of $\Delta Q > 80 \text{ W/m}^2$ are very rare occurrences (probability of occurrence $P = 0.0004$ these were not included for further consideration.

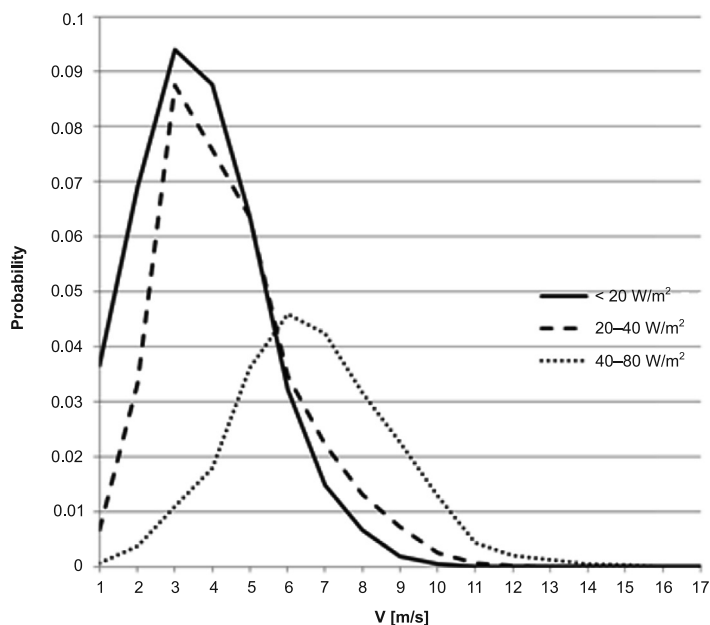


Fig. 3. Probability density function levels for the occurrence of thermal loads, depending on wind speed

Figure 5 illustrates how the wind speed and temperature ranges for comfort conditions were established. Instances where the probability of occurrence was less than 0.001 did not form part of the analysis.

As illustrated in Fig. 5, comfortable conditions ($\Delta Q < 20 \text{ W/m}^2$) occur mainly when the temperature ranges between 8 and 22°C and wind speed is up to 5m/s. Such conditions correspond to probability $P = 0.37$.

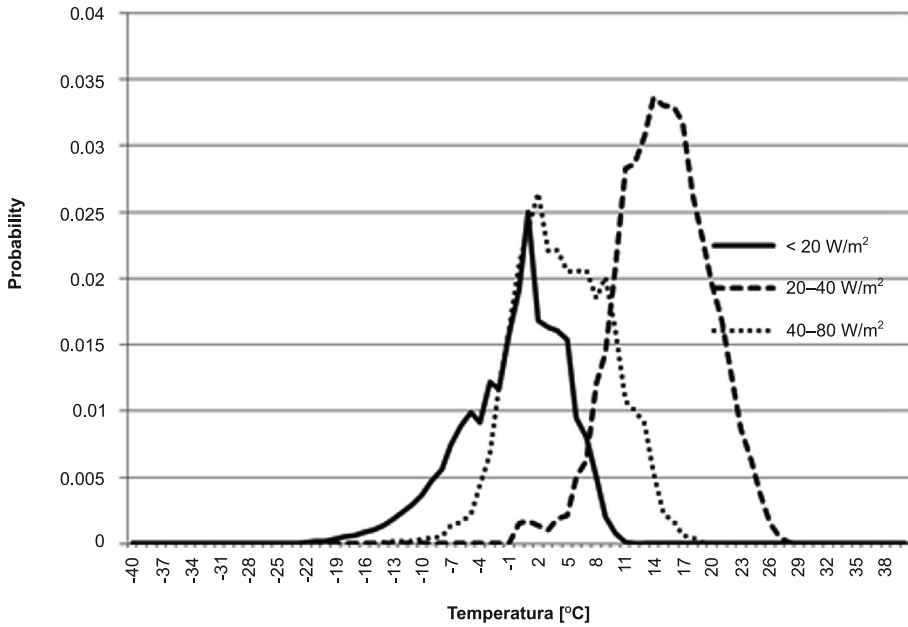


Fig. 4. Probability density function levels for the occurrence of thermal loads, depending on temperature

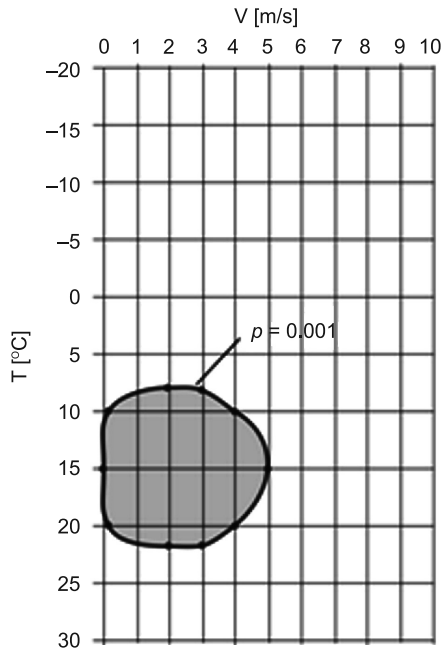


Fig. 5. Wind speed and temperature ranges providing comfortable conditions ($\Delta Q < 20 \text{ W/m}^2$)

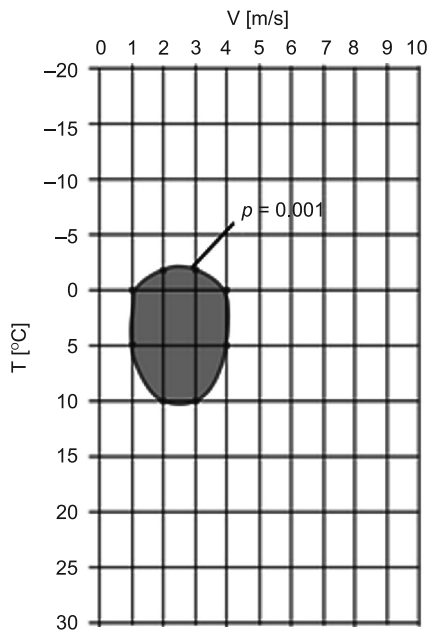


Fig. 6. Ranges of wind speed and temperature providing conditions of discomfort
 $\Delta Q = 20 - 40 \text{ W/m}^2$

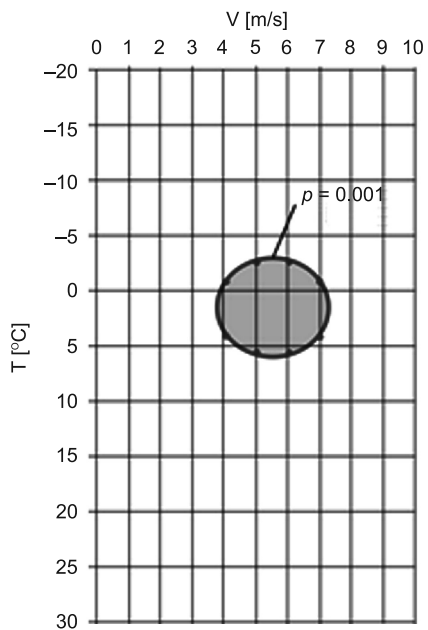


Fig. 7. Ranges of wind speed and temperature providing strong conditions of discomfort
 $(\Delta Q = 40 - 80 \text{ W/m}^2)$

Conditions in which unfavorable loads on the body occur ($\Delta Q = 20 - 40 \text{ W/m}^2$) are presented in Fig. 6. As in the previous instance, only situations with a probability exceeding 0.001 were taken into account.

In the case of uncomfortable conditions, the temperature reaches a value between -2 and $+10^\circ\text{C}$ and wind speed varies between 1 and 4 m/s. The probability of an occurrence of discomfort in such conditions over the 30-year analysis period is at a level of 0.26.

The third of the proposed thresholds refers to strong unfavorable loads, in which $\Delta Q = 40 - 80 \text{ W/m}^2$. Figure 7 presents the ranges of temperature and wind speeds in which such conditions of discomfort may occur.

The analysis establishes that strong conditions of discomfort will occur when air temperature acquires values between -3 and $+5$ and wind speed reaches between 4 and 7 m/s. In such meteorological conditions, the probability of an individual experiencing strong discomfort is approximately equal to 0.15.

5. Conclusions

The analysis drew on data from the open suburban area of Lodz, located near a meteorological station, and reflects only climatic influences on comfort conditions. In the case of a built-up area, the problem becomes more complicated. The most important factor, which significantly affects microclimatic conditions (and thereby human comfort) are buildings. Depending on the arrangement of buildings and the location in relation to Compass North, different wind speeds can be expected. Particular attention has to be paid to high buildings above 20m, which generate strong winds in their vicinity. In order to assess conditions for human comfort in urban areas, a detailed analysis should be carried out taking heat and mass transfer into account.

References

- [1] Strategiczny plan adaptacji dla sektorów i obszarów wrażliwych na zmiany klimatu do roku 2020 z perspektywą do roku 2030, Ministerstwo Środowiska, Warszawa 2013.
- [2] Błażejczyk K., *Wymiana ciepła pomiędzy człowiekiem a otoczeniem w różnych warunkach środowiska geograficznego*, Prace Geograficzne PAN, nr 159, 1993, 71-75.
- [3] Klemm K., *Kompleksowa ocena warunków mikroklimatu w luźnych i zwartych strukturach urbanistycznych*, Polska Akademia Nauk Komitet Inżynierii Lądowej i Wodnej, studia z zakresu inżynierii, Nr 75, Warszawa 2011, 172.

DOMINIKA KNERA*, ELIZA SZCZEPAŃSKA-ROSIAK*, DARIUSZ HEIM*

PROVIDING AN INTERIOR DAYLIGHT ENVIRONMENT THROUGH THE USE OF LIGHT PIPES

KSZTAŁTOWANIE WEWNĘTRZNEGO ŚRODOWISKA OŚWIETLENIOWEGO ZA POMOCĄ ŚWIETLIKÓW RUROWYCH

Abstract

The paper presents the effect of using additional daylight illumination of building interiors using tubular skylight systems. Interior illuminance distribution was analysed using a combination of two daylight sources – window and skylight pipes. The results were obtained for cloudy weather conditions. Final remarks concern the effectiveness of supplementary daylighting of interiors using different configurations of light pipes.

Keywords: daylight, tubular skylights, interior illuminance, simulation

Streszczenie

W artykule omówiono możliwość wykorzystania doświetlenia wewnątrz światłem dziennym za pomocą systemów świetlików rurowych. Przeanalizowano rozkłady natężenia oświetlenia wewnątrz przy zastosowaniu kombinacji okna ze świetlikami rurowymi. Wyniki otrzymano dla warunków nieboskłonu zachmurzonego. Określono skuteczność doświetlenia w przypadku zastosowania różnych rozwiązań i konfiguracji świetlików.

Słowa kluczowe: światło dzienne, świetliki rurowe, oświetlenie wewnętrzne, symulacja

* M.Sc. Eng. Dominika Knera, Ph.D. Eng. Eliza Szczepańska-Rosiak, Ph.D. D.Sc. Eng. Dariusz Heim, Department of Environmental Engineering, Faculty of Process and Environmental Engineering, Lodz University of Technology.

1. Introduction

Daylight utilization in the design of a healthy building environment is a crucial point, not only with regard to the indoor environment quality but also from an energy efficiency point of view. People spend a majority of time during the day in selected types of the non-residential buildings e.g. offices. Therefore, it is necessary to provide high indoor comfort parameters including the lighting quality. Daylight distribution and directionality of light determine the main parameters of visual comfort and comfort indexes. The main visual comfort indexes are based on two parameters: luminance and illuminance. Daylight illuminance inside the building is changeable and depends on external parameters like weather, time, season and urban development. Similarly, the amount of light inside the building strongly depends on architecture design, geometry, size of windows and surface properties (transmission and reflection characteristics). Nowadays, the starting point for daylight design is some simple guidelines which are giving inaccurate results. This approximation is based on the percentage of glazing, the ratio of glazing area to floor area or the maximum depth of the room which should not be exceeded. It is a relatively easy but a too imprecise approximation. In some cases, creating an appropriate lighting environment does not simply need horizontal windows, but also untypical solutions like a light shelf [1], light breakers [2], light pipes or optical fibers [3]. These solutions are used due to limitations of architecture, spatial condition and the unique character of natural light.

The aim of this study is the analysis of interior illuminance distribution in the room illuminated by a combination of window and light pipes. The paper presents the results of simulations of the different optical properties of windows and various positions of light pipes. Subsequently, an analysis was carried out for the selected combination of windows and light pipes.

2. Visual comfort

Use of daylight for lighting building interiors is a prerequisite to ensure a comfortable and healthy working environment [4]. Daylight is the healthiest kind of light for the human eye because of its colour and continuous spectrum. Lighting condition has an impact on speed, accuracy and effort associated with activity. It has also a great influence on health, well-being and life quality. Therefore, it is important to create a visually comfortable interior of the room by providing lighting of a suitable quality and quantity. It should be emphasized that comfort depends on many parameters, but it is also very subjective.

An appropriate light environment which ensure the visual comfort, visual effectiveness as well as security, is mainly associated with following values [5]: lighting intensity, luminance distribution and glare. In the following paper, only one of these parameters – illuminance was considered. Ensuring an adequate level of illuminance and its spatial distribution affects how quickly and easily visual tasks may be carried out. Insufficient lighting causes tiredness, sleepiness, worsening mood of the observer and additionally, it may be the cause of accidents. The required average illuminance in the field of work and on the immediate surroundings of the workspace are given in standard EN 12464-1 Light and lighting. Lighting

jobs. Part I. Indoor work places. For most scenarios, the illuminance on the work area should be in the range of 20 lux (noticeable human traits) to 2000 lux. In the immediate surroundings of the workspace, the illuminance value might be slightly lower. Another important parameter is the uniformity of illuminance (ratio of the smallest measured illuminance on a given surface to the average illuminance on the plane), which should be at least 0.7 on the work plane and 0.5 on the immediate surroundings for continuous operations. Lack of uniformity of illumination causes ocular muscle fatigue, which is related to the need to adapt to changing light intensity.

3. Light pipes vs. windows

There have been some research works on the performance of light pipes over past decades [6, 7]. The main task of light pipes is to supply natural light into areas of the building with limited or zero access to daylight. They can be also situated in the rooms with shape, dimensions or optical properties of existing windows causing insufficient light distribution. Light pipes consist of three parts: outside collector installed on the roof, tube to transport daylight and diffuser. The transport tube can be rigid or flexible. The main goal of the light pipes is to collect the solar radiation through the cupola, its transporting by tube and dissipating in the room. The type of the lower glazing, matt or transparent, determines the interior daylight distribution. Matt glazing causes a more regular distribution of light while for transparent, it is more diverse. Light pipes provide less light than traditional windows due to losses in the transport tube. However, in dimly lit rooms, especially with north oriented windows, light pipes can be used to increase the illumination. Besides, the application of light pipes allows for a decreased surface area of windows which consequently reduces the threat of a glare effect or overheating problems in the summer period. Previous analyses of combination system of windows and light pipes are available in the literature [8].

4. Case study

The test cell analysed here was 3 m high, 3 m wide and 9 m deep. The external surface was 9 m². For the purpose of analysis, the representative types of glazing have been selected. The visible transmittance for ten types of glazing components rises gradually by 10% from 10% to 100%. In this case, the whole external surface was treated as a transparent area which is 1/3 of the total floor area. In the second case, only the size of the window has been changed gradually by 10% from 100% (totally glazed surface) to 10%. For each transmittance and size of window, six variations of light pipes' geometry with a diameter of 0.35 m and 0.85 m were assessed. In the paper, two types of the emitter were analysed – matt (mat) and transparent (tran). Transmittance for collector and both types of emitters was assumed as 0.9. The analysed tube was 1.0 m long and has internal reflectance at a level of 0.95. Analysis was performed for six cases due to the number and position of the light pipes (Fig. 1). In the first three cases, one light pipe located on the 1.5 m (1.1), 4.5 m (1.2) or 7.5 m (1.3) depth was analysed. Next two cases were performed for two light pipes situated on the 1.5 m



Fig. 1. Position of the light pipes according to the window

and 4.5 m (2.1) or 4.5 m and 7.5 m (2.2) depth. In the last case (3.1) three light pipes were located on the 1.5 m, 4.5 m and 7.5 m depth.

The analysed part of the building was located at a point with central Europe climatic conditions (longitude, latitude and meridian respectively 52.25N, 21.0E, -15.0) and south oriented. The luminance of the sky was assumed according to the Standard Overcast Sky Distribution developed by the *Commission Internationale de l'Eclairage* (CIE) [9]. Results were saved and analysed for 21st of March at 12:00.

The numerical calculation for vertical windows has been done using RADIANCE- which is based on Ray-tracing methodology [10]. Analysis of the daylight distribution supplied by light pipes was performed using the calculation program, HOLIGILM (**H**ollow **L**ight **G**uide **I**nterior **i**llumination **M**ethod). The calculation method of this program is based on the analytical solution and the Ray-tracing method [11].

5. Results analysis

The analysis was divided into two parts. In the former part, the interior daylight distribution was performed due to the different optical properties of the glazing partition as well as the position and diffusivity of the light pipes (Fig. 2). It can be noticed that for most of the analysed cases of the façade optical properties, interior illuminance is sufficiently high across the whole surface of the room (> 500 lux). Additional light from light pipes is required in only four cases. The first two were characterized by visible transmittance equal to 100% and a small area of the window with a size of 10% and 20% of the glazing. The next cases for the fully glazed façade with visible transmittance at a level of 10% and 20% were chosen. According to the analysis of the light pipes, the maximum values of the illuminance for matt and transparent light pipes (Fig. 2. c, d) are comparable and reach almost 600 lux. The significant difference between them is visible due to the distribution. The matt diffuser caused more even light than the transparent one. For further research, three cases (1.3, 2.2, 3.1) were adopted both for the matt and the transparent diffuser. Illuminance resulting from window light is the highest near the window and low in the opposite side of the room. Therefore, additional lighting was chosen for light pipes located deep in the room (1.3, 2.2). Furthermore, case 3.1 was analysed with three light pipes uniformly illuminating the whole analysed surface. Additionally, in the second part of the analysis, a study of the illuminance for a light pipe with a 0.35 m diameter was included. Graphs in Fig. 3 present illuminance distribution in the room illuminated by a combined system of window and 0.35 m diameter light pipes. It can be noticed that additional illuminance from light pipes is slight at a maximum of 100 lux. Therefore, light distribution for analysed cases is insufficient (< 500 lux), except for the combination system of 20% glazed surface of the façade and three light pipes with matt diffusers.

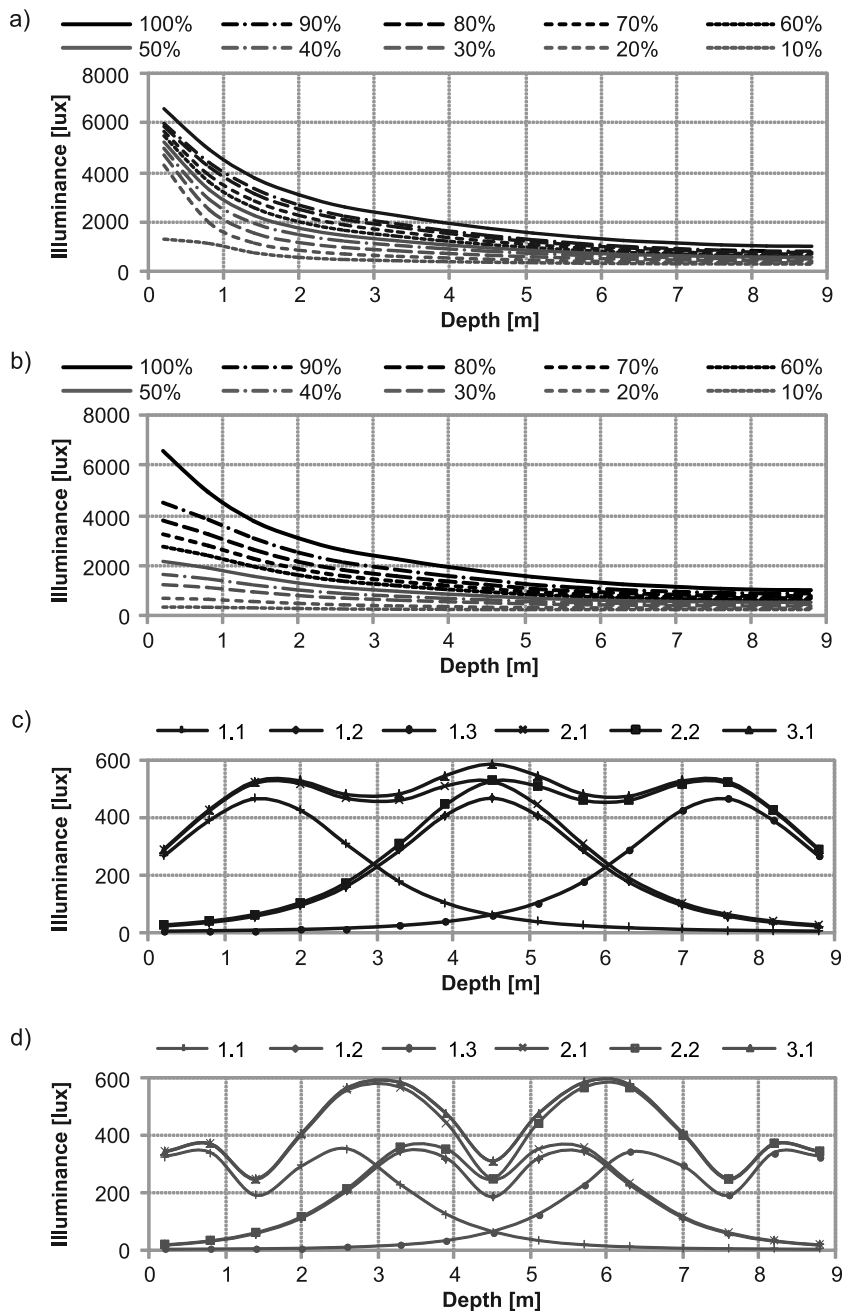


Fig. 2. Interior illuminance for different: a) size of the window, b) visible transmittance of the window, c) position of 0.85 m diameter light pipes with transparent diffuser, d) position of 0.85 m diameter light pipes with matt diffuser

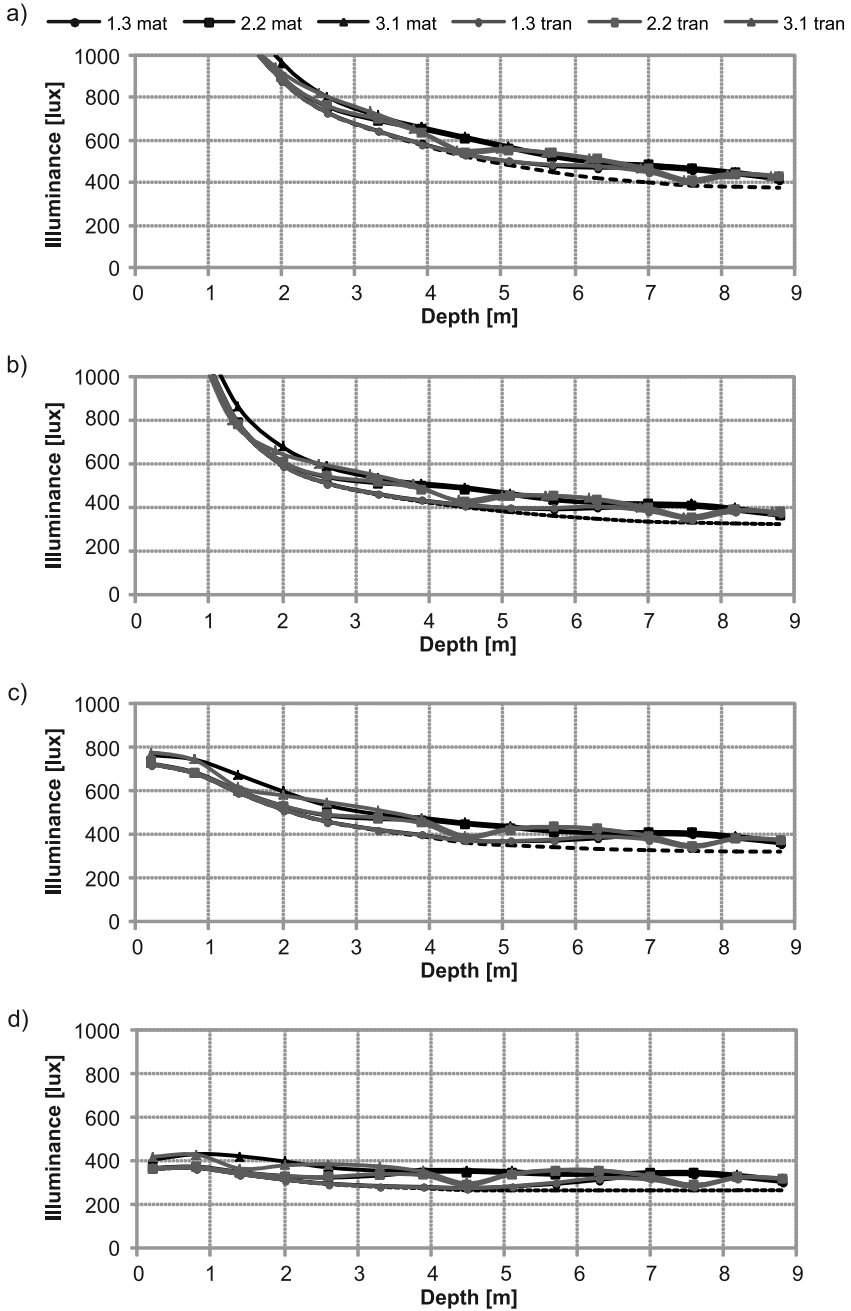


Fig. 3. Interior illuminance for light system combined from the 0.35 m diameter light pipes and window of: a) 20% glazing surface of the facade, b) 10% glazing surface of the facade, c) 20% visible transmittance, d) 10% visible transmittance

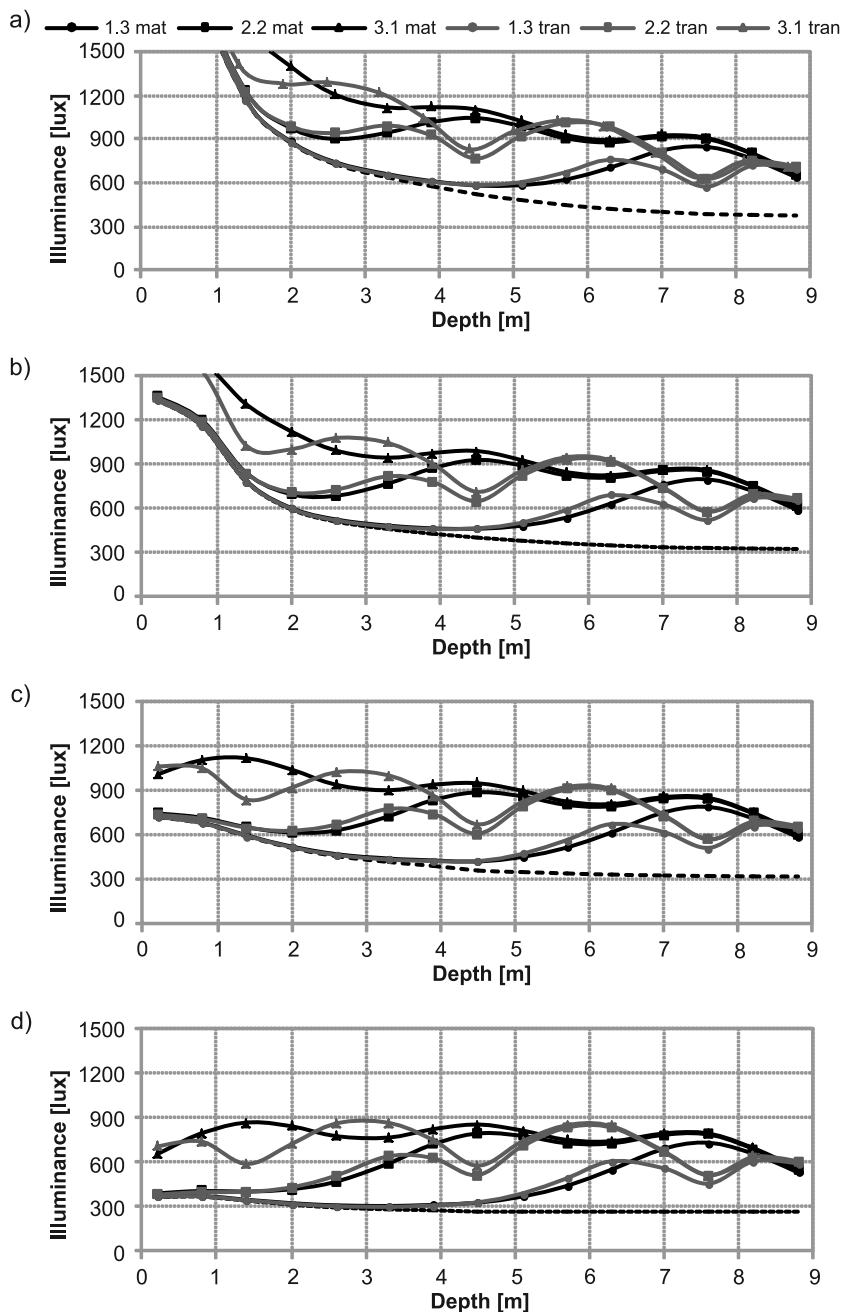


Fig. 4. Interior illuminance for light system combined from the 0.85 m diameter light pipes and window of: a) 20% glazing surface of the facade, b) 10% glazing surface of the facade, c) 20% visible transmittance, d) 10% visible transmittance

Figure 4 presents results due to the application of bigger light pipes with a diameter of 0.85 m. All combined systems with a 20% glazing surface provide minimum illuminance in the whole room. In other cases, the use of two or three light pipes is required to ensure 500 lux.

6. Conclusions

In the paper, analyses of the interior illuminance for individual and combined systems of window and light pipes in the longitudinal room were performed. Windows with high visible transmittance or a large surface area ensure sufficient illuminance distribution in the whole room. Additional lighting from the light pipes is reasonable only for windows with a low visible transmittance ($< 30\%$) or small surface ($< 30\%$). Light passing through these kinds of windows does not provide required illuminance distribution in the opposite side of the room. Consequently, application of light pipes as a source of additional illuminance in the deep parts of the room can solve the problem. Furthermore, high levels of illuminance from light pipes with matt and transparent diffuser are comparable for overcast sky distribution. However, the matt diffuser causes more uniform light distribution. Therefore, it is recommended to use light pipes with a matt diffuser to ensure high visual comfort. Additionally, on preliminary examination, light pipes with a diameter of less than 0.35 m result in low additional light and application of them in combined systems with windows is inefficient.

References

- [1] Heim D., Kieszkowski K., *Wpływ zastosowania poziomych pól świetlnych na komfort wizualny we wnętrzach budynków*, Zeszyty Naukowe Politechniki Rzeszowskiej, Budownictwo i Inżynieria Środowiska z. 40, Energia Odnawialna – innowacyjne idee i technologie dla budownictwa, nr 229, Rzeszów 2006, 197-202.
- [2] Balcerzak W., Heim D., *Badania wybranych parametrów wizualnych żaluzji typu FISH*, Fizyka Budowli w Teorii i Praktyce, Tom 2, 2007, 11-14.
- [3] Darula S., Kittler R., Kocifaj M., Plch J., Mohelnikova J., Vajkay F., *Osvetlovani Svetlovody*, Grada Publishing, 2009.
- [4] Heim D., Klemm P., Narowski P., Szczepańska E., *Komputerowa analiza oświetlenia dziennego i ocena parametrów komfortu wizualnego w pomieszczeniach*, red. D. Heim, Katedra Fizyki Budowli i Materiałów Budowlanych, Politechnika Łódzka, Łódź 2007.
- [5] Bąk J., Pabiańczyk W., *Podstawy techniki świetlnej*, Wydawnictwo Politechniki Łódzkiej, 1994.
- [6] Oakley G., Riffat S.B., Shao L., *Daylight performance of lightpipes*, Solar energy, vol. 69, 2000, 89-98.
- [7] Mohelnikova J., *Tubular light guide evaluation*, Building and environment, vol. 44, 2009, 2193-2200.
- [8] Jin Oh S., Chun W., Riffat S.B., Il Jeon Y., Dutton S., Joo Han H., *Computational analysis on the enhancement of daylight penetration into dimly lit spaces: Light tube vs. fiber optic dish concentrator*, Building and environment, vol. 59, 2013, 261-274.

- [9] Praca zbiorowa, CIE, *Guide on Daylighting of Building Interiors*, CIE Technical Committee TC-4.2 Daylighting, 1990.
- [10] Larson G.W., Shakespeare R., *Rendering with Radiance – The Art and Science of Lighting Visualization*, Morgan Kaufman Publishers Inc., San Francisco, California, 1998.
- [11] Kocifaj M., Darula S., Kittler R., *HOLIGILM: Hollow light guide interior illumination method – An analytic calculation approach for cylindrical light-tubes*, Solar energy, Vol. 82, 2008, 247-259.

PIOTR KONCA*, ALEKSANDRA KUBACKA**, DARIUSZ GAWIN*

EFFECT OF TITANIUM DIOXIDE ON THE SELF-CLEANING PROPERTIES OF PAINTS FOR ETICS

WPLYW DWUTLENKU TYTANU NA WŁAŚCIWOŚCI SAMOCZYSZCZĄCE FARB DO BEZSPOINOWYCH SYSTEMÓW OCIEPLEŃ

Abstract

The influence of a nano-particle addition on the self-cleaning properties of exterior paints for External Thermal Insulation Composite Systems is analyzed. The effect of UV radiation on the color change of paints containing normal pigments and the photo-catalyst titanium dioxide is laboratory tested. To evaluate self-cleaning properties of the paints and their color change due to accelerated weathering processes spectro-photometric tests were performed.

Keywords: External Thermal Insulation Composite Systems, facade paints, nanotechnology, photocatalyst titanium dioxide

Streszczenie

W artykule przeanalizowano wpływ nano-dodatku na właściwości samoczyszczące farb elewacyjnych stosowanych w systemach ETICS. Badano zmiany barwy powłok zawierających zwykłe pigmenty i foto-katalityczny dwutlenku tytanu wskutek działania promieniowania UV. Samoczyszczące właściwości zabrudzonych powierzchni farb i zmiany ich barwy podczas przyspieszonego procesu starzenia zbadano ilościowo za pomocą techniki spektrofotometrycznej.

Słowa kluczowe: Bezspoinowe Systemy Ociepleń, farby do elewacji, nanotechnologia, fotokatalityczny dwutlenek tytanu

* Ph.D. Piotr Konca, Prof. D.Sc. Dariusz Gawin, Department of Building Physics and Building Materials, Faculty of Civil Engineering, Architecture and Environmental Engineering, Lodz University of Technology.

** M.Sc. Aleksandra Kubacka, Graduate of Faculty of Civil Engineering, Architecture and Environmental Engineering, Lodz University of Technology.

1. Introduction

Nanotechnology is a promising field of research, allowing for significant improvements and/or modifications of physical and service properties of many materials used in building structures. Examples of such products, obtained by addition of nano-particles of silver, copper and/or titanium dioxide are: external renders, key coats, finishing coats, plaster-boards, polymer based or gypsum finishing systems, decorative renders, paints, grouts, self-cleaning glass, air conditioners, etc., see e.g. [1–3].

Different amounts of some additives, including pigments and nano-particles, are used in paints in order to obtain the required color and/or self-cleaning properties. The purpose of this study is to examine self-cleaning properties of silicone façade paints, containing different amounts of photo-catalyst titanium dioxide. The specimens of ETICS system were tested. First accelerated weathering of the paints with the UV irradiation and water vapor condensation was applied in the fluorescent UV device ATLAS UV2000. This is a screening device for reproducible, accelerated weathering testing of the sun's damaging effects on various coatings. Then the color tests were performed by means of a spectro-photometer Konica Minolta CM-2500d, in order to assess the self-cleaning properties and resistance of the surface to the UV irradiation.

2. Materials

The specimens of External Thermal Insulation Composite System with the dimensions 20 cm × 5 cm, were made in the laboratory.

The tested paints were prepared on a basis of silicone dispersion. The composition of different types of paints varied in content from titanium white, photo-catalyst titanium dioxide UVLP 7500, organic pigment powder (pink or yellow). The specimen symbols and the contents of chemical components are given in Table 1.

Table 1

Symbol of specimen and contents of each chemical components

Specimen symbol	Titanium White [%]	UVLP 7500 [%]	Organic Pigment [%]
S1	6.3	–	0.2 (pink)
S2	6.3	0.5	0.2 (pink)
S3	6.3	0.5	–
S4	6.3	–	0.2 (yellow)
S5	6.3	–	–
S6	6.3	0.5	0.2 (yellow)
S7	–	–	–
5	–	5	–
6	–	10	–
7	–	15	–

The paint components were weighed and mixed. Then, the paints were applied on the surface of base coat of ETICS and then stored for at least 14 days at $(23\pm 2)^{\circ}\text{C}$ and $(50\pm 5)\%$ RH. The UVLP 7500 nano-powder content of 0.5% is a standard quantity in façade paints produced in the factory. This powder contains no addition of pigments and it is a pure titanium dioxide (TiO_2). The UVLP 7500 is a photo-catalyst designed to improve paint durability against UV radiation. It is also suitable for eliminating unwanted odors such as vehicle emissions; for air purification from organic compounds such as nitrogen oxides, sulfoxides and chlorinated hydrocarbons [4]. The photo-catalyst titanium dioxide also eliminates soiling or contamination on the façade surfaces from substances like e.g. soot.

The next step of specimen preparation was the application of different types of dirt, in order to check self-cleaning properties of the tested paints. The upper part of the specimens remained clean and was used to test the effects of solar irradiation and water vapor condensation. The rest of the specimens' surface were covered with three types of contaminants, most commonly encountered on real building façades.

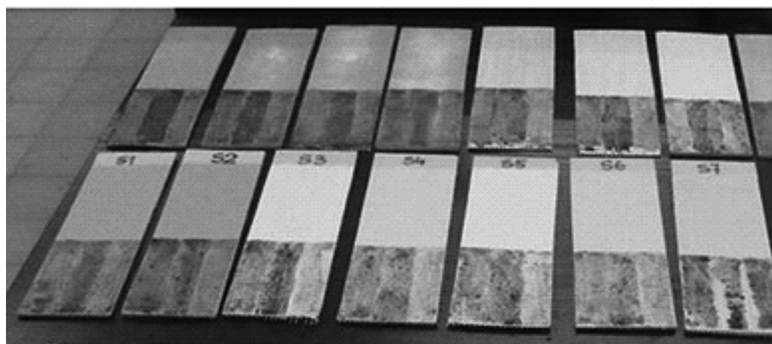


Fig. 1. The test samples before application of the UV radiation

The three types of contaminant were applied by means of painting with 10% 'dirt solutions' in distilled water. One sixth of each sample surface was covered with the carbon soot contamination, one sixth with the carbon ash contamination, and one sixth with the dust contamination. The dust was collected from the facades and windows of the university buildings, at a height of about 3 meters from the ground level. This is probably the kind of contamination which the facades of buildings are mostly exposed to.

3. Test methods

For testing the radiation resistance and self-cleaning properties, the fluorescent UV devices ATLAS UV2000 were used. The heated reservoir below the test chamber produced water vapor that was rising to the upper chamber, where specimens were exposed to the UV irradiation and uniform wetting at 100% RH. One test cycle consisted of irradiation of the samples by the fluorescent UV lamp and then condensation of water vapor. The samples were tested according to the Polish standard PN-C-81913:1998 [5] after the 50 cycles, consisting of the following phases:

- 4 hour UV-A (340 nm) irradiation of the intensity 0.65 W/m^2 at a temperature of $60 \pm 2^\circ\text{C}$,
- 4 hour water vapor condensation at a temperature of $40 \pm 2^\circ\text{C}$.

Hence, the total testing time in the chamber was equal to 400 hours. Next macroscopic color of the samples' surface was evaluated by means of the spectrophotometer Konica Minolta CM-2500d.

Color space CIELab has been normalized by CIE (the International Commission on Illumination (also known as the CIE from its French name, the Commission Internationale de l'Eclairage) is devoted to worldwide cooperation and the exchange of information in all fields of science and art concerning light and lighting, color and vision, photobiology and image technology. The color space defined by the CIE is based on one channel for Luminance (lightness) (L) and two color channels (a and b) [5]. A problem related to a XYZ color system, is that colorimetric distances between the individual colors do not correspond to perceived color differences. For example the difference between green and greenish-yellow is relatively large, whereas the distance distinguishing blue and red is quite small. The CIE solved this problem in 1976 with the development of the three-dimensional Lab color space (or CIELab color space). In this model, the color differences which are perceived correspond to the distances measured calorimetrically. The ' a axis' extends from green ($-a$) to red ($+a$) and the ' b axis' from blue ($-b$) to yellow ($+b$). The brightness (L) increases from the bottom to the top of the three-dimensional model. This color space is currently the most popular method for describing the color and forms a basis of modern color management systems [6]. In the CIELab color space, the color difference can be expressed as a single numerical value, ΔE , which indicates the size of the color difference, but not in what way the colors are different. ΔE is defined by the following equation [6]:

$$\Delta E = \sqrt{(\Delta L)^2 + (\Delta a)^2 + (\Delta b)^2} \quad (1)$$

and is the simple Euclidean distance between two points in three-dimensional space.

It can be assumed that the color difference noted by the standard observer can be described as follows:

- $0 < \Delta E < 1$ – the difference cannot be noticed,
- $1 < \Delta E < 2$ – the difference can be noted only by an experienced observer,
- $2 < \Delta E < 3.5$ – the difference can be also noted by an inexperienced observer,
- $3.5 < \Delta E < 5$ – a clear difference of color can be noted,
- $5 < \Delta E$ – the impression of two different colors is noted.

In the research a three-dimensional classification was used, based on the relative spectral power distribution of the CIE standard illuminant D_{65} and the 10° supplementary standard observer. The symbol D_{65} suggests that the related color temperature should be 6500 K, while in reality it is closer to 6504 K [7].

Our perception and interpretation of color are highly subjective. Color measurement is the determination of the characteristics of electromagnetic radiation entering an eye. It is difficult to describe objectively any particular color to someone without the same type of standards. The solution is application of a measuring instrument that explicitly identifies the color. Spectrophotometer is an instrument that differentiates any given color from all the others and assigns it a numeric value.

4. Results

The three color components were measured in the three points on the surface of every specimen and the results were averaged. The samples were tested with the spectrophotometer, before and after 50 cycles of aging. Results for clean paints are shown in Table 2.

Table 2

The difference in color and lightness after exposition to the UV radiation - clean paints

Symbol of specimen	The difference in color ΔE after the UV cycles	The difference in lightness ΔL after the UV cycles	Color of paint
S1	1.58	0.71	pink
S2*	2.39	0.88	pink
S3*	1.18	-0.92	white
S4	1.79	-0.45	yellow
S5	1.04	-0.84	white
S6*	1.02	-0.81	yellow
S7	2.46	-1.88	transparent
5*	2.82	2.72	white
6*	2.29	1.83	white
7*	2.35	1.64	white

* The paint contains the nano-powder

The results obtained for sample S7 indicate an important effect of the UV irradiation on the color change for the pure silicone dispersion without any pigments, what influenced also the other results. To show character of the change, another parameter showing the difference in lightness/darkness value ΔL (positive ΔL means lighter, negative – darker colour) was used. The difference ΔL is defined by the following equation:

$$\Delta L = L_1 - L_2 \quad (2)$$

where:

L_1 – lightness sample after aging UV radiation,

L_2 – lightness sample before aging UV radiation.

After the UV irradiation, the surface painted with pure silicone dispersion (sample S7) darkened. Application of larger amounts of the photocatalyst titanium dioxide caused significant brightening of the surface. This may mean destruction of the silicone dispersion in presence of the UVLP 7500. The 0.5% admixture of nano-powder had not a significant influence on the results obtained. For the color change both the pigment and the dispersion were responsible.

The color measurement results in the case of surfaces soiled with different pollutants are shown in Fig. 2. The results show that the color aging depends on the type of pollution.

The results clearly indicate that admixture of the photo-catalyst titanium dioxide to the paints in the amount of 0.5% does not activate the self-cleaning properties. In this case

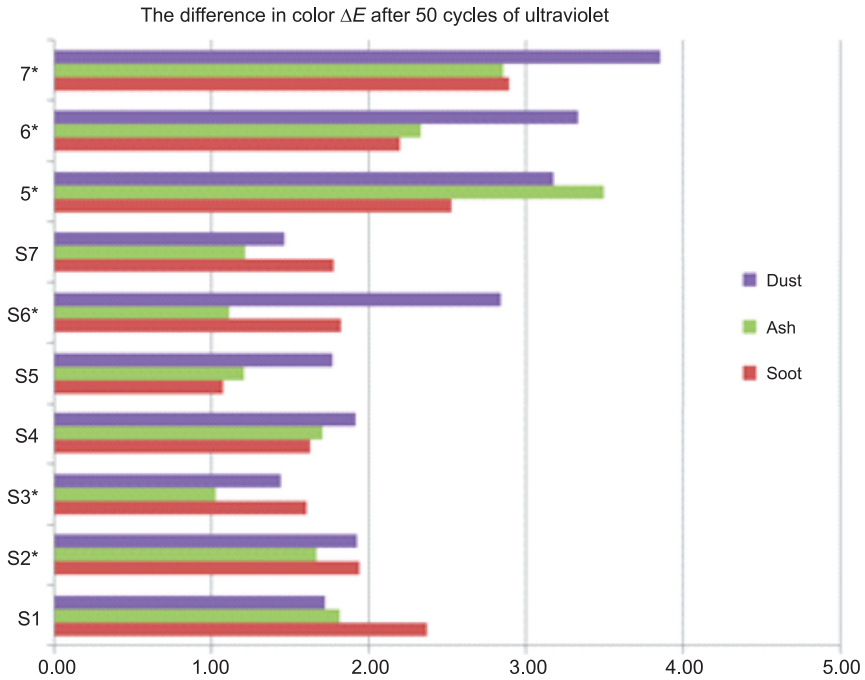


Fig. 2. The differences in color of polluted paints after the UV irradiation

the nano-powder is too dispersed within volume of the paint. A noticeable self-cleaning effect can be obtained only after adding several times larger amount of the UVLP 7500 (Fig. 3).

Figure 3 indicates, that obtaining self-cleaning properties of the façade surface is possible by adding the photo-catalyst titanium dioxide to the silicone paint. It is important to properly select the paint composition. The nano-powder applied in too small amounts does not work,

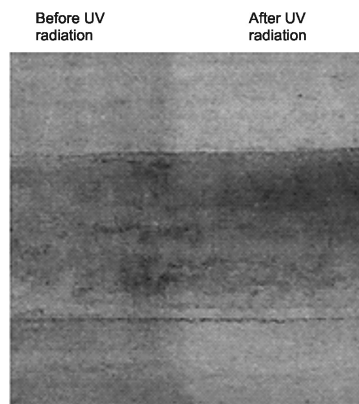


Fig. 3. Photo of the sample No 6 with 10% UVLP 7500, before and after exposition to the UV radiation

while the amounts exceeding a certain level can destroy the paint organic binder. Obtaining the self-cleaning paints may depend on other factors as well. For example the sample S7 showed a hydrophobic (water resistant) behavior and it was even very difficult to apply

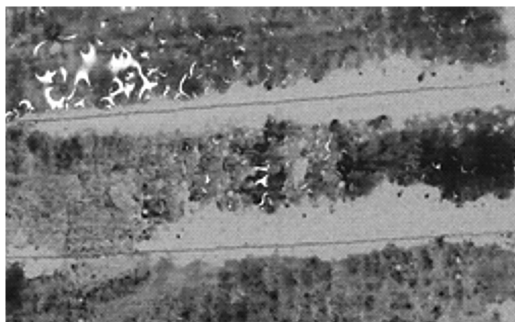


Fig. 4. Photo of sample No S7, the polluted surface of the clean silicon dispersion

soiling on its surface (Fig. 4). During pollutant painting, drops of water and soiling did not adhere to the surface, but flowed down freely. The sample showed a greater resistance to attempts of soiling than the dispersions with pigments.

5. Conclusions

There is lack of standardized methods for testing the self-cleaning properties for facade paints. The surface of the tested silicone paints, without and with different additions of the nano-powder, after weathering by means of UV irradiation and water vapor condensation, exhibited visible aging effects for the all paints.

The studies performed revealed that the properties of 'self-cleaning surface' have been measured for the paints containing at least 5% of the photo-catalyst titanium dioxide, and were clearly visible for its amount in the paint of at least of 10% by weight.

References

- [1] Czarniecki L., *Nanotechnologia w budownictwie*, Przegląd Budowlany 1/2011.
- [2] Kaiser J.-P., Zuin S., Wick P., *Science of the Total Environment*, 442, 2013, 282-289.
- [3] Nakatani H., Miyazaki K., *Journal of Applied Polymer Science*, 2013, 3490-3496 (DOI 10.1002/APP.39101).
- [4] KRONOS, *TiO₂, Grades and applications*, Kronos Information 2.1, March 2009.
- [5] Polish Standard PN-C-81913:1998 *Farby dyspersyjne do malowania elewacji budynków*.
- [6] Mielicki J., *Zarys wiadomości o barwie*, Fundacja Rozwoju Polskiej Kolorystyki, Łódź 1997.
- [7] Konica Minolta, *User manual Spektrophotometer CM – 2600d/2500d*.

OL'GA KORONTHÁLYOVA*, L'UBOMÍR BÁGEL*, MARTA KULLIFAYOVÁ*,
TOMÁŠ IFKA*

HYGRIC PERFORMANCE OF CONTEMPORARY AND HISTORICAL CREAMIC BRICKS

HIGROSKOPOWA ANALIZA WSPÓŁCZESNYCH ORAZ HISTORYCZNYCH CEGIEŁ CERAMICZNYCH

Abstract

This paper analyses the effect of microstructure, mineralogical composition and possible salt contamination on parameters of moisture accumulation and transport. Analysis is done for three types of contemporary and two types of historical bricks.

Keywords: sorption isotherm, water vapour permeability, ceramic brick, microstructure, salt

Streszczenie

W artykule przedstawiono wpływ mikrostruktury, składu mineralnego oraz możliwego występowania soli na akumulację i transport wilgoci. Analizy zostały przedstawione dla trzech typów elementów ceramicznych: materiału współcześnie stosowanego oraz dwóch stosowanych w przeszłości.

Słowa kluczowe: sorpcja, przepuszczalność pary wodnej, cegła ceramiczna, mikrostruktura, sól

* Ph.D. Oľga Koronthályová, RNDr Ľubomír Bágel, Eng. Marta Kullifayová, Ph.D. Eng. Tomáš Ifka, Institute of Construction and Architecture, Slovak Academy of Science, Bratislava, Slovakia.

1. Introduction

Moisture transport and accumulation parameters are key factors in evaluation of hygro-thermal performance of building structures. Generally, moisture transport and accumulation parameters depend on actual pore structure of the building material. In cases when moisture accumulation only can be attributed to physisorption of water vapour on the material pore system and the material does not contain very fine pores, inaccessible to nitrogen (e.g. common ceramic bricks), the hygroscopic moisture content (HMC) can be evaluated from nitrogen sorption [5, 6]. However, in case of historical bricks, which have been exposed for a long-time to interaction with chemicals from the surrounding air or water, contamination with water soluble salts is very probable. Presence of hygroscopic salts significantly increases the HMC of ceramic bricks [6, 8]. Therefore measurement of the HMC of brick samples can be used as an indication of the salt contamination [7]. In case of material contaminated with single salt relative reliable results, also on the quantity of the present salt, can be obtained from the HMC because of the linear relation between HMC and salt content. However, in case when a mix of unknown salts is present, as it is usual in reality, the relation between the HMC and the salt content is not clear [7, 8].

In this work, parameters of moisture accumulation and transport, namely water vapour sorption and water vapour permeability moisture dependence for three types of contemporary and two types of historical ceramic bricks were determined. Based on the obtained results, the effects of microstructure, mineralogical composition and possible salt contamination on the parameters of moisture accumulation and transport were analysed.

2. Materials and methods

The tested samples were three types of contemporary burnt clay bricks produced by Slovak manufacturers and two types of historical brick (nineteenth century) from western part of Slovakia.

The tested bricks were characterised by following basic parameters: bulk density, density, total porosity, open porosity and capillary moisture content. The bulk density was calculated from volume and mass of the dried out specimens (oven drying at 105°C). The density of ceramic body was determined by gas (N_2) pycnometer Pentapyc 5200e. The total porosity was calculated from density and bulk density. The open porosity was determined from water saturation test, the capillary moisture content from one dimensional time-controlled capillary water uptake experiment.

Mineral composition was determined by X-ray diffractograf Philips. The device is equipped with goniometer PW 1050 and Ni filter, and use Cu-K α radiation in the range of angles 4–62° 2 Θ . X-ray tube works at 35 kV and 20 mA. Velocity of record is 2°/min 2 Θ . The data were analysed using software BedeZDS Search/Match.

Nitrogen adsorption measurements were performed with the volumetric ASAP2400 instrument, enabling isotherms in the 0.01–0.98 relative pressure range to be obtained. Prior to the measurement the samples were degassed overnight at 150°C and 2 Pa. The specific surface area of pores was determined by the BET method.

Water vapour sorption isotherms were determined by the standard gravimetric desiccator method, which consists of conditioning the samples in desiccators under constant relative humidity (RH) and temperature until the static equilibrium is achieved [2]. The samples were oven dried beforehand at 105°C.

The water vapour permeability of the brick specimens was measured by the standard cup method [3]. Mass of the samples was checked before and after each cup test. At the end of all cup measurements the samples were oven dried at temperature of 105°C in order to determine actual moisture contents of the samples. All water vapour permeability measurements were performed in an air-conditioned room at temperature of $23 \pm 0.5^\circ\text{C}$ and RH equal to $53 \pm 1\%$. The required RH inside the cup was established by using silica-gel, water or saturated salt solutions.

3. Results and discussion

The basic material parameters and the BET specific surface area of the tested bricks are presented in Table 1. The crystal phases identified in brick specimens by X-ray diffractometry are summarized in Table 2. As follows from the data, the tested bricks had practically identical mineral composition, with an exception in the case of illite, which was identified in bricks D, BA1 and BA2 and of montmorillonite, identified in brick BA2. The presence of illite and montmorillonite indicates an imperfect heating regime in the furnace, common for historical bricks [1]. The X-ray diffractometry results did not confirm presence of hygroscopic salts. This result does not fully exclude the possibility of salt contamination but it guarantees that in case of contamination the amount of particular salt is below of 1 wt %.

Figure 1 and 2 show the measured nitrogen and water vapour adsorption isotherms for tested bricks. In case of all three contemporary bricks very good correspondence between nitrogen and water vapour adsorption isotherms was found. The nitrogen results showed significant dissimilarity of the tested bricks microstructure. Correspondingly the HMC of brick D was practically negligible up to the RH of 94%. The determined HMC of brick S was noticeable but relatively low while the HMC of brick P was quite significant (Fig. 1). The good agreement between the water and nitrogen adsorption curves indicated that the contemporary bricks did not contain hygroscopic salts.

Table 1

Basic material parameters and BET specific surface area of tested bricks

Brick	Bulk density [kg/m ³]	Density [kg/m ³]	Total porosity [-]	Open porosity [-]	Capillary moisture content [m ³ /m ³]	Specific surface area [m ² /g]
P	1370	2752	0.51	0.42	0.37	14.2
S	1460	2788	0.50	0.44	0.39	4.7
D	1780	2752	0.35	0.30	0.24	1.13
BA1	1710	2708	0.37	0.34	0.29	4.4
BA2	1700	2790	0.39	0.36	0.25	9.3

Crystal phases identified in tested bricks

Brick	Identified phases
D	Quartz, illite, muscovite, feldspars, enstatite (Fe, Mg), hematite
P	Quartz, muscovite, feldspars, enstatite (Fe, Mg), hematite
S	Quartz, muscovite, feldspar, esseneite (Ca, Fe), enstatite, hematite
BA1	Quartz, illite, muskovite, feldspars, calcite, hematite
BA2	Quartz, Illite, montmorillonite, muscovite, calcite, feldspars, hematite

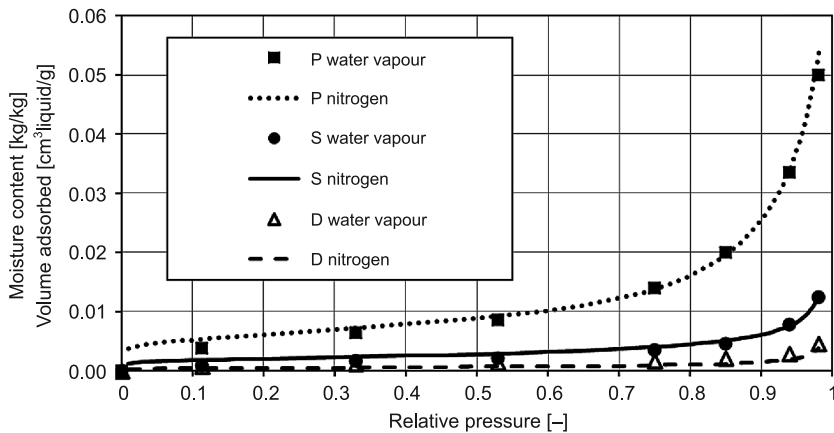


Fig. 1. Water vapour and nitrogen adsorption isotherms of contemporary bricks D, P and S

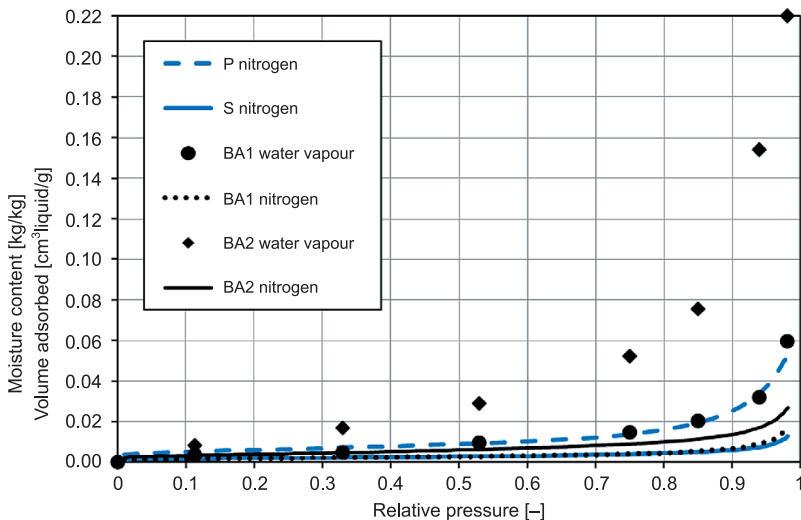


Fig. 2. Water vapour and nitrogen adsorption isotherms of historical bricks BA1 and BA2 compared with nitrogen adsorption isotherms of contemporary bricks P and S

Table 3

Identified concentration of salt anions and evaluated total salt concentration (historical bricks)

Brick	Cl ⁻ [kg/kg]	SO ₄ ²⁻ [kg/kg]	NO ₃ ⁻ [kg/kg]	Total salt amount [kg/kg]
BA1	0.0014	0.0014	0.0035	0.011–0.015
BA2	0.0038	0.0002	0.01	0.023–0.03

The nitrogen adsorption curve of historical brick BA1 was practically identical with the one of brick S, the nitrogen adsorption curve of historical brick BA2 was somewhere between the ones of brick S and P. However, the obtained HMC values of the historical bricks were significantly higher than the corresponding nitrogen isotherms. This discrepancy could result from their possible salt contamination. Therefore the BA1 and BA2 samples were put to qualitative, and after receiving positive results, also quantitative chemical analysis for determination of chloride, sulphate and nitrate anions. The analysis confirmed medium chloride, low sulphate and high nitrate salt contents in BA1 sample. In case of brick BA2 the analysis showed high chloride, practically negligible sulphate and very high nitrate salt content in the samples (Tab. 3). With the aim to estimate the total amount of hygroscopic salts in the samples, the presence of ammonium salts was tested but result of the test was negative. Taking into account occurrence of the most probable salts (NaCl, KCl, CaCl₂, CaSO₄, Na₂SO₄, K₂SO₄, KNO₃ and NaNO₃ for BA1 and NaCl, KCl, CaCl₂, KNO₃ and NaNO₃ for BA2) and the actual concentration of the salt anions (Tab. 3), total amount of the salts was evaluated. The minimum total salt amount was evaluated supposing only the salts with the lowest ratio of molar mass per one salt anion are present (CaCl₂, CaSO₄, NaNO₃). The maximum total salt amount was correspondingly calculated from the salts with the highest value of molar mass per one salt anion (KCl, K₂SO₄, KNO₃). The evaluated total salt amount was from 1.1 to 1.5 wt % in case of BA1 and from 2.3 to 3.0 wt % in case of BA2 (Tab. 3). However it is necessary to point out that the values presented are only approximate. Nevertheless it is possible to note that the estimated considerably higher total salt amount of BA2 is in good agreement with the significantly higher HMC of this brick. From the estimated values of the total salt amount and the results of X-ray diffractometry also follows that mixture of at least two different salts was present in bricks BA1 and BA2.

The measurements of the water vapour permeability of contemporary bricks were performed under different RH differences (0–53%, 11.3–53%, 33–53%, 53–75.4%, 53–84.7%, 53–94% and 53–100%) with the aim to get water vapour resistance factor values for the broadest possible range of moisture contents, including the transition zone from the higher value of water vapour resistance factor, corresponding to the water vapour diffusion without the surface diffusion, to the lower value, following from cumulated effect of the water vapour diffusion and the surface diffusion. The water vapour permeability of the historical bricks was measured under RH differences of 0–53%, 53–94% and 53–100% (Fig. 3). Analysis of the measured water vapour resistance factor/moisture content relations of contemporary bricks has shown that they can be approximated by following hyperbolic function:

$$\mu = \mu_0 - a \cdot \frac{\exp\left(\frac{u_m - u_{m1}}{u_{m2}}\right) - \exp\left(\frac{u_{m1} - u_m}{u_{m2}}\right)}{\exp\left(\frac{u_m - u_{m1}}{u_{m2}}\right) + \exp\left(\frac{u_{m1} - u_m}{u_{m2}}\right)} \quad (1)$$

where:

u_m – moisture content [kg/kg],
 μ_0, a, u_{m1}, u_{m2} – parameters.

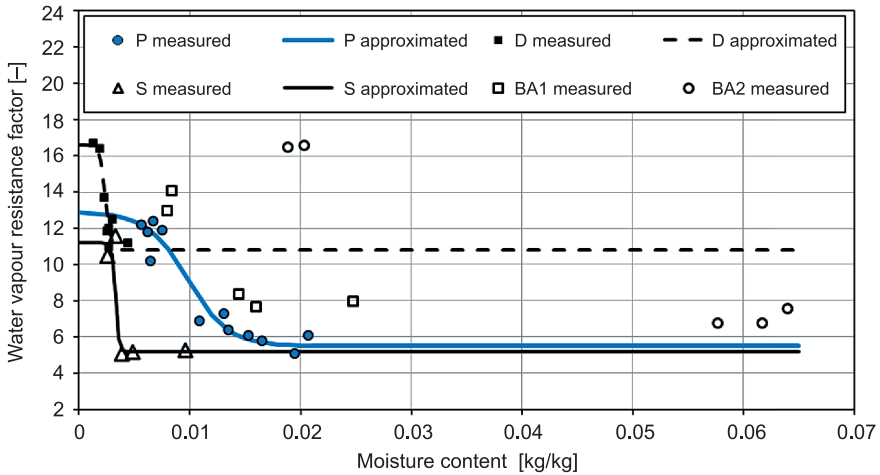


Fig. 3. Water vapour resistance factor vs. moisture content for contemporary bricks P, S and D and historical bricks BA1 and BA2

The mean moisture content at which the transition from higher to the lower value of water vapour resistance factor occurs corresponds to parameter u_{m1} . The width of the transition zone is expressed by the parameter u_{m2} and corresponds to value of $2 \cdot u_{m2}$. The parameter μ_0 expresses the mean value of water vapour resistance factor and value of $2a$ corresponds to the difference between maximum and minimum vapour resistance factor value. The applied parameters are in Tab. 4.

Table 4

Applied parameters of hyperbolic function (1)

Brick	μ_0	a	u_{m1}	u_{m2}
P	9.2	3.7	0.0098	0.0037
S	8.2	3.0	0.0033	0.0003
D	13.7	2.9	0.0024	0.0005

During the dry cup measurements of saline samples an efflorescence occurrence is often reported on the dry sides of samples [4, 6]. The created salt crust then causes an increase

of the dry cup water vapour resistance factor value. However, the salt crust formation depends on many factors (e.g. type of salt or salts, salt concentration, way of drying) and therefore is hardly predictable. In case of the measured historical bricks a weak efflorescence was noticed in case of one sample but noticeable salt crust was not created. The presence of salt has caused slightly higher values of vapour resistance factor of BA2 samples (Fig. 3, 4).

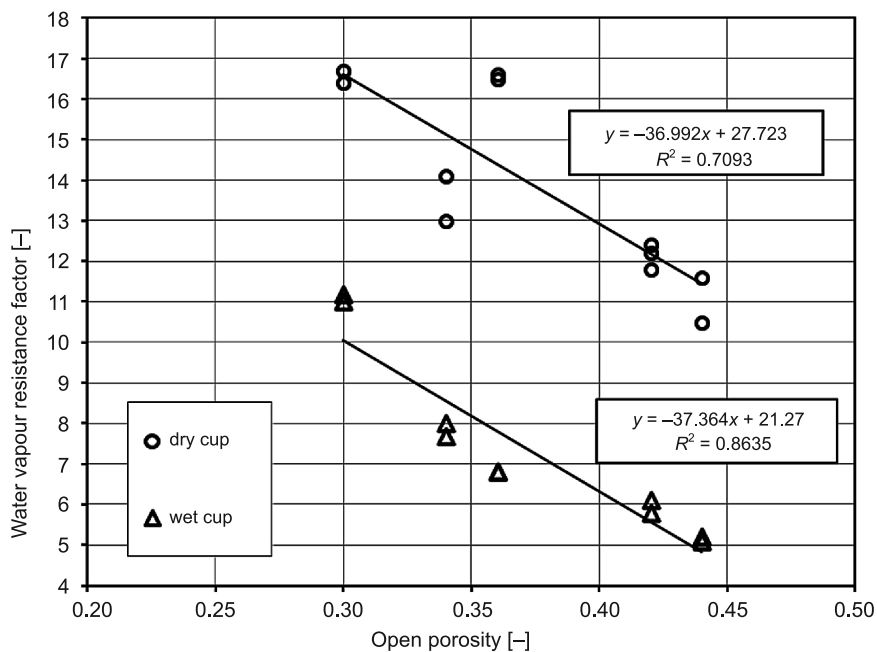


Fig. 4. Dry cup and wet cup water vapour resistance factor values vs. open porosity. Presented linear approximations involve all tested bricks

In case of contemporary bricks good correlation between the dry cup water vapour resistance factor values (measured at RH difference 0–53%) and open porosity of the bricks was obtained (Fig. 4). Compared to the contemporary salt free bricks the corresponding moisture contents of historical bricks are shifted towards the higher values (Fig. 3). This effect was significant especially for wet cup measurements of historical brick BA2 and corresponded to the high salt content as was determined. On the other hand it seems that this salt bounded moisture had minor effect on water vapour and surface diffusion. For wet cup measurements (RH difference 53–100%) relative good correlation between the water vapour resistance factor and open porosity was obtained for the whole set of tested bricks (Fig. 3, 4).

4. Conclusions

The microstructure, mineralogical composition, hygroscopic moisture content and water vapour permeability moisture dependence were determined for three types of contemporary and two types of historical ceramic bricks.

The tested bricks had very similar mineralogical composition. The microstructure of the tested contemporary bricks differed significantly. Correspondingly the potential hygroscopicity of the bricks varied from the practically negligible to the relative significant. The determined potential hygroscopicity of the historical bricks pore structure did not exceed the range determined for contemporary bricks.

Good compatibility between the nitrogen and water vapour adsorption was confirmed for salt free bricks. On the other hand it was showed that the discrepancy between nitrogen and water vapour results could indicate a contamination by hygroscopic salts.

On the whole, the water vapour permeability of the tested bricks was directly proportional to the open porosity of the bricks. However in case of historical brick BA2 the present amount of salts caused slightly lower dry cup water vapour permeability.

This research was supported by the Slovak Grant Agency VEGA (Grant No. 2/0145/13).

References

- [1] Cultrone G., Rodriguez-Navarro C., Sebastian E., Cazalla O., De La Torre M.J., *Carbonate and silicate phase reactions during ceramic firing*, *European Journal of Mineralogy*, Vol. 13, Iss. 3, 2001, 621-634.
- [2] EN ISO 12571:2000 Hygrothermal performance of building materials and products – Determination of hygroscopic sorption properties.
- [3] EN ISO 12572:2001 Hygrothermal performance of building materials and products – Determination of water vapour transmission properties.
- [4] Kiessl K., *Bauphysikalische Einflüsse bei der Krustenbildung am Gestein alter Bauwerke*, *Bauphysik*, Vol. 11, Iss.1, 1989, 44-49.
- [5] Koronthályová O., *Moisture storage capacity and microstructure of ceramic brick and autoclaved aerated concrete*, *Construction and Building Materials*, Vol. 25, Iss. 2, 2011, 879-885.
- [6] Koronthályová O., Bagel L., Kullifayova M., Ifka T., *Effect of presence of salt on moisture accumulation and transport in burnt clay bricks*, [In:] NSB 2014, 10th Nordic Symposium on Building Physics, 15–19 June, Lund University, Lund 2014, 443-450.
- [7] Lubelli B., van Hees R.P.J., Brocken H.J.P., *Experimental research on hygroscopic behaviour of porous specimens contaminated with salts*, *Construction and Building Materials*, Vol. 18, 2004, 339-348.
- [8] Nielsen C.B., *Salts in Porous Building Materials*, Technical Report 243/91, Technical University of Denmark 1991.

PIOTR KOSIŃSKI*

AIR THERMAL BRIDGES**POWIETRZNE MOSTKI CIEPLNE****Abstract**

The paper presents the phenomenon of air thermal bridges. The results of thermal simulation are presented. The impact of air infiltration on the surface temperature adjacent to air thermal bridges is discussed.

Keywords: air thermal bridge, infiltration, air tightness of building envelope

Streszczenie

W artykule przedstawiono zjawisko powietrznych mostków cieplnych. Przedstawiono wyniki symulacji cieplnych. Omówiono wpływ infiltracji powietrza na zmiany pola temperatury znajdującego się w pobliżu powietrznego mostka cieplnego.

Słowa kluczowe: powietrzne mostki cieplne, infiltracja, szczelność powietrzna budynków

* M.Sc. Piotr Kosiński, Chair of Building Engineering and Building Physics, Faculty of Technical Sciences, University of Warmia and Mazury in Olsztyn.

1. Introduction

Thermal Bridges in a building envelope can be defined as those parts of a construction in which the thermal resistance is significantly less than the adjacent portions. The reason for this may be the total or partial occurrence of a material with higher thermal conductivity or a decreased thickness of the building envelope. Both situations often occur simultaneously. Thermal bridges are situated in the connections between building components or in places where the building structures alter the composition. Thermal bridges in building constructions cause changes in heat flow rates and surface temperatures compared with those of the unbridged sides and also cause three-dimensional or two-dimensional heat flows. In recent years, the interest in a new type of thermal bridges that were previously marginalized in the building heat calculations has been growing. These are places of increased air infiltration and are named in the article as air thermal bridges (in brief ATP). The paper presents selected issues relating to the identification of technical and computing issues in these types of defects in building envelopes and highlights the importance of air infiltration in the heat balance of buildings.

2. The issue of air thermal bridges

Air thermal bridges are a special type of heat loss problem whose driving force is the movement of air. This phenomenon may apply to both linear and point zones, as in the case of structural thermal bridges. ATBs differ from structural bridges with regard to the complexity of the heat transfer, since their impact on increasing the heat demands in buildings is much larger. There are two types of ATB. The first type concerns the case of channel flow in which the air flows through the entire thickness of the construction with the inlet and outlet, so the bridge may be described as a slotted air bridge. The air flow, at a specified temperature and humidity, changes the magnitude of the local heat flux and temperature in the vicinity of the channel. The second type concerns the case in which the air affects one side of the element without the possibility of channel flow, so the bridge may be described as a one-sided air bridge. It particularly applies to porous and fibrous materials exposed both locally or to the wind. Due to the prevalence of this case, it will be discussed first.

2.1. One-side air thermal bridge

This type of heat disorder occurs primarily in the outer layers of the building envelope in cases where a wind barrier was damaged or incorrectly constructed. One-sided air bridges concern porous and fibrous materials protected faulty or not protected against wind force. This problem particularly affects improperly made lightweight constructions, mainly in the attic zones, where poor protection against air filtration is the most frequently appearing failure. One-sided ATBs arise as a result of the wind pulsation action, however, higher temperatures during summer cause the air movement as well. The impact of one-sided ATBs on heat transfer through the building envelope, despite its prevalence, is so far little explored



Fig. 1. Picture of poorly constructed roof and corresponding thermogram illustrating the impact of one-sided ATBs on heat transfer. Interior temperature $t_i = 18^\circ\text{C}$, exterior $t_e = -10^\circ\text{C}$

apart from a few works [1] rarely seen in the literature. Fig. 1 presents a poorly constructed roof (no continuity of a windproof membrane) and its corresponding thermogram.

2.2. Slotted air thermal bridge

Slotted ATBs arise as a result of pressure differences on both sides of the building envelope and can be caused by natural forces, i.e., thermal buoyancy or wind, or by an internal air distribution system. Air leaks can occur in many zones of the building envelope, i.e., gaps occurring in the joinery window and door, construction joints, contacts of materials of different structures and textures, holes for the installation cables and many others. Potential leaks gaps and cracks in a building envelope may be caused by building exploitation or due to improper manufacture of elements.

Slotted ATBs are often investigated by scientists, but the main issue is the impact of air filtration on natural ventilation effectiveness, moisture degradation of porous elements and the distribution of contaminants in buildings. The impact of air filtration on heat transfer processes and temperature distribution in the vicinity of the cracks is rarely discussed. Dufour, Derome and Zmeuranu used thermography to measure the surface temperature of single-layer walls subjected to air flow through surrogates of cracks in laboratory conditions. The authors solved an inverse problem using developed image-processing methods of recorded thermograms, i.e., using the edge detection technique and correlations for peak height and missing attenuation to estimate the widths of cracks with an error of less than 4% [2].

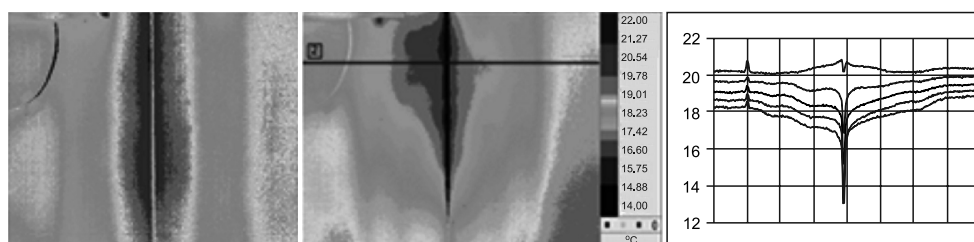


Fig. 2. Thermograms and graph illustrating the impact of slotted ATBs on surface temperature of the inner side of the frame wall

Fig. 2 presents thermograms of a defective board contact zone on the inner side of the frame wall filled with loose mineral wool, unprotected against air filtration. A model investigation, with highly sensitive (20 mK temperature) infrared camera FLIR SC 7200, was conducted in a non-isothermal climatic chamber in a Building Physics Laboratory at the University of Warmia and Mazury in Olsztyn. The thermograms present the impact of the slotted ATBs on surface temperature in a contact zone of gypsum boards. The boundary conditions are: interior temperature $t_i = 21^\circ\text{C}$; exterior $t_e = 0^\circ\text{C}$; wind speed by the colder side $v = 2$ m/s. The presented thermograms were recorded at 0 and 40 minutes. The temperature curves in the graph illustrate cooling of the crack and the adjacent area at 0, 10, 20, 30 and 40 minutes.

3. Thermal bridge calculation in the heat flux through the building envelope

Existing procedures address structural thermal bridges: linear and point in the calculation of the heat flux through the building envelope. Thermal transmittance of linear thermal bridges can be approximately substituted from catalogues of thermal bridges in ISO 14683 [3] or calculated using more advanced computational methods according to ISO 10211 [4]. These procedures include an error up to 20%. Neither of them include an infiltration phenomenon. Even the ISO standard 10077-2 [6] for thermal calculations for window frames do not take into account this phenomenon. The only form of taking air flow into account in energy calculation is using a convective coefficient on the internal and external surfaces of the construction according to ISO 6946 [5].

Air filtration significantly changes the temperature and heat transfer process on the surface of air permeable construction, this is caused by a certain amount of heat moving by air flux. During infiltration, air flows through the construction in the opposite direction to the conducted heat flow, so the air receives part of the heat, therefore, the intensity of heat transfer on the internal surface of construction is reduced. The heat flux on the internal surface of the construction reaches its maximum value, but the closer to the outer surface, the smaller the heat flux is. It is due to the recovery of heat that warms up the air flowing toward the internal side.

During the exfiltration process, air flow and conducted heat has the same direction therefore, the heat transfer intensity on the internal surface increases.

4. A case study of air thermal bridges

A new apartment envelope was chosen for this investigation. The wall consists of autoclaved aerated concrete ($\lambda = 0.17$ W/mK) with a width of 24 cm and expanded polystyrene EPS ($\lambda = 0.040$ W/mK) with a width of 15 cm, plastered and painted both sides. In the construction layer, PVC windows with 6-ventricular frames (width 7 cm), double glazing (thickness 4 mm) and packed with 16 mm of argon were mounted.

The thermogram, made by infrared camera FLIR B335 with thermal sensitivity 50 mK, was recorded on the inner side of the apartment with the conditions: $t_e = -8^\circ\text{C}$, $t_i = 23^\circ\text{C}$;

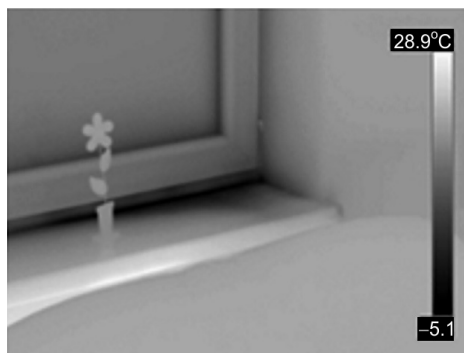


Fig. 3. An analyzed thermogram

wind speed of 0 kilometers per hour; RH inner – 50%; distance – 1 m; emissivity – 0.91. The lowest temperature in the contact zone of the window frame and window sill was 4.4°C.

A thermal simulation of this wall area based on the construction details was computed. For the purpose of simulation, a model of the wall and window was simplified, i.e., frame and glazing were changed by substitutes with the same thermal resistance. Plaster and painted layers were omitted. An air gap, 2 mm thickness, was placed under the external windowsill and between the window frame and PUR foam under the frame sealing the window's joint with the wall. Such a gap width, according to ISO 10077-2, qualifies it as a non-ventilated.

The simulation was performed on the basis of ISO 10211 in Autodesk Simulation Multiphysics with selected steady-state heat transfer model, based on the fundamental equations of heat conduction. The calculations that were performed for the two cases differ in the values of heat transfer resistance on the internal and external surfaces designated in accordance with ISO6946. In the first case, the default values of the heat transfer resistance

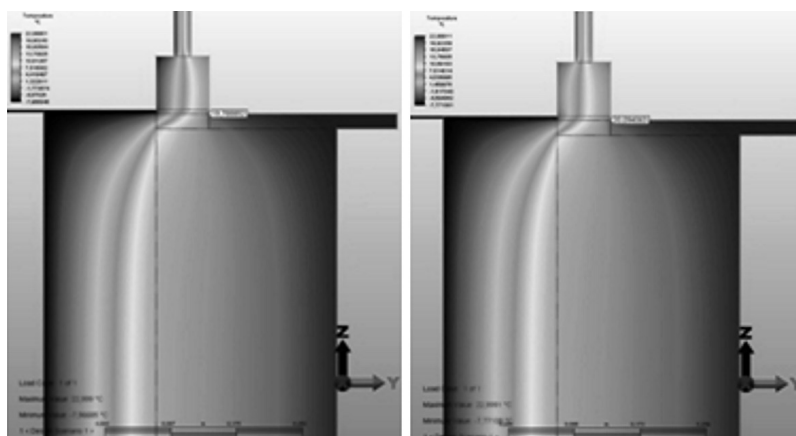


Fig. 4. The results of the simulation performed in the steady-state conditions, on the left side $R_{se} = 0.04 \text{ m}^2\text{K/W}$, $R_{si} = 0.13 \text{ m}^2\text{K/W}$, on the right $R_{se} = R_{si} = 0.128 \text{ m}^2\text{K/W}$. Thermal load applied to edges adjacent to environment

for the horizontal direction of heat flow were used: $R_{se} = 0.04 \text{ m}^2\text{K/W}$, $R_{si} = 0.13 \text{ m}^2\text{K/W}$, while in the second case, the values were calculated for the boundary conditions: $R_{se} = R_{si} = 0.128 \text{ m}^2\text{K/W}$. The heat transfer coefficients and temperature were applied only to the edges adjacent to the internal and external environment. No load was applied to the air gap. In the first case, the temperature at the contact zone of the window frame and windowsill is 19.79°C while in the second, it is 20.09°C .

The results were different from those in reality, so the model was modified by applying an external heat transfer coefficient and temperature to the air gap surfaces. The phenomenon of heating the air flowing into the room was omitted. In the first case, there was a temperature of 14.29°C in the contact zone, in the second, 14.35°C . R_{se} , R_{si} are the same as in the previous step.



Fig. 5. The results of the simulation performed in the steady-state conditions, on the left side $R_{se} = 0.04 \text{ m}^2\text{K/W}$, $R_{si} = 0.13 \text{ m}^2\text{K/W}$, on the right $R_{se} = R_{si} = 0.128 \text{ m}^2\text{K/W}$. Thermal load applied to edges adjacent to the environment and the air gap

The results of simulations performed in both of the above cases do not reflect the real problem. In the next approximation step, the thermal simulation was performed for a wall cross-section using the test based on the extended equation of heat and mass balance. For this purpose, the calculation software Delphin 5 was used. Initially, the simulation was performed in analogy to the Autodesk based solely on the fundamental laws of heat conduction, omitting the air filtration. In analogy to the previous step, the heat transfer resistance was the same, in the first case: $R_{se} = 0.04 \text{ m}^2\text{K/W}$, $R_{si} = 0.13 \text{ m}^2\text{K/W}$, while in the second: $R_{se} = R_{si} = 0.128 \text{ m}^2\text{K/W}$. In the first case, there is a temperature of 17.93°C in the contact zone, in the second, 18.50°C .

In the next step, the extended equation of heat and mass balance was used. A pressure difference of 5 Pa was calculated for the boundary conditions. The simulation included the same R_{se} and R_{si} as in the previous step. In the first case, the temperature was -6.34°C in contact zone, while in the second, -5.83°C .

The study supports the notion that in addition to the traditionally conceived structural thermal bridges resulting from the change of material or structure of the barrier, there are air

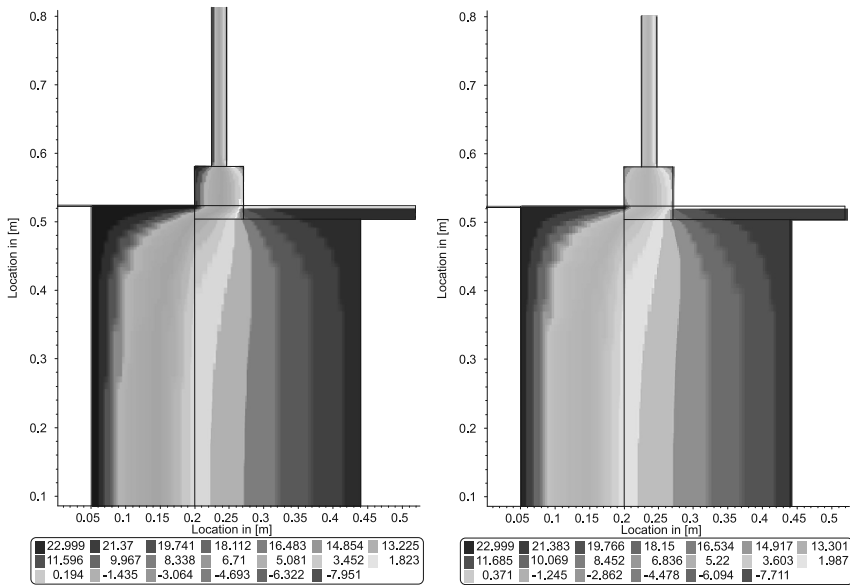


Fig. 6. The results of the simulation performed with the extended balance equation, on the left side $R_{se} = 0.04 \text{ m}^2\text{K}/\text{W}$, $R_{si} = 0.13 \text{ m}^2\text{K}/\text{W}$, on the right $R_{se} = R_{si} = 0.128 \text{ m}^2\text{K}/\text{W}$. Thermal load applied to edges adjacent to environment

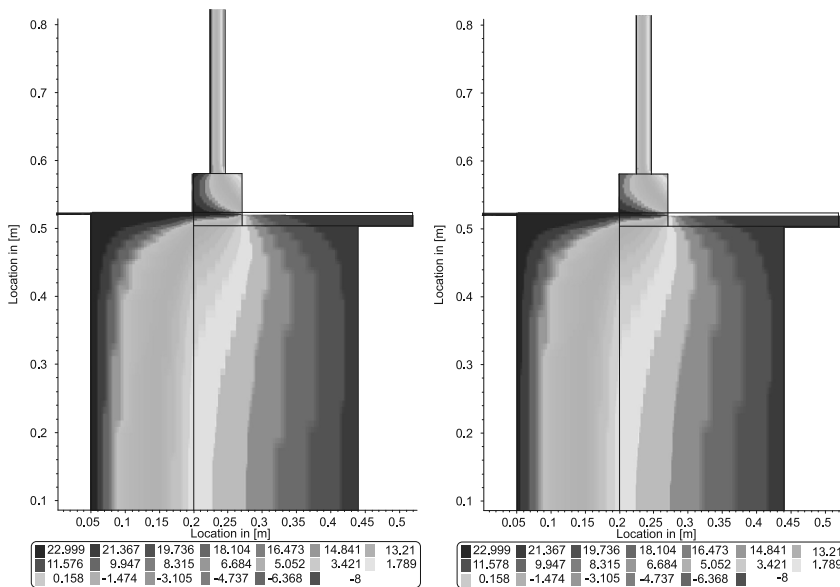


Fig. 7. The results of the simulation performed with the extended balance equation, on the left side $R_{se} = 0.04 \text{ m}^2\text{K}/\text{W}$, $R_{si} = 0.13 \text{ m}^2\text{K}/\text{W}$, on the right $R_{se} = R_{si} = 0.128 \text{ m}^2\text{K}/\text{W}$, $\Delta p = 5 \text{ Pa}$

thermal bridges, caused by the movement of air. In winter, when the air temperature inside the rooms and exterior differ considerably, a thermal buoyancy phenomenon in air permeable compartments occurs almost all the time. It is only mitigated during the airing of rooms. Wind is another causative factor of air filtration, but in buildings equipped with an exhaust ventilation system, there is an additional driving force causing air channel flows.

Currently, in the Building Physics Laboratory at the University of Warmia and Mazury in Olsztyn, there are conducted researches on one-sided ATBs of fibrous materials, one side exposed to wind forces. So far, achieved results show that heat loss resulting from pulsed wind force in areas not protected against wind is at least several times more than in the adjacent protected areas. In parallel, there are conducted researches underway to repair the existing air gaps under difficult of only one-sided possible access to them (internal or external).

5. Conclusions

The implementation of this simulation should enhance the knowledge about the impact of air thermal bridges on the temperature of surfaces adjacent to them. The difference between results in the last step and reality may be due to variable dimensions of air gaps. The differences between models are due to different balance equations. Air thermal bridges should be included in heat balance calculations. In most cases, the air tightness measurements are obligatory in order to determine the presence of such defects in the building envelope.

References

- [1] Deseyve C., Bednar T., *Wind induced airflow through lightweight pitched roof construction: Test roof element – measurements and model validation*, 8th Symposium on Building Physics in the Nordic Countries, Kopenhaga 2008.
- [2] Dufour M.B., Derome D., Zmeuranu R., *Analysis of thermograms for the estimation of dimensions of cracks in building envelope*, Infrared Physics & Technology, Vol. 52, 2009, 70-78.
- [3] ISO 14683:2007 Thermal Bridges in Building construction – Linear thermal transmittance – Simplified methods and default values, EU.
- [4] ISO 10211:2007 Thermal Bridges in Building construction – Heat flows and surface temperatures – Detailed calculations, EU.
- [5] ISO 6946:2007 Building components and building elements – Thermal resistance and thermal transmittance – Calculation method, EU.
- [6] ISO 10077-2:2012 Thermal performance of windows, doors and shutters – Calculation of thermal transmittance – Part 2: Numerical method for frames, EU.
- [7] ISO 13789:2007 Thermal performance of buildings – Transmission and ventilation heat transfer coefficients – Calculation method, EU.

MARTIN KOVAC*, KATARINA KNIZOVA*, ANNA SEDLAKOVA*

HEAT LOAD ELIMINATION BY USING DISPLACEMENT VENTILATION IN A CLASSROOM

OGRANICZENIE OBCIĄŻENIA CIEPLNEGO W SALI LEKCYJNEJ PRZY ZASTOSOWANIU WENTYLACJI WYPOROWEJ

Abstract

The target of this contribution is to know if we can use displacement ventilation for the so-called free cooling of a room. What flow rate of air do we need in order to sufficiently reduce the thermal loads in the classroom? We search for the answer to this question by using CFD tools. We only use air from the exterior without any cooling system.

Keywords: displacement ventilation, free cooling, CFD

Streszczenie

Celem pracy jest analiza zastosowania wentylacji wyporowej w tzw. swobodnym chłodzeniu pomieszczenia. Jaka ilość wymian powietrza jest wymagana, aby wystarczająco zmniejszyć obciążenia termiczne w klasie? Szukamy odpowiedzi na to pytanie za pomocą narzędzi CFD. Używamy jedynie powietrza zewnętrznego bez układu chłodzącego.

Słowa kluczowe: wentylacja wyporowa, swobodne chłodzenie, CFD

* Ph.D. Eng. Martin Kovac, Ph.D. Eng. Katarina Knizova, Doc. Ph.D. Eng. Anna Sedlakova, Institute of Architectural Engineering, Civil Engineering Faculty, Technical University of Kosice.

1. Introduction

The object of this analysis is the classroom of the Civil engineering faculty in Kosice. This room is situated on the fourth floor in the loft of the building. The heat loads from students and solar radiation cause the indoor temperature to increase greatly during the summer months (for example May or June) of the academic year. The classroom is currently only naturally ventilated (i.e. by opening the windows). This method of ventilation is very inefficient. For this reason we would like to use displacement ventilation in the classroom in order to achieve efficient air exchange. We could also use this method of ventilation to reduce heat load from students and solar radiation.

2. Experiment

The classroom used in our CFD analysis is shown below. It has been modelled using the software package ANSYS/CFX (ANSYS 2012). The base proportions of the room are: length 11.0 m, width 6.0 m and height from 1.9 to 4.5 m. The slope of the roof is 23°. The classroom commonly accommodates 30 students. We can see the placement of the desks in Fig. 1. We compare two variants in our CFD analysis of displacement ventilation. The first is variant A where the rate of air exchange is 6 times per hour (volume flow rate is 1 260 m³/h (mass flow rate is 0.42 kg/s) across 4 inlets). In variant B we calculate with the rate of air exchange at 20 times per hour (volume flow rate is 4 200 m³/h (mass flow rate is 1.4 kg/s) across 4 inlets).

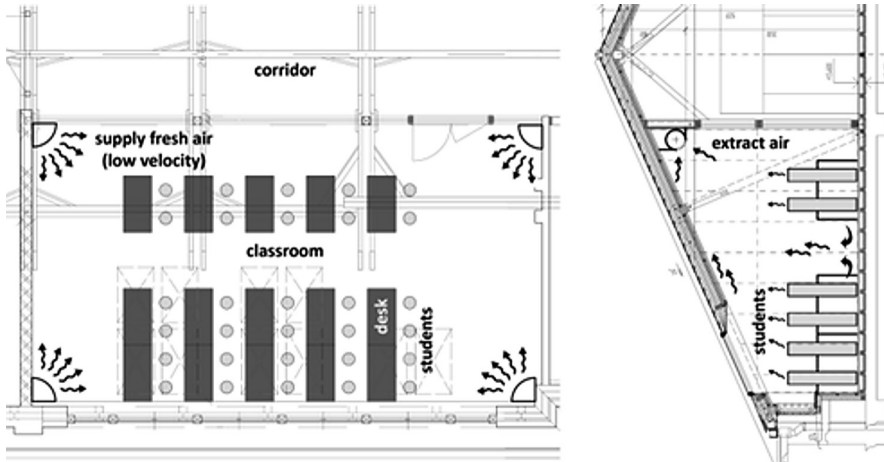


Fig. 1. Scheme of the classroom with displacement ventilation

2.1. Geometrical and physical model

Students sitting in the classroom were approximately modelled as cylinders with a height of 1.4 m and a volume of 75 litres – the volume of the average human body. The boundary and initial conditions of the task are written in the table below (Table 1). For CFD calculation,

unstructured tetrahedral mesh was used in the domain (Fig. 2) with non-isothermal flow, heat transfer by convection and radiation S2S, gravitation model and k -epsilon turbulence model. The calculation process was ended when the residual target 1E-4 was achieved.

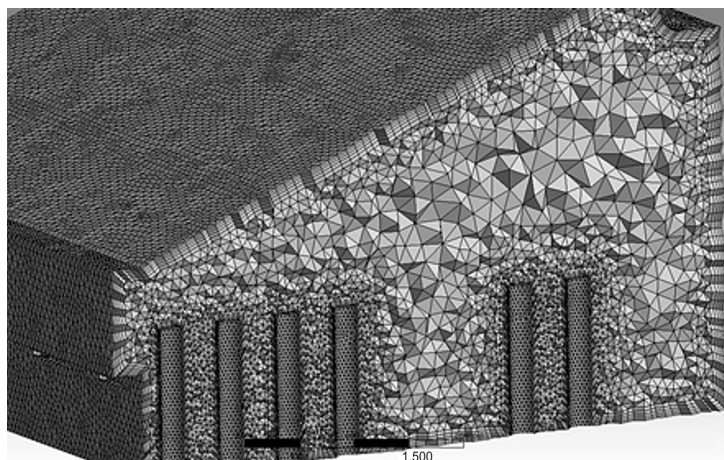


Fig. 2. Tetrahedral mesh

Table 1

Boundary and initial conditions for CFD analysis

External wall	$U = 0.29$ [W/(m ² ·K)], surface emissivity = 0.91	
Roof	$U = 0.20$ [W/(m ² ·K)], surface emissivity = 0.91	
Windows	$U = 2.5$ [W/(m ² ·K)], surface emissivity = 0.15, surface transmissivity = 0.75	
Roof windows	$U = 2.0$ [W/(m ² ·K)], surface emissivity = 0.15, surface transmissivity = 0.75	
	Variant A	Variant B
Exterior	Air temperature = 22 [°C] Air density = 1.197 [kg/m ³]	Air temperature = 22 [°C] Air density = 1.197 [kg/m ³]
Inlets	Number = 4 Total mass flow rate = 0.42 [kg/s] Air temperature = 22 [°C]	Number = 4 Total mass flow rate = 1.4 [kg/s] Air temperature = 22 [°C]
Outlet	Average static pressure	Average static pressure
Students	Number = 30 Heat flux = 60 [W/m ²] Body volume = 75 [litres] Body surface area = 1.8 [m ²] Surface emissivity = 0.93	Number = 30 Heat flux = 60 [W/m ²] Body volume = 75 [litres] Body surface area = 1.8 [m ²] Surface emissivity = 0.93
Solar gain	On the floor plane after transmission of windows = 4 056 [W]	On the floor plane after transmission of windows = 4 056 [W]

In our CFD simulation the body of a student was approximately modelled as a cylinder with heat flux 60 W/m².

3. Discussion of the CFD results

The density of the supply air is higher than the air density in the classroom. Why? Because the temperature of the supply air is lower than the air temperature in the classroom. The supply air falls to the floor from the low velocity inlets (large area) and it is consequently distributed within the room. The mass flow rate in the first variant A is 0.105 kg/s across each inlet. In this case the supply air falls quickly to the floor surface as we can see in Fig. 3. In variant B the supply air also falls to the floor, but more slowly. The mass flow rate of supply air is 0.35 kg/s across each inlet: higher than in variant A. Supply air at 22°C can reach further from the air inlet than in variant A (Fig. 4).

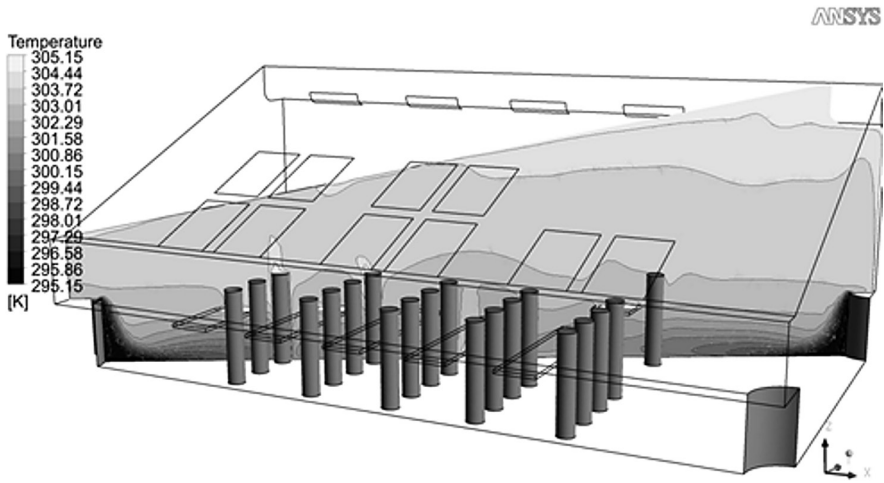


Fig. 3. Reach of supply air at 22 °C in the classroom (rate of air exchange is 6 times per hour)

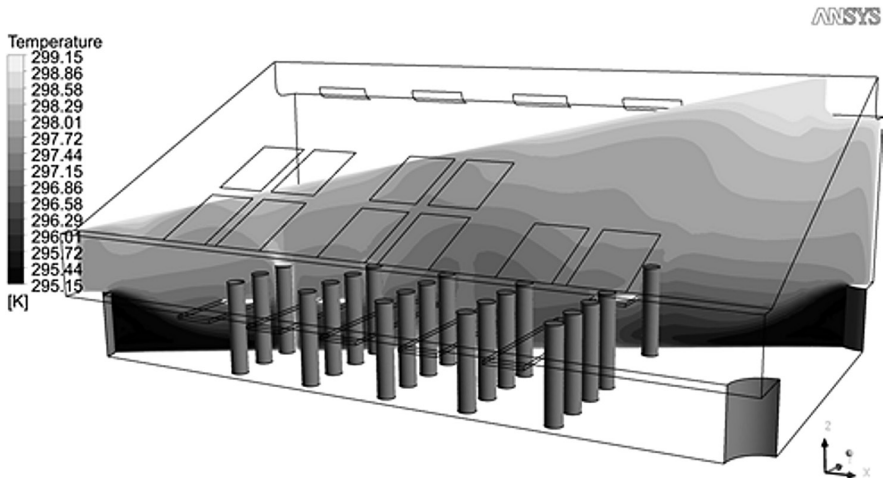


Fig. 4. Reach of supply air at 22°C in the classroom (rate of air exchange is 20 times per hour)

The main advantage of displacement ventilation is the air buoyancy that is formed from the air temperature gradient. The air at a higher temperature (caused by the heat load) is moved directly upwards to the ceiling of the classroom. We can see this effect in Figures 5 and 6. The mass flow rate of supply air and heat load from students and solar radiation are the main factors that influence the temperature gradient of air in the classroom. If we look at Figure 5, where the rate of air exchange is 6 times per hour we can see a change in air temperature from 26°C to 32°C between ankle and head level. If we increase the mass flow rate of the supply air (to a rate of air exchange of 20 times per hour), the air temperature in the classroom decreases, ranging from 22.5°C to 25°C between ankle and head level (Fig. 6).

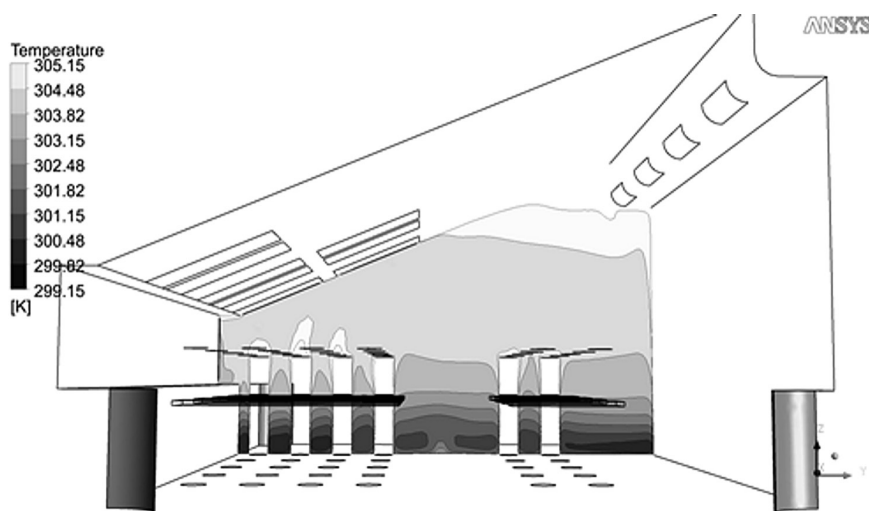


Fig. 5. Air temperature gradient in the classroom (rate of air exchange is 6 times per hour)

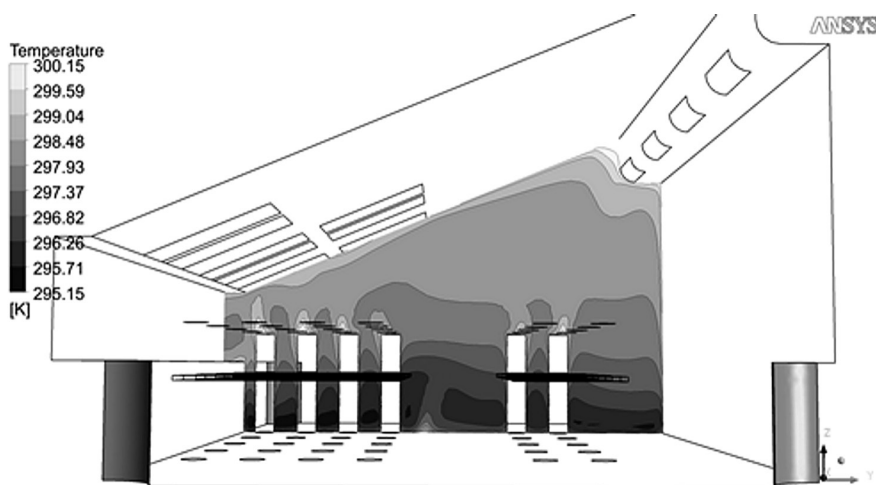


Fig. 6. Air temperature gradient in the classroom (rate of air exchange is 20 times per hour)

The next figures (Fig. 7, 8) show air temperature at the plane which is 200 mm above the floor. If we use a higher rate of air exchange we can stop the extreme rise in air temperature in the room. However, the question is: what will the air velocity be around the students? Figures 9 and 10 can offer the answer to this question.

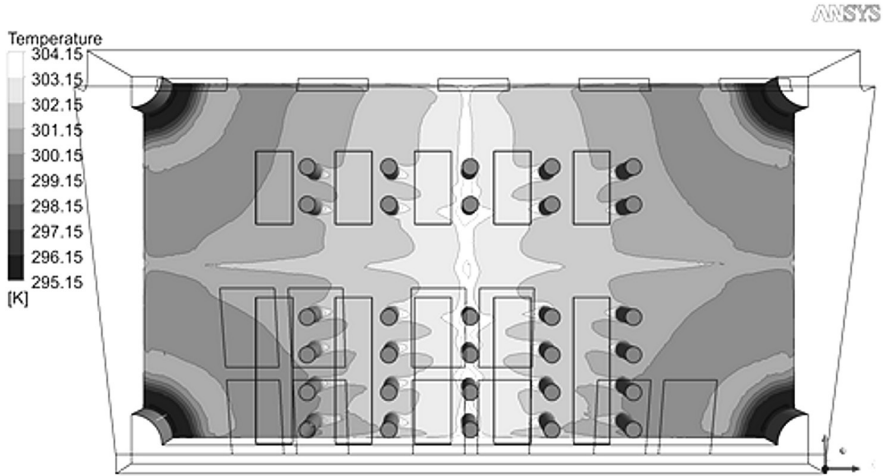


Fig. 7. Air temperature at the plane 200 mm above the floor (rate of air exchange is 6 times per hour)

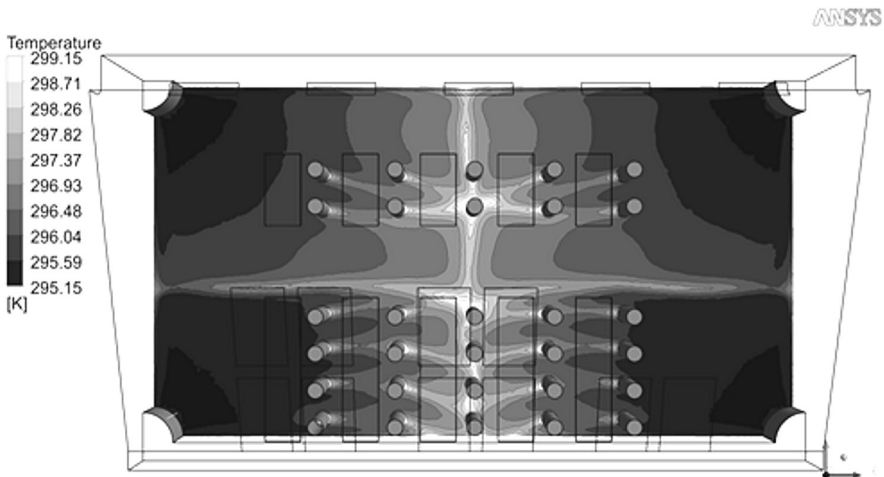


Fig. 8. Air temperature at the plane 200 mm above the floor (rate of air exchange is 20 times per hour)

The air velocity in variant A achieves values from 0.075 to 0.15 m/s around the students (Fig. 9). The air velocity in variant B is between 0.1 and 0.3 m/s (Fig. 10). These values are measured at the plane 200 mm above the floor. Our regulations state that the maximum air velocity around the students is 0.25 m/s for this activity (teaching). On the basis of these

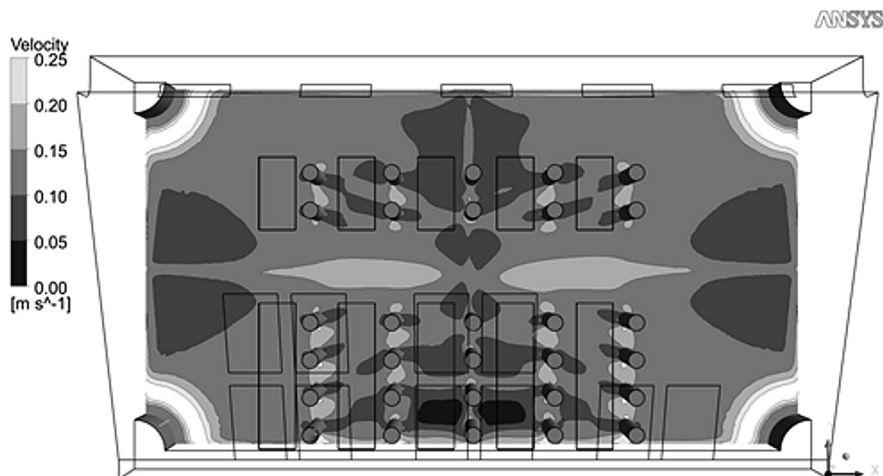


Fig. 9. Air velocity at the plane 200 mm above the floor (rate of air exchange is 6 times per hour)

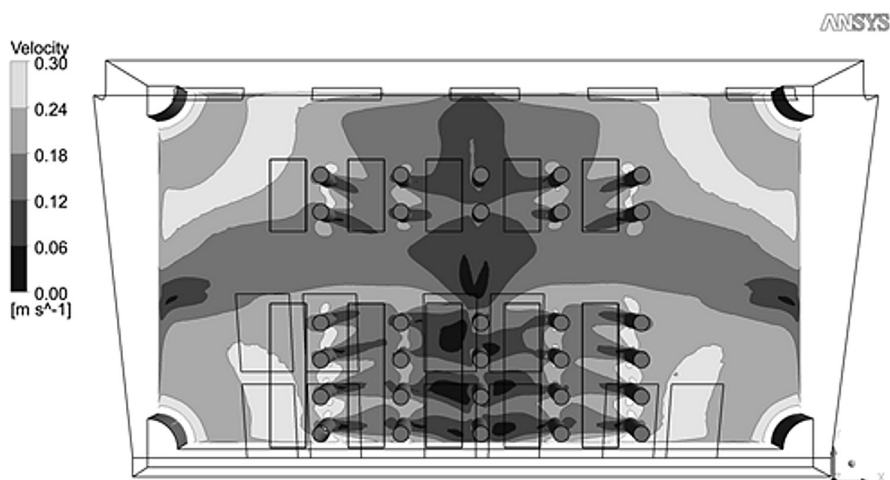


Fig. 10. Air velocity at the plane 200 mm above the floor (rate of air exchange is 20 times per hour)

results we can predict that some students in the front section of the room near the air inlets could theoretically experience some discomfort.

4. Conclusions

The results from this CFD simulation show that an air exchange rate of 6 times per hour is insufficient to stop the extreme rise in air temperature in the classroom. We can stop this rise in air temperature if we use the higher rate of air exchange of 20 times per hour (0.35 kg/s across each inlet). The supply air temperature is constantly 22°C in both compared variants.

Currently, we only use natural ventilation through the windows in the classroom. This system is very inefficient. The working conditions in the classroom are very difficult for the students and teachers during the summer months (May and June). If we used displacement ventilation with sufficient rate of air exchange we could provide for effective air exchange in the room, and in parallel we could reduce the heat load from students and solar radiation. It would be free cooling. The target is not to reduce the air temperature in the classroom below the outside temperature, but to reduce it to the value of the outside temperature.

This work was funded by project KEGA 052 TUKE-4/2013 "The implementation of a virtual laboratory for designing energy-efficient buildings".

References

- [1] Knizova K., Kovac M., *Influence of natural and mechanical ventilation on elimination of heat load in the loft space*, Visnik Nacional'nogo universitetu Evivska politechnika: Teorija i praktika budivnictva, vol. 756, 2013, 95-100.
- [2] ANSYS CFX Introduction, Release 12.0, 2012, ANSYS Inc., Canonsburg, USA.

KATARINA KOVACOVA*, MARTIN KOVAC*, DANICA KOSICANOVA*

EVALUATING THE ENERGY AND COST BENEFITS OF HEAT PUMPS IN MULTI-OCCUPANCY DWELLINGS

ANALIZA ENERGETYCZNYCH ORAZ KOSZTOWYCH KORZYŚCI STOSOWANIA POMP CIEPŁA W BUDOWNICTWIE WIELORODZINNYM

Abstract

This paper provides a tabular analysis of an “outdoor air-water” heat pump in heating and domestic hot water system inside a multi-occupancy dwelling house. The study set out to compare a conventional system using the city’s district heat supply with one using an “outdoor air-water” heat pump. One part of the analysis is the energy performance of the renewable energy source. The study is also addressed the benefits of saving on conventional heat source and the period of financial return on the heat pump investment.

Keywords: energy consumption, heat pump, savings, period of financial return, multi-occupancy domestic property/building/dwelling house

Streszczenie

W artykule opracowano tabelaryczną analizę systemu ogrzewania i ciepłej wody użytkowej w domu wielorodzinnym, z zastosowaniem pompy ciepła „woda-powietrze”. Badania przeprowadzono dla porównania konwencjonalnego miejskiego systemu ogrzewania z systemem pompy ciepła „woda-powietrze”. Jedną z części analizy jest charakterystyka energetyczna źródła energii odnawialnej. Analizy przedstawiają korzyści z oszczędzania przy zastosowaniu konwencjonalnego źródła ciepła oraz okres zwrotu finansowego z inwestycji w pompę ciepła.

Słowa kluczowe: zużycie energii, pompa ciepła, oszczędność, okres zwrotu, budynek wielorodzinny

* Ph.D. Eng. Katarina Kovacova, Ph.D. Eng. Martin Kovac, Doc. Ph.D. Eng. Danica Kosicanova, Institute of Architectural Engineering, Civil Engineering Faculty, Technical University of Kosice.

1. Description of the selected multi-dwelling house

A multi-dwelling house (comprising 8 floors above ground) was selected for the study. It has a flat roof; the total heated floor area is 2.189 m². There are 32 flats in the building, with a total of 96 occupants. The building is supplied with thermal energy through the city's district heating system. This energy supply is used for heating and domestic hot water system within the property. The city's energy supply is fuelled by natural gas and black coal. The building's pre-renovation construction did not provide for sufficient heat transmittance values (U -values), when measured against the relevant standard requirements [1] (Table 1).

Table 1

U -values of the building constructions (before renovation)

Building constructions	Current value	Standardized value
	U [W/(m ² ·K)]	U_N [W/(m ² ·K)]
External wall	0.46	0.32
Flat roof	0.52	0.20
Ceiling above the unheated floor	1.24	0.75
Old windows	2.40	1.70
New windows	1.45	1.70

The average consumption of domestic hot water in the selected house was calculated as 35 litres per person per day. Table 2 contains the actual thermal energy consumption figures for the heating and the domestic hot water system in the multi-occupancy dwelling house.

Table 2

Actual thermal energy consumption in multi-dwelling house (before renovation)

Period	Thermal energy consumption [kWh/year]	
	Heating system	Domestic hot water system
2010	216.778	129.159
2011	190.527	121.313
2012	185.250	117.172
Average value	197.518	122.548

2. Energy balance

The first task was to identify what energy savings could be achieved by improving the U -values of the building's construction in this property. The occupants had vacated the premises to enable a detailed survey to be conducted, with a view to the complete renovation of the building, including thermal insulation of the external walls (ETICS system), the flat roof and the ceiling above the unheated basement floor (Table 3).

On the basis of the results of this survey of the building's constructions, heating system energy savings of 32% are anticipated. Thermal energy consumption levels in the domestic hot water system are unchanged.

Table 3

U-values of building's constructions (after renovation)

Building constructions	Projected value	Standardized value
	U [W/(m ² ·K)]	U_N [W/(m ² ·K)]
External wall	0.21	0.32
Flat roof	0.15	0.20
Ceiling above unheated floor	0.60	0.75
New windows	1.45	1.70

The occupants were invited to consider the advantages of using electric heat pumps (air-water) for their domestic hot water and general heating system needs in place of the existing source. These proposed alterations, forming part of the building renovation work are examined in the second stage of the energy balance. A new heating supply system was designed to meet this purpose (Fig. 1). The plans called for a set of 4 heat pumps (air-water) to act as the primary heat source with the city's district heating system serving as the back-up heating source.

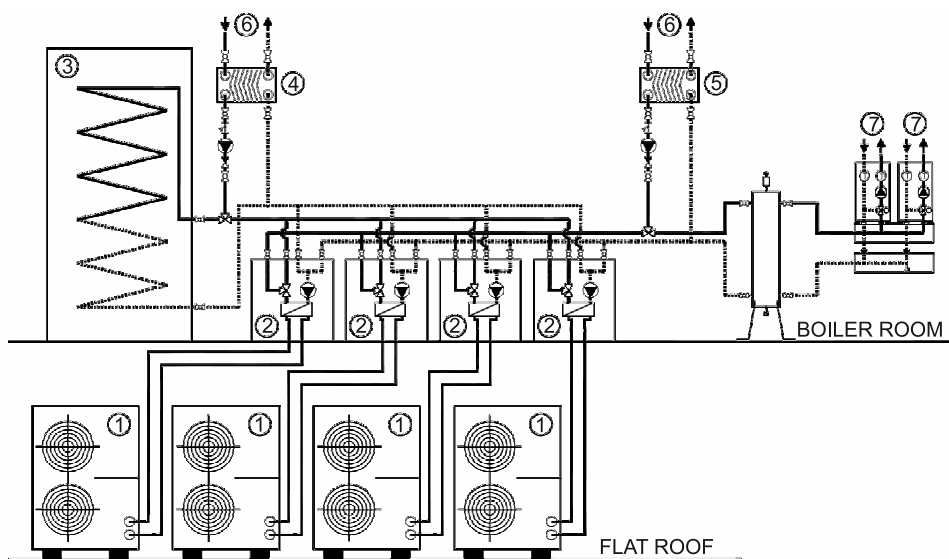


Fig. 1. New heating supply system for the selected multi-occupancy property. Legend: 1 – heat pump (outdoor units), 2 – heat pump (indoor units), 3 – domestic hot water storage, 4 – brazed plate heat exchanger (for the domestic hot water system), 5 – brazed plate heat exchanger (for the heating system), 6 – city's district heating system, 7 – heating system of the multi-dwelling house

Four sets of electric-powered high-temperature heat pumps were designed to act as the primary heating source, with a total heating capacity of 64 kW. The plan is to place the outdoor units on the flat roof of the building, and the indoor units in the boiler room (at the basement level). These heat pumps are capable of warming the water to a temperature of up to 80°C. Improving the thermal insulation of the building's constructions offered further reductions in the level of heat loss from the house. It is therefore possible to reduce the temperature of heating medium. For the purposes of this case study, a maximum output temperature of 65°C at from the heat pumps is considered to be appropriate. The number of heat pumps was set to a bivalent point of -5°C . The heat pumps were designed to work in combination with the city's district heating system, in order to provide the capacity for heating the property when outdoor temperatures fell to lower levels. Heat from the city's district heating system is delivered by designed brazed plate heat exchanger (Fig. 1, Item 5). A domestic hot water storage system was designed, to hold domestic hot water to a volume ratio of 1.500 liters, according to the ČSN 06 0320 standard [2]. Hot water consumption was set at 35 litres per person, per day. When required, the domestic hot water storage system can be supplemented with supplies from the proposed brazed plate heat exchanger connected to the city's district heating system (Fig. 1, Item 4). When these primary and secondary heating sources are combined, the heat provided through the city's district system accounts for only 5.9% of the building's total thermal energy demand. The electricity energy demand

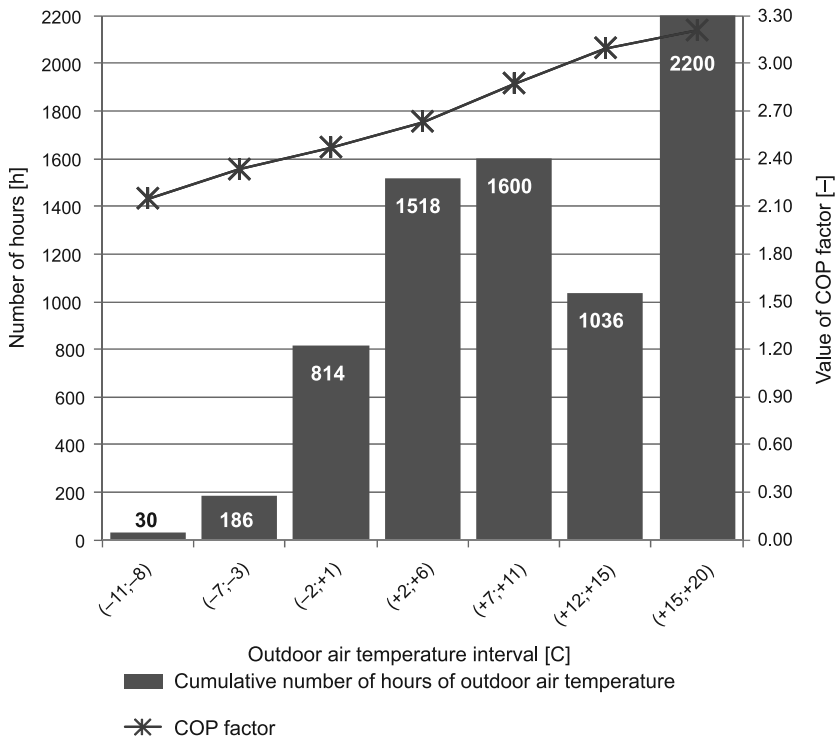


Fig. 2. Frequency of selected outdoor temperature readings and COP factor values

of the heat pumps was assessed on the basis of a COP factor set at 2.89. This value was calculated as the weighted average, based on outdoor temperature readings [3] for heating period (Fig. 2, Table 4).

Table 4

**Capacity parameters of the heat pump with water
at 65°C ($\Delta\theta = 10$ K, 22.9 l/min)**

Outdoor temperature [°C]	Heating capacity [kW]	Power input [kW]
-15	14.0	6.52
-7	15.8	6.78
-2	16.0	6.48
2	16.0	6.08
7	16.0	5.57
12	16.0	5.17
15	16.0	4.99

The graph below shows the energy consumption (current state) and energy demand (1st and 2nd variant) for the domestic hot water and heating system in the building (Fig. 3).

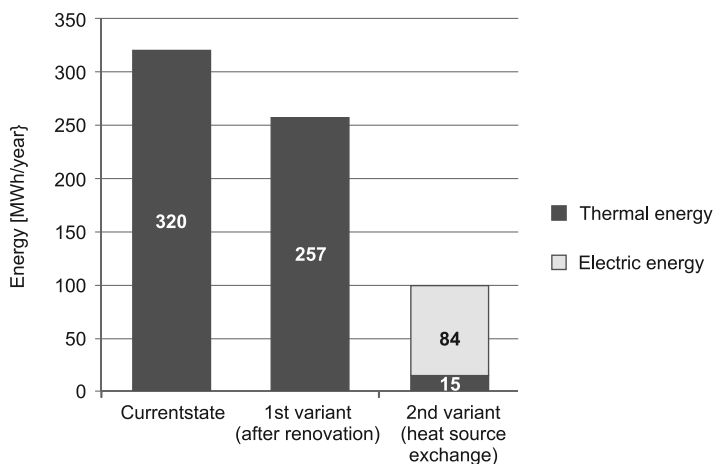


Fig. 3. Energy consumption (current state) and energy demand (1st and 2nd variant) for the domestic hot water and heating system in the building

Implementing the first (renovation) variant can bring energy savings of 20% in terms of the total energy consumption for the domestic hot water and heating system. Further improvements in terms of the heat pump technology can result in progressive energy savings of up to 69%.

3. Financial costs and benefits

It is necessary to conduct a full financial cost and benefits assessment in order to calculate the level of investment required to carry out the necessary renovation work in such a multi-occupancy property; to identify potential financial savings and to determine the financial return on the resources outlayed. In terms of the first variant, the proposed renovation work requires an investment of 186.264 Euros. This amount includes the necessary building materials and the price of the works. If the heat source exchange is included in the price, then the investment level rises by a further 63.403 Euros. This total sum covers the cost of the heat pumps, the domestic hot water storage, the brazed plate heat exchangers, the circulation pumps, piping, thermal insulation and installation of the above. The investment figure also includes VAT.

In order to calculate the energy prices for the domestic hot water and general heating system in the building, energy suppliers's current prices were applied (Table 5) [4–5].

Table 5

The price of thermal and electricity energy including VAT

Thermal energy prices from the city's district heating supply		Electricity energy prices	
Variable price [Euro/kWh]	Fixed price [Euro/kW]	Variable price [Euro/kWh]	Fixed price [Euro/point of supply]
0.04992	262.9393	0.115	5.123

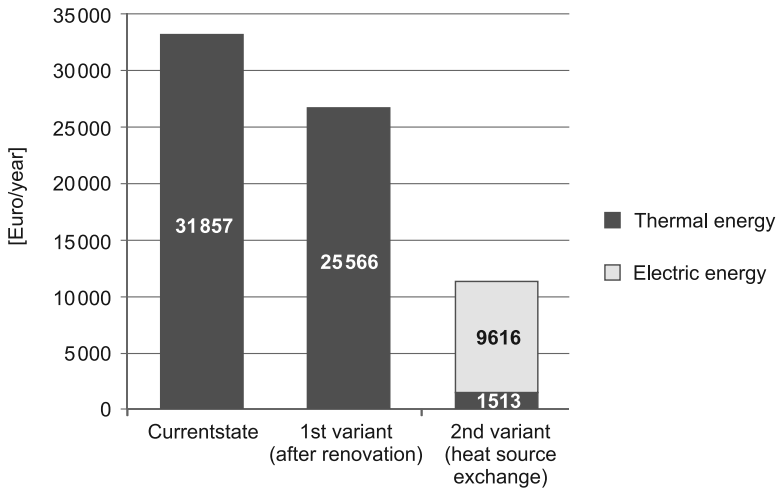


Fig. 4. Energy prices for the domestic hot water and heating system in the multi-occupancy building

Implementing the first (renovation) variant can bring about financial savings of 20% on the total operational costs of running the domestic hot water and heating system. Installing the heat pumps should reduce these operating costs by 65%, in relation to current amounts.

4. Conclusions

Implementing the first variant raises the prospect of achieving 30% energy savings – which is sufficient, but this requires a considerable commitment to invest in the necessary resources. Consequently the return on investment outlayed period is of the order of 29 years. If energy prices were to rise by 4% [6], then the investment return period is estimated to be 19 years.

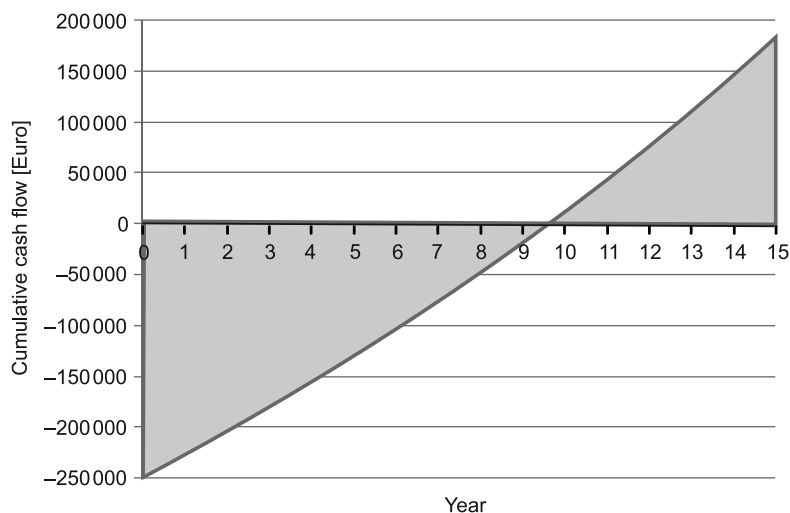


Fig. 5. The return on investments (building renovation work combined with the installation of heat pumps)

In the case of this particular property, a suitable solution is to combine the installation of heat pumps for the domestic hot water and heating system with renovation work on the building. It offers the potential to deliver clear energy and financial savings within a shorter investment return period of some 12 years. Should energy prices rise by 4% [6], then the investment return period reduces to 10 years (Fig. 5). The heat pumps are assumed to have operating lifespans of about 15 years.

This paper was funded by the following projects: KEGA 052 TUKE-4/2013 – “The implementation of a virtual laboratory for designing energy-efficient buildings”; and ITMS 26220220064 – “Research centre for renewable energy resources, integration and performance efficiency”.

References

- [1] STN 73 0540-2:2012. Thermal protection of buildings. Thermal performance of buildings and components. Part 2: Functional requirements. Slovakia.
- [2] Krippelova Z., Perackova J., *Comparison of the Design of the Storage Water Heaters According to the Technical Standards of Central European Countries*, CLIMA 2013, 11th REHVA World Congress and the 8th International Conference on IAQVEC, Energy Efficient, Smart and Healthy Buildings, Prague, 16–19 July 2013, 1436-1445.
- [3] STN EN 15 316-4-2:2007. Heating systems in buildings – Method for calculation of system energy requirements and system efficiencies – Part 4-2: Heat generation systems, heat pump systems. Brussels, Belgium.
- [4] <http://www.teho.sk/odberatelia/cena-tepla/cena-tepla-v-roku-2014>
- [5] http://www.vse.sk/wps/PA_Minnesota/content/vse.D1100/doc/VSE_Cennik_elektriny_domacnosti_od01012014.pdf
- [6] Kovac M., Knizova K., *The analysis of energy consumption and operation costs of the system with using solar collectors in apartment building*, Structura stavebni trendy 2013, Ostrava, 7–8 November 2013, 127-132.

PAWEŁ KRAUSE*, TOMASZ STEIDL*, BOŻENA ORLIK-KOŹDOŃ*,
DOMINIK WOJEWÓDKA*

ENERGY ANALYSIS OF NF40 RESIDENTIAL BUILDINGS ON SELECTED EXAMPLES

ANALIZA ENERGETYCZNA BUDYNKÓW MIESZKALNYCH NF40 NA WYBRANYCH PRZYKŁADACH

Abstract

The paper presents an energy analysis of single and multi-family residential buildings in terms of achieving the NF40 standard defined by NFOŚiGW. Obtaining financing from the investor for the construction of energy efficient buildings must meet a number of technical criteria. In this paper, examples of the practical process of fulfilment of the above requirements for the building enclosure will be presented.

Keywords: energy efficient buildings, linear thermal bridges

Streszczenie

W artykule przedstawiono analizę energetyczną budynków mieszkalnych jednorodzinnych i wielorodzinnych w aspekcie osiągnięcia standardu NF40 określonego przez NFOŚiGW. Otrzymanie przez inwestora dofinansowania do budowy budynków energooszczędnych wymaga spełnienia szeregu kryteriów technicznych. W niniejszym opracowaniu zostaną przedstawione przykłady praktyczne procesu spełnienia powyższych wymagań w zakresie obudowy budynku.

Słowa kluczowe: budynki energooszczędne, liniowe mostki cieplne

* Ph.D. Eng. Paweł Krause, Ph.D. Eng. Tomasz Steidl, Ph.D. Eng. Bożena Orlik-Koźdoń, Ph.D. Eng. Dominik Wojewódka, Department of Buildings and Buildings Physics, Faculty of Civil Engineering, The Silesian University of Technology.

1. Introduction

The subject of the study is a designed complex of a single-family house in a terrace building development in Wrocław.

The aim of the study is to analyse the design documentation and execution of necessary energy and numerical calculations leading to the implementation of recommendations allowing to achieve, by the designed complex of buildings, a standard low-energy NF40, or NF15, building as defined by the NFOŚiGW (National Fund for Environmental Protection and Water Management) in specific provisions.

For the adopted purpose of the work, a scope of activities was submitted including:

- presentation of the general requirements of NFOŚiGW,
- selection of typical details related to the existence of linear thermal bridges,
- examples of detailed solutions along with thermal analysis, designed to meet the requirements of NFOŚiGW.

2. NFOŚiGW requirements for buildings of the NF type

The standard for a single-family low-energy NF40 building, as specified by NFOŚiGW (designer) in detailed provisions, is published on the designer's website. This standard assumes that for the analysed single-family building, a unit energy demand for heating and ventilation of 15 or 40 kWh/m² of heated surface is not exceeded (EUco indicator).

The minimum technical requirements for single and multi-family buildings, in terms of housing and technical equipment, have been included in the detailed instructions. The requirements for the building enclosure, including thermal insulation of opaque external walls – walls, roof, floor on the ground, and other partitions including windows, doors and garage doors, are shown in the table. Moreover, the requirements were placed in the scope of:

- linear thermal bridges,
- air tightness of the enclosure.

Confirmation that the building fulfils the energy standard requirements in a specific group (NF15 or NF40) must be documented by means of a presentation of the verification document regarding the construction project for which building permits had been obtained on the basis of the provisions of the Building Act. Additionally, necessary trade implementation projects are verified to enable practical implementation of the designed building. All projects must be prepared in accordance with the relevant provisions of the Building Act, and they should have the appropriate calculations confirming the achievement of the specific energy standard by the building. The whole should have a designer's statement that the project is executed in accordance with the Regulation of the Minister of Transport, Construction and Maritime Economy of 25 April 2012, in the scope and form of the construction project (Journal of Laws 2012, No. 0 pos. 462) [2], and in accordance with the guidelines of NFOŚiGW.

A construction project and trade executive projects must be prepared taking into account the minimum technical requirements set out in the guidelines by NFOŚiGW, including requirements relating to housing and all facilities associated with the production and transport of thermal energy. Part of such requirements relating to a building's enclosure is shown in Table 1.

Table 1

Minimum technical requirements mandatory for a single-family building – NFOŚiGW

No.	Requirement		NF15	NF40
			Single-family building	
1.	Block/construction of the building			
1.1	Linear values of partitions' heat transfer coefficients U_{max} [W/m ² K]			
a)	– external walls	I, II and III climatic zone IV and V climatic zone	0.10 0.08	0.15 0.12
b)	– roofs, flat roofs and ceilings under unheated attics or above level crossings	I, II and III climatic zone IV and V climatic zone	0.10 0.08	0.12 0.10
c)	– ceilings above unheated basements and underfloor enclosed spaces, floors on the ground	I, II and III climatic zone IV and V climatic zone	0.12 0.10	0.20 0.15
d)	– windows, skylights, balcony doors and non-opening opaque surfaces	I, II and III climatic zone IV and V climatic zone	0.80 0.70	1.00 0.80
e)	– exterior and garage doors	I, II and III climatic zone IV and V climatic zone	0.80 0.70	1.30 1.30
1.2	Limit values of thermal bridges' linear coefficients of heat loss [W/mK]			
a)	Balcony panels		0.01	0.20
b)	Remaining thermal bridges		0.01	0.10
1.3	Air tightness of the building n50 l/h		0.6	1.00

Table 2

Minimum technical requirements mandatory for a multi-family building – NFOŚiGW

No.	Requirement		NF15	NF40
			Single-family building	
1.	Block/construction of the building			
1.1	Linear values of partitions' heat transfer coefficients U_{max} [W/m ² K]			
a)	– external walls	I, II and III climatic zone IV and V climatic zone	0.15 0.12	0.20 0.15
b)	– roofs, flat roofs and ceilings under unheated attics or above level crossings	I, II and III climatic zone IV and V climatic zone	0.12 0.12	0.15 0.15
c)	– ceilings above unheated basements and underfloor enclosed spaces, floors on the ground	I, II and III climatic zone IV and V climatic zone	0.15 0.15	0.20 0.20
d)	– windows, skylights, balcony doors and non-opening opaque surfaces	I, II and III climatic zone IV and V climatic zone	0.80 0.80	1.30 1.00
e)	– exterior and garage doors	I, II and III climatic zone IV and V climatic zone	0.80 0.80	1.50 1.50
1.2	Limit values of thermal bridges' linear coefficients of heat loss [W/mK]			
a)	Balcony panels		0.01	0.20
b)	Remaining thermal bridges		0.01	0.10
1.3	Air tightness of the building n50 l/h		0.6	1.00

3. Energy analysis of designed solutions

The building energy analysis was performed via a computer program serving to determine the building's energy characteristics, in accordance with the guidelines of the Minister of Infrastructure of 6 November 2008, based on the methodology for calculating the building's energy characteristics constituting a self-contained, technical-functional whole and the method of producing certificate models of their energy characteristics [3] – program Arcadia Termo version: 4.2.

3.1. Assumptions for energy calculations

The energy calculations assume the following:

- weather conditions for the city of Poznań,
- temperature in living and service quarters: 20°C,
- temperature in the staircases: 12°C,
- a coefficient of shielding against wind 'e' was adopted for the shielding class – average shielding, at a level of 0.07,
- degree of air tightness for a multi-family building – average – standard windows with double glazing,
- number of persons: 3 persons adopted for 1 flat,
- window frames: the heat transfer coefficient for input shaft: $U = 1.0 \text{ W}/(\text{m}^2\text{K})$, wooden frame, calculated resultant heat transfer coefficients for all sets of windows, unheated glazed lifts and garages,
- ventilation of flats, staircases and service quarters (natural ventilation assisted by exhaust units), according to the standard,
- heating efficiency ($\eta_e = 0.95$; $\eta_d = 0.95$; $\eta_s = 1.0$; $\eta_g = 0.99$).

All calculations of the partitions' thermal insulation were performed using the computational coefficients of thermal heat transfer λ for the materials and values declared by the manufacturers.

3.2. Results of calculations of heat transfer coefficients

Calculations of heat transfer coefficients for partitions limiting the zone of adjustable temperature were calculated on the basis of the applicable standards: PN-EN ISO 6946 [3], PN-EN ISO 13370 [4] (for floors and walls on the ground) and PN-EN ISO 10077 (for windows and doors) [5].

In the calculations, standard heat transfer coefficients λ were used (PN-EN 12524) for the materials and values declared by the manufacturer.

3.2.1. Windows

According to PN-EN ISO 10077-1:2002 "Thermal properties of windows, doors and shutters – Calculation of heat transfer – Part 1: Simplified method" [6]. For each window, the heat transfer coefficient was calculated using the formula:

$$U_w = \frac{A_g U_g + A_f U_f + I_g \Psi_g}{A_g + A_f} \quad (1)$$

For all windows, an equal framework width was adopted, i.e. 12 cm. The results of the calculations are presented in the following table:

Table 3

Results of calculations of the heat transfer coefficient for windows

Window symbol	Window dimensions W-H [m]	Frame coefficient U_f [W/m ² K]	Glass coefficient U_g [W/m ² K]	Linear coefficient of heat transfer Ψ_g [W/mK]	Glazing perimeter l_g [m]	Glass surface A_g [m ²]	Frame surface A_f [m ²]	Window coefficient U_w [W/m ² K]
01	2.20–0.75	0.74	0.50	0.03	4.94	1.00	0.65	0.68
02	1.30–2.20	0.74	0.50	0.03	6.04	2.08	0.78	0.63

The described boundary value of the heat transfer coefficient U_{\max} for windows according to the NF15 standard is: 0.8 W/m²K. The designed heat transfer coefficient U_w for all windows and balcony doors in the building will be less than 0.8 W/m²K, provided that windows with the following parameters will be used:

- heat transfer coefficient of the glazing: $U_g \leq 0.50$ W/m²K,
- permeability coefficient of the total solar radiation of the glass: $g \geq 0.5$,
- coefficient of linear heat loss of the frame: $\Psi_g \leq 0.03$ W/mK,
- window profiles with a heat transfer coefficient of the frame $U_f \leq 0.74$ W/m²K.

3.2.2. External walls

The values of the heat transfer coefficient for opaque partitions were calculated in accordance with PN-EN ISO 6946:2008 [5].

The results of the calculation of the heat transfer coefficients for partitions limiting a temperature-controlled zone are shown in Tale 4 along with a reference to the current requirements of NFOŚiGW. Meeting these requirements means the simultaneous fulfilment of the requirements of the Minister of Infrastructure of 12 April 2002, on technical conditions, buildings and their location, which should correspond with Journal of Laws No. 75, pos. 690, with amendments [1].

Table 4

Results of calculations of the heat transfer coefficient for external walls

Block/construction of the building – third climatic zone			
1.	Limit values of partitions' heat transfer coefficient [W/m ² K]	Value	
		Required	Designed
a)	External walls	0.10	0.075
b)	Flat roof	0.10	0.084
	Ceiling under unheated attic		0.084
c)	Floor on the ground	0.12	0.096
d)	Windows	0.80	0.063–0.069
	Balcony doors		0.061–0.065
e)	Exterior doors	0.80	0.70

3.3. Analysis of selected design details for the presence of linear thermal bridges

In a low-energy construction, the enclosure limiting the temperature-controlled zone, except for good thermal insulation, should be characterised by a high quality of thermal connections. This is to minimise uncontrolled heat loss through so-called linear thermal bridges. A parameter characterising the effect of this heat loss is the coefficient of linear heat loss by the transmission of ψ_e for thermal bridges in relation to the external dimensions. Analyses are performed using numerical calculations in accordance with PN-EN ISO 10211 on thermal bridges in a building – heat fluxes and surface temperatures, with detailed calculations [7].

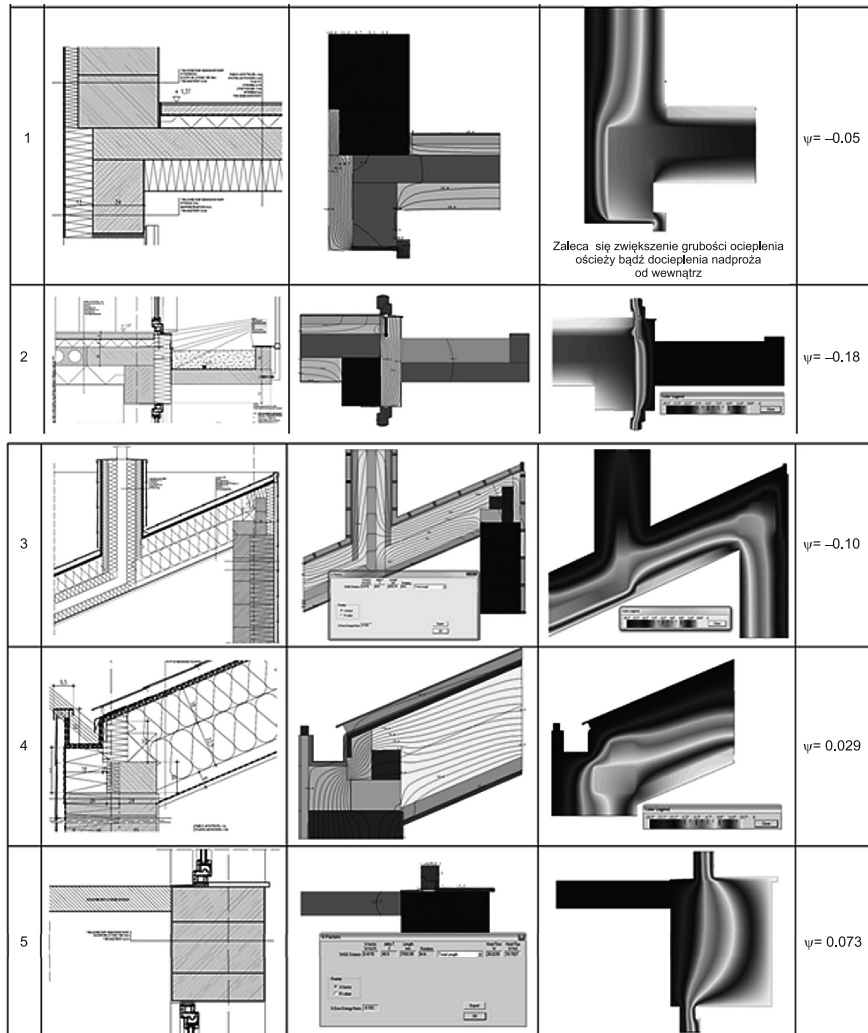


Fig. 1. Summary of the calculation results of the linear thermal bridge values of selected design details with the assessment of fulfilment of standard NF40 requirements

Coefficients of the linear heat loss by the transmission ψ_e were determined using specialised software based on the finite element method. For solutions of standard components connections – the Cobra program; in the case of non-standard solutions –the Therm 7.1.19 program.

It is recommended that in a low-energy construction, the coefficient of linear heat loss through transmission ψ_e be as low as possible, and NF0SiGW requirements set the limit value at a level of 0.01. This requirement is not a standard regulated by law but only a requirement for the participants in the support programme cited earlier. After a detailed analysis of the project, several architectural details were selected for further analysis that were considered as potential linear thermal bridges. Analysis of the earlier adopted architectural solutions, after introducing minor changes associated with localised thickening of the insulation and the use of insulation in several places that was lower than anticipated in the original project, allowed for the qualification of all the buildings to the NF40 standard. Due to the inability to make all recommended changes to the enclosure and changes in installation techniques due to the lack of permits by the architect and investor, the NF15 standard was not reached, although some partitions, such as windows, have met the conditions of this standard. Figure 1 shows example results of the calculations of selected details.

4. Summary and conclusions

4.1. Summary

Calculated according to the formula (2) [3], the EUco indicator for the complex of buildings in Wrocław was:

- before the introduction of changes to the building's enclosure: $E_{uco} = 62.3 \text{ kWh/m}^2\text{a}$,
- after the analysis of architectural details and amendments: $E_{uco} = 38.8 \text{ kWh/m}^2\text{a}$.

$$E_{uco} = \frac{Q_{H,nd}}{A_f} \quad (2)$$

where:

- $Q_{H,nd}$ – annual demand for usable energy for heating and ventilation,
- A_f – a temperature-controlled surface in a building.

4.2. Conclusions

Project activities in the obtaining appropriate values of E_{uco} at an appropriately low level should be carried out during the creation of the architectural design and not after its completion.

Matching the existing project to relatively high requirements is possible provided there is close cooperation between the architect, investor and designer in the field of Building Physics, but additional costs incurred by the investor due to the changes should be expected.

References

- [1] Rozporządzenie Ministra Infrastruktury z dnia 12 kwietnia 2002 r. w sprawie warunków technicznych, jakim powinny odpowiadać budynki i ich usytuowanie (Dz. U. Nr 75, poz. 690 z późniejszymi zmianami).
- [2] Rozporządzeniem Ministra Transportu, Budownictwa i Gospodarki Morskiej z dnia 25 kwietnia 2012 r. w sprawie szczegółowego zakresu i formy projektu budowlanego (Dz.U. 2012, nr 0, poz. 462).
- [3] Rozporządzenie Ministra Infrastruktury z dnia 6 listopada 2008 r. w sprawie metodologii obliczania charakterystyki energetycznej budynku i lokalu mieszkalnego lub części budynku stanowiącej samodzielną całość techniczno-użytkową oraz sposobu sporządzania i wzorów świadectw ich charakterystyki energetycznej.
- [4] PN-EN ISO 13370:2008. Ciepłne właściwości użytkowe budynków. Wymiana ciepła przez grunt. Metody obliczania.
- [5] PN-EN ISO 6946:2008. Komponenty budowlane i elementy budynku. Opór cieplny i współczynnik przenikania ciepła. Metoda obliczania.
- [6] PN-EN ISO 10077:2007. Ciepłne właściwości użytkowe okien, drzwi i żaluzji. Obliczanie współczynnika przenikania ciepła. Część 1: Metoda uproszczona.
- [7] PN-EN ISO 10211:2008 Mostki cieplne w budynkach – Strumienie ciepła i temperatury powierzchni – Obliczenia szczegółowe.

PAWEŁ KRAUSE*, DOMINIK WOJEWÓDKA*, BOŻENA ORLIK-KOZDOŃ*
TOMASZ STEIDL*

ANALYSIS OF SOLUTIONS OF LIGHTWEIGHT CASING MADE FROM SANDWICH PANELS IN THE ASPECT OF THERMAL INSULATION

ANALIZA ROZWIĄZAŃ LEKKIEJ OBUDOWY Z PŁYT WARSTWOWYCH W ASPEKCIE IZOLACYJNOŚCI TERMICZNEJ

Abstract

The paper relates to the issue of improving the thermal insulation of external walls of industrial buildings using a lightweight curtain wall with a folded metal sheet filled with mineral wool.

Keywords: linear thermal bridge, thermal insulation, lightweight casing

Streszczenie

W artykule przedstawiono problematykę poprawy izolacyjności cieplnej ścian zewnętrznych budynków przemysłowych wykonanych z blachy fałdowej z wypełnieniem z wełny mineralnej.

Słowa kluczowe: liniowy mostek cieplny, izolacyjność termiczna, lekka obudowa

* Ph.D. Eng. Paweł Krause, Ph.D. Eng. Dominik Wojewódka, Ph.D. Eng. Bożena Orlik-Kozdoń, Ph.D. Eng. Tomasz Steidl, Department of Buildings and Buildings Physics, Faculty of Civil Engineering, The Silesian University of Technology.

1. Introduction

The thermal insulation of external walls made in the form of wall panels partially depends on the method of connection between them and the method of attachment to the metal structural elements. The method of wall panels connection has two main consequences:

- 1) it effects the casing tightness,
- 2) it significantly effects the value of the linear U -value.

The paper presents the possibility of improving the thermal protection state of wall claddings by changing the method of connecting the casing's metal surface with the metal structural element – load-bearing bolt. Measurements were performed of the two-dimensional heat flow for the selected example of the connection and mounting of sandwich panels in a social-heated part of a warehouse.

2. Research subject

The sandwich panel used as the subject of this investigation has the following specifications:

- profiled sheet $d = 0.088$ cm/internal,
- rock wool $d = 15.0$ cm; $\lambda = 0.037$ W/mK,
- T35 trapezium sheet $d = 0.07$; $\lambda = 50$ W/mK /external,
- vapor and windproof foils (omitted in the calculations),
- profiles of (wall bolts) omega type spaced every 60 cm; $d = 0.01$ cm; $\lambda = 50$ W/mK.

The system of layers and mounting of the analyzed sandwich panel is presented in the figure below, alongside is the thermograph of a warehouse fragment with a built-in wall panel [1].

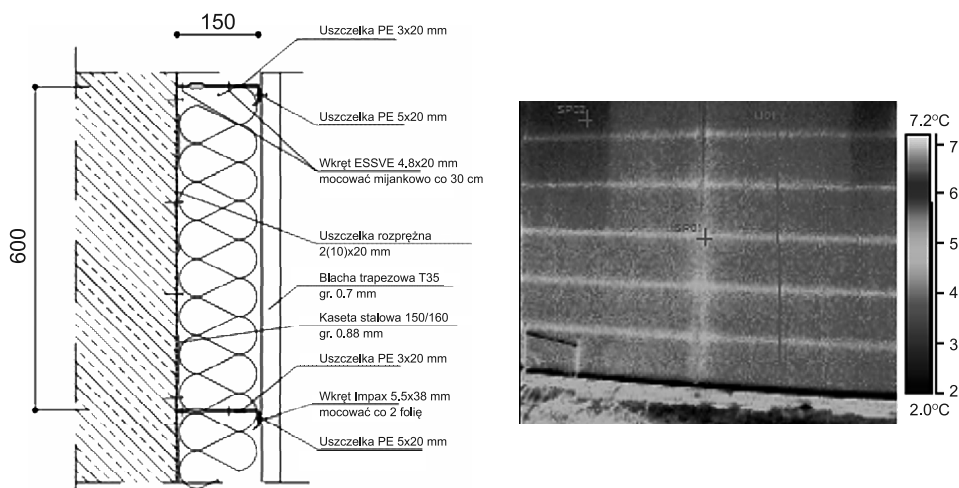


Fig. 1. Layout of the wall sandwich panel layers with mineral wool filling, on the right thermograph of the wall with a sandwich panel

3. Scope and boundary conditions of the analysis

For the tested external walls, the following measurements were performed: the total thermal resistance of the partition; temperature distribution; heat flux density; linear thermal transmittance ψ . Measurements were performed using the Therm 7.1.19 software, based on the use of MES for calculations of any two-dimensional construction element model. The results are shown in graphical form – temperature distribution in the cross-section, the distribution of the heat flux and the results of numerical calculations. Boundary conditions adopted for the calculations: calculation temperatures – as for the climate zone III $t_e = -20^\circ\text{C}$. For the internal environment, normal operating conditions were adopted $t_i = +20^\circ\text{C}$, film coefficient $h_e = 25.0 \text{ W}/(\text{m}^2\text{K})$; $h_i = 7.69 \text{ W}/(\text{m}^2\text{K})$. For calculations, surface emissivity was adopted – as for the light color, i.e. $\epsilon = 0.86$ [2].

4. Partition models adopted for measurements

A geometric model of the wall's connection was constructed on the basis of the manufacturer's specifications. The program allows the obtaining of temperature values at any point of the wall's cross section, the total heat flux and thermal transmittance $U \text{ (W}/\text{m}^2\text{K})$, and for the conditions of one and two-dimensional heat flow. The model was created in accordance with the guidelines contained in [3]. The actual length of the model adopted for calculations is $L = 1.00 \text{ m}$.

For numerical analysis, two models were adopted:

- 1) the output model (Fig. 1),
- 2) the modified model.

The modification of the output model involves making a connection in a security panel over the entire length of the panel's connection in the form of additional strip of mineral wool with a width of 15.0 cm. Both computational models are shown in Fig. 2.

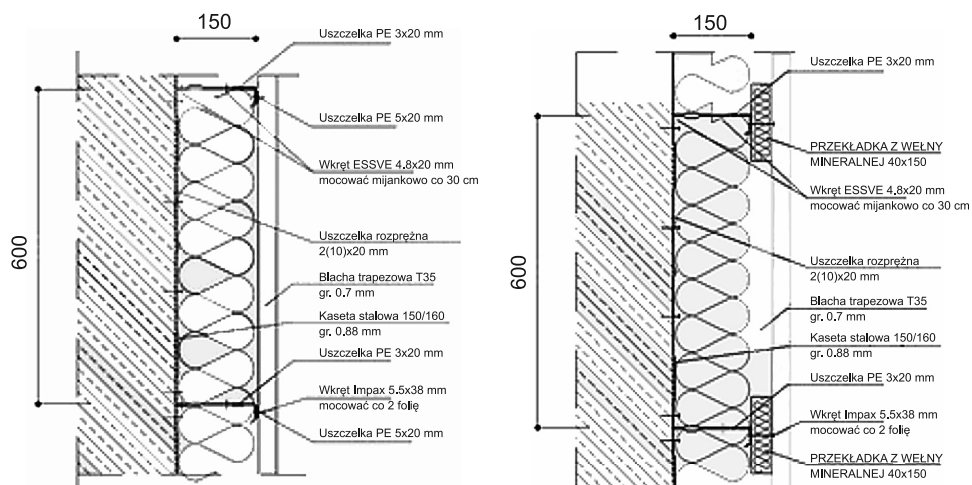


Fig. 2. Models of a wall panel adopted for the calculations, both standard and modified

5. Analysis results

The calculation results are shown in graphical form and summarized in Table 1. The results in both tested models include:

- temperature field distribution,
- heat flux density distribution,
- U -value.



Fig. 3. Calculation results of a wall panel – temperature field distribution in wall's cross-section, standard (left) modified (right)

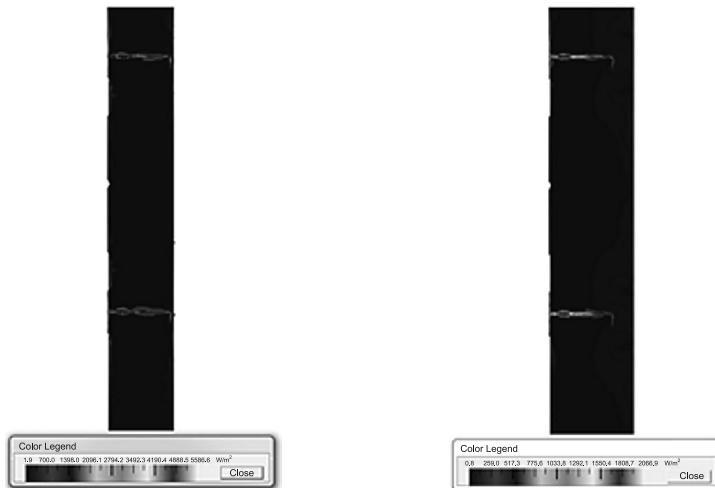


Fig. 4. Calculation results of a wall panel – heat flux density distribution in wall's cross-section, standard (left) modified (right)

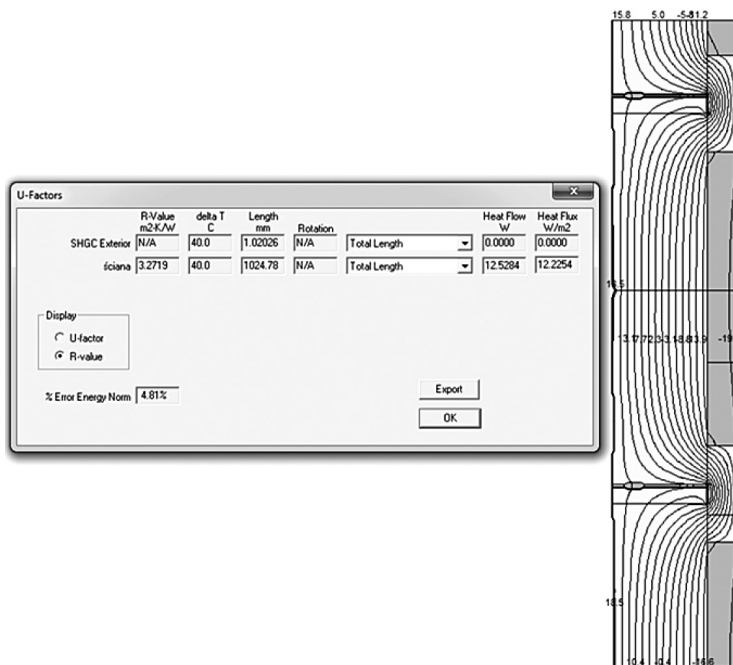


Fig. 5. Exemplary result of the U -value calculation. Modified model

In addition, the calculated results of the heat loss are included in the form of the heat flow and heat flux density.

Table 1

Summary of the calculated results

	Thermal transmittance U [W/(m ² K)]	Value of linear thermal bridge ψ [W/m]	L – model's linear value [m]	Heat flux [W]	Heat flux density [W/m ²]
Standard model	0.454	0.006	1.00	20.02	20.02
Modified model	0.308	0.002	1.00	12.55	12.35

6. Conclusions

The improvement of the thermal insulation of a building wall is usually associated with housing construction and the construction process understood as thermal modernization. The tightening of rules relating to the thermal protection of building walls applies equally to residential and industrial construction. The reduction of heat loss through external walls is not only due to the increase of the material thickness to thermal insulation. As shown in the analyzed example, equally good results can be gained through the inclusion

of additional partial protection of the fragments that are most vulnerable to heat loss. Such elements in the sandwich walls of wall panels type, are panels connections between them and structural elements, load-bearing steel bolts. Using the appropriate thermal pads, U -value for the wall panel (caskets) was reduced by more than 35%. On the basis of simple calculations, i.e. the calculation of SPBT rate, it can be proved that such action is economically justified. For the analyzed case, $SPBT < 0.8$ per year.

References

- [1] Krause P., Steidl T., Wojewódka D., *Ocena stanu ochrony cieplnej hali przemysłowej*, Praca niepublikowana, Mikołów 2012.
- [2] Branson A.M., *Infrared: A Handbook for Applications*, Plenum Press, 1966.
- [3] EN ISO 10211: 2008 Thermal bridges in building constructions – Calculations of heat flows and surface temperatures-Detailed calculations.

MAREK KUŠNÍR*, DANICA KOŠIČANOVÁ*, ZUZANNA VRANAYOVÁ*,
FRANTIŠEK VRANAY*, JÁN LOJKOVICS*

ZERO ENERGY BALANCE PROPOSAL FOR OFFICE BUILDINGS

BUDYNEK BIUROWY O ZEROWYM BILANSIE ENERGETYCZNYM

Abstract

The paper discusses the issue of prediction of electric energy production using a photovoltaic system which is directly installed at the administrative building. The problem with solar energy, which has been transformed using photovoltaic systems for electricity, is the low capacity to accumulate an excess of produced electricity. This excess of electricity we link within the power grid to send outside the building where the energy was produced to be consumed elsewhere. In this way, we achieve the highest possible utilisation of electricity produced within the boundaries of the building itself. One option is to create opportunities to recharge electric vehicles during working hours, at the time when the production of electricity is the highest but the consumption of electricity is not.

Keywords: photovoltaic system, solar energy, heat pump, synergy

Streszczenie

W artykule przedstawiono analizę przewidywanej produkcji energii elektrycznej z system fotowoltaicznego zainstalowanego bezpośrednio w budynku administracyjnym. Problemem z energią słoneczną, zamienianą przy użyciu systemów fotowoltaicznych w energię elektryczną, jest niska zdolność gromadzenia nadmiaru produkowanej energii elektrycznej. Ten nadmiar energii elektrycznej możemy przy połączeniu z siecią energetyczną wysłać poza granice budynku, w którym energia została wytworzona i zastosować w innym miejscu. W ten sposób możemy najlepiej wykorzystać energię elektryczną wytwarzaną w granicach budynku. Jedną z opcji jest stworzenie możliwości ładowania pojazdów elektrycznych w czasie godzin pracy, kiedy poziom produkcji energii jest najwyższy, a zapotrzebowanie na energię nie jest na wysokim poziomie.

Słowa kluczowe: system fotowoltaiczny, energia słoneczna, pompy ciepła, synergia

* Ph.D. Eng. Marek Kušník, Doc. Ph.D. Eng. Danica Košičanová, Doc. Ph.D. Eng. Zuzana Vranayová, Ph.D. Eng. František Vranay, Eng. Ján Lojkovics, Department of Technical Building Equipment, Institute of Architectural Engineering, Faculty of Civil Engineering, Technical University of Košice, Slovakia.

1. Introduction

Renewable energy comes from natural resources that are all around us. It is up to us to discover how we can use these resources to our advantage. Through the right choice and combination of different sources of energy, we can achieve zero energy balance conditions for a building. In this article, we will deal with the synergy of renewable energy sources and how it affects and reduces energy consumption in buildings. Heat pumps and photovoltaics offer the most energy-efficient way to provide heating and cooling in many applications, as they can use the renewable heat sources in our surroundings. The experimental workplace of our Faculty of the “Economic Research Centre for Renewable Energy Sources and Distribution Systems” was founded with the purpose of investigating the possibilities to reduce the energetic costs of buildings tied to economy. The realised project of the Centre creates a real environment for effective implementation research of technologies in laboratory and operative conditions: technologies of co-generative elements, heat pumps, photovoltaic elements, thermal capillaries and technologies in the field of measurement and regulation. The solution is a project with the possibility to repeat this on other similar applications as well as the utilisation of experience and determination of the economical expedience of implementation of researched technologies. In the contemporary phase of the research, we evaluate the operative behaviour of a zero energy balance building, interaction with building constructions and a study of the inner climate parameters and overall results for a central heat supply system.

At the heart of the ZEB concept is the idea that buildings can meet all their energy requirements from low-cost, locally available, non-polluting, renewable sources. At the strictest level, a ZEB generates enough renewable energy on site to equal or exceed its annual energy use. The following concepts and assumptions have been established to help guide the definitions for ZEBs.

2. Research methods of renewable energy sources – photovoltaic system

The existing photovoltaic system, made of monocrystalline photovoltaic panels, from which the measurements were taken, is located on the flat roof of an administrative building in Košice, Slovakia. Monocrystal photovoltaic panels have a rated efficiency of solar energy transformation at a level of around 20%. The system itself consists of 40 photovoltaic panels that are attached to two electric power converters. These converters record the measurement values of the amount of produced electricity at 5-minute intervals. Photovoltaic panels (2×2×10 pc.) are placed in rows on the flat roof of the building, supported by a metal frame structure. The resulting DC power from the photovoltaic panels is transformed into DC voltage with 2 inverters for a single-phase AC voltage and an automatically phased inverter for a single phase AC voltage to two phases of a low voltage distribution grid. Each inverter is equipped with fuses, which automatically disconnect the photovoltaic solar generator from the distribution network when subjected to critical deviations of the monitored parameters from the limits of standard values. The photovoltaic solar system is composed of 40 units of photovoltaic panels. The peak power of one photovoltaic panel is 230 Wp (Fig. 1).



Fig. 1. Installed photovoltaic system

The PVGIS simulation program was used to simulate the photovoltaic system. In order to quantify the amount of energy produced, a mathematical method was developed to calculate the amount of incident solar energy on the Earth's surface for any location and the inclination of solar panels. The measured and simulated values of produced electric energy are set for comparison with the calculated values. This methodology for calculating the amount of electricity produced by the photovoltaic system partly used the measured values for the city of Košice (cloud cover, ambient temperature and direct sun glare).

Produced electric energy comparison

When comparing the all results from different sources (measurement, simulation and calculation) of the produced electricity during the year, there are clear variations in the amount of energy produced each month.

But when we look at the yearly produced electric energy balance of the measured values, we obtain approximately identical results. These results are processed in the following table, where the methodology of calculating the amount of electricity produced for the selected location is more favourable (Table 1).

Table 1

Comparison of measured data

Data collection methods	electric energy [kWh/year]	variation [%]
Measurement	8752.505	–
Simulation	8920.000	1.88
Calculation	8840.974	1.00

3. Research methods of renewable energy sources – progressive indoor environmental system

The heating and cooling system incorporates a separate electricity meter. The electricity meter records the consumption of the electric energy source as well as the circulation pumps in the building. The area includes the heating source heat pump (HP), submersible pump (P1) and circulation pumps (P2-P5). The source cooling circuit includes a submersible pump (P1) and circulation pump source (P2 – P5) (Fig. 2). During the heating season, the largest consumer of electricity in the system is the heat pump. During the cooling period, water from the source well is used for cooling; thus, we are not producing cooling in the building, and in this case, the heat pump is decommissioned. On the other hand, we are also measuring the consumption of electricity in the heating system (Fig. 2).

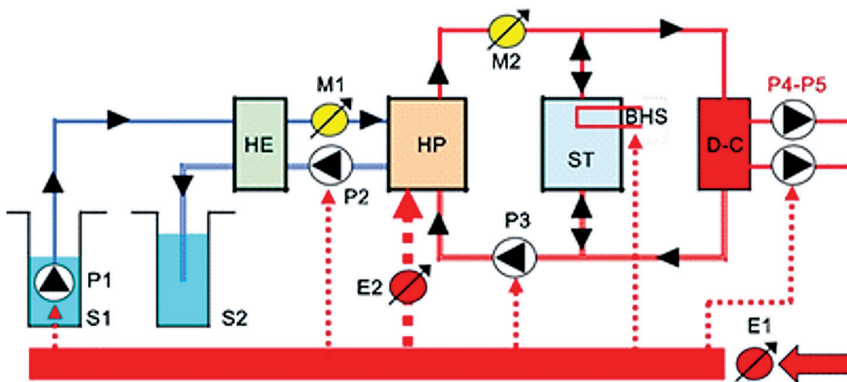


Fig. 2. Depicted scheme of the connection of water/water heat pump and electricity consumption

where:

- HE – heat exchanger
- HP –water/water heat pump, 0°C/35°C COP 3.8; heat performance 95.3 kW
- M1-2 – heat meter
- E1-2 – electricity meter
- ST – heating storage tank
- BHS - bivalent/backup heat
- S1-2 – source/suction well
- P1 – submersible pump
- P2-3 – circulation pumps – engine room
- P4-5 – circulation pumps – building
- D-C – distributor-collector

Requirements for supply of heat and cooling to the office building

1. Heat:

- Energy loss during the heating season: 1,000 GJ
- Requirement for maximum output power supply: 125 kW

2. Cooling:

- Energy loss during the summer: 330 GJ
- Requirement for maximum output power supply: 50 kW

Energy performance and technological annual energy input of energy source wells

Energy potential of the water source was measured via a hydrological test. Given the nature of the ground and the building above it, the test of a part of the sedimentation showed that the ground motion is not detected until the yield point of the water source at 7 l/s. A test for 7 days \times 24 hours showed that suction wells are capable of such absorption of a volume of continuously pumped water. For the purposes of supply of heat, it is then possible to determine the energy performance of the wells as follows:

- Coverage of water source: 7 l/s
- Water temperature: 14°C
- Two heat pumps connected in series
- The temperature difference for each heat pump: 4°C
- The number of heating days: 204
- Days of cooling: 153
- Temperature difference: 4°C

Proposal of a photovoltaic system in the evaluated administrative building

One part of the photovoltaic system will be placed in rows on the flat roof of the building on a metal framework structure, and the other part of the photovoltaic system will be placed on the inclined metal structure on the south side of the administrative building. This design increases the number of installed photovoltaic panels and also fills in the blank and unused space of the office building. The resulting DC power from photovoltaic panels is transformed into DC voltage with inverters for single-phase AC voltage and an automatically phased inverter for single phase AC voltage to two phases of a low voltage distribution grid. Each inverter is equipped with security protection, which in the case of deviations of the monitored parameters from the limits of standard values automatically disconnects the photovoltaic solar generator from the distribution network. The photovoltaic solar system will be composed of 365 photovoltaic panels. The peak power of one photovoltaic panel will be 230 Wp. Depending on the weather conditions for Slovakia, the entire photovoltaic system is inclined at an angle of 35° (Fig. 3).

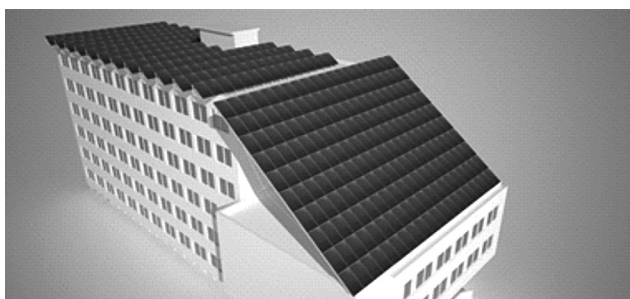


Fig. 3. Photovoltaic system proposal and design

4. Conclusions

The electric energy demand for the administrative building during the heating season is 65 MWh per year, and during the cooling season, it is 19.4 MWh per year. Overall electric energy demand to drive the heat pump and other circulation pumps in the system is about 84.4 MWh per year. The calculated amount of electricity produced by photovoltaic system is 80.7 MWh. According to the annual energy balance of the heating and cooling system, we can say that energy demand will be 96% covered by the electric energy produced with the proposed photovoltaic system. If the parameters of photovoltaic panels increase in the future, there is the possibility to say that the entire system during the year will be fully covered by the electric energy that is produced through the photovoltaic system. On the other hand we should say that we need to cover additional energy demands for lighting as well as for electric equipment in the offices. This could be possible if the peak power of one photovoltaic panel is around 300 Wp. After these system modifications, we will be able to say that the evaluated administrative building will be a building with a zero-energy balance, which mean that the administrative building will be completely self-sustaining. This is effective if we could cover the energy consumption on the basis of the yearly energy balance.

This work was supported by VEGA 1/0450/12 Energy balance research on rainwater management in cities of the future; VEGA 1/0748/11 Theoretical and experimental analysis of building services and HVAC systems from the point of view of microbiological risk and regarding the effective use of renewable sources.

References

- [1] Torcellini, P. et al., *Zero energy buildings: A critical look at the definition*, ACEEE Summer study, 2006, 1-12.
- [2] Huld, T. et al., *Estimating average day time and daily temperature profiles within Europe*, Environmental Modelling & Software, Vol. 21, 2006, 1650-1661.
- [3] Huld, T. et al., *Mapping the performance of PV modules, effects of module type and data averaging*, Solar Energy, vol. 84, 2010, 324-338.
- [4] Masters G.M., *Renewable and Efficient Electric Power Systems*, Stanford University, A John Wiley & Sons, Inc. publication, 676.
- [5] Shenck, N., *PV PowerSystems*, PV Theory, Vol. 2, 5.
- [6] Available from the Internet at: http://re.jrc.ec.europa.eu/pvgis/apps3/PVcalchelp_en.html
- [7] Tauš, P., Taušová M., *Ekonomická analýza fotovoltaiických elektrární podľa inštalovaného výkonu*, Acta Montanistica Slovaca, Vol. 14 (1), 2009, 92-97.
- [8] Kapalo, P., *Využitie solárnej techniky pri vetraní budov*, Plynár, Vodár, Kúrenár + Klimatizácia, vol. 2, 2011, 37-38.
- [9] Domnit, F., Muntea, C., Kapalo, P., *Riadené centrálné vetracie systémy s využitím rekuperácie doskovým rekuperátorom a tepelným čerpadlom*, Plynár, Vodár, Kúrenár + Klimatizácia, Vol. 4, 2012, 21-22.

AGNIESZKA LECHOWSKA*, JACEK SCHNOTALE*

CFD MODELLING AND ANALYTICAL CALCULATIONS OF THERMAL TRANSMITTANCE OF MULTI-LAYER GLAZING WITH ULTRATHIN INTERNAL GLASS PARTITIONS

MODELOWANIE CFD ORAZ OKREŚLANIE METODAMI ANALITYCZNYMI WSPÓŁCZYNNIKA PRZENIKANIA CIEPŁA WIELOWARSTWOWEGO OSZKLENIA Z WEWNĘTRZNYMI ULTRACIENKIMI SZYBAMI

Abstract

In recent times, there has been a demand for developing new technologies for glazing with superior thermal performance, good optical quality and of the lowest possible weight. In the paper, CFD modeling and analytical calculation of the thermal performance of multi-layer glazing with ultrathin internal glass partitions is presented.

Keywords: fenestrations, CFD modelling

Streszczenie

Obecnie istnieje potrzeba rozwoju technologii okien z bardzo niskimi wartościami współczynników przenikania ciepła i jednocześnie posiadających dobre walory optyczne, a także niską wagę. W artykule zaprezentowano wyniki symulacji CFD wieloszybowego oszklenia z ultracienkimi wewnętrznymi szybami, które następnie porównano z wynikami obliczeń analitycznych wykonanymi zgodnie ze stosowną normą.

Słowa kluczowe: oszklenia, modelowanie CFD

* Ph.D. Eng. Agnieszka Lechowska, Prof. D.Sc. Ph.D. Eng. Jacek Schnotale, Department of Environmental Engineering, Institute of Thermal Engineering and Air Protection, Cracow University of Technology.

1. Introduction

The Ansys Fluent numerical CFD tool allows for the simulation of the behavior of systems, processes and equipment involving the flow of gases and liquids, heat and mass transfer, chemical reactions and related physical phenomena and can be used for simulating energy efficient building systems and components including the thermal performance of windows [1, 2, 4]. In the paper, the heat transfer through multi-layer glazing has been analyzed. The glazing consists of two standard glass panes (internal and external) and 11 ultra-thin organic glass panes separated by 12 argon gaps. The study of heat transfer through the glazing was conducted using Ansys Fluent CFD software [1, 2, 4].

The glazing geometry was represented by a two-dimensional CFD model. The numerical simulation results have been compared to analytical calculation results based on the PN-EN 673 procedure [6].

2. CFD model of glazing

2.1. Geometry and materials

The modeled glazing consists of two 4 mm glass layers (internal and external) with the emissivity of 0.837 on both outer surfaces and with low emissivity coatings of 0.037 on both surfaces of the internal gas gaps. The other 11 organic glass layers have a thickness of 0.4 mm and an emissivity of 0.837 on every surface. The spacer is made of steel with an emissivity of 0.2. The twelve 13 mm width gas gaps are filled with a mixture of argon (90%) and air (10%). The dimensions of the glazing are 623 mm (width), 622 mm (height) and 163 mm (thickness).

Table 1

Material properties applied in the calculations

Material	ρ [kg/m ³]	λ [W/(mK)]	c_p [J/(kgK)]	ε [-]
Glass	2500	1	840	0.837
Glass with low emissivity coating	2500	1	840	0.037
Organic glass	1180	0.19	1260	0.837
Steel	2719	16.3	871	0.2

The investigated glazing prototype made by the Vis Inventis company was placed in a Styrofoam frame. A view of the analyzed glazing is given in Fig. 1.

The CFD model geometry is presented in Fig. 2. Thermal properties of the glazing construction materials applied for calculation are listed in Table 1, while gas thermal properties are presented in Table 2.

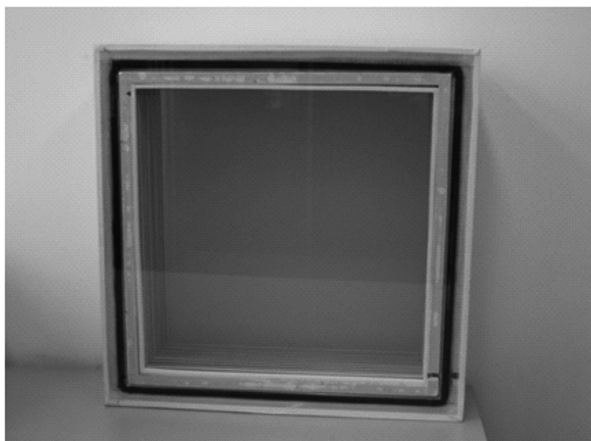


Fig. 1. The view of the glazing

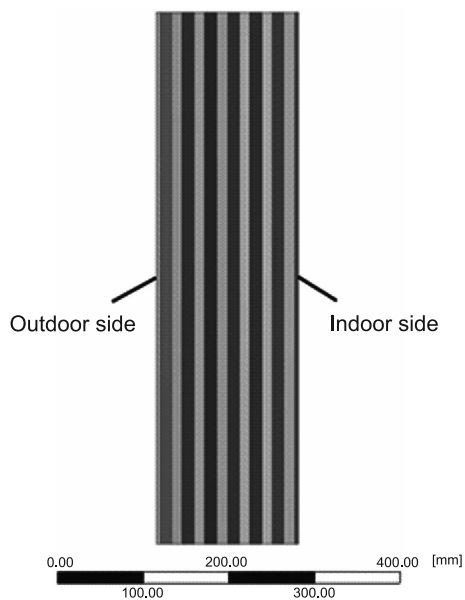


Fig. 2. The cross-section of the glazing

Table 2

90% Argon, 10% air mixture thermal properties applied in the calculations

θ [°C]	ρ [kg/m ³]	λ [W/(mK)]	c_p [J/(kgK)]	μ [kg/(ms)]
0	1.7135	0.01712	567.9	$2.062 \cdot 10^{-5}$
10	1.6523	0.01765	567.9	$2.124 \cdot 10^{-5}$
20	1.5949	0.01818	567.9	$2.186 \cdot 10^{-5}$

2.2. Boundary conditions

Boundary conditions have been set as prescribed for analytical calculations by the PN-EN 673 [6] standard. Free external air stream heat transfer coefficients of $7.6 \text{ W}/(\text{m}^2\text{K})$ and $21.4 \text{ W}/(\text{m}^2\text{K})$ were assumed for the internal and external glass surfaces respectively. The indoor and outdoor temperatures were set at 20°C and 5°C .

2.3. CFD settings and mesh

The settings for the finite element CFD model for the convective and radiative heat transfer are listed in Table 3 [4].

The calculations have been performed with a mesh of $\sim 400\,000$ elements. The solution was grid independent. The cells' quality was checked by factors – aspect ratio (max. 2.1) and skewness (max. $1.3 \cdot 10^{-10}$). Part of the mesh in the lower left portion of the glazing is presented in Fig. 3.

Table 3

CFD model settings

Solver	Stationary	
Viscous model	Laminar	
Fluid thermal properties	Density, conductivity and dynamic viscosity	Piecewise-linear
	Specific heat	Constant
Discretization schemes	Gradient	Least squares cell based
	Pressure	Body force weighted
	Momentum	Second order upwind
	Energy	Second order upwind
Radiation model	Discrete Transfer Radiation Model (DTRM)	

2.4. Simulation results

With regard to the total thermal transmittance of glazing, the overall heat transfer coefficient calculated with the use of CFD model was equal to $0.297 \text{ W}/(\text{m}^2\text{K})$. The value of the transmittance is relatively low, at a level comparable with thermal transmittance of solid walls in EU buildings.

The calculated temperature and the 90% argon, 10% air mixture velocity distribution in all the modeled glazing and in the lower part of the glazing are presented in Figures 4 and 5 respectively.

The velocity vectors of the 90% argon, 10% air mixture in the lower left hand corner of the glazing are presented in Fig. 6.

As it can be seen in Figure 6, the intensity of convection gas movements depends on the gap location.

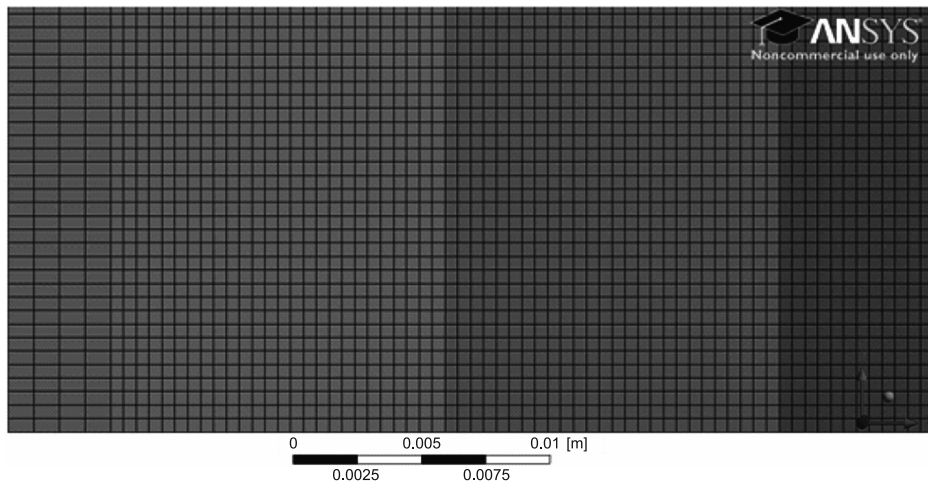


Fig. 3. The cross-section of the glazing with mesh - the lower left part of the glazing

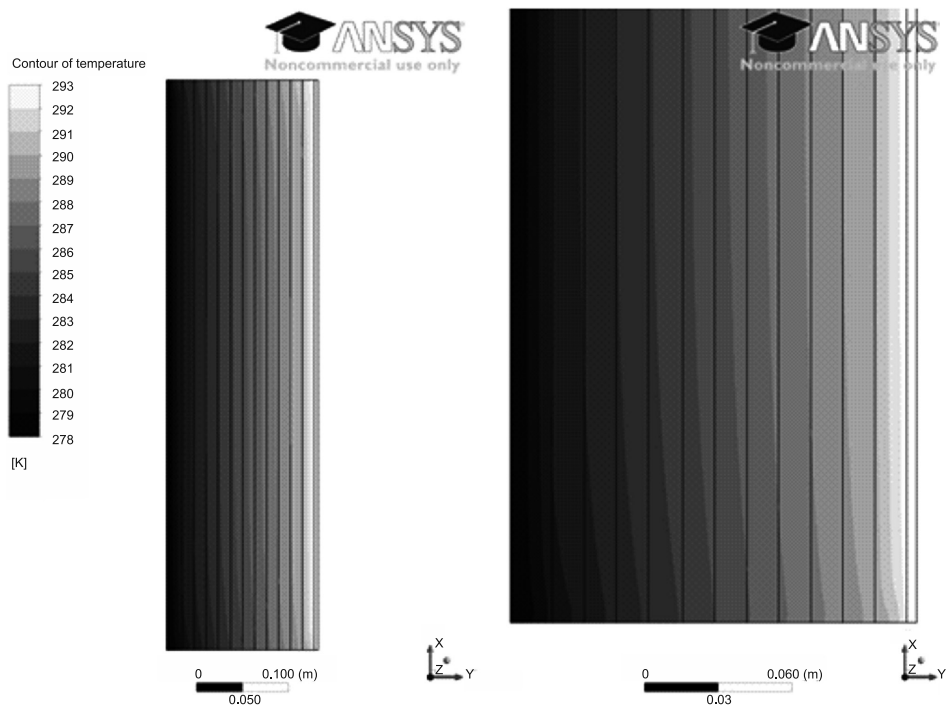


Fig. 4. Contours of temperature in the overall model and in the lower part of the glazing

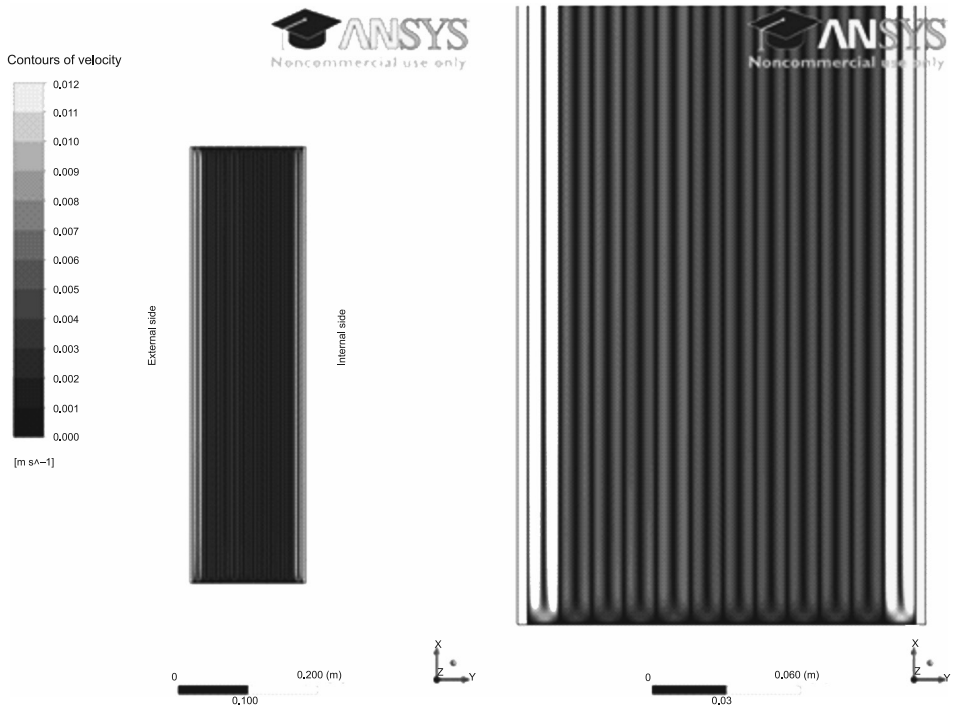


Fig. 5. Contours of gas velocity in the overall model and in the lower part of the glazing

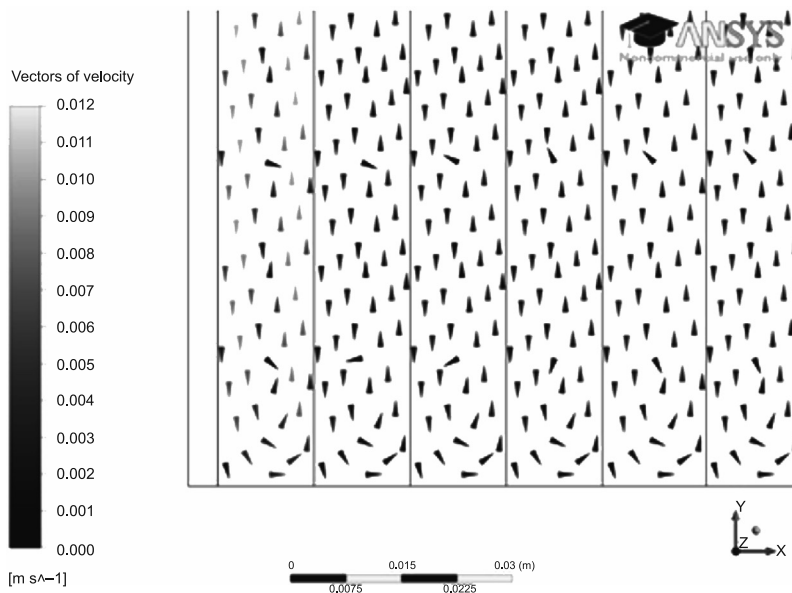


Fig. 6. Vectors of gas velocity in the lower left hand corner of the glazing

3. Analytical calculations

The overall heat transfer coefficient of glazing can be calculated analytically with the use of the PN-EN 673 [6] standard for flat and parallel surfaces in the central area of glazing. The standard does not take into account thermal bridges through the spacer or through the window frame.

The standardized boundary conditions assumed for the analytical calculations are listed in table 4.

Table 4

Boundary conditions assumed for analytical calculations

Thermal resistivity of soda lime glass	1 [mK/W]
Thermal resistivity of organic glass	5.26 [mK/W]
Temperature difference between bounding glass surfaces	15 [K]
External heat transfer coefficient for uncoated soda lime glass surfaces	23 [W/(m ² K)]
Internal radiative heat transfer coefficient for uncoated soda lime glass surfaces	4.4 [W/(m ² K)]
Internal convective heat transfer coefficient for uncoated soda lime glass surfaces	3.6 [W/(m ² K)]
Constant in Nusselt number for vertical glazing	0.035
Exponent in Nusselt number for vertical glazing	0.38

The calculation results of the glazing according to the PN-EN 673 standard [6] are as follows:

- total thermal conductance of the glazing $h_t = 0.187$ [W/(m²K)],
- thermal transmittance of the glazing $U = 0.181$ [W/(m²K)].

The thermal transmittance of the glazing calculated with the PN-EN 673 standard is 39% lower than the value calculated with the Ansys Fluent CFD program, which is a very significant difference.

There is a need to assess if CFD simulations or analytical calculations lead to proper results. That is why experimental validation has been performed using the calorimetric hot box test stand described in [3]. The measurement results as well as the analytical and CFD calculation results are presented in Table 5 [3].

Table 5

Measured and calculated results of thermal transmittance (U -value) of multi-layer glazing

Calculated U -value of glazing – CFD numerical simulation	0.3 (0.297) [W/(m ² K)]
Measured by a calorimetric hot box CHB system U -value of glazing – measurement results according to PN-EN ISO 12567-1 [6, 10]	0.3 (0.319) [W/(m ² K)]
Analytically calculated U -value of glazing – calculation according to PN-EN 673 [6, 11]	0.2 (0,181) [W/(m ² K)]

It is easily noticed, that a very good agreement between CFD simulations and experiment has been achieved. The discrepancy is about 7%. It should be also mentioned, that the value obtained by the use of the PN-EN 673 [6] standard leads to unsatisfactory results.

4. Conclusions

The U -value calculation results of multi-layer glazing with ultrathin internal glass partitions have been presented. The CFD simulations as well as the analytical calculations prescribed in the PN-EN 673 [6] standard have been applied. A significant difference between the results has been achieved. The measurement results gained with the use of the calorimetric hot box test stand have been applied in order to validate the results [3].

The CFD simulation and measurement results show that the method described in the PN-EN 673 [6] standard is not appropriate for such a kind of multi-layered glazing that was investigated.

The obtained data stipulates that the CFD approach can provide good agreement between the measured and the calculated thermal transmittance (U -value) of multi-layer glazing.

References

- [1] Dalal R., Naylor D., Roeleveld D., *A CFD study on convection in a double glazed window with an enclosed pleated blind*, Elsevier, Energy and Buildings, 41, 2009, 1256-1262.
- [2] Flaga-Maryńczyk A., Schnotale J., Radon J., Was K., *Experimental measurements and CFD simulation of a ground source heat exchanger operating at a cold climate for a passive house ventilation system*, Energy and Buildings, 68, 2014, 562-570.
- [3] Lechowska A., Schnotale J., Fedorczyk-Cisak M., Paszkowski M., *Measurement of thermal transmittance of multi-layer glazing with ultrathin internal glass partitions*, Wydawnictwo Politechniki Krakowskiej, Technical Transactions, 3-B/2014, Cracow 2014, 273-280.
- [4] Vendelboe M.V., Svendsen S., Nielsen T.R., *CFD modelling of 2-D heat transfer in a window construction including glazing and frame*, Proceedings of the 8th Symposium on Building Physics in the Nordic Countries, Copenhagen, 16–18 June 2008.
- [5] PN-EN ISO 12567-1, Thermal performance of windows and doors – Determination of thermal transmittance by the hot-box method – Part 1: Complete windows and doors, Ciepłne właściwości użytkowe okien i drzwi – Określanie współczynnika przenikania ciepła metodą skrzynki grzejnej – Część I: Kompletne okna i drzwi, 2010.
- [6] PN-EN 673. Glass in building – Determination of thermal transmittance (U -value) – Calculation method, Szkło w budownictwie – Określenie współczynnika przenikania ciepła (wartość U) – Metoda obliczeniowa, 2011.

AGNIESZKA LECHOWSKA*, JACEK SCHNOTALE*,
MAŁGORZATA FEDORCZAK-CISAK**, MARIUSZ PASZKOWSKI***

MEASUREMENT OF THERMAL TRANSMITTANCE OF MULTI-LAYER GLAZING WITH ULTRATHIN INTERNAL GLASS PARTITIONS

POMIAR WSPÓŁCZYNNIKA PRZENIKANIA CIEPŁA WIELOWARSTWOWEGO OSZKLENIA Z WEWNĘTRZNYMI ULTRACIENKIMI SZYBAMI

Abstract

Currently, the most technologically advanced building walls have an overall heat transfer coefficient U at a level of $0.10 \text{ W}/(\text{m}^2\text{K})$ which corresponds to the passive house standard. Less demanding requirements are set for building windows for which the thermal performance has not yet been significantly improved. Therefore, there is a demand for developing new technologies for glazing with superior thermal performance, good optical quality and of the lowest possible weight. In the paper, measurements of thermal performance of multi-layer glazing with ultrathin internal glass partitions are presented.

Keywords: fenestrations, calorimetric hot box, thermal transmittance measurement

Streszczenie

Obecnie współczynnik przenikania ciepła ścian w budynkach energooszczędnych jest rzędu $0.10 \text{ W}/(\text{m}^2\text{K})$, co odpowiada standardowi budynków pasywnych. Z kolei mniej rygorystyczne wymagania w standardzie pasywnym dotyczą okien, gdzie współczynnik przenikania ciepła wynosi około $0.7 \text{ W}/(\text{m}^2\text{K})$. Tak więc istnieje potrzeba rozwoju technologii okien z bardzo niskimi wartościami współczynników przenikania ciepła i jednocześnie posiadających dobre walory optyczne a także niską wagę. W artykule zaprezentowano wyniki pomiarów izolacyjności cieplnej wielowarstwowego oszklenia z wewnętrznymi ultracienkimi szybami wykonane w komorze klimatycznej zgodnie z odpowiednimi normami.

Słowa kluczowe: oszklenia, komora kalorymetryczna, pomiar współczynnika przenikania ciepła

* Ph.D. Eng. Agnieszka Lechowska, Prof. D.Sc. Ph.D. Eng. Jacek Schnotale, Department of Environmental Engineering, Institute of Thermal Engineering and Air Protection, Cracow University of Technology.

** Ph.D. Eng. Małgorzata Fedorcza-Cisak, Department of Civil Engineering, Institute of Materials and Building Constructions, Cracow University of Technology.

*** Ph.D. Mariusz Paszkowski, Institute of Geological Sciences, Polish Academy of Sciences, Krakow.

1. Introduction

In recent times, there has been an increased focus on lowering the energy demands in buildings [1, 8, 9] leading to a reduction of transmission heat losses through the building envelope and the development of buildings that are almost air tight. However windows, to a large degree, still contribute to the total building heat loss with respect both to the cooling and heating demands [1].

The triple glazed windows are readily available on the market. Their thermal transmittance is about $U_w = 0,7 \text{ W}/(\text{m}^2\text{K})$. In the paper, the heat transfer through multi-layer glazing has been analyzed. The glazing consists of two standard glass panes (internal and external) and 11 ultra-thin organic glass panes separated by 12 argon gaps. The investigated glazing prototype made by the Vis Inventis Company was placed in a Styrofoam frame. The view of the analyzed glazing is given in Fig. 1. The calorimetric hot box instruments were used to determine the thermal transmittance of the analyzed glazing [1–5, 7]. The measurements were based on PN-EN ISO 12567-1 procedure [10].

2. Measurement test stand

Experimental work focusing on measurements of the thermal transmittance of glazing presented in Figure 1 was performed in order to validate the simulation and calculation results. All investigations were carried out at Cracow University of Technology. The calorimetric hot box (CHB) was used with the test method in compliance with the PN-EN ISO 12567-1 [10] standard [3].

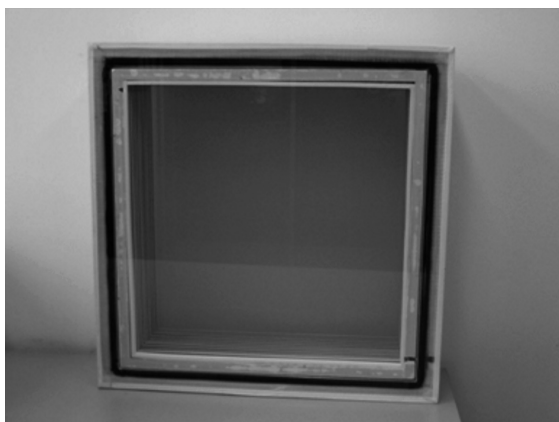


Fig. 1. The view of the glazing

The CHB system consists of a metering box, simulating the indoor environmental condition (warm side), and a climate box, simulating the outdoor environmental condition (cold side). The metering box is surrounded by a guarding box in order to minimize the heat flow rate through the metering box walls. The test specimen glazing is mounted into

the opening of a surround panel. The tested glazing and surround panel are placed between the metering box and the climate box. The steady state heat flow rate through the glazing due to the constant indoor and outdoor temperature difference is measured in order to calculate the thermal transmittance [3, 10]. Figure 2 shows the schematic cross-section of the CHB system in thermal transmittance measurement mode [3, 10]. The view of the CHB system is presented in Fig. 3.

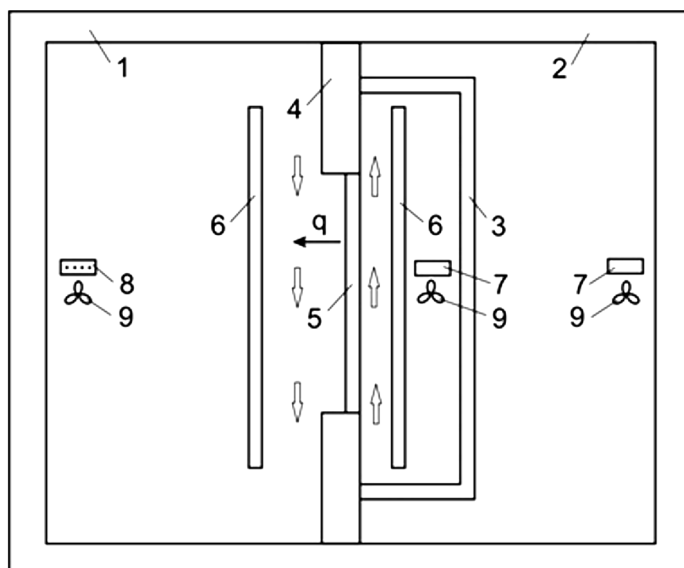


Fig. 2. CHB system scheme: 1 – climate box (outdoor side), 2 – guarding box (indoor side), 3 – metering box, 4 – surround panel, 5 – tested specimen, 6 – isothermal baffle, 7 – heater, 8 – cooling element, 9 – fan



Fig. 3. General view of calorimetric hot box (CHB) system

A PID-controller based upon the measured temperature difference across the metering box walls controlled the environment in the guarded box. The cold side temperature was kept at a 0.1°C with 0.5% discrepancy of the overall temperature difference in a steady state condition. It was assumed that the stability was attained if within two hours, the measurement results were stable with fluctuations of $\pm 0.05\%$ in the measured values.

The metering box was kept at an environmental temperature of 19.9°C using the same kind of PID-controller as the guarded box. The surface resistance on the cold side was established by controlling the air speed along the specimen using a set of regulated ventilators - a similar arrangement as on the warm side of the specimen in the metering box. Measurements were performed with an accuracy that meets the demands specified in the PN-EN ISO 8990 standard [7, 12].

3. Measurement results

Measurement results with the calorimetric hot box (CHB) apparatus are listed in Table 1.

Table 1

Measurement results

Air temperature in the metering box (warm side)	19.9°C
Baffle surface temperature in the metering box	19.°C
Surround panel surface temperature on the metering box side	19.5°C
Air temperature in the climate box (cold side)	0.1°C
Baffle surface temperature of the surround panel on the climate box side	0.5°C
Reveal surface temperature in the climate box	1.2°C
Surround panel surface temperature on the climate box side	0.9°C
Input power in hot box	13.81 W
Air speed on the warm side, down	0.1 m/s
Air speed on the cold side, up	1.7 m/s

The calculation results of the glazing according to the EN ISO 12567-1 [10] standard are as follows:

- environmental temperature on the warm side $\theta_{ni} = 19.8^\circ\text{C}$,
- environmental temperature on the cold side $\theta_{ne} = 0.3^\circ\text{C}$,
- total surface resistance $R_{s,t} = 0.253 \text{ m}^2\text{K/W}$,
- thermal transmittance of the glazing (measured) $U = 0.310 \text{ W}/(\text{m}^2\text{K})$,
- total surface resistance (standardized) $R_{(s,t)st} = 0.17 \text{ m}^2\text{K/W}$,
- thermal transmittance of the glazing (standardized) $U_{st} = 0.319 \text{ W}/(\text{m}^2\text{K})$.

A total surface resistance of 0.253 m²K/W was calculated according to measured air velocities and adjacent air temperatures on the warm and cold side. With known total surface resistance, the U value of the glazing calculated according to the measurement results was equal to 0.310 W/(m²K). The measured total surface resistance is then replaced by

0.04 m²K/W on the cold side and 0.13 m²K/W on the warm side in thermal transmittance calculation procedure [10] to achieve the standardized U value which was finally equal to 0.319 W/(m²K).

4. Uncertainty analysis

With the CHB system, the heat flow through the specimen can be obtained with certain accuracy. The accuracy in each separate measurement not only depends upon the complexity of the construction being measured, but also on heat exchange with the surroundings, errors of temperature and input power measurements etc. The measurement error is not constant from specimen to specimen.

To determine the uncertainty of the calculated heat transfer coefficient, the uncertainty in each performed measurement was estimated and then combined to give a single value according to the law of propagation based on the root square formula [1–4, 10]. The thermal transmittance U is a function of n independent variables x_k , which are known with an uncertainty Δx_k . The global uncertainty of the thermal transmittance ΔU can be written as follows [2]:

$$\Delta U = \sqrt{\sum_{k=1}^n \left[\frac{\partial U(x_k)}{\partial x_k} \right]^2 \Delta x_k^2} \quad (1)$$

The glazing thermal transmittance uncertainty depends on the following values of parameters and their uncertainties:

$$\Delta U = \Delta U(H_{sp}, w_{sp}, d_{sp}, H_{sur}, w_{sur}, d_{sur}, \theta_{ci}, \theta_{ce}, \theta_{si,b}, \theta_{se,b}, \theta_{si,sur}, \theta_{se,sur}, \theta_{se,p}, \Phi_{in}) \quad (2)$$

where:

- U – overall heat transfer coefficient [W/(m²K)],
- θ_{ci} – air temperature on hot side [°C],
- θ_{ce} – air temperature on cold side [°C],
- $\theta_{si,b}$ – baffle surface temperature on hot side [°C],
- $\theta_{se,b}$ – baffle surface temperature on cold side [°C],
- $\theta_{si,sur}$ – surround panel surface temperature on hot side [°C],
- $\theta_{se,sur}$ – surround panel surface temperature on cold side [°C],
- $\theta_{se,p}$ – reveal surface temperature on cold side [°C],
- d_{sp} – specimen thickness [m],
- d_{sur} – surround panel thickness [m],
- H_{sp} – specimen height [m],
- H_{sur} – surround panel height [m],
- w_{sp} – specimen width [m],
- w_{sur} – surround panel width [m],
- Φ_{in} – input power in hot box [W].

The U -value uncertainty is connected with the measurement errors of dimensions, temperatures and input power in the hot box, equal to 0.001 m, 0.1 K or 0.01 K and 0.52 W respectively.

The calculated value of the glazing overall heat transfer coefficient measurement uncertainty is equal to 0.070 W/(m²K), this means a measurement error of about 20%.

5. Conclusions

The U -value measurement results of multi-layer glazing with ultrathin internal glass partitions have been presented. The calorimetric hot box method has been applied as prescribed in the PN-EN ISO 12567-1 [10] standard.

The measurement results can be compared to CFD simulation results as well as analytical calculation results given in [6]. The comparison is presented in Table 2.

Table 2

Measured and calculated results of thermal transmittance (U -value) of multi-layer glazing

Calculated U -value of glazing – CFD numerical simulation	0.3 (0.297) [W/(m ² K)]
Measured by a calorimetric hot box CHB system U -value of glazing – measurement results according to PN-EN ISO 12567-1 [6, 10]	0.3 (0.319) [W/(m ² K)]
Analytically calculated U -value of glazing – calculation according to PN-EN 673 [6, 11]	0.2 (0,181) [W/(m ² K)]

On Table 2, one can see a very good correlation between thermal transmittance values obtained from measurements done at the hot box calorimeter test stand and those obtained from CFD simulations. The deviation between them is about 7%.

The calculation and measurement results show that the method described in the PN-EN 673 [11] standard is not appropriate for the kind of multi-layered glazing that was investigated.

The obtained data stipulates that the CFD approach can provide a good agreement between the measured and calculated thermal transmittance (U -value) of multi-layer glazing. The investigation points out that it is possible to obtain a significant improvement in the thermal transmittance value of glazing that can lead to an even further lowering of heat demand of residential and commercial buildings without compromising comfort expectations.

References

- [1] Appelfeld D., Svendsen S., *Experimental analysis of energy performance of a ventilated window for heat recovery under controlled conditions*, Elsevier, Energy and Buildings, 43, 2011, 3200-3207.
- [2] Asdrubali F., Baldinelli G., *Thermal transmittance measurements with the hot box method: calibration, experimental procedures and uncertainty analyses of three different approaches*, Energy and Buildings, 43, 2011, 1618-1626.
- [3] Chen F., Wittkopf S.K., *Summer condition thermal transmittance measurement of fenestration systems using calorimetric hot box*, Elsevier, Energy and Buildings, 53, 2012, 47-56.

- [4] Elmahdy A. H., *Heat transmission and R-value of fenestration systems using IRC hot box – procedure and uncertainty analysis*, Transactions of ASHRAE, 98, 2, 1992.
- [5] Fang Y., Eames P.C., Norton B, Hyde T.J., *Experimental validation of a numerical model for heat transfer in vacuum glazing*, Solar Energy, 80, 5, 2006, 564-577.
- [6] Lechowska A., Schnotale J., *CFD modeling and analytical assessment of thermal transmittance of multi-layer glazing with ultrathin internal glass partitions*, Wydawnictwo Politechniki Krakowskiej, Technical Transactions, 3-B/2014, Cracow 2014, 265-272.
- [7] Rose J., Svendsen S., *Validating numerical calculations against guarded hot box measurements*, Nordic Journal of Building Physics, 4, 2004, 9.
- [8] Directive 2010/31/EU of the European Parliament and of the Council of 19 May 2010 on the energy performance of buildings, Dyrektywa Parlamentu Europejskiego i Rady w sprawie charakterystyki energetycznej budynków z dnia 19 maja 2010, 2010/31/UE.
- [9] Directive 2012/27/EU of the European Parliament and the Council of 25 October 2012 on energy efficiency, Dyrektywa Parlamentu Europejskiego i Rady w sprawie efektywności energetycznej z dnia 25 października 2012, 2012/27/UE.
- [10] PN-EN ISO 12567-1. Thermal performance of windows and doors – Determination of thermal transmittance by the hot-box method – Part 1: Complete windows and doors, Ciepłote właściwości użytkowe okien i drzwi – Określanie współczynnika przenikania ciepła metodą skrzynki grzejnej – Część I: Kompletnie okna i drzwi, 2010.
- [11] PN-EN 673. Glass in building – Determination of thermal transmittance (U -value) – Calculation method, Szkło w budownictwie – Określenie współczynnika przenikania ciepła (wartość U) – Metoda obliczeniowa, 2011.
- [12] PN-EN ISO 8990. Thermal insulation – Determination of steady-state thermal transmission – Calibrated and guarded hot box, Izolacja cieplna – Określanie właściwości związanych z przenikaniem ciepła w stanie ustalonym. Metoda kalibrowanej i osłoniętej skrzynki grzejnej, 1998.

PIOTR LIS*, ANNA LIS**

THE SEASONAL HEAT DEMAND FOR HEATING, CALCULATED ON THE BASIS OF PEAK POWER VALUES IN EDUCATIONAL BUILDINGS

SEZONOWE ZAPOTRZEBOWANIE NA CIEPŁO DO OGRZEWANIA OBLICZONE NA PODSTAWIE MOCY SZCZYTOWEJ W BUDYNKACH EDUKACYJNYCH

Abstract

This paper presents the selected results of examinations connected with a seasonal heat consumption (Q) and thermal power (q) for heating in educational buildings. The purpose of the analysis presented here was to examine the influence of possible occurrence and level of differences between the seasonal heat consumption (Q) and the seasonal heat demand (Q_q) for heating, calculated on the basis of q values. A modification in the method for determination of Q_q for room heating on the basis of available data on q was introduced. A linear function, describing the changes in ($Q_q - Q$) depending on the changes in q values, which was applied for that purpose, made it possible to improve the consistency of obtained heat demand values in relation to measured consumption of heat for heating by 65.6%.

Keywords: educational buildings, heating, thermal power, heat demand, heat consumption

Streszczenie

W artykule przedstawiono wybrane wyniki analiz związanych z sezonowym zapotrzebowaniem na ciepło (Q) i mocą szczytową (q) do ogrzewania budynków edukacyjnych. Celem tej analizy było ustalenie wystąpienia różnic pomiędzy sezonowym zużyciem ciepła (Q) a sezonowym zapotrzebowaniem na ciepło (Q_q) do ogrzewania, obliczonym na podstawie znanej wartości szczytowej mocy cieplnej q . Realizacja ww. analizy stanowiła podstawę do zaproponowania zmiany w metodzie obliczania wartości zapotrzebowania na ciepło Q_q do ogrzewania pomieszczeń na podstawie dostępnych danych. Wykorzystanie tutaj funkcji liniowej opisującej zmiany ($Q_q - Q$) w zależności od zmian wartości q umożliwiło zmniejszenie rozbieżności pomiędzy obliczonymi wartościami zapotrzebowania na ciepło a zmierzonym zużyciem ciepła do ogrzewania o 65,6%.

Słowa kluczowe: budynki edukacyjne, ogrzewanie, moc cieplna, zapotrzebowanie na ciepło, zużycie ciepła

* Prof. D.Sc. Ph.D. Eng. Piotr Lis, Department of District Heating, Heating and Ventilation, Faculty of Environmental Engineering and Biotechnology, Czestochowa University of Technology.

** Ph.D. Eng. Anna Lis, Department of General Construction and Building Physics, Faculty of Civil Engineering, Czestochowa University of Technology.

1. Introduction

The calculative methods, which are applied in various fields of engineering, are usually a certain kind of theoretical approximation of reality.

Estimated and simplified calculations of the seasonal heat demand (Q_q) based on the known value of thermal power (q) are used quite often in engineering practice [5]. The using of available base quantities for calculation of sought quantities, the physical interpretation of which is often different from the “base”, is not a new phenomenon [2, 4–7] and, despite its disadvantages, it will probably still be applied. Despite the simplifications introduced in such cases, the obtained results of calculations should correlate with the results of measurements. It should be so also in case of theoretical heat demand (Q_q) for heating, calculated on the basis of the thermal power (q) and the actual (measured directly or indirectly) seasonal heat consumption (Q) for heating.

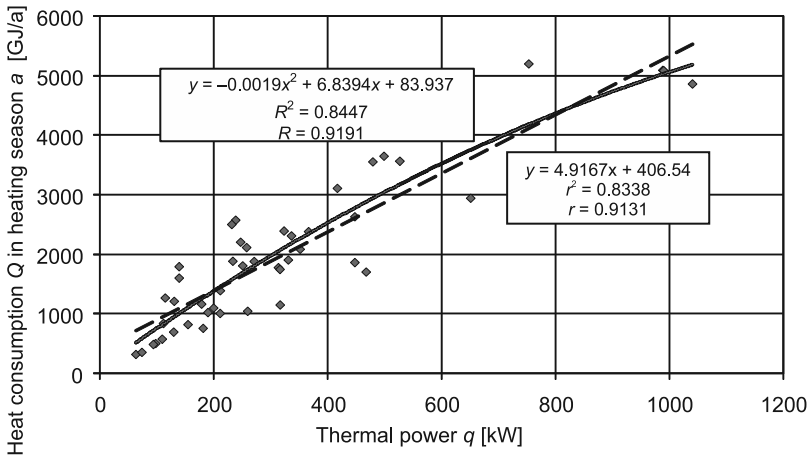


Fig. 1. Graph for the relationship between heat consumption Q and thermal power q for heating

The association between Q for heating and the calculated q as well as the discrepancies appearing here and the aforementioned use of q values for estimating of the heat demand (Q_q) in engineering practice were the main reason inducing the undertaking of the examinations and analyses, the results of which will be presented.

2. Description of the conducted examinations and analyses

The material presented in this work is a fragment of wider analysis and relates to 46 of 50 educational buildings, which were constructed in 1913–1992 (data for 4 objects were questionable in the author’s opinion). The basic characteristic of these buildings is presented in the Table 1.

The statistical description of this group does not differ significantly from the description of the entire group of 50 buildings [6]. Difference from this analysis of heat consumption

in educational buildings is also presented, inter alia, Butala V. and Novak P. [1], Corgnati S. P., Corrado V., Filippi M. [2], Desideri U., Proietti S. [3].

Table 1

Selected measures of statistical description for the values characterizing 46 of 50 educational buildings forming the municipal group of objects of this type

Value x	Selected measures of statistical description			
	Average value x_{sr}	Standard deviation $s(x)$	Limits of typicality x_{yp}	Coefficient of variation $v_k(x)$ [%]
Cubic capacity V [m ³]	14682.37	9674.55	5007.82 – 24356.92	65.89
A/V [m ⁻¹]	0.40	0.09	0.31 – 0.50	23.43
Thermal power for heating q [kW]	323.38	235.15	88.23–558.54	72.72
q/V [W/m ³ a]	21.93	5.11	16.81–27.04	23.32
Heat consumption for heating in stand. heating seas. Q [GJ/a]	1996.52	1266.14	730.38–3262.66	63.42
Q/V [GJ/m ³ a]	138.36	39.26	99.10–177.62	28.37

The heating season used in the analyses can be considered as typical for multiannual period in statistical respect (min. 30 years). In the examined group, 23 educational buildings were provided with heat for heating by HPC (Heat Power Company), while 27 buildings had their own boiler-rooms.

Returning to the relationship shown in the Fig. 1, it was noticed that about 84% of changes in Q depends on the changes in q , while 16% does not depend on the changes of this quantity. This state can be caused by not very accurate consideration of the actual conditions of buildings' heating in the methodology of thermal power (q) calculation.

Bearing in mind the practice that the demand for heat needed for buildings' heating is estimated on the basis of thermal power (q) as well as the conclusion formulated above, the following important question arises: Will the relationships and discrepancies revealed in the analysis of graphs in Fig. 1 be analogous in calculating the heat demand for buildings' heating (Q_q) on the basis of thermal power (q) (should it be expected)?

3. Results of examinations

In order to give an answer to the question, the values of Q_q for examined buildings, which are a "representative" of the buildings' thermal needs mentioned in the title and connected with heating in calculation – theoretical conditions, were calculated and they were compared graphically with the corresponding values of heat consumption (Q) for heating in the actual conditions (Fig. 2).

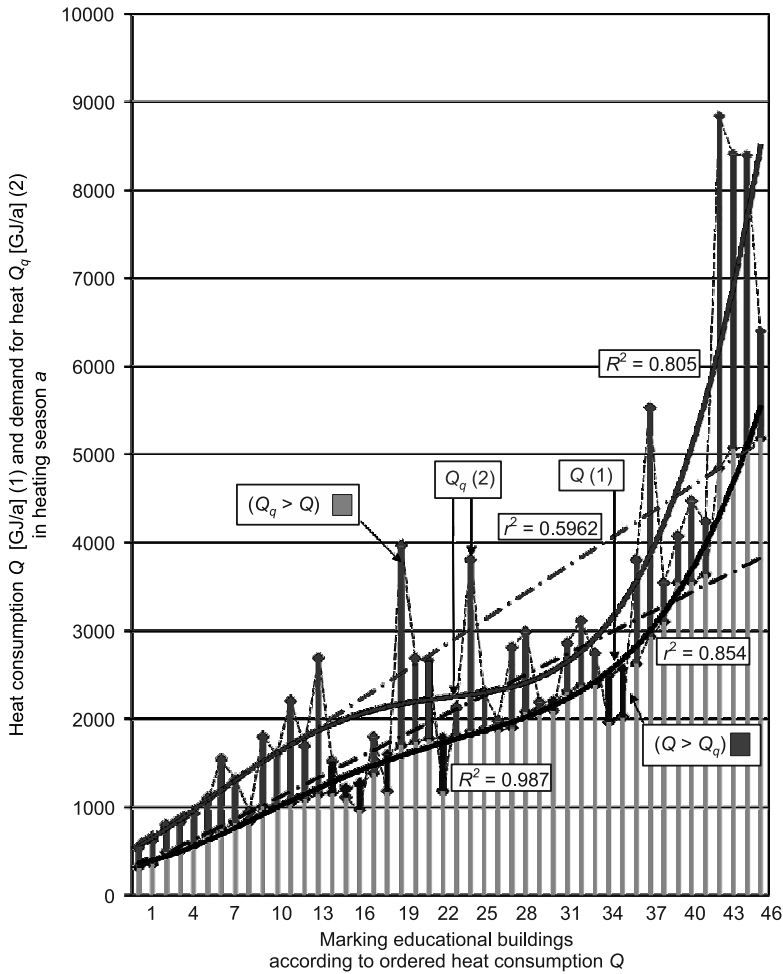


Fig. 2. Graph for the relationship between heat consumption Q and thermal power q for heating

The heat demand (Q_q) in analysed heating season for a given building calculated with the use of known value of thermal power (q), on the basis of equation (1), which is quoted, directly or indirectly, also in other publications [4–6]:

$$Q_q = q \cdot Nd \cdot 24h \cdot \frac{(T_{ical} - T_{eav})}{(T_{ical} - T_{emin})} \cdot 0.0036 \quad (1)$$

where:

- Q_q – heat demand for heating in heating season a [GJ/a],
- q – thermal power [kW],
- Nd – number of heating days in the considered heating season [days],
- $24h$ – duration of a day [h],

- $T_{i\,cal}$ – calculative temperature of air inside of heated building assumed in the considered case ($T_{i\,cal\,av} = +20^{\circ}\text{C}$) [$^{\circ}\text{C}$],
 $T_{e\,av}$ – average temperature of air outside in the heating season for the considered period and for determined area (town) ($T_{e\,av} = +2.9^{\circ}\text{C}$) [$^{\circ}\text{C}$],
 $T_{e\,min}$ – calculative temperature of air outside, ($T_{e\,min} = -20.0$) [$^{\circ}\text{C}$],
 0.0036 – conversion factor for values expressed in various physical units.

In the analysed case this relationship will have the following form:

$$Q_q = q \cdot 230 \cdot 24h \cdot \frac{(20^{\circ}\text{C} - 2.9^{\circ}\text{C})}{(20^{\circ}\text{C} - (-20^{\circ}\text{C}))} \cdot 0.0036 \quad (2)$$

The equation (2) is the result of comparison of algorithms for calculation of heat demand for heating in the conditions of the previously characterized heating season and thermal power necessary for fulfilling these needs in extreme conditions. Obviously, it is an imperfect comparison due to the applied “conversion factor”, which “eliminates” only the difference of temperatures outside of a heated building, included in the considered algorithms.

4. Discussion of examination results

An indirect target of the analysis was to establish if there are essential differences between the actual seasonal heat consumption (Q) for heating of the examined buildings and the seasonal heat demand (Q_q) for heating, calculated on the basis of thermal power (q) value. The realization of such formulated task should make it possible to achieve the direct target, i.e. proposing a modified version of the method for calculating the seasonal heat demand (Q_q). The modification should make it possible to reduce the differences between the thermal needs of educational buildings in actual and theoretical conditions, in case when these needs are estimated on the basis of known values of thermal power (q).

The analysis of relationships (Fig. 2) reveals the differences between seasonal heat consumption (Q) for heating and calculated (with the use of known values of thermal power (q)) seasonal heat demand (Q_q). Occurrence of these differences confirms the divergence of trends for changes in the analyzed quantities, which are shown on the graph.

The described differences could be considered as resulting only from the discrepancies between the calculative assumptions and the actual conditions of heating season. However, it seems that their level (Fig. 2) in the examined educational buildings and the course of trend line do not incline towards such a statement. The calculated heat demand (Q_q) is bigger by 41.6%, on the average, than the actual consumption (Q). However, there are objects (7 of 46), in which the situation is opposite, i.e. $Q > Q_q$ (Fig. 2). In the analysed group of buildings the maximal discrepancy between the values of Q and Q_q amounted to 134% ($Q_q > Q$), while minimal discrepancy amounted to (-34)% ($Q > Q_q$). A percentage relation of the difference's value ($Q_q - Q$) to the value of Q is diverse in individual objects.

5. The proposal of reducing discrepancies between the thermal needs of educational buildings in actual and calculation conditions

The relationships presented in the Figs. 3, 4 and 5 were used to propose a method for calculation of modified heat demand ($Q1_q$). For some of them $r^2 = 1$, which is a result of Q_q and $Q1_q$ calculation using thermal power, and not of an “ideal” adjustment of function to the points of data on a graph. Using functional description of changes in the ($Q_q - Q$)

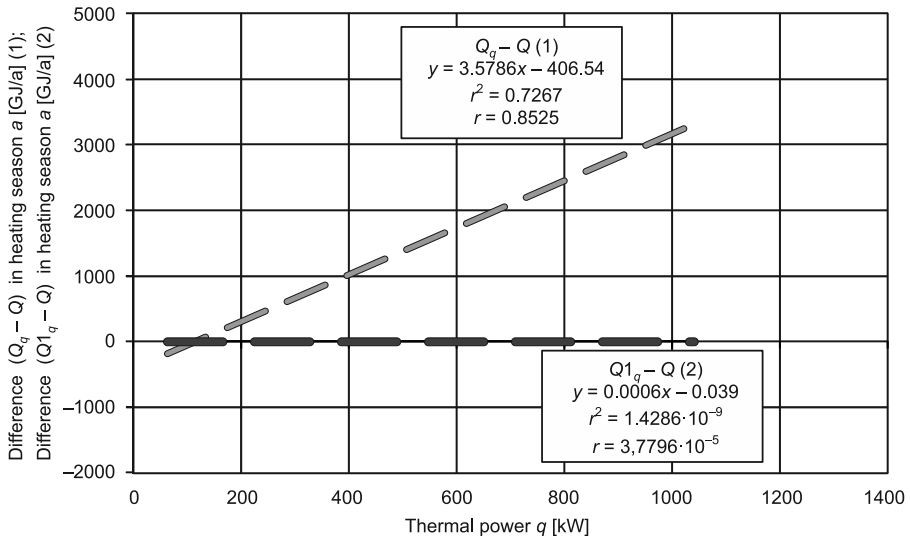


Fig. 3. Graph for the relationship between differences ($Q_q - Q$), ($Q1_q - Q$) and thermal power q

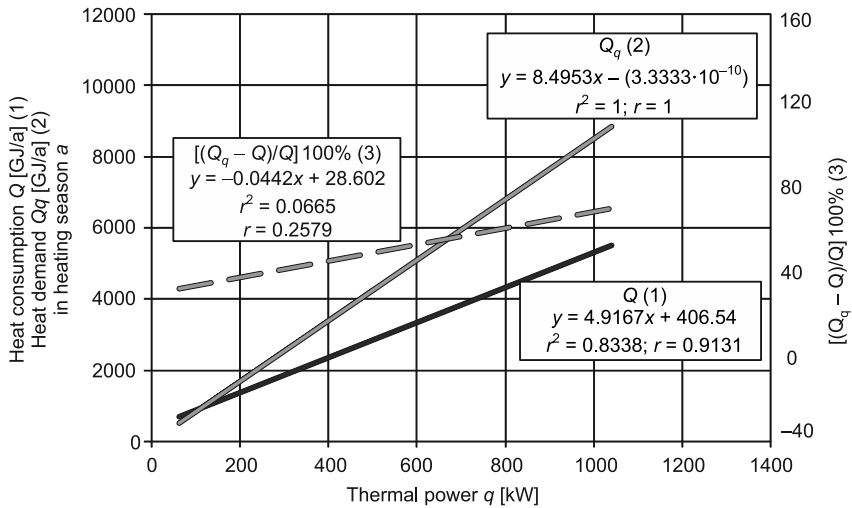


Fig. 4. Graph for the relationship between Q , Q_q , $[(Q_q - Q)/Q]$ 100% and thermal power q

difference depending on the changes in the thermal power (q) (Fig. 3) made it possible to create the relationship allowing the theoretical $Q1_q$ to be determined. A similar, but quantitatively worse effect, can be achieved by replacing the mentioned functional notation with a multiplier, equal to the average difference between Q_q and Q , which in the analysed case amounted to 0.416. The method of $Q1_q$ determination allowed making the difference ($Q1_q - Q$) independent of the changes in thermal power (q) (Fig. 3).

Bearing in mind the results of previous analyses, in the next stage a trial to modify the relationship (1) was undertaken. The effect of such modification should be determining a method for calculating the values of seasonal heat demand for heating ($Q1_q$), which would, on the average, differ less from the heat consumption (Q) in the examined objects in relation to the difference occurring if the Q_q quantity is used (Fig. 4). Its course in the graph (Fig. 3) was described by using the linear function $y = 3.5786x - 406.54$ for that purpose. The determination of the difference in form of decimal fraction 0.416 is simple, but not sensitive to the changes in the thermal power. Therefore, in further part, the mentioned linear function was used for quantitative determination of differences between the heat demand (Q_q) and the heat consumption for heating of educational buildings, including the changes in thermal power (q), according to the following equation:

$$(Q_q - Q) = 3.5786q - 406.54 \quad (3)$$

Equation (3) was used to create the relationship allowing for calculation of a modified seasonal heat demand for heating $Q1_q$:

$$Q1_q = Q_q - (Q_q - Q) \quad (4)$$

By substituting the relationships (1) and (3) to the equation (4), we obtain:

$$Q1_q = q \cdot Nd \cdot 24h \cdot \frac{(T_{ical} - T_{eav})}{(T_{ical} - T_{emin})} \cdot 0.0036 - (3.5786q - 406.54) \quad (5)$$

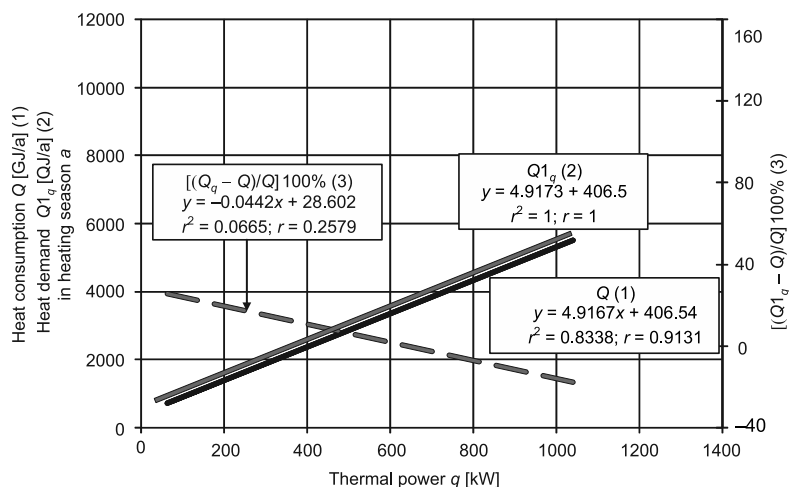


Fig. 5. Graph for the relationship between Q , $Q1_q$, $[(Q1_q - Q)/Q] 100\%$ and thermal power q

The symbols used in equation (5) are the same as in case of equation (1) and they were described above. The values of Q_q and $Q1_q$, calculated with two various methods, were compared and differentiated in relation to Q (Fig. 3), in order to determine if the performed transformations allowed for reduction (mentioned in the title) of the differences between the thermal needs of educational buildings in actual and theoretical conditions. The qualitative effect of the described actions is presented in the Fig. 5, in the form of graph.

6. Conclusions

To sum up, it can be repeated that the occurrence of differences between the seasonal heat consumption (Q) and the seasonal heat demand (Q_q) for schools heating, calculated in the proposed manner, was found. The quantitative level ($Q_q - Q$) is different in the analysed educational buildings. It does not result only from the differences between the methodology of Q_q calculation and the actual heating process, which results in generating the seasonal heat consumption (Q) for heating of the examined buildings. If it is so, then it seems that the points of data for individual buildings should overlap with the trend of changes in Q_q and Q values (Fig. 2).

The comparison of graphs presented in Fig. 4 and 5 make it possible to state, that if the equation (4) is applied for calculating heat demand ($Q1_q$) on the basis of thermal power (q), then the obtained difference of theoretical values in relation to the heat consumption (Q) is smaller than it was in case of using the equation (1) and calculation of Q_q . An average level of the mentioned differences amounted to 14.3% and 41.6%, respectively. A modification in the method for determination of heat demand for room heating on the basis of available data on thermal power (q) was introduced. A linear function, describing the changes in ($Q_q - Q$) depending on the changes in thermal power (q) values, which was applied for that purpose, made it possible to improve the consistency of obtained heat demand values in relation to the measured consumption of heat for heating by 65.6%. An even better effect can be expected by applying a function in the form of a polynomial, which is better adjusted to the data included in the Fig. 3. However, the selection of such a function is connected with complication of the calculation method, which is "simplified" by assumption.

The proposed comparison of the Q and Q_q values and the graphical methods applied in the analysis may be used in order to determine the scope of such incorrectness, in the analysis of the heating of similar groups of educational buildings and also as a help in providing other information connected with the specificity of heating of such objects'.

References

- [1] Butala V., Novak P., *Energy consumption and potential energy savings in old school buildings*, Energy and Buildings, Vol. 29, 1999, 241-246.
- [2] Corgnati S.P., Corrado V., Filippi M., *A method for heating consumption assessment in existing buildings: A field survey concerning 120 Italian schools*, Energy and Buildings, 40, 2008, 801-809.
- [3] Desideri U., Proietti S., *Analysis of energy consumption in the high schools of a province in central Italy*, Energy and Buildings, 34, 2002, 1003-1016.

- [4] Karperkiewicz K., *Building heating needs assessment based on monitoring of the supplied energy*, Cracow University of Technology Technical Journal 5B, 2006, 251-258.
- [5] Lis P., *Interpretation of differences between the thermal needs of educational buildings in the real world and theoretical*, Modern solutions in engineering and environmental protection, Publisher Institute for Air Conditioning and Heating Faculty of Environmental Engineering Technical University of Wroclaw, Vol. II, Wroclaw 2011, 35-41.
- [6] Lis P., *Compatibility of the theoretical and actual conditions of heating in educational buildings*, Energy and Building, 11, 2011, 44-48.
- [7] Lis P., *The actual and calculated thermal needs of educational buildings*, Environmental Engineering, Taylor & Francis Group, UK, London 2013, 405-416.

ANNA MACHNIEWICZ*, ARTUR BOROWCZYŃSKI*, DARIUSZ HEIM*

TRANSPARENT INSULATION EFFICIENCY DETERMINED BY DIFFERENT METHODS

OBLICZENIOWA EFEKTYWNOŚĆ IZOLACJI TRANSPARENTNYCH WYZNACZANA RÓŻNYMI METODAMI

Abstract

The paper summarizes the methods of calculating heat gain by transparent insulation using two national standards. The energy balance of the partition was evaluated taking its orientation into account. A comparison was conducted into the methods of assessing the effectiveness of transparent insulation.

Keywords: transparent insulation, heat gains, energy balance

Streszczenie

W artykule przedstawiono metody wyznaczania zysków ciepła uzyskiwanych poprzez zastosowanie izolacji transparentnej z wykorzystaniem dwóch norm. Wyznaczono bilans energetyczny przegrody uwzględniający warunki klimatyczne charakterystyczne dla danej orientacji. Przeprowadzono porównanie metod ze względu na efektywność izolacji transparentnej.

Słowa kluczowe: izolacja transparentna, zyski ciepła, bilans energetyczny

* M.Sc. Eng. Anna Machniewicz, M.Sc. Eng. Artur Borowczyński, Ph.D. D.Sc. Eng. Dariusz Heim, Department of Environmental Engineering, Faculty of Process and Environmental Engineering, Lodz University of Technology.

1. Introduction

The concept of transparent insulation (TI) refers to a transparent material or a composition of several materials placed on the external layer of a building envelope. It is an effective technology that aims to reduce the heating demand by enhancing solar energy conversion and the capability of thermal energy storage [3]. Therefore, transparent insulation not only reduces heat loss by conduction but, unlike the traditional thermal insulation, also provides additional solar heat gains [4].

The heat gains are achieved through an appropriate transparent insulation construction and its utilization varies depending on the system [16]. The typical arrangement of components comprises the outer glass (or a layer of glass plaster), a transparent insulation material which allows solar radiation to be transmitted to the absorber, and transfers heat directly to the storage layer (massive wall). Effective transparent insulation materials used in such an application are made of plastics, such as polycarbonate with a structure of honeycomb or acrylic foam, or inorganic materials, which include fiber glass and aerogel. The diversified structure of transparent insulation allows for the design of an aesthetic façade components which easily combine with traditional insulation systems.

Transparent insulation enables heat to accumulate on the surface of the absorber and, by warming the accumulation layer, to transfer heat to the building [6]. Nevertheless, on cloudy days or during the night the insulation should have appropriate thermal insulation properties to minimize heat loss. Therefore, the TI is usually characterized by a low thermal transmittance U , a high solar energy transmittance g and low emissivity ϵ [2].

Many studies have examined the overall performance and heat transfer through TI [7, 13]. Furthermore, different numerical models to evaluate the thermal behaviour of these kinds of insulation materials can be found in this literature [17, 18]. These models differ in terms of their complexity and also take into account specific variables, in accordance with the model's application. Moreover, the effectiveness of the application of TI in external walls can be evaluated more precisely by a dynamic simulation using ESP-r [11], TRNSYS [10], tsbi3 software [15] or experimentally [12, 14].

In the latter paper, the efficiency of transparent insulation was calculated using two methods described in the Polish (ISO) and German (DIN) national standards. Both methods are based on the monthly, steady-state energy balance but also take into account different weather and material parameters. The study was designed to investigate the impact of the model's complexity on the accuracy of the results.

2. Calculation methods

2.1. The Polish Standard calculation method

An energy efficiency evaluation can be formulated using different calculation methods characterized by different levels of accuracy and complexity. In order to determine the overall energy performance of the building, and of its components, the monthly balance method can be applied. The effect of the transparent insulation application can be estimated according to the difference in heat fluxes (between gains and losses). Heat loss by the external envelope utilising TI can be calculated likewise as for usual elements. It can be stated that,

for the purpose of TI performance evaluation, transmission of the heat transfer coefficient can be limited to the direct heat transfer coefficient by the transmission to the external environment. Flux caused by neglect of linear and point thermal bridges heat loss can be expressed as:

$$Q_{tr} = A \cdot U_T \cdot \Delta\theta \cdot 24 \cdot n_i \quad (1)$$

where:

- A – total area of partition,
- U_T – total thermal transmittance,
- $\Delta\theta$ – average difference between indoor and outdoor air temperature,
- n_i – number of days in a month.

Despite the specific structure and optical characteristics, heat loss through a TI wall can be calculated in the same way as for a typically insulated wall. Nevertheless, heat gains are quite difficult to estimate and different approaches need to be applied.

The Polish national and European Standard [8] provides the basic guide for an assessment of the overall energy performance of a building. It applies to whole zone energy balance calculations but can be also be used to evaluate the performance of a specific part of a building's construction. The energy performance of transparent insulation can be estimated by reference to the difference between heat gain and heat loss, and calculations can be extrapolated for subsequent months.

Taking into account the effective collecting area and solar irradiance for a specific orientation and month, the calculation method detailed in the Annex to the National Standard allows the effect of additional solar heat gains during the whole year to be quantified. For non-heating zones, solar heat gain can be calculated as:

$$Q_s = I_{si} \cdot A_s \cdot 24 \cdot n_i \quad (2)$$

where:

- A_s – effective collecting area,
- I_{si} – solar irradiance on vertical surface at the given orientation.

Solar heat gains calculated by ISO depend on the orientation of the surface and shading by other external structures. The method takes account of climate, time and also location-dependent factors such as the Sun's position, and the ratio between direct and diffuse solar radiation. The solar energy-effective collecting area is equal to the area of a black-clad body having the same solar heat gain as the surface in question:

$$A_s = A_{TI} \cdot F_s \cdot F_F \cdot \frac{U_T}{U_{te}} \cdot g_T \quad (3)$$

where:

- A_{TI} – total area of the transparent insulation,
- F_s – shading coefficient,
- F_F – frame area coefficient (ratio of transparent insulation area to total area),
- U_{te} – thermal transmittance from the surface facing the transparent insulation to the external environment,
- g_T – total solar energy transmittance of the transparent insulation:

$$g_T = \alpha(g_{h,T} - c_{j,m} \cdot g_{n,T}) \quad (4)$$

where:

- $g_{h,T}$ – total diffuse solar energy transmittance of transparent insulation,
- $c_{j,m}$ – coefficients for the calculation of total solar energy transmittance,
- $g_{n,T}$ – total direct solar energy transmittance of transparent insulation,
- α – solar radiation absorption coefficient of a surface.

2.2. The German Standard calculation method

The German Standard [1] assume the same heat loss calculation method as in the ISO, but the heat gains by TI are determined in a different way. DIN assumes there to be a distinction in calculation methods for opaque constructions and envelopes with transparent insulation.

The general equation for solar heat gain in the case of opaque partitions is in two parts. The first addresses the energy yield as a result of energy absorption of solar radiation on the exterior surface of an opaque element. The calculation depends on the absorption coefficient of a surface, for solar radiation α and also for solar irradiance I_s . The second part of the formula concerns the thermal radiation loss due to heat emission, which depends on the average surface temperature and the atmospheric temperature $\Delta\theta_{er}$.

The heat gain of the partition with the transparent insulation is determined in a similar way, but taking into account the transparent insulation efficiency coefficient α_e and the shading coefficient F_s :

$$Q_{S, TI} = \sum (U \cdot A_{TI} \cdot R_{se} \cdot (\alpha \cdot \alpha_e \cdot F_s \cdot I_{si} - F_l \cdot h_r \cdot \Delta\theta_{er}) \cdot t_M) \quad (5)$$

The transparent insulation efficiency coefficient is determined by:

$$\alpha_e = \frac{g_{TI} \cdot R_{TI} \cdot F_F}{R_{se}} \quad (6)$$

where:

- h_r – surface coefficient of the transfer of radiative heat of the exterior surface,
- F_l – slope coefficient of the element,
- T_{TI} – thermal resistance of transparent insulation,
- g_{TI} – total effective solar transmittance,
- $\Delta\theta_{er}$ – average surface temperature and atmospheric temperature.

The substitution of (6) into (5) gives the overall formula for the heat gain generated by transparent insulation:

$$Q_{S, TI} = \sum (U \cdot A_{TI} \cdot (\alpha \cdot g_{TI} \cdot R_{TI} \cdot F_F \cdot F_s \cdot I_{si} - R_{se} \cdot F_l \cdot h_r \cdot \Delta\theta) \cdot t_M) \quad (7)$$

In certain cases the share of absorption coefficient α and/or shading coefficient F_s can be omitted from the equation. This depends on the transparent insulation system in question. The type of transparent insulation also influences the means of determining the total effective solar energy transmittance g_{TI} . In this type of TI there is no air gap (thermal resistance of an air gap R_{sp} is omitted) – so it can be assumed:

$$g_{TI} = g_T \quad (8)$$

3. Case study

For the purpose of a comparative analysis of the methods described, the single partition was taken into account. The dimensions were assumed to be 5.0 m in length and 2.4 m in height, reaching a total area of 12 m². The geometry was defined in such a way that the modeled wall matched the dimensions of the transparent insulation panels (1.0 × 1.2 m). The external wall was constructed from cellular concrete with a thickness of 0.24 m and 0.125 m of transparent insulation. It was assumed that TI covered the whole area of the partition to determine its energy balance precisely. The physical properties of the transparent insulation (thermal conductivity, solar energy transmittances) were adopted in accordance with the technical specifications of the material.

To determine the heat transfer through the partition, the climatic data developed for the EBPD certificate system [9] was used in the calculations. The interior air temperature was set at 20°C and one calendar year was assumed to be the calculation period. The monthly

Table 1

Material and weather parameters used in calculations

Parameter					Method	
No.	Description	Symbol	Unit	Value	ISO	DIN
1	total area of the transparent insulation	A_{TI}	[m ²]	12.0	V	V
2	absorption coefficient	α	[-]	0.95	V	X
3	solar energy transmittance coefficient	$c_{j,m}$	[-]	[8]	V	X
4	thickness of the wall (excluding TI)	d	[m]	0.24	V	V
5	thickness of transparent insulation	d_{TI}	[m]	0.125	V	V
6	frame area coefficient	F_F	[-]	1.0	V	V
7	slope coefficient	F_I	[-]	0.5	X	V
8	shading coefficient	F_S	[-]	1.0	V	V
9	total solar energy transmittance	g_T	[-]	0.54	X	V
10	total direct solar energy transmittance	$g_{n,T}$	[-]	0.6	V	X
11	total diffuse solar energy transmittance	$g_{h,T}$	[-]	0.4	V	X
12	surface coefficient of radiated heat transfer of the outer surface	h_r	[W/m ² K]	4.0	X	V
13	solar irradiation on vertical surface	I_{si}	[W/m ²]	Fig. 1	V	V
14	thermal conductivity of the wall	λ	[W/mK]	0.29	V	V
15	equivalent thermal conductivity of the transparent insulation	λ_{TI}^{eq}	[W/mK]	0.09	V	V
16	calculation period	t_M	[h]	[9]	V	V
17	average surface and atmospheric temperature (DIN allowing the adoption of a constant value for a moderate climate zone)	$\Delta\theta_{er}$	[K]	10.0	X	V

average values of the solar irradiation (depending on orientation) and the average differences between the indoor and external air temperature are shown in Fig. 1. All the parameters used in the calculations are detailed in Table 1.

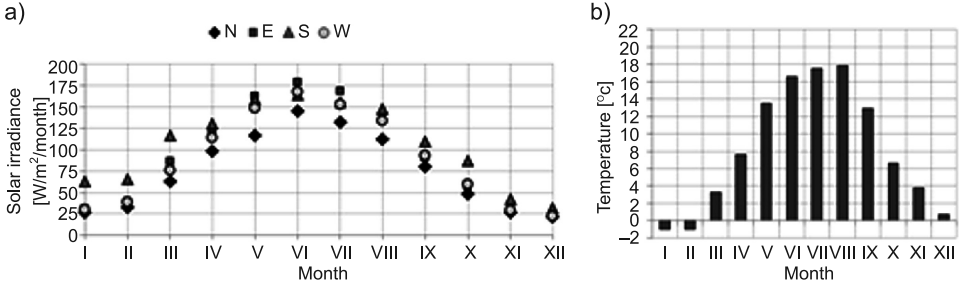


Fig. 1. Climatic data for Lodz: a) solar irradiance, b) outdoor air temperature

4. Results

Analysis showed that the energy balance obtained for a wall insulated with TI is positive for almost an entire year. Heat loss is almost equal to solar heat gain even during the coldest winter months, except for southwards facing orientations.

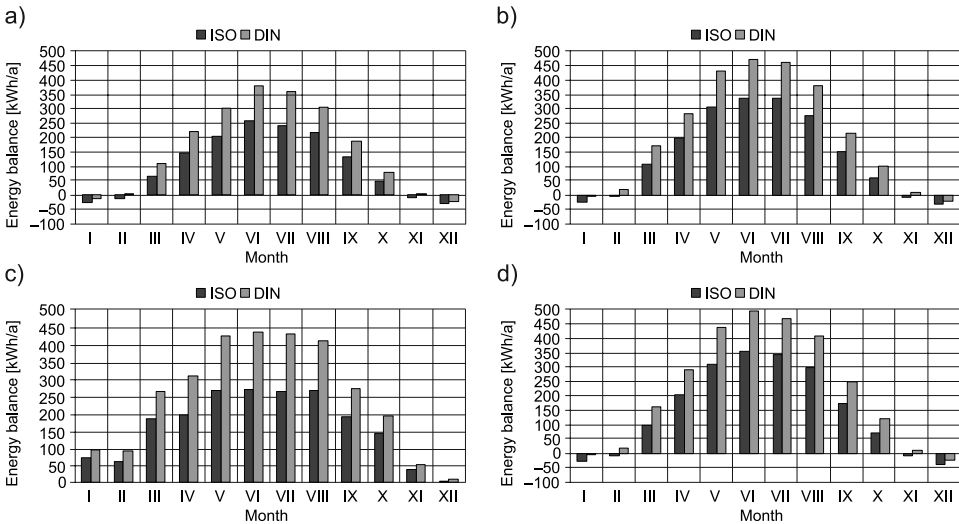


Fig. 2. Monthly energy balances for: a) north, b) east, c) south, d) west orientated insulated walls

Furthermore, it is noted that during these months, values obtained by both calculation methods are similar (Fig. 2). Nevertheless, calculations in accordance with DIN noticeably overestimate heat gain in comparison to values obtained by the ISO calculation method (Fig. 3).

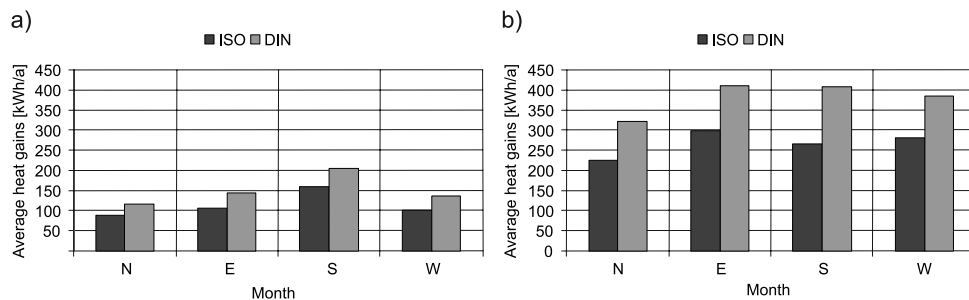


Fig. 3. Average monthly heat gains during: a) heating season, b) cooling seasons

The differences in the results obtained are mainly caused by the values of total solar energy transmittance of TI. The ISO method assumes that these values depend on the orientation and are different for specific months, while a constant value is used in the DIN calculation method (Fig. 4).

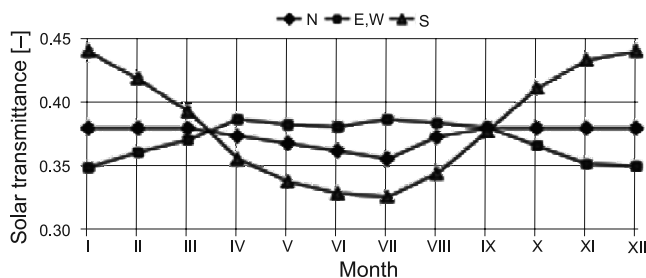


Fig. 4. Values of total solar energy transmittance used in the ISO calculation method

5. Conclusions

The analysis demonstrates that calculations for the energy balance for the partition with the transparent insulation varies depending on the method used. Despite some similarities in heat gain calculations and in the means of determining heat loss in results obtained, differences are apparent and significant. Both methods take into account the thermal resistance of the insulation, shading and frame area coefficients. Nevertheless, the ISO method separately includes diffuse and direct solar energy transmittance and absorption coefficient of the materials. On the other hand, the DIN method includes the heat loss share by thermal radiation (due to the emission) by the introduction of the h_r and $\Delta\theta_{er}$ parameters.

For all the months in question, heat gains recorded using the Polish Standard calculation method are lower than those recorded using the German Standard. Nevertheless, it is noted that heat gains are only desirable at certain times of the year and during the summer months effective insulation should provide protection from overheating. Therefore, it is not possible to make a clear declaration as to which method allows for more precise calculations. Therefore, more complex and dynamic analysis, including experimental tests, should be undertaken [5].

References

- [1] DIN 4108-6:2000-11: Wärmeschutz und Energie-Einsparung in Gebäuden – Teil 6: Berechnung des Jahresheizwärme- und des Jahresheizenergiebedarfs.
- [2] Dudko K., *Izolacje transparentne w systemach pasywnego ogrzewania słonecznego*, Izolacje, 1/2004.
- [3] Kaushika N.D., Sumathy K., *Solar transparent insulation materials: a review*, Renewable&Sustainable Energy Reviews, Vol. 7, 2003, 317-351.
- [4] Kisilewicz T., *Computer Simulation in Solar Architecture Design*, Architectural Engineering and Design Management, Vol. 3/2007.
- [5] Kisilewicz T., *Experimental field testing of transparent insulation*, Archives of Civil Engineering, Vol. 54, 2008, 493-508.
- [6] Lewandowski W.M., Lewandowska-Iwaniak W., *The external walls of a passive building: A classification and description of their thermal and optical properties*, Energy and Buildings, Vol. 69, 2014, 93-102.
- [7] Platzer W.J., *Total heat transport data for plastic honeycomb-type structures*, Solar Energy, Vol. 49, 1992, 351-358.
- [8] PN-EN ISO 13790: Energy performance of buildings – Calculation of energy use for space heating and cooling.
- [9] Polish Ministry of Infrastructure and Development (<http://www.mir.gov.pl>).
- [10] Sick F., Kummer J.P., *Simulation of transparently insulated buildings*, Solar Energy, Vol. 49, 1992, 429-434.
- [11] Strachan P.A., Johnstone C.M., *Solar Residences with transparent insulation: predictions from a calibrated model*, Proc. North Sun '94, Glasgow, 1994, 347-353.
- [12] Suehrcke H., Daldehog D., Harris J.A., Lowe R.W., *Heat transfer across corrugated sheets and honeycomb transparent insulation*, Solar Energy, Vol. 76, 2004, 351-358.
- [13] Verbeeck G., Hens H., *Radiative and Conductive Heat Transfer through Transparent Insulation Material and the Effect on the λ -value*, Building Physics '96 – 4th Nordic Symposium.
- [14] Wallner G.M., Hausner R., Hegedys H., Schobermayr H., Lang R.W., *Application demonstration and performance of a cellulose triacetate polymer film based transparent insulation wall heating system*, Solar Energy, Vol. 80, 2006, 1410-1416.
- [15] Wittchen K.B., *Simulation Solar Walls with tsbi3*, Building Physics '93 – 3th Nordic Symposium.
- [16] Wong I.L., Eames P.C., Perera R.S., *A review of transparent insulation systems and the evaluation of payback period for building applications*, Solar Energy, Vol. 81, 2007, 1058-1071.
- [17] Yang H., Zhu Z., Burnett J., *Simulation of the behaviour of transparent insulation materials in buildings in northern China*, Applied Energy, Vol. 67, 2000, 293-306.
- [18] Zanghirella F., Perino M., Serra V., *A numerical model to evaluate the thermal behaviour of active transparent facades*, Energy and Buildings, Vol. 43, 2011, 1123-1138.

ANTONI MALINOWSKI*, WOŁODYMYR TURKOWSKI*, ANDRIY MUZYCZAK*

THERMAL CONDITIONS OF BUILDINGS: MATHEMATICAL MODELING BY POWER CIRCUIT THEORY

MODELOWANIE MATEMATYCZNE STANU CIEPLNEGO BUDYNKU METODAMI TEORII OBWODÓW ENERGETYCZNYCH

Abstract

The object of this study is to produce a mathematical model for heat conditions in a building, expressed as a complex power circuit. The building is characterized as a power circuit, complete with a detailed description of those components responsible for heat loss, using formal methods to make circuit calculations. Representing a building as a power circuit provides a powerful mathematical modelling tool for assessing heat processes (heat conditions) in separate rooms and in the building in a whole.

Keywords: heat conditions, heat loss, power circuit, flow, effort, mathematical modelling

Streszczenie

W niniejszym artykule przedstawiana jest budowa jako obwód energetyczny ze szczegółowym odtwarzaniem różnych składowych strat cieplnych budynku. Obliczenia takiego obwodu są wykonywane formalizowanymi metodami. Odtwarzanie stanu cieplnego budynku przez obwód energetyczny daje potężny instrument modelowania matematycznego procesów cieplnych (stanu cieplnego) zarówno pomieszczeń pojedynczych, jak i budynku w całości.

Słowa kluczowe: stan cieplny, straty cieplne, obwód energetyczny, strumień, natężenie, modelowanie matematyczne

* Prof. D.Sc. Ph.D. Eng. Anton Malinowski, Assoc. Prof. D.Sc. Eng. Wołodymyr Turkowski, M.Sc. Eng. Andriy Muzyczak, Department of Electrical Supply to Industry, Cities and Agriculture, Lviv Polytechnic National University.

1. Introduction

The modern building has a complex architectural and structural system with various spatial and engineering elements. The traditional method for calculating energy balance is to calculate the thermal conditions of the building [1, 2]. The demand for heating must take account of the heat loss through the enclosure, infiltration of external air or conditions affecting heat loss as well as heat gains from solar energy, human and household activity.

The energy balance approach does not provide a tool for the analysis of complex air conditioning systems, such as heating, cooling and ventilation. To apply a modern approach, it is necessary to apply power circuit theory to our methods.

2. Simulating the thermal conditions of a building using power circuit theory in our methodology

Traditionally, calculating heat loss from a building had to take into account heat transfer through interior heated rooms [1, 2]:

$$P = F \frac{T_{in} - T_{out}}{R_{ht.s}} \quad (1)$$

where:

- F – enclosure area [m^2],
- $R_{ht.s}$ – heat transfer resistance [$m^2 \cdot K/W$],
- T_{out}, T_{in} – interior air and environmental temperatures.

In addition to heat loss caused by heat transfer through the building's interior, heat loss is also caused by infiltration (condition):

$$Q_i = ck_{ch}m(T_{in} - T_{out}) = ck_{ch} \rho V(T_{in} - T_{out}) \quad (2)$$

where:

- c – specific heat capacity of air, $c = 1.005$ kJ/(kg·K),
- k_{ch} – number of air changer per hour, $k_{ch} = 1/h$,
- ρ – air density, $\rho = 1.2255$ kg/ m^3 ,
- V – volume of heated room.

Applying the theory that a building should be represented by a power circuit, passive (resistive) and active components [3] are required. Resistive components reflect heat loss through the enclosed building spaces (their resistances are determined by heat transfer resistance $R_{ht.s}$) and air infiltration or deterioration in the condition of the building.

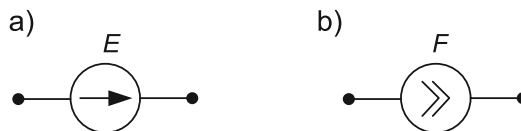


Fig. 1. Sources of heat energy: a) Source of Effort, b) Source of Flow

Sources of heat energy in power circuits are replaced by ‘Source of Effort’ E (Fig. 1a) or ‘Source of Flow’ F (Fig. 1b).

Source of effort can represent a heating system which provides a stable temperature inside the building. Source of flow can represent an appliance which provides a certain amount of heat for a building (e.g. fireplace).

3. Example of comparative calculation of building heat loss

The thermal conditions of a building with two rooms (Fig. 2) can be calculated. In particular, a heated room and an un-heated annex will be compared in terms of their efficiency according to the traditional method and the power circuit method.

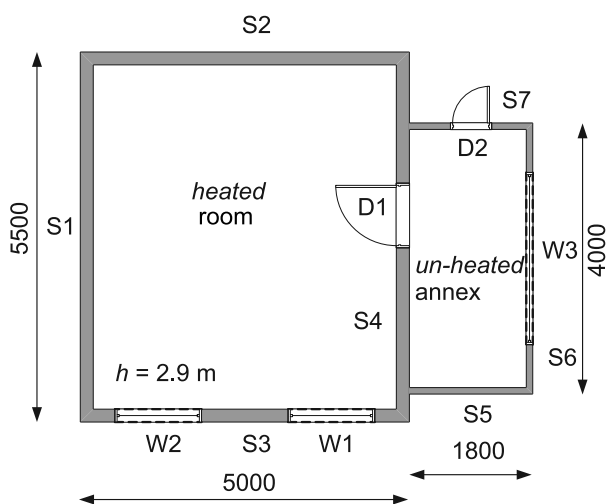


Fig. 2. Plan of building

We will consider heat loss through the following enclosures – walls (S1, S2, ..., S7), windows (W1, W2, W3), doors (D1, D2) and air infiltration losses. The floor and ceiling are not included in this exercise.

3.1. Calculations using the heat balance method

According to [1, 2] heat loss from an enclosed heated room in a building is determined by equation (1).

If the heated room is connected to an un-heated annex, then heat loss, through enclosures separating these rooms are multiplied by an additional empirical factor k [1, 2]. Then, the equation (1) is expressed as:

$$P = F \frac{T_{in} - T_{out}}{R_{ht.s}} k \quad (3)$$

Measurements and calculations for heated rooms of varying dimensions are shown in Table. 1. Here, we see the results of calculations for heat loss through surfaces applying equations(1) and (3). We assume that $T_{out} = -19^{\circ}\text{C}$, $T_{in} = 20^{\circ}\text{C}$.

The next step is to substitute numerical values (volume of a heated room $V = 79.8 \text{ m}^3$):

$$Q_i = 1.005 \cdot 1.2255 \cdot 79.8(20 - (-19)) = 3830.7 \text{ kJh,}$$

this equation corresponds to a power rating of 1064.1 W.

Table 1

Measurements of heated rooms and heat loss calculations

Enclosures	Dimensions		F	$R_{h.l.s}$	k	P
	a [m]	b [m]	[m^2]	[$\text{m}^2 \cdot \text{K}/\text{W}$]		[W]
S1	5.5	2.9	15.95	1.10		565.5
S2	5.0	2.9	14.50	1.10		514.1
S3	5.0	2.9	8.74	1.10		309.9
W1	1.6	1.8	2.88	0.42		267.4
W2	1.6	1.8	2.88	0.42		267.4
S4 (environment)	5.5	2.9	4.35	1.10		154.2
S4 (annex)			11.60	1.10	0.4	164.5
D1	1.4	2.5	3.50	0.64	0.4	85.3
Sum total						2328.3

Thus, the building’s total heat loss expressed in terms of power is 3392.4 W.

3.2. The power circuit calculation method

In the simplest of cases, the circuit that is equivalent to a heated room is shown in Fig. 3. In this basic circuit, each enclosed space/room is represented by its equivalent resistive

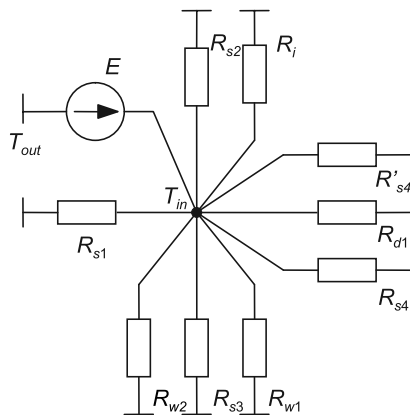


Fig. 3. Circuits representing a heated room

component. The index of the component corresponds to the description of the enclosed space/room. The wall (S4) is represented by two components: R_{s4} – as the part of the wall that is connected to the environment, and R'_{s4} – as the part of the wall that is connected to the un-heated annex. Heat loss through air infiltration is represented by component R_i .

The motive power of the equivalent circuit relates to the temperature difference between the air inside the building T_{in} and the environmental temperature T_{out} :

$$E = T_{in} - T_{out} \quad (4)$$

In theory, any power circuit can be described according to the following sets of equations [3, 4]:

$$\begin{cases} \mathbf{\Pi} \vec{X} = -\vec{F} \\ \mathbf{\Gamma} \vec{Y} = 0 \\ \vec{Y} = \vec{E} - \mathbf{R} \vec{X} \end{cases} \quad (5)$$

where:

- $\mathbf{\Pi}, \mathbf{\Gamma}$ – incidence and circle matrixes,
- \vec{X}, \vec{Y} – column vectors of flows (serial variables) and efforts (parallel variables) of branches,
- \vec{E}, \vec{F} – column vectors of effort and flow sources,
- \mathbf{R} – resistance matrix of the resistive components.

The first equation in the system (the nodal equation) represents the compliance of the flows (serial variables) under Kirchhoff's first law. The second equation in the system (the circle equation) represents the compliance of efforts (the parallel variables) under Kirchhoff's second law. The third equation of the system (pole equation) depicts the connections between the main variables of the power circuit branches.

It is important to determine the actual terms of the main variables – flow X and effort Y . In engineering terms, heat is expressed using the temperature difference ΔT for effort Y , measured in K. Flow X takes heat flow q and is measured by W. Conveniently, this corresponds to the accepted methods for calculating heat loss in buildings [1, 2].

In this case, the measurement of resistance of the resistive components of the equivalent circuit is equal to K/W. The values are determined by the division of heat transfer resistance of the enclosed room by the area $R = R_{ht.s}/F$.

We apply the following equation to determine the resistance of the resistive component, which represents heat loss infiltration:

$$R_i = \frac{3.6}{cmk_{o1}} = \frac{3.6}{c\rho V k_{o1}} \quad (6)$$

Similarly, we can consider the loss caused by air conditioning systems. The parameters of the resistive components of the equivalent circuit (Fig. 3) are shown in Table 2.

The motive effort of the source in compliance with (4) is the same as $E = 20 - (-19) = 39$ K.

The parameters of the power circuit can be determined through direct equation calculations (5). However we can also use more effective methods, for example the nodal

voltage method. This proposed method is analogous to the nodal voltage method used in electrical engineering [5].

The results of calculations of the flows in circuit branches are shown in Table 2.

The total power of heat loss from the heated room is equal to the sum of the flows (serial variables) of all resistive components of the power circuit.

Table 2

Parameters of the components of the equivalent circuit of a heated room and the parameters of the main mode

Resistive component	$R_{ht,s}$	F	k	$R = R_{ht,s}/F$	X
	[m ² ·K/W]	[m ²]		[K/W]	[W]
R_{s1}	1.10	15.95		0.069	565.5
R_{s2}	1.10	14.50		0.076	514.1
R_{s3}	1.10	8.74		0.126	309.9
R_{w1}	0.42	2.88		0.146	267.4
R_{w2}	0.42	2.88		0.146	267.4
R_{s4}	1.10	4.35		0.253	154.2
R'_{s4}	1.10	11.60	0.4	0.237	164.2
R_{d1}	0.64	3.50	0.4	0.457	85.3
R_i	—	—	—	0.037	1064.1
Sum total					3392.4

This example shows that the same results occur when applying both methods to the same elements of the building (see Table 1 and Table 2). However, the advantages of the power circuit theory became apparent after all of the relevant elements of the building were represented in more detail in the equivalent circuit. If all of the enclosed rooms in the building (both heated and unheated rooms) are represented in the equivalent circuit (Fig. 4), it follows that we should not use the empirical factor k (3).

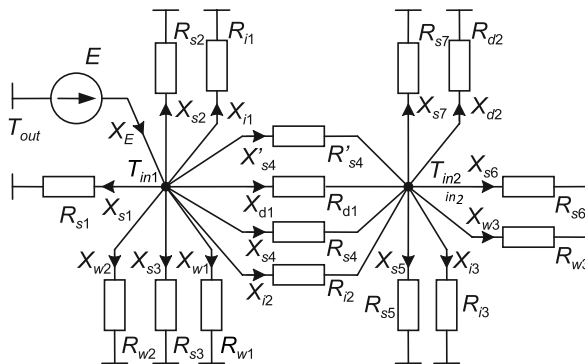


Fig. 4. Equivalent circuit of the building

The parameters of the resistive components of the equivalent circuit (Fig. 4) and the main mode parameters are shown in Table 3.

Table 3

Parameters of the components of the equivalent circuit of the building and the main mode parameters

Resistive component	$R_{ht.s}$	F	$R = R_{ht.s}/F$	X	Y
	[m ² ·K/W]	[m ²]	[K/W]	[W]	[K]
	1.10	15.95	0.0690	134.17	-24.54
R_{s2}	1.10	14.5	0.0759	565.28	-39.00
R_{s3}	1.10	8.74	0.1259	513.83	-39.00
R_{w1}	0.42	2.88	0.1458	309.77	-39.00
R_{w2}	0.42	2.88	0.1458	267.49	-39.00
R_{s4}	1.10	4.35	0.2529	267.49	-39.00
R_{s4}^*	1.10	11.6	0.0948	953.55	-39.00
R_{d1}	0.64	3.5	0.1829	97.03	-24.54
R_{t1}			0.0409	258.86	-24.54
R_{t2}			0.3500	70.11	-24.54
R_{s5}	0.86	5.22	0.1648	87.75	-14.46
R_{s6}	0.86	6.2	0.1387	104.26	-14.46
R_{w3}	0.38	5.4	0.0704	205.41	-14.46
R_{s7}	0.86	2.97	0.2896	49.93	-14.46
R_{d2}	0.64	2.25	0.2844	50.85	-14.46
R_{t3}			0.2333	61.98	-14.46

In addition to calculating the flows and efforts of the circuit branch potentials (i.e. temperatures) all nodes of the power circuit (i.e. the rooms of the building) must be determined:

$$\vec{T} = eT^* + \mathbf{R}_\rho \vec{Y}_\rho \quad (7)$$

where:

- T^* – potential (temperature) of the basic node of power circuit,
- e – unit vector,
- \mathbf{R}_ρ – path matrix,
- \vec{Y}_ρ – column vector of efforts of the linked circuitbranches.

According to (7), the temperature of an un-heated room is equal to -5.5°C . The calculation is not governed by the heat balance method.

It is important to note that, in this example, the total sum of the flow (i.e. serial variables) of all resistive components (7435 W) is greater than the heat flow source (3437.5 W).

On first examination, the balance between the power levels of the source and receiver is not maintained. This is explained due to an inconsistency between Trent’s third condition and the selected measurements for flow [W] and effort [K]. According to [6], the measurement of flow (serial variable) and effort (parallel variable) must be physically compatible, in order to provide power:

$$P = XY \tag{8}$$

This equation corresponds to the Bond Graph theory, the main principle of which is that power between two element combinations of is transferred by the combination of effort (parallel variable) and flow (serial variable) [7].

Therefore, heat loss in separate rooms can be determined as an algebraic sum of the flow of the resistive components which are incidental to the node of the placement in the equivalent circuit:

$$P_{np} = X_{s1} + X_{s2} + X_{s3} + X_{w1} + X_{w2} + X_{s4} + X'_{s4} + X_{d1} + X_{i1} + X_{i2} = 3437.52 \text{ W.}$$

In order to determine the heat loss of the building, it is necessary to add the flow of the resistive components that are incidental to the environmental node (corresponding to the external facade of the building) to the algebraic formula.

4. Heat equivalent circuits of wall enclosure

Heat is transferred through the building’s exterior enclosure by processes such as conduction, convection and radiation. A plan of heat transfer through a one-layered wall of a building [1] is shown in Fig. 5, where the lined dashess how the conditional margins for the air layer near the wall.

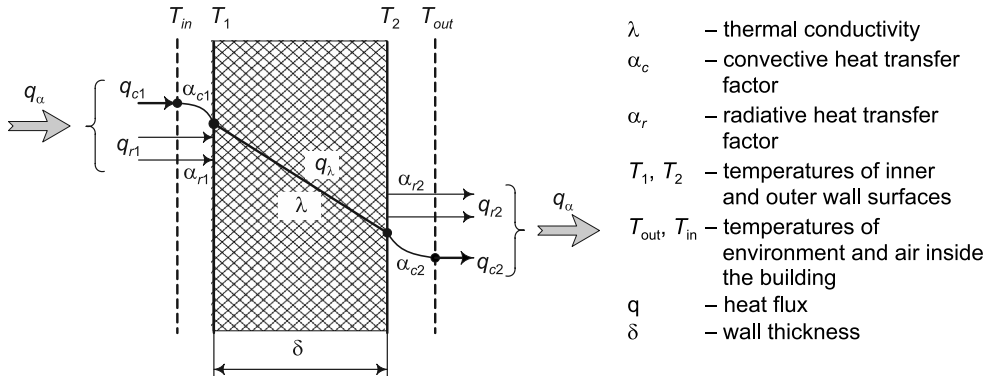


Fig. 5. Scheme of heat transfer through a one-layered wall

The wall enclosure can be represented by heat equivalent circuits, of different specifications (Fig. 6).

Firstly, we must consider the mechanism of heat transfer between the wall enclosure and the air as well as the heat conductivity mechanism.

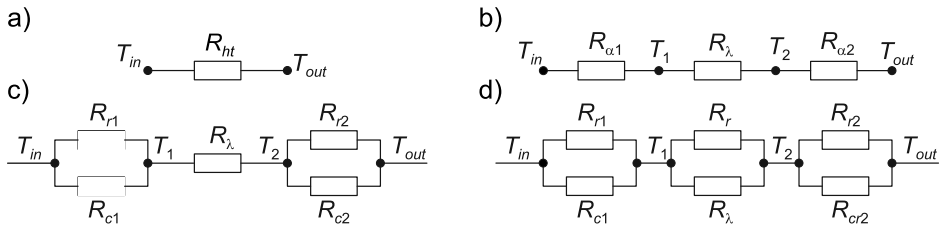


Fig. 6. Heat equivalent circuits of a one-layered wall

Static heat flux through a wall with thickness δ and the temperature difference between its surfaces $T_1 - T_2$ is calculated applying Fourier's equation:

$$q_\lambda = \lambda \frac{T_1 - T_2}{\delta} = \frac{T_1 - T_2}{R_\lambda} \quad (9)$$

where:

- λ – thermal conductivity of the wall material [W/(m·K)],
- δ – wall thickness [m].

Heat flux from the air inside the building to the wall enclosure $q_{\alpha 1}$ and then to the external environment $q_{\alpha 2}$ is equal to:

$$q_{\alpha 1} = \alpha_1(T_{in} - T_1), \quad q_{\alpha 2} = \alpha_2(T_2 - T_{out}) \quad (10)$$

where:

- α_1, α_2 – convective heat transfer factor on the internal air-wall boundary and wall-environment [W/(m²·K)].

The equivalent circuit for the wall enclosure (Fig. 6a) may be transformed as in Fig. 6b. The resistive components regarding the K/W relationship will be equal to:

$$R_{ht} = R_{\alpha 1} + R_\lambda + R_{\alpha 2} = \frac{1}{\alpha_1 F} + \frac{\delta}{\lambda F} + \frac{1}{\alpha_2 F} \quad (11)$$

where:

- R_{ht} – heat transfer resistive component [K/W],
- R_λ – thermal resistive component, $R_\lambda = \delta/(\lambda F)$ [K/W],
- $R_{\alpha 1}, R_{\alpha 2}$ – resistive components of heat transfer between the wall surface and the air inside and outside the building $R_{\alpha 1} = 1/(\alpha_1 F)$, $R_{\alpha 2} = 1/(\alpha_2 F)$ [K/W].

Heat transfer factors α on the margin between the wall and the air are divided into two components – convective α_c and radiative α_r :

$$\alpha_1 = \alpha_{r1} + \alpha_{c1}, \quad \alpha_2 = \alpha_{r2} + \alpha_{c2} \quad (12)$$

The equivalent heat transfer resistance circuit is shown in Fig. 2a, taking all components into account. The resistive components (radiative and convective) are defined as:

$$R_{r1} = \frac{1}{\alpha_{r1} F}, \quad R_{c1} = \frac{1}{\alpha_{c1} F}, \quad R_{r2} = \frac{1}{\alpha_{r2} F}, \quad R_{c2} = \frac{1}{\alpha_{c2} F} \quad (13)$$

The equivalent circuit (Fig. 6d) applies to transparent wall enclosures. Here, heat conduction takes place through radiation as well as by thermal conduction [1]. The corresponding resistive component R_r regarding the K/W relationship is equal to:

$$R_r = \frac{mk\delta}{16\sigma_0 n^2 \left(\frac{T_1 + T_2}{2}\right)^3} \frac{1}{F} \quad (14)$$

where:

- m – opto-geometrical parameter,
- k – attenuation coefficient [m^{-1}],
- σ_0 – Stefan–Boltzmann constant,
- n – refractive index.

The thermal conditions of buildings, constructed of modern materials, can be analysed by the proposed, detailed equivalent circuit enclosure method.

5. The problem of measuring variables

In order to apply the general rule of power balance for the heat circuit, we must use another system of main variables. Accordingly [6] selecting main variables [4, 7] is recommended:

- serial variable (flow) – flow of entropy S [W/K],
- parallel variable (effort) – temperature differences ΔT [K].

In this case, the measurement of the resistance of the resistive component of the equivalent circuit is equal to K^2/W . However, the question of how to determine the resistance of the resistive component, using such a measurement, remains unsolved.

6. Conclusions

The application of power circuit theory methods for calculating the thermal conditions of a building provides a powerful tool for mathematical modeling of thermal processes (i.e. thermal conditions) both for separate rooms as for the building as a whole. A detailed representation of the building's wall enclosures and its heating sources allows for empirical factors to be discounted and for the closest possible approximations to be obtained in terms of the parameters of the building's actual and required thermal conditions.

References

- [1] Блази В., *Справочник проектировщика. Строительная физика*, М.: Техносфера, 2004, 480 с.
- [2] *ДБН В.2.6-31:2006 Теплова ізоляція будівель*, Київ: Міністерство будівництва, архітектури та житлово-комунального господарства України, 2006, 70 с.
- [3] Бердников В.В., *Прикладная теория гидравлических цепей*, М.: Машиностроение, 1977, 192 с.: ил.

- [4] Саух С.Е. *Математическое моделирование энергетических цепей*, Электронное моделирование, 2011, Т33, №3 С.3-12.
- [5] Перхач В.С., *Математичні задачі електроенергетики*, Вид. 3-є, перероб. і доп. – Львів: Вища школа. Вид-во при Львівському університеті, 1989, 464 с.
- [6] Trent H.M., *Isomorphisms between oriented linear graphs and lumped physical system*, J. Acoustic America, vol. 27, May 1955, 500-527.
- [7] Borutzky W., *Bond Graph Methodology – Development and Analysis of Multidisciplinary Dynamic System Models*, Springer–Verlag, UK, London 2010.

GABRIEL MARKOVIČ*, MOHAMED AHMIDAT*

PARAMETERS OF RAINWATER COLLECTION AND STORAGE – MEASUREMENT AND EVALUATION

PARAMETRY ZWIĄZANE Z GROMADZENIEM I PRZECHOWYWANIEM WODY OPADOWEJ – POMIARY I OCENA

Abstract

This paper describes the experimental evaluation of the effect of using different roofing materials affecting the quality and quantity of the amount of rainwater collected and stored in the Kosice city area. The two sites that were tested were located at the TUKE (Technical University of Kosice) campus site. Two models serving as data sources were located on the roof of the University library and a third source of data was an actual school building (PK6). The results obtained were then inputted to create a simulation. This article provides a detailed analysis of the factors at play in relation to the quality of rainwater collected and drained off from the PK6 building roof, and also an evaluation of an experimental model relating to a ceramic tiled roof. The results show that both roofing materials tested are suitable for systems collecting and storing rainwater. Ceramic tiles are suitable for the purpose without any complications concerning further treatment; Ceberit needs additional treatment and disinfection. The findings shall be used to inform the next step – modelling data.

Keywords: rainwater, quality, quantity

Streszczenie

Artykuł opisuje ocenę eksperymentalną efektu użyciu różnych materiałów dachowych wpływających na jakość i ilość ilości wody deszczowej gromadzonej i przechowywanej na terenie miasta Koszyce. Dwa testowane obiekty znajdowały się na terenie kampusu TUKE (Uniwersytet Techniczny w Koszycach). Dwa źródła danych znajdowały się na dachu Biblioteki Uniwersyteckiej, natomiast trzecim źródłem danych był rzeczywisty budynek szkoły (PK6). Otrzymane wyniki zostały następnie użyte do symulacji. Artykuł zawiera szczegółową analizę jakości wody deszczowej zebranej i odprowadzanej z dachu budynku PK6, a także ocenę modelu doświadczalnego opisującego dach pokryty dachówką ceramiczną. Wyniki pokazują, że oba badane materiały dachowe są odpowiednie dla systemów zbierania i przechowywania wody deszczowej. Płytki ceramiczne są odpowiednie do tego celu, bez żadnych dalszych działań; Ceberit wymaga dodatkowych zabiegów oraz odkażenia. Wyniki powinny zostać wykorzystane w kolejnym etapie – modelowaniu.

Słowa kluczowe: woda deszczowa, jakość, ilość

* Ph.D. Eng. Gabriel Markovič, Eng. Mohamed Ahmidat, Faculty of Civil Engineering, Institute of Architectural Engineering, Technical University of Košice.

1. Introduction

Stormwater management is a relatively new issue in Slovakia. There is no legal framework giving standards or guidelines as to how to apply sustainable stormwater management techniques. As a result of repeated flooding incidents, we are mindful of the need to adopt more effective stormwater handling procedures. There are numerous techniques and approaches applied worldwide to support sustainable stormwater management, especially in urban areas where stormwater can cause significant damage. Nowadays we are more open to these new approaches especially in cases where the issue concerns sustainability in stormwater management such as flood prevention / protection and pollution reduction measures. The aim is to manage stormwater as close to the source as possible (termed as source control) which encompasses a number of measures. The ‘harvesting’ (collection and storage) of rainwater within these source control measures may also contribute to stormwater management sustainability, by promoting portable water conservation measures and water management sustainability in general [1].

2. Measurements of the quality of rainwater run-off

This article describes the experimental evaluation of the effect of using different roofing materials affecting the amount of rainwater in the Kosice city area. The two sites that were tested were located on the TUKE (Technical University of Kosice) campus site. Two models serving as data sources were located on the roof of the University library and a third source of data was an actual school building PK6 (Fig.1). This article provides a detailed analysis of the factors in play in relation to the quality of rainwater draining off the PK6 building roof and also an evaluation of an experimental model with a ceramic tiled roof [2].

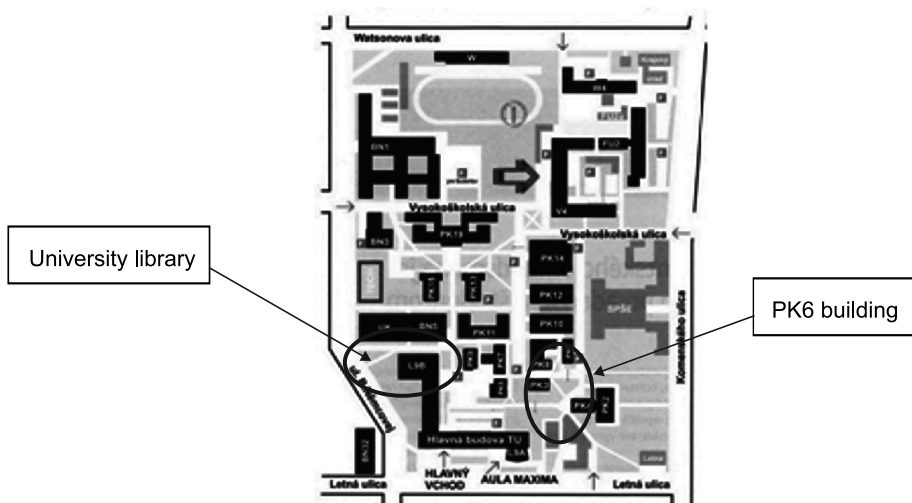


Fig. 1. Location of the research points at the TUKE campus site

2.1. Models located on the library roof

Two identical roofing models were placed on the University library rooftop (Fig. 2). The design allows for the pitch angle to be adjusted and also for the model roofing material to be exchanged for other materials. All components required to collect RHSR data may be fastened to the models (Figs. 3, 4). Ceramic tiles, lakoplastic, and concrete roof tiles have been used. X marks the angle of slope at which readings are first taken. The objective



Fig. 2. Models located on the roof of the University library

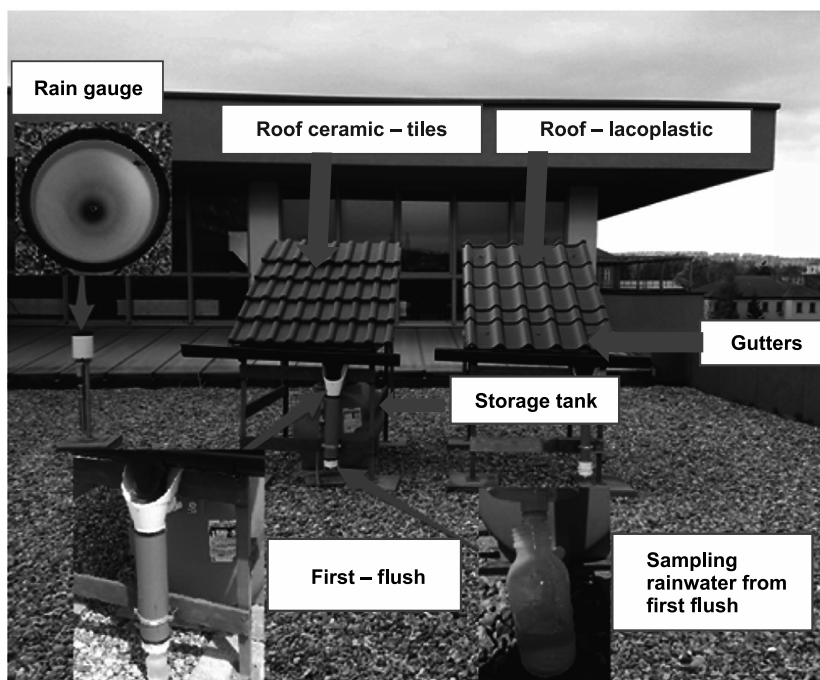


Fig. 3. The model's components

of the exercise is to identify the material best suited for the collection of RHSR in the Kosice city area. This is done by using a simple flow meter, a precipitation measuring station, and by conducting rain water quality analysis. Models are still being constructed. At present, one model with a ceramic tiled surface continues in operation.



Fig. 4. The model's components

Roofing materials are chosen according to the most commonly used roofing materials in Slovakia, but the choice also depends on suitability of use for of the collection and storage of RHSR.

The qualitative indicator results for RHSR collected from a model fitted with ceramic tiling are presented in Figs. 5, 6. The RHSR quality was monitored between June and December in 2012. Water samples were taken regularly on the 3rd, 15th and 30th days of the month from a 100 litre tank. Two parameters were examined: pH and conductivity.

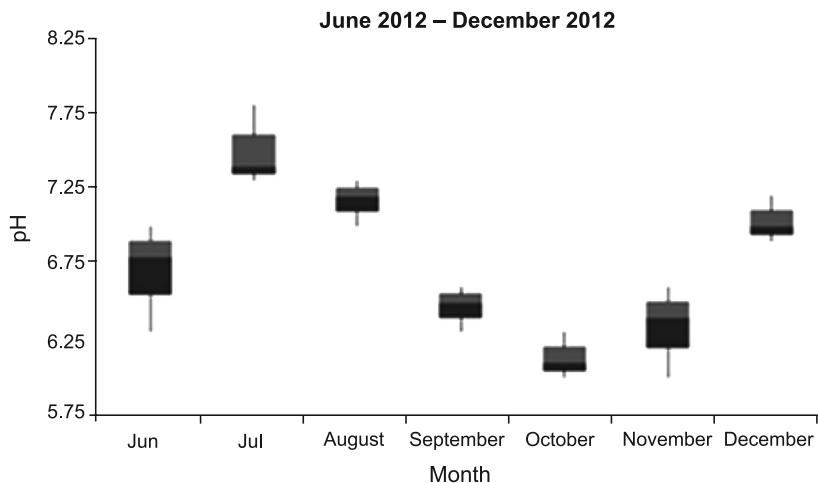


Fig. 5. pH values of the model with ceramic roof tiling

These values were obtained through the collection and subsequent chemical analysis of rainwater samples. The pH values of the water during the 2012 sample period are shown in Fig. 5. The mean pH value, at 25°C, was 6.7, the maximum pH was 7.8 and the minimum was 6.1. According to the NV SR regulation (number 269/2010 Z.z.), the pH value should be in the range of 6 to 8.5. In fact, the pH values obtained during the June to December observation period were at a standard level.

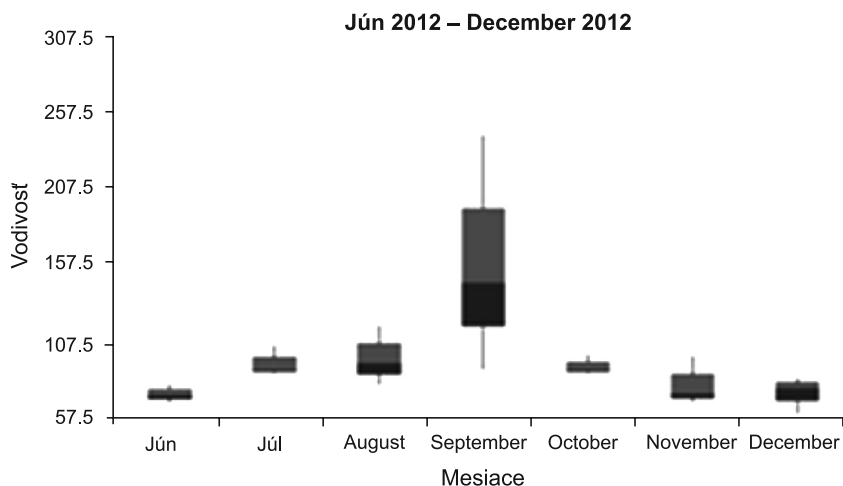


Fig. 6. Conductivity values of the model fitted with ceramic roof tiling

The water conductivity values during the 2012 survey period are shown in Fig. 6. According to the NV SR regulation (number 269/2010 Z. Z), the conductivity limit for water in portable storage represents 100 mS/m which is equal to 1000 mg/l. In optimum conditions, portable water supplies should be less soluble in substance, i.e. 200–400 mg/l (about 25–50 mS/m). In most cases, the conductivity values did not exceed the standard value of 100 mS/m [14]. September was an exception with higher conductivity values recorded. The average conductivity value of is 96 mS/m.

2.2. Building PK6

The PK6 building at the Technical University of Kosice campus was selected for research into the quality and volume of rainwater draining into existing underground drainage shafts. Two vertical shafts are located next to the PK6 building. All of the run-off rainwater falling onto the roof flows into these underground pipes (Fig. 7).

A multiparameter water sensor took qualitative measurements of pH and conductivity readings from late 2011 onwards. The sensor was installed in a measurement flume inserted in one of the drainage shafts (Fig. 8). Values for pH and conductivity were recorded on a continuous basis.

The Box-Plot graph shown in Fig. 9 depicts the pH values of the rainwater from the PK6 building throughout 2012. Figure 9 shows that the average pH value varied each month. The pH values in June and October indicated RHSR levels of acidity.

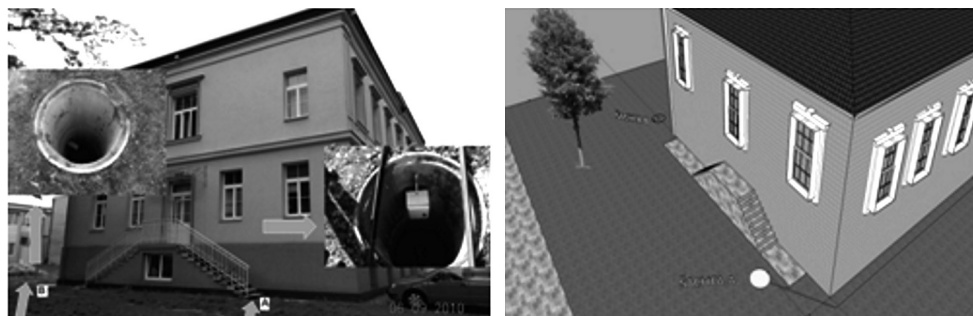


Fig. 7. Location of drainage shafts near the PK6 building [3]

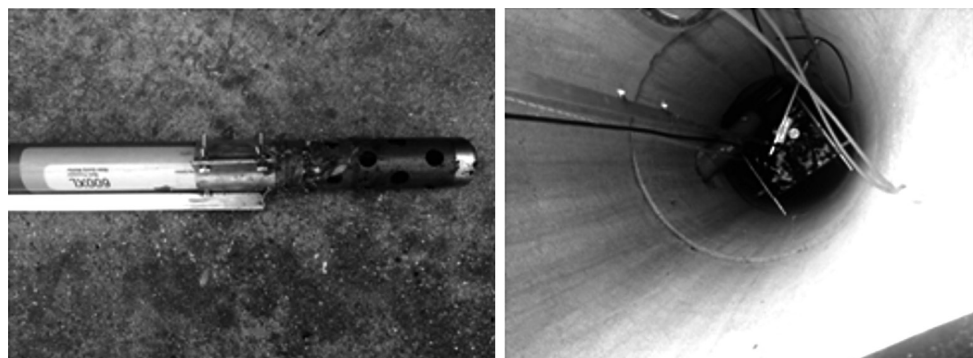


Fig. 8. The multi-parameter water sensor in the drainage shaft near the PK6 building

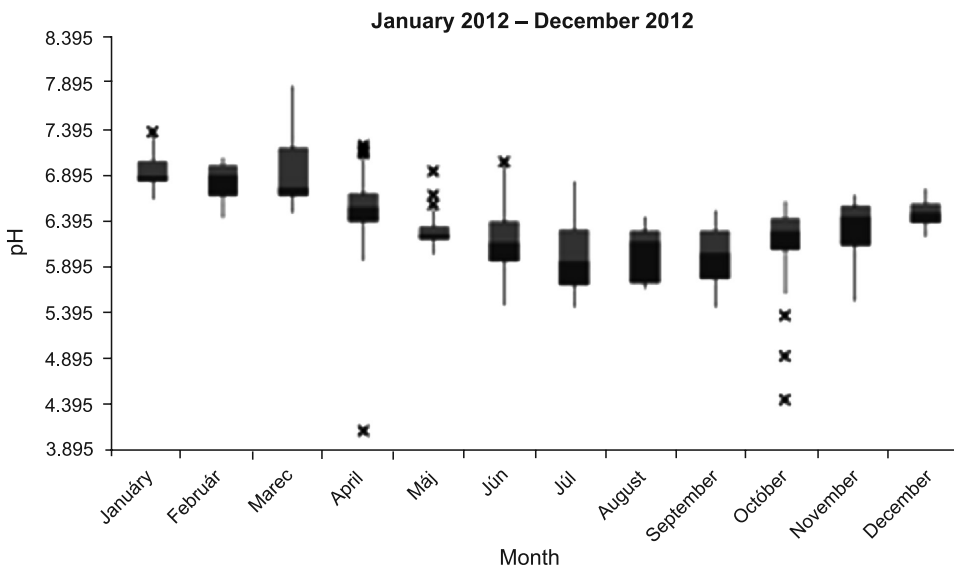


Fig. 9. pH values of rainwater collected from the PK6 building during 2012

Another water quality indicator is the conductivity of the water collected from the PK6 building. As with the pH values, the conductivity levels were also measured on a continuous basis using the same multi-parameter sensor (Fig. 8).

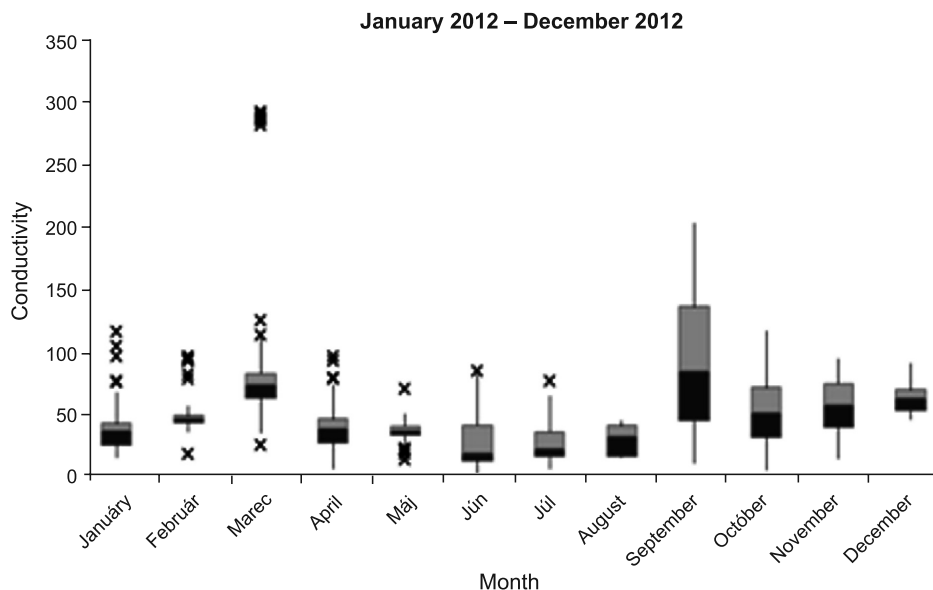


Fig. 10. Conductivity values of the rainwater from the PK6 building during 2012

Conductivity refers to the approximate rate of the concentration of electrolytes in water. Conductivity values of rainwater during the 2012 period are shown in the Box-Plot graph in Fig. 10. From this graph, we can see that the average value for each month varied, but in most months the values were satisfactory. Limits were exceeded during periods of rainfall, however on most occasions the conductivity levels were within acceptable standards and were occasionally satisfactory. September was an exception, when the limit was exceeded [2].

3. Conclusions

The storage and re-use of rainwater collected from rooftops of buildings in the Slovak Republic is not so commonplace as it is in the USA, Western Europe, Australia etc. The limiting factors are lower prices of drinking water and high initial investment costs of technological equipment required to turn rainwater into a re-usable resource.

The rainwater quality measurements taken from the PK6 building roof, and from the roofing models sited on top of the university library, demonstrate that the rainwater meets quality standards for the purposes of collection, storage and re-use, as well as for the purposes of rainwater infiltration.

Clearly, it is necessary to take each project on a case-by-case basis, because rainwater collection and storage systems are sensitive to, and dependant on, local site and building design conditions [6].

This work was supported by the Slovak Research and Development Agency under contract (No. SUSPP-0007-09). "Increasing rainwater management efficiency for the purpose of minimizing energy demand".

VEGA 1/0450/12

Rainwater management and energy balance research in the cities of the future.

References

- [1] Karellová Z., *Stormwater Management in Compliance With Sustainable Design of Buildings and Environmental Conception*, Doctoral thesis – theory, Technical University, Košice 2010.
- [2] Ahmidat M., Vranayová Z., Kaposztasova D., *The Impact of Roof Materials on the Quality and Quantity of Harvested Rainwater in Experimental Conditions*, [In:] CIBW062 Symposium 2013.
- [3] Markovič G., Vranayová Z., *Infiltration as a means of surface water drainage*, TU, Košice 2013, 137 s.
- [4] Vranayová Z., *Posúdenie trvalej udržateľnosti systémov využitia vôd z povrchového odtoku*, Habilitačná práca, Košice 2003.
- [5] Slys D., *Potential of rainwater utilization in residential housing in Poland*, Water and Environment Journal, Vol. 23, Issue 4, DEC 2009, 318-325.
- [6] Vrana J., Oslejskova M., *Rainwater conservation in the Czech Republic*, Environmental Engineering, Vol. 1-3, 2011, 709-712.
- [7] Zeleňáková M., Purcz P., Gargar I.A.K., Helena H., *Comparison of precipitation trends in Libya and Slovakia*, [In:] *River Basin Management 7*, Southampton: WIT Press, 2013, 365-374.
- [8] Gaňová L., Zeleňáková M., Purcz P., Kuzevičová Ž., Hlavatá H., *A rainfall distribution and their influence on flood generation in the eastern Slovakia*, [In:] *Acta Universitatis Agriculturae et Silviculturae Mendelianae Brunensis*, Vol. 61, No. 6, 2013, 1645-1652.
- [9] Zeleňáková M., Purcz P., Gargar I., Hlavatá H., *Research of Monthly Precipitation Trends in Libya and Slovakia*, Proceedings of the 2014 International Conference on Environmental Science and Geoscience (ESG'14), Venice, Italy, 15–17 March 2014, 46.
- [10] Markovič G., Zeleňáková M., *Measurements of quality and quantity of rainwater runoff from roofs in experimental conditions – 2014*, [in:] ICITSEM 2014: International conference on innovative trends in science, engineering and management 2014: 12th and 13th February 2014, Dubaj, UAE [Bangalore]: Mudranik Technologies, 2014, 145-151.
- [11] Fuller C.O., Martin T.J., Walters R.P., *Quality aspects of water stored in domestic rainwater tanks*, Engineering and Water Supply Department, South Australia 1981.
- [12] Heaber R.H., Waller D.H., *Water duality of rainwater collection système in the Eastern Caribbean*, Third International Rainwater Catchment System Conference Proceedings, 1987.
- [13] Yaziz M.I., Gunting H., Sapari N., Ghazali A.W., *Variations in rainwater quality from roof catchments*, Water Research, Vol. 23, 1989, 761-65.
- [14] The government regulation of Slovak Republic (NV SR), no. 269/2010 Z. z. from May 25th 2010 which sets the requirements for optimal state of water, Surface water drainage.

HENRYK NOWAK*, ŁUKASZ NOWAK*

THE USE OF ACTIVE THERMOGRAPHY TO DETECT MATERIAL INCLUSIONS IN THE WALLS

ZASTOSOWANIE TERMOGRAFII AKTYWNEJ DO DETEKCJI WTRĄCEŃ MATERIAŁOWYCH W ŚCIANACH

Abstract

One of the non-destructive testing methods of building envelope of unknown structure is active thermography in reflective mode. This method was used to test a model of the concrete wall with the material inclusions with significantly different thermal properties. The study performed in climatic chambers consisted of heating the model wall with a 7.2 kW heat pulse, and then recording the thermograms during wall cooling, at regular intervals, using a thermal imaging camera. Based on the recorded temperature distribution on the thermograms the thermal properties and location of subsurface defects were concluded.

Keywords: external wall, material inclusions, thermography survey, active thermography in reflective mode

Streszczenie

Jedną z nieniszczących metod badania przegród budowlanych o nieznannej strukturze jest termografia aktywna w trybie odbiciowym. Metodę tę zastosowano do badania modelu ściany betonowej z wtrąceniami materiałowymi o znacznie różniących się właściwościach cieplnych. Badanie w komorach klimatycznych polegało na nagrzewaniu modelu ściany impulsem ciepła o mocy 7,2 kW, a następnie rejestrowaniu termogramów podczas stygnięcia ściany w stałych odstępach czasu za pomocą kamery termowizyjnej. Na podstawie zarejestrowanego na termogramach rozkładu temperatury wnioskowano o właściwościach cieplnych i położeniu defektów podpowierzchniowych.

Słowa kluczowe: ściana zewnętrzna, wtrącenia materiałowe, badania termowizyjne, termografia aktywna w trybie odbiciowym

* Prof. Henryk Nowak, Ph.D. Łukasz Nowak, Institute of Building Engineering, Faculty of Civil Engineering, Wrocław University of Technology.

1. Introduction

Traditional infrared surveys of buildings and other building structures consists of the identification of the temperature distribution on the boundary surfaces, i.e. on the exterior and interior surfaces, without the externally controlled interference and the thermal stimulation into their thermodynamic state [2]. There can be places with discontinuity or lack of thermal insulation in the building envelope, around the heated (or cooled) volume of the building. In these places, there are varied temperature fields on the boundary surfaces, which can be used for the identification of material inclusions. In addition, one thing should be noted, not every difference seen in the temperature field of the wall surfaces is because of its thermal insulation defects [6]. Based on the surface temperature distribution (thermograms) of an analyzed wall we can draw conclusions about its thermal insulation properties (as a qualitative assessment). In practice, this means that the building thermal envelope is tested “in a state as it is”, without any controlled thermal force. Of course, research should be done in accordance with the IR camera measurement rules in the buildings. In this case, the detection of internal material inclusions in the building envelope with the thermographic method is based on the relationship between the external temperature field of the wall with its thermal conductivity and temperature difference on both sides of the wall. This type of the thermographic survey is typical and has been widely used from many years. In practice, it is rarely called “passive thermography” and is usually referred as “infrared thermography” or simply “thermvision survey” (or “thermographic investigation”).

The active thermography is used to detect material defects or inclusions in the superficial layer of the tested material (building component) and for determining the unknown thermal characteristics of the tested element materials. The active method of infrared thermography is based on two things:

- controlled external thermal forcing of tested wall by a high-power (several kW) heat source to create thermal contrast between areas containing defects (inclusions) and the area of homogeneous material,
- periodically recorded thermal images of the element during its cooling, after turning off the heat stimulation sources [1, 3, 4].

The essence of active thermography is a time function analysis of the wall’s (material’s) thermal response to controlled heat pulse stimulation. Material inclusions in the construction are shown as different temperature areas, where the surface temperature differs from the temperature of the remaining part of the tested wall, due to their different properties of the heat conduction. The tested wall response, during its cooling, is periodically recorded using a thermal imaging camera. Thermograms of a cooling surface, in other words the time sequence of the temperature distribution on the test surface, contain information about the subsurface defect location and enable the depth and size identification of these defects (material inclusions) and material discontinuities. Temperature distribution measurements on the surfaces of the tested wall can be carried out on the heat pulse stimulated side (so-called reflective mode) as well as on the other side (so-called transmission mode) [5, 7].

The active thermography in transmission mode is applied for detecting material inclusions (defects) located deeper, i.e. located closer to the other “colder” side of the tested wall. In contrast, reflective mode is used to detect defects (material inclusions) located

near the heated surface. Thermograms of wall surface cooling are carried out at regular intervals, which allows to for the observation of the dynamics of surface temperature changes in the homogeneous material and in the heterogeneous parts. With proper processing and interpretation of the wall surface cooling thermal images it is possible to obtain information about the areas where there is discontinuity of the material and to identify these places.

The article presents the exemplary results of the first stage of research for wall made of concrete blocks with the inclusion of different materials using the method of active thermography in reflective mode. The material inclusions had significantly different thermal conductivity coefficients and were placed at different depths in the wall. The aim of the study was to evaluate the effectiveness of this method for identifying the size and depth of the material defects in the wall. The next stage of research will be to solve the inverse heat conduction problems for the tested wall.

2. Description and test results

The study was performed in climatic chambers in the laboratory of the Institute of Civil Engineering at Wroclaw University of Technology. A wall made of concrete blocks (with dimensions of $120 \times 250 \times 380$ mm) with material inclusions ($100 \times 200 \times 20$ mm) was placed in the connecting sleeve between the 'warm' and 'cold' chamber (air temperatures respectively $+20^\circ\text{C}$ and -10°C) (Fig. 1).

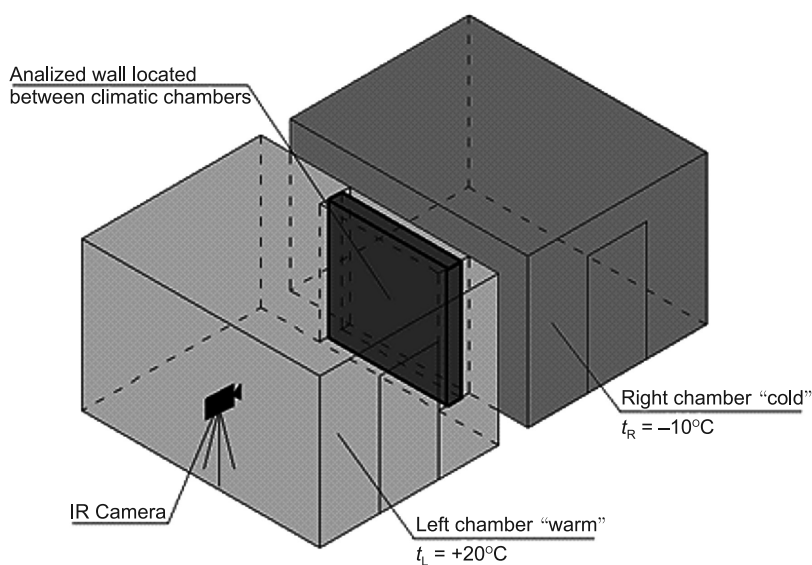


Fig. 1. Wall testing scheme in climatic chambers

Material inclusions in the wall were made by placing materials with significantly different thermal conductivity coefficient λ . Materials used:

- extruded polystyrene (XPS foam) , $\lambda = 0.033$ [W/(m K)],
- granite, $\lambda = 3.500$ [W/(m K)],
- steel, $\lambda = 50.000$ [W/(m K)].

These were placed at two different depths in the concrete block wall. Inclusions were located, at two depths, 6 cm – in the existing wall layer, 4 cm – in the glued after thinner plate layer of the same material. Schematic layouts of material inclusions are shown on Fig. 2 and 3. During the measurements, the following were recorded:

- air temperature, relative humidity and air velocity in the chambers by:
 - NiCrNi thermocouples,
 - FVA935 – TH4K2 and FVA605 – TA50 anemometers,
 - FHA646 – E1 and FHA646 – E1C temperature and humidity sensors connected to the Ahlborn ALMEMO datalogger types 2690-8, 2890-9 and 5690-2M09,
- wall surface temperature on the warm and cold sides by NiCrNi thermocouples,
- temperature inside the wall between the existing wall and concrete plates by means of NiCrNi thermocouple and RTD Pt100 sensor,
- thermograms using the thermal imaging camera FLIR P65 and FLIR B360.

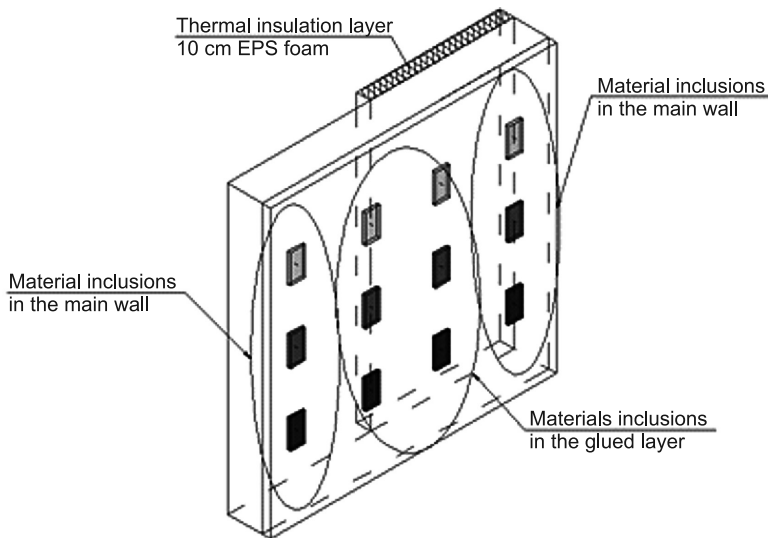


Fig. 2. Analyzed wall with material inclusions scheme

The research of the wall with inclusions started with heating their surface from the inclusions side (warm side) with infrared radiators with the summary power of 7.2 kW, shown on Fig. 4. The time of wall heating was 40 min and the uniformity of the heating surface of the wall of 2.0×2.0 m was carried out by placing an arm stand with infrared radiators in three positions in 5 min cycles.

After wall heating, the next step was to start the surface temperature recording with the thermal imaging camera while the wall started to cool down. In order to accelerate the process of wall cooling and to direct the heat flow the right ('cold') climate chamber was

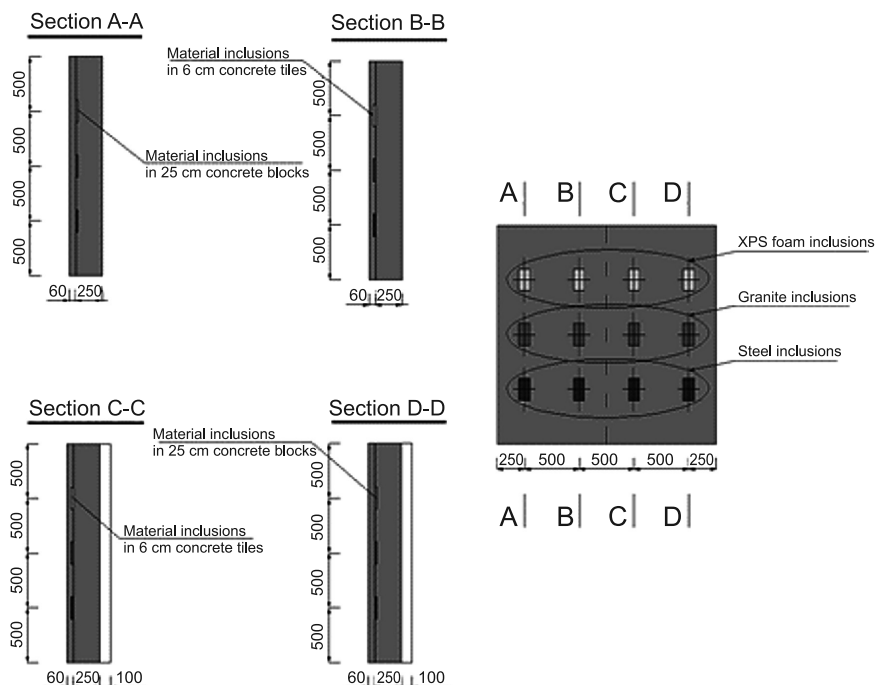


Fig. 3. Placement of XPS foam, granite and steel inclusions in wall made of concrete blocks



Fig. 4. Heating surface of the test wall by infrared radiators with power 7,2 kW

set in the cooling mode to the air temperature $t_e = -10^\circ\text{C}$. The thermograms were recorded with 15 min intervals (with FLIR P65 and FLIR B360 cameras).

Exemplary results of the study performed in climate chambers the concrete blocks wall with material inclusions are shown in Figs. 5 and 6, in which are thermograms of the wall after the infrared radiators were turned off ($t = 0$ min) and during the cooling of the wall after 60, 120 and 250 minutes. Additionally, under the thermograms are shown surface temperatures of the wall along the horizontal lines at the level of material inclusions.

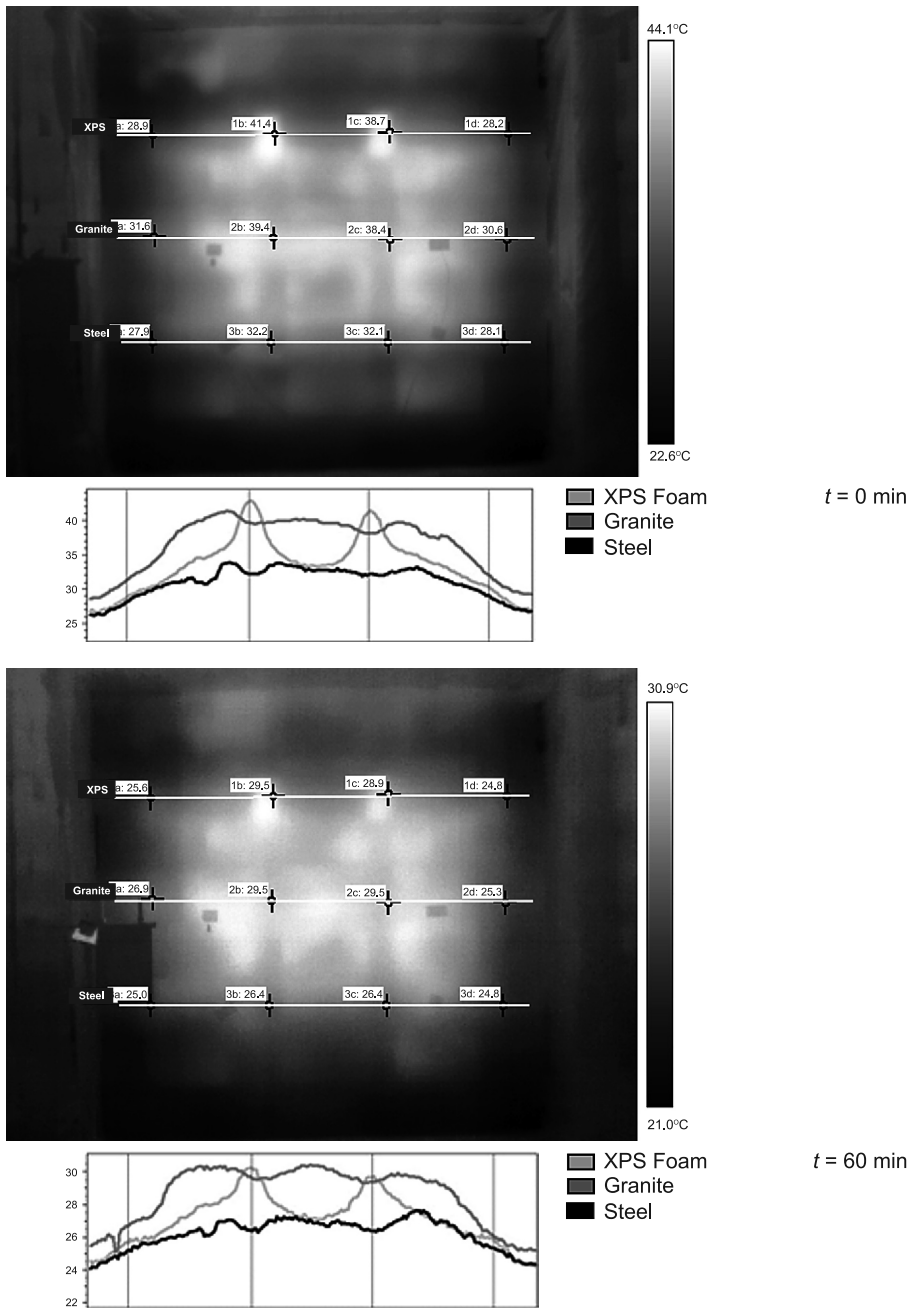


Fig. 5. Thermograms of analyzed wall with surface temperatures in place of material inclusions and temperature distribution along inclusion lines in time of wall cooling ($t = 0$ and $t = 60$ min)

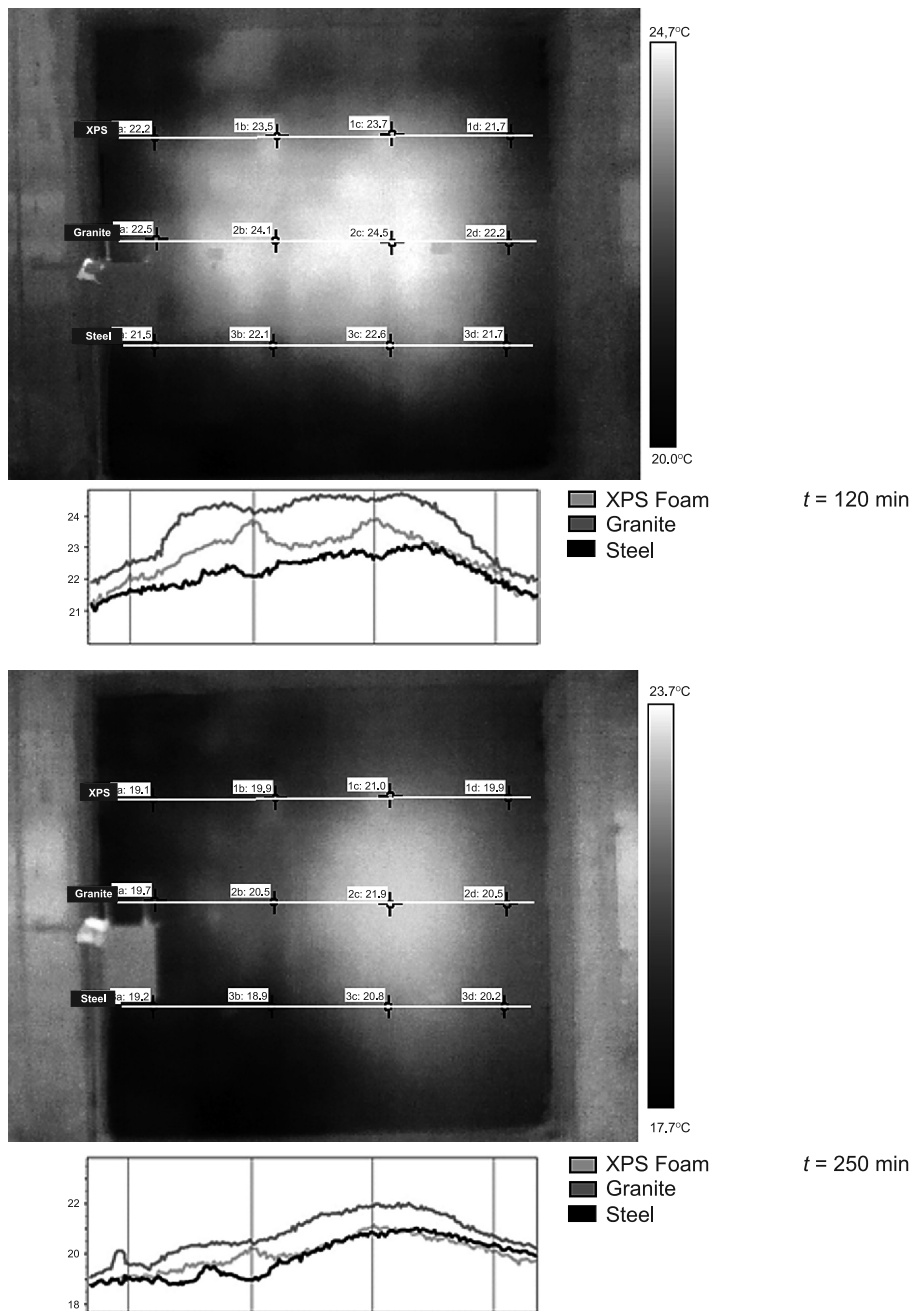


Fig. 6. Thermograms of analyzed wall with surface temperatures in place of material inclusions and temperature distribution along inclusion lines in time of wall cooling ($t = 120$ and $t = 250$ min)

The results analysis leads to the conclusions that:

- The surface temperature of the wall, at the place of inclusions, is depending on the type of material inclusion. For the inclusion material with better thermal properties than wall (e.g. extruded polystyrene) the surface temperature is always between the temperature lines for the inclusions with worse thermal properties than wall (e.g. granite, steel). It is seen in all graphs in the lower part drawings.
- The surface temperature of the wall, at the place of inclusions, for inclusions having worse thermal properties (e.g. granite, steel) is lower than the surface temperature of the remaining wall ('temperature peaks turned down' in the lower graphs on Fig. 5, 6).
- The surface temperature of the wall, at the place of inclusions, for inclusions having better thermal properties (e.g. extruded polystyrene) is higher than the surface temperature of the remaining wall ('temperature peaks turned up' in the lower graphs on Fig. 5, 6).
- The above mentioned temperature trend lasted up to 2 hours after the wall started cooling. From the 3rd hour of cooling, till the end of measurements, the surface temperatures of the wall, in the part of wall with thermal insulation, where inclusions were placed were higher than on in the uninsulated part
- The first clear signs of the material inclusions' impact on the wall surface temperature distribution could be seen at the time the heating was turned off and the wall started to cool down.
- The effect of the material inclusions in the form of different surface temperatures of the concrete wall was still visible in the 3rd hour of measurements. Wherein, the steel and granite inclusions in the wall without thermal insulation can be identified even in the 7th hour of wall cooling.
- This gives the practical conclusion that in the case of walls made of concrete or concrete blocks, to be successful, searches for material inclusions should be done within 3 hours of heating the wall for 40 minutes with infrared radiators (with a capacity of about 7.0 kW). It is also possible to identify these inclusions even after a long time, up to 7 hours, but careful interpretation of the obtained test results is necessary.

These conclusions and observations are formulated for walls with concrete blocks. Probably some other proposals will be for walls with different thermal parameters, such as brick walls or aerated concrete blocks, especially when it comes to seeing temperature differences above materials inclusions.

3. Conclusions

Infrared thermography is a very powerful and effective tool for locating hidden material defects in the building envelope by searching for surface temperature anomaly distribution on boundary surfaces of walls. In every case, the heat flow through the individual parts of the walls with material inclusions causes differences in the surface temperatures of building partitions, which is correlated with different thermal conductivity, specific heat capacity of materials and their geometries.

Each anomaly in the temperature distribution of the wall surface, identified by infrared camera, should be thoroughly analyzed in conjunction with the design and structure

of partitions, the materials used, the conditions of the temperature coercion and the performed examination conditions.

This research, which was carried out for concrete blocks wall with various material inclusions (steel, granite and extruded polystyrene differs in thermal conductivity rate) in climate chambers with use of active thermography in reflective mode allows to get conclusions for practical use:

Principles of applying the method of active thermography in reflective mode to locations of material inclusions being built in masonry or cast concrete walls are as follows:

- the method is effective in locating the material inclusions inside the wall to a distance of 5 to 6 cm from the heated side of the wall surface,
- it is recommended that, for uniform heating of the wall, the infrared heating device should use a few lamps with the total heating power of 6–7 kW, and the wall heating time should not be less than 40–45 minutes made from a distance of about 1.0 m from its surface,
- if the wall has glued sensors, such as thermocouples, attention must be paid that the wall surface temperature does not exceed 70–75°C, due to the attachment stability of thermocouples,
- it is recommended to record the thermograms of the wall cooling in 10 min. steps, and should last, depending on the thermal mass of wall, at least 8 hours.
- analysis of thermograms should be performed in a professional computer software application, such as ThermaCAM Researcher Pro.

The article presents the results of experimental studies. The next stage of research is the analysis of inverse problems of heat conduction. To identify the size and depth of the material of the inclusions in the wall by active thermography in reflective mode, is necessary to use a mathematical model describing the relationship between the time-spatial distribution of the diagnostic output and the diagnostic signal [8, 9].

Theoretical analysis of heat conduction in solids is associated with the solution of the so-called simple and inverse problems of mathematical physics, and the simple problems correspond to numerical modeling and inverse problems with experimental data processing. A simple solution to the problem is to determine the temperature field based on the established model of heat exchange with the defined boundary conditions, adopted geometry and knowledge of the thermo-physical properties of materials. In contrast, the inverse problem of heat conduction is to identify the thermo-physical parameters on the basis of the adopted model of heat transfer, temperature observations at selected measuring points, and knowledge of the distribution of the surface heat flux.

We are currently working on solving the inverse heat conduction problems, in order to identify the location and depth of the thermal properties of the material inclusions in the studied concrete wall and the sensitivity analysis for the experiment.

The study has been worked out as part of the research project N N506 107138 "Infrared identification of thermal properties of building partitions". Project was financed by the Ministry of Science and Higher Education and the final report was prepared at the request of National Science Centre.

References

- [1] Maierhofer Ch., Arndt R., Rolling M., Rieck C., Walther A., Scheel H., Hillemeier B., *Application of impulse-thermography for non-destructive assessment of concrete structures*, Cement and Concrete Composites, Vol. 28, Issue 4, April 2006.
- [2] Maldague X., *Theory and practice of infrared technology for nondestructive testing*, John Wiley & Sons, Inc., 2001.
- [3] Nowak H., Kucypera M., *Application of active thermography for detecting material defects in the building envelope*, Infrared Camera Applications Conference: InfraMation 2010, Proceedings Vol. 11, 8–12 November 2010, Las Vegas, NV, USA, 369-380.
- [4] Nowak H., Kucypera M., *Wybrane problemy badań przegród budowlanych metodą termografii aktywnej*, Inżynieria i Budownictwo 12/2010, 682-687.
- [5] Nowak H., Kucypera M., *Zastosowanie termografii aktywnej w nieniszczących badaniach przegród budowlanych*, Energia i Budynek, Nr 7, 2011, 13-18.
- [6] Nowak H., *Zastosowanie badań termowizyjnych w budownictwie*, Oficyna Wydawnicza Politechniki Wrocławskiej, Wrocław 2012.
- [7] Oliferuk W., *Termografia podczerwieni w nieniszczących badaniach materiałów i urządzeń*, Biuro Gamma, Warszawa 2008.
- [8] Ozisik M.N., Orlande H.R.B., *Inverse Heat Transfer, Fundamentals and Application*, Taylor&Francis, 2000.
- [9] Taler J., Duda P., *Rozwiązywanie prostych i odwrotnych zagadnień przewodzenia ciepła*, WNT, Warszawa 2003.

KATARZYNA NOWAK*, KATARZYNA NOWAK-DZIESZKO*

IMPACT OF PREPARATION PROCEDURES ON RESULTS OF AIRTIGHTNESS TESTS

WPLYW PRZYGOTOWANIA BUDYNKU NA WYNIKI BADAŃ SZCZELNOŚCI

Abstract

Requirements connected with the designing of low-energy and passive buildings impose an obligation to conduct airtightness tests during the building process and after the completion of building works. Proper building preparation is required before initiating an airtightness test. In case of commercial buildings with complicated HVAC systems, the proper preparation may appear to be very complicated and can unfavorably affect the tests results. On the example of tests conducted in the low-energy office buildings in Wrocław, the authors describe the problems met during airtightness tests.

Keywords: air leakage, fan pressurisation method, airtightness of the buildings, n_{50} coefficient, low-energy buildings

Streszczenie

Wymagania związane z projektowaniem budynków energooszczędnych oraz pasywnych narzucają obowiązek przeprowadzania badań szczelności budynków w czasie procesu budowy oraz po jego zakończeniu. Do rozpoczęcia badań szczelności wymagane jest poprawne przygotowanie budynku. W przypadku budynków użyteczności publicznej ze skomplikowanymi systemami ogrzewania, wentylacji oraz chłodzenia poprawne przygotowanie budynku może okazać się bardzo skomplikowane oraz może bardzo niekorzystnie wpływać na wyniki testów. Na przykładzie badań dwóch energooszczędnych budynków biurowych zlokalizowanych we Wrocławiu autorki opisały problemy napotkane w czasie prób szczelności.

Słowa kluczowe: badania szczelności budynków, współczynnik n_{50} , metoda wentylatorowa, budownictwo energooszczędne

* Ph.D. Eng. Katarzyna Nowak, M.Sc. Eng. Katarzyna Nowak-Dzieszko, Institute of Building Materials and Structures, Faculty of Civil Engineering, Cracow University of Technology.

1. Polish requirements regarding building airtightness

Requirements regarding airtightness of the buildings described in the Polish national standards are just recommendations not obligations. Based on the experience of other countries it is obvious that the airtightness measurements give the possibility of field work control and a reduction of the building energy usage.

At present according to Polish building legislation, airtightness measurements are not obligatory. According to national standard Rozporządzenie w sprawie warunków technicznych jakim powinny odpowiadać budynki i ich usytuowanie [1], it is recommended that all detached buildings, commercial buildings, as well as industrial buildings and all building joints between walls and connections between windows and the building envelope should be designed and constructed to ensure the total airtightness.

However, Polish regulations recommend the airtightness measurements and determining the n_{50} coefficient, which describes the number of air changes per hour at a 50 Pa pressure difference. The recommended maximum values of n_{50} are as follows:

- a) For buildings with natural ventilation 3.0 h^{-1} .
- b) For buildings with mechanical ventilation 1.5 h^{-1} .

Building measurements are however obligatory in case of passive buildings where the n_{50} coefficient should not exceed 0.6 h^{-1} . Also, in case of low-energy buildings, the airtightness of the envelope is determined at the designing stage and must be controlled in the building process and after completion of building works.

2. Airtightness measurements according to PN-EN 13829

The airtightness measurements should be conducted according to standard PN-EN 13829 'Thermal performance of buildings. Determination of air permeability of buildings. Fan pressurization method' [2].

In the standard, two different methods are acceptable depending on the purpose:

- a) Method A – test of the building in use.
- b) Method B – test of the building envelope.

In both methods, all openings in the building envelope such as windows, doors and chimney ducts should be closed. All interconnecting doors within the building should be opened during the entire air leakage test. All heating systems taking air from the outside, mechanical ventilation and air conditioning must be turned off. The open chimneys should be cleaned of ash. All air intake and exhaust mechanical ventilation and air-conditioning ducts should be sealed. Openings for natural ventilation should be opened in the case of method A and closed in the case of method B.

3. Analyzed buildings

Authors conducted the airtightness test of two low-energy office buildings, called Centrum Ekologiczne, located in Wrocław after the completion of building works:

1. Building A (Fig. 1a) – two storey office building, building volume 1074 m³, usage area 377,5 m².
2. Building B (Fig. 1b) – two storey office building, building volume 305,5 m³, usage area 108 m².



Fig 1a. Building A



Fig. 1b. Building B

Tests were conducted using the Blowerdoor set (Fig. 2) with the digital controller Retrotec 3000 and Fantastic program to analyze test data.



Fig. 2a. Blowerdoor fan – external view



Fig. 2b. Blowerdoor set –internal view

Per requirements regarding building airtightness, specified in the building project, n_{50} should not exceed 1.5 h⁻¹. The measurements must have been conducted two times due to the incorrect building preparation and inaccurate construction works.

The authors conducted the first measurements in July.

The measurements were conducted in the following weather conditions:

- external air temperature: 20°C,
- wind speed on the Beaufort scale based on own observation: 1,
- air temperature inside the flat: 18°C.

The buildings were prepared for the tests (method B), all openings in the building envelope such as windows, doors, ventilation ducts and openings next to the lightning devices were closed. Inside the building with the mechanical ventilation system, there is a lift shaft with a separate mechanical ventilation system. For the purpose of testing, the elevator shaft was cut off from the analyzed building volume. Figs. 3, 4 present the preparation of different building parts.



Fig. 3. Preparation of lighting fixtures



Fig. 4. Preparation of lift shaft

Tests were conducted in two pressure states: pressurisation and depressurisation (per [2]). Results of the first test were very unfavorable. Index n_{50} in the first pressurisation test was equal to $n_{50} = 2.98 \text{ h}^{-1}$. The value was almost two times higher than the project limit value of $n_{50} = 1.5 \text{ h}^{-1}$. Those negative conditions were caused by both inaccurate building erection and inaccurate building preparation. After the tests, all preparation works were checked carefully and all unsealed or ineffectively sealed openings were corrected. The tests in building A were repeated five more times. Results of all tests are presented in Table 1.

In all conducted tests, the results were higher than $n_{50} = 1.5 \text{ h}^{-1}$ however the correction of building preparation works improved the first result by 30% (from $n_{50} = 2.98 \text{ h}^{-1}$ to $n_{50} = 1.94 \text{ h}^{-1}$).

In case of building B the first test results were also much higher than $n_{50} = 1.5 \text{ h}^{-1}$. Results are presented in Table 2.

Table 1

Results of airtightness tests of building A conducted in July

	Test 1 pressurisation	Test 2 pressurisation	Test 3 pressurisation	Test 4 pressurisation	Test 5 pressurisation	Test 6 depressurisation
n_{50} [1/h]	2.98	2.25	2.01	1.95	1.94	2.58

Table 2

Results of airtightness tests of building B conducted in July

	Test 1 pressurisation	Test 2 depressurisation
n_{50} [1/h]	2.96	2.94

During the tests, all air leakages were monitored using a fog generator, an anemometer and an infrared camera. It allowed for the detection of both openings in the building envelope caused by inaccurate erection as well as the inaccurate building preparation (Figures 5 and 6). To make the monitoring possible and to increase the air flow through the openings, a pressure difference of up to 100 Pa was forced. It revealed the location of leaks but also loosened the sealed openings. This is the reason why the constant monitoring of all sealed openings should be done.



Fig. 5. Detection of leakages with fog generator and anemometer



Fig. 6. Detection of leakages with infrared camera



Fig. 7. Loosened sealed opening during the airtightness test



Fig. 8. Loosened sealed opening during the airtightness test

The problem of a too high n_{50} value in both buildings was mainly connected with the suspended ceilings in the buildings. Unfortunately, the roof construction above the ceiling was not tight – the air leakages were noticeable next to lighting fixtures mounted in the ceiling construction, however, direct monitoring of the roof construction was not possible.

The next set of tests was conducted in November after the repair works of the building envelope tightness and after proper building preparation. The results of those tests were significantly better, Table 3 presents the results of the final tests conducted in buildings A and B.

Table 3

Results of final measurements of building A and B

	Building A	Building B
Number of air changes at 50 Pa, n_{50} [1/h] pressurisation	1.3	2.13
Number of air changes at 50 Pa, n_{50} [1/h] depressurisation	1.46	1.96
n_{50} [1/h]	1.38	2.04

The measurements were conducted in the following weather conditions:

- external air temperature: 22°C,
- wind speed on the Beaufort scale based on own observation: 1,
- air temperature inside the flat: 20°C.

In the case of building A, $n_{50}=1,38\text{h}^{-1}$ was smaller than the permissible value of $n_{50} = 1,5\text{h}^{-1}$. Unfortunately, in case of building B, even after the caulk works, results were still not acceptable.

4. Conclusions

Airtightness field tests require the extensive and very precise preparation of the building. In the case of commercial buildings, it appears to be one of the most important aspects which can significantly affect the final tests results. The field tests conducted by the authors and described in the article showed that the incorrect preparation of the building envelope can unfavorably affect the n_{50} value even by up to 30%. The conducting of tests must be connected with the simultaneous monitoring of all sealed openings with infrared cameras, using fog generator and anemometer.

The work reported in this paper has been partially funded by the project L-1/115/DS/2013.

References

- [1] Rozporządzenie Ministra Infrastruktury w sprawie warunków technicznych, jakim powinny odpowiadać budynki i ich usytuowanie z dnia 12 kwietnia 2002.
- [2] PN-EN 13829 Właściwości cieplne budynków. Określenie przepuszczalności powietrznej budynków. Metoda pomiaru ciśnieniowego z użyciem wentylatora.
- [3] PN-EN 15242 Wentylacja budynków – Metody obliczeniowe do określania strumieni objętości powietrza z uwzględnieniem infiltracji.
- [4] Nowak K., Nowak-Dzieszko K., *Badania szczelności budynków metodą ciśnieniową*, Czasopismo Techniczne, 2-B/2012, 305-313.
- [5] Delmotte Ch., *Proper building preparation for envelope airtightness testing*, The REHVA European HVAC Journal 1/2013, 17-19.
- [6] Nowak K., Nowak-Dzieszko K., *Trudności związane z przeprowadzaniem badań szczelności budynków*, Izolacje 2/13, 16-19.

KATARZYNA NOWAK*, MAŁGORZATA ROJEWSKA-WARCHAŁ*

THERMAL COMFORT OF OFFICE ROOMS WITH A LARGE AREA OF GLAZING

KOMFORT CIEPLNY POMIESZCZEŃ BIUROWYCH O DUŻEJ POWIERZCHNI PRZESZKLEŃ

Abstract

The paper presents an attempt at assessing the impact of how the type of construction of a building influences the thermal comfort of office rooms with a large area of glazing, in summer months. The results of simulations are presented for a two-storey office building. The calculations were carried out in the Design Builder program. Simulations were carried out for the climate in Poland, which allowed for assessment of the conditions for the thermal comfort of the building in the spring and summer. The main aim of the analysis was to determine how the material and design solutions as well as the applied glazing and shades influence the protection of the building against overheating and the thermal comfort conditions.

Keywords: thermal comfort, energy – efficient windows, overheating rooms

Streszczenie

W artykule podjęto próbę oceny wpływu rodzaju konstrukcji budynku na warunki komfortu cieplnego panującego w okresie letnim w pomieszczeniach biurowych z dużymi powierzchniami przeszkleń. Przedstawione zostaną wyniki obliczeń symulacyjnych dla dwukondygnacyjnego budynku biurowego. Obliczenia wykonano przy użyciu programu Design Builder. Dla polskich warunków klimatycznych przeprowadzone zostały symulacje pozwalające na ocenę warunków komfortu cieplnego budynku w okresie wiosenno-letnim. Głównym celem przeprowadzonych analizy było określenie, w jaki sposób rozwiązania materiałowo-konstrukcyjne oraz zastosowane przeszklenia i osłony słoneczne wpłyną na ochronę budynku przed przegrzaniem i na poprawę warunków komfortu cieplnego.

Słowa kluczowe: komfort cieplny, okna energooszczędne, przegrzanie pomieszczeń

* Ph.D. Eng. Katarzyna Nowak, M.Sc. Eng. Małgorzata Rojewska-Warchał, Institute of Building Materials and Structures, Faculty of Civil Engineering, Cracow University of Technology.

1. Introduction

The architectural solutions in modern design office buildings are characterized by large glazed facades. They form large external glazed surfaces and generate high heat losses in winter causing a greater increase of energy demand for the heating of the buildings and influencing the development of unfavourable conditions with regard to thermal comfort in summer.

The parameters that strongly influence the climate conditions in a room are: the air temperature; the temperature of the surfaces of the partitions; the velocity of air movement. They are dependent not only on the architectural and construction solutions such as the thermal capacity of the partitions and the size and type of the glazing, but also on the installation systems and service load of the rooms.

2. The object of simulation calculations

Computational analysis was performed for the two-storey office building in Fig. 1. It is a two-storey building measuring $6.8 \text{ m} \times 18.5 \text{ m} \times 5.4 \text{ m}$. The building has seven offices with a surface area of approximately 18 m^2 each and a conference room with a surface area of 25 m^2 . The windows in the rooms are primarily facing the south and their total area is approximately 60% of the facade (Table 1). The northern part of the building is the communication zone in which there are no glazed surfaces provided (Fig. 2)

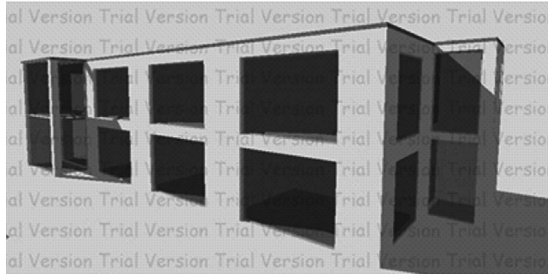


Fig. 1. Building visualization

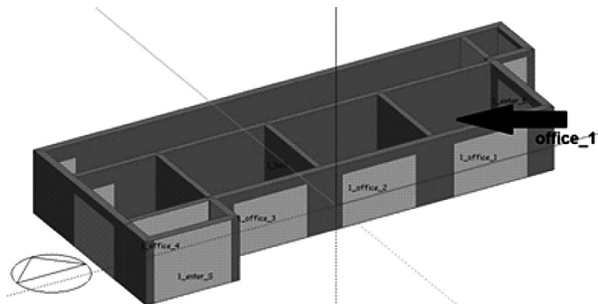


Fig. 2. Building zones visualization

Table 1

Summary of the flooring space and windows in each room

room	Ground floor				First floor			
	office 1	office 2	office 3	office 4	office 1	office 2	office 3	conference room
Flooring area [m ²]	18.7	19.0	18,4	14.3	18.7	18.7	18.7	25.4
Volume[m ³]	50.5	51.3	49.6	38.7	50.5	50.5	50.5	68.58
Window area S [m ²],	7.36	7.36	7.36	9.3	7.36	7.36	7.36	9.13
External wall [%]	57	56	58	100	57	57	57	100
Window area E [m ²],	6.20	–	–	–	6.20	–	–	–
External wall [%]	58	–	–	–	58	–	–	–
Window area W [m ²],	–	–	–	6.90	–	–	–	6.90
External wall [%]	–	–	–	63	–	–	–	41

The building is characterized by proper insulation of individual partitions. They meet the requirements imposed by Technical Requirements [2]. For initial analysis, a window of thermal transmittance $U = 1.1$ [W/m²K] and solar heat gain coefficient of 0.63 were used. The glazing used is characterized by a visible radiation transmittance coefficient of 0.8.

The building has only natural ventilation and is heated by convection heaters with the use of a gas boiler.

Simulation calculations were made with the use of the Design Builder v.3 program. The climate data from the database of the Energy Plus program was used and the calculation simulations were done for a building located in Kraków. The aim of the analysis was to determine the air operative temperature in spring and summer in separate areas of the building depending on the thermal capacity of the rooms and the extent of the glazing. A dominant aspect of the calculations was the assessment of thermal comfort. External heat gains connected with the functions of the rooms were taken into account for the individual rooms and such factors influencing the thermal comfort as the physical activity of the persons working in the rooms and the insulation features of their clothing. The thermal isolation of the clothing of $clo = 0.5$ was adopted for summer time.

3. The results of the analyses conducted.

The following assumptions were adopted for the purposes of the simulation analysis: offices of 18 m² each, 3 persons working from 8.00 in the morning to 7.00 in the evening; a conference room with 10 persons present there from 10.00 in the morning to 2.00

in the afternoon; 3 persons present during the remaining hours; at weekends the building is not in use. An air exchange of 20 m³/h for person in accordance with norm specifications was assumed.

A comparative analysis was conducted with reference to the described office building constructed using three different types of technology. Two of the variants adopted were two-layer walls with an insulation layer of polystyrene. One variant was a load-bearing wall made of aerated concrete and another was a heavy monolithic concrete wall. The third technology was a light-frame wooden construction. An in-depth analysis was conducted concerning the office rooms located on the first floor with the glazing facing south and east (Office_1) – Fig. 2.

Table 2

A summary of the thermal capacity of individual rooms in the analysed technologies

room	Ground floor				First floor			
	office 1	office 2	room	office 1	office 2	room	office 1	office 2
Enclosure – aerated concrete								
Heat capacity [kJ/K]	4709	4780	4658	3865	4244	4244	3718	5627
Heat capacity/area	251.82	251.57	253.15	270.28	226.95	226.95	198.82	221.54
Enclosure – concrete								
Heat capacity [kJ/K]	10518	10099	9853	8368	13272	13272	12732	17643
Heat capacity/area	562.46	531.5	535.5	585.17	709.73	709.73	680.86	694.61
Enclosure – light core								
Heat capacity [kJ/K]	3409	3365	3269	2683	2276	2276	2144	2961
Heat capacity/area	187.31	177.1	177.66	187.62	121.71	121.71	114.65	116.6

The initial simulations for the construction of light aerated concrete that were carried out allow for a positive assessment of the thermal comfort of this room through the whole period tested (Fig. 3).

Based on the results presented in Fig. 3 it may be observed that, during the period from 15 May to 15 September, there are days when the PMV thermal comfort index reaches short-term values of much over 5. Such conditions of the microclimate in the building greatly exceed the optimum temperature for summer which is 25°C and the recommended value of the coefficient $-0.5 < PMV < +0.5$.

During the period which was analysed, the greatest thermal load caused by the external temperature for the location in Kraków takes place in the first half of August. The coolest days

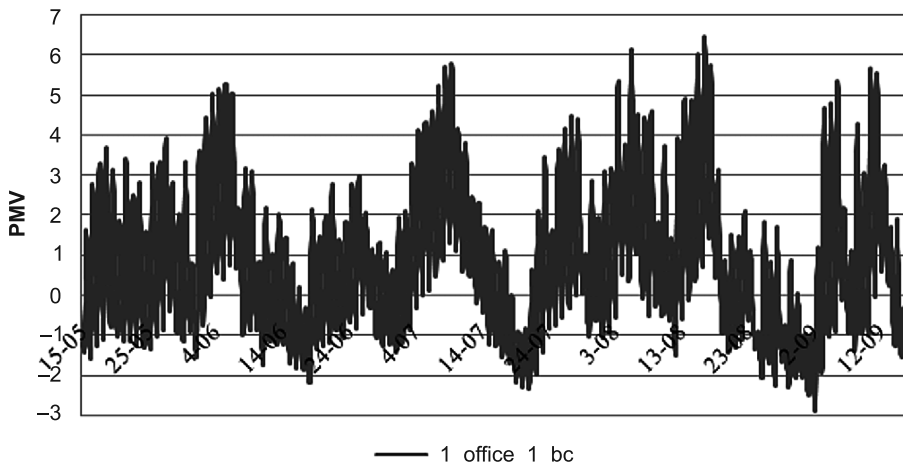


Fig. 3. Hourly flow of the PMV comfort index for an office room (Office_1) in the period from 15 May to 15 September

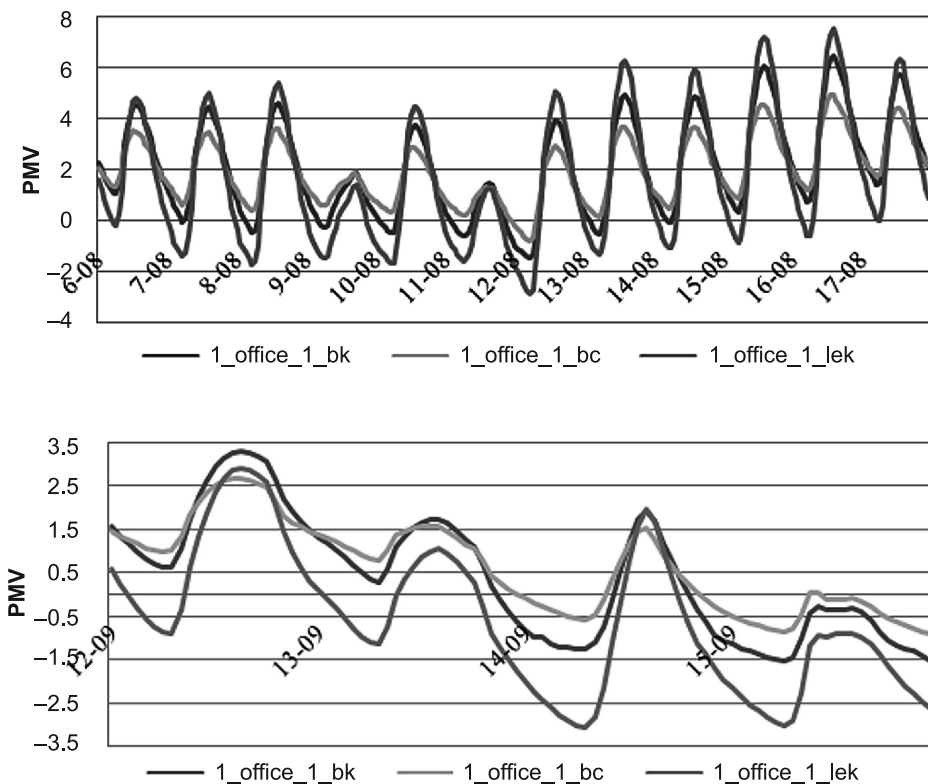


Fig. 4. Hourly flow of the PMV comfort index for an office room (Office_1) in the period from 6 August to 17 August and from 12 September to 15 September

come in the second half of September. Hourly graphs for the analysis, both of the operative temperature that may be in the room, and for the flow of the PMV thermal comfort index for the cases studied were shown for the period from 6 August to 17 August and for the period from 12 September to 15 September.

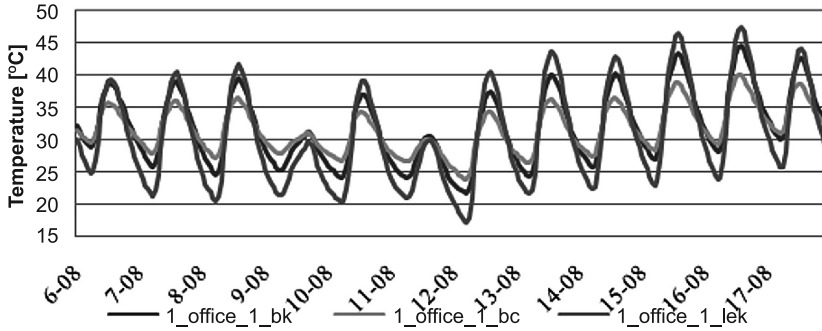


Fig. 5. Hourly flow of the operative temperature for an office room (Office_1) in the period from 6 August to 17 August

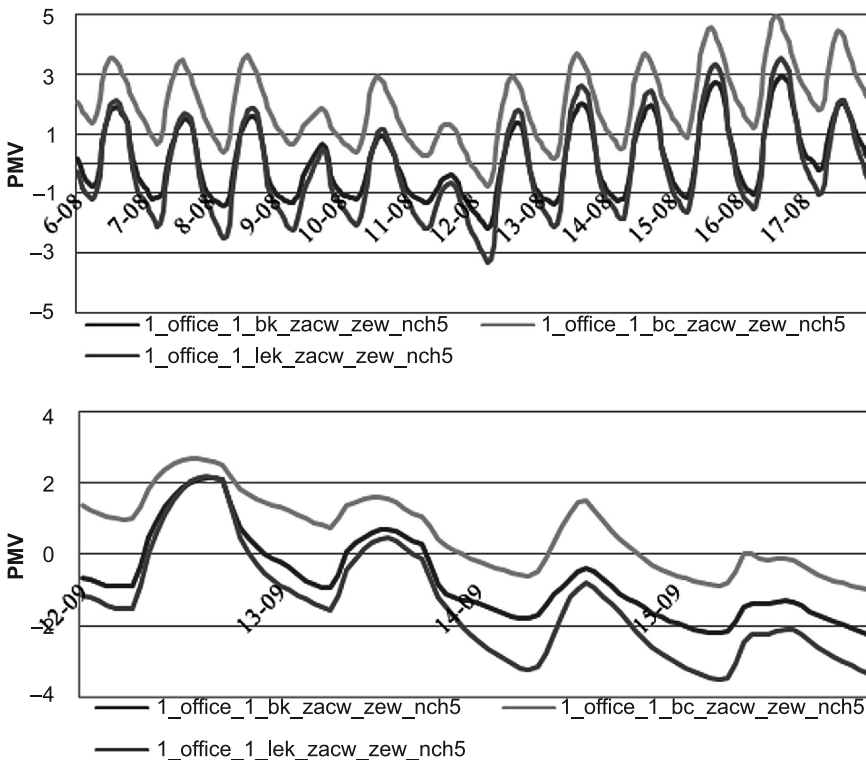


Fig. 6. Hourly flow of the PMV comfort index for an office room (Office_1) with shading and night cooling in the period from 6 August to 17 August and from 12 September to 15 September

In order to observe the influence of the heat capacity of the construction on the possibility of shaping the internal microclimate, in Fig. 4 and 5 the authors prepared a summary of comparative flows of the PMV thermal comfort index and the operative temperature for all the analysed technologies.

The results of the simulations presented in Fig. 4 and 5 show that in the complex conditions of usage, the most favourable parameters of the microclimate are present in a building with a heavy construction of monolithic concrete.

For the existing buildings, a crucial aspect is the actions which allow for a decrease in the operative temperature in the rooms. Such activities include the possibility of intensive ventilation of the premises at night time and the possibility of using shades. In order to perform an assessment of the influence of those actions, simulations were performed that took into account the night ventilation in the amount of 5 exchanges of air per hour in the rooms.

The limitation of solar gain was achieved through the use of both external and internal shades. The results of the simulation are presented in Fig. 6.

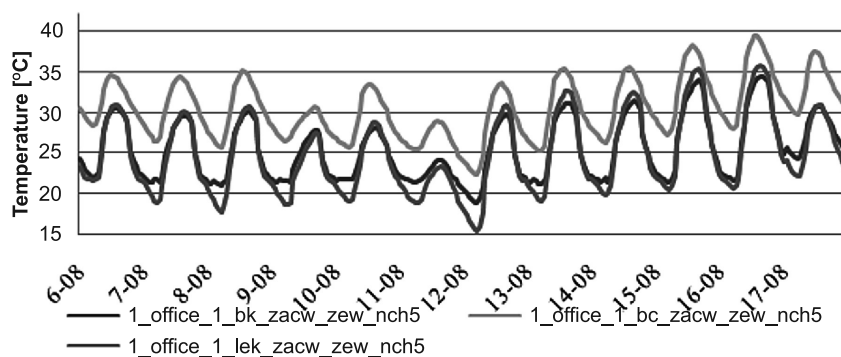


Fig. 7. Hourly flow of the operative temperature for an office room (Office_1) with shading and night cooling in the period from 6 August to 17 August

The results of the simulation presented in Fig. 6 and 7 show that in the case of greater limitation of the solar gains and intensive night ventilation, partitions of a lower thermal capacity are a more beneficial solution.

4. Conclusions

Many newly designed office buildings and buildings of public service are characterized by extensive glazing, despite the use of appropriate insulation of separate elements of a building, the size of the glazing generates solar gains that are too big in summer and so create uncomfortable working conditions.

When such architectural solutions for the facades are proposed, it seems necessary to determine the conditions of thermal comfort not only for the whole building, but especially for particular work stations at the stage of developing the concept of the building.

The results of the simulations that are presented in the article constitute an initial stage of the work on the impact the thermal capacity of housing, the type of the glazing how to limit the availability of solar gains on the thermal comfort in the rooms with extensive glazed surfaces.

This stage of the studies and analyses allows the following conclusions to be posed:

1. In the case of the application of the solutions that limit thermal gains, it is more beneficial to use construction solutions of lower thermal capacity. Such building enclosures enable the dynamic reaction of the partitions to the change of environmental conditions.
2. With an extensive surface of glazing in a building it is necessary to apply solar shadings in order to achieve comfortable thermal conditions.
3. The lack of shading systems (external or internal) may result in the necessity to cool the in order to avoid overheating.

The work reported in this paper has been partially funded by the project L-1/115/DS/2013.

References

- [1] PN-EN ISO 7730 Ergonomics of the thermal environment. Analytical determination and interpretation of thermal comfort using calculation of the PMV and PPD indices and local thermal comfort criteria.
- [2] Rozporządzenie Ministra Transportu, Budownictwa i Gospodarki Morskiej z dnia 5 lipca 2013 r. zmieniające rozporządzenie w sprawie warunków technicznych, jakim powinny odpowiadać budynki i ich usytuowanie.
- [3] Lyons P. Arasteh D., *Window Performance for Human Thermal Comfort 2000*, ASHRAE Winter Meeting, Dallas, TX, February 5–9, 2000 LBNL-44032TA-412.
- [4] Huizenga Ch., Zhang H., Mattelaer P., Yu T, Arens E., Lyons P., *Window performance for human thermal comfort*, Final Report to the National Fenestration Rating Council, February 2006.
- [5] Nowak K., Nowak-Dzieszko K., Rojewska-Warchał M., *Thermal comfort of the rooms in the designing of commercial buildings*, Research and Applications in Structural Engineering, Mechanics and Computation. SMEC Cape Town, 2013, 651-652.
- [6] Nowak K., Nowak-Dzieszko K., Rojewska-Warchał M., *Thermal comfort of individual rooms in the design of commercial buildings*, 2nd Central European Symposium on Building Physics, Vienna, Austria, September 9–11, 2013, 343-349.

KATARZYNA NOWAK*, ANNA ZASTAWNA-RUMIN*

THE POSSIBILITY OF USING PCM IMPREGNATED GIPSUM BOARDS OF DIFFERENT TEMPERATURE PHASE CHANGE

MOŻLIWOŚĆ STOSOWANIA PŁYT GISPOWO-KARTONOWYCH Z DODATKIEM PCM O RÓŻNEJ TEMPERATURZE PRZEMIANY FAZOWEJ

Abstract

The paper presents results of experimental studies on components containing phase change materials. The subject of research was the simultaneous usage of two different PC materials: gypsum-carton boards with paraffin capsules of change temperature 23°C and a board with a melting temperature of 26°C. The tests were carried out in a climatic chamber for a light skeleton wall lined with inner facing consisting of a traditional gypsum-carton and a layer of PCM board. Measurements of temperature course were taken as well as heat flux density distribution on the surfaces of the boards for variable conditions in the climatic chamber. The results presented in the article are one of the aspects of widely planned and realized measurements aimed at evaluating and choosing the optimal material solutions, using available phase change materials.

Keywords: phase change material, PCM, heat capacity, heat accumulation

Streszczenie

W artykule przedstawiono wyniki badań eksperymentalnych przegród zawierających materiały fazowo zmienne. Przedmiotem badań było jednoczesne zastosowanie dwóch rodzajów materiałów PCM: płyt gipsowo-kartonowych z kapsułkami z parafiną o temperaturze przemiany 23°C oraz płyty z temperaturą przemiany 26°C. Badania przeprowadzono w komorze klimatycznej dla lekkiej ściany szkieletowej, wyłożonej okładziną wewnętrzną z tradycyjnej płyty gipsowo-kartonowej oraz jedną warstwą płyty z PCM. Przeprowadzono pomiary przebiegu temperatury oraz rozkładu gęstości strumieni ciepłych na powierzchniach płyt dla zmiennych warunków panujących w komorze klimatycznej. Zaprezentowane w artykule wyniki badań stanowią jeden z aspektów szeroko zaplanowanych i realizowanych pomiarów mających na celu ocenę i dobór optymalnych rozwiązań materiałowych z zastosowaniem dostępnych materiałów fazowozmiennych.

Słowa kluczowe: materiał fazowo zmienny, PCM, pojemność cieplna, akumulacja ciepła

* Ph.D. Eng. Katarzyna Nowak, M.Sc. Eng. Anna Zastawna-Rumin, Institute of Building Materials and Structures, Faculty of Civil Engineering, Cracow University of Technology.

1. Introduction

Energy used in both commercial and apartment buildings is largely spent on their heating and cooling.

One of the solutions which makes it possible to decrease its consumption is to use phase change materials. They take heat during phase change from solid into liquid and release it when changing from a liquid state into a solid state.

When building, the use of products that contain phase change materials may contribute to the decrease of daily temperature fluctuations inside the rooms and in this way to improve the heat comfort and decrease the energy demand of buildings. In case of buildings with no cooling installations it is a passive solution which may decrease the risk of overheating.

1.1. The aim of research

The subject of the undertaken research is comparative analysis of the behavior of a light wall in which inner finishing boards were used in variable air temperature conditions. The main aim of the analysis is evaluation of accumulative possibilities of gypsum-carton boards which contain phase change materials of different change temperature.

2. Description of a measurement stand

A measurement stand was installed in a laboratory climatic chamber. A light skeleton wall of 195 cm × 210 cm was placed between the so called “cold chamber” and a “warm one”. The basic layers of the partition were: expanded polystyrene board of 16 cm and an inner gypsum-carton board cladding. In order to exclude the possibility of air circulation between the thermal insulation and the gypsum-carton board, the board was additionally sealed with silicone on its perimeter.

On the partition surface from the side of the “warm chamber” three test gypsum-carton boards of 50 cm × 60 cm were mounted. Two of them contained phase change material, the third one was an ordinary board with no additions. The arrangement of the boards were made according to the scheme presented in Fig. 2. The boards mounted in the top row contained an organic material called Micronal which has an adequate melting temperature of 23°C for the board placed on the left and the melting temperature of 26°C for the board on the right. The phase change heat of the material used was 110 kJ/kg (according to the producer). PCM was about 30% of the board mass (about 3 kg of dry Micronal per 1 m² of the board. All the test boards were also sealed with silicone on their perimeters.

2.1. Testing equipment

Temperature and heat flux density were the quantities measured both on the surface and between the layers of the partition. On the surface of the expanded polystyrene and on each of the fastened boards three temperature sensors (type K thermocouple) were placed and a heat meter (a square one of 120 mm × 120 mm), (Fig. 2a, 2b). Air temperature inside the chambers was measured by temperature sensors Pt 100 and Pt 1000. Registering

of the measured quantities took place through data collecting system Ahlborn Almemo connected to the computer. Measurement data were written down with the aid of data collecting system Data-Control 4.2. Further data processing was conducted in Excel programme.

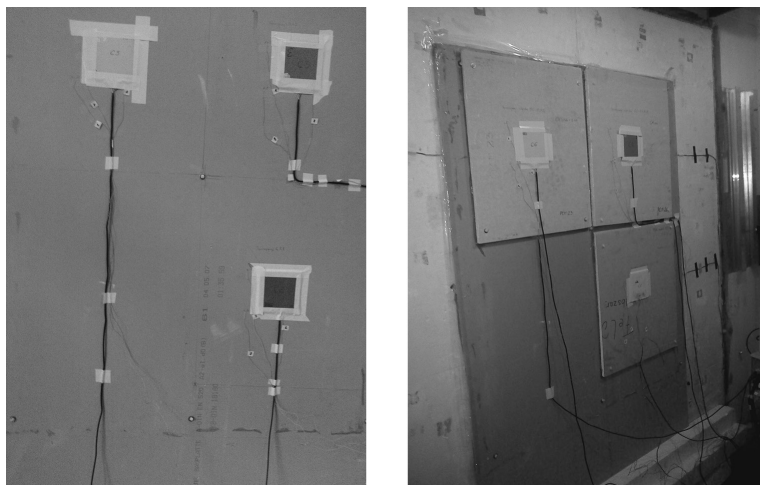


Fig. 1. Picture of the board with sensors attached to the surface

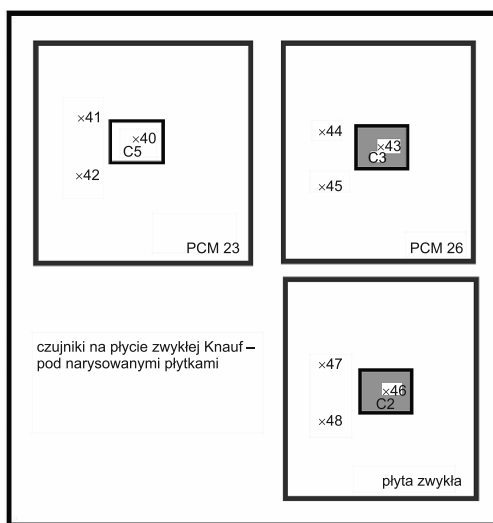


Fig. 2a. Sensor distribution scheme under the surfaces of the boards: 40, 41, 42 – temperature sensors under the surface of PCM23 board; 43, 44, 45 – temperature sensors under the surface of PCM26 board; 46, 47 – temperature sensors under the surface of gypsum-carton board with no phase change material; C5, C3, C2 – square heat meters of 120 mm × 120 mm placed adequately under the surfaces of the boards: PCM23, PCM26 and an ordinary board

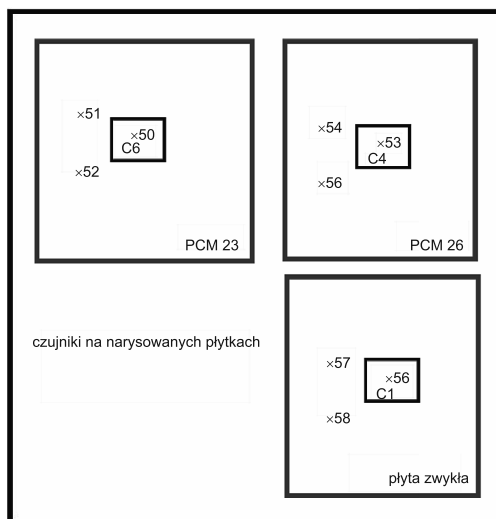


Fig. 2b. Sensor distribution scheme on the surfaces of the boards: 50, 51, 52 – temperature sensors on the surface of PCM23 board; 53, 54, 55 – on the surface of PCM26 board; 56, 56, 57 – temperature sensors on the surface of gypsum-carton board with no phase change material; C6, C4, C1 – square heat meters of 120 mm × 120 mm placed adequately on the surfaces of the boards: PCM23, PCM26 and an ordinary board

3. Procedure of the carried out tests

3.1. Tests in a climatic chamber

The tests were carried out in a few stages. In the article the research results were analysed for the case of nonstationary temperature conditions existing in a heat chamber. Temperature change range inside the chamber was selected in a way that would correspond to the conditions that may occur in rooms during summer. The tests were carried out in 24 hour cycles, which would reflect the actual temperature course in a sunny room.

When taking measurements all three tested gypsum-carbon plates were subjected to the same conditions.

The first stage of testing aimed at observing changes in temperature and in heat flux on the front and back surfaces of the boards.

During twelve hours in a heat chamber there was an increase of temperature from 18°C to 36°C, and then a decrease of air temperature down to initial conditions. In a test cycle high temperature, above 35°C, remained in the heat chamber for about four hours. In a cold chamber there was a steady temperature of about 18°C. Air temperature increase in the chambers, due to technical possibilities of the controlling equipment, could reach six degrees an hour. Because of this, temperature increase was not continuous but it agreed with the scheme presented in Fig. 3. The scheme presents the course of temperature distribution for one cycle.

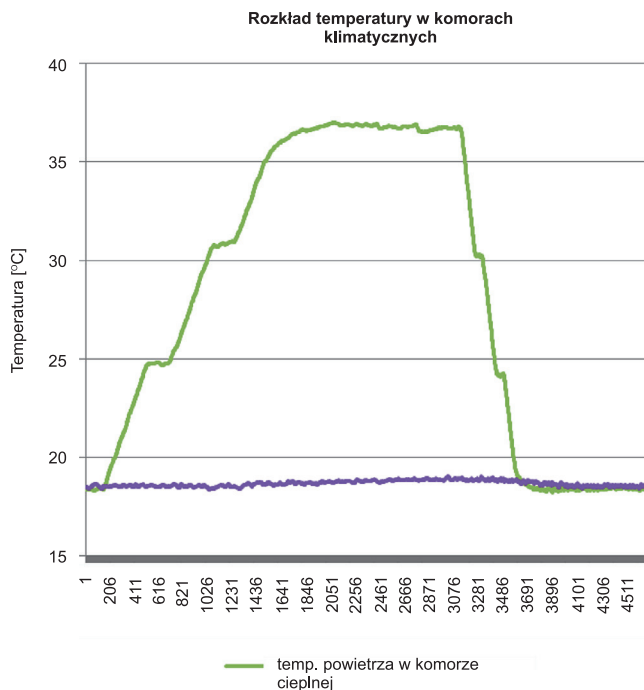


Fig. 3. Measurement of the air temperature distribution in the hot and cold chamber during testing

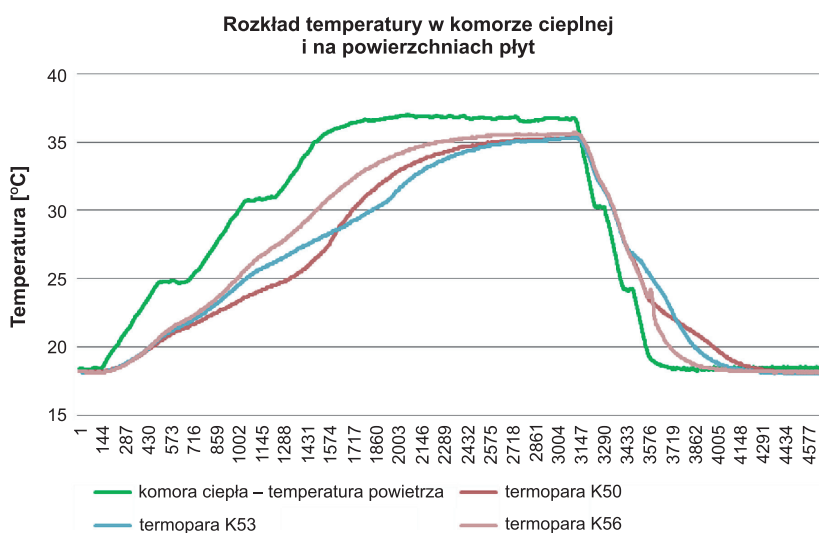


Fig. 4. Course of air temperature changes in the hot chamber and temperature distribution on the surfaces of the analysed boards. On PCM23 board – thermocouple K50, on PCM26 board – thermocouple K53, on the ordinary board – thermocouple K56

Taking into consideration heat comfort of the rooms it is essential to have information about the difference between the air temperature value in a room and the temperature of the finishing surfaces. The graph in Fig. 5 allows us to observe the course of temperature difference that could be noticed on the plate surface of an ordinary gypsum-carton board and on the surfaces of board containing PCM23 and PCM26. In the process of air temperature growth the temperature on the surfaces of the boards containing PCM was lower maximally 3.6°C than on the surface of an ordinary board. This is beneficial for a PCM board temperature course and is connected with bigger possibilities of excess heat accumulation in such a material. It can be observed in the graph presented in Fig. 4 that in the case of boards containing phase change materials it is the temperature change that beneficially influences temperature distribution. In the analysed example, during air temperature growth from 18°C to 36°C it is more advantageous to use PCM23 board whose surface temperature is 3.5°C lower than of an ordinary plate and 1.8°C lower than in the case of PCM26 plate. After the heating cycle is finished and when air temperature stabilizes above 35°C the arrangement is reversed. There follows temperature increase (over 28°C) on the surfaces of PCM plates. Therefore, in this case, it is better to use plates of higher temperature change (the temperature of the PCM26 surface is maximally 3.2 degree lower than in an ordinary plate).

An essential aspect connected with the possibility of storing energy in PCM was the measurement of the difference in temperature that occurred in a given time period between the front and the back surfaces of all analysed boards. Fig. 6 presents temperature distribution for the case discussed.

Figure 6 presents the temperature course on the surface behind the boards containing PCM. It can be observed that the indications are 4.8°C lower than on the surface behind an ordinary plate. These lower values are caused by absorption of heat flux penetrating this material and reaching the surface of the back board at a much slower rate. It is also important that the maximum difference of temperature indications between the back PCM23 board and an ordinary board occurs in the neighbourhood of phase change temperature (23.3°C), while for PCM26 board it is shifted to 27.3°C.

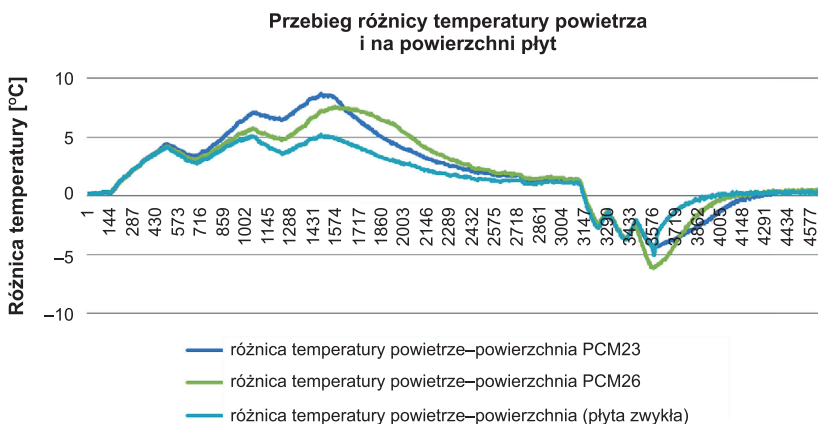


Fig. 5. Differences in air temperature course and on the surfaces of an ordinary plate and the plates containing PCM

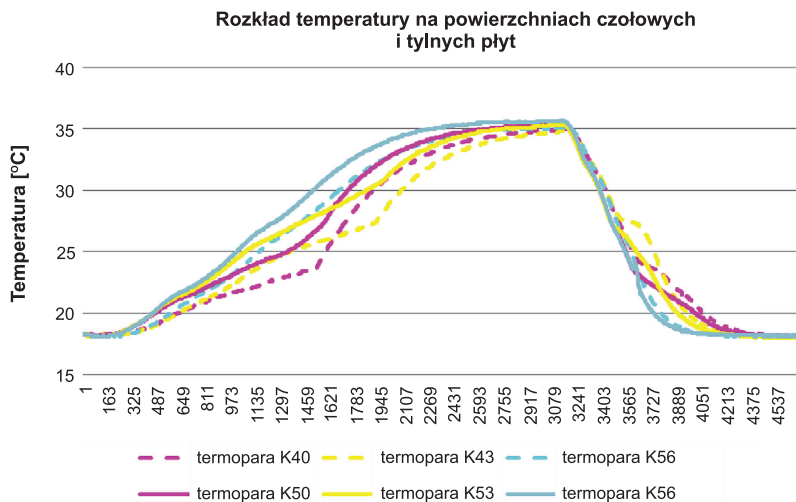


Fig. 6. Temperature change course on and under the surfaces of the analysed boards. The sensors: on PCM23 board – thermocouple K50, under PCM23 – thermocouple K40; On PCM26 board – thermocouple K53, under PCM26 board – thermocouple K43; on an ordinary board – thermocouple K56, under an ordinary board – thermocouple K46

The accumulative possibilities of the analysed boards are more clearly shown by heat flux density taken and given up by particular surfaces. The measurement results are presented in Fig. 7. The graphs show distinctly greater heat absorption for boards containing phase change materials. Due to different change temperature (23°C and 26°C) a clear shift in time of the extremes can be observed in the compared materials.

The integration results of the heat flux density taken by three analysed plates in the studied time period show greater possibility of heat accumulation by a plate containing PCM26. During the heating cycle it accumulates 3.5 times more heat than a gypsum-carton plate with

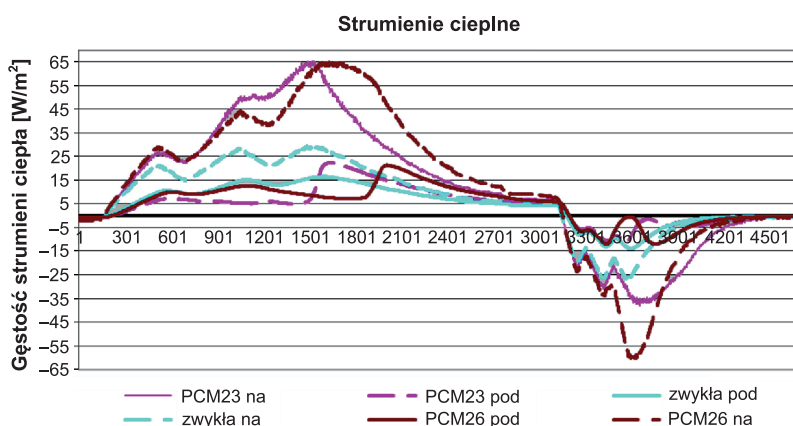


Fig. 7. Thermal flux density measurement on the front and back surfaces of gypsum boards

no addition of phase change materials. The board PCM23 was equally advantageous – during testing it accumulated nearly 3.11 times more heat than an ordinary board.

4. Conclusions

The integration results of the heat flux density taken by the two boards containing phase change materials in the studied time period indicate much greater possibility to accumulate heat than an ordinary board. It is therefore evident that it is possible to significantly increase the heat volume of a room while using the same amount of finishing material but with the addition of PCM. A partition working in the conditions of extreme temperatures of the summer time was analysed. The results presented allow us to state that phase change temperature will have a significant influence on its effectiveness. When choosing a very high maximum air temperature for the tests it seems justified to use boards of lower and higher phase change temperature.

Such analyses will be the subject of further studies.

The work reported in this paper has been partially funded by the project L-1/115/DS/2013.

References

- [1] Wnuk R., Jaworski M., *Badania charakterystyk cieplnych elementów budowlanych akumulujących ciepło zawierających materiały PCM (Phase Change Materials)*, Polska Energetyka Słoneczna 2, 4/2010, 1/2011, 5-11.
- [2] Wnuk R., *Magazynowanie ciepła, pozyskanego z energii promieniowania słonecznego, z wykorzystaniem materiałów fazowo-zmiennych, w budownictwie*, II Konferencja SOLINA 2008, Innowacyjne Rozwiązania Materiały i Technologie dla Budownictwa.
- [3] Soares N., Costab J.J., Gasparb A.R., Santosc P., *Review of passive PCM latent heat thermal energy storage systems towards buildings' energy efficiency*, Energy and Buildings 59, 2013, 82-103.
- [4] Wnuk R., *Bilans energetyczny pomieszczenia ze strukturalnym, funkcjonującym w cyklu dobowym, magazynem ciepła z materiałem fazowo-zmiennym*, Czasopismo Techniczne, 1-B/2009, 269-277.
- [5] Berrouga F., Lakhala E.K., Omania M.El, Faraji M., Qarniac H.El, *Thermal performance of a greenhouse with a phase change material north wall*, Energy and Buildings 43, 2011, 3027-3035.
- [6] Peippo K., Kauranen P., Lund P.D., *Multicomponent PCM wall optimized for passive solar heating*, Energy Build, 17(4), 1991, 259-70.
- [7] Kuznik F., David D., Johannes K., Roux J., *A review on phase change materials integrated in building walls*, Renewable and Sustainable Energy Reviews, 15, 2011, 379-391.
- [8] Neeper D.A., *Thermal dynamics of wallboard with latent heat storage*, Solar Energy, 68(5), USA 2000, 393-403.
- [9] Heim D., Clarke JA., *Numerical modelling and thermal simulation of PCM-gypsum composites with ESP-r*, Energy Build, 36(8), UK 2004, 795-805.

- [10] Jiang F., Wang X., Zhang Y., *A new method to estimate optimal phase change material characteristics in a passive solar room*, Energy Conversion and Management 52, 2011, 2437-2441.
- [11] Chwieduk D., *Wybrane aspekty stosowania materiałów zmiennofazowych w przegrodach zewnętrznych w polskich warunkach klimatycznych*, Zeszyty Naukowe Politechniki Rzeszowskiej, Budownictwo i Inżynieria Środowiska, z. 59, 2/2012/II.
- [12] Scalat S., Banu D., Hawes D., Paris J., Haghghata F., Feldman D., *Full scale thermal testing of latent heat storage in wallboard*, Solar Energy Materials and SolarCells, 44 (1), 1996, 49-61.
- [13] Kooa J., Sob H., Honga S.W., Honga H., *Effects of wallboard design parameters on the thermal storage in buildings*, Energy and Buildings 43, 2011, 1947-1951.
- [14] Soaresa N., Costab J.J., Gasparb A.R., Santosc P., *Review of passive PCM latent heat thermal energy storage systems towards buildings' energy efficiency*, Energy and Buildings 59, 2013, 82-103.
- [15] Zalba B., Marin J.M., Cabeza L.F., Mehling H., *Review on thermal energy storage with phase change materials, heat transfer analysis and applications*, Applied Thermal Engineering 23, 2003, 251-283.
- [16] Sharma A., Tyagi V.V., Chen C.R., Buddhi D., *Review on thermal energy storage with phase change materials and applications*, Renewable and Sustainable Energy Reviews 13, 2009, 318-345.
- [17] Kosny J., Kossecka E., Brzeziński A., Theoubaer A., Yarbrough D., *Dynamic thermal performance analysis of fiber insulations containing bio-based phase change materials (PCMs)*, Energy and Buildings 52, 2012, 122-131.
- [18] Shukla N., Fallahi A., Kosny J., *Performance characterization of PCM impregnated gypsum board for building applications*, Energy Procedia 30, 2012, 370-379.
- [19] Kosny J., Yarbrough D., Miller W., Petric T., Childs P., Mohiuddin Syed A., *PCM-Enhanced Building Envelopes in Current ORNL Research Project*.

ŁUKASZ NOWAK*, KRZYSZTOF CEBRAT**, ANNA BAĆ***

DOUBLE SKIN HOUSE CONCEPT – A STUDY OF BUFFER ZONE USAGE IN A SINGLE FAMILY HOME

DOUBLE SKIN HOUSE – STUDIUM WYKORZYSTANIA STREFY BUFOROWEJ W DOMU JEDNORODZINNYM

Abstract

The Double Skin House concept presents an attempt at using a building's opaque double façade as a buffer zone. Due to more stable temperatures, these unconditioned areas around the building reduce heat losses during the heating season and present better overheating protection in the summer. In this concept the exterior skin protects building from the weather conditions and the interior skin gives thermal insulation. This paper presents the concept and the simulation results run in order to determine its influence on building energy demand.

Keywords: double façade, buffer zones, energy efficiency, passive house

Streszczenie

Koncepcja Double Skin House jest przykładem wykorzystania podwójnej, nieprzezroczystej fasady jako strefy buforowej w budynku. Takie nieogrzewane przestrzenie wokół budynku, ze względu na mniejsze wahania temperatury, zmniejszają straty ciepła w sezonie grzewczym oraz lepiej zabezpieczają budynek przed przegrzewaniem w lecie. W tej koncepcji zewnętrzna powłoka zabezpiecza budynek przed działaniem czynników zewnętrznych, a wewnętrzna daje właściwą ochronę cieplną. W artykule zaprezentowano koncepcję budynku oraz wyniki przeprowadzonych symulacji w celu określenia jej wpływu na zapotrzebowanie budynku na energię.

Słowa kluczowe: podwójna fasada, strefy buforowe, efektywność energetyczna, budynki pasywne

* Ph.D. Eng. Łukasz Nowak, Division of Building Physics and Computational Design Methods, Faculty of Civil Engineering, Wrocław University of Technology.

** Ph.D. Eng. Arch. Krzysztof Cebzat, Division of Environmental Development, Faculty of Architecture, Wrocław University of Technology.

*** Ph.D. Eng. Arch. Anna Bać, Division of Housing Design, Faculty of Architecture, Wrocław University of Technology.

1. Introduction

1.1. Double façades in buildings

The vast majority of studies on heat flow in the buffer zones are those of glazed double façades used in high-rise buildings. What can also be found is research into the issues of building physics of objects such as greenhouses integrated with buildings. The impact of non-ventilated, non-glazed and unheated buffer zones adjacent to exterior walls of zones with controlled air temperature is not as strongly represented as the aforementioned topic.

There can be some utility areas in a building which due to the nature of their functions, or the period of their use have lower temperature requirements. Therefore, these zones are suitable for the creation of thermal buffers which would reduce static heat loss in spaces where the maintenance of higher temperatures is obligatory. Reducing the temperature difference between the two sides of a partition decreases the heat flux between the rooms. Therefore, temperature zoning of spaces inside a building is one of the basic principles of passive constructions. It appears that locating thermal buffers, regardless of their orientation, should bring a reduction in static heat loss.

This type of solution is part of a long tradition in regional architecture. Often, regardless of the size of a cottage [1], areas exposed to extreme conditions to the north, east or west (depending on the region) were often separated and used as chambers, stores or even barns. In turn, locating glazed buffer zones in areas facing south – the equivalent of traditional porches – was to achieve greater energy gains from solar radiation. In general, the gains were greater as the surface area of glazing increased, as did its thermal resistance. Additional introduction of air circulation between the buffer zone and the interior of the heated space was to improve the energy balance of the building.

Brown and DeKay [2], and Goulding et al. [3] distinguish three variants of glazed buffer zones, which impact the indirect solar gains of a building. These solutions differ in thermal resistance of the buffer zone's exterior glazing and the interior glazing of the heated spaces.

Profits arising from the creation of this glazed buffer zone are defined as a linear function the values of which depend on:

- the difference between the computed outside and inside temperatures of the building and the heated zone respectively,
- the proportion of glazed surfaces in the outer wall of the buffer zone and the wall separating the buffer zone from the heated space, and
- the thermal resistance of the glazing.

However they do not depend on the size (volume) of the buffer zone.

Hegger et. al. [4] indicates that the static heat loss can be reduced through the use of non-ventilated and not glazed buffer zones. Energy savings depend on the location of a zone within the structure of a building, which in turn influences the calculation of outdoor temperature (the temperature in the buffer zone). The reported values of the temperature correction coefficient in the buffer zone to the outdoor temperature are as follows:

- for confined spaces above the ceiling of heated rooms – 0.8,
- for confined spaces adjacent to the walls of heated rooms – 0.5, and
- for confined spaces under floors of heated rooms (recessed into the ground) – 0.6.

Temperature correction coefficients do not depend on the orientation of the building nor was a value for the glazed buffer zones specified.

1.2. Double Skin House – concept and design features

The design premise was to have an outer skin to create a heat buffer, reducing temperature fluctuations in cold periods and protecting technical equipment (Fig. 1a). In summertime, the outer skin provides shading for the house (Fig. 1b). A buffer zone created in this way limits the daily temperature fluctuations and protects technical equipment. This translates also into a continuous thermal insulation around the residential area (no structural breaks), good air tightness and minimized appearance and influence of thermal bridges.

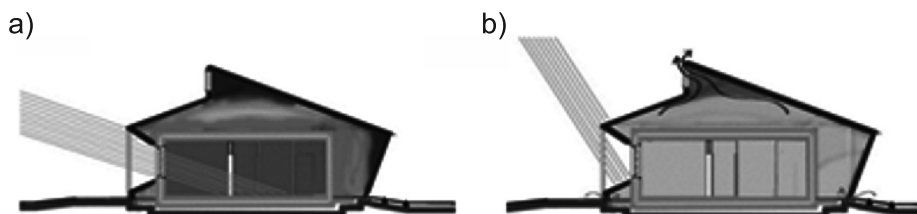


Fig. 1. Building section – buffer zone functions: a) winter heat loss reduction and passive solar gains, b) summer overheating protection [5]

Additional window niches facing south, east and west are working like shading devices, which protect from heat during summer, but provide solar gains during winter (Fig. 2). Furthermore, the roof shaped like a solar chimney and equipped with an awning window provides natural ventilation and cooling of the intermediate cavity between skins during cooling periods.

Being aware that the temperature in the space between the two shells shall not be less than that in the external environment and not more than the temperature inside the heated zone during the heating period assumes that to some extent this will limit the static heat losses of the house. By contrast, during the summer the assumption is that the opening of the outer shell should provide both a cooling effect and reasonable thermal comfort almost without the need to use air conditioning.

High energy performance standard requirements are met using double skin, both for the façades and the roof. The outer skin of the walls is made of wood – a material of low ecological cost, which is easily accessible, and can be obtained through recycling or be recycled later. The outer skin of the roof is made of metal sheets. The outer layers are presumed to protect the internal shell from weather conditions while the internal layers provide thermal insulation.

A single storey house was designed with a net area of 122.83 m², with a built-up area of 255.26 m² and an internal volume of 331.64 m³. It was functionally divided into a common open space and a private area [5]. A kitchen that opens onto a living room is conducive to the integration of its inhabitants (Fig. 2). Additionally, during warm periods of the year, a covered, louvered terrace expands the living area. The compact nature of the house, with its built-in terrace allows for the house to be placed on relatively small plots. The house

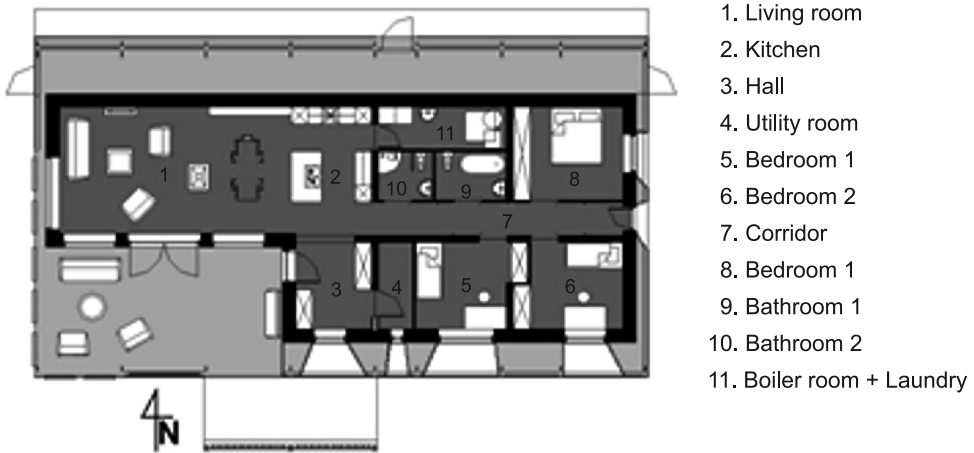


Fig. 2. Double Skin House – building plan and room layout: dark grey – residential area, light grey – buffer zones

was divided into zones based on temperature requirements: rooms necessitating the highest internal temperature (i.e. two bathrooms) were placed in the centre. The buffer located in the northern part of the house conceals a storage space. The orientation of the house toward the south facilitates the installation on its rooftop area of both solar hot water panels and solar panels for the generation of electricity. The building has a compact shape (its A/V ratio being at 0.83) and no glazing at the north façade.

1.3. Double Skin House – energy performance

The heated residential zone of the building (dark grey area in Fig. 2) was enclosed with the following partitions (each described from its outermost to its innermost layer):

- external walls ($U = 0.09 \text{ W/m}^2\text{K}$) – 1 cm cement plaster, 20 cm stone wool boards between wooden spacers, a 20 cm timber frame structure filled with stone wool, a PVC vapour barrier, an OSB and gypsum plasterboard,
- flat roof ($U = 0.07 \text{ W/m}^2\text{K}$) – 15 cm stone wool, a 30 cm timber frame structure filled with stone wool, a PVC vapour barrier, and a gypsum plasterboard,
- ground floor ($U = 0.12 \text{ W/m}^2\text{K}$) – 20 cm hard Styrofoam, a 20cm reinforced concrete slab, PVC foil, 5 cm Styrofoam elements for underfloor heating, 7 cm levelling layer, flooring.

The internal walls were also constructed around a timber frame so the thermal mass was located mainly in the ground floor slab. The buffer zone (light grey area in Fig. 2) was bounded by external walls made of 20 mm wooden facade boards ($U = 3.47 \text{ W/m}^2\text{K}$) and a roof made of trapezoidal steel sheets placed on a wooden roof construction. Windows and doors are designed to be mounted in a layer of thermal insulation; the calculated U_w values for the windows are within the 0.67–0.78 $\text{W/m}^2\text{K}$ range while the U_d values for the doors in the 0.76–0.77 $\text{W/m}^2\text{K}$ range. Glazing involves a triple pane set – 4 mm Low-E glass/14 mm Argon gap/4 mm float glass/14 mm Argon gap/4 mm Low-E glass and their properties are: $U_g = 0.6 \text{ W/m}^2\text{K}$, SHGC = 0.49 [–] and LT = 0.71 [–].

The numerical calculations for the heat flow in the construction details were performed using THERM software and the linear thermal transmittance coefficient values, Ψ_e , ranged from -0.056 to 0.025 W/mK. The high air tightness value set at $n_{50} = 0.6$ ac/h, was achieved through a minimization of structural breaks, proper window assembly and the use of vapour control membranes and appropriate sealing tapes. The house is equipped with heat recovery ventilation with 90% efficiency.

A house designed in such a way fulfils the requirements of the so-called NF15 standard [7]. In order to be deemed in compliance with the National Fund for Environmental Protection and Water Management an object must maintain the usable energy demand index (EA) for heating and ventilation at a level below 15 kWh/m²a [6]. The EA index for this particular building, calculated according to Polish energy performance certification (EPC) calculation regulations [7] for the Wroclaw location, equals 13.97 kWh/m²a.

2. Analyzed building cases in energy simulations

The building was located in Wroclaw (TMY weather data was used) and had heating system temperatures set to 24°C in bathrooms and to 20°C in other rooms (there was no air conditioning system in the building). The mechanical ventilation air flow rate was at 0.6 [ac/h] and the heat recovery efficiency was at 90%. The air tightness of the heated zone partitions was set as a passive building standard at $n_{50} = 0.6$ [ac/h]. Two design cases were analyzed (Fig. 3):

Case 1 – a building with a single skin façade (i.e. only an internal skin with thermal insulation), where the heat loss through the building envelope was calculated as for the external environment; in order to maintain the same shading conditions window overhangs and sidefins were modelled on the case of the double skin façade.

Case 2 – a building with a double skin façade (i.e. an internal skin with thermal insulation and an external skin made of wooden panels and a steel roof), which means that the heat loss through the building envelope was calculated for unconditioned buffer zones, taking into account that the double façade thickness varies from 0.3 to 1.6 m. The unheated buffer zones were modelled as cavities, so they were ventilated by the infiltrating outside air and gained heat from adjacent internal partitions. The air tightness of the external skin was set low at $n_{50} = 10.0$ [ac/h], due to its construction (wooden and steel panels only). There was also

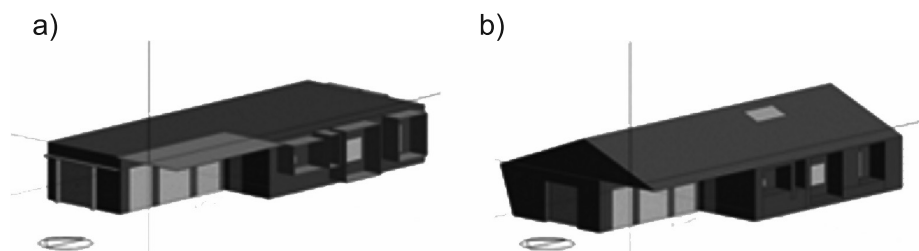


Fig. 3. Analyzed building cases: a) Case 1 – single skin, shading, no buffer zones, b) Case 2 – double skin, shading and unconditioned buffer zones

a roof window which was set as opened in the summer and closed in the winter. Shading conditions were the same as in Case 1.

Both cases were analyzed by two different methods: Method 1 – calculations according to Polish EPC regulations, Method 2 – DesignBuilder software simulations (ver. 3.2.0.073).

3. Results

3.1. Usable energy demand index – EA

The results from energy simulations (Method 2) were compared with previously made EPC calculations (Method 1) with and without buffer zones being taken into account. The changes in the usable energy demand EA indices, calculated for a Wroclaw location, are at a 2% level for the EPC method and at a level of 8 % for simulations in favour of cases with buffer zones. There are also visible differences due to the method of calculation, but there is need for further testing if Method 2 is more reliable. Some of the energy simulation knowledge resources [8], indicate that there should be an increase of between 5% to 20% of energy savings due to using buffer spaces, thus the results obtained by simulations look appropriate.

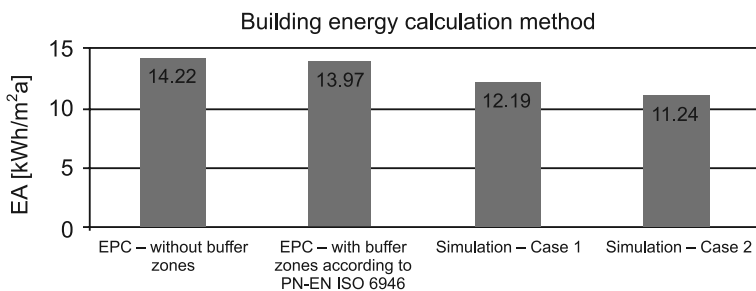


Fig. 4. Usable energy index for heating and ventilation purposes according to calculation method: EPC – energy performance certificate, Simulation – DesignBuilder software

3.2. Air temperatures

Besides slightly better energy performance of buildings incorporating a buffer zone, the other important reason for using them is their ability to stabilize air temperatures. This should mean less heat loss in the winter and less overheating (lower inside air temperatures) in the summer. According to the air temperature charts in the sample winter week (Fig. 5), the air temperature in the buffer zone is 2–3°C higher than the outside air temperature. This has significant influence on lowering the inside air temperature fluctuations connected with heating system specificity.

Looking at the air temperature charts in the summer week (Fig. 6), it can be observed that Case 2 (building with buffer zones) can have up to a 2.5°C (average 1°C) lower inside air temperature compared to Case 1 (building without buffer zones). The thermal buffer effect

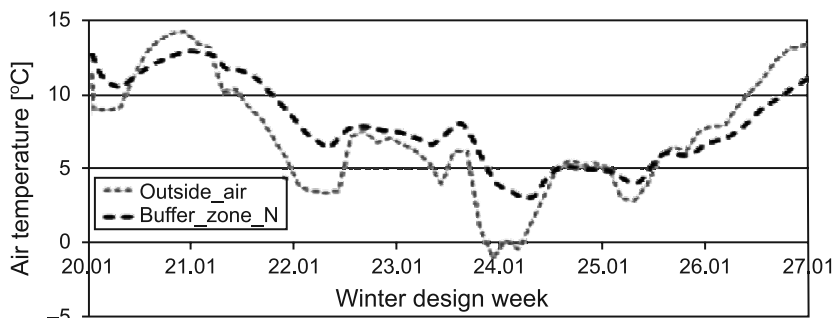


Fig. 5. Air temperatures in the buffer zone from the north side during a winter week (20–26th January)

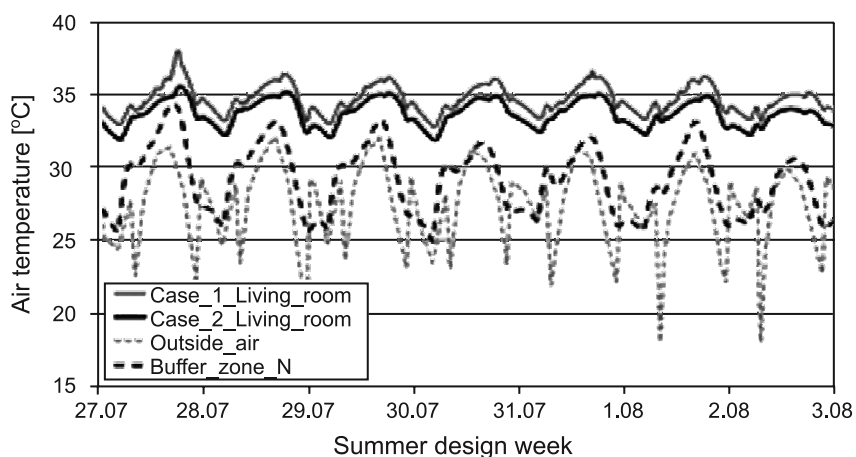


Fig. 6. Air temperatures in living room facing the south and in the adjacent buffer zone from the north side during a summer week (27th June–3rd August)

and scheduled natural ventilation in the summer, which rejects warm air from the space between the skins, reduces the temperatures (mainly the peak ones), even in the rooms facing south.

3.3. Future plans – in situ measurements

Further research will be focused on attempting to measure the value of the heat flow in the buffer zones of buildings: both in the existing building, as well as in matching computer models designed to obtain empirical data. It is assumed that the first step is the measurement of an existing single-family residential building. The building is a single storey, occupied, single-family house, built with timber frame technology. The buffer zone is a greenhouse with western exposure, with the outer wall and the greater part of the roof glazed (wall – openable windows and solid roof – polycarbonate). The measurement will be carried inside

the building's heated zone (with temperature and humidity sensors), in the buffer zone (measuring temperature and humidity) and outside with weather data station (air temperature, humidity, wind speed and direction and solar irradiation measurement).

4. Conclusions

The use of buffer zones gives real benefits in terms of noticeable influences on the energy performance of buildings. Even when there are no glazed areas in the exterior skin (the outside façade), the more stable temperatures of unheated thermal buffers lead to less heat loss through building fabric in the heating season and give slightly better overheating protection in the summer. Nevertheless, there is a need to conduct further evaluation of this design combined with other factors such as natural ventilation scheduling and thermal mass in order to achieve better results. Also, as mentioned earlier, planned in situ measurements of collected values will be compared with simulation models to obtain an optimal modelling approach of such buffer zones.

Building regulations, which are currently being implemented, aim towards near-zero energy demands, and are a serious challenge for modern architecture of both small and of large scale objects. Solutions presented in the design of the Double Skin House concept are an original reaction to the demand for a modern energy-efficient house, allowing for widely understood comfort of use (functional, spatial and climatic) and low maintenance costs [5].

Architecture of the proposed house conforms to the energy efficiency and minimal energy consumption, manifesting in the selection of building materials and a simple, compact volume which can easily be adapted for a specific site as well as the needs of the investor, changing over the years.

Design Team: architecture: grupa synergia: Cebzat K., Bać A. energy performance: Nowak Ł.; structure: Miś G., cost estimation: Fantaziński S., visualizations: Stec W., graphical layout: Gałwiaczek A.. The Double Skin House project received an honorable mention of Isover, a sponsor in the Murator competition for Energy Efficient Affordable Houses 2013.

References

- [1] Bogusz W., *Projektowanie architektoniczne i budownictwo regionalne*, WSiP, Warszawa 1996.
- [2] Brown G.Z., DeKay M., *Sun, wind, light. Architectural design strategies*, John Wiley & Sons, New York 2001.
- [3] Goulding J.R., Lewis O., Steemers T.C., *Energy in architecture. The European passive solar handbook*, B.T. Batsford, London 1992.
- [4] Hegger M., Fuchs M., Stark T., Zeumer M., *Energy manual. Sustainable architecture*, Birkhauser 2008.
- [5] Bać A., Cebzat K., Nowak Ł., *Double Skin House – propozycja rozwiązania dla dostępnych domów blisko-zeroenergetycznych*, [In:] *Kierunki rozwoju budownictwa energooszczędnego*

i wykorzystania odnawialnych źródeł energii na terenie Dolnego Śląska, (ed.) A. Bać, J. Kasperski, Oficyna Wydawnicza Politechniki Wrocławskiej, Wrocław 2013, 215-224.

- [6] www.nfosigw.gov.pl/gfx/ees/userfiles/files/inteligentne_sieci_energetyczne/wytyczne_do_programu_domow_energooszczednych.pdf – 13.03.2014.
- [7] Dz. U. 2008, Nr 201, poz. 1240, Rozporządzenie Ministra Infrastruktury z dnia 6 listopada 2008 r. w sprawie metodologii obliczania charakterystyki energetycznej budynku stanowiącej samodzielną całość techniczno-użytkową oraz sposobu sporządzania i wzorów świadectw ich charakterystyki energetycznej.
- [8] www.designbuilder.co.uk/helpv3.2/#solar_technology_solutions.htm?Highlight=passivesolar – 13.03.2014.

KATARZYNA NOWAK-DZIESZKO*, JACEK DĘBOWSKI*

INFLUENCE OF THE THERMAL MODERNIZATION OF PANEL BUILDINGS ON TRANSMISSION HEAT LOSSES

ANALIZA WPŁYWU TERMOMODERNIZACJI BUDYNKU WIELKOPLYTOWEGO NA STRATY CIEPŁA PRZEZ PRZENIKANIE

Abstract

It is commonly known that the thermal modernization of existing buildings reduces the energy requirements for heating. In the last twenty years many large panel blocks of flats built in the sixties and seventies have been insulated. In one example of an 11-storey building the heating energy demand before and after thermal modernization was analyzed. The transmission heat losses before and after thermal modernization, including the thermal bridges simulated in AnTherm program, were included in the calculations.

Keywords: large panel buildings, W-70 system, thermal modernization, system joints

Streszczenie

Powszechnie wiadomo, że zabiegi termomodernizacyjne istniejących budynków prowadzą do redukcji zużycia energii na cele ogrzewania. W ostatnich kilkudziesięciu latach tymże zabiegom poddano tysiące budynków wielorodzinnych wzniesionych w technologii wielkiej płyty w latach 60. i 70. XX wieku. W artykule przeanalizowano redukcję zużycia energii na cele grzewcze przed i po termomodernizacji, na przykładzie 11-piętrowego budynku wielorodzinnego. W obliczeniach uwzględniono straty przez przenikanie obudowy budynku, z uwzględnieniem występowania mostków cieplnych, których analizę przeprowadzono z użyciem programu AnTherm.

Słowa kluczowe: budynki wielkopłytowe, system W-70, termomodernizacja, połączenia systemowe

* M.Sc. Eng. Katarzyna Nowak-Dzieszko, Ph.D. Eng. Jacek Dębowski, Institute of Building Materials and Structures, Faculty of Civil Engineering, Cracow University of Technology.

1. Prefabricated buildings in Poland

In the nineteen-fifties, the erection of large panel-system buildings began in Poland. Over the following decades about 4 million flats were built in this way. The thermal insulation of these buildings was low and the seasonal heating energy demand was usually 50% higher than the national requirements [1]. In the eighties, loans for removing the technological defects were taken out and the subsidization of energy prices was ended. At the beginning of the nineties, the Building Research Institute started to tackle thermal modernization issues. As a result of the Act on Supporting Thermo-insulation Works, December, 1998 [3], investment loans covering projects reducing heating energy demands become available. It was the beginning of extensive thermal modernization of panel buildings.

At present more than 10 million Poles live in these buildings. That is the main reason why thermal modernization problems became so prevalent.

2. W-70 System

System W70 is the “open” system used for the erection of multi-family buildings, in which, contrary to the “closed” system, all construction walls within the flats were eliminated. It allowed for changes of the partition wall pattern and therefore enabled the design of flats with different areas and room arrangements. It is estimated that about 15% of all panel-system buildings were erected using this system.

Prefabricated system elements were made of B15 crushed gravel concrete, while the connection joints used concrete of at least B15 grade. The elements were reinforced with welded wire meshes made of steel, grade 34GS, 18GS, St0 or St0S. As thermal insulation for the multi-layer external walls, a layer of Styrofoam “15” or mineral wool “120”, 4 to 6 cm thick was used.

Regarding the building envelope, during the design process and the initial construction stages, PN-64/B-03404 [6] was the applicable standard. Based on this standard (depending on climate zone) the maximum permissible thermal transmittance coefficients were $k = 1.25 \text{ W/m}^2\text{K}$ and $k = 1.42 \text{ W/m}^2\text{K}$ (this coefficient is now denoted as “ U ”). In the nineteen-eighties, the new standard PN-82/B-02020 [7] reduced the value to $k = 0.75 \text{ W/m}^2\text{K}$. The next revision, standard PN-91/B-02020, limited the value to $k = 0.55 \text{ W/m}^2\text{K}$.

Per the current national standard [1,2] since 1st of January the max. U value of external walls should not exceed $U = 0.25 \text{ W/m}^2\text{K}$ (since the end of 2013, the max. U value has been $U = 0.3 \text{ W/m}^2\text{K}$). The European Energy Performance of Buildings Directive Recast states that buildings designed and modernized after 2020 should be zero-energy buildings. According to those regulations, after 1st of January 2021 the thermal transmittance U of the heated building components should not exceed $0.20 \text{ W/m}^2\text{K}$.

Based on the information above, it can be concluded that none of the panel system buildings would meet the current thermal requirements. However, those requirements can be met after specific thermal modernization such as: additional insulation of the walls, replacing the windows, insulation of the roof and the ceiling above the basement, as well as the modernization of heating and ventilation systems.

3. Description of the analyzed building

The analyzed multi-family building, built using the W70 system, is located in the Krowdrza district of Cracow, and has been used since 1974 (Fig. 1)

Building description:

1. Number of storeys: 11.
2. Dimensions: 21.5 m × 13.2 m.
3. Area: 2279 m².
4. Basement below entire building.
5. Flat roof.
6. Depth of building below ground: 2.5 m.
7. Ground floor 1.0 m above surrounding ground



Fig. 1. North and East elevations of analyzed building

According to the building administrator, for the first 30 years of the building's life no thermal modernization has been carried out.

In 2004 and 2005 the windows in all apartments were replaced. The new ones have a thermal transmittance of between 1.5 and 1.8 W/m²K. In 2006, partial thermal modernization of the building was carried out; the external walls were insulated with 10 cm of Styrofoam (thermal conductivity $\lambda = 0.04$ W/m²K). The applied solutions were not complex, as the roof and the ceiling above the unheated basement were not insulated. So far none of the installed systems have been modernized.

4. Analysis of transmission heat losses through the building envelope

In the empirical analysis the transmission losses through the building envelope, before and after thermal modernization, were taken into consideration, with a particular emphasis on the influence of panel joints which act as additional thermal bridges and affect the value of transmission losses.

Figure 2 shows joints between prefabricated panels; Fig. 3 shows additional thermal losses through the panel connections, and Fig. 4, temperature distribution in the connections based on computer analysis.



Fig. 2. Panel connection joint – external view

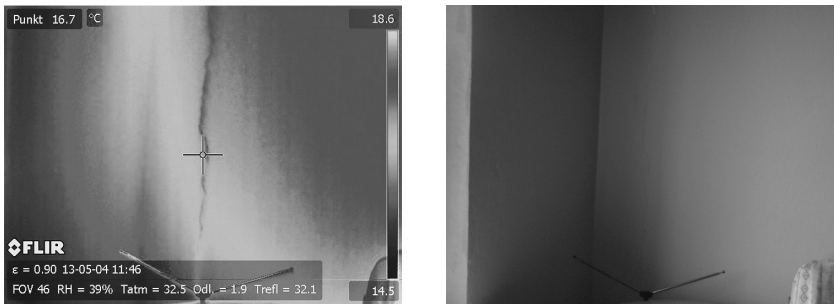


Fig. 3. Thermogram with additional thermal losses at panel joint

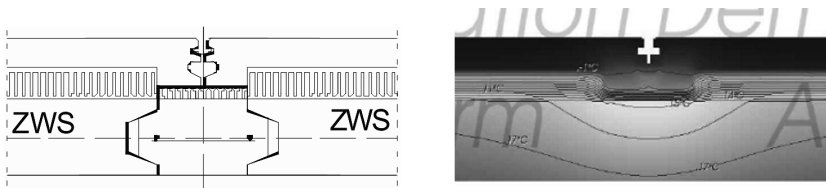


Fig. 4. Panel joint. Temperature distribution in the panel connection (from AnTherm program)

Based on standard EN ISO 13789 [5] and [9], the heat transfer by transmission coefficient H_{tr} was calculated. It describes the transmission losses through the building envelope. The ventilation losses were omitted in the analysis as the ventilation system has not been modernized.

$$H_{tr} = \sum_i \left[b_{tr,i} \cdot \left(A_i \cdot U_i + \sum_j l_j \cdot \psi_j \right) \right], \quad [\text{W/K}]$$

where:

- b_{tr} – coefficient describing reduction of temperature difference [non-dimensional]
- A_i – area of the building component i [m²],
- U_i – thermal transmittance of the specific i component [W/m²K],
- l_i – length of linear i thermal bridge [m],
- Ψ_i – linear thermal transmittance of thermal bridge [W/mK].

Thermal transmittances of all building components were calculated based on standard PN-EN 6946 [8] – Table 1: values of linear thermal transmittances based on computational analysis in AnTherm (Table 2).

Table 1

Thermal transmittances of building components

Building component	U [W/m ² K] before thermal modernization	U [W/m ² K] after thermal modernization
External walls	0.69	0.25
Roof	0.50	0.50
Ceiling above basement	0.35	0.35
Windows	2.80	1.40
Entrance door	2.80	1.80

Table 2

Linear thermal transmittances for different thermal bridges

Description of thermal bridge	Ψ_e – before thermal modernization	Ψ_e – after thermal modernization
Window frame in the curtain wall – window head	0.047	0.007
Window frame in the curtain wall – window sill	0.205	0.089
Horizontal connection of curtain wall with ceiling slab	0.293	0.029
Horizontal connection of gable with ceiling slab	0.276	0.029
Vertical connection of curtain wall and basement wall with floor slab	0.160	0.200
Balcony slab and external wall	0.764	0.253
Balcony slab with balcony door and external wall	1.034	0.315
Vertical connection of gable with internal partition wall	0.169	0.019
Vertical connection of curtain wall with internal partition wall	0.198	0.020

The heat transfer coefficient was calculated for five different stages of the building's modernization. All results are presented in Table 3.

Table 3

Heat transfer by transmission coefficient for different calculation steps

	Modernization stage	Htr [W/K]	Share of transmission losses through the building envelope $A_i U_i$ in H_{tr}	Share of losses through thermal bridges $\Sigma l_i \psi_i$ in H_{tr}
1	Building before thermal modernization	3490.6	2091.0 (60%)	1399.6 (40%)
2	Building before thermal modernization with windows replaced	2995.8	1596.2 (53%)	1399.6 (47%)
3	Building with existing windows but with insulated external walls	2047.7	1771.0 (84%)	276.7 (14%)
4	Building with windows replaced and with insulated external walls	1419.2	1142.5 (80%)	276.7 (20%)
5	Building with windows replaced and with insulated external walls – U of external walls 0,20 W/m ² K, as per standard that will be in force from 1st of January 2021	1014.9	808.0 (80%)	206.9 (20%)

The conclusions based on the results listed in Table 3 are as follows:

- Both replacing the windows and the insulation of the external walls significantly reduced the value of the heat transfer by transmission coefficient from 3490.6 [W/K] to 1419.2 [W/K], i.e. by almost 60%.
- Replacement of windows and doors lessened the transmission losses by about 15%, while the insulation of external walls alone decreased the H_{tr} value by about 40%. This proves that insulating the walls is a more effective measure.
- The insulation of the external walls significantly decreased the transmission losses due to thermal bridges from 1399.6 [W/K] to 276.7 [W/K]; an 80% decrease compared with the building as originally designed. The tight insulation layer closes the connection joints between panels.
- Comparing percentage share of losses through thermal bridges in the insulated building with the original windows and with the replacement windows (steps 3 and 4), the influence of thermal bridges is higher when the windows are replaced (14% in step 3 and 20% in step 4). It proves that the influence of thermal bridges is greater after complex thermal modernization.
- Thermal modernization of the building to the 2021 standard would lower the thermal losses in the already insulated building by a further 30%. In the case of buildings which have yet to undergo any thermal modernization processes, a decrease of transmission losses of almost 80% could be expected.

5. Actual energy consumption for heating

In the period of time between 2000 and 2008 the monitoring of energy use for heating was carried out by the building administrator. The results are presented in Table 4 and confirm the reduction of heating costs after thermal modernization.

Replacing the windows in 2004 and 2005 reduced amount of energy usage by about 20%, while the insulation of external walls, conducted in 2006, reduced this by a further 20%. The percentage values cannot be compared with the calculation results as real energy demand is also affected by ventilation and infiltration losses.

Table 4

Energy consumption for heating in the analyzed building

Year	Heating costs of the building [zł/year]	Energy usage in GJ
2000	71350	1615
2001	70751	1558
2002	71065	1569
2003	76095	1736
2004	64850	1476
2005	61912	1263
2006	56344	1077
2007	51553	988
2008	50220	962

6. Conclusions

Based on the conducted analysis it can be concluded that both the replacement of windows and the insulation of walls significantly improved the building's energy parameters, reducing transmission losses by up to 70%. The calculation results are confirmed by the monitoring of energy consumption in the analyzed building.

In the case of large panel buildings, the insulation of external walls significantly lessens the influence of thermal bridges as it tightens the building envelope.

In this analysis, only the modernization of the building's external walls was taken into consideration. Additional reductions in heat loss could be achieved by the modernization of the ventilation system and the insulation of the roof and the ceiling above the basement.

References

- [1] Rozporządzenie Ministra Infrastruktury w sprawie warunków technicznych, jakim powinny odpowiadać budynki i ich usytuowanie z dnia 12 kwietnia 2002.
- [2] Rozporządzenie Ministra Transportu, Budownictwa i Gospodarki Morskiej z dnia 5 lipca 2013 r. zmieniające rozporządzenie w sprawie warunków technicznych, jakim powinny odpowiadać budynki i ich usytuowanie (Dz. U. z 13 sierpnia 2013 r., poz. 926).
- [3] Ustawa z dnia 18 grudnia 1998 r. o wspieraniu przedsięwzięć termomodernizacyjnych (Dz. U. Nr 162, poz. 1121, z późn. zm.)
- [4] Ostańska A., *Wpływ dotychczasowych termomodernizacji budynków mieszkalnych na oszczędność energii i planowanie programów rewitalizacji na przykładzie jednego z lubelskich osiedli*, Budownictwo i Architektura 7, 2010, 89-103.
- [5] EN ISO 13789 Thermal performance of buildings – Transmission and ventilation heat transfer coefficients – Calculation method.
- [6] PN-64/B-03404 – Współczynnik przenikania ciepła K dla przegród budowlanych.
- [7] PN-91/B-02020 – Ochrona cieplna budynków. Wymagania i obliczenia.
- [8] PN-EN 6946 Building components and building elements. Thermal resistance and thermal transmittance. Calculation method.
- [9] Rozporządzenie Ministra Infrastruktury w sprawie metodologii obliczania charakterystyki energetycznej budynku i lokalu mieszkalnego lub części budynku stanowiącej samodzielną całość techniczno-użytkową oraz sposobu sporządzania i wzorów świadectw ich charakterystyki energetycznej z dnia 6 listopada 2008 roku.

KATARZYNA NOWAK-DZIESZKO*, MAŁGORZATA ROJEWSKA-WARCHAŁ*

INFLUENCE OF SHADING SYSTEMS ON THE MICROCLIMATE CONDITIONS IN LARGE PANEL BUILDINGS

WPLYW ZACIENIEŃ NA WARUNKI MIKROKLIMATU W BUDYNKU WIELKOPŁYTOWYM

Abstract

The thermal comfort conditions of multi-family buildings, including large panel buildings, are rarely analyzed. Simulations of large panel buildings conducted by authors in the Design Builder program show very unfavorable microclimate conditions in buildings after thermal modernization. The simulation results of the influence of internal and external shadings on the thermal comfort of dwellings in multi-family large panel building are presented in this article.

Keywords: large panel building, internal and external shading system, thermal comfort of the panel buildings, PMV (Predicted Mean Vote), PPD (Predicted Percentage of Dissatisfied)

Streszczenie

Warunki komfortu cieplnego wielorodzinnych budynków mieszkalnych, w tym budynków wielkopłytowych, są analizowane bardzo rzadko. Symulacje budynków wielkopłytowych przeprowadzone przez autorów w programie Design Builder wykazały bardzo niekorzystne warunki mikroklimatu w budynkach po termomodernizacji. W artykule przedstawiono wyniki symulacji wpływu zacienień wewnętrznych oraz zewnętrznych na komfort cieplny lokali mieszkalnych w wielorodzinnym budynku wielkopłytowym.

Słowa kluczowe: budynek wielkopłytowy, zacienienia zewnętrzne i wewnętrzne, komfort cieplny w budynkach wielkopłytowych, PMV, PPD

* M.Sc. Eng. Katarzyna Nowak-Dzieszko, M.Sc. Eng. Małgorzata Rojewska-Warchał, Institute of Building Materials and Structures, Faculty of Civil Engineering, Cracow University of Technology.

1. Description of problem

In considering and designing thermal modernization, no one takes into consideration the thermal comfort and overheating issues which seem to be very important from the occupants' point of view. The thermal modernization of the large panel buildings is usually limited to the insulation of external walls and the replacement of windows, which significantly reduces the energy demand. Unfortunately, those treatments negatively affect the microclimate conditions inside buildings. The modernization process should be more complex and solutions for reducing the problem of overheating should be taken into consideration. The usage of internal and external shading was analyzed based on the simulations conducted in the Design Builder program.

Analysis of thermal comfort is based on international standard PN-EN ISO 7730 "Ergonomics of the thermal environment. Analytical determination and interpretation of thermal comfort using calculation of the PMV and PPD indices and local thermal comfort criteria" [1].

2. Description of analyzed building

Conducted simulations allowed the influence of internal and external shadings on the thermal comfort in the particular parts of the analyzed five-storey large panel building to be analyzed. The simulations were conducted for a part of a W70 multi-family panel building – basement below entire building, flat roof. Visualizations of different building elevations are presented in Fig. 1.

The building has natural ventilation and a central heating system with convection heaters. There is a communication area located in the central part of each building level. In the analyzed part of the building, there are three flats on every level. Exterior walls made of prefabricated panels in the W70 system, insulated with 15 cm of styrofoam with plasters at both sides: $U = 0.20$ [W/m^2K], double glazed windows: $U = 1.5$ [W/m^2K].



Fig. 1. South-east and south elevations of analyzed building

The calculations were carried out in the Design Builder v.3. This program has been specifically developed around Energy Plus allowing the simulation of the building envelope and building interiors. The simulations conducted for the Polish climatic conditions (building located in Cracow) allowed for the evaluation of the microclimate conditions of the entire building as well as of particular dwellings.

3. Simulation settings

The main aim of simulations was to determine the temperature and PMV index of the particular flats at different elevations during the summer months. Figure 2 presents a typical arrangement of dwellings on the building storey.

Every single flat was modeled as a separate thermal comfort zone due to the small usage area of different flats. It was assumed that the doors between rooms are usually opened. Three different flats were analyzed:

1. Flat M1 – usage area 56 m², balcony at south elevation.
2. Flat M2 – usage area 31 m², balcony at south elevation.
3. Flat M3 – usage area 36 m², balcony at east elevation.

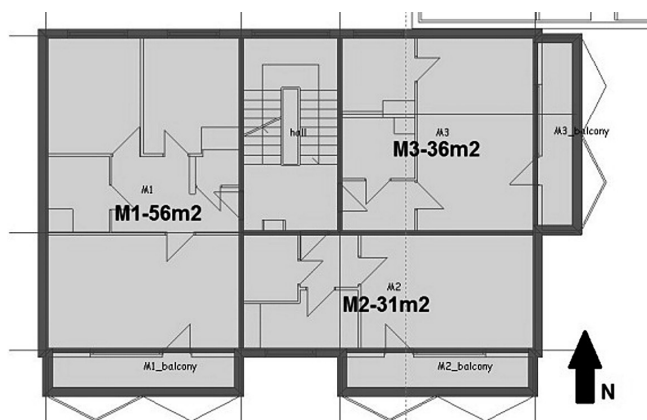


Fig. 2. Typical zones' visualization at every building level

According to the recast to the European Energy Performance of Buildings Directive, buildings designed and modernized after 2021 should be zero-energy buildings. In connection with those provisions, since 1st of January 2014, the new requirements regarding building envelope thermal insulation were introduced in Warunki Techniczne 2013 [4]. According to those regulations, thermal transmittance U of the heated building components cannot exceed 0.25 W/m²K and after 1st of January 2021, 0.2 W/m²K.

The starting point for further analyzes was the simulation of the building with the external walls modernized to the standard being in force since 2021.

The assumptions for the simulations:

1. Heating system on from September to March (22°C), 7 days a week, 24 hours a day.
2. Occupancy density: flats – about 1 person per 15 m²,
3. Operating schedule: flats – 100% occupancy density between 4 pm and 7 am, 5 days a week; between 6 pm and 9 am at the weekends; 50% reduced occupancy between 9 am and 6 pm.
4. Metabolic activity: 1.2 met, winter clothing – clo = 1.0, summer clothing clo = 0.5.
5. Ventilation requirements per polish national standards PN-83/B-03430 [2], in every flat 70 m³/hour for kitchens and 50 m³/hour for bathrooms.

Table 1 presents the number of discomfort hours in the analyzed period of time between 15th of May and 15th of September hours in all analyzed dwellings on different levels. In this particular period of time in Poland, there is the highest risk of overheating.

Table 1

Number of discomfort hours for all analyzed flats at different levels

		Number of overheating hours
M1	1st level	946
	2nd floor	1235.5
	3rd floor	1477
	4th floor	1746.5
M2	1st level	1391.5
	2nd floor	1916
	3rd floor	2225.5
	4th floor	2392
M3	1st level	1377
	2nd floor	1718
	3rd floor	1985
	4th floor	2153.5

The worst thermal conditions can be observed on the fourth level in flat M2 at the south-east corner of the building. The total number of hours in the analyzed period of time is 2952 which means that for more than 80% of hours in flat M2, temperatures are above the acceptable value of 25°C. Those conditions are very uncomfortable for the occupants. In practice, those hours are being lessened by night cooling of the internal space through the opening of windows. At the lowest levels however, due to security reasons, this kind of solution cannot be used widely.

In many flats, occupants use the internal shading systems (shading panels) to decrease the solar gains. In the next step of simulations, the influence of internal shadings on the microclimate conditions was analyzed.

Figures 3a and 3b present the number of overheating hours for flat M2 at different levels with and without internal shading. The number of discomfort hours decreased as follows:

- at the first floor – from 1391 to 1307 – 6% decrease,
- at the second floor – from 1916 to 1829 – 5% decrease,
- 3rd floor – 2225 to 2126 – 4% decrease,
- 4th floor – 2392 to 2348 – only 2% decrease.

Internal shading systems only slightly decreased the number of overheating hours.

The next step of simulating the external shading system consisted of four steel louver blades (width 20 cm) covering 1m height of all windows. This solution again improved the thermal comfort conditions and decreased the number of overheating hours. Table 2 shows the number of overheating hours in three simulation steps.

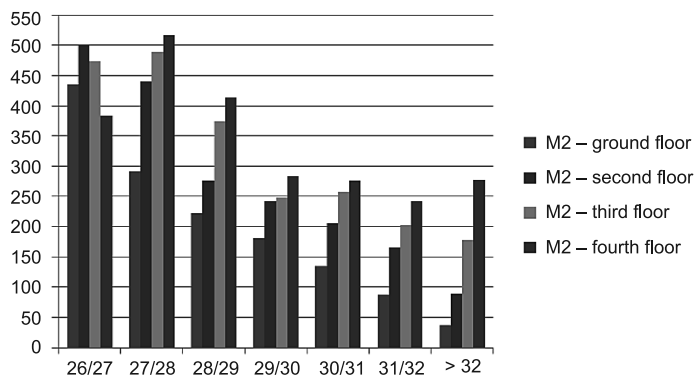


Fig. 3a. Number of overheating hours for flat M2 at different levels – without any shading

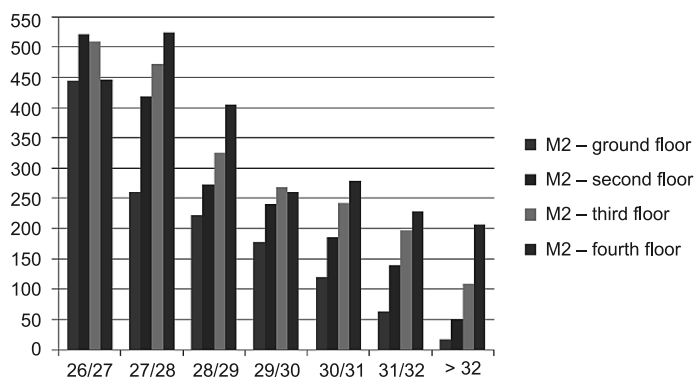


Fig. 3b. Number of overheating hours for flat M2 at different levels – with internal shading

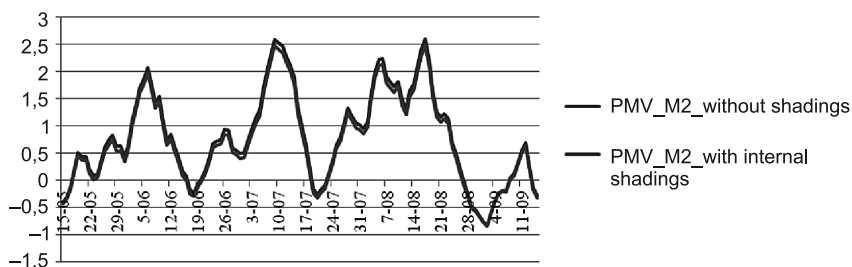


Fig. 4. PMV comfort indexes for flat M2 without any shading and with internal shading system

In case of flat M2 on the fourth floor, the number of discomfort hours was lessened by a further 2%, which gives a total decrease of only 4% from 2392 to 2304.

The most significant improvement of thermal conditions, about 14% decrease of discomfort hours from 1235.5 to 1064, can be noticed in flat M1 due to the biggest usage area of this particular flat. However, this is still not a considerable improvement compared to the installation cost of external shading systems.

Number of discomfort hours for all analyzed flats without any shading, with internal shading and with both internal and external shading systems

		Number of discomfort hours – without any shadings	Number of discomfort hours – with internal shadings	Number of discomfort hours – with internal and external shadings
M1	1st level	946	891,5	836,5
	2nd floor	1235,5	1135,5	1064
	3rd floor	1477	1388,5	1314
	4th floor	1746,5	1656,6	1581,5
M2	1st level	1391,5	1307,5	1218
	2nd floor	1916	1829,5	1727
	3rd floor	2225,5	2126	2055,5
	4th floor	2392	2348	2304
M3	1st level	1377	1305	1246
	2nd floor	1718	1638,5	1572,5
	3rd floor	1985	1916	1852,5
	4th floor	2153,5	2081	2038,5

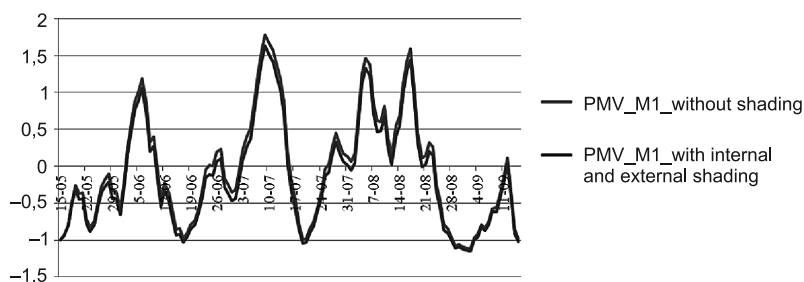


Fig. 5. PMV comfort indexes for flat M1 without any shadings and with internal and external shading systems

4. Conclusions

The results of the conducted analysis show that the microclimate conditions in all flats of the building after thermal modernization are very uncomfortable and the parameters describing thermal comfort exceed the acceptable values. Using different shading systems, internal and external ones, only slightly reduce the number of overheating hours during summer months. The smaller the usage area of the analyzed dwelling, the lower the reduction of discomfort hours.

The work reported in this paper has been partially funded by the project L-1/116/DS/2013.

References

- [1] PN-EN ISO 7730 Ergonomics of the thermal environment. Analytical determination and interpretation of thermal comfort using calculation of the PMV and PPD indices and local thermal comfort criteria.
- [2] PN-83/B-03430 Wentylacja w budynkach mieszkalnych zamieszkania zbiorowego i użyteczności publicznej – Wymagania.
- [3] Rozporządzenie Ministra Infrastruktury z dnia 12 kwietnia 2002 w sprawie warunków technicznych, jakim powinny odpowiadać budynki i ich usytuowanie (Dz.U. nr 75, poz. 690 z późn. zm. ogłoszonymi w Dz.U. z 2003 r. Nr 33, poz. 270, z 2004 r. Nr 109, poz. 1156, z 2008 r. Nr 201, poz. 1238, z 2009 r. Nr 56, poz. 461, z 2010 r. Nr 239, poz. 1597, z 2012 r. poz. 1289 oraz z 2013 r., poz. 926).
- [4] Rozporządzenie Ministra Transportu, Budownictwa i Gospodarki Morskiej z dnia 5 lipca 2013 r. zmieniające rozporządzenie w sprawie warunków technicznych, jakim powinny odpowiadać budynki i ich usytuowanie (Dz.U. z 13 sierpnia 2013 r., poz. 926).
- [5] Nowak K., *Modernizacja budynków a komfort cieplny pomieszczeń*, Energia i Budynek, 29-33.
- [6] Dębowski J., *Cała prawda o budynkach wielkopłytowych*, Przegląd budowlany 9/2012.
- [7] Nowak K., Nowak-Dziesko K., Rojewska-Warchał M., *Thermal comfort of the rooms in the designing of commercial buildings*, Research and Applications in Structural Engineering, Mechanics and Computation, SMEC Cape Town 2013, 651-652.

KATARZYNA NOWAK-DZIESZKO*, MAŁGORZATA ROJEWSKA-WARCHAŁ*

SIMULATION ANALYSIS OF MICROCLIMATE CONDITIONS IN A MULTI – FAMILY LARGE PANEL BUILDING

ANALIZA SYMULACYJNA WARUNKÓW MIKROKLIMATU W WIELORODZINNYM BUDYNKU WIELOPŁYTOWYM

Abstract

When analyzing large panel buildings, it is very rare to take into consideration the requirements connected with the overheating effect. This issue is closely related to the thermal comfort of the building, especially during the summer months. Based on the simulations conducted in the Design Builder program, the authors determined the influence of building orientation, individual flat location and thermal insulation on the thermal comfort of the different flats of a large multi-family panel building.

Keywords: large panel building, thermal comfort of the panel buildings, PMV (Predicted Mean Vote), PPD (Predicted Percentage of Dissatisfied)

Streszczenie

W analizie budynków wielopłytowych bardzo rzadko uwzględnia się problem przegrzania pomieszczeń. Problem ten jest ściśle związany z komfortem cieplnym budynku, szczególnie w miesiącach letnich. W oparciu o symulacje przeprowadzone w programie Design Builder autorzy określili wpływ orientacji, lokalizacji poszczególnych lokali oraz termomodernizacji na komfort cieplny w mieszkaniach wielopłytowego budynku wielorodzinnego.

Słowa kluczowe: budynek wielopłytowy, komfort cieplny w budynkach wielopłytowych, PMV, PPD

* M.Sc. Eng. Katarzyna Nowak-Dzieszko, M.Sc. Eng. Małgorzata Rojewska-Warchał, Institute of Building Materials and Structures, Faculty of Civil Engineering, Cracow University of Technology.

1. Description of problem

Based on statistical information, about 4 million flats in Poland are made of prefabricated elements in different systems. Moreover, almost a quarter of Poles live in large system panel buildings. That is why the issues related to this subject are very important and common. The most important aspect is the improvement of the building energy certificate of those buildings. It is connected with the thermal modernization of the building envelope.

Unfortunately, when considering and designing the thermal modernization, no one takes into consideration the thermal comfort and overheating issues which seems to be very important from the occupants' point of view. The average usable area of dwelling in a prefabricated building is about 55 m² and the average number of occupants is 4, which gives less than 15 m² for one person [8]. It makes those issues even more essential.

2. Thermal comfort

Thermal comfort is related to the thermal balance of the body which is affected by different parameters: personal and environmental such as human activity; clothing insulation; environmental parameters (air temperature, average radiation temperature, air flow speed and relative humidity). These factors make up what is known as the 'human thermal environment'. Evaluation of thermal comfort is based on the PMV (Predicted Mean Vote) and PPD (Predicted Percentage of Dissatisfied) indexes.

International standard PN-EN ISO 7730 (Ergonomics of the thermal environment. Analytical determination and interpretation of thermal comfort using calculation of the PMV and PPD indices and local thermal comfort criteria) uses Fanger's method to estimate thermal comfort. The Predicted Mean Vote (PMV) model stands among the most recognized thermal comfort models. It was developed using principles of heat balance and experimental data collected in a controlled climate chamber under steady state conditions. Fanger's method combines the following environmental features: air temperature, air velocity, mean radiant temperature and relative humidity and two personal variables (clothing insulation and activity level) into the index that can be used to predict the average thermal sensation of a large group of people. Also, psychological parameters such as individual expectations may affect thermal comfort. The thermal sensation 7 level scale with values between -3 and 3 describes the thermal sensation between 'hot' and 'cold'.

Occupants can control their thermal environment by means of clothing, operable windows, fans, heaters, internal and external sun shades.

3. Description of analyzed building

The aim of the building simulations was to analyze the influence of thermal insulation and flat location on the thermal comfort of particular parts of the panel building. The simulations were conducted for part of W70, a 5 storey large panel dwelling building, the usage area of analyzed building part was 150 m². The basement is below entire building and the building has a flat roof. Visualizations of different building elevations are presented in Fig. 1.

The building has natural ventilation and a central heating system with convection heaters. A communication area is located in the central part of each building level. In the analyzed part of the building, there are three flats at every level. Exterior walls made of prefabricated panels in the W70 system, insulated with 15 cm of styrofoam with plasters at both sides: $U = 0.20$ [$\text{W}/\text{m}^2\text{K}$] (before thermal modernization $U = 0.75$ [$\text{W}/\text{m}^2\text{K}$]), double glazing windows: $U = 1.5$ [$\text{W}/\text{m}^2\text{K}$].



Fig. 1. South-east and south elevations of analyzed building

The calculations were carried out in Design Builder v.3. The program has been specifically developed around Energy Plus, allowing the simulation of the building envelope and building interiors. The simulations conducted for the Polish climatic conditions (building located in Cracow) allowed the evaluation of the microclimate conditions of the entire building as well as of particular dwellings.

4. Simulation settings

The main aim of simulations was to determine the temperature and PMV index of particular flats at different elevations during the summer months. Figure 2 presents typical arrangements of dwellings on a storey of the building.

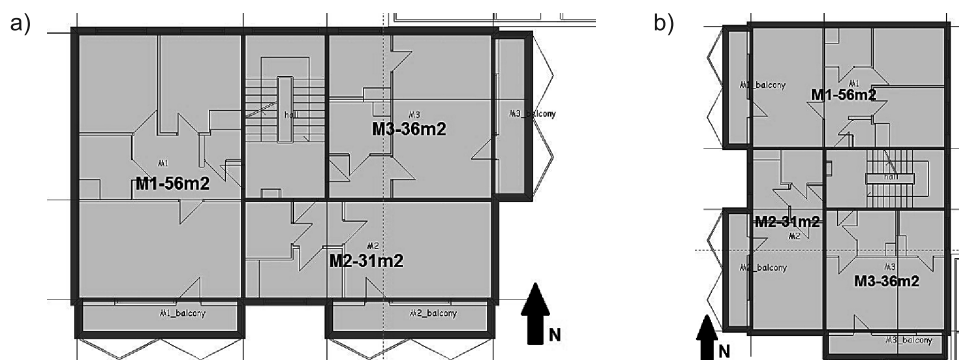


Fig. 2. Typical zones' visualization on every building level: a) Two rows of balconies at south elevation, b) Building rotated 90 degrees clockwise – two rows of balconies at west elevation

Every single flat was modelled as separate thermal comfort zone due to the small usage area of different flats. It was assumed that the doors between rooms are usually opened. Three different flats were analyzed:

1. Flat M1 – usage area 56 m², balcony at south elevation.
2. Flat M2 – usage area 31 m², balcony at south elevation.
3. Flat M3 – usage area 36 m², balcony at east elevation.

Area of balcony windows is 5.2 m².

Three simulation steps were analyzed – the building model before thermal modernization (two different building rotations, as shown in Fig. 2) and the building model after thermal modernization. Data for three different flats located at four different levels were compared. The period of time between 15th of May and 15th of September was taken into consideration because at this time in Poland, there is a risk of overheating.

The assumptions for the simulations:

1. Heating system on from September to March (22°C), 7 days a week, 24 hours a day.
2. Occupancy density: flats – about 1 person per 15 m²,
3. Operating schedule: flats – 100% occupancy density between 4 pm and 7 am, 5 days a week; at the weekends and between 6 pm and 9 am; 50% reduced occupancy between 9 am and 6 pm.
4. Metabolic activity: factor 1.2 met, winter clothing – clo = 1.0, summer clothing clo = 0.5.
5. Ventilation requirements per polish national standards PN-83/B-03430 [2], in every flat 70 m³/hour for kitchen and 50 m³/hour for bathroom.

5. Test results

All simulation results presented below, have shown that during few days between 15th of May and 15th of September the average interior air temperatures of different dwellings exceed 30°C and the PMV factor is higher than 2. Those microclimate building conditions exceed the optimal internal summer temperature of 25°C and recommended value $-0.5 < PMV < +0.5$.

5.1. Building before thermal modernization – base case

Simulations of the building before thermal modernization have shown that in all dwellings, on all levels the operative temperature for most of the time is significantly higher than 25°C. The daily maximum interior temperature is 33.80°C (flat M2) and the PMV value is above 2.9. The number of discomfort hours, with the temperature above 25°C, in the assumed period of time is 1555. Those negative flat conditions continue almost for the entire day and do not change significantly during the night. The flats can be cooled by occupants during the night through the opening of windows.

Figures 3a, 3b and 3c present the number of discomfort hours for all three flats at different levels. The most unfavorable microclimate conditions are noticeable in flat M2 where the number of discomfort hours with temperatures above 32°C is the highest. Regarding the influence of the building storey, the worst conditions can be observed on the fourth floor (Fig. 4).

Comparing flats M1 and M2, both with balcony windows at the south elevation, thermal comfort conditions are worse in flat M2 due to its smaller usage area (31 m² compared to 56 m²).

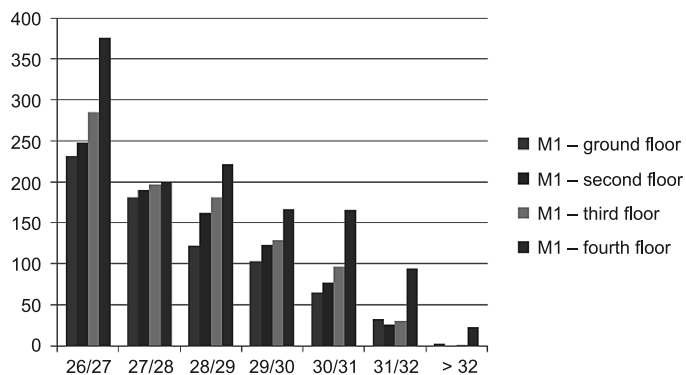


Fig. 3a. Number of overheating hours for flat M1 (south-west) at four levels – base case

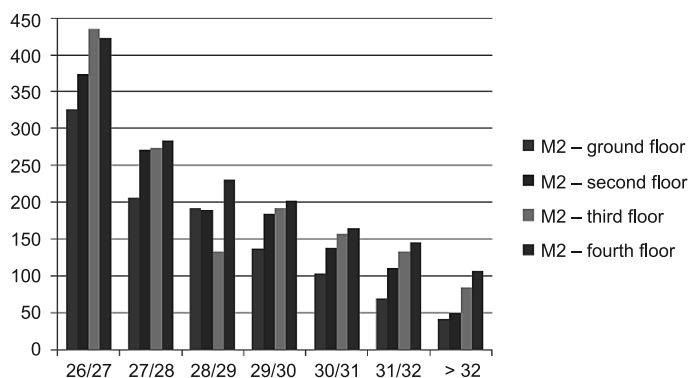


Fig. 3b. Number of overheating hours for flat M2 (south-east) at four levels – base case

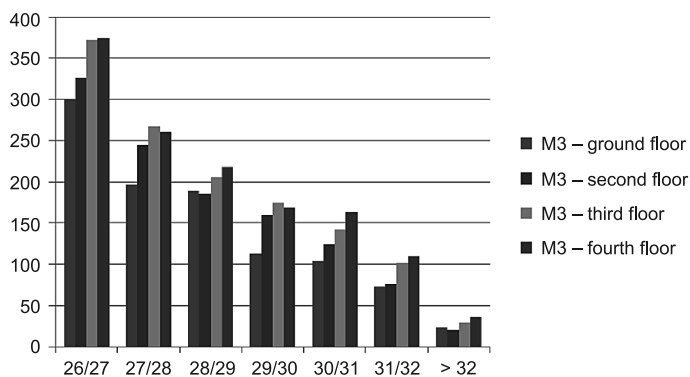


Fig. 3c. Number of overheating hours for flat M3 (east) at four levels – base case

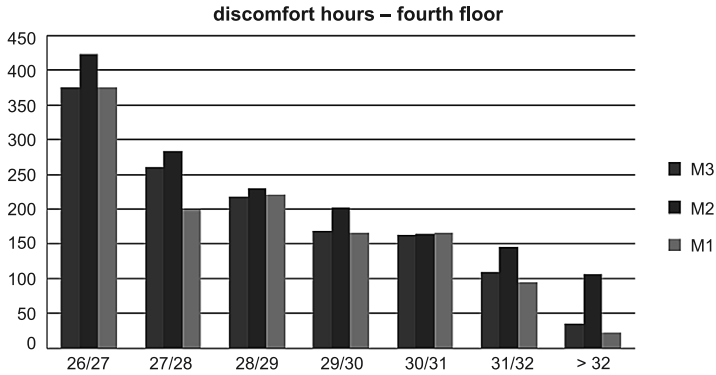


Fig. 4. Number of overheating hours for different flats at fourth floor – base case

5.2. Building before thermal modernization rotated 90 degrees clockwise

The overheating problems are closely related to the orientation of glazing and the worst thermal conditions are usually observed in rooms with windows oriented to the west. It is connected with the angle of solar radiation. In the analyzed building, the windows located at south elevation are shaded by the balconies at higher levels which lessen the solar gains. In the next step of simulation, the building was rotated 90 degrees clockwise to analyze the microclimate conditions in the rooms with balcony windows located at the west.

After rotation of the buildings the worst microclimate conditions are also observed in flat M2, the number of discomfort hours increased from 1555 to 1618. Again, comparing the M2 with flat M1 (balcony windows at the same elevations), less favorable results are noticeable in flat M2 due to its smaller usage area. Figure 5 presents the number of discomfort hours for flat M2 and Figure 6, a comparison of PMV indexes for all three flats located on the fourth floor. The daily maximum interior temperature is 34.70°C and the PMV value is above 3.1.

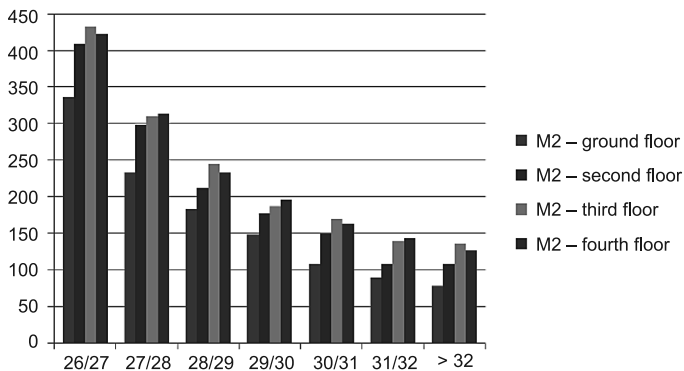


Fig. 5. Number of overheating hours for flat M2 by floors – rotated building

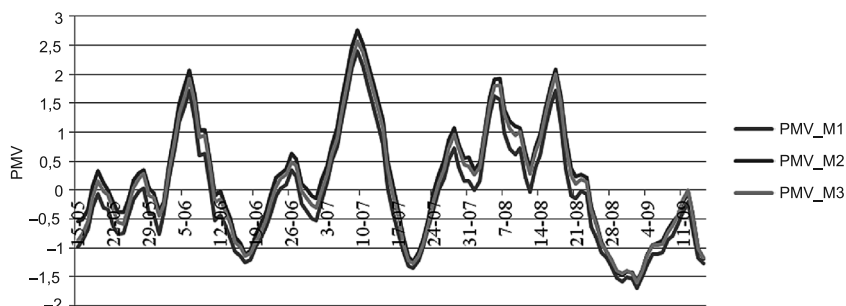


Fig. 6. PMV comfort indexes for three flats located on the fourth floor – rotated building

5.3. Building after thermal modernization

Due to the recast to the European Energy Performance of Buildings Directive, buildings designed and modernized after 2021 should be zero-energy buildings. In connection with those provisions, since 1st of January 2014, the new requirements regarding building envelope thermal insulation were introduced Warunki Techniczne 2013 [4]. According to those regulations, thermal transmittance U of the heated building components cannot exceed $0.25 \text{ W/m}^2\text{K}$ and after 1st of January 2021, $0.2 \text{ W/m}^2\text{K}$.

In the next step, the simulations were conducted for the building after thermal modernization fulfilling the requirements of the standard [4] being in force since 2021. Only external walls were insulated with 15cm of styrofoam ($\lambda = 0.04 \text{ W/mK}$).

Figure 7 presents the number of discomfort hours for flat M2 with the most unfavorable microclimate conditions. The worst conditions are again on the fourth floor (Table 1). The daily maximum interior temperature is 34.5°C and the number of discomfort hours in the assumed period of time is 2392. After thermal modernization, the number of overheating hours in flat M2 on the fourth floor increased from 1555 to 2392.

Table 1 presents the number of overheating hours in all flats, at all analyzed levels before and after thermal modernization. A significant increase can be observed in all flats of even up to 60%.

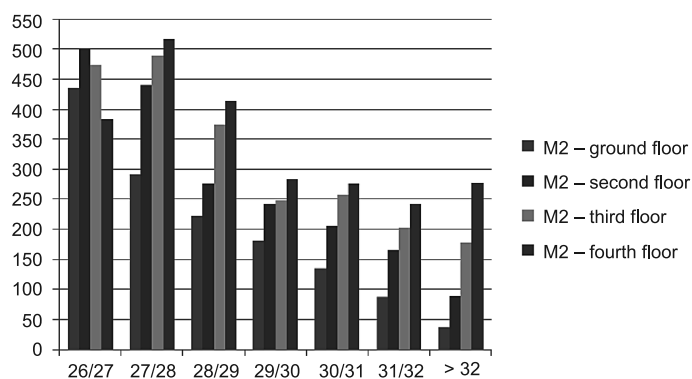


Fig. 7. Number of overheating hours for flat M2 at different levels

It appears that the reduction of heat losses connected with the thermal modernization of the building envelope unfavorably affects the microclimate conditions in the leaving spaces.

Both before and after thermal modernization, the worst conditions for all flats, are noticeable on the fourth floor, however, the percentage increase in case of flat M1 and M2 is noticed on the third floor. It can be explained by the fact that the roof was not insulated so the transmission gains through this part of the building stay at the same level.

Table 1

Number of discomfort hours for all analyzed flats before and after thermal modernization

		Number of discomfort hours – before thermal modernization	Number of discomfort hours – after thermal modernization	Percentage increase [%]
M1	1st level	736	946	29
	2nd floor	827	1235,5	49
	3rd floor	920,5	1477	60
	4th floor	1245	1746,5	40
M2	1st level	1073	1391,5	30
	2nd floor	1317,5	1916	45
	3rd floor	1409	2225,5	58
	4th floor	1555	2392	54
M3	1st level	999,5	1377	38
	2nd floor	1137	1718	51
	3rd floor	1293,5	1985	53
	4th floor	1329	2153,5	62

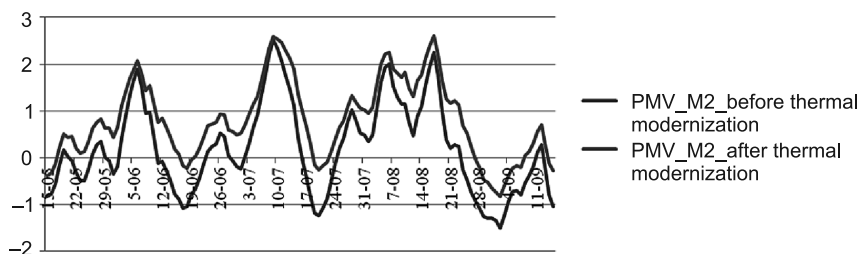


Fig. 8. PMV comfort indexes for flat M2 before and after thermal modernization

6. Conclusions

The results of the conducted analysis show that the overheating problem appears in large panel buildings, both before and after thermal modernization. Windows in the prefabricated panel buildings in most cases are poorly shaded from solar radiation. Glazing is the source of the excessive heat gains and results in the overheating of the dwellings. The microclimate

conditions in all flats are very uncomfortable and the parameters describing thermal comfort exceed the acceptable values.

Modernization of the building should be preceded by the extensive analysis of how the changes influence thermal comfort of the particular flats. The priority is heating cost reduction in the winter season. The conducted analyses show that improvement of the building envelope thermal insulation alone can unfavorably affect the internal conditions during the summer season. In the process of thermal modernization of panel buildings, use of internal or external shadings to reduce summer overheating should be taken under consideration. Those solutions are the subject of the authors' further researches.

The work reported in this paper has been partially funded by the project L-1/116/DS/2013.

References

- [1] PN-EN ISO 7730 Ergonomics of the thermal environment. Analytical determination and interpretation of thermal comfort using calculation of the PMV and PPD indices and local thermal comfort criteria.
- [2] PN-83/B-03430 Wentylacja w budynkach mieszkalnych zamieszkania zbiorowego i użyteczności publicznej – Wymagania.
- [3] Rozporządzenie Ministra Infrastruktury z dnia 12 kwietnia 2002 w sprawie warunków technicznych, jakim powinny odpowiadać budynki i ich usytuowanie (Dz.U. nr 75, poz. 690 z późn. zm. ogłoszonymi w Dz.U. z 2003 r. Nr 33, poz. 270, z 2004 r. Nr 109, poz. 1156, z 2008 r. Nr 201, poz. 1238, z 2009 r. Nr 56, poz. 461, z 2010 r. Nr 239, poz. 1597, z 2012 r. poz. 1289 oraz z 2013 r., poz. 926).
- [4] Rozporządzenie Ministra Transportu, Budownictwa i Gospodarki Morskiej z dnia 5 lipca 2013 r. zmieniające rozporządzenie w sprawie warunków technicznych, jakim powinny odpowiadać budynki i ich usytuowanie (Dz.U. z 13 sierpnia 2013 r., poz. 926).
- [5] Nowak K., *Modernizacja budynków a komfort cieplny pomieszczeń*, Energia i Budynek, listopad 2013, 29-33.
- [6] Dębowski J., *Cała prawda o budynkach wielkopłytowych*, Przegląd budowlany 9/2012.
- [7] Nowak K., Nowak-Dzieszko K., Rojewska-Warchał M., *Thermal comfort of the rooms in the designing of commercial buildings*, Research and Applications in Structural Engineering, Mechanics and Computation. SMEC Cape Town 2013, 651-652.
- [8] Wierzbiński S.M., *Problemy modernizacji budynków wielkopłytowych*, Materiały Konferencji Naukowo-Technicznej ITB, Mrągowo 1999.

BOŻENA ORLIK-KOŹDOŃ*, AGNIESZKA SZYMANOWSKA-GWIŹDŹ*

THE EFFECT OF TRADITIONAL STRUCTURAL
ELEMENTS OF PARTITION WALLS
IN RESIDENTIAL BUILDINGS ON THE QUALITY
OF THE USE OF THE PREMISES

WPŁYW CHARAKTERYSTYCZNYCH
ELEMENTÓW KONSTRUKCJI PRZEGRÓD
BUDYNKÓW MIESZKALNYCH
NA JAKOŚĆ UŻYTKOWANIA POMIESZCZEŃ

Abstract

This paper describes the phenomenon of mould growth on the inner surface of partition walls of multi-block constructed residential buildings. An assessment was undertaken of the impact of the resulting damage, in terms of health and safety of residential premises.

Keywords: humidity levels in partitions, industrialized construction, thermal quality

Streszczenie

W artykule opisano zjawisko występowania pleśni na powierzchni wewnętrznej przegród budynków mieszkalnych, wykonanych w technologii wielkoblokowej. Wykonano ocenę wpływu występujących uszkodzeń w aspekcie bezpiecznego użytkowania lokali mieszkalnych.

Słowa kluczowe: zawilgocenia przegród, budownictwo uprzemysłowione, jakość ciepła

* Ph.D. Eng. Bożena Orlik-Koźdoń, Ph.D. Eng. Agnieszka Szymanowska-Gwiźdź, Department of Buildings and Buildings Physics, Faculty of Civil Engineering, The Silesian University of Technology.

1. Introduction

The phenomenon of mould growth on the surfaces of partitioned walls in residential premises occurs in buildings with different material and structural characteristics. Among other building types, it affects properties built in the 1970's and 1980's. Nowadays, residents in these housing estates report problems associated with poor level insulation of partition walls and instances of mould spore corrosion. Maintaining an indoor climate (temperature and humidity) at a certain level is not an insignificant factor in terms of health and safety in these dwellings.

This paper analyses the results of research into surface condensation, using humidity measurements taken on site.

2. Research subject and scope

The study focused on one of the buildings of the Bytom housing estate. The selected property is a multi-block technology construction, using the WBS system – Big Silesian Block. The external construction walls are comprised of light-coloured concrete blocks, 32 cm thick, and are insulated with 12 cm PGS cladding. The curtain walls and canopy hooded walls of the vented flat roof were fortified with PGS blocks with a thickness of 24 and 19 cm. During its period of use, the building has been insulated with 5 cm thick mineral fibre panels and exterior wooden panels have been coated with asbestos-cement.



Fig. 1, 2. Bytom, view of the surveyed building, north-west elevation (1) and south-east elevation (2)

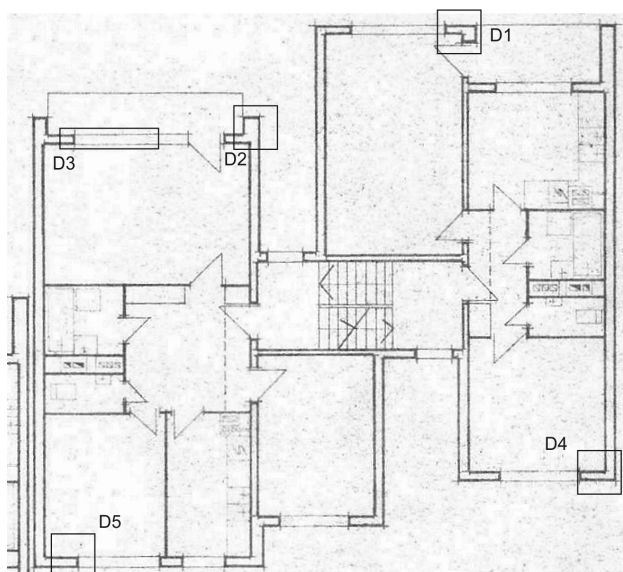
In June 2013, the building was subject to a visual inspection, in response to residents reporting a problem with mould affecting partition walls in part of the premises. The surveys confirmed that mould had affected the inner surfaces of the walls and small areas next to ceilings. Spores were located in corner positions, at the juncture of the curtain walls and external structural walls, mostly next to loggias (recessed balconies on the south-east elevation), but also on the north-west elevation.

At locations where mould had appeared, humidity readings were carried out (17 locations in all) using a TESTO 635-2 tool with a probe to measure actual humidity (manufacturer's

calibration protocol No. 02356831). Moisture values were given as a percentage value expressed in relation to dry material mass. The level of humidity present on the inner surfaces where mould damage had occurred, ranged between 1.3% to 2.8%. An increase in humidity of 3.2% to 5.4% was recorded at the north-west side on the second and fourth floors.



Fig. 3, 4. The view on mould outbreaks on external walls: detail D1 (3) and D5 (4) in flats on second floor



- Detail_1: connection of recessed balcony wall with curtain wall
- Detail_2: connection of recessed balcony wall with curtain wall
- Detail_3: connection of balcony panel with curtain wall
- Detail_4: corner of wall (juncture of block wall and PGS block wall)
- Detail_5: juncture of ceiling and curtain wall

Fig. 5. Sites of mould occurrence and details

This paper deals only with readings where further analysis was conducted.

Of all the spore-corroded sites, 5 construction joints were selected (Fig. 3) in order to check the likelihood of mould formation on the inner surfaces of the partition walls, using the PN-EN ISO 13788 [1] standard procedure. The temperature distribution across the surfaces/joints of the partition walls was calculated using a computer simulation, representing each of the joints. A temperature factor of f_{Rsi} was applied to calculate temperature values at the selected locations. In the simulated models, details were taken from archived project records as well as information available from the relevant standard and technical approvals.

The following thermal conductivity coefficient values were applied [1, 4]:

- Concrete blocks of light aggregate: 0.75 [W/mK],
- Gravel concrete: 1.45 [W/mK],
- Reinforced concrete: 2.20 [W/mK],
- PGS blocks 0.30 [W/mK],
- Swarf-cement panels 0,14 [W/mK],
- Cement-lime plaster 1.00 [W/mK].

Table 1

Measured moisture values, depicted by percentage weighting in relation to dry material mass

Detail	Site of occurrence	Floor	Humidity
D1	wall	1	1.8–1.9%
		3	1.9%
		4	1.7–1.8%
D2	wall	1	1.9–2.5%
		2	1.8–2.1%
		4	2.5–2.7%
D3	wall	1	1.6%
		2	1.3–1.8%
D4	wall	4	5.4%
D5	ceiling	2	5.0–5.2%

3. Measurement method

A computer program THERM 7.19 was used to assess the thermal-humidity at selected locations in the building. Temperature values for the cross-section of the partition in the joints were obtained, as were the total heat flux density and the heat transfer coefficient U (W/m²K). The geometry and readings are shown in Table 2. The computer program readings were used to assign a temperature factor for the inner surface of the external wall: i.e. f_{Rsi} ; in order to determine the risk of surface condensation. Calculations were made in accordance with [1]. This process was performed for two variants: for the first variant using data from

PN-82/B-02402 [2] and PN-82/B-02403 [3]; and for the second variant with local climate parameters used at the meteorological station in Katowice. The results were as follows:

- Outside air temperature: $t_{e1} = -20^{\circ}\text{C}$; $t_{e2} = -2.4^{\circ}\text{C}$ (annual mean temperature for the coldest month);
- Internal air temperature: t_{i1} i $t_{i2} = +20^{\circ}\text{C}$;
- Heat transfer coefficient $h_e = 25 \text{ W}/(\text{m}^2\text{K})$; $h_i = 7,69 \text{ W}/(\text{m}^2\text{K})$; providing the conditions for surface condensation $4.0 \text{ W}/(\text{m}^2\text{K})$.

If we apply the relevant Technical Conditions [4] for a residential building with an internal temperature $t_i = 20^{\circ}\text{C}$, and an average monthly relative 50% internal air humidity value, then we can adopt the required temperature factor value on the inner surface of external wall (of f_{Rsi}). This is equal to 0.72 and is acceptable. For the calculation of the condensation risk, an internal humidity level of 50% was adopted.

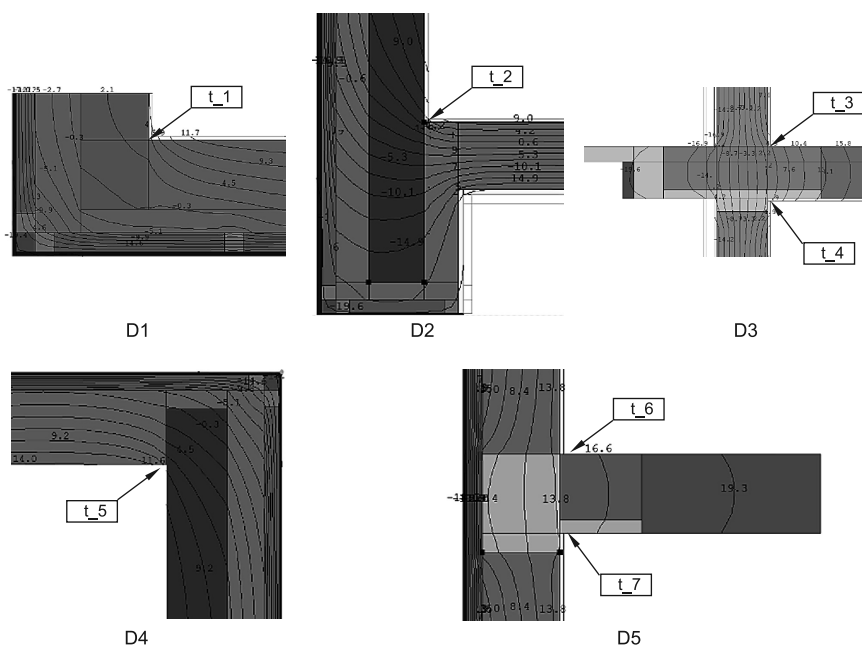


Fig. 6. Geometric models of details and locations of temperature readings

The minimum value of the temperature coefficient $f_{Rsi,\min}$ was calculated using the formula j :

$$f_{Rsi,\min} = \frac{\theta_{si,\min} - \theta_e}{\theta_i - \theta_e} \quad (1)$$

where:

- $\theta_{si,\min}$ – minimum temperature value of the inner surface of the partition walls,
- θ – external temperature,
- θ_e – internal temperature.

4. Summary and results analysis

The values of the minimum temperatures in the selected joints, and the calculated temperature factors, are shown in Table 2.

Table 2

Summary of calculation results

Scheme	Surface temperature determination method	Temperature in joint [°C]		Temperature factor f_{Rsi}	
		Variant_1 $t_i = 20^\circ\text{C}$ $t_e = -20^\circ\text{C}$	Variant_2 $t_i = 20^\circ\text{C}$ $t_e = -2.4^\circ\text{C}$	Variant_1 $t_i = 20^\circ\text{C}$ $t_e = -20^\circ\text{C}$	Variant_2 $t_i = 20^\circ\text{C}$ $t_e = -2.4^\circ\text{C}$
Detail D1	t_1	4.8	11.5	0.62	0.62
Detail D2	t_2	6.7	12.4	0.66	0.66
Detail D3	t_3	4.5	11.2	0.61	0.60
	t_4	3.7	10.8	0.59	0.58
Detail D4	t_5	8.6	13.6	0.71	0.72
Detail D5	t_6	14.7	17.0	0.86	0.86
	t_7	14.4	16.6	0.86	0.84

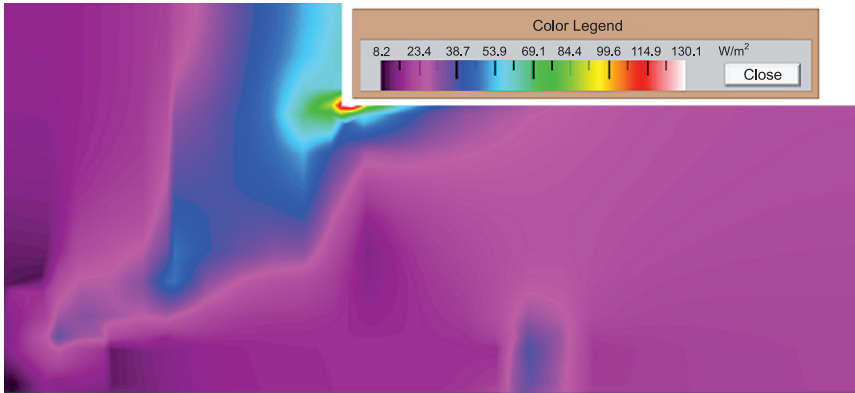


Fig. 7. An example of the heat flux density distribution in the cross-section – Detail D_1

The calculation results indicate there is a risk of surface condensation and of the formation of mould in both of the computed variants, in the joints marked D_1, D_2, and D_3. These partitions have complex material elements and characteristics. A concrete (class B20 according to the old marking) core joint, reinforced with plain bars, with favourable thermal parameters (shown in details D_1 and D_3), is in place alongside the light concrete elements of the wall. In comparison to the temperature reading of the D_1 structural wall and curtain wall combination (i.e. wall blocks with PGS blocks but without a column

in the corner), the temperature at the joint was almost 2°C higher. The beneficial impact on the thermal parameters of the joint, by using gravel concrete at the juncture of the balcony panel and the external wall (detail D_5), is also apparent.

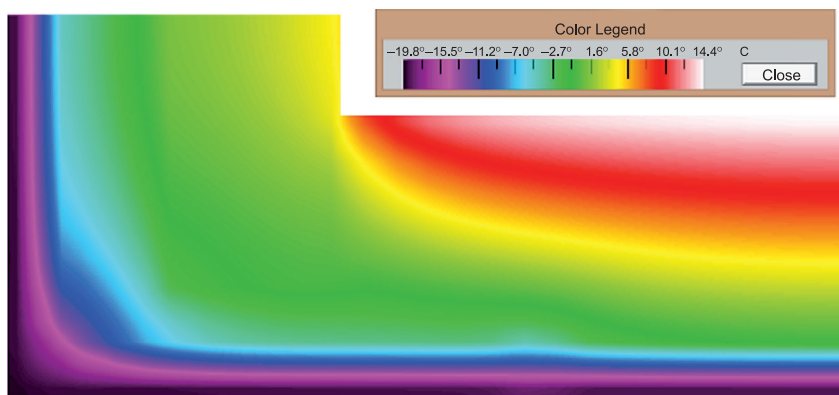


Fig. 8. An example of the field temperature distribution in the cross-section – Detail D_1

However, regardless of the theoretical computer-generated results obtained for all of the analyzed fragments of the partition walls, mould corrosion outbreaks were observed, and in the case of D_4 and D_5 ($f_{Rsi} > f_{Rsi,max}$), humidity levels were greater on the partition wall's surface (up to 5.4%). Such high humidity levels on partition walls indicate considerable proclivity to exceptional humidity levels in the winter months when the heating system is fully functional and a lack of opportunity for drying out in the spring and summer. Operating conditions in domestic properties during these periods may differ significantly from those indicated in these calculations. This means that temperatures inside residential properties may be lower than 20°C and operating humidity levels may be higher than 50%.

The effect of partition wall design features on the quality of use of the premises, becomes more noticeable during short-term or long-term periods where relatively adverse air humidity levels are present in flats and apartments. It may also result from a lack of effective drainage of hot water vapour generated by users (e.g. due to an insufficient or inadequate air ventilation supply or a lack of a proper air outlet from the premises).

The computer model forecasts indicate that the minimum temperature factor, calculated for the local weather conditions, may reach values far higher than 0.72. As far as average monthly temperatures are concerned, the most adverse conditions occur in February, according to the meteorological station in Katowice. The temperature factor $f_{Rsi,max}$ reaches a value of 0.832 in this period. For the D_4 building joint, such conditions favour the development of mould on the inner surface of a partition wall.

The joints most prone to humidity are located at the north-west elevation, and this may also indicate that weather conditions (rainfall and lack of sunlight) have a physical impact on the partition wall due to gaps, cracks and leaks in the building facade.

5. Conclusions

The inner surfaces of partition walls in the premises inspected suffer local and irregular occurrences of mould and excess humidity levels, which may be the result of:

- low thermal insulation of external walls;
- ineffective insulation of joints or the lack of insulation;
- adverse operational conditions at the premises, including operational temperatures lower than 20°C and relative air humidity levels inside the premises at levels higher than 50%;
- a lack of effective ventilation in the premises;
- cracks, leaks and gaps in the partition walls at the north-west elevation.

Material and structural features of partition walls can affect the quality of use of the premises. The accumulation of negative factors is most unfavourable. Residential construction works carried out in the 1970's and 1980's saw insufficient thermal insulation of external walls. This (coupled with utility factors associated with occupants' individual activities in, and use of, the premises) has encouraged the formation of mould.

References

- [1] PN-EN ISO 13788 Ciepłno-wilgotnościowe właściwości komponentów budowlanych i elementów budynku. Temperatura powierzchni wewnętrznej dla uniknięcia krytycznej wilgotności powierzchni i kondensacji międzywarstwowej.
- [2] PN-82/B-02402: Temperatury ogrzewanych pomieszczeń w budynkach.
- [3] PN-82/B-02403: Temperatury obliczeniowe zewnętrzne.
- [4] Rozporządzenie Ministra Infrastruktury z dnia 12 kwietnia 2002 r. w sprawie warunków technicznych, jakim powinny odpowiadać budynki i ich usytuowanie, wraz z późniejszymi zmianami.

KRZYSZTOF PAWŁOWSKI*, FABIAN LEWANDOWSKI*

THERMAL DESIGN OF EXTERIOR WALLS MADE OF WOODEN BEAMS

PROJEKTOWANIE CIEPLNE PRZEGRÓD ZEWNĘTRZNYCH Z BALI DREWNIANYCH

Abstract

In the paper were shown the calculation results of thermal parameters of exterior walls made of wooden beams and their joints. The selected joints of wooden beam walls were analysed numerically. On the basis of the calculation and analyses, an evaluation was made according to the requirements formulated in the Regulation [1] and the directives of the National Centre for Environment Protection and Water Management [2] concerning buildings of NF15 and NF40 standards.

Keywords: beam, hydro-thermal analysis

Streszczenie

W artykule przedstawiono wyniki obliczeń parametrów cieplnych ścian zewnętrznych z bali drewnianych i ich złączy. Przeprowadzono analizę numeryczną wybranych złączy ścian z bali drewnianych. Na podstawie obliczeń i analiz dokonano oceny wg wymagań sformułowanych w Rozporządzeniu [1] oraz wytycznych Narodowego Funduszu Ochrony Środowiska i Gospodarki Wodnej [2] w zakresie budynków w standardzie NF15 i NF40.

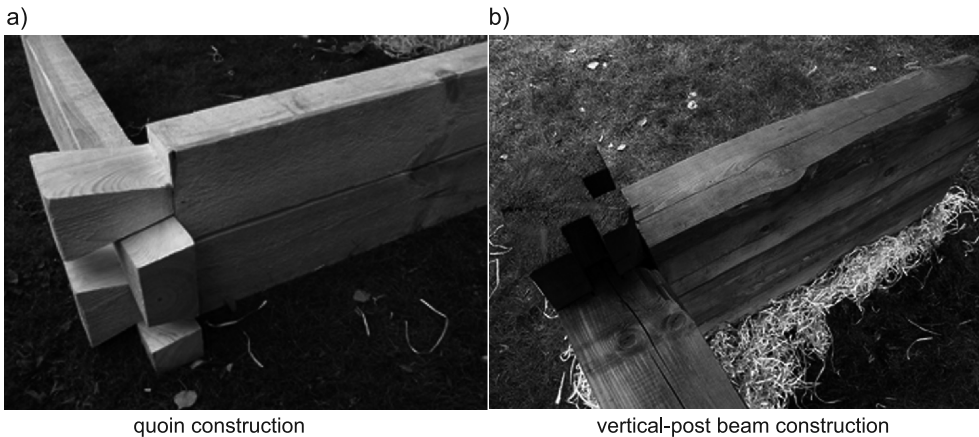
Słowa kluczowe: bale drewniane, analiza cieplno-wilgotnościowa

* Ph.D. Eng. Krzysztof Pawłowski, M.Sc. Eng. Fabian Lewandowski, Department of Building Construction and Building Physics, Faculty of Civil and Environmental Engineering and Architecture, University of Technology and Life Sciences in Bydgoszcz.

1. Introduction

A building and especially its casing, in an essential manner, take part in providing thermal comfort for the needs of humans, separating the unfavourable and constantly changing external environment from the interior. It is the wall construction that shapes the physical parameters of a particular building, and this cannot be accidental. Undoubtedly, the most popular in Poland is masonry technology. We can distinguish single and multi-layer walls in which some layers fulfil a construction function and others for insulation. However, it can be noticed that on the Polish market, there is a growing offer of housing utilising wooden technology. The material used for the main construction of such houses is spruce or pine wood. Depending on the applied wood type, humidity and thermal insulation, the insulation properties can vary. Every year, specialised companies erect about four thousand single-family houses using wooden frame technology. Additionally, there are approximately one thousand more built from solid and insulated beams. Thus, in a period of one year, five thousand houses of wooden construction are built. Development of this kind of construction is a result of investor belief in its energy-saving and ecological properties. Most often, two basic construction systems are used for erecting outer walls made from solid beams:

- Quoin construction,
- Vertical-post beam construction [3].



quoin construction

vertical-post beam construction

Fig. 1. Example of construction system of wooden beam walls [4]

Often, because of thermal protection requirements, buildings are made of insulated solid beams. In a subsequent part of the article, calculations of the thermal parameters of solid wooden beam and insulated beam walls will be shown.

In the following of the paper presents the calculation of the thermal parameters of the external walls of solid and isolated beams.

2. Own tests and calculations

At the first stage of calculations of thermal transmittance U_c [W/(m²·K)], two variants of outer walls of wooden beams were selected (Fig. 2):

- variant I (outer wall of solid beams),
- variant II (outer wall of insulated beams).

Calculations were done according to procedure PN-EN ISO 6946:2008 [5].

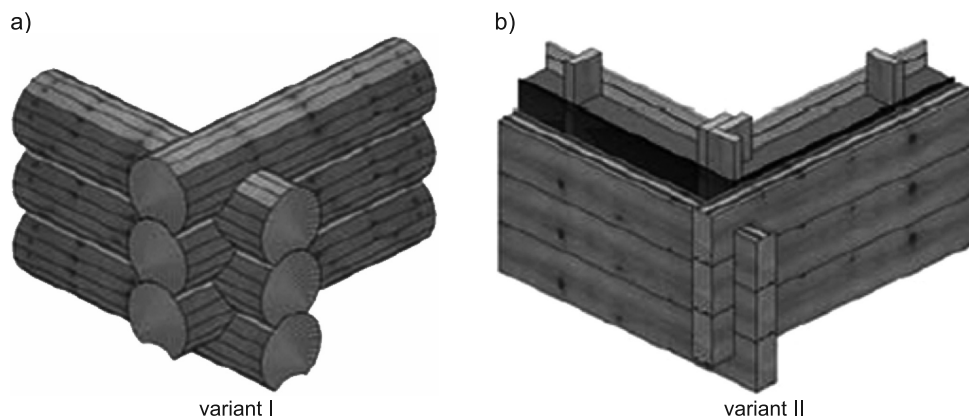


Fig. 2. Example of material solutions of walls from wooden beams [3]

For the second stage of calculations, 6 joints of the outer walls of the wooden beams analysed in the two variants were chosen (Fig. 2):

- connection of outer walls in the corner (M1),
- connection of the outer wall with a window in a cross section of a window frame (M2),
- connection of the outer wall with a window in a cross section of the breast of a window (M3),
- connection of the outer wall with window in a cross section of a wall rim (M4),
- connection of the outer wall with window in a cross section of a wall plate (M5),
- connection of the outer wall with roof in a cross section of a wall rim and lintel (M6).

Calculations of the basic parameters of thermal bridges were done:

- linear thermal transmittance Ψ [W/(m·K)] according to inside measurements (Ψ_i) and outside measurements (Ψ_e); in the case of bridge M4, M5 and M6, branch thermal transmittance concerning heat loss by corresponding parts of the connection was also defined,
- minimal temperature on an inside partition surface at the thermal bridge t_{\min} [°C],
- temperature factor f_{Rsi} [-] on the base of minimal temperature t_{\min} [°C].

The following assumption were made for calculation:

- the building was localised in zone III – temperature of outside air $t_e = -20^\circ\text{C}$, temperature of inside air $t_i = +20^\circ\text{C}$,
- values of the thermal conductivity coefficients of building materials λ [W/(m·K)] were assumed based on tables in [6, 9],

- thermal transmittance U_c [$W/(m^2 \cdot K)$] was calculated according to PN-EN ISO standard No 6946:2008 [5],
- conditions of heat reception on the inside and outside surface of a partition were assumed according to PN-EN ISO 6946:2008 [5] for calculation of heat flux and according to PN-EN ISO 13788:2003 [7] for calculation of temperatures and temperature factor f_{Rsi} ,
- modelling of the analysed connections was done according to principles formulated in PN-EN ISO 10211:2008 [8].

The procedures of calculation of the construction connection require setting principles of modelling, which means setting the geometric criteria, an instruction for setting the heat conductance of materials, margin conditions, manner and method of calculations and the methodology of the setting of temperature distribution [9].

Calculation by use of the TRISCO computer program is possible after definition of geometrical models. They can be obtained by dividing the building into many parts using the so-called cutting planes. The section should be created in such way that the results gained by the assumed models do not differ substantially from the results that are obtained when treating the building as a whole. Each geometric model of a connection consists of a central part or parts, side parts and, if necessary, a base. A single model is always limited by section planes and can contain more than one heat bridge. Below is shown the detailed procedure of setting the parameters of an outer wall connection with the roof in a cross section of a wall rim and lintel with a window (Fig. 3).

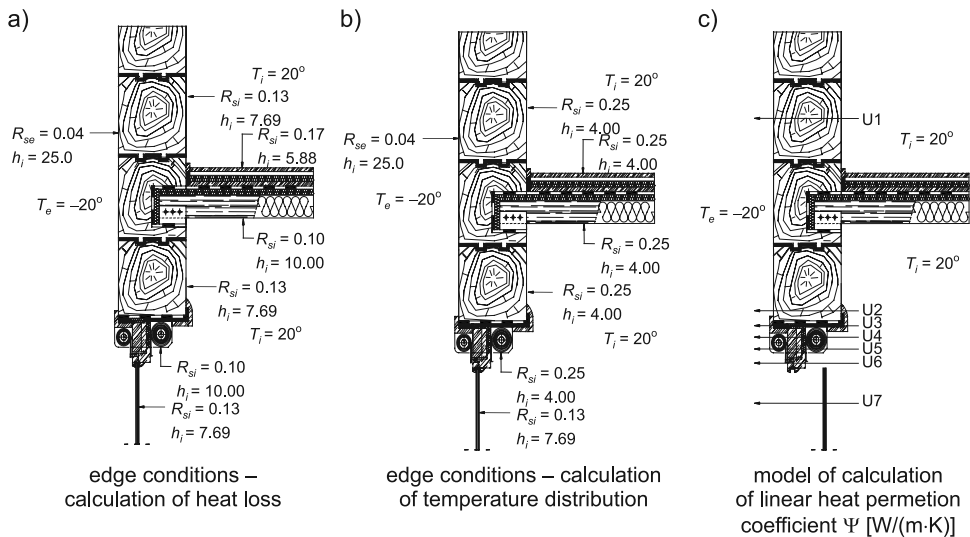


Fig. 3. Connection of an outer wall of wooden beams with a roof in a cross section of a wall rim and lintel with a window [3]

Based on the performed calculations using the TRISCO program, the values of inflow heat flux were defined as:

- window wood surface $\Phi_o = 27.83$ W, $L_o^{2D} = 0.695$ W/(m · K),

- lower part of a connection (below roof surface) $\Phi_d = 9.05 \text{ W}$, $L_d^{2D} = 0.226 \text{ W}/(\text{m} \cdot \text{K})$,
- upper part of a connection (above roof surface) $\Phi_g = 16.05 \text{ W}$, $L_g^{2D} = 0.266 \text{ W}/(\text{m} \cdot \text{K})$.

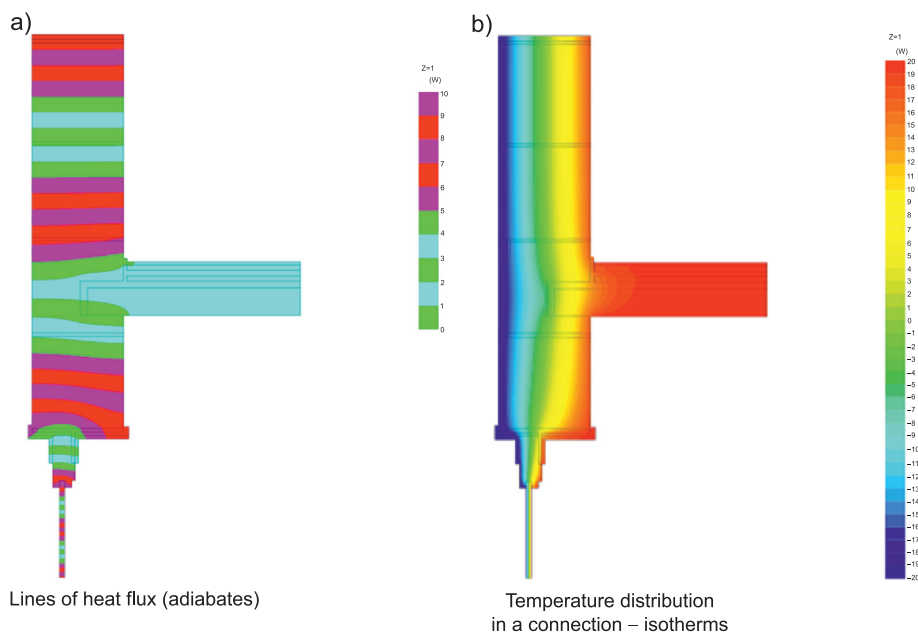


Fig. 4. Results of the numeric analysis of the connection [3]

Next were defined the values of linear heat permeation coefficient Ψ_i [W/(m·K)] (according to outer measurements), defined according to the procedures described in [6, 9], for a particular parts of a connection:

- branch thermal transmittance through a window: $\Psi_{iO} = 0.056$ [W/(m·K)],
- branch thermal transmittance through a lower part of the connection: $\Psi_{id} = 0.076$ [W/(m·K)],
- branch thermal transmittance through an upper part of the connection: $\Psi_{ig} = 0.022$ [W/(m·K)],
- linear thermal transmittance for the whole connection: $\Psi_i = 0.154$ [W/(m·K)].

In the range of humidity parameters, the minimal temperature t_{\min} [°C] in the connection and temperature factor f_{Rsi} [–] were set:

- minimal temperature in the connection was set based on calculations using the TRISCO computer program – $t_{\min} = 15.95^\circ\text{C}$,
- the value of the temperature factor is $f_{Rsi} = 0.898$.

Based on the calculations of a particular connection, it is possible to work out catalogue cards of sections made of wooden beams necessary for calculations and heat and humidity analyses. The detailed results of the calculations of selected connections are presented in Table 1.

Results of the physical parameters of selected connections of walls made of wooden beams

Heat bridge	variant I ($U_c = 0.287$ [W/(m ² ·K)])				variant II ($U_c = 0.195$ [W/(m ² ·K)])			
	Solid pine beam 53 cm thick				Solid pine beam 27 cm thick Mineral wool 15 cm thick GKF board 2.2 cm thick			
	Ψ_i [W/(m·K)]	Ψ_e [W/(m·K)]	t_{\min} [°C]	f_{Rsi} [-]	Ψ_i [W/(m·K)]	Ψ_e [W/(m·K)]	t_{\min} [°C]	f_{Rsi} [-]
M1	0.06	-0.27	13.32	0.83	0.04	-0.15	15.25	0.88
M2	0.07	0.07	13.19	0.83	0.07	0.07	14.91	0.87
M3	0.07	0.07	13.32	0.83	0.06	0.06	14.57	0.86
M4	$\Psi_i = 0.04$ $\Psi_{id} = 0.01$ $\Psi_{ig} = 0.03$	$\Psi_e = -0.05$ $\Psi_{ed} = -0.01$ $\Psi_{eg} = -0.04$	16.84	0.92	$\Psi_i = 0.05$ $\Psi_{id} = 0.06$ $\Psi_{ig} = -0.01$	$\Psi_e = -0.06$ $\Psi_{ed} = -0.03$ $\Psi_{eg} = -0.03$	16.99	0.92
M5	$\Psi_i = 0.07$ $\Psi_{id} = 0.02$ $\Psi_{is} = 0.05$	$\Psi_e = -0.15$ $\Psi_{ed} = -0.03$ $\Psi_{es} = -0.12$	14.79	0.87	$\Psi_i = 0.09$ $\Psi_{id} = 0.05$ $\Psi_{is} = 0.04$	$\Psi_e = -0.09$ $\Psi_{ed} = -0.07$ $\Psi_{es} = -0.02$	14.62	0.87
M6	$\Psi_i = 0.15$ $\Psi_{iO} = 0.06$ $\Psi_{id} = 0.08$ $\Psi_{ig} = 0.02$	$\Psi_e = 0.05$ $\Psi_{eO} = 0.04$ $\Psi_{ed} = -0.05$ $\Psi_{eg} = 0.06$	13.89	0.85	$\Psi_i = 0.12$ $\Psi_{iO} = 0.06$ $\Psi_{id} = 0.04$ $\Psi_{ig} = 0.02$	$\Psi_e = 0.06$ $\Psi_{eO} = 0.06$ $\Psi_{ed} = 0.03$ $\Psi_{eg} = -0.03$	13.38	0.83

Denotation concerning branch coefficients of heat permeation coefficient:
 Ψ_{id} – linear thermal transmittance of lower connection part [W/(m·K)],
 Ψ_{ig} – linear thermal transmittance of lower connection part [W/(m·K)],
 Ψ_{iD} – linear thermal transmittance of the roof [W/(m·K)],
 Ψ_{is} – linear thermal transmittance of lower connection part and outer wall [W/(m·K)],
 Ψ_{iO} – linear thermal transmittance of the window [W/(m·K)].

3. Calculation results analysis

The basic characteristic parameters of outer walls of wooden beams and their connections are:

- thermal transmittance U_c [W/(m²·K)], defining the heat loss through a flat (solid) outer wall,
- linear thermal transmittance Ψ_i [W/(m·K)], defining additional heat loss resulting from the existence of heat bridges,
- temperature factor f_{Rsi} [-], serving the evaluation of condensation on the inside surface of a partition (risk of fungi and mildew development) in the location of a heat bridge.

Based on the performed calculations and analyses, the following conclusions can be formulated:

- outer walls of housing made of wooden beams must fulfil the same requirements of thermal protection that are set for all outer partitions. According to regulations binding until the end of 2013 ($U_{c(max)} = 0.30$ [W/(m²·K)]), walls made of homogenous wooden beams should have an average thickness of 53 cm. However, according to more strict requirements from 2014 ($U_{c(max)} = 0.25 - 0.20$ [W/(m²·K)]), their thickness should be a minimum of 78 cm. In accordance with the above, an alternative construction of a wall of pine beam 27 cm thick with a 15 cm thick layer of mineral wool insulation from the inside was proposed. Accordingly, was suggested an alternative construction of a pine beam wall of thickness 27 cm with a layer of 15 cm insulation of mineral wool inside. tools (professional computer programs) let us establish correct heat loss and temperature distribution in the analysed connections (Table 1).
- the values of the linear heat permeation coefficient (Ψ_i) according to PN-EN ISO 14683:2008 [10] are approximate values (without taking into account the thickness of an outer partition and thermal insulation); in the table are gathered the results of the (Ψ_i) parameter for the selected connections obtained according to own calculations and based on PN-EN ISO 14683:2008 [10].
- Based on a value of thermal factor f_{Rsi} , it can be stated that in the analysed connections (Table 1), there is no risk of development of mildew and fungi. In all analysed connections, there is a condition observed for avoiding condensation on the inner partition surface (risk for mildew and fungi development) ($f_{Rsi} \geq f_{Rsi(kryt)}$). The edge (critical) value of the temperature factor, concerning the parameters of internal and external air, of the analysed calculation variants are $f_{Rsi(kryt)} = 0.778$.
- The analysed connections of walls of wooden beams (except the M6 connection) fulfilled the requirements of the guidelines from the National Centre for Environment Protection and Water Management [2] in the range of buildings of the NF40 standard, as they are characterise with values of Ψ [W/(m·K)] smaller than $\Psi_{max} = 0.10$ [W/(m·K)] (in the case of balcony boards $\Psi_{max} = 0.20$ [W/(m·K)]). The connections do not fulfil the requirement within the range of buildings of the NF15 standard ($\Psi_{max} = 0.01$ [W/(m·K)]).

Table 2

Results of physical parameters of selected connections of walls made of wooden beams

Analysed connections of outer walls	Values of linear thermal transmittance Ψ_i [W/(m·K)]			
	Own calculations		Catalogue cards PN-EN ISO 14683:2008 [10]	
	variant I	variant II		
M1	0.06	0.04	(C4)	0.10
M2	0.07	0.07	(W10)	0.10
M3	0.07	0.06	(W10)	0.10
M4	0.04	0.05	(IF4)	0.80

*) for analyses, catalogue cards for framing wooden walls were taken according to PN-EN ISO 14683:2008 [10]
 *) for analyses, only the M1, M2, M3, M4 connections were chosen (in the PN-EN ISO 14683:2008 [10] standard, there is lack of equivalents for M5, M6 connections)

4. Conclusions

The design of exterior walls of buildings made of wooden beams is a complex issue. Comprehensive evaluation of a building casing (outer partitions) should concern the partitions as well as their connections. The selection of construction and insulating materials should not be accidental, but should be based on detailed calculations and analyses. What is particularly significant is the correct design of the outer partition connection when it comes to minimising heat loss and eliminating heat loss and condensation on the inner partition surface.

Besides of heat and humidity issues of outer partitions of wooden beams and their connections there is a need to work out particular detailed design and executive guidelines within the range of acoustic insulation and fire protection.

References

- [1] Regulation of the Ministry of Transport, Building and Marine Economy amending the regulation on the technical conditions that buildings and their location should fulfil.
- [2] Guidelines setting forth the basic requirements necessary for achievement of expected energy standards for housing constructions and the manner of verification of designs and checking of energy-saving houses built (www.nfosigw.gov.pl).
- [3] Lewandowski F., *Analiza numeryczna parametrów cieplnych przegród zewnętrznych i ich złączy budynku z bali drewnianych*, MSc degree thesis written the under direction of Krzysztof Pawłowski, PhD, UTP in Bydgoszcz, Bydgoszcz 2013.
- [4] www.malanowicz.eu
- [5] PN-EN ISO 6946:2008 Komponenty budowlane i elementy budynku. Opór cieplny i współczynnik przenikania ciepła. Metoda obliczania.
- [6] Pawłowski K., *Projektowanie przegród zewnętrznych w świetle nowych warunków technicznych dotyczących budynków WT-2013*, Wydawnictwo MEDIUM, Warsaw 2013.
- [7] PN-EN ISO 13788:2003 Ciepłno-wilgotnościowe właściwości komponentów budowlanych i elementów budynku. Temperatura powierzchni wewnętrznej konieczna do uniknięcia krytycznej wilgotności powierzchni i kondensacja międzywarstwowa. Metody obliczania.
- [8] PN-EN ISO 10211:2008 Mostki cieplne w budynkach. Strumienie ciepła i temperatury powierzchni. Obliczenia szczegółowe.
- [9] Dylla A., *Praktyczna fizyka ciepła budowli. Szkoła projektowania złączy budowlanych*, Wydawnictwo Uczelniane UTP, Bydgoszcz 2009.
- [10] PN-EN ISO 14683:2008 Mostki cieplne w budynkach. Liniowy współczynnik przenikania ciepła. Metody uproszczone i wartości orientacyjne.

JAN RADOŃ*, KRZYSZTOF WĄS*, AGNIESZKA FLAGA-MARYAŃCZYK**,
FLORIAN ANTRETTNER***

THERMAL PERFORMANCE OF SLAB ON GRADE WITH FLOOR HEATING IN A PASSIVE HOUSE

ZJAWISKA CIEPLNE W PŁYCI NA GRUNCIE Z OGRZEWANIEM PODŁOGOWYM W DOMU PASYWNYM

Abstract

Extensive experimental investigations have been carried out in the passive house in Boruszowice for several years. The building foundation interface consists of a 25 cm reinforced concrete slab situated on a 40 cm layer of Styrofoam. The analysis of experimental results as well as theoretical calculations made it possible to determine the thermal performance of the applied slab on grade with floor heating during the whole year.

Keywords: slab on grade, floor heating, thermal performance, passive house

Streszczenie

W ciągu kilku ostatnich lat w budynku pasywnym w Boruszowicach przeprowadzono obszerne badania eksperymentalne. Fundament przedmiotowego budynku stanowi płyta żelbetowa o grubości 25 cm położona na 40 cm warstwie styropianu utwardzonego. Analiza wyników pomiarowych oraz obliczenia teoretyczne pozwoliły określić zjawiska cieplne występujące w płycie z ogrzewaniem podłogowym w skali całego roku.

Słowa kluczowe: płyta na gruncie, ogrzewanie podłogowe, zjawiska cieplne, dom pasywny

* Assoc. Prof. Ph.D. Jan Radoń, M.Sc. Krzysztof Wąs, Department of Rural Building, Faculty of Environmental Engineering and Land Surveying, University of Agriculture in Cracow.

** Ph.D. Agnieszka Flaga-Maryańczyk, Institute of Thermal Engineering and Air Protection, Faculty of Environmental Engineering, Cracow University of Technology.

*** M.Sc. Florian Antretter, Fraunhofer Institute for Building Physics, Holzkirchen.

1. Introduction

The detached, single-family house in Boruszowice was constructed in 2010 using pre-fabricated, lightweight technology. It has a floor area of approximately 120 m² located on two stories and approximately 311 m³ of internal volume. The length of the building is 10.58 m, its width is 7.77 m and its height is about 8 m. After the verification process, the building was granted the passive house standard certificate by the end of 2011. Since April 2011, it has been inhabited by a four-person family (parents + 2 children). Starting from the 1st May 2011, extensive experimental investigations are being carried out in the building. Passive, hygrothermal performance of outer partitions as well as energy use in active systems is continuously monitored [1, 2].

The foundation interface of the building consists of a 25 cm reinforced concrete slab situated on a 40 cm layer of Styrofoam. This reduces thermal-bridge effect while enabling even mechanical load distribution from load-bearing walls. Integration of floor heating with the concrete slab makes thermal insulation crucial for heat losses to the ground. Floor heating pipes were put at the bottom of the slab for better use of heat accumulation. Fig. 1 shows the passive house in Boruszowice and slab on grade during construction.



Fig. 1. Passive house in Boruszowice (left) and slab on grade during construction (right)

The reinforced concrete slab has the largest heat capacity in the building. This property is very important in terms of better use of internal and external heat gains and mitigation of air temperature fluctuation in the building.

The presented structural and functional solution of foundation and flooring has not yet been tested in Poland under real operating conditions. Measurement results and overall calculations were used to determine thermal performance of the applied slab on grade with floor heating during the whole year.

2. Experimental investigation

To get a full picture of the development of thermal conditions in the floor area, the temperature was measured at 21 points located along 7 vertical lines. One vertical is located in the middle of the building and two each at the outer edge of two rooms

and the outer corner (Fig. 2). Floor structure with location of measurements points is presented in Fig. 3.

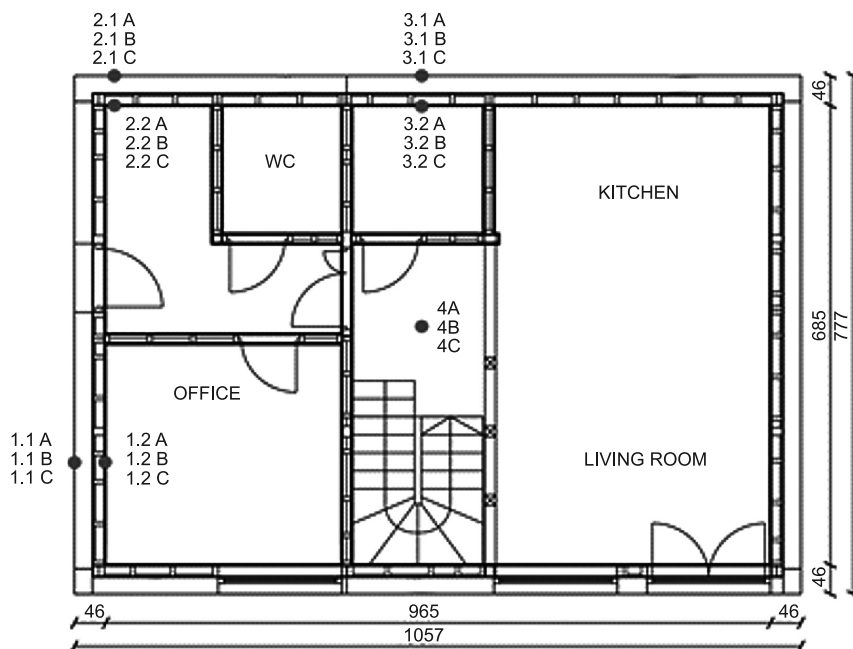


Fig. 2. Location of temperature measurement sections (dimensions in cm)

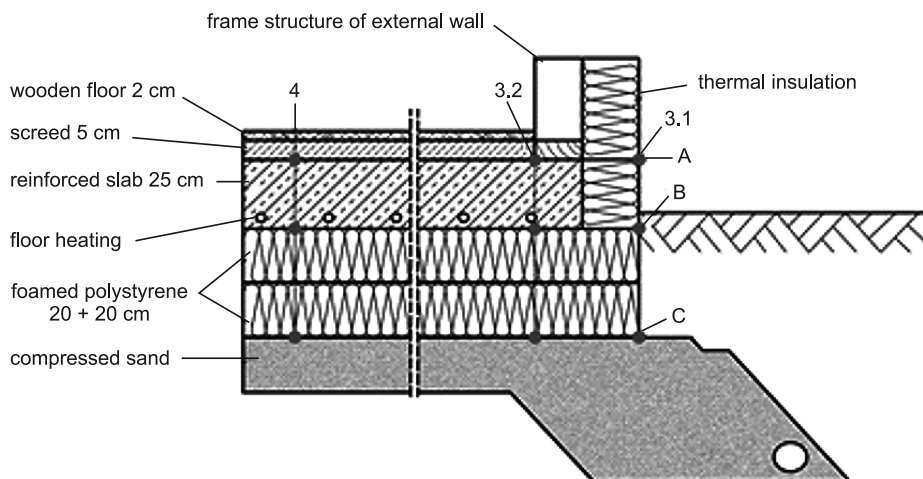


Fig. 3. Vertical section of foundation interface with measurement points

The PT100 sensors (TOP1068 class) with an accuracy of 0.1°C were used (together 21 measurement points).

The energy demand for space-heating of the building and domestic hot water is covered by a ground source heat pump. The heat is stored in a 500-litre water storage tank, from which hot water is supplied to the air heater and the floor heating system (Fig. 4).

Both supply and return water temperature as well as water flow for floor heating were measured. TP100 sensors for temperature and JS90-06_NC flow meter (accuracy above 95%) for water flow were used. The results allow for calculating the energy provided to the slab by the heating system.

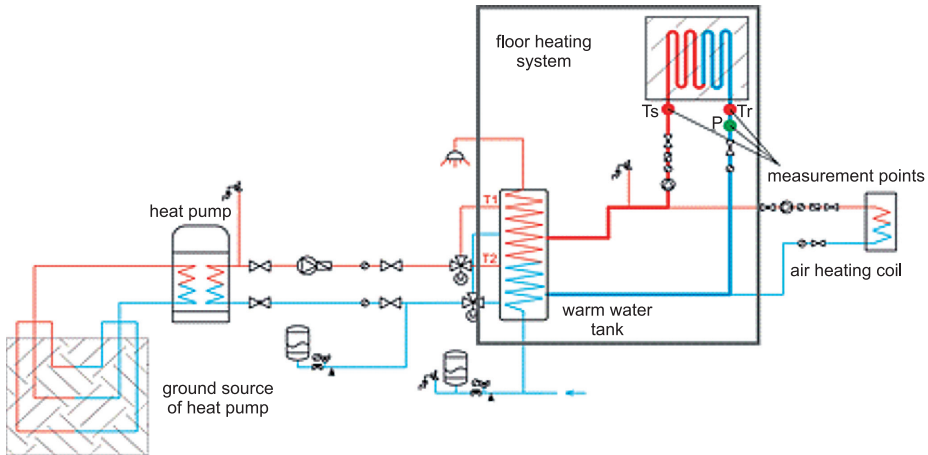


Fig. 4. Heating system with measurement points of supply (T_s), return temperature (T_r) and water flow (P) for floor heating

In order to maintain a continuous record of the outer climate, a local meteorological station was built next to the building. Outdoor air temperature and relative humidity, solar radiation, wind velocity and direction were also measured.

All measurements were carried out with the time step of 1 minute. Short time step is necessary for the monitoring of energy flow into floor heating. For temperature measurements, 1h would have been enough, but applied measurement techniques required the same time step for all channels.

At present, the results for more than two years are available. However, due to gap-free data set (no breaks caused by failure of measurement system), an analysis was carried out for the year 2012. Fig. 5 presents measurement results for outer and inner air temperature as well as temperature at the top of the concrete slab at the edge (section 3.2) and in the center of the building (section 4), for 90 days (from 1st January to 30th March 2012).

The winter of 2012 started with mild outer temperature gradually dropping at the end of January. The first half of February was very cold with temperatures reaching almost -30°C . Floor heating operated intermittently till the end of February. Based on the measured supply and return temperature as well as water flow, heat supply into the slab was calculated (Fig. 5).

The indoor air temperature oscillated mostly between 20°C and 22°C (to a maximum of 24°C during sunny days). The temperature at the slab top was about 20°C with small

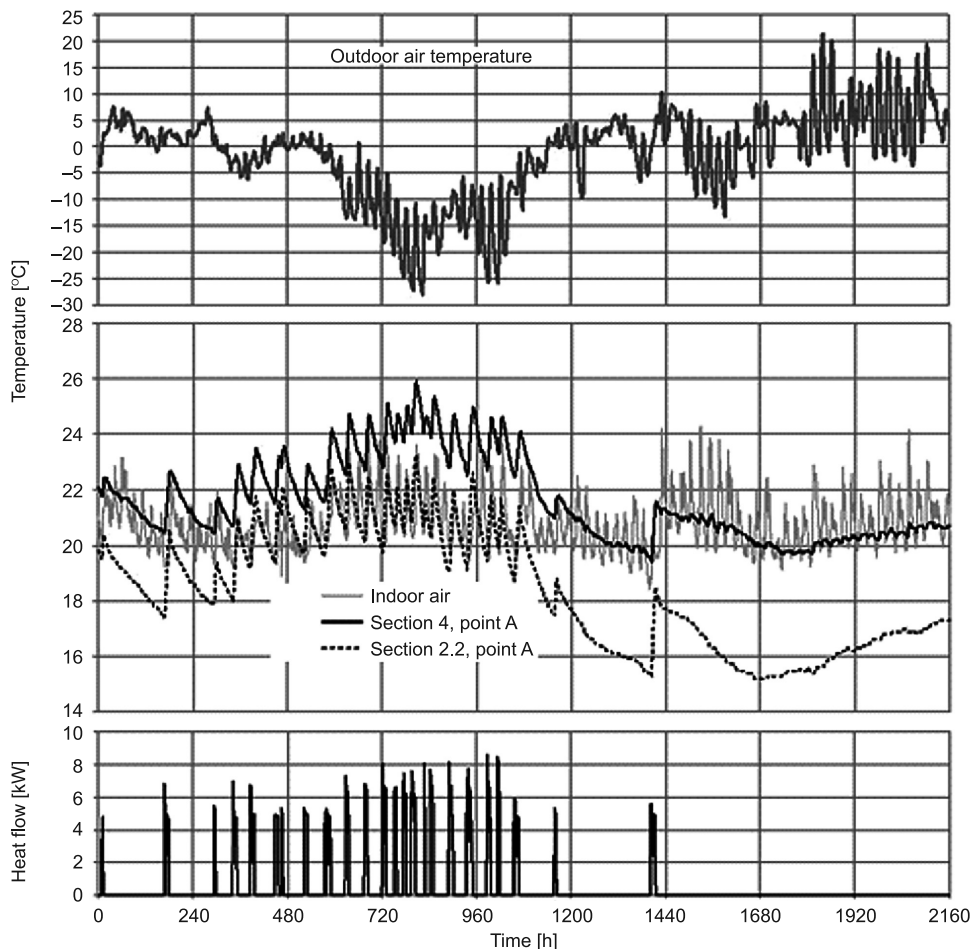


Fig. 5. Pattern of outdoor (top diagram) and indoor temperature, temperature measured at points 4A, 2.2A (lower diagram), and heat supply to floor, 1st Jan.–30th March, 2012 (measurement points location shown on Figs. 2, 3)

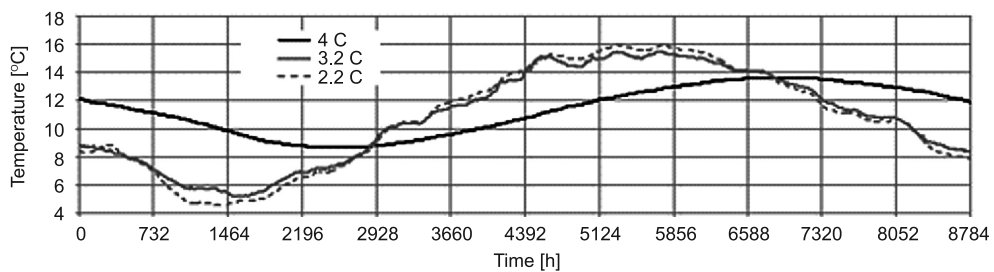


Fig. 6. Measured, yearly temperature pattern at the bottom of thermal insulation (measurement points location shown on Figs. 2, 3)

changes following the indoor temperature. The temperature at the corner (section 2.2) was lower than in the middle of the building by about 3–4°C. No significant temperature difference between the slab top and bottom (points A and B, see Fig. 3) was observed during the measurement period.

Over the course of the heating period, slab temperature rose to 2–3°C above indoor temperature. Despite intermittent heating, floor temperature also remained higher than air temperature during the cut off time. Due to a relatively high heat capacity, temperature drop was about 1°C during a 1 day break. Along with floor heating, air heaters were also used during most cold periods.

Measurements below the insulation layer showed a very stable temperature pattern during the whole year (Fig. 6). In the middle of the building, an almost ideal sinusoidal course (mean value 11.3°C, amplitude 5°C) was observed. At the edge and corner, a similar pattern with about 10.5°C mean value and 11°C amplitude occurred.

3. Numerical analysis

Numerical analysis of transient 3D heat flow in the system with measured boundary conditions was carried out using the hygrothermal whole building simulation software WUFI®Plus [3]. To account for 2 and 3 dimensional thermal bridges in thermal coupling with the building, the software was supplemented with the so-called 3D-objects. Transient heat flow is calculated using the finite balance method. The calculation method was recently validated against DIN EN ISO 10211 standard (DIN 2008) and cross-validated with ZUB Argos® software [4, 5]. WUFI®Plus software was also used for calculation of heat exchange between building and ground [6, 7].

The latest software development concentrates on the integration of active systems within a building [8]. This includes wall and underfloor heating. The modelling of integrated heating pipes would require the application of advanced calculation methods, which is still limited by the capability of contemporary PCs. Therefore, simplified methods, possibly not compromising calculation accuracy, are tested and validated.

The applied algorithm does not reflect the exact arrangement of heating pipes in the slab. Instead of modelling liquid flow and heat exchange in the slab, the model assumes a heat source at certain places of assembly. In the case of floor heating, it is the plane of piping. This assumption can only be made by spiral pattern piping arrangements where the heat source can be regarded as even across the horizontal plane (mean flow and return temperature are constant in the nearby pipes. In the analyzed floor, 3 loops with a spiral pattern are used. Material data used for calculation are collated in Table 1.

Based on the assumed calculation model, the calculation of yearly heat flow in the floor and ground was carried out. The measured indoor and outdoor temperature and heat supplied into the system were used as boundary conditions. Results, for section 4, point A, are presented in Fig. 7 (upper diagram). After about 10 days, quite a good match between calculated and measured temperature could be achieved. The impact of the initial conditions (initial temperature assumed 12°C) can be seen in a relatively short time (about 10 days), this is due to high thermal insulation of the slab from the ground. Similar accuracy was obtained for the remaining measurement points.

Table 1

Assumed material data for calculation

Material	Thermal conductivity [W/mK]	Heat capacity [kJ/m ³]
Concrete slab and screed	2.0	1887
Floor (panels)	0.6	600
Styrofoam	0.04	22.5
Compressed sand	1.3	1530
Ground	1.6	1600

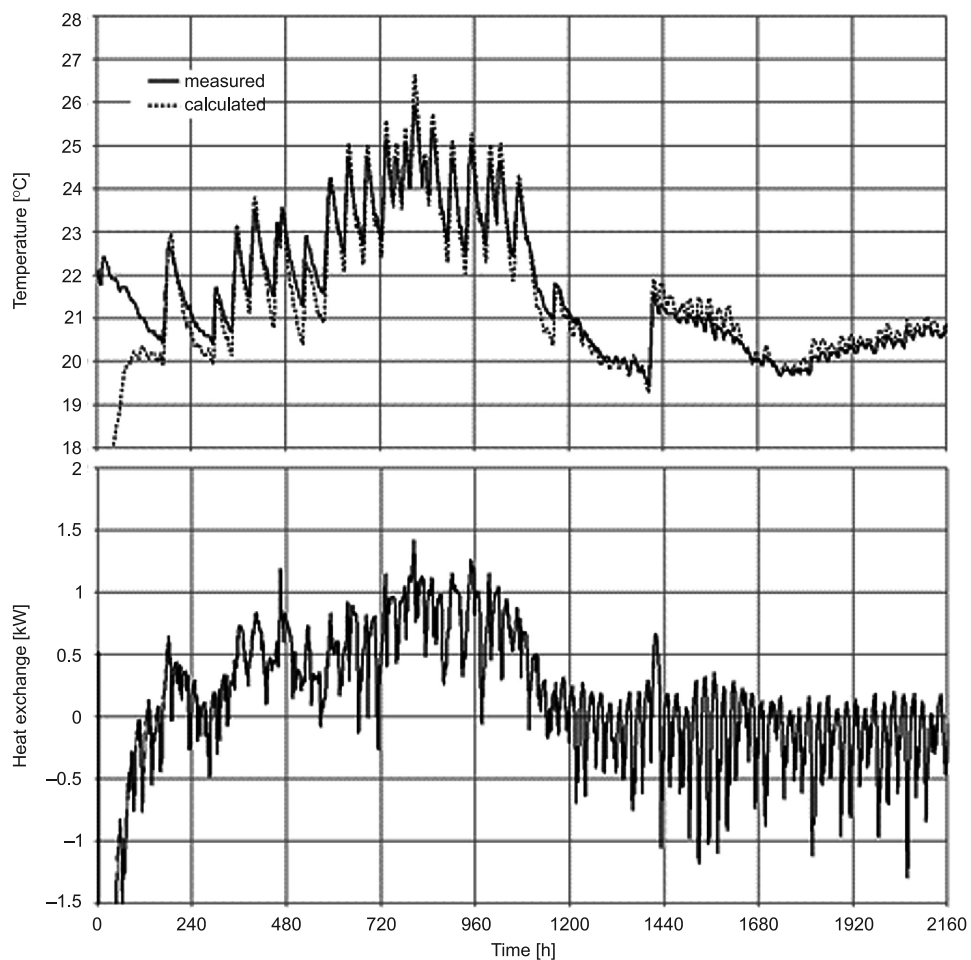


Fig. 7. Measured and calculated temperature pattern at section 4, point A (measurement points location shown on Fig. 2, 3) and total heat exchange between inner air and floor, 1st January–30th March, 2012

Inner air temperature is determined dynamically by heat balance of the analyzed zones. One of the significant factors is heat exchange between inner air and the floor. The results for 90 days are presented in Fig. 7 (lower diagram). As presented, inner diurnal temperature changes of 2–4°C cause more than 1 kW heat exchange in the whole building. This is the contribution of the massive concrete slab to the stabilization of inner air fluctuations. The obtained pattern of heat flux also allows for the assessment of the thermal efficiency of the system. Taking into consideration the time period between 480 and 1000 h (about a 3-week heating period), the energy consumed by floor heating (538 kWh) and the sum of heat gained by inner air from the floor (376 kWh), it could be estimated that efficiency of floor heating was about 70%. For most of the time, outside heating periods, heat loss into the ground was about 250 W ($\sim 3 \text{ W/m}^2\text{K}$).

4. Conclusions

The paper presents results of whole year measurements of a foundation interface in a passive house, including concrete slab with floor heating. Beside valuable, objective information about the thermal performance of the system, the results were used for the validation of a simplified calculation model of floor heating. Overall, calculations supplemented results by heat exchange and led to more general conclusions.

During the measurement time, excluding the heating period, indoor air temperature oscillated between 20°C and 22°C (to a maximum of 24°C). The temperature at the slab top was about 20°C in the middle of the building and lower by 3–4°C in the corners. No significant temperature difference at the slab top and bottom was observed. Below the thermal insulation, the ground temperature remained very stable revealing a sinusoidal pattern.

Diurnal fluctuations of inner air caused heat exchange with floor of about 1 kW for the whole building. For most of the time, heat loss into the ground was about 250 W ($\sim 3 \text{ W/m}^2\text{K}$). The estimated thermal efficiency of floor heating was about 70%. However, this value was obtained under very cold weather conditions.

References

- [1] Wąs K., Radoń J., Globlicki M., Pawliczek B., *Badania cieplno-wilgotnościowe oraz energetyczne budynku pasywnego w Boruszowicach*, Czasopismo Techniczne 2-B/2012, 453-460.
- [2] Flaga-Maryańczyk A., Schnotale J., Radoń J., Wąs K., *Experimental measurements and CFD simulation of a ground source heat exchanger operating at a cold climate for a passive house ventilation system*, Energy & Buildings, Vol. 68, 2014, 562-570.
- [3] Holm, A., Radon J., Künzel H.M., Sedlbauer K., *Berechnung des hygrothermischen Verhaltens von Räumen*, WTA Schriftenreihe H. 24, 2004, 81-94.
- [4] Antretter F., Radon J., Pazold M., *Coupling of Dynamic Thermal Bridge and Whole-Building Simulation*, Thermal Performance of the Exterior Envelopes of Whole Buildings, XII International Conference ASHRAE, Clearwater/USA, 2013.
- [5] Antretter F., Pazold M., Radon J., Künzel H., *Kopplung von dynamischer Wärmebrückenberechnung mit hygrothermischer Gebäudesimulation*, Bauphysik 35, Heft 3, 2013, 181-192.

- [6] Staszczuk A., Radoń J., Holm A., *Evaluation of simplified calculation method of heat exchange between building and ground*, Proceedings of the 1st Central European Symposium on Building Physics, Research on Building Physics, Kraków 2010, 371-376.
- [7] Staszczuk A., Kuczyński T., Radoń J., *Effect of hot weather periods in moderate climate regions on approach to slab thermal design in residential buildings*, 9th Nordic Symposium on Building Physics – NSB, Tampere, Finland, Proceedings, Vol. 2(3), 2011, 825-832.
- [8] Pazold M., Burhenne S., Radoń J., Herkel S., Antretter F., *Integration of Modelica models into an existing simulation software using FMI for Co-Simulation*, Proceedings of the 9th International MODELICA Conference, 3–5 September 2012, Munich, 2012, 949-954.

AGNIESZKA SADŁOWSKA-SALĘGA*, JAN RADOŃ*

EXPERIMENTAL AND THEORETICAL STUDY OF MICROCLIMATE IN HISTORICAL CHURCH IN WIŚNIOWA

EKSPERYMENTALNE I TEORETYCZNE BADANIE MIKROKLIMATU W KOŚCIELE W WIŚNIOWEJ

Abstract

The paper presents a comparison of calculation and measurement results of interior air temperature and humidity in the historical wooden church in Wiśniowa. WUFI@plus software was used for these calculations. A concurrence between calculated and measured parameters allows the presupposition that calculation accuracy is sufficient for the purposes of determining thermal comfort in buildings where the indoor climate is shaped passively. Statistical analysis of the trend changes seems to also be sufficient to assess dynamic impact.

Keywords: microclimate, comparative calculations, historical churches

Streszczenie

W artykule przedstawiono porównanie wyników pomiarów i obliczeń wewnętrznej temperatury i wilgotności powietrza wykonanych w zabytkowym kościele w Wiśniowej. Zbieżność obliczonych za pomocą programu WUFI@plus i zmierzonych parametrów pozwala przypuszczać, że dokładność obliczeń jest wystarczająca do celów określenia komfortu cieplnego w budynkach z pasywnym kształtowaniu klimatu. Analiza statystyczna zmiany trendu wydaje się być wystarczająca do oszacowania dynamiki zmian mikroklimatu.

Słowa kluczowe: mikroklimat, obliczenia porównawcze, kościoły zabytkowe

* M.Sc. Agnieszka Sadłowska-Sałęga, Assoc. Prof. Ph.D. Jan Radoń, Department of Rural Building, Faculty of Environmental Engineering and Land Surveying, University of Agriculture in Cracow.

1. Introduction

Historical buildings constitute an essential part of our cultural heritage. Valuable objects such as wall paintings, sculptures and other furnishings form an integral part of a building. Scientific research shows that the preservation of artefacts and building components is particularly sensitive to the microclimate. High temperature and relative humidity both increase biological risks. Too low humidity often causes cracks due to the shrinkage of the painting substratum and leads to other mechanical damages.

Current valuations of the microclimate in historical buildings show that the indoor air parameters often exceed restoration demands. Global climate change and its negative potential impact constitutes another challenge. The preservation measures, therefore, need reliable calculation results of a building's hygrothermal performance nowadays and in the future.

The software used for calculating hygrothermal performance of the building's envelope is state-of-the-art. However, historic buildings differ from each other in their usage and design. Hygrothermal conditions often shape passively, as in unheated churches. The physical properties of the materials historic building are constructed of differ from contemporary materials. Also, defining internal heat and moisture sources proves difficult due to the specific uses of historic buildings, such as tourism, and so the number of tourists in the museums, their age, weight, clothing, etc., need to be considered.

The paper presents a comparison of calculation and measurement results of interior air temperature and humidity in a historical wooden church in Wiśniowa. WUFI@plus software was used for these calculations.

2. Historical wooden church in Wiśniowa

Wiśniowa village is located in the Małopolska province, 50 km south of Krakow. The church of Saint Martin in Wiśniowa was built around 1730 on the site of a previous one, which burned down. The church was renovated and expanded in the early twentieth century. The church has a wooden log construction. From the outside, the building is boarded with larch paneling. The church is oriented east to west. The church's interior is decorated in Baroque style. The walls bear colorful paintings made in 1910 (Fig.1). The church is located on the so-called "Wooden Architecture Route" in Małopolska province.



Fig. 1. Church of St. Martin in Wiśniowa

It is heated using seven electric storage heaters (only during extreme cold, and immediately before the services). Mass is celebrated at 7 am on weekdays, and at 6pm every Saturday (in wintertime, from October to April – at 5 pm). Four church services are held every Sunday at the following times: 7 am, 9 am, 11 am and 6 pm (in wintertime – at 5 pm).

3. Measurements

Experimental studies in the church in Wiśniowa have been conducted within the scope of “Possibilities and limitations of computational designation of temperature and humidity in historical buildings”, research project funded by Narodowe Centrum Nauki (2011/01/N/ST8/02534).

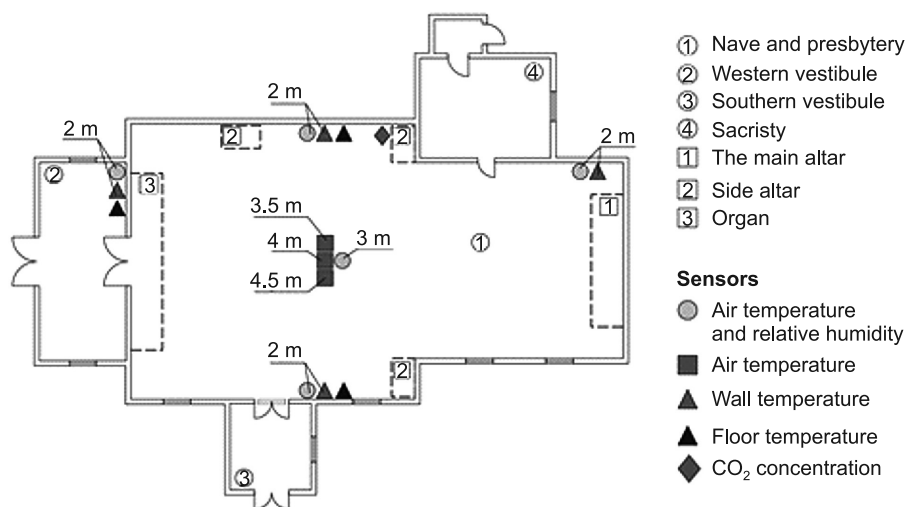


Fig. 2. Placement of sensors in the church in Wiśniowa

The measuring system, due to the historic character of the building, has been based mostly on battery powered measuring devices with radio communication features. The measuring elements have been arranged in two locations – inside the church (measuring internal parameters, see Fig. 2), and outside the church (evaluating external parameters).

The temperature and relative humidity are measured at six points:

- against the southern and northern walls of the nave (at a height of 2.0 m),
- against the northern wall of the presbytery (at a height of 2.0 m),
- in the middle of the nave (sensor hidden in the chandelier at a height of 3.0 m),
- against the western wall of the vestibule,
- and in the central part of the attic (at a height of 1.5 m).

In addition, to recording the vertical temperature stratification in the middle aisle, three supplementary temperature sensors have been mounted (at 3.5 m, 4.0 m and 4.5 m heights), which are hidden in the chandelier as temperature and relative humidity sensors.

Floor temperature is measured at three points: near the southern and northern walls of the nave and in the vestibule (against the wall connecting the vestibule with the nave). The surface temperature is measured at the southern and northern walls of the nave (at 2.0 m height) and at the northern wall of the presbytery (at 2.0 m height). At the northern wall a CO₂ concentration sensor has been mounted.

The weather station was placed in the vicarage, just about 100 m in a straight line from the church. The choice of the location was limited due to numerous trees (the church is surrounded by a historic linden avenue) and other buildings. The weather station includes air relative humidity and temperature sensors and converters of solar radiation (diffuse and global).

4. Theoretical calculations

Hygrothermal conditions in the church in Wiśniowa were calculated using the WUFI®plus software designed for whole building simulations [1, 2].

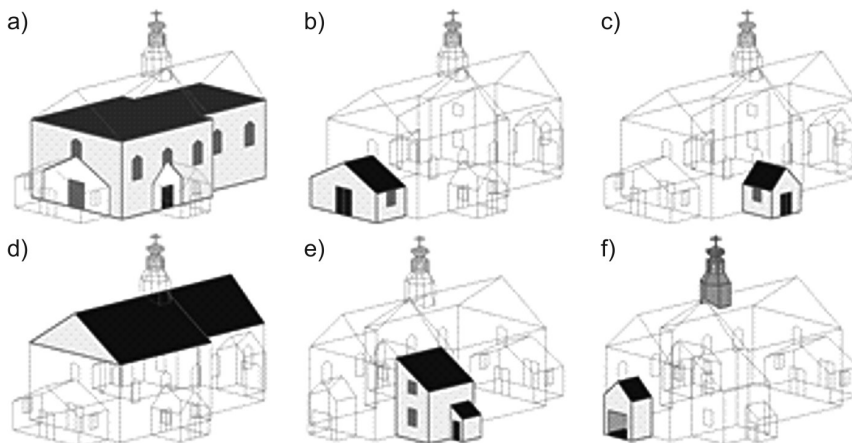


Fig. 3. Division of the church in Wiśniowa by zone: a) nave and presbytery, b) western vestibule, c) southern vestibule, d) the attic, e) sacristy, f) outer altar

The model of the building model takes into account one simulated zone (nave and presbytery: its cubic capacity – 1883.2 m³, and area – 243.7 m²) and 5 attached zones (western and southern vestibules, sacristy and the attic). An additional outer altar is attached to the eastern façade (Fig.3). Material data for particular assemblies was obtained from the WUFI®plus database.

Based on the data obtained from the rector of the Wiśniowa Parish, the number of participants at church services was estimated as outlined in Table 1. The simulation also includes church services such as “Midnight Mass”, which involved far more participants. Heat and moisture gains from people were taken from the WUFI®plus database (activity – 0.97 met).

Based on the CO₂ concentration, the air change rate in the church was estimated as summarised in [3]. At the closed door, the air change rate was about 0.8 h⁻¹. Before each service, and in the summer time, the air change rate increased (Table 1).

Two versions of the boundary conditions were taken into account for the purposes of the calculations (see Table 2). The first set involved statistical data only, i.e. Typical Meteorological Year (TMY), while the second set consisted of parameters measured in 2013. Comparing these calculation results obtained using statistical climate data with the measurement results does not make much sense. The authors, however, wanted to show the extent of the differences when measurement results are not available and TMY is used as a boundary condition. This, on the other hand, is common practice nowadays.

Table 1

Number of participants (A) and ventilation rate (B) during mass in St. Martin church in Wiśniowa (times provided are consistent with daylight saving time)

January–March and November–December					April–October				
Time	Saturdays		Sundays and holidays		Time	Saturdays		Sundays and holidays	
	A [-]	B [h ⁻¹]	A [-]	B [h ⁻¹]		A [-]	B [h ⁻¹]	A [-]	B [h ⁻¹]
6 am		0.8	30	0.9	7 am		0.8	30	1.0
7 am		0.8	80	0.8	8 am		0.8	80	0.9
8 am		0.8	30	0.9	9 am		0.8	30	1.0
9 am		0.8	100	0.8	10 am		0.8	100	1.0
10 am		0.8	30	0.9	11 am		0.8	30	1.1
11 am		0.8	300	0.8	12 am		0.8	300	1.1
12 am		0.8	50	0.9	13 pm		0.8	50	1.1
4 pm	25	0.9	30	0.9	18 pm	25	1.0	30	1.1
5 pm	50	0.8	200	0.8	19 pm	50	0.9	200	1.1
6 pm	5	0.9	10	0.9	20 pm	5	1.0	10	1.1

Table 2

Number of participants (A) and ventilation rate (B) during mass (times consistent with daylight saving time)

Simulation	Outer climate	Ground parameters	Climate in attached zones
1	TRM for Kraków from WUFI@plus database	– Temperature – sine curve (9.2 ± 7.2; max 01.08.2013) – 100% RH	Outer climate
2	From measurements: – temperature – relative humidity – solar radiation	– Temperature of the floor in the church – 100% RH	From measurements: – temperature – relative humidity

To ensure proper initial conditions, the calculations started at the beginning of November 2012 although the results were evaluated starting on January 1st 2013. Calculation time was 12 months (until the end of December 2013).

5. Results and discussion

As a result of the simulation the hourly patterns of temperature and relative humidity inside St. Martin church in Wiśniowa have been obtained. Figure 4 shows a comparison of the simulation results with the measured values for sample winter and summer months, December, 2013 and July, 2013, respectively. Statistical analyses were conducted separately for seasonal, weekday, Saturday and Sunday data sets (Fig. 5–7 and Table 3). A correlation was calculated based on the Spearman R test (the distribution of variables differs from a normal distribution) [4].

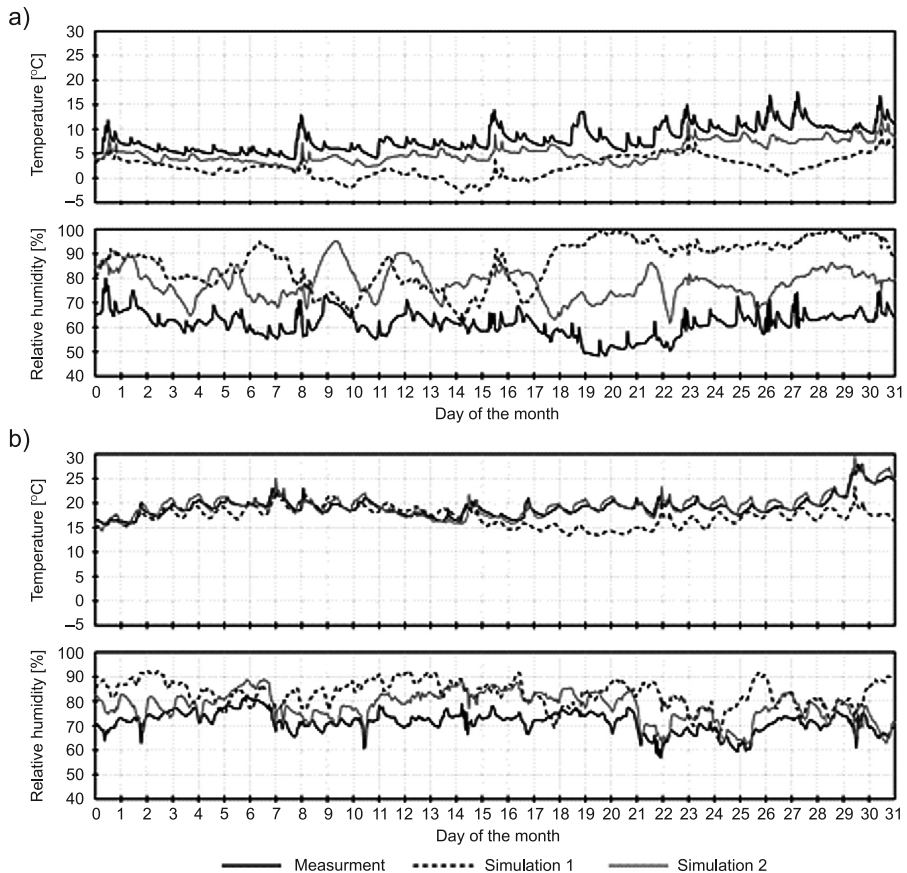


Fig. 4. Measurement results of temperature and relative humidity inside St. Martin church in Wiśniowa and simulation results for: a) December, 2013 b) July, 2013

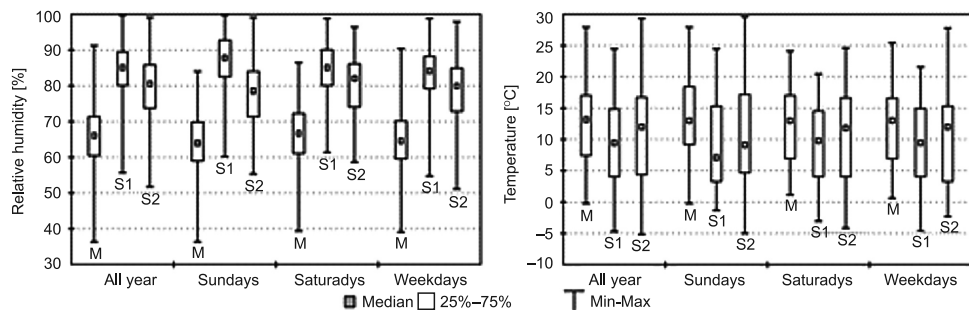


Fig. 5. Median, 25–75% percentile and min.-max. scope of measured (M) and calculated (S1, S2) inside air relative humidity and temperature

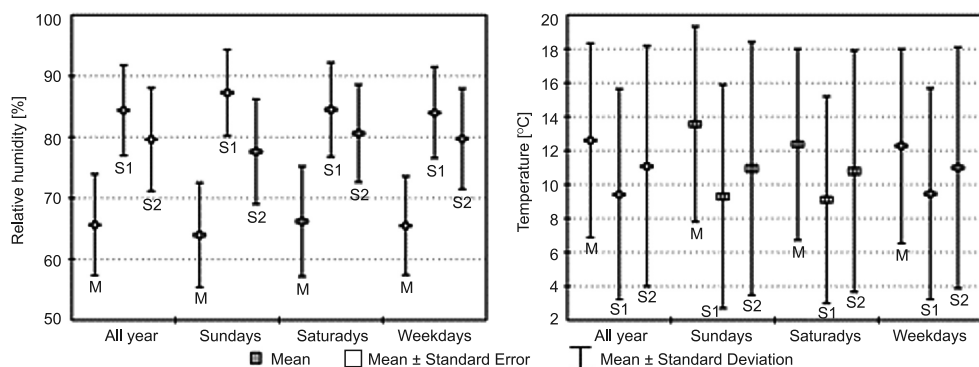


Fig. 6. Average, standard error and deviation of measured (M) and calculated (S1, S2) inside air relative humidity and temperature

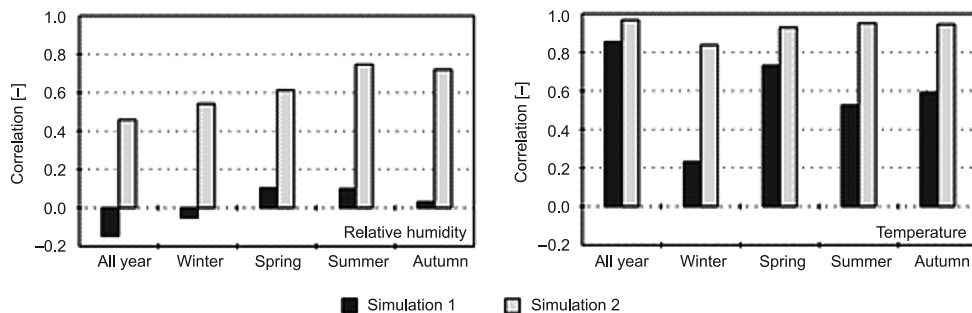


Fig. 7. Correlation between measurement and simulation for indoor air temperature and relative humidity depending on the season

Temperature calculations demonstrate a better agreement with the measurements. In all of the analyzed cases the correlation is positive. Over the course of a year, statistical climate correlation can be described as average-strong to strong, while real climate as strong. In both cases there are fewer errors than the average error rate of more than 62%.

Clear differences can be noted between the accuracy of the calculations for the summer and winter. For weekdays, the mean absolute error, in the case of statistical climate for the winter, is equal to 3.9°C, while for the summer it is 2.3°C. For external climate – on the basis of measurements – the mean absolute errors for the winter and summer are equal to 3.3°C and 0.9°C respectively.

Table 3

Correlation, mean and maximal absolute error

	All year		Sundays		Saturdays		Weekdays	
	Sym 1	Sym 2	Sym 1	Sym 2	Sym 1	Sym 2	Sym 1	Sym 2
Temperature								
Mean absolute error [°C]	3.6	1.9	4.5	2.8	3.7	1.9	3.4	1.8
Max. absolute error [°C]	17.3	12.1	17.3	11.5	13.9	12.1	14.7	12.1
Correlation	0.85	0.97	0.85	0.95	0.87	0.97	0.86	0.97
Relative humidity								
Mean absolute error [%]	19.3	14.2	23.4	13.9	19.3	14.5	19.0	14.4
Max. absolute error [%]	54.1	42.7	51.8	35.7	48.2	35.2	54.1	42.7
Correlation	-0.14	0.46	-0.34	0.51	-0.31	0.50	-0.12	0.42

In the case of relative humidity calculation accuracy is lower. Over the period of one year, in the case of statistical climate, the correlation proves negative. For the climate based on measurements, the correlation is positive and it can be describes as average-strong. Analogous to the temperature, clear differences between the accuracy of calculations for summer and winter can be noted. For weekdays, mean absolute error, in the case of statistical climate for the winter is equal to 30.6%, while for the summer it is 14.9%. For external climate – on the basis of measurements – the mean absolute errors for the winter and summer are equal to 24.0% and 8.1% respectively.

6. Conclusions

The concurrence of the calculated and measured parameters allows the presupposition that calculation accuracy is sufficient for the purposes of determining thermal comfort in buildings where the indoor climate is shaped passively. A statistical analysis of the trend changes seems to also be sufficient to assess the dynamic impact. Absolute temperature and humidity values, however, depend strongly on the accuracy of the definition of boundary conditions.

The authors were able to reach a much better agreement by modifying some parameters slightly (e.g. heat and/or moisture sources) and applying a more precise heat and moisture exchange model of the floor. Nevertheless, the presented results are very likely to be obtained based on partly rough estimated data, when exact solutions (in the form of measurement data) are unknown.

References

- [1] Holm A., Radon J., Künzel H.M., Sedlbauer K., *Berechnung des hygrothermischen Verhaltens von Räumen*, WTA Schriftenreihe H., 24, 2004, 81-94.
- [2] Karagiozis A., Künzel H.M., Holm A., *WUFI-ORNL/IBP – A North American Hygrothermal Model*, Contribution to “Performance of Exterior Envelopes of Whole Buildings VIII”, 2–7 Dec. 2001, Clearwater Beach, Florida.
- [3] Mattsson M., Lindström S., Linden E., Sandberg M., *Tracer Gas Techniques For Quantifying The Air Change Rate In Churches – Field Investigation Experiences*, 12th International conference on air distribution in rooms, Paper No 235, Trondheim, Norway 2011.
- [4] Aczel A.D., *Statystyka w zarządzaniu* (original title: *Complete Business Statistics*), Wydawnictwo Naukowe PWN, Warszawa 2011.

ANNA SEDLÁKOVÁ*, PAVOL MAJDLEN*, LADISLAV ŤAŽKÝ*

ENERGY EFFICIENT BUILDINGS – LOWER STRUCTURE

BUDYNKI ENERGOOSZCZĘDNE – STREFA KONTAKTU Z GRUNTEM

Abstract

Part of the package of low-energy and passive houses is the basement and foundation too. A correct proposal of construction detail of buildings that lying on the soil is one of the steps that contribute to reducing energy requirements for heating and operation of building. At the same time increase the quality of the indoor environment as well as performance at work. In the construction of the lower structure, the most delicate point is the contact of walls, foundations and floor structure with the soil and subsoil, this frequently leads to inconsistent solutions of the design detail, resulting in the formation of thermal bridges with subsequent condensation

Keywords: building construction, ground floor, thermal insulation, buildings on the terrain

Streszczenie

Poprawne rozwiązanie szczegółów budynku będących w kontakcie z ziemią jest jednym z istotnych kroków, które przyczyniają się do zmniejszenia zapotrzebowania na energię do ogrzewania i eksploatacji budynku. Jednocześnie poprawie ulega jakość środowiska wewnętrznego i wydajności pracy. W dolnej części budynku najbardziej wrażliwe są miejsca styku ścian, fundamentów oraz podłogi z gruntem i podłożem, są one często niewłaściwie rozwiązywane, powodując powstawanie mostków termicznych i dalej kondensację pary wodnej.

Słowa kluczowe: konstrukcja budynku, podłoga na gruncie, izolacja termiczna, budynki na terenie

* Assoc. Prof. Ph.D. Anna Sedláková, M.Sc. Pavol Majdlen, M.Sc. Ladislav Ťažký, Department of Building Physics, Institute of Architectural Engineering, Civil Engineering Faculty, Technical University of Košice, Slovakia.

1. Introduction

The correct proposal of construction details is one of the steps which will contribute to reducing energy requirements for the heating and operation of the buildings which are situated on the terrain whilst at the same time, increasing the quality of the indoor environment as well as performance at work.

In our case within the construction solution of a detail where the wall, foundation and floor are in contact we must consider many requirements. In addition to the structure and thermal protection must be taken into account requirements as follow as: waterproofing, fire safety, antiradon measures, statics, economy and impact of outdoor and indoor environment.

The quantity and type of thermal insulation material is very important too. Compliance with this requirements is the deciding factor that contributes to the optimization of the construction details.

1.1. The design possibilities of a new generation of ground floors for energy efficient buildings

1.1.1. Boundary conditions for the calculation

Outside winter air temperature shall designate the location of the building, depending on the geographic location according to maps of temperature fields and, depending on altitude **Košice 297 m above sea level** (2. temperature region), $\theta_e = -13^\circ\text{C}$. The relative humidity of ambient air is determined by the ambient temperature as calculated: $\varphi_e = 84\%$. Calculation of the internal air temperature for the residential part of the building: $\theta_i = 20^\circ\text{C}$. Relative humidity of indoor air: $\varphi_i = 50\%$. Surcharge for heating temperatures dipped to decrease indoor air: **to 5 K**.

1.2. Results of 2D modeling of details for new generation of the lower structure for energy efficient buildings

Distribution of temperatures and heat flows under the buildings (as you can see below) and its immediate vicinity is closely linked with the correct calculation of the total heat loss of assessed buildings. The detailed analysis of the building structure show us what impact the location of insulation has and its mutual combination as well as the overall solution of the detail. In our case we're speaking about the detail where are external wall, basement and floor in contact with a soil as yiu see below.

Here are the following variants:

- establishment with thermal insulation of basis and external wall,
- establishment with special block and plinth insulation,
- establishment on block of foam glass and plinth insulation,
- establishment on brash of foam glass,

Variant 1: Establishment with thermal insulation of basis and external wall. This method (Fig. 1) is the most used in Slovakia for ordinary houses in the energy standard. Thermal insulation of the external wall continues up to the lower edge of the base strip. Thermal

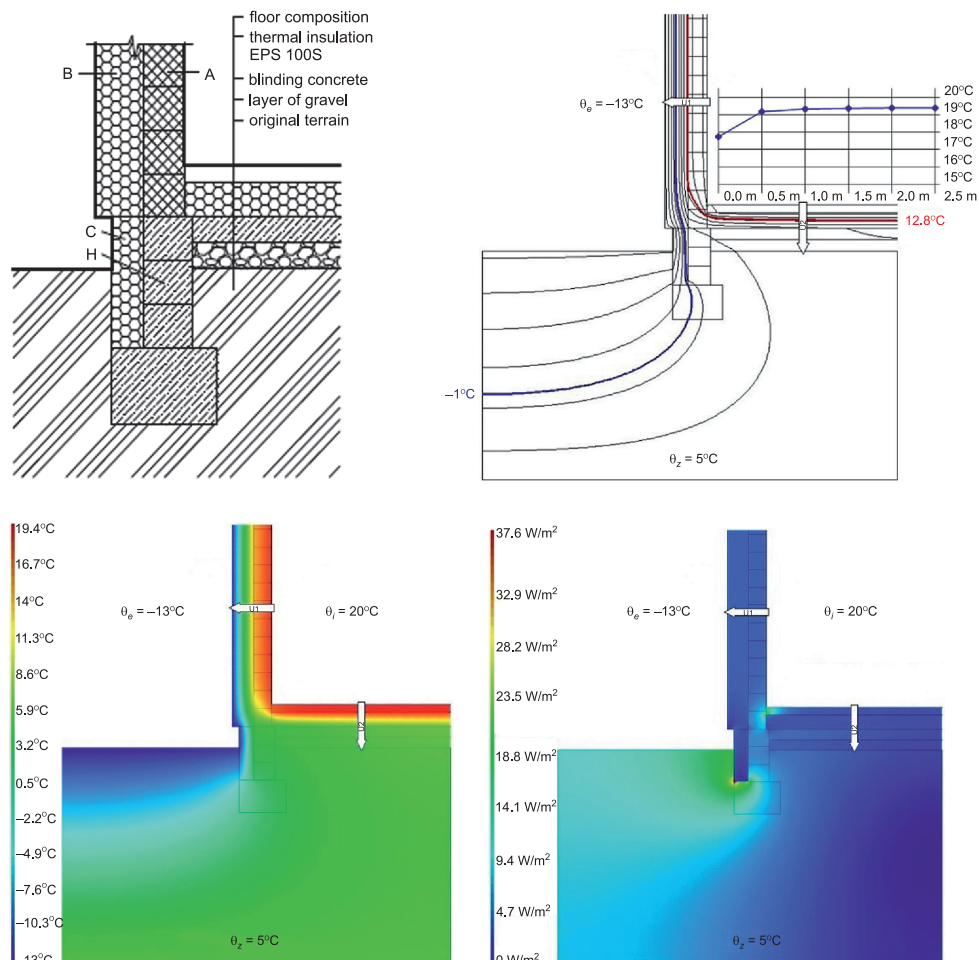


Fig. 1. Establishment with thermal insulation of basis and external wall (A – Ytong P2-400, B – expanded polystyrene EPS 70F, C – extruded polystyrene Styrodur 2800C, H – form block DT30) – results of 2D modeling of detail and cours of temperature

insulation in the floor is laid on the upper surface of the base plate (slab). Thermal insulation of external walls and in the floor is separated by external construction.

Variant 2: Establishment with special block, with plinth insulation. The thermal bridge, which forms the cladding in contact with the base plate (slab) can be interrupted by polystyreneconcrete shapes KS-ISO KIMMSTEIN. This method can be still combined with plinth insulation or without this insulation (Fig. 2).

Variant 3: Establishment with special block, with plinth insulation. The thermal bridge, which forms the cladding in contact with the base plate (slab) can be interrupted by block of foam glass PERINSUL. This method can be still combined with plinth insulation or without this insulation (Fig. 3).

Variant 4: Establishment on brash of foam glass. Establishment on brash of foam glass is a relatively new solution. Brash of foam glass is poured into the tub which is lined with extruded polystyrene boards. Backfill is compacted at a ratio of 1:1.25. Thereafter is situated reinforced concrete base plate (slab) on backfill of foam glass (Fig. 4).

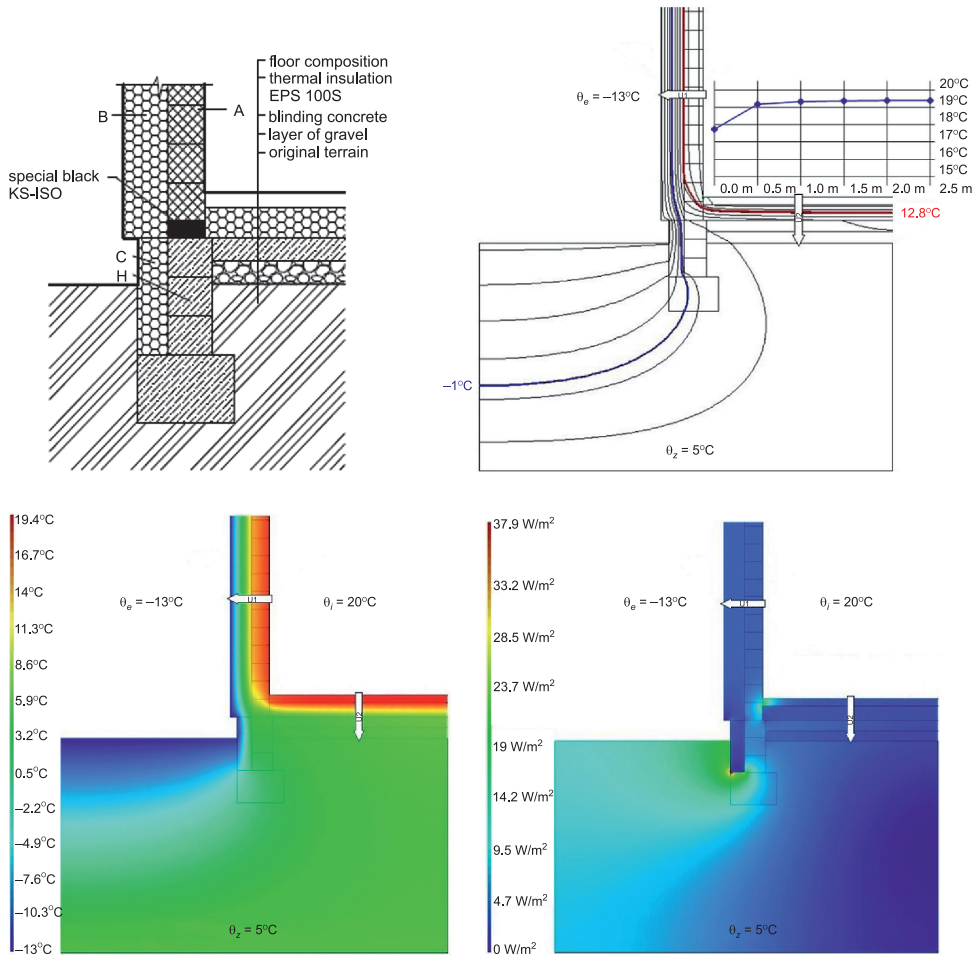


Fig. 2. Establishment with special block – KS-ISO, with plinth insulation (A – Ytong P2-400, B – expanded polystyren EPS 70F, C – extruded polystyren Styrodur 2800C, H – form block DT30,) – results of 2D modeling of detail and course of temperature

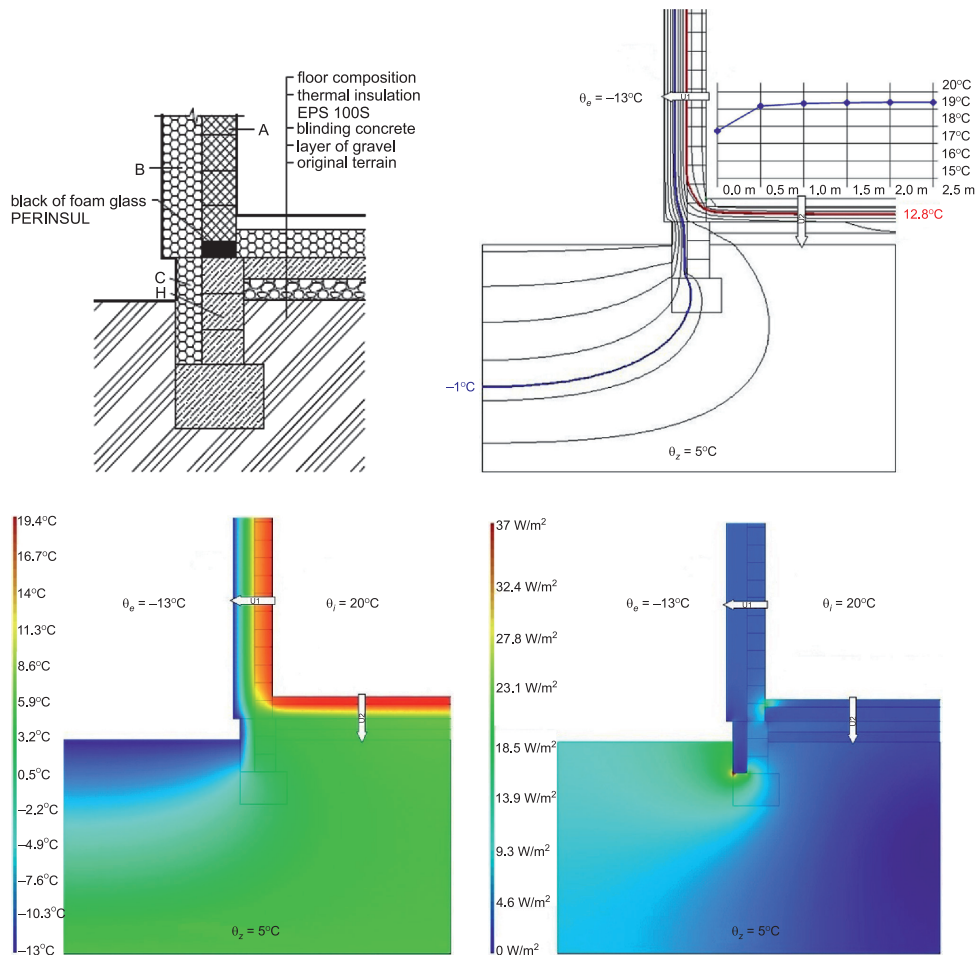


Fig. 3. Establishment with special block – PERINSUL, with plinth insulation (A– Ytong P2-400, B – expanded polystyren EPS 70F, C – extruded polystyren Styrodur 2800C) – results of 2D modeling of detail and course of temperature

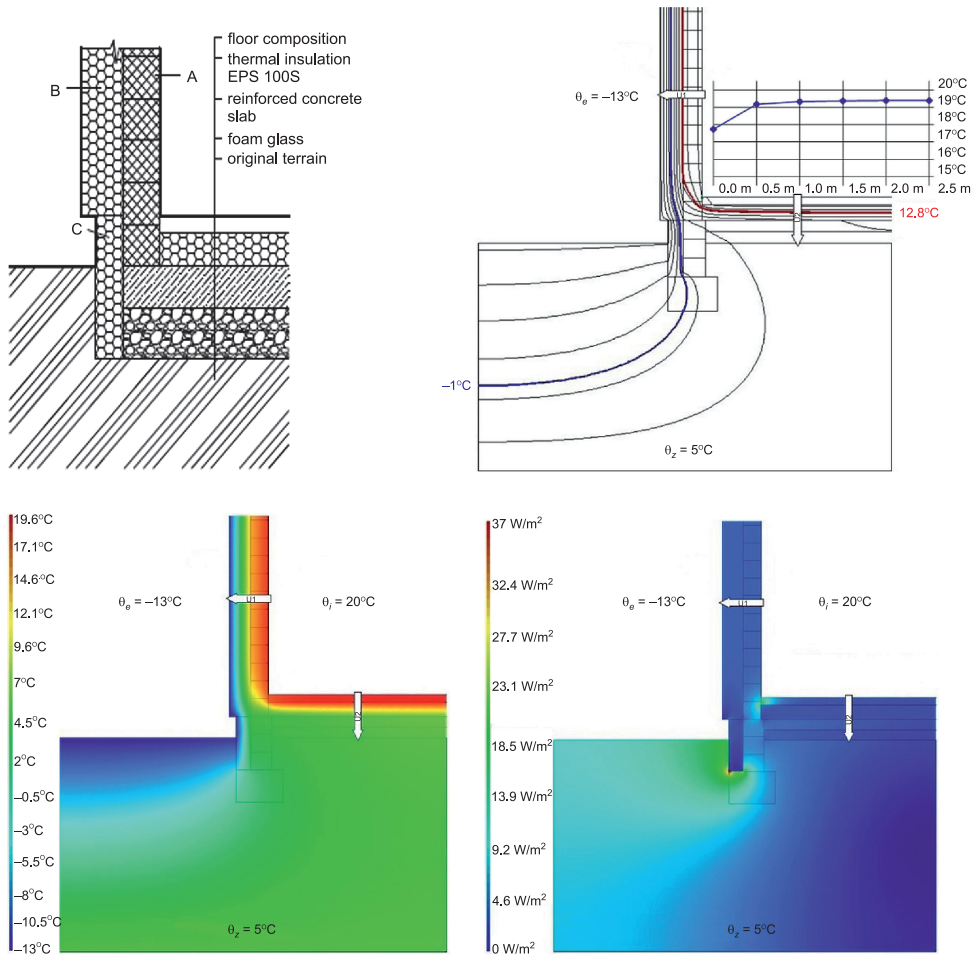


Fig. 4. Establishment on brush of foam glass (A – Ytong P2-400, B – expanded polystyren EPS 70F, H – form block DT30) – results of 2D modeling of detail and course of temperature

2. Conclusion

Thermal insulation is now a word that we hear all around, particularly with respect to rising energy prices in line with the long-term strategic goals of reducing emissions and improving energy efficiency in buildings. This is the subject of European Parliament and Council 2013/31/EU of 19th May 2010 on the energy performance of buildings. The European Union has committed to reduce overall greenhouse gas emissions by 20% of what it was in 1990 by 2020. By the same date, to reduce energy consumption in EU countries by 20% and to achieve 20% share of renewable energy sources of total energy consumption. This can also contribute to solving the lower structure for a new generation of energy efficient buildings. The simulation model will be compare with measurement in situ [2]. Based on the results of measurements and after fine-tuning simulations of the experimental building will be to obtain relevant results applicable in practice for the design of passive buildings. It will be in compliance with basic hygienic requirements in terms of structures, indoor environment and in terms of design and use of heating or ventilation systems.

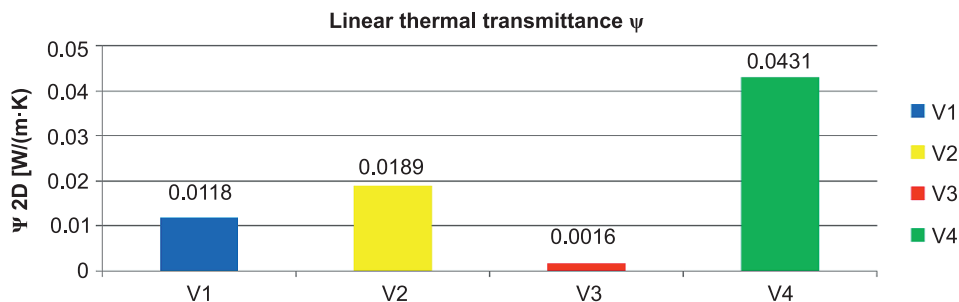


Fig. 5. Linear thermal transmittance

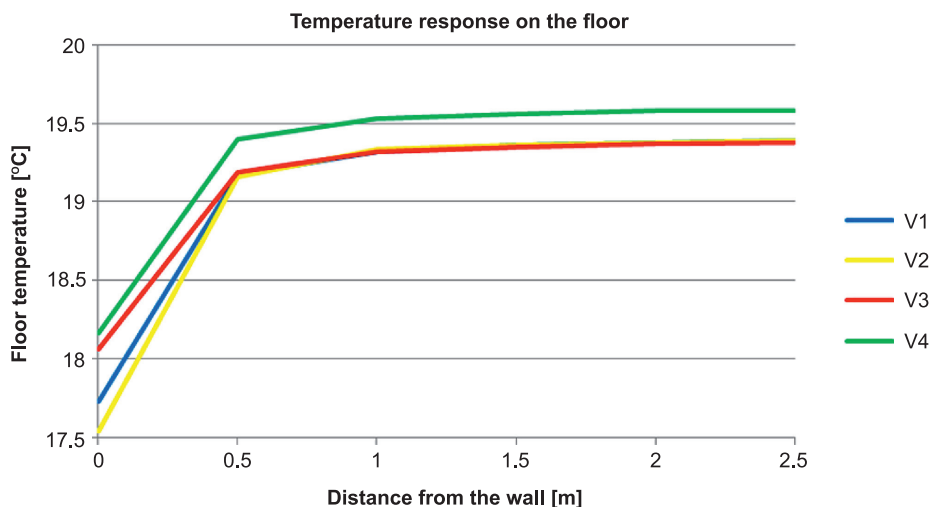


Fig. 6. Temperature response on the floor of variant 1–4

Representation of the structural modifications for each variants detail

Sign	U_{wall} [W/(m ² ·K)]	U_{floor} [W/(m ² ·K)]	θ_{si} [°C]	f_{Rsi} [-]	L_{2D} [W/(m·K)]	$L_{2D,wall}$ [W/(m·K)]	$L_{2D,floor}$ [W/(m·K)]	Ψ_{2D} [W/(m·K)]
Variant 1	0.104	0.17	17.73	0.93	0.527	-0.26	-0.256	0.0118
Variant 2	0.104	0.17	17.54	0.93	0.534	-0.26	-0.256	0.0189
Variant 3	0.104	0.17	18.06	0.94	0.514	-0.26	-0.256	0.0016
Variant 4	0.104	0.099	18.16	0.94	0.452	-0.26	-0.149	0.0431

This article was written as a project solution entitled "The use of the virtual laboratory for designing energy-efficient buildings" Project code: 052TUKE-4/2013.

References

- [1] Sedláková A., Al Ali M., *Composite materials based on lightweight concrete*, [in:] *Chemické listy*, Vol. 105, no. Special issue 16, 2011, 445-447.
- [2] Passive House Solutions, *Concept of building structure design and environmental assessment for consumer model of research in order to force the integration of renewable energy sources*, May 2006, 50.
- [3] Smola J., *Architektura pasivních domů*, Pasivne domy 2011.
- [4] Pacson T., *Introduction to Phase Change Materials: Building Applications*, 8.04.2011.
- [5] Lstiburek J., *Building Science*, Passive Getting Active.
- [6] Pifko H., *Čo je energeticky pasívny dom*, Konferencia Energetický pasívny dom 2006, 14.06.2006, Bratislava, 22-26.
- [7] Antonova A., *Passive house for Latvia, Energy efficiency and technical-economic aspects*, Thesis for the Degree of Master of Science, June 2010.

MARIUSZ SOBOLEWSKI*

A STUDY OF THICK THERMAL INSULATION WITH DENSITY FOAM POLYSTYRENE (EPS)

BADANIA CIEPLNE GRUBYCH IZOLACJI Z POLISTYRENU SPIENIONEGO (EPS) O MAŁEJ GĘSTOŚCI

Abstract

Energy-efficient construction requires the use of thermal insulation materials of high thickness compared to traditional construction. Thus, there is a need to conduct research for thick insulation products. The paper presents the results of the measurements of thermal parameters for foam polystyrenes (EPS) with low density and of different thicknesses. The experimental work has been carried out in the Water Center Laboratory WULS-SGGW.

Keywords: lightweight thermal insulations, thick thermal insulations, low density insulation products, expanded polystyrene (EPS), HFM apparatus

Streszczenie

Budownictwo energooszczędne wymaga stosowania izolacji cieplnych o dużych grubościach w porównaniu z budownictwem tradycyjnym. Istnieje więc potrzeba prowadzenia badań dla grubych wyrobów termoizolacyjnych. W artykule przedstawiono rezultaty pomiarów parametrów cieplnych polistyrenów spienionych EPS o małej gęstości i różnej grubości. Prace badawcze zostały wykonane w Laboratorium Centrum Wodne SGGW w Warszawie.

Słowa kluczowe: lekkie materiały termoizolacyjne, grube izolacje cieplne, wyroby izolacyjne o małej gęstości, polistyren ekspandowany (EPS), aparat płytowy HFM

* Ph.D. Mariusz Sobolewski, Department of Civil Engineering, Faculty of Civil and Environmental Engineering, Warsaw University of Life Sciences (SGGW).

1. Introduction

The need for research into thick thermal insulation in engineering practice arises from the need to check insulation products with a high thickness (i.e. more than 100–150 mm range) and low-density products, in which the effect of the thickness occurs (i.e. dependence of the measured thermal conductivity coefficient on material thickness). As there are more and more thermal design requirements, it is essential to use increasingly thick layers with traditional insulation products. The two above research cases concerning control of insulation products are of particular importance due to the thermal protection of low energy-consuming buildings e.g. passive. Providing reliable thermal values of thick insulating products' performance with their actual thickness is very important. The author of this article narrows down the subject to presenting research for low density insulation products with different thicknesses only.

For this study, we employ appropriate measuring equipment that allows for the measurement of samples with thicknesses exceeding 100 mm. Currently, among the existing plate apparatus on the market, the best apparatus to study thick samples with high accuracy (error of measurement less than 2%) have a large measuring field. Large dimensions of the measuring section enable an appropriate volume of the sample to take an active part in the research. In addition, the maximum thickness of the sample in each plate apparatus is limited to the edges of the samples-boundary conditions and related edge error heat loss. According to the guidelines contained in standards [5–7] the maximum thickness of the sample in the plate apparatus with the heat flux sensors, in symmetrical configuration with a single sample of the measuring section 300 mm, should not exceed the value of 135 mm. The permissible thickness of the sample (135 mm) is important for low density materials, for which it is recommended not to exceed the maximum permissible value of the thickness given in the standards. Generally, it is assumed that in low density material, the thickness of the sample should be greater than that for which the transfer factor (ζ) of material, product or system does not change by more than $\pm 2\%$ with continued growth.

2. Thermal insulations with low density

Most thermal insulations, including low density insulations, have a porous body with closed or open pores, filled with gas. Insulating plastics are heterogeneous in terms of the structure and may not be treated as the thermo-homogeneous medium. However, it is assumed in the standards that products with high thermal resistance are homogeneously porous. Such products can be investigated in terms of heat properties when the maximal nominal pores' size, granules or grains do not exceed one tenth of the specimen thickness [6, 7].

For the above reasons, the actual transport of heat inside the insulating products is very complex and may take place by conduction both in the solid and gas phase radiation, convection and mutual interactions. This phenomenon is often called the measured, the equivalent, the apparent or the sample effective heat conduction and the parameter describing this phenomenon is called the measured thermal conductivity coefficient (λ). The process of heat

flow in thermal insulations is not fully recognized due to a lack of sufficiently accurate, quantitative description of heat transfer mechanisms. Insulations, where the heat exchange takes place by conduction and radiation, are products with medium and high thermal resistance and low bulk density ($\rho < 40 \text{ kg/m}^3$). Heat transfer by radiation in insulations characterized by density ($\rho < 20 \text{ kg/m}^3$) is quantitatively significant. In recent times, it has been noted that thermal radiation could be responsible for a significant part of heat transport in very light foam and fibred insulations, even at temperatures of functioning insulation which is little above room temperature [3].

The characteristic feature of thermal insulation products is an increase of thermal conductivity with a decrease in the density of the product. From the point of view of the thermal insulation of building partitions, the observed dependence of the measured thermal conductivity as a function of bulk density is unfavourable. In order to preserve a specific level of the insulation of building partitions which have been analysed, there is a need to apply a thicker layer of lightweight insulation as opposed to heavier insulation [1, 4]. In the case of polystyrene (EPS), an inversely proportional dependence of conductivity and density occurs throughout the range of density of the EPS. i.e. $10 - 45 \text{ kg/m}^3$. We can observe the stabilization of the measured thermal conductivity at density $\rho \geq 40 \text{ kg/m}^3$ [1, 2, 4].

The aim of the experimental research performed on thermal insulations is to obtain information on the size of thermal parameters and a correlation between measured values. In studies of the perfectly conductive heat solids, i.e. thermally isotropic and homogeneous in the direction of the heat flow by the product, we can usually consider the average thermal conductivity coefficient (λ) of samples. In the complex conditions of heat flow and the research of real materials with complex construction, we apply the concept of the transfer factor (\mathfrak{Z}), which is not always the intrinsic feature of the material. In products in which the heat flow results not only from conduction, the transfer factor may be dependent on the test conditions. This parameter may be greatly determined by the thickness of the sample, the temperature difference for the same mean temperature test, emissivity of the apparatus etc. In light thermal insulations (i.e. low density products) specifying the thermal transmissivity (λ_r) is more relevant because this parameter deals with cases when the heat flow is only a combination of conduction and radiation. With regard to the heat flow the thermal transmissivity is the parameter which the most precisely describes very light insulations, because it does not depend on the thickness of the sample. On the basis of an analysis of simultaneous heat conduction and radiation in low density insulations, it has been shown that the apparent thermal conductivity coefficient (λ) of the insulation type varies with the layer thickness. This effect was experimentally observed in foam insulations (polystyrene and polyurethane, phenols), fibred insulations (wools) and light weight aerated concrete [1–4]. The apparent thermal conductivity of insulations increases gradually with increasing the thickness of insulation. Starting from a thickness limit (d_m), this conductivity reaches asymptotic values corresponding to the total sum of thermal conductivity and thermal radiation [3]. The thickness effect is caused by the partial transparency of thin samples of material with low density for thermal radiation. Only with sufficient thickness, does light-weight material have a sufficiently large density for thermal radiation to be absorbed and diffused within the sample. As a result of the heat radiation absorption and the dissipation, the fixing

of the values for the measured thermal conductivity coefficient succeeds. Along with a further increase in the sample thickness, there are no changes in the value of the measured thermal conductivity coefficient. On the basis of the literature [1] we can assume that with the increase in density of polystyrene the thermal conductivity coefficient should be defined for material thickness being reduced gradually. The asymptotic values of the apparent thermal conductivity coefficient can correspond to the thermal transmissivity, defined in the standards [5–7]. If the thickness effect does not occur, then the transfer factor takes the value equal to the thermal transmissivity of the material [6]. According to the standard [8], the thickness effect is negligible for EPS products with a thickness of at least 50 mm and a declared thermal conductivity coefficient of $\lambda_d \leq 0.038$ W/mK.

The evaluation of the significance of the thickness effect is possible on the basis of the experimental procedure, by means of calculation [6] or by using charts and tables [6]. The last two methods have limitations and boil down to the formulated cases assigned to selected types of products. This work concerns the experimental way of determining the thickness effect in the analysed EPS samples.

The thermal characteristics of the samples can also be described by thermal resistance (R). When research clearly shows that the thermal resistance of samples does not depend on the temperature variations in the given test average temperature, then it may be additive. The average thermal conductivity coefficient and transfer factor do not depend on the test conditions and characterise the product. However, the thermal resistance in apparent low density insulations at any mean temperature may be a function of the temperature difference determined by the sample thickness. This behaviour in this case is not due to convection because it does not participate in heat flow. Therefore, in the light type insulations, the smallest thickness of the sample (d_m) is needed – furthermore, it can be possible to define the thermal properties of the product. Then, the transfer factor is different in relation to the thermal transmissivity by less than 2% [6]. In any case, whether the effect of thickness is significant or not, it is necessary to specify the representative value, i.e. the thermal transmissivity or thermal resistance for products with low density.

The total thermal resistance of a thick product with low bulk density is determined on the basis of the thinner plasters cut from the product. There are two ways to deal with thin samples. It should be assessed experimentally which way is appropriate for the tested product. The first way involves dividing the product into a few plasters which are equal in thickness and measuring the thermal resistance of only one layer that represents the product. The total thermal resistance of the product is calculated, assuming that the other plasters have the same thermal resistance. The second option is based on separate examination of the thermal resistance of each plaster which is cut from the thick product. The total thermal resistance is calculated as the sum of the thermal resistance of the plasters. If the thickness effect is significant, then the total thermal resistance of the thick product cannot be calculated in some cases as the sum of the thermal resistance of the layers which are cut from the product [5, 6]. Then, there are possible two situations in the course of an experiment – when the sample thickness exceeds or does not exceed the measuring capabilities of the apparatus (the distance between the heating and the cooling plates). When the sample thickness exceeds the measuring capabilities of the apparatus, the transfer factor and thermal resistance are calculated from the existing formulas for low density insulating

products presented in the standards. In this situation, the research is conducted for one layer and the transfer factor is determined using the interpolated equations for the full thickness of the sample, then on the basis of the transfer factor, we can calculate the total thermal resistance of the target thickness of a product. If the sample thickness does not exceed the measurement capabilities of the apparatus, the thermal parameters of the product for the thickest sample (put in the apparatus) can be determined experimentally. Hence, there is not any further need to experimentally determine the thermal conductivity coefficient for thinner samples. Thermal resistance is calculated on the basis of the determined thermal conductivity coefficient and thickness of the products concerned.

The thermal resistance, the transfer factor and the thermal transmissivity may be a result of a measurement on one sample in the test conditions for the isolation of fitting the homogeneity conditions (thermal, structural). The heat flow characteristics measured for many samples of the same material may vary due to the variety of material composition or the diversity of samples. These properties can change with the mean temperature test, can change over time or be dependent upon previous thermal history.

3. The characteristics of the analysed low density polystyrenes (EPS)

The research was conducted for three different types (A, B, C) of commercial expanded polystyrenes (EPS) with low density, produced by Polish firms. All tested types of warming plates are designed to perform the external thermal insulation of walls, including the thermal insulation of facades.

The tests have been subjected to plates A – white expanded polystyrene EPS 70, average bulk density 16.9 kg/m^3 , with the declared thermal conductivity coefficient 0.040 W/mK , flexural strength above 115 kPa . Plates were cut from one polystyrene block, directly on the production line. Eleven different thicknesses of samples ranging from 20 mm to 160 mm were prepared. The product was subjected to systematic control of thermal performance for a period of 20 months from the date of manufacturing. Instability of the thermal parameters was observed at an early product in the early years of its seasoning.

The second analysed product was plates B – with the so-called expanded polystyrene in the black dot, characterized by the declared value of the thermal conductivity coefficient 0.040 W/mK at the temperature 10°C and flexural strength at least 100 kPa . The average bulk density of the tested insulation in dots was 14.2 kg/m^3 . Nine samples of the thickness ranging from 20 mm to 180 mm have been tested.

The experiment also included plates C – with the so-called silver-gray expanded polystyrene. The declared thermal conductivity coefficient at 10°C is equal to 0.032 W/mK , the level of flexural strength being at least 75 kPa . The average density of polystyrene with improved insulation by graphite was 14.6 kg/m^3 . Seven samples have been tested in the thickness range 20 mm to 130 mm .

During the entire period of the experiment, all the samples of the three types of products were conditioned in standard laboratory conditions, i.e. in equilibrium with temperature $(23 \pm 2)^\circ\text{C}$ and the relative air humidity $(50 \pm 10) \% \text{ RH}$.

4. The results of experimental research

In order to determine the performance of the analysed polystyrenes, the importance of the effect of the product thickness has been verified. The phenomenon was proved to be important in two cases: EPS (A) and (B). In the case of EPS (A) the minimum thickness of the product at which the effect of the thickness did not matter (d_m) was 108 mm and in the case of EPS (B) it was 60 mm (see Figure 2 and 3). Theoretically, it has been calculated that the absence of the thickness effect occurs at 218 mm (A) and 120 mm (B). In the case of EPS (C), the thickness effect did not take place in the whole population of the samples. This is also confirmed by the results presented in the literature [1].

Studies carried out for EPS (A) showed that this product in terms of thermal insulation, do not comply with the declared values for this type of expanded polystyrene. Thermal resistance (R) calculated on the basis of the thermal conductivity coefficient and thermal transmissivity for almost all the samples turned out to be less than that given by the manufacturer. Also, the conversion of the measured thermal conductivity coefficient due to the effect of the thickness, carried out in accordance with the standard [8] (in samples with smaller thicknesses), exceeded the declared value for this parameter. Values of measurements in which conversion is taken into consideration further in the article are called the converted thermal conductivity coefficient and are shown on Fig. 2. Consequently, in thicker samples, above the thickness limit (d_m) of the specimen, where it is possible to define the thermal properties of the product, the declared value of the thermal conductivity coefficient was exceeded. The measurements of the bulk density of the research material (A) showed its heterogeneity comparing to other polystyrenes, as illustrated on Fig. 1.

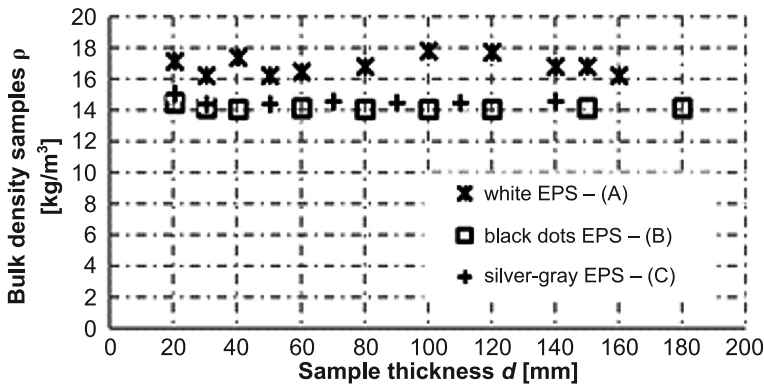


Fig. 1. The distribution of medium bulk density as a function of the change in the samples' thickness for lightweight EPS

The influence of heterogeneity in terms of bulk density is revealed in studies of thermal conductivity by the irregular arrangement of thermal conductivity coefficient points as a function of the thickness. The dependence of the measured thermal conductivity coefficient (λ) as a function of the samples thickness cutting from one block is shown on Fig. 2. The nature of the changes in the calculated transfer factor, which approximates

thermal transmissivity, was also presented. The difference between the measured values of the thermal conductivity coefficient for extreme thickness is significant and is equal to 7.4%. The maximum difference between the measured thermal conductivity coefficient and the transfer factor is small and equal to 3.2%.

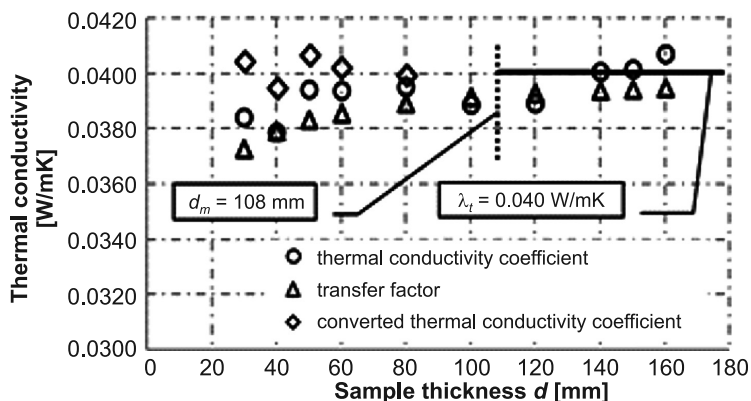


Fig. 2. The effect of the samples' thickness and density for the result of the λ measurement at the temperature of 10°C for product (A)

In the case of EPS (B) – black dots, the obtained dependency of the measured thermal conductivity coefficient as a function of the samples thickness shows no abnormalities arising from the heterogeneity of the samples (Fig. 3). The difference between the measured values of the thermal conductivity coefficient for extreme thickness is equal to 5.5%, which is significant. The biggest difference between the measured thermal conductivity coefficient and the transfer factor was 1.6%.

Mechanism of heat flow in the EPS plates (C) – the silver-gray colour compared to (A) and (B) is different. Addition of graphite causes absorption of radiant heat and contributes

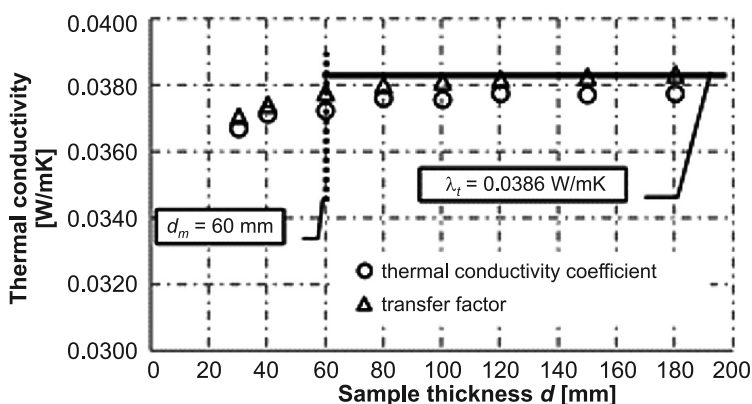


Fig. 3. The influence of the samples' thickness on the measured thermal conductivity coefficient at an average temperature of 10°C for product (B)

to the peculiar nature of the transfer factor course. The values of this parameter are being reduced with the thickness of samples tending asymptotically to thermal transmissivity (Fig. 4). The difference of the measured thermal conductivity coefficient for extreme thickness is very small – equal to 0.6%, reflecting the absence of the effect of thickness. The thermal conductivity of plates (C) is more than 20% lower compared to plates (B) with similar bulk density.

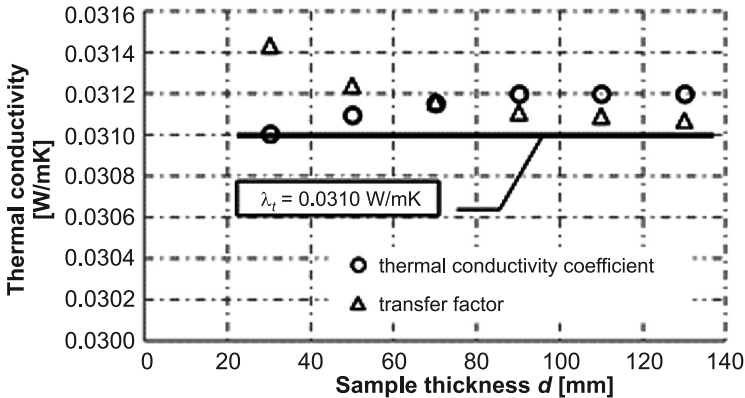


Fig. 4. The dependence of thermal parameters as a function of the samples' thickness for product (C)

5. Conclusions

Thick insulating products (EPS) with low density usually revealed the lack of thickness effect because they are non-transparent to thermal radiation. In any case, especially in new products, it is important to determine their thickness limit (d_m) experimentally. About this thickness limit thermal parameters are the intrinsic material feature. Lower density products in comparison with higher density products may show lower values of the thickness limit. In modern plate apparatus, it is possible to perform samples' tests with thicknesses exceeding the maximum acceptable thickness recommended in the standards. Studies carried out with plates apparatus FOX 600 show that the results obtained from measurements at sample thicknesses above 135 mm are reliable for EPS analysed products with low density (light).

Product control in terms of determining the thermal properties in insulations should be carried out on a number of samples of the same material and not on just one sample – then proper evaluation of the consistency of the product concerned becomes possible. Products from expanded polystyrene should have a constant bulk density. The author's suggestion is the following: a preliminary conformity assessment of the tested insulation plates with the type of product should contain control of thermal parameters and constant bulk density of the product. The visible jumps in the value of this parameter on Fig. 1 for product (A) indicate the high heterogeneity of density that can cause the dispersion of the values for the measured thermal conductivity coefficient. It could also be one of the reasons for

the lack of preservation of the declared values of thermal parameters. In view of the above, easy control becomes possible at any production site to ensure the quality of the products (by checking the bulk density) without purchasing expensive apparatus by manufacturers.

The author would like to thank Ms Ruslana Giczewska for proofreading the manuscript.

References

- [1] Flirkowicz-Pogorzelska K., *Transport ciepła przez promieniowanie w lekkich materiałach termoizolacyjnych*, Energodom 2002, Kraków–Zakopane, 13–16 października 2002, 83-90.
- [2] Flirkowicz-Pogorzelska K., Pogorzelski J.A., *Wykorzystanie baz danych przy określaniu cech cieplnych materiałów budowlanych*, XLVIII Konf. Nauk. Problemy Naukowo-Badawcze Budownictwa, t. 3, Opole–Krynica, 15–20 września 2002, 89-96.
- [3] Furmański P., Wiśniewski T.S., Banaszek J., *Izolacje cieplne Mechanizmy wymiany ciepła, właściwości cieplne i ich pomiary*, ITC – Politechnika Warszawska, Warszawa 2006, 17-93.
- [4] Pogorzelski J.A., *Zagadnienia cieplno-wilgotnościowe przegród budowlanych*, [w:] Klemm P. et al (Eds.), *Budownictwo ogólne*, T. 2, Arkady, Warszawa 2006, 139-148.
- [5] CEN: EN 12667:2001. Thermal performance of building materials and products – Determination of thermal resistance by means of guarded hot plate and heat flow meter methods – Products of high and medium thermal resistance.
- [6] CEN: EN 12939: 2000. Thermal performance of building materials and products – Determination of thermal resistance by means of guarded hot plate and heat flow meter methods – Thick products of high and medium thermal resistance.
- [7] ISO-EN 8301:1991. Thermal insulation – Determination of steady – state thermal resistance and related properties – Heat flow meter apparatus + ISO: EN 8301:2010 Amendment 1.
- [8] CEN: EN 13163:2012. Thermal insulation products for buildings – Factory made expanded polystyrene (EPS) products – Specification.

NINA SZCZEPANIK*, JACEK SCHNOTALE*

CFD MODELLING OF AIR FLOW AND TRANSPORT OF CONTAMINANTS IN A PASSIVE HOUSE

MODELOWANIE METODĄ CFD (KOMPUTEROWEJ DYNAMIKI PŁYNÓW) PRZEPIYWU POWIETRZA I TRANSPORTU ZANIECZYSZCZEŃ W DOMU PASYWNYM

Abstract

Rising costs of energy have caused the building envelope in the living sector to become tighter to improve energy efficiency. This raises questions about the quality of the indoor air as in traditional housing fresh air is supplied not only by ventilation system but also by infiltration through cracks in the building envelope. If a building is not properly ventilated, contaminants could accumulate within it and their levels could become hazardous to human comfort and health.

Keywords: CONTAMW, passive house, mechanical ventilation, modelling of contaminant concentrations

Streszczenie

Wzrastające koszty energii spowodowały, że przegrody zewnętrzne w budynkach stały się coraz bardziej szczelne, aby polepszyć efektywność energetyczną. Rozpoczęło to szereg dyskusji na temat jakości powietrza w pomieszczeniach, ponieważ w tradycyjnym budownictwie świeże powietrze jest dostarczane poprzez infiltrację przez nieszczelności w budynku. Jeśli budynek nie jest odpowiednio wentylowany, zanieczyszczenia gromadzą się w nim, co może tworzyć niekomfortowe warunki, które mogą być niebezpieczne dla zdrowia.

Słowa kluczowe: CONTAMW, dom pasywny, wentylacja mechaniczna, modelowanie stężeń zanieczyszczeń

* M.Sc. Eng. Nina Szczepanik, Prof. D.Sc. Ph.D. Eng. Jacek Schnotale, Institute of Thermal Engineering and Air Protection, Faculty of Environmental Engineering, Cracow University of Technology.

1. Introduction

Due to the growing costs of energy and environmental consideration, great effort is nowadays made to build more and more energy efficient buildings which under certain requirements can be named as passive houses. Such buildings are not only built from materials providing better insulation, but they are also becoming more “airtight” to prevent infiltration energy losses via building infrastructure and ventilation systems. This raises questions about the quality of indoor air in such airtight structures, for which natural ventilation is no longer the optimal solution to provide proper air quality. The reason why natural ventilation is not adequate for the energy efficient building is because it is (apart from ducts) based on airflows through leakages throughout the building envelope.

This paper reports a study based on computer simulation to examine this issue in an airtight passive house located in Poland. The simulations were performed using CONTAMW software, a computer program designed to analyse a ventilation systems, indoor air quality and occupant exposure in a multi-zone structure [5]. The program was used to analyse and compare three ventilation systems: natural ventilation, demand control ventilation based on occupant schedules and demand control ventilation based on the concentration of contaminants. The contaminants included in these simulations are: carbon dioxide, carbon monoxide, nitrogen dioxide, total volatile organic compounds and water vapour. As an indicator to compare the energy consumption of the proposed mechanical ventilation systems, their air flow rates through each air handling unit were compared.

2. Methods

This study shows the impact of three different ventilation systems within a passive house on the indoor air quality assessed by computer simulation. The chosen program was CONTAMW, a computer program designed to analyse ventilation systems, indoor air quality and occupant exposure in a multi-zone structure [5]. The tested ventilation systems include:

- A natural ventilation system where the air flows into the house through infiltration leakages and with two outlet fans in the bathroom and kitchen.
- A mechanical ventilation system based on zone occupancy. The airflow is maintained by an air handling unit connected to a series of inlets and outlets within the house. The proper inlets and outlets are activated when an occupant is within a zone/room and are switched off when the zone is empty.
- A mechanical ventilation system based on contaminant control. The airflow is maintained by the same system as in the one based on zone occupancy but it is activated when the concentration of carbon dioxide exceeds the maximum the permissible level, which is 1000 ppm.

2.1. Considered parameters

The test object is a one-story house located in Boruszowice, Poland, occupied by a family of four (two adults and two children). The house is heated by a heat pump system and has a central air-conditioning system [4, 9].

The contaminants considered in the study are airborne contaminants. The CONDAMW program allows the user to define traceable and non-traceable contaminants. The concentration of the latter is constant and is used to define the ambient contaminant influence [4]. Outdoor air composition is considered constant and consists of: 75.54% nitrogen, 23.14% oxygen, 1.27% argon and 0.05% CO₂ [5]. On the other hand traceable contaminants are variable and include: carbon dioxide, carbon monoxide, nitrogen dioxide, water vapour and total volatile organic compounds.

The only considered indoor source of CO₂ is human respiration. As mentioned earlier, a family of four occupy the house and they include: two adult family members, a male and female working full time, two children, which are aged 16 (child_1) and 10 (child_2). Each member has an assigned schedule. Such timetables define the whereabouts of each occupant as well as specify the amount of time spent by him or her in each room and outside of the house. This option allows to track the amount of contaminants within a zone that are produced by each individual during the day. In the following simulations the amounts of CO₂ generated by the adult male and female are 9.1 mg/s and 8.0 mg/s respectively while they are awake. The children's CO₂ generating rates when awake are lower and equal 7.8 mg/s for child_1 and 5.5 mg/s for child_2. While sleeping, the amount of CO₂ generated by occupants is equal to 66% of the rate when they are awake [1].

It was decided that a gas cooking stove would be taken under consideration as cooking on both gas and electrical stoves are equally popular in Poland and many EU countries and gas stoves generate more contaminants. Cooking on such a stove generates mostly water vapour, carbon monoxide (CO) and nitrogen dioxide (NO₂). Other contaminants caused by cooking were not taken into consideration. The generation rate depends on the time of day and its example is displayed in the table below (Table 1).

Table 1

Generation level of CO and NO₂ for gas cooking [1]

weekdays		
	Carbon monoxide [µg/s]	Nitrogen dioxide [µg/s]
6:30–7:30 am	210	28
17–17:30 pm	420	56
17:30–18 pm	830	111

Besides cooking, sources of water vapour include bathing and occupant respiration. The estimated amount of water vapour generated while showering is 3 dm³/h. Each occupant takes a 10 minute shower daily based on his or her daily schedule [8]. The amount of moisture released by cooking breakfast or supper is equal 0.45 dm³/h, while cooking dinner 1.33 dm³/h [8]. Furthermore, the ratio of humidity generation from each person during the day is equal to 0.03 dm³/h [8]. The generation rate of volatile organic compounds is considered to be steady as they are emitted by building materials and furnishings. Their amount was estimated on the basis of the area of each room and is equal to 250 µg/h per each cubic meter of the house space [3].

2.2. Simulation approach

The tool used to present the contaminant migration and concentration is the computer program CONTAMW developed by NIST (National Institute of Standards and Technology, which is a part of the Technology Administration of the U.S. Department of Commerce). CONTAMW is a multi-zone indoor air quality and ventilation analysis program that helps to define airflows and pressure drops, concentration of airborne contaminants and occupant exposure to them [5]. Each zone created in the program has the assigned name, temperature, initial contaminant concentration and assigned contaminant sources. Airflow paths are created between zones to connect zones with other zones or with the outdoor space, allowing air to move between two neighbouring zones. The external air paths can be defined for example as: leakages through windows, doorways or cracks in the building envelope. The airflow through the majority of these paths is determined by the flow characteristics of the path itself and the air pressure difference between the zones [5]. The sources of contaminants can be assigned to a specific zone, as for example kitchen and bathroom appliances, or can be connected to the occupants who generate contaminants while migrating through zones. CONTAMW defines the concentration of contaminants in each room by calculating the airflow characteristics through a zone and estimating contaminant migration between zones.

2.3. Natural ventilation

The first simulation was undertaken for a natural ventilation system which consists of extraction fans that are placed in the bathroom and room_1 (which contains kitchen appliances). Fresh air is supplied through leakage paths through the building envelope. Each air vent is turned on by a schedule that lines up with occupant usage of the room. The air vent in the kitchen is turned on when cooking occurs. As the house is a passive one, the air leakages are much smaller than in a standard one, the pressure drops through the leakage paths are quite high and probably cause a draft inside of the house. To prevent this, an additional inlet flow path was placed in the bathroom and room_1 (Fig. 1).

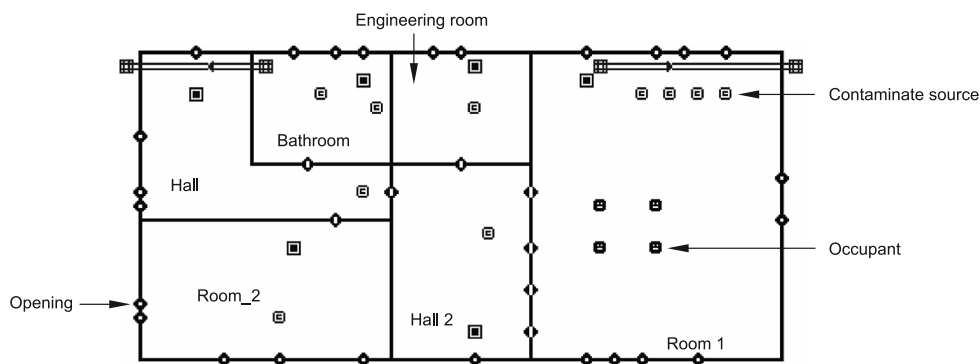


Fig. 1. Natural ventilation system

2.4. Demand control ventilation based on zone occupancy

This type of demand control ventilation system is accomplished by supplying zones with fresh air through a single air intake and divided into room_1, room_2, and the hallway. Contaminated air is removed through exhaust duct, which is connected through valves with room_1, the bathroom. The activity of the system depends on occupant schedule. When an occupant is inside of a room, the proper valves are opened and the room is ventilated. Because the occupants only attend the hallway on a limited basis, the ventilation system in this room is scheduled to activate briefly before occupants enter the room and is deactivated a period of time after the occupants exit the room. As a result, the sufficient amount of contaminants would not have been removed. The supply and exhaust fans used inside of each room have an equal capacity for maintaining air pressure balance within the building. This simulation approach does not depend on the contaminate concentration within a room and is not affected by it. According to Polish standards, when occupants are outside of a zone the ventilation system maintains a 20% airflow through the ducts [12]. The ventilation system in the engineering room is not altered as its main purpose is to ventilate the monitoring system (Fig. 2).

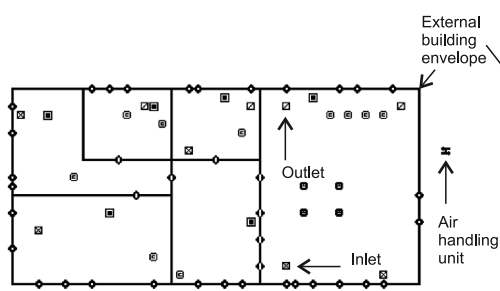


Fig. 2. Demand control ventilation based on zone occupancy

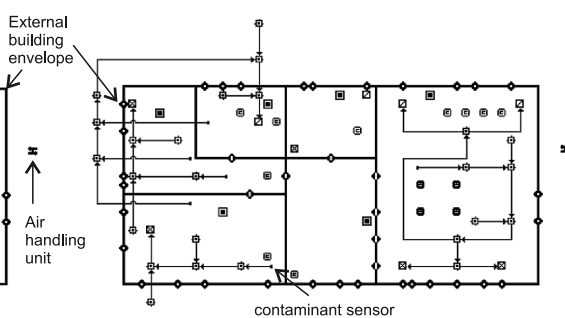


Fig. 3. Demand control ventilation based on CO_2 concentration

2.5. Demand control ventilation based on indoor air quality

This ventilation system is designed in the same way as the duct system in the previous simulation approach (Demand control ventilation based on zone occupancy). In this approach, the ventilation system was activated on the basis of the indoor air quality. The contaminate chosen as an indicator was carbon dioxide (CO_2). Carbon dioxide was chosen not only because of its negative effect on the human organism but also because it is the most variable contaminant. Its amount depends on occupant activity. Each room was equipped with a CO_2 sensor that sent a signal to proper valves when the CO_2 level was higher than the project assumptions. The CO_2 limit is equal to 1000 ppm. According to Polish standards, when occupants are outside of a zone the ventilation system maintains a 20% airflow through the ducts [12]. The ventilation system in the engineering room is not altered as its main purpose is to ventilate the monitoring system (Fig. 3).

3. Results

As explained above, the ventilation system is run by controlling it either on occupant schedules or on the concentration of carbon dioxide. This resolves the problem of altering the concentration of all of the contaminants in the building in comparison to their concentration when natural ventilation is used. The room that contains the most altering contaminant rate as well as the highest concentration of pollutants is room_1. All cooking activities take place here, and the two adult family members sleep in this room. This is why the concentrations from this room will be used to display the difference between the efficiency of the three ventilation methods. The contaminants displayed below include: carbon dioxide (CO₂), carbon monoxide (CO), nitrogen dioxide (NO₂) and volatile organic compounds (VOC). These are vital contaminants that affect a person’s health, efficiency and comfort level, which is why they were used in all of the simulations.

3.1. Carbon dioxide

When analysing Fig. 4, it is clear that the natural ventilation system does not meet the stated criteria and constantly exceeds the allowable maximum contaminant (CO₂) level which is 1000 ppm. However, as expected, both types of mechanical ventilation (demand control based on occupant schedules as well as contaminant concentration) meet the indoor air criteria for the maximum amount of this contaminant. Constant, higher than 1000 ppm,

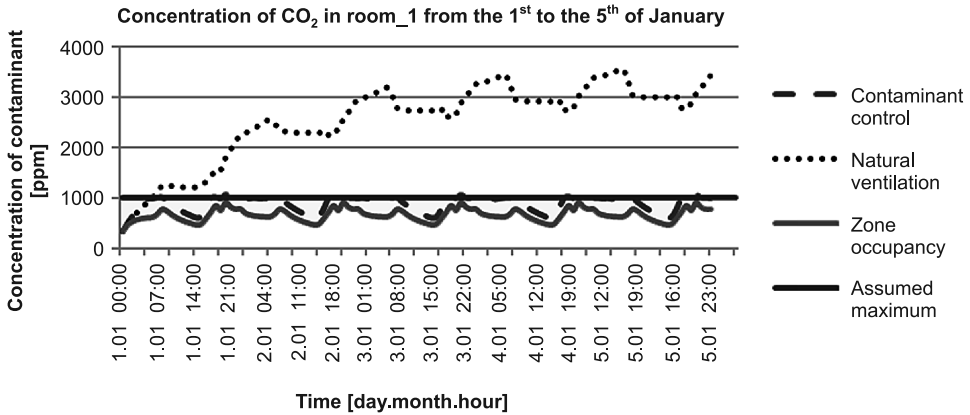


Fig. 4. Concentration of CO₂ in room 1

concentration rate of carbon dioxide may cause, among others, headaches, tiredness, dizziness, elevated heart rate and in extreme cases suffocation [13]. Though the concentrations less than 3500 ppm of carbon dioxide dose not threaten the human wellbeing, it is important to remember that the source of carbon dioxide inside of this house is strictly associated with occupant physical activity.

3.2. Carbon monoxide

Since carbon monoxide is a toxic gas it is vital to keep its concentration below a certain level. Even at low concentrations it causes mild effects that are often mistaken for the flu, which include dizziness, disorientation, nausea and headaches [13]. In higher concentrations it is deadly. Furthermore, because of the lack of colour and smell it is practically impossible for humans to detect increased CO levels without instruments.

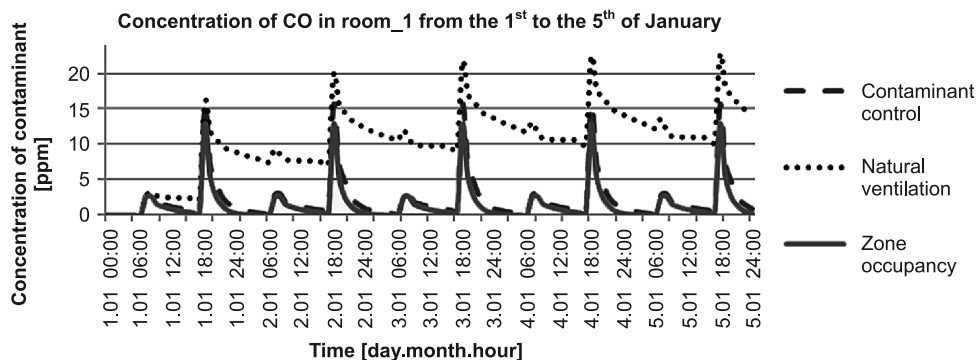


Fig. 5. Concentration of CO in room 1

Figure 5 shows, that the maximum established rate of CO – 4.3 ppm [2] is constantly exceeded while using the natural ventilation system and occasionally by both mechanical ventilation systems (demand control based on occupants schedules and the one based on contaminant concentration) while cooking dinner. This is why natural ventilation is not an acceptable option if a gas stove is used inside an air-tight house as the one considered in this research.

3.3. Nitrogen dioxide

In Figure 6 it is noticeable that the rate of nitrogen dioxide is almost instantly and constantly surpassed while using natural ventilation as its limit was specified as 0.058 ppm [2].

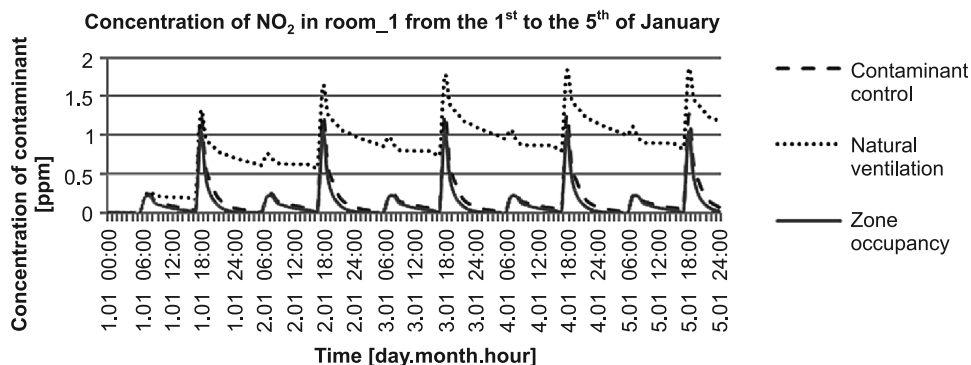


Fig. 6. Concentration of NO₂ in room 1

Similarly to the Fig. 5 for carbon monoxide, nitrogen dioxide rates are occasionally exceeded for both mechanical ventilation systems (demand control based on occupant schedules and contaminant concentration). It takes place while cooking dinner. Nitrogen dioxide may cause irritations of the respiratory system and can be hazardous to young children causing respiratory infections [13]. This is why natural ventilation is not an acceptable option if a gas stove is used inside an airtight house as it is in this case.

3.4. Water Vapour

In Figure 7 it is visible that the rate of water vapour concentrations are almost instantly and constantly exceeded while using natural ventilation, as its limit was specified between 30–60% [11]. On the other hand, the relative humidity inside of the house, while using the mechanical ventilation systems, is below the lower limit. When a house is too dry, the occupants may experience aggravation of allergy and asthma symptoms, frequent colds, flu, sore throats, nose bleeds, dry skin and dry coughs [14]. This can be easily altered by using a humidifier.

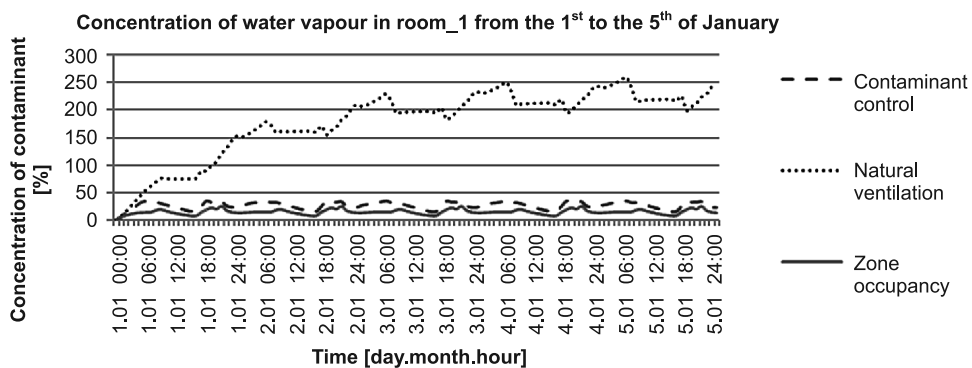


Fig. 7. Concentration of water vapour in room_1

The symptoms of excess indoor moisture are more hazardous. They include: odours, frost and ice on cold surfaces (such as windows), surface discoloration and texture changes and deformations of wooden surfaces [15]. It is common for mould and mildew to appear when the relative humidity is above 70%. Mould can lead to a series of health problems that include: development of asthma, coughs, allergic reactions, and respiratory ailments [15].

3.5. Total volatile organic compounds

The indoor concentration of volatile organic compounds is higher (up to ten times higher) than outdoors [13]. The reason for this is that these compounds are emitted by a wide range of products such as: paints and lacquers, paint strippers, cleaning supplies, pesticides, building materials, furnishings, etc. At high concentration they may cause: nausea, headaches throat, eye and nose irritation, damage vital organs such as the kidneys, liver and central nervous system [13]. They can also be carcinogenic. The maximum assumed in this paper is 0.95 ppm [2] which is exceeded when using natural ventilation.

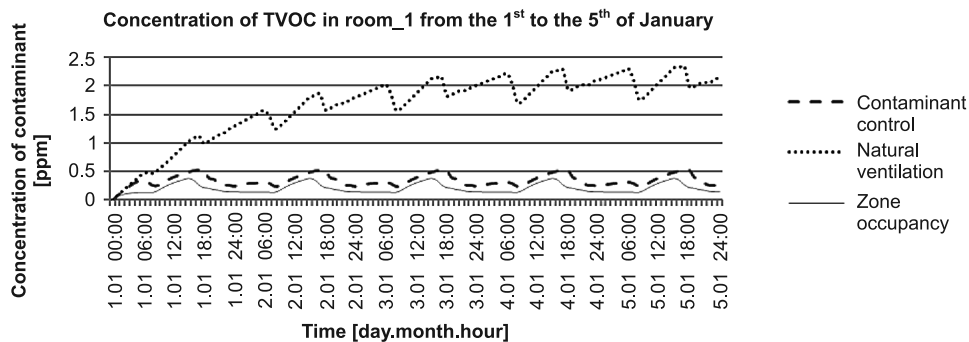


Fig. 8. Concentration of TVOC in room_1

Figures 4 to 8 show contaminant concentration in the room_1 zone. It can be concluded that the natural ventilation system does not provide proper indoor air quality for the simulated passive house. Both mechanical ventilations systems provide proper indoor air quality, but the ventilation system based on zone occupancy is more efficient when it comes to removing contaminants. The same trend was noticed in the other rooms within the house.

The concentration of the contaminants in each room is not only determined by the contaminant sources inside each room but also by the arrangement of ventilation inlets and outlets within the house. The effect of this arrangement can be observed by analysing the concentrations of carbon monoxide (CO) and nitrogen dioxide (NO₂) when using the mechanical ventilation systems. These contaminants are generated only in room_1 while cooking but because of the large openings between room_1 and hall_2 as well as the outlets in room_2 and the bathroom, contaminants migrate from room_1 throughout the house with the movement of the air. While in room_1 cooking causes the level of CO to increase over 15ppm (Fig. 5) in hall_2 its concentration is also over limit ranging from 10ppm to 12ppm. The same tendency can be seen for NO₂, the concentration of which in room_1 is around 1ppm (Fig. 6) and 0.9 in hall_2. The lowest concentration of both CO and NO₂ are in room_2 and reach range around 4ppm and 0.3ppm respectively. This simple analysis shows, how the arrangement of inlets and outlets can influence contaminant concentration throughout a building. This is why a proper spacing and location of the ventilation inlets and outlets is needed, since otherwise contaminants could accumulate in certain areas where air exchange is not sufficient.

3.6. Air flow rate through the ventilation system

The flow rate of the mechanical ventilation systems was taken under consideration, as the natural ventilation system does not provide proper air quality (the concentrations of the examined contaminants are exceeded and do not meet the established standards). Based on Fig. 9, in which the airflow rate through the air handling unit is displayed, it is quite clear that the contaminant control ventilation system is more energy efficient than the zone occupancy based one. It would also be more justifiable to use it when it is expected that several more occupants could be inside of the house (ex. during a party).

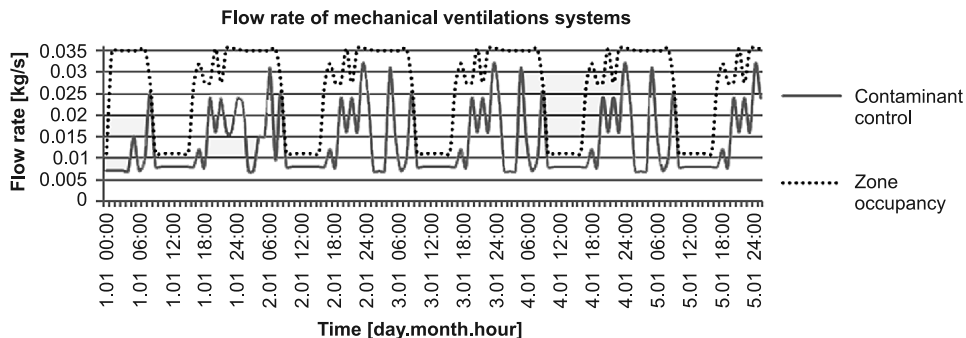


Fig. 9. Flow rate of mechanical ventilation systems

4. Conclusions

The performed simulations, which were generated using CONTAMW software, show that natural ventilation is not an adequate option in the examined passive house, as the main source of fresh air is provided through infiltration leakages through the building envelope which are not sufficient in a passive house. This fact limits possible airflows causing the highest contaminant levels among all the examined systems. The natural ventilation is also the least energy efficient as it has no heat recuperation system.

Even though the ventilation system controlled by occupant schedules is the most efficient when it comes to removing contaminants, it is also less energy efficient than the other considered mechanical ventilation system. Another problem would be with the estimation of the number of people for which the system would be designed. It is common for family members to entertain guests in a house. This is why the most optimal solution seems to be the application of the ventilation demand system based on carbon dioxide concentration. It is independent on occupant activity, which makes it the most reliable ventilation system.

To conclude, multi zone CFD simulation programs like CONTAMW can be used to determine, which ventilation system is the best to maintain indoor air quality at the lowest energy consumption. However detailed CFD calculation coupled with multi zone approach of the whole building would be required to determine which configuration of ventilation inlets and outlets are the most effective in removing contaminants.

References

- [1] Persily A.K., *A modelling Study of Ventilation, IAQ and Energy Impacts of residential Mechanical Ventilation*, NIST, 1998.
- [2] Pelech A., *Wentylacja i klimatyzacja*, Wydanie III, Oficyna Wydawnicza Politechniki Wrocławskiej, Wrocław 2010, 16-18.
- [3] Jones A.P., *Indoor air quality and health*, School of environmental Sciences, University of East Anglia, 18 May 1998, 12-13, 323.
- [4] Flaga-Maryńczyk A., Schnotale J., Radon J., Was K., *Experimental measurements and CFD simulation of a ground source heat exchanger operating at a cold climate for a passive house ventilation system*, *Energy and Buildings* 68, 2014, 562-570.

- [5] Walton G.N., *CONTAM User Guide and Program Documentation*, Naval Surface Warfare Center, October 2005.
- [6] Walton G.N., *AIRNET – A Computer Program for Building Airflow Network Modeling*, U.S. DEPARTMENT OF COMMERCE National Institute of Standards and Technology Gaithersburg, MD 20899, April 1989.
- [7] Järnström H., Saarela K., Kalliokoski P., Pasanen A.-L., *Reference values for indoor air pollutant concentrations in new residential buildings in Finland*, Environment national, 2006.
- [8] Christian J.E., *Moisture Control in buildings*, American Society for Testing and Materials, 1994, 176-178.
- [9] Radoń J., *Sprawozdanie z wykonania badań w domu pasywnym w ramach projektu „dom pasywny dla każdego – badania i rozwój przedsiębiorstwa Multicomfort”*, ETAP I, 2011, 3-7.
- [10] Justo Alonso M., Malvik B., Mathisen H.M., Haugen E.N., *Energy Efficiency and Indoor Climate: Modelling Of Ventilation Systems Using ContamW (Ii)*, Icr 2011, August 21–26, Prague, Czech Republic.
- [11] Szczepanik N., *ContamW as a Tool for Modelling Indoor Air Quality for Assorted Ventilation Systems in a Passive House*, Masters Theses, Kraków 2013.
- [12] PN-83 B-03430 Az3 2000, Wentylacja w budynkach mieszkalnych i zamieszkania zbiorowego i użyteczności publicznej.
- [13] www.epa.gov/iaq/co.html – 26.03.2013.
- [14] <http://extension.oregonstate.edu/catalog/pdf/ec/ec1437.pdf> – 20.06.2013.
- [15] http://www.euro.who.int/__data/assets/pdf_file/0017/43325/E92645.pdf, 89-92 – 20.06.2013.

AGNIESZKA SZYMANOWSKA-GWIŹDŹ*, TOMASZ STEIDL*

ANALYSIS OF TEMPERATURE AND HUMIDITY PROCESSES IN EXISTING HALF-TIMBERED PARTITIONS

ANALIZA PROCESÓW CIEPLNO-WILGOTNOŚCIOWYCH W ISTNIEJĄCYCH PRZEGRODACH Z MURU PRUSKIEGO

Abstract

The paper presents the analysis of the inner surface of half-timbered walls in multi-family residential houses created in the early twentieth century. The analysis was made in order to avoid the possibility of mold. The analysis of partition's moisture growth was performed at the existing state and after designed thermal insulation from the inner side. The measurements and analyzes are a prelude to further research and analysis of such types of objects.

Keywords: mold fungi, partitions' humidity, surface temperature

Streszczenie

W artykule dokonano analizy temperatury powierzchni wewnętrznej ścian z muru pruskiego w wielorodzinnych domach mieszkalnych powstałych na początku XX wieku pod kątem możliwości powstania pleśni. Przeprowadzono analizę przyrostu zawilgocenia przegrody w stanie istniejącym oraz po projektowanym dociepleniu od strony wewnętrznej. Pomiar i analizy są wstępem do dalszych badań i analiz tego typów obiektów.

Słowa kluczowe: grzyby pleśniowe, zawilgocenia przegród, temperatura powierzchni

* Ph.D. Eng. Agnieszka Szymanowska-Gwiźdź, Ph.D. Eng. Tomasz Steidl, Department of Buildings and Buildings Physics, Faculty of Civil Engineering, The Silesian University of Technology.

1. Introduction

A characteristic feature of residential buildings from the turn of nineteenth and twentieth century in the Upper Silesia region is the presence of multi-family building associated with the nineteenth century industrial revolution and historical changes taking place at that time. With the development of the century, colonies and housing estates were formed, including industrial ones, built also by the owners of developing industrial plants. One of the characteristics of such construction is locating in the highest floors (mostly unused attics), walls of half-timbered structure. At present, attempts are being made to adapt attics for living space, connected with the necessity to improve thermal comfort.

The paper presents the research results conducted into a housing estate of railwaymen in Pyskowice. The aim of this study was to determine temperature and humidity phenomena in partitions for the cases of their insulation from the inside with homogeneous material for thermal insulation. Research will be continued and the final goal will be to broaden the knowledge in the field of possibilities to reduce heat loss in these types of objects.

2. Object of study

The construction of the housing estate in Pyskowice began after the launch of the railway line from Opole to Gliwice via Pyskowice. Already in 1910, along the railway line, there were 12 family railwaymen houses. After World War I, new buildings for railwaymen were built, but also for miners and steelworkers working outside Pyskowice [1].

In the housing estate, there are multi-family buildings with three residential floors, with flats of fairly low standard, and single-family housed in detached and terraced buildings. The buildings are currently inhabited. The housing standards in both types of buildings are similar [4].

Buildings described and analyzed in this paper are three-floor basement residences, covered with wooden roof rafter framings. Construction material of external and foundation walls is of ceramic brick. Wall thickness depends on the floor level, traditionally, in the ground it is most commonly 52 cm, decreasing towards the top. Dormer's peaks, in their entirety



Fig. 1, 2. Pyskowice, examples of the building development of railway housing estate, visible frame construction of the attic's walls (photo by authors)

or in parts, were made with the use of tier wooden frames, filled with ceramic brick. In this case, brick wall thickness was 12 cm. This type of wall was used for floor housing without residential function – non-used attics and the highest levels of staircases. Areas between wooden elements were usually plastered.

In recent years, due to the large increase in heating costs, the residents decided to improve the insulation of external walls. Thermomodernization treatments of various kinds were performed. There were also attempts to adapt lofts for residential purposes.

For such adaptations, the essential importance for the thermal comfort of premises and technological possibilities of construction works, has the specific nature of half-timbered walls. Attempts at insulating partitions from the inside were made, which may have entailed the occurrence of adverse phenomena in the partition [3].

3. The scope of research

The scope of research was adapted to the needs of the carried out analyses of thermal humidity processes, and included:

- measurements of brick layers and wooden elements, and humidity measurements in situ, on the inner surface of external partitions, which were used to determine the boundary conditions of existing partitions for further analysis,
- determination of thermal insulation and possibility of condensation on the inner surface of existing external partitions,
- a forecast of condensation possibility on the inner surface of external partitions, in the case of their insulation from the premises side,
- analysis of humidity changes of the partition in the existing state and after the design of thermal insulation from the inside,

The forecast of humidity changes covered a period of 1 statistical year.

4. Research method

Analyses of temperature and humidity processes were performed for two-dimensional theoretical models, with consideration of the actual conditions of external climate, parameters of premises' internal climate, in accordance with their purpose and actual humidity of the partitions. Geometric models of selected parts of the partitions were performed on the basis of in-situ measurements. For temperature and humidity estimates of selected locations in the building, program THERM 7.19 was used, based on the use of FEM, for the calculation of any two-dimensional model of building element. The program allows to obtain temperature values at any point of partition's cross section, total heat flux and heat transfer coefficient U [$W/(m^2K)$]. Values obtained in the program were used to determine temperature coefficient on the inner surface of the external partition, i.e. f_{Rsi} , determining the risk of surface condensation. Preliminary calculations were made in accordance with PN-EN ISO 13788 [2]: Temperature and humidity properties of building components and building elements. The temperature of the inner surface to avoid the critical surface

humidity and interlayer condensation. The assignment of temperature coefficient was made for the parameters of the local climate, i.e. the nearest weather station in Katowice

For the calculation, the boundary conditions were adapted:

- Outside air temperature: $t = -2.4^{\circ}\text{C}$ (annual average temperature for the coldest month),
- Inside air temperature: $t = +20^{\circ}\text{C}$,
- Heat transfer coefficients $h_e = 25 \text{ W}/(\text{m}^2\text{K})$; $h_i = 7.69 \text{ W}/(\text{m}^2\text{K})$; for the surface condensation condition $4.0 \text{ W}/(\text{m}^2\text{K})$.

For the calculation of the risk of condensation, premises humidity was adopted in accordance with the Technical Conditions, i.e. 50%.

The analysis of changes in partition's humidity at the period of 1 year for the existing state and after the design of insulation from the inner side, was performed with the use of a custom program for the calculations of humidity increase in building partitions. The program operates in EXCEL and is based on an algorithm contained in the Standard [2]. The calculations were made on the basis of data from the meteorological station in Katowice, using, for the standard meteorological year monthly average temperatures, monthly minimum and maximum temperatures. As for the inside temperature, standard conditions were adapted, i.e. $t_i = 20^{\circ}\text{C}$ and $\varphi = 50\%$.

5. Partition models adapted for the calculations

Calculations included the partitions of attics, characterized with the construction typical for half-timbered walls and their modifications consisting of partitions insulation from the premises side.

For the calculation of the critical temperature, flat partition was selected with the cross-section of wooden pillars $14 \times 14 \text{ cm}$ and thickness of the brick filling 12 cm , with lime plaster and structural knot-angle of the external wall. As insulation material, Remmers SLP lime-silicate plates were adopted. Coefficient of thermal conductivity under normal conditions, of lime-silicate plates is $\lambda = 0.0626 \text{ (W/mK)}$, diffusion resistance coefficient $\mu = 4.4$ (based on Technical Instruction No. 0223 Remmers).

The markings of analyzed partition models were adopted (as in Fig. 3):

- detail_P1: flat partition, a combination of ceramic filler with a wooden pillar,
- detail_P2: flat partition, a combination of ceramic filler with a wooden pillar, with insulation of 6 cm from the premises side,
- detail_P3: flat partition, a combination of ceramic filler with a wooden pillar, with insulation of 8 cm from the premises side,
- detail_P4: flat partition, a combination of ceramic filler with a wooden pillar, with insulation of 10 cm from the premises side,
- detail_N1: corner of the external partition with corner wooden pillar,
- detail_N2: corner of the external partition with corner wooden pillar, with insulation of 6 cm from the premises side,
- detail_N3: corner of the external partition with corner wooden pillar, with insulation of 8 cm from the premises side,
- detail_N4: corner of the external partition with corner wooden pillar, with insulation of 10 cm from the premises side.

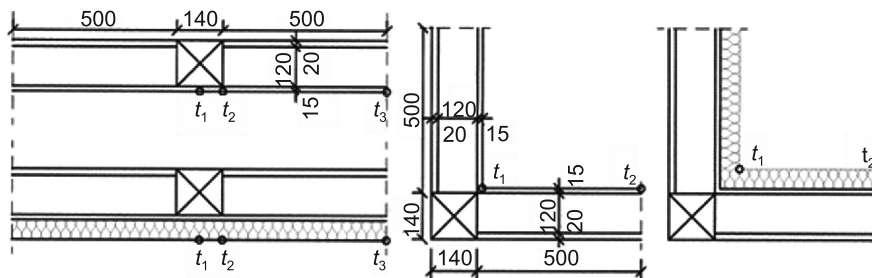


Fig. 3. Models of analyzed partitions and places of calculated temperatures

Adapted values of the thermal conductivity coefficient λ [W/mK]: pine wood (0.16), ceramic brick (0.77), lime plaster (0.88), lime-silicate plates (0.063).

The analysis of changes in humidity of the partition at the period of 1 year, was carried out for the brick element of the partition existing, for variants: w0 (existing state), and with plates insulation of 6, 8, and 10cm (respectively variants w1, w2, w3).

6. Measurements of partitions humidity in situ

In order to check the level of humidity of partition's inner surface in non-used premises in the existing state, humidity measurements were performed. They were made using a measuring instrument Testo 635-2 with a probe to measure materials humidity (manufacturer's calibration protocol No. 02356831, measuring accuracy $\pm 1\%$). Moisture values, showed by weight percent in relation to dry material mass. Too high humidity may be a problem when mounting newly designed insulation from the inner side. Its size affects the performance of computational prediction of climate and microclimate effect on the future temperature and humidity state. The measurements were carried out on the inner surface of half-timbered partition (wall plastered from the inside). The measurements will be used for further analysis and should be treated as preliminary. Measuring points at the wood level were highlighted in gray.

The measurements are summarized in Table 1.

Table 1

Measured values of moisture, showed by weight percent in relation to dry material mass

Point No.	1	2	3	4	5	6	7	8	9	10
Humidity value [%]	1.9	1.6	1.9	1.6	1.8	1.8	1.9	2.5	1.5	1.8
Point No.	11	12	13	14	15	16	17	18	19	20
Humidity value [%]	3.2	3.1	4.0	2.2	0.8	2.4	1.4	1.0	1.3	0.5

Slightly higher humidity occurred in the brick wall, in the part with the window.

7. Analysis results

The surface temperatures of selected knots were marked t_1 , t_2 i t_3 . They occur in (Fig. 1), the calculated values are summarized in Table 2 and 3.

Table 2

Values of temperatures [°C] depending on the detail (flat partitions) and places of appearing

Temperature markings in selected knots	Details			
	Detail_P1	Detail_P2	Detail_P3	Detail_P4
t_1	14.0	16.7	17.1	17.5
t_2	9.8	16.3	17.0	17.4
t_3	8.1	16.1	16.8	17.3

Table 3

Values of temperatures [°C] depending on the detail (corners) and places of appearing

Temperature markings in selected knots	Details			
	Detail_N1	Detail_N2	Detail_N3	Detail_N4
t_1	7.2	13.1	14.0	14.3
t_2	8.1	16.1	16.2	17.3

In accordance with WT requirements, the size of $f_{Rsi,min}$ temperature coefficient, determined in accordance with the procedure PN-EN ISO 13788, in heated rooms to a temperature of at least 20°C, assuming the average relative inside air humidity $\varphi_i = 50\%$, can be adapted at the level of 0.72. Such value, with properly designed partition, for the minimum inside temperature of partition surface, at which there is no likelihood of mold (called the critical temperature), should be exceeded. From the calculation practice it shows that the minimum temperature factor, calculated for local climatic conditions, may reach much higher values, and thus increase design requirements. By adopting the calculation procedure, contained in [2], the value of minimum temperature factors for all months of the year, were set. The most unfavorable conditions for the assumptions occur in the winter months – in February (Table 4). For critical conditions (month of February), calculated on the basis of the available climate data base, the inner surface temperature cannot be less than 16.2°C. This will prevent condensation on the inner surface of the corner. State requirements, contained in the Regulation [5] require that the minimum surface temperature was 13.8°C.

Table 4

Values of the minimum factor $f_{Rsi,min}$ for the critical month, for a meteorological station in Katowice

Month	p_e [Pa]	$p_{sat}(\theta_{si})$ [Pa]	$\theta_{si,min}$ [°C]	ΔP [Pa]	$f_{Rsi,min}$
February	478	1844	16.2	907	0.832

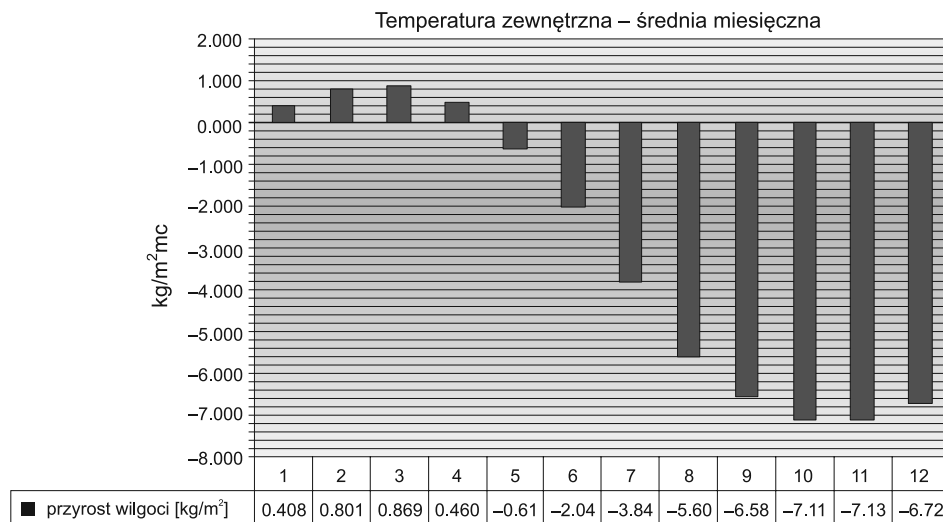


Fig. 4. Humidity increase in the wall for average monthly temperatures (variant w1)

Table 5

Values of humidity increases [kg/m²] in individual months of the year

		Months											
		1	2	3	4	5	6	7	8	9	10	11	12
W0	av	-0.61	-1.15	-2.02	-3.17	-4.77	-6.56	-8.59	-10.5	-12.1	-13.3	-14.2	-14.8
	min	-0.16	-0.32	-0.79	-1.44	-2.33	-3.29	-4.39	-5.59	-6.37	-6.97	-7.48	-7.67
	max	-1.12	-2.24	-3.95	-6.55	-9.44	-13.0	-17.1	-21.1	-24.3	-27.1	-28.9	-30.2
W1	av	0.41	0.80	0.87	0.46	-0.61	-2.04	-3.84	-5.60	-6.58	-7.11	-7.13	-6.72
	min	0.95	1.81	2.41	2.77	2.82	2.72	2.45	2.03	2.19	2.63	3.16	4.09
	max	-0.25	-0.63	-1.78	-4.45	-7.57	-12.0	-17.2	-22.4	-26.0	-29.0	-30.4	-30.9
W2	av	0.41	0.80	0.94	0.69	-0.11	-1.19	-2.57	-3.92	-4.64	-4.98	-4.92	-4.50
	min	0.85	1.61	2.18	2.54	2.66	2.66	2.52	2.26	2.46	2.90	3.41	4.24
	max	-0.13	-0.37	-1.24	-3.35	-5.83	-9.42	-13.6	-17.8	-20.7	-23.1	-24.1	-24.5
W3	av	0.39	0.76	0.91	0.74	0.11	-0.67	-1.88	-2.98	-3.54	-3.79	-3.70	-3.31
	min	0.76	1.43	1.95	2.30	2.44	2.48	2.40	2.23	2.44	2.85	3.31	4.05
	max	-0.07	-0.24	-0.94	-2.70	-4.77	-7.79	-11.3	-14.8	-17.3	-19.3	-20.1	-20.4

av – average temperatures, min – minimum temperatures, max – maximum temperatures,
partition variants: w0 – existing partition, w1 – 6 cm of insulation, w2 – 8 cm of insulation, w3 – 10 cm of insulation.

The value of the critical temperature, determined for the local conditions, will be exceeded in all indicated points with insulation thickness of min. 8cm, in the case of flat partition. In order to obtain a temperature higher than 16.2°C in the corner, the insulation thickness would have to be larger.

For the average monthly temperatures, a lack of humidity increase in the insulated partition will occur during the calculation period (one year), despite periodic monthly increases. The annual permanent increase of wall's humidity may occur with the appearing of minimum temperatures.

8. Conclusions

The measurements and calculations indicate the necessity for precise analysis in the case of insulating the half-timbered walls from the inside. The type of insulating material, thickness, and attachments method should be selected referring to the local conditions in each case separately.

It is suggested that temperature and humidity calculations, due to the rather problematic humidity calculation model contained in [2], should be carried out not only for the average conditions but mostly for critical conditions, including maximum and minimum outside temperatures, and increased humidity of inside air, i.e. not less than 60%. Such actions will allow the design of internal insulation with the likelihood of avoiding the risk of condensation on the inner surface and minimize possible, even short-term, presence of external conditions conducive to the formation of mold and humidity accumulation in the partition. The number of conducted measurements was considered insufficient to perform statistical analyzes. Further studies of the phenomena occurring in the contact surface of wooden elements with brick, for different variants of internal insulation, will be conducted in the next heating season. The authors of this paper treat presented tests and calculations as preliminary due to the imperfection of the calculation method set in [2]. However the method used provides a good solution to the problem. The moisture content, calculated by [2] will be more extensive than is necessary and more successful. It was recognized that phenomena appearing in the joint plane of wooden elements with brick, for different variants of internal insulation, require analysis related to the two-dimensional coupled heat and moisture flow. Final calculations will be performed using AnTherm program with the use of carried out tests.

Reference

- [1] Chrząszcz J., *Historia miast Pyskowice i Toszek*, przeł. Hepa M., Wydawnictwo Wokół Nas, Gliwice 1994.
- [2] PN-EN ISO 13788: Ciepłno-wilgotnościowe właściwości komponentów budowlanych i elementów budynku. Temperatura powierzchni wewnętrznej dla uniknięcia krytycznej wilgotności powierzchni i kondensacji międzywarstwowej.
- [3] Radoń J., Kuncel H., Olesiak J., *Problemy ciepłno-wilgotnościowe przy renowacji ścian budynków z muru pruskiego*, [In:] Acta Scientiarum Polonorum, Architektura, Kraków 2006, 45-53.

- [4] Tomanek M., Szymanowska-Gwiżdż A., Dębowski J., *Pyskowskie zespoły urbanistyczne jako przykład projektowania zespołów mieszkaniowych w okresie przemian politycznych, funkcjonalnych i obyczajowych*, [In:] Materiały z Międzynarodowej Konferencji Znaki Tradycji w Architekturze, Nysa 2008, 233-239.
- [5] Rozporządzenie Ministra Infrastruktury z dnia 12 kwietnia 2002 r. w sprawie warunków technicznych jakim powinny odpowiadać budynki i ich usytuowanie; Dz. U. Nr 75, poz. 690 z późniejszymi zmianami.

MICHAŁ SZYMAŃSKI*, RADOSŁAW GÓRZEŃSKI*, KAMIL SZKARŁAT**

AUTOMATION RETROFITTING AS A FIRST STAGE OF COMPLEX RENOVATION OF DISTRICT HEATING SUBSTATIONS IN PUBLIC BUILDINGS

ROZBUDOWA UKŁADÓW AUTOMATYKI JAKO PIERWSZY ETAP KOMPLEKSOWEJ MODERNIZACJI WĘZŁÓW CIEPŁA W OBIEKTACH UŻYTECZNOŚCI PUBLICZNEJ

Abstract

Automation systems modernization in selected district heating substations in university campus buildings were described in the article. Replacement of the control valves and application of heat meters for each circuits were the scope of the renovation. Local automation systems were integrated within Building Management System. Conclusions resulted from the operation of renovated heat substations will be used in the future for further complex and optimized heating substations modernization. Analysis of the work of the heating substations in buildings built in the past few years were also presented in the paper.

Keywords: district heating substations, automation systems, thermal renovation

Streszczenie

W artykule opisano proces rozbudowy układów automatyki w wybranych węzłach ciepła budynków uniwersyteckich. Zakres remontu obejmował wymianę zaworów regulacyjnych oraz zastosowanie liczników ciepła na poszczególnych obiegach instalacji grzewczych. Układy automatyki zintegrowano w systemie zarządzania BMS. Wnioski wynikające z eksploatacji zmodernizowanych węzłów mają w przyszłości posłużyć do dalszej, kompleksowej, zoptymalizowanej modernizacji węzłów ciepła. W artykule przedstawiono również analizę pracę węzłów obsługujących budynki wybudowane w ciągu ostatnich kilku lat

Słowa kluczowe: węzły ciepła, układy automatyki, termomodernizacja

* Ph.D. Michał Szymański, Ph.D. Radosław Górzeński, Institute of Environmental Engineering, Faculty of Civil and Environmental Engineering, Poznan University of Technology,

** Ph.D. Kamil Szkarłat, Department of Applied Informatics, Faculty of Physics, Adam Mickiewicz University in Poznań.

1. Introduction

In recent years many buildings were thermally renovated. Thermal insulation of external walls was improved, windows replaced, central heating (CH) and hot water distribution systems (DHW) modernized. Changes in heat bills, use of electronic heat cost allocators, and the heat meters along with billing of individual tenants, as well as public institutions, led to a more conscious operation of buildings, reduced heat demand for heating and hot water preparation.

The existing buildings technical documentation, after numerous modifications of buildings' envelopes and HVAC systems, is not a significant help in determining the actual buildings' heat demand. Analytical methods for existing buildings are affected by substantial errors [3]. Measurements of heat transfer coefficients or airtightness of buildings, although technically feasible, are seldom used. Very difficult to assess is the influence of natural ventilation and operation of the buildings.

Costs of delivered heat depend on the contracted heat demand, which is typically declared by the building administrator. Heat suppliers have precise knowledge of peak capacities, thanks to heat meters with the data transmitters. Unfortunately, this information is usually not available for the customers. A typical configuration of heating substation is equipped with only the main heat meter and no individual circuits are measured. Real heat demand is not known, that is why comprehensive modernizations of heating substations are difficult to conduct properly.

The solution is staged modernization. First step consists of replacing the automation control system, main actuators and valves; integrating it within the Building Management System (BMS) and installing heat meters. After one period of operation, knowing real heat demand, one can proceed to the second phase of modernization, which consists of replacing the substation's hydraulic components. This solution allows for a selection of a heating substation well-fitted to building needs, and results in distributing the financing in time.

2. Modernization of automation systems and metering of heating substations

In 2013, 12 heating substations in the Poznan University of Technology (PUT) campus were selected for modernization. Buildings are summarized in Table 1. Among them are dormitories (A11–A19), the canteen (A20), administration and educational buildings (the rest). Additionally, for comparative purposes, Mechatronics, Biomechanics and Nanoengineering R&D Centre (CM), built in 2011, are presented.

The heating substations have been in use since 1980/1990. The newest one was made in 2003. During this operation a number of fittings, valves, sensors and actuators have been replaced. They were equipped, only, with main heat meters (district heating circuit). Heating substations generally worked properly with weather based controls, but have the ability neither to remotely control the heating parameters, nor reading the circuits' heat consumption.

Staged modernization was proposed, with the first step consisting of the automation systems replacement and metering the substations circuits: CH, DHW, air handling units



Fig. 1. Analyzed PUT campus buildings (source: Google Maps)

heaters (VH) and hot water circulation (HWC). New valves with actuators for CH, VH and DHW circuits were installed; damaged fittings were replaced; and thermal insulation of pipelines completed.

The total net specific cost of upgrade was around 20 € per 1 kW of contracted heat demand.

3. Operation of retrofitted heating substations

Information about real peak heat demands is important to determine the modernization strategy for the campus buildings and is essential to reduce the contracted capacities as to decrease fixed costs associated with the heat delivery.

Minister of Economy ordinance [1] sets detailed rules for calculation of tariffs and settlements of heat supply. In accordance with §2.18 [1] contracted heat demand is set by the administrator of the building. It is the peak capacity calculated for design conditions. Heat suppliers enforce the contracted heat demand with use of flow limiters. In case of exceeding the contracted heat demand, heat suppliers may charge the customer twice the rates.

Heat demand is determined (§43.3 [1]) as 1/24 of the difference of the heat meter readings (MWh) made in a period of 24 hours. Contracted head demand is calculated as follows (§41.3 [1]):

$$N_C = \frac{Q_{dCH}}{24} \cdot \frac{t_i - t_e}{t_i - t_{av}} + \frac{Q_{dHW}}{24} \quad (1)$$

where:

- Q_{dCH} – amount of heat supplied for CH+VH in 24 hours period [MWh],
- Q_{dHW} – amount of heat supplied for DHW+HWC in 24 hours period [MWh],
- N_C – calculated contracted heat demand [MW],

- t_i – indoor temperature [°C],
- t_e – design temperature [°C],
- t_{av} – average ambient temperature for 24 hours period [°C].

Q_{dCH} and Q_{dHW} values should be determined with use of dedicated heat meters. If only the main heat meter is available it is impossible to determine in practice the Q_{dHW} at ambient temperature t_{av} .

The impact of contracted heat demand on fixed heat costs is particularly evident in the case of new, low energy buildings connected to the district heating network. Connection heat demand defined in the application for connection to the network based on the HVAC design in general practice is often two or even three times higher than the actual heat demand, which occurs during operation. CM building, with measured specific heat demand for CH and VH of 26 W/m² and 14.000 m² of heated area is equipped with a substation of 1.21 MW heating capacity. With contracted heat demand set with the use of connection heat demand, instead of the real demand (about 400 kW), would result in an increase in total annual heat cost from 2.30 €/m²/annual to 4.00 €/m²/annual (data calculated for the year 2012). In many cases, technical and administrative heat customer staff, used to the higher specific heat costs for typical buildings, pay no special attention to low energy buildings heat costs.

Heat demand for an existing building can be estimated using the consumption readings from the main heat meter for longer time periods (e.g. monthly invoices), divided by the number of hours of the measurement period. It results in determination of heat capacity smaller than actual values, due to averaging of peak demands.

Accurate determination of the heat capacity of a substation is possible with use of long-term metering of heat power. It requires the use of individual heat meters for each circuit,

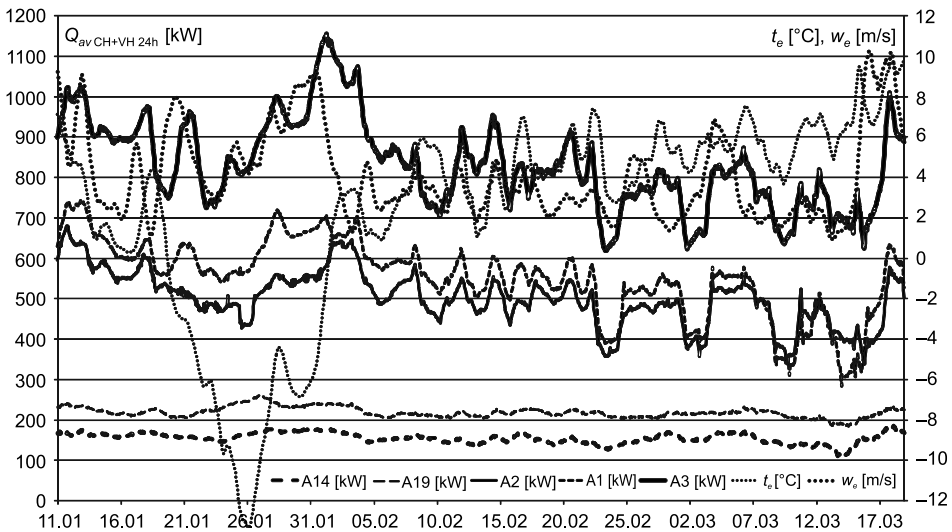


Fig. 2. Thermal capacities of selected buildings, averaged over 24-hour periods related to design conditions ($t_e = -18^{\circ}\text{C}$, $t_i = 20^{\circ}\text{C}$), wind speed (w_e) and outside temperature (t_e) for the analyzed period 10.01–18.03.2014

integrated into the BMS, which enables archiving of measured parameters. Substation heat demand is the sum of the maximum DHW+HWC demand and CH+VH demand, related to design conditions, selected from the list of 24-hour mean demands.

Figure 2 presents the thermal capacity measurements averaged over 24-hour periods and related to design conditions. The measurements were made using the CH and VH heat meters and archived in BMS.

Heat demand reduction observed on weekends for some buildings (B1, A2, A1, A3, C1) is the result of internal temperature setback. The analysis does not take into account lowered temperature in the rooms (assumed constant 20°C). In dormitories (A14, A19) these reductions were not applied, what resulted in flat curves for the buildings.

Table 1

Contracted and estimated heat demands

object	A_f [m ²]	N_{OH}	N_{24}			N_{MH}			ΔN_{OH} [%]	ΔN_{MH} [%]	q_{24} [W/m ²]
		Σ	CH	HW	Σ	CH	HW	Σ			
A11	6560	422	374	66	440	355	31	386	-4	-12	57
A12	5420	294	235	73	308	209	47	256	-4	-17	43
A13	5420	260	188	54	242	154	40	193	8	-20	35
A14	5420	256	187	69	256	155	47	202	0	-21	35
A18	7180	526	256	86	341	172	75	247	54	-28	36
A19	7180	526	261	88	349	218	69	286	51	-18	36
B1	4300	487	472	2	474	344	2	347	3	-27	110
A20	2000	230	134	15	149	98	12	110	55	-26	67
A2	6340	586	680	13	693	489	13	502	-16	-28	107
A1	13700	788	743	20	763	541	25	566	3	-26	54
A3	14900	1005	1155	19	1173	824	22	845	-14	-28	77
C1	3210	318	336	2	339	237	1	238	-6	-30	105
CM	14000	400	362	9	371	254	8	262	8	-29	26
$\Sigma/\bar{s}r.$	95630	6096			5897			4441	3.4	-24.7	61

Abbreviations: A_f – heated area, CH – central heating (CH and VH taken into account), HW – hot water preparation (DHW and HWC taken into account), Σ – total power, N_{OH} – contracted heat demand, N_{24} – maximum heat power averaged over 24 hours periods, N_{MH} – maximum heat power averaged over monthly periods, ΔN_{OH} – contracted heat demand over-sizing relative to the actual value (N_{24}), ΔN_{MH} – maximum heat power excess averaged over monthly periods relative to the actual value (N_{24}), q_{24} – specific heat demand (CH+VH)

Due to the 24-hour averaging, capacity increases after the reduction period are not particularly noticeable on the chart. In practice, increased power periods last approximately a few hours.

For high-rise buildings (A1, A3) and for older buildings with poor airtightness (A2, B1, C1) the influence of wind, even in ambient temperature rising periods, can be clearly observed.

For the 10.01–18.03.2014 period analysis of the heat meters readings was conducted and presented in Table 1, which compares the ordered heat demand (subscript OH), heat power averaged in the 24 hours period (subscript 24) and during the month (subscript MH). Analysis was performed using the CH, VH, DHW and HWC circuits heat meters archived in the BMS database. Average ambient air temperature was 2.5°C. CH and VH capacities were related to the design ambient temperature –18°C.

It should be noted that determination of the heat demand using monthly averages (MH) results in underestimating the power of up to 30%, with average of almost 25%. Dormitories, thermally renovated in recent years, are characterized by a specific heat demand of 35–36 W/m² (with the exception of buildings A11 and A12 due to their different operation: adjacent sports hall and conference auditorium). Not thermally renovated buildings (C1, A2 and B1 – prohibited by Old Monuments Law), are characterized by a specific heat power demand of 105–110 W/m². Buildings A1 and A3, erected in the 70's, thermally renovated, but with large number of thermal bridges, exposure to wind and equipped with additional mechanical ventilation systems with poor controls (for A3) are characterized by an 54–77 W/m². Low energy building CM, erected in 2012, is characterized by the value of 26 W/m². Very good performance is the result of proper thermal insulation, good airtightness (measured $n_{50} = 0.3 \text{ h}^{-1}$) and the demand controlled ventilation (DCV) all over the building.

By comparing the heat demand of A1 and A3 buildings, with the same structure and similar operation, attention was paid to, not metered so far and thus not conscious by the technical staff – the heat demand of the auditorium building located in between A1 and A3 buildings. The building is supplied with heat from A3 building substation, which includes the lecture halls, with an area of 1.200 m². Heat demand for CH+VH is nearly 400 kW, which represents about 40% of the heat demand of A3 building (with an area of 13.700 m²). The reasons are: lack of insulation, high heat losses to the ground, low efficiency heating system and most of all primitive automation system often resulting in a continuous operation of air handling units, without dependence on the auditoriums' occupancy profile.

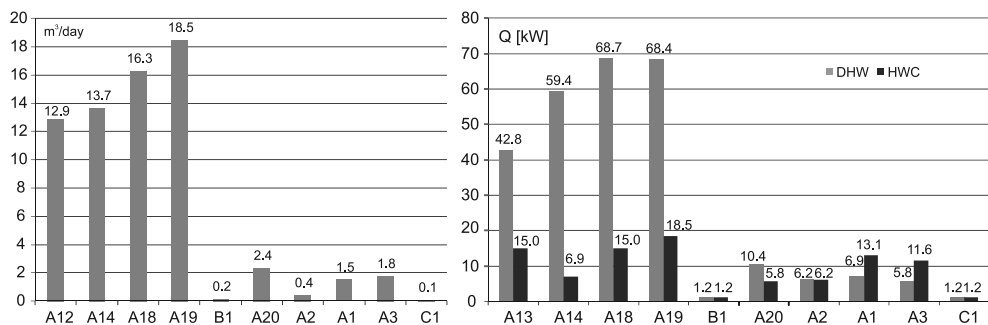


Fig. 3. Hot water consumption (left) and comparison of DHW and HWC heat demand (right) in selected PUT campus buildings

Measurements proved a very low consumption of DHW (100 to 400 dm³/day) in B1, A2 and C1 buildings. A change should be considered from central hot water preparation with circulation system to local electric water heating.

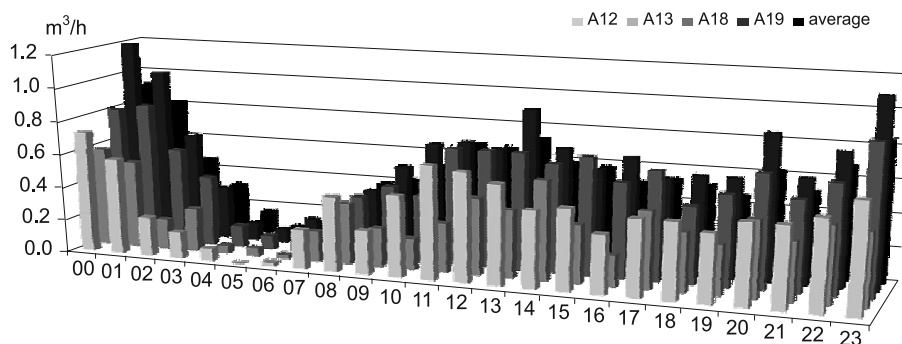


Fig. 4. Hourly averaged DHW consumption in selected dormitories

The higher hot water consumption compared to the buildings' floor area results in less HWC contribution in total DHW+HWC heat losses. For dormitories HWC ratio is about 18.3%, while for rest of the campus (except A20 – canteen) it exceeds 56%. Very large heat losses were observed in high-rise A1 and A3 buildings, where HWC ratio is more than 66%. As a result of the observations strict schedules and hot water temperature reductions (setbacks) were set for the DHW circulation systems.

In the dormitories, a reduction of hot water consumption was observed in the hours 3:00–7:00. For the period temperature reduction to 45°C (compared to standard temperature of 55°C) was set.

4. Conclusions

The paper presents the concept, scope and effects of the first stage of a complex retrofitting of heating substations for 12 buildings located on the PUT campus. Common problems of operation of the heating substations being in use for years were described. Capabilities of BMS control, schedules, reductions and the adjusting of parameters were also discussed.

Particular attention was paid to the method of estimating the contracted heat demand. It was concluded, that design oversizing of heat exchangers may indirectly and substantially increase the heat cost for low energy buildings. A number of heating substations operation phenomena, not noticed till now due to lack of instrumentation, were described and analyzed.

Benefits of automation systems retrofit, as a first stage of complex modernization was presented. Customer obtains knowledge of the peak heat demands, heat losses, hot water consumption and operation profiles. This is a very good step towards optimal complex retrofitting in next stages. BMS allows to control the operation parameters of heating substations, set schedules and reductions.

References

- [1] Rozporządzenie Ministra Gospodarki z dnia 17 września 2010 r. w sprawie szczegółowych zasad kształtowania i kalkulacji taryf oraz rozliczeń z tytułu zaopatrzenia w ciepło (Dz.U. 2010, nr 194, poz. 1291).
- [2] Rozporządzenie Ministra Gospodarki z dnia 15 stycznia 2007 r. w sprawie szczegółowych warunków funkcjonowania systemów ciepłowniczych (Dz.U. 2007, nr 16, poz. 92).
- [3] Basińska M., Koczyk H., *Analiza zmienności stopniodni dynamicznych okresu ogrzewania w rzeczywistych warunkach klimatu zewnętrznego*, XLVII Konferencja Naukowa Komitetu Inżynierii Lądowej i Wodnej PAN i Komitetu Nauki PZTIB, Wrocław 2001.

ADRIAN TRZĄSKI*, ALEKSANDER PANEK*, JOANNA RUCIŃSKA*

IMPACT OF WINDOWS PARAMETERS ON THE THERMAL PERFORMANCE OF A MULTI-FAMILY BUILDING

WPŁYW PARAMETRÓW OKIEN NA CHARAKTERYSTYKĘ ENERGETYCZNĄ BUDYNKU WIELORODZINNEGO

Abstract

The paper presents an analysis of the influence of various window types on the thermal performance of a multi-family building. In the analysis several different fenestration system configurations were considered. For these systems, heating and cooling demand of the building was estimated according to the simple hourly method proposed in ISO 13790. The results were used to compare, both the overall thermal performance of the building, as well as the actual thermal energy balance of analyzed windows.

Keywords: windows, fenestration, energy performance

Streszczenie

W artykule przedstawiono wyniki analizy wpływu zastosowania różnych rodzajów okien w charakterystyce energetycznej budynku wielorodzinnego. W analizie rozpatrzono zastosowanie kilku różnych systemów okiennych. Dla analizowanych systemów obliczono zapotrzebowanie na ciepło oraz chłód, posługując się prostą metodą godzinową zgodną z ISO 13790. Wyniki obliczeń wykorzystano do porównania zarówno całkowitego zapotrzebowania na energię budynku, jak i do określenia rzeczywistego bilansu badanych okien.

Słowa kluczowe: okna, przeszklenie, charakterystyka energetyczna

* Ph.D. Eng. Adrian Trząski, Ph.D. Eng. Aleksander Panek, Ph.D. Eng. Joanna Rucińska, Department of Heating and Ventilation, Faculty of Environmental Engineering, Warsaw University of Technology.

1. Introduction

New regulations, such as the European Directive 31/2010 Recast, impose new demands on the construction industry and investors. New low-energy buildings should be built using advanced technology and design techniques.

Windows play an important role in ensuring the comfort of indoor climate conditions. Commonly used factor for windows thermal efficiency is the heat transfer coefficient U . This factor, however, does not describe the full energy balance of the window. In fact, windows are also a source of solar heat gains and allow air infiltration. That means that the lowest U -factor does not guarantee the best thermal performance.

2. Methodology

In order to analyze the influence of thermal parameters of the fenestration system on the energy characteristic of a multi-family building, a two stage method has been used. The first step of the analysis was to calculate the energy characteristics of a reference multi-family building for various fenestration systems. The energy characteristic was calculated according to the simple hourly method of the ISO 13790 standard. Obtained heating/cooling energy demand was used to compare the overall building thermal characteristic depending on the fenestration parameters. To analyze the results on a window scale windows energy performance was calculated for both heating and cooling seasons. The general concept of the calculation procedure is presented in Fig. 1.

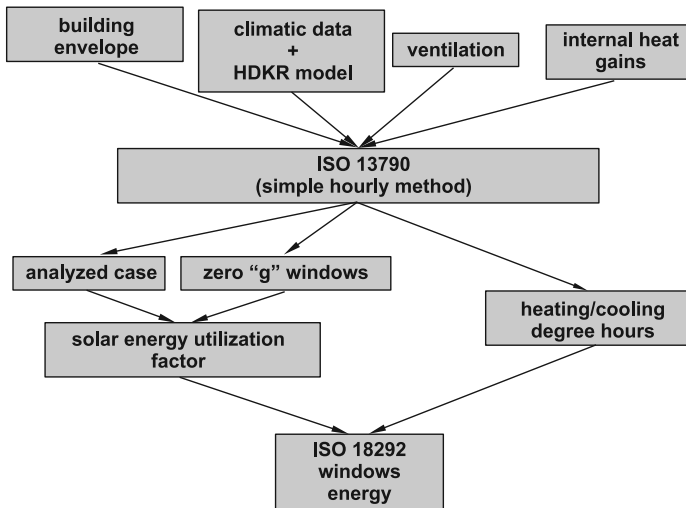


Fig. 1. Calculation algorithm

The assessment procedure in ISO 18292 requires data on both solar heat gains and heat loss through windows. Since both of these parameters depend largely on the climate and the energy characteristic of a building; detailed calculations for each reference building located

in the three climate zones in accordance with the procedure proposed in ISO 13790 have been conducted. As not all of the available solar energy can be utilized for heat demand reduction, utilized fraction of the available solar energy is calculated on an hourly basis for the reference house. Solar energy utilization factor is calculated as a ratio of the effective reduction of the heating demand (calculated as a difference of the heating demand of the reference building and the building with windows for which solar energy transmittance equals 0) to the total solar irradiation through windows. Finally, the energy performance of windows is calculated as a difference between the utilized transmitted solar energy and the thermal heat losses during the heating and cooling seasons.

$$E_{\text{ref,heating}} = I_{\text{heating}} \cdot g - D_{\text{heating}} \cdot U \quad (1)$$

$$E_{\text{ref,cooling}} = I_{\text{cooling}} \cdot g - D_{\text{cooling}} \cdot U \quad (2)$$

where:

$E_{\text{ref,heating}}$	– window energy balance for the heating season [kWh/m ²],
$E_{\text{ref,cooling}}$	– window energy balance for the cooling season [kWh/m ²],
I_{heating}	– utilizable solar irradiation during the heating season [kWh/m ²],
I_{cooling}	– utilizable solar irradiation during the cooling season [kWh/m ²],
g	– solar energy transmittance of the window [–],
U	– heat transfer coefficient of the window [W/(m ² ·K)],
D_{heating}	– heating degree hours [kKh],
D_{cooling}	– cooling degree hours [kKh].

3. The reference building

The energy performance of windows may vary in various building mostly due to a different solar energy utilization potential (as a result of various heat gains/heat loss factor). The selection of the reference building is not random, residential buildings play an important role in the overall national energy consumption. That makes optimization of their construction a very important factor for the national energy policy. Therefore in this study, an average sized multi-family building was chosen. In order to include in the study the impact of the building's overall energy performance on the windows, two different constructions were considered. One for a building constructed in 1970s and the other constructed according to current standards (Technical Requirements 2008); the general building construction for both reference building construction types was the same:

- heated/cooled space – 4466.17 m²,
- building volume – 14960 m³,
- number of floors – 4,
- ground floor/roof area – 1298.30 m²,
- roof pitch – 0°.

The most important thermal properties of the building envelope are presented in Table 1. The values were taken according to respective standards, that is:

- in case of current standard (TR 2008) – Ordinance of the Minister of Infrastructure on the technical requirements for buildings and their location building design from 2008,

- building from 70s – PN-64/B-03404 and PN-74/B-03404 polish standards representative for most of existing buildings.

Table 1

Selected construction types			
Construction type	Walls U [W/m ² K]	Roof U [W/m ² K]	Ground floor U [W/m ² K]
TR2008	0.3	0.25	0.45
70s standard	1.16	0.5	0.7

One of the factors that may influence the energy performance of windows is their area and distribution. However due to practical requirements in case of residential buildings windows fraction on facades is similar in most buildings. In the study, windows distribution for the reference building was assumed according to the Table 2.

Table 2

Windows distribution and facades	
Orientation	Window fraction on a facade [%]
N	31.3%
E	9.2%
S	31.3%
W	9.2%

Other important factors, that may influence thermal performance of buildings are:

- ventilation airflow – the airflow was calculated in accordance with the norm PN-83/B-03430/AZ3:2000. The design ventilation airflow equals 11200 m³/h,
- building's thermal capacity – typical for polish conditions building construction is traditional masonry construction and concrete/masonry construction. Therefore the reference building's thermal capacity was assumed to be $C = 260\,000$ J/(K·m²),
- internal heat gains – Internal heat gains were estimated according to the ordinance of the Minister of Infrastructure on the methodology of building energy performance calculation [2], assuming floor area distribution: living room and kitchen – 35%, bedroom – 35%, other – 30%, giving in average heat flow of 4.1 W/m².
- climate – as climate in various regions of Poland does not differ significantly, the relative differences in the energy performance of windows is insignificant, meaning that a good window in a colder region should also be good in a warmer region. To represent average climate as a representative dataset of weather; data was chosen for Warsaw.

4. Analyzed window types

Windows, substantially, influence the building's thermal performance in two ways: on one hand by an increase of transmission heat loss through the envelope and on the other

by an increase of solar heat gains. That means that comparison of windows based only on one parameter (usually thermal energy transmittance for the whole window U_w) may not be optimal and may lead to incorrect window selection. If we want to make a reliable comparison of windows we should take into account both the U_w factor and the g_w coefficient that describes solar energy transmittance of windows. Both values may vary considerably depending on used materials and window construction. In order to analyze the influence of the parameters on the energy performance of the reference building six, different window types were taken into account (Table 3).

Table 3

Selected window types		
No.	U_w [W/m ² K]	g_w [-]
1	1.6	0.40
2	1.6	0.55
3	1.4	0.35
4	1.4	0.46
5	1.0	0.20
6	1.0	0.27

5. Results

For the selected window types the reference building energy performance was calculated for both heating and cooling seasons. In order to unify calculations, building energy demand for heating was calculated with an assumption of a set length of the heating season (from 26 September to 5 May). This assumption allowed calculation of the solar energy utilization factor during the heating season, required for further analysis. In case of the cooling demand such unification was not possible. However, it wasn't necessary as there is no need for solar energy utilization factor calculation as this energy is not utilized, but must be removed from the building. Moreover, the impact of windows on the number of hours when the set temperature would be exceeded, in case of cooling, is much more significant than in case of heating. Therefore this impact should be included in calculations.

Table 4 presents heating and cooling demand values for selected window types and building construction standards. Note that better energy performance was not necessarily achieved through selection of windows with a lower U_w value. In particular the heating demand for the window type #2 ($U_w = 1.6$ W/m²K) was lower than for the window type #5 ($U_w = 1.0$ W/m²K). This difference was a result of a much lower solar energy transmittance of the window type #5. The results shows the importance of this factor for energy performance optimization. On the other hand the results confirm that regardless of the construction standard the classification of thermal performances is the same therefore windows' performance should behave in the same manner.

Table 4

**Building energy performances for selected window types
and building construction standards**

No.	U_w W/m ² K	g_w [-]	TR2008		1970s	
			E_h [kWh]	E_c [kWh]	E_h [kWh]	E_c [kWh]
1	1.6	0.40	416 091	-16 059	649 321	-15 431
2	1.6	0.55	394 055	-30 008	628 639	-25 265
3	1.4	0.35	409 018	-13 542	643 098	-13 505
4	1.4	0.46	392 662	-22 719	627 782	-20 108
5	1.0	0.20	402 522	-6 339	637 791	-7 864
6	1.0	0.27	391 827	-10 282	627 816	-10 911

In order to classify windows, energy performances for selected window types was calculated on the basis of ISO 18292 standard. Required for the calculations values of degree hours and irradiation were calculated for selected window types and building construction standards.

Table 5

**Values of heating/cooling degree hours and irradiation for selected window types
and building construction standards**

No.	TR2008				1970s			
	D_h [kDh]	I_h [kWh/m ²]	D_c [kDh]	I_c [kWh/m ²]	D_h [kDh]	I_h [kWh/m ²]	D_c [kDh]	I_c [kWh/m ²]
1	87.7	197.7	0.8	66.3	87.7	183.9	0.5	49.6
2	87.7	195.8	2.2	103.1	87.7	182.5	1.1	70.5
3	87.7	198.9	0.6	58.4	87.7	184.8	0.3	45.1
4	87.7	197.5	1.4	84.8	87.7	183.8	0.8	61.7
5	87.7	201.8	0.1	34.4	87.7	187.1	0.1	30.1
6	87.7	200.9	0.4	48.6	87.7	186.5	0.2	38.8

For the calculated heating/cooling degree hours and irradiation values windows energy balances were calculated.

The results (Table 5) indicate that due to a set heating season length the utilizable irradiation varies only slightly. In case of cooling the differences were much higher, however, as using various datasets for windows classification might be difficult; therefore a similar analysis for a reference dataset based on averaged values was conducted.

Comparison of results (Tables 6 and 7) indicate that there are differences in the reference heating/cooling energy balances depending on the used dataset. However it does not change

the general classification of windows meaning that windows could be compared on a basis of a reference dataset of heating/cooling degree hours and irradiation values.

Table 6

Heating/cooling balances for selected window types and building construction standards

No.	TR2008				1970s	
	U_w [W/m ² K]	g_w [-]	E_h [kWh/m ²]	E_c [kWh/m ²]	E_h [kWh/m ²]	E_c [kWh/m ²]
1	1.6	0.40	-61.2	25.2	-66.8	19.1
2	1.6	0.55	-32.6	53.3	-39.9	37.0
3	1.4	0.35	-53.2	19.5	-58.1	15.3
4	1.4	0.46	-31.9	37.0	-38.2	27.3
5	1.0	0.20	-47.3	6.8	-50.3	5.9
6	1.0	0.27	-33.4	12.7	-37.3	10.2

Table 7

Heating/cooling balances for selected window types and a reference climatic data set

No.	U_w [W/m ² K]	g_w [-]	D_h [kDh]	I_h [kWh/m ²]	D_c [kDh]	I_c [kWh/m ²]	E_h [kWh/m ²]	E_c [kWh/m ²]
1	1.6	0.40					-63.6	21.9
2	1.6	0.55					-34.8	30.6
3	1.4	0.35	87.7	191.8	0.7	57.6	-55.7	19.2
4	1.4	0.46					-34.6	25.5
5	1.0	0.20					-49.3	10.8
6	1.0	0.27					-35.9	14.8

6. Conclusions

U -value of windows cannot be used to compare energy performance of windows. Therefore, in order to provide decision makers information on the actual performance of windows, it is necessary to develop a windows rating scheme based on an overall energy performance during both heating and cooling seasons. The development of a such system is possible as the performance of windows does not differ significantly for various building construction standards.

Thermal performance of windows is not the only aspect that should be taken into account; windows are an important source of natural daylight that allows for reduction of electricity consumption for lighting, therefore a method of daylight potential implementation into

the windows rating system should be developed. Windows are also providers of natural ventilation, thus improving the indoor thermal climate and reducing cost/energy consumptions for mechanical ventilation. These effects should be considered in future studies.

References

- [1] PN-83/B-03430/AZ3:2000 Wentylacja w budynkach mieszkalnych, zamieszkania zbiorowego i użyteczności publicznej. Wymagania.
- [2] Rozporządzenie Ministra Infrastruktury z dnia 6 listopada 2008 r. w sprawie metodologii obliczania charakterystyki energetycznej budynku i lokalu mieszkalnego lub części budynku stanowiącej samodzielną całość techniczno użytkową oraz sposobu sporządzania i wzorów świadectw ich charakterystyki energetycznej
- [3] Panek A., Rucińska R., Trząski A., *Energy certification of windows*, International Sustainable Building Conference 2011, Helsinki 2011.
- [4] Panek A., Rucińska R., Trząski A., *Energy energy performance of windows in various building types*, Sustainable buildings construction products & technologies, Graz 2013.
- [5] Maccari A., Zinzi M., *Simplified algorithms for the Italian energy rating scheme for fenestration in residential buildings*, Solar Energy, Vol. 69 (Suppl.), Nos. 1-6, 2000, 75-92.
- [6] Duer K., et al., *Energy labelling of glazings and windows in Denmark: calculated and measured values*, Solar Energy, Vol. 73, No. 1, 2002, 23-31.
- [7] Karlsson J., Roos A., *Evaluation of window energy rating models for different houses and European climates*, Solar Energy, 76, 2004, 71-77.
- [8] Karlsson J., Karlsson B., Roos A., *A simple model for assessing the energy performance of windows*, Energy and Buildings, 33, 2001, 641-651.

MARIA WESOŁOWSKA*, PAULA SZCZEPANIAK*

SELECTED PROBLEMS OF THERMAL BRIDGES IN CONTEMPORARY MULTI-OCCUPANCY BUILDINGS

WYBRANE PROBLEMY MOSTKÓW TERMICZNYCH WE WSPÓŁCZESNYCH WIELORODZINNYCH BUDYNKACH MIESZKALNYCH

Abstract

In contemporary multi-occupancy buildings, each architecture studio has its own uniform and trademarked design for the external appearance of the structure. Façade features such as breaks, bays, balconies and cornices often generate energy and humidity problems. These require detailed analysis, both in terms of construction as well as physical aspects, so that elements are appropriately designed.

Keywords: thermal bridge, thermal quality, architectural detail

Streszczenie

We współczesnych budynkach wielorodzinnych stosowane detale elewacji urozmaicające monotonię bryły stają się wizytówką określonej pracowni architektonicznej. Wychodzące z płaszczyzny elewacji ryzality, wykusze, balkony i gzymsy często stwarzają problemy ciepłno-wilgotnościowe. Prawidłowe zaprojektowanie tych elementów wymaga szczegółowej analizy detalu zarówno pod względem konstrukcyjnym, jak i fizykalnym.

Słowa kluczowe: mostek termiczny, jakość cieplna, detal architektoniczny

* Ph.D. Eng. Maria Wesołowska, Ph.D. Eng. Paula Szczepaniak, Faculty of Civil and Environmental Engineering, University of Technology and Life Sciences in Bydgoszcz.

Denotations

- $v_{i,\min}$ – minimum internal surface temperature [$^{\circ}\text{C}$]
 t_s – point temperature [$^{\circ}\text{C}$]
 f_{Rsi} – temperature factor at the internal surface [-]
 $f_{Rsi,\text{kryt}}$ – critical value of temperature factor at the internal surface [-]
 $\Theta_{si,\min}$ – minimum acceptable surface temperature of the joint [$^{\circ}\text{C}$]
 Ψ_i – linear heat transport coefficient for internal dimensions [W/mK]

1. Introduction

The move away from uniform and prefabricated techniques for the construction of multi-occupancy buildings properties has allowed architects to experiment with individual and distinctive building facades which acquire considerable value as trademarked designs. A wide availability of building materials allows for the creation of more refined architectural details: balconies, cornices, breaks, bays, roofs and screens [7]. On the other hand, proven partition methods and solutions have remained in use: two-layered external walls, ventilated two-sectional ceilings [2] and rooves. Linking traditional solutions and developing new concepts can have unexpected consequences [1, 3]. Instead of enhancing comfort levels, problems arise with maintaining proper temperatures in a room and mould growth can result. Highly sensitive points for concern are the roof joints, ceilings and outer walls as well as the cornices.

In the photograph and cross section diagrams of a joint (Fig. 1, 2) we can see examples of solutions to this problem. Occupants in upper floors often report problems with maintaining proper internal temperatures even where controls are set at maximum level. In some apartments, tell-tale signs of mould growth appear on internal surfaces of the joint and on parts of the wall, and along the length of the cornice (Fig. 3).

In most cases, the problem is attributed to improper exploitation more precisely through excessive attempts to save on heating costs. Apartment users are often blamed for limiting the amount of ventilation and switching off heating for long periods. However, an analysis of heating costs in these particular apartments indicates otherwise. The cost of heating a 1 m^2 area can be as much as 50% higher than for a flat on the floor below.



Fig. 1. Examples of building facades erected after 2000

In order to establish the reasons for the problem occurring, it was necessary to examine the design, application and construction stages. Inspections of a group of buildings (Fig. 1, 2a) highlighted discrepancies between execution and design. Although the basic internal partition layers were constructed and fitted to the design, the construction firm used a more traditional set of materials for the wall, ceiling and roof joint, as shown in Fig. 4.

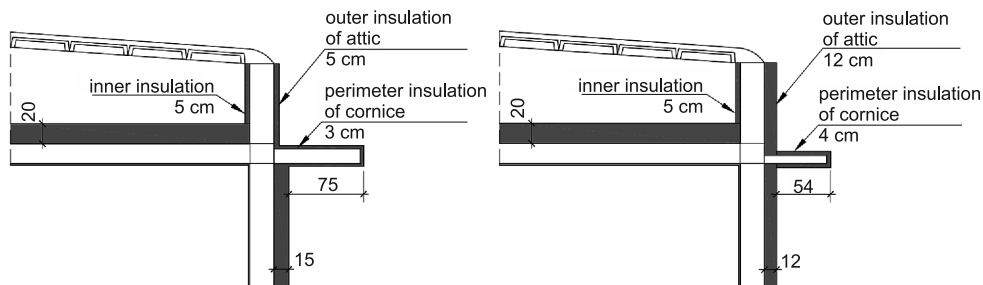


Fig. 2. Solutions for joints

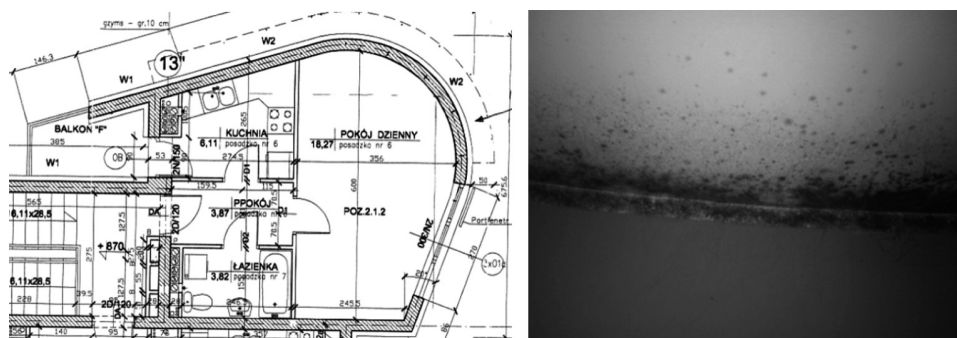


Fig. 3. A diagrammatic and photographic view of the surface of a ceiling in the section of the building

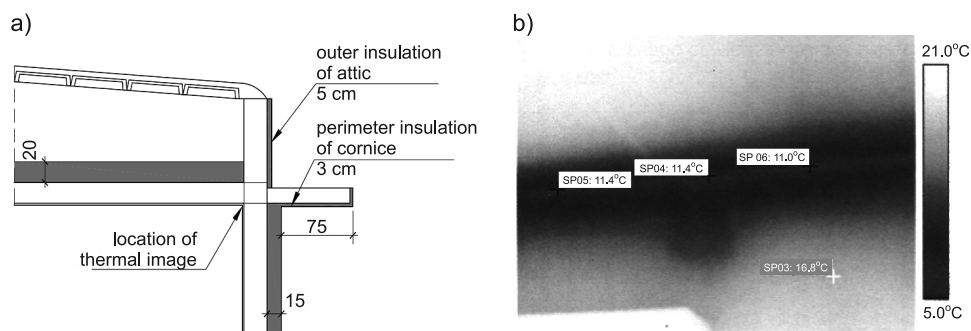


Fig. 4. The outside wall, ceiling and roof as currently configured: a) diagram showing materials, b) thermal image where the outside temperature was -11°C

After intervention of owners of apartments in summer period an additional layer of mineral wool was added in the roofspace against the outside walls, with thicknesses of 10 cm, and 25 cm on the attic wall.

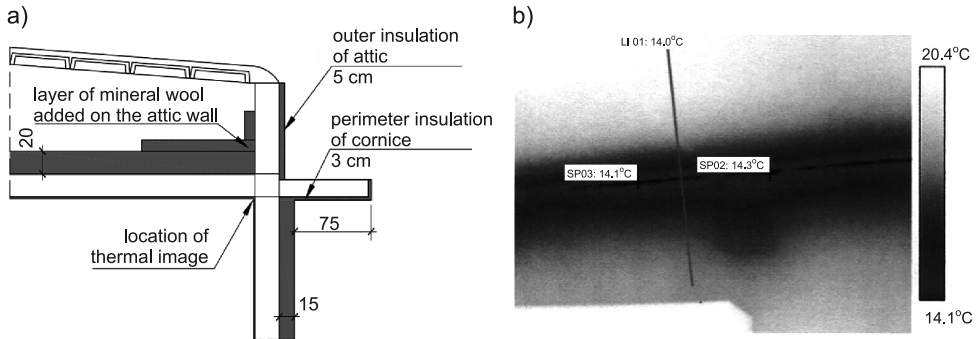


Fig. 5. Insulating the roof and ceiling: a) diagram showing materials, b) thermal image with the insulation in place, where the outside temperature was -10°C

This remedial work only partially limited this thermal bridge effect – the junction of outside wall with the ceiling and roof continued to experience heat losses from the apartment. Therefore, it was necessary to perform a more detailed analysis of the problematic structure.

2. Thermal protection requirements

According to the binding regulations (WT 2008) [6] concerning thermal insulation of building partitions (in force until the end of 2013), there is a requirement to provide maximal value of heat permeation at a value of factor U . The effects of thermal bridges were not taken into account in the heat demand calculations, and the required thermal quality levels for a solid structure were instead defined according to a moisture point (Eq. 1). It is necessary to calculate the temperature of the internal surface of the partition where a thermal bridge occurs, through experimentation or by using a numeric program.

$$v_{i,\min} \geq t_s + 1 \quad (1)$$

In 1997, this condition was incorporated into a regulation on the technical requirements of buildings and their locations [6] which remained in effect until the end of 2008. According to this calculation procedure, the dew point temperature value used to assess the humidity levels (Eq. 1) changed depending on how the room was used. In domestic properties, a room with a temperature of $+20^{\circ}\text{C}$ and $\phi_i = 55\%$ gives a reading (Eq. 1) of

$$v_{i,\min} \geq 11,7^{\circ}\text{C} \quad (2)$$

In the subsequent re-drafting of this regulation in November 2008, conditions giving rise to surface vapour condensation were modified – ‘on an internal surface of a non-transparent internal partition, there can be no condensation of vapour allowing for the development

of mould growth'. Checks to ensure that this condition is adhered to are carried out using temperature factor $f_{R_{si}}$, as defined in the PN-EN ISO 13788 standard [1]. In regard to external partitions of housing blocks, communal group buildings, civic and industrial buildings, the following approach should be taken in relation to external partitions and the main part of the building. The temperature factor $f_{R_{si}}$ should not be less than the required critical value, calculated according to the PN-EN ISO 13788 standard.

The required value should be calculated according to section 5 of the standard, and it is within acceptable parameters to fix the required value of the factor at the level of 0.72.

3. Analysis of the solution for the selected construction's joint

3.1. Pre-calculation values

The wall is constructed of 24 cm thick SILKA E blocks. The wall insulation is 15 cm thick foamed polystyrene. The walls are covered with gypsum plaster – assumed to be 2 cm thick. The ventilated ceiling and roof have the following layers: 2 cm thick gypsum plaster, 20 cm steel-concrete Filigran plates, vapour insulating foil, mineral wool mats, 2 cm \times 10 cm \times 10 cm height, width and length, roof space at 60 to 136 cm pitched height (the height of the ceiling to the roof at the point of analysis is 60 cm). Assumptions were made in terms of edge of area conditions and thermal properties of materials, according to [1, 4] as shown in Fig. 6.

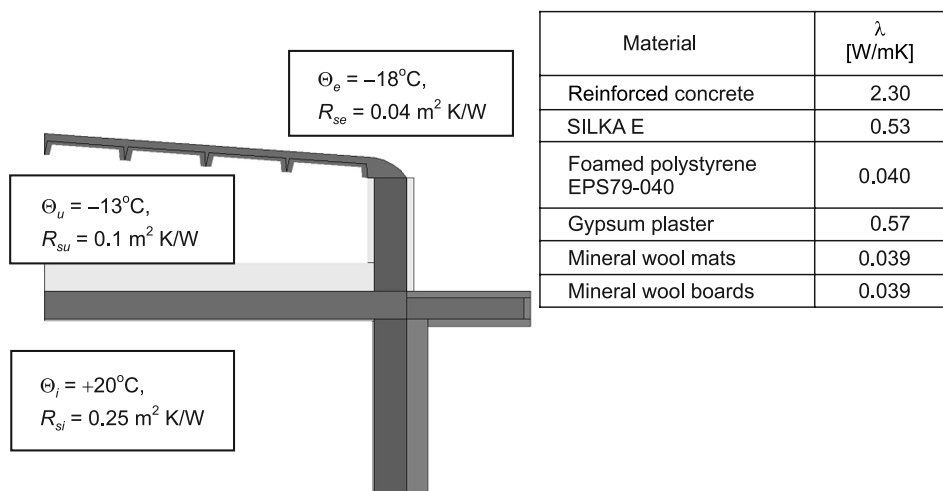


Fig. 6. Calculations assumed for the cross section of the joint

Insulation at this joint was examined under three different conditions:

- Following the work: lack of edge-to-edge insulation of the attic walls and lack of insulation on the upper surface of the cornice,
- Thermal insulation work carried out – laying of additional, horizontal edge-to-edge insulation of the roofspace with 25 cm overlaying on the attic wall,

- Bringing the joint up to its design specifications – filling missing spaces with additional, edge-to-edge thermal insulation on the attic wall using 5 cm thick mineral wool layers, and 3 cm thick foamed polystyrene on the upper surface of a cornice.

3.2. Calculation results and discussion

Measurements were taken for minimum temperatures in the joint ($\theta_{si,min}$) and the thermal factor f_{Rsi} . The results are shown in Table 1.

Table 1

Thermal quality of the analyzed joint

Joint insulation conditions	$\theta_{si,min}$ °C	Adherence to the dew point condition	f_{Rsi}	Adherence to the WT2008 standard	
				$f_{Rsi, kryt} = 0,72$	$f_{Rsi, kryt}$, for class 3 humidity conditions
After-work state	7.7	No	0.676	No	No
Insulation work completed	8.0	No	0.684	No	No
At design specifications	9.9	No	0.734	Yes	No

These readings show that the joint is at risk of internal condensation, according to the requirements for humidity protection which are binding up to 2008, but that the WT2008 standards give cause to dispute that outcome. Adherence to the requirement standard depends on the assumed critical value of $f_{Rsi,crit}$.

In view of this, the thermal quality of the joint should be improved to avoid any conceivable risk of mould growth.

4. Proposals for improving the joint's thermal quality

For internal partitions with high thermal insulation parameters, the effect of a thermal bridge generated by a solid structure is very great. Changes need to be made to the joint and two options should be considered:

- Proper thermal insulation of the existing thermal bridge, without the need for expensive construction solutions
- A design-based solution to the problem.

In the case of a joint in the existing building, there is a need to increase the thickness of edge-to-edge insulation including the attic walls. The best results are obtained by supplementing the external insulation of the attic and the upper and lower surface of a cornice (Fig. 7)

Such action will partially limit the effect of the thermal bridge – the minimum temperature will increase by 12°C. The linear heat transport coefficient ψ_i will also decrease (Table 2).

Significant improvement is only possible through construction intervention – at the building design stage. Isothermal connectors should be used as brackets and the typical solution used for the foundations of houses – ie: spacer layer of foamed dark glass (Fig. 8) – should be applied to the attic wall.

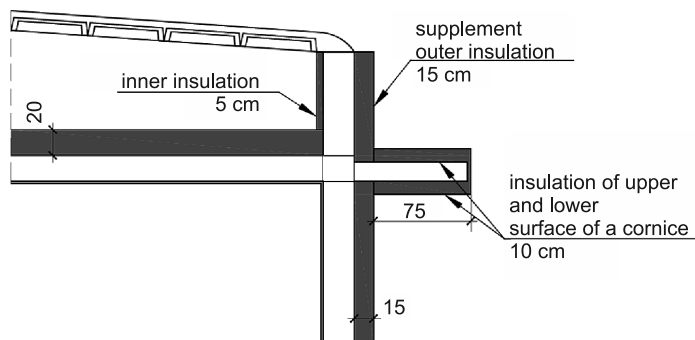


Fig. 7. Proposal for insulation the existing joint

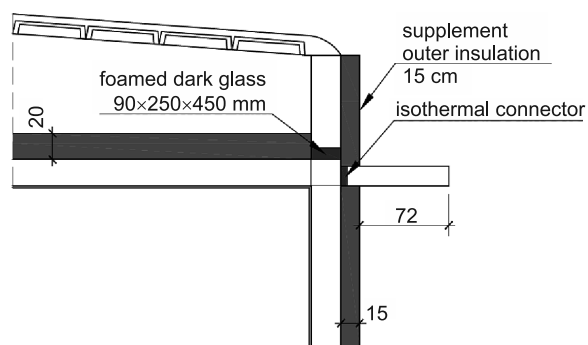


Fig. 8. Proposal for a construction solution

Table 2

Thermal characteristics of the modified joint

Variant of joint solution	Design solution Used	Proposed joint insulation	Proposed change of joint construction
$\theta_{si, min}$ [°C]	9.9	12.0	14.5
Ψ_i [W/mK]	0.419	0.284	0.123

5. Conclusions

In the light of the thermal and humidity conditions of rooms surveyed in the housing blocks, for ventilated ceilings and attics are necessary – possibly double-sectional. In such a construction, the connection between the exterior walls with features such as cornices

need special attention. The geometry of the structure examined in this paper is especially unfavourable – there is an attic and a supported cornice at the juncture of the ceiling and the roof. Both act as cooling elements – removing heat from the structure. Consequently, the temperature is significantly lower on the internal surface and the heat permeation factor is high for such a thermal bridge. In the case of a building in situ, it is only possible to insulate particular surfaces of the thermal bridge, but at the project design stage it is worthwhile considering changes in the construction of the structure, leading to an increase in the thermal quality of the building shell. This action is necessary from the perspective of consecutive regulations which restrict the permitted thermal protection ranges.

Attention should be paid to an evaluation of the quality of thermal bridges where the only parameter is the thermal factor, f_{Rsi} . According to technical and binding conditions [6], the critical value can be assumed to be 0.72. This has led to the adoption of solutions which were judged to be unfavourable or even defective, in terms of the physics – as well as the art and design – of building construction.

References

- [1] Byrdy A., *Analysis of insulation solutions for attics, illustrated by the example of a complex of steel structure swimming pool (in Polish)*, Izolacje 3/2014.
- [2] Byrdy C., *Dachy i stropodachy ocieplone i nieocieplane*, Wydawnictwo PK, Kraków 2003.
- [3] Pierce M., Causes and Cures of Attic Condensation and Roof Ice Dampening Problems Housing Fact Sheet, 2005.
- [4] PN-B-02403:1982 Ogrzewnictwo. Temperatury obliczeniowe zewnętrzne.
- [5] PN-EN ISO 13788:2003 Hygrothermal performance of building components and building elements - Internal surface temperature to avoid critical surface humidity and interstitial condensation – Calculation methods.
- [6] Regulation of the Ministry of Infrastructure, 12 April 2002 w sprawie warunków technicznych jakim powinny odpowiadać budynki i ich usytuowanie (with later changes).
- [7] Simons L.H., *Olin's construction*, John Wiley & Sons, 2001.

KINGA ZĘBALA*

REACTIVE POWER COMPENSATION AND ENERGY SAVING

KOMPENSACJA MOCY BIERNEJ A OSZCZĘDNOŚĆ ENERGII

Abstract

The issue of energy saving in workplaces where multiple machines are in use, and consequently there is high energy consumption, is discussed in this paper.

Keywords: compensation, reactive power, active power, energy efficiency

Streszczenie

W niniejszym artykule podjęto temat energooszczędności w zakładach pracy, w których wykorzystywane są maszyny, acz za tym idzie, bardzo duże zużycie energii

Słowa kluczowe: kompensacja, moc bierna, moc czynna, kondensator, energooszczędność

* M.Sc. Eng. Kinga Zębala, Institute of Building Materials and Structures, Faculty of Civil Engineering, Cracow University of Technology.

1. Introduction

Issues surrounding energy-saving, passive, or even zero-energy construction techniques, are commonly debated these days, particularly when we consider the use of new technology in house-building. The practice is regulated in law, which describes in precise terms how walls of buildings should be constructed so that: thermal heat loss is as low as possible; and energy requirements are at the minimum required to heat the building. However, the question of how to save energy in factories with higher machinery and lighting energy demands is discussed less frequently. Practically speaking, it is possible to limit electrical energy consumption in any business, factory and office block without any harm being done to the normal operation and function of the building. Rising prices in electrical energy, further legislation and regulations, and increasing fuel costs will not affect this situation, which explains why we need to consider all feasible means of reducing the amount of electrical energy used and the associated costs. This is why an analysis of reactive power compensation is necessary.

2. Reactive power compensation

Power, or more specifically induction reactive power, occurs only in alternating current circuits. The flow is between the source and the recipient/customer. This energy is required to generate alternating magnetic fields for engines, for magnetizing core convertors and for charging supplies carried in overhead and cable transmission lines to capacity levels. Reactive power does not readily convert into work energy, but it is often necessary to do so and all machines must utilize reactive power.

All induction machines run on reactive power, however, a-synchronic engines (especially idle engines), low-demand convertors, welding machines, low-demand transmission lines and long cable lines absorb the most reactive power. Electrical devices supplied with alternating current may also require reactive power, except where these require real/actual power. Reactive power must be used to create magnetic fields in engines, convertors, gland/shell-cased seals or electrical fields in capacitors. Additionally, reactive power is used in other capacities such as cables and non-linear devices such as fluorescent compact lamps, in which the current shifts in a time-frame to generate voltage, or devices that are not sinusoid.

Unfortunately, the energy flow of reactive power also has disadvantages. The flow from the source to the recipient/customer places a burden on electrical cables and lines, lowering the flow capacity and resulting in additional voltage levels, falls and losses of actual electrical power.

That is why electrical energy suppliers require consumption of reactive power to be limited. The suppliers make money from the amount of actual power delivered to the user, so wish to supply as much energy as possible, but with minimum losses and within the required parameters. As far as the measurement of losses is concerned, the value of the current flowing through the net elements depends upon the parameter of what is known as the apparent power – referred to as S .

$$S = \sqrt{3} \cdot U \cdot I \quad (1)$$

where:

- U – root mean square of strain,
- I – root mean square of current intensity.

The apparent power is the geometric sum of real/actual power P and reactive power Q :

$$S = \sqrt{P^2 + Q^2} \quad (2)$$

where:

- Q – reactive power,
- P – real power.

Figure 1 shows a graphic interpretation of the dependence between powers, depicting the ‘so called’ triangle of powers.

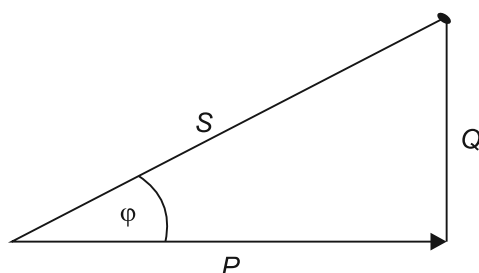


Fig. 1. The triangle of powers [3]: Q – reactive power, S – apparent power, P – real power, φ – the angle of difference (in degrees) between current and voltage

It would be ideal if the apparent power S was equal to real/actual power P , so that reactive power Q would be worth 0. In order to get such a result, the following is applied: reactive power compensation is represented as the relationship between the reactive power consumed by the recipient/customer and the reactive power of an identical or approximate value but with an opposite sign. Figure 2 presents a graphic illustration of reactive power compensation.

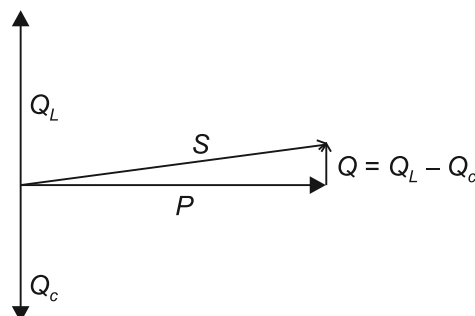


Fig. 2. Reactive power compensation [3]: Q – reactive power, Q_L – induction reactive power consumed e.g. by engines, Q_c – capacity reactive power absorbed by capacitor, S – apparent power, P – real power

After compensating, the amount of power absorbed from the network is much lower than would otherwise be the case.

Practically, there is no need to compensate to an extent that reactive power is zeroed out. The reason is that the increase in current is not significant when only real/actual power is consumed, and is also within a low value in terms of the difference in angle between the current and the voltage. The bigger the angle, then the faster is the current generated. As a result, fixed limits are established and losses are relatively slight and acceptable. The limits are described in terms of the tangent of the angle of difference between the current and the voltage, which is given as 0.4.

It is important to limit reactive power consumption by an appropriate choice of (work) load for converters in order to limit the energy expended by idle engines, to limit welding work on idle engines and for the maintenance of engines.

Reactive power compensation also plays an important role. It is generated by means of a synchronic capacitor. Therefore, there is no need for it to be sent from the supplier to the receiver, which explains why a greater amount of actual power can be carried along the same electrical power lines.

3. Capacitor batteries

A capacitor battery is a device used to compensate induction reactive power. It usually consists of a few capacitors, a regulator and various accessories. The regulator automatically switches on the appropriate number of devices, depending on the reactive power needs, to maintain a power factor cosine φ at the required level. The capacitor module consists of an electrical capacitor, a contactor, protection and glands/shells (in some types of batteries).



Fig. 3. Capacitor models (with various capacities) which set the 'heart' of each battery used for reactive power compensation

Capacitor batteries create capacitive reactive power (compensating induction reactive power) whose unit is expressed as a kilovar (kVAr).

Capacitor battery applications are commonplace, but a relatively recent solution, mostly popular in medium and large-scale factories, as only these receivers can be charged to provide additional reactive power consumption. As a result of the fact that modern electrical power meters became more commonly used, so smaller induction reactive power receivers must be taken into consideration for setting induction reactive power. Battery effectiveness

is considered to be 100%; the only preconditions for success being the appropriate choice of device and correct installation. Therefore each recipient, who is billed on the basis of their usage of induction reactive energy according to their contract terms, is free to fit a capacitor battery. This should only be considered if the investment is economically profitable, and a decision is taken on the basis of when it will pay for itself.

Kinds of capacitors

In view of the fact that networks and receivers have various characteristics in particular factories, four basic kinds of capacitors are considered here:

- Common batteries – batteries of the simplest construction, which may be applied only in places where the current and voltage are not adversely affected to a large extent and where the phenomenon of resonance with the network does not occur. If these requirements are not satisfied, then the battery will deteriorate and expire rapidly.
- Amplified batteries – these batteries are constructed in a similar way to common ones. However, they contain more durable capacitors. Such batteries may be applied in an environment where there is a higher level of deterioration, but cannot be used where there is resonance between the battery and the network.
- Batteries with thyristor linkages – batteries in which a thyristor is used instead of a contraction device. Therefore these react very quickly to any change in the power burden. These batteries are very expensive and are used only where large changes of reactive power occur in short periods and where traditional batteries would not provide the required results.
- Protective shell (glands) batteries – batteries with additional shells which protect capacitors from decay caused by current and voltage fluctuations. These batteries may be used wherever significant current and voltage fluctuations are observed and where there is a risk of resonance with the network.

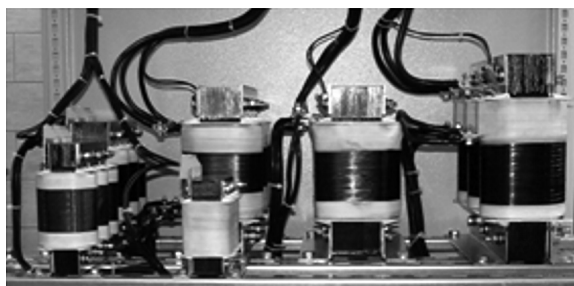


Fig. 4. Batteries with additional shells which protect capacitors from decay due to current and voltage fluctuations

Appropriate choice of batteries

When purchasing batteries, it is important to know which to choose. There are many kinds of batteries, which may be used for various purposes. All brands of batteries differ in both construction and price. If an inappropriate choice is made, the battery will deteriorate

very quickly and may also pose a risk. Therefore, people with specialist knowledge should be responsible for selecting the batteries. In order to make an appropriate choice, the power profile and any rate of deterioration must first be taken into account. Once this is done, the power of the device and its other parameters must be taken into consideration. Only such an approach will guarantee that the device will be of good quality with a long life span. On the basis of the demands for electrical power, it is possible to make an approximate calculation of the cost of the device. However, this approach will not give us any information about the fluctuations of the current and voltage, the risk posed by resonance or degradation.

There is no obligation for the electricity supplier to agree on the choice and use of a battery, and there is no requirement to inform the supplier about the fittings. It is perfectly within the rules to use batteries, and they do not interfere with instruments designed to measure the amount of electrical power supplied.

Batteries are self-contained and fully functional and they do not require continual maintenance. An operator monitoring the readings will control the amount of power to the capacitor modules so that the required power factor (cosine φ) is maintained (the battery operator is guided by the cosine – but on the print-out the tangene φ is shown because it allows for easier and clearer calculations to be made). It is necessary to carry out regular maintenance such as changing the filters.

The installation of a battery will not lead to an increased consumption of actual power. The battery only generates reactive power, at the same time compensating for induction reactive power absorbed by the receiver. The battery does not take much real power, at the same time reducing the amount of loss of electrical energy in power lines and convertors. It is expected that actual power consumption will be unchanged, or will decrease to a slight degree.

Usually applying capacitor batteries completely eliminates reactive power induction costs. Generally, prices are reduced by about 90%.

The cost of installing such a battery usually pays for itself after a few months. Considering the fact that the life span of an appropriately-selected device extends to 12 or so years, it is an excellent investment which should return on its investment cost as many as 20 times over, throughout its useful working span.

4. Penalties for higher reactive power consumption [1, 2]

If excessive reactive power induction consumption occurs, then the additional levy is calculated on the basis of the value of the actual factor $\text{tg}\varphi$ (tangene φ). This is calculated as a quotient of the reactive power to the actual power consumed within the chargeable billing period. If the power factor is higher than the required factor $\text{tg}\varphi_0$ (usually 0.4), then the cost for the additional reactive power induction consumption is calculated on the basis of the following formula:

$$O_b = k \times C_{rk} \times \sqrt{\frac{1 + \text{tg}^2\varphi}{1 + \text{tg}^2\varphi_0} - 1} \times A \quad (3)$$

where:

- O_b – the fee for additional reactive power consumption in PLN,
- k – the price factor C_{rk} as set out in the scale of charges. For the customers supplied at the low voltage level, factor k usually amounts to 3 and for customers supplied at the medium voltage level, factor k is set at 1,
- C_{rk} – average price of electrical power on the open competition market set on the day that the tariff was approved,
- $\text{tg } \varphi_0$ – power factor under the contract (usually 0.4),
- $\text{tg } \varphi$ – the power factor arising from the reactive power consumption,
- A – actual power consumed on a 24 hour basis or for the time period during which the consumption of reactive power took place.

Fees for additional consumption of reactive power:

- Increase the distribution service costs of electrical power leading to an increase in the average price;
- Should encourage the customers to take up compensation measures for the reactive power induction levels consumed;
- Reflect on the high prices charged to customers using the nN network, and the lower prices of electricity meters measuring the consumption of reactive power induction; reactive power prices to be paid by small-scale customers, who mainly use induction, single-phase devices, refrigerated units, ventilators, air conditioners etc.

5. Real savings

Capacitor batteries are deployed in almost all kinds of situations. In the past, these devices were almost solely used in industry, but nowadays are in common usage in shops, municipal buildings, office blocks, hotels, sewage treatment plants etc. Generally speaking, capacitor batteries are in place where energy distributors provide for the additional consumption of reactive power, and the recipient/customer possesses a significant number of machines, pumps, old types of lighting units etc. Examples include companies producing furniture pots, soles for shoes, and engaged in metalworking. In each case, once the device has been installed, the customer is in a position to control the effects. In around 90% of cases, the costs associated with reactive power are eliminated. In the remaining 10% of cases, the additional amount to be paid does not exceed 10% of the total amount billed for reactive power – prior to the installation of the device. The majority of batteries pay for themselves after 6–10 months. Information was gleaned from one company, in relation to the choice and fitting of batteries. To take the example of the town swimming pool in Silesia, the monthly net costs prior to the battery being fitted into position were about 1800 PLN. Excess costs were completely offset once capacitor batteries were fitted (shell-protected batteries in this instance because measurements showed resonance with pumps supplied occurring). The entire cost of the device and its fittings amounted to approximately 9600 PLN net. The investment cost paid for itself within nearly 6 months.

As mentioned earlier, a good choice of batteries eliminates the costs associated with reactive energy. As far as the excess fees are concerned much depends on the power factor – which is between 10% and 60% of the distribution bill. In turn, this may account for between 5% and 30% of the entire chargeable energy bill.

6. Conclusions

- The customer is not required to obtain the agreement of the electricity power supplier to fit the battery.
- The amount of actual energy consumed does not increase.
- The application of batteries to supply capacitors either completely off-sets the financial cost of induction reactive power, or at least significantly decreases it by at least 90%.
- Batteries are fully automated and do not require ongoing service. It is necessary to change the filters.
- Installing a battery does not carry any financial penalty in terms of any additional consumption of reactive energy.

The paper detailed in this paper has been partially funded by the project L-1/115/DS/2013 “Building compatible with Sustainable Development”. This financial support is gratefully acknowledged.

References

- [1] A Minister of Economy decree of 18 August 2011 Dz.U. (legal daily record) no. 189 in relation to detailed rules of development and calculations of the scale of charges and settlements of accounts for electrical energy.
- [2] A Minister of Economy decree of 27 April 2012 Dz.U. (legal daily record) no. 535 amending the existing decree in relation to detailed rules concerning the development of and calculations for the scale of charges for electrical power.
- [3] <http://www.korporacjasystem.pl/>
- [4] <http://www.elektroinstalacje.info/>

CONTENTS

Adamski M., Siergiejuk J., Ojczyk G.: Heat pump installation (John Paul II Centre, Krakow).....	3
Bandurski K., Mielczyński T., Koczyk H.: Thermal comfort and energy consumption of the ecological house – simulation analysis of <i>DOMTRZON</i>	11
Belok J., Wilk-Słomka B.: Energetic effectiveness of a building with a surface heating system.....	23
Bielek B.: Concept of the new physical-energy quantification of buildings in the development of technology in architecture for sustainable society	31
Bielek B.: New classification of renewable energy sources in the development of technology in architecture for a sustainable society.....	41
Byrda A.: Point thermal bridges in walls with external stone layer	49
Bzowska D.: The effect of thermal resistance of building's opaque elements and windows surface on air exchange intensity during the summer season	57
Chwieduk D., Grzebielec A., Rusowicz A.: Solar cooling in buildings	65
Dudzińska A.: The role of anti-solar protection in the reduction of solar gains in the passive sports hall	75
Đurica P., Janiková M., Cangár M., Štaffenová D.: Long time testing of thermal parameters in selected windows.....	83
Đurica P., Šuštiaková M., Ponechal R., Rybárik J.: Measured and simulated parameters of wooden lightweight external walls.....	91
Fieducik J., Godlewski J.: The low energy house using an air solar collector – a case study.....	99
Firląg S.: Pre-war public utility buildings – results of surveys.....	107
Gałek P.: Optimising energy produced by photovoltaic cells	117
Gavlík M., Böszörményi L.: Determine the optimal system structure of the combined production of electricity and heat	125
Gumuła S., Staniszk K.: An experimental evaluation of resources and the potential for using the kinetic energy of wind to produce electricity	133
Heim D., Janicki M., Kubacka E.: A model of infiltrating air flow and its distribution in a room with a double skin façade	143
Ickiewicz I.: White certificates – legal, technical and economic aspects	153
Jaglarz G., Ciesielski F.: Feasibility analysis of upgrading an old building to the standard requirement of a low energy requirement building	163
Kapalo P., Sedláková A., Vilčeková S., Dominta F.: Energy efficiency of ventilation system in apartment buildings	173
Kaposztasova D., Vranayova Z., Purcz P.: Rainwater harvesting system and risk management application	179
Klemm K.: An assessment of conditions of human comfort in open landscaped areas of Lodz.....	187
Knera D., Szczepańska-Rosiak E., Heim D.: Providing an interior daylight environment through the use of light pipes	195
Konca P., Kubacka A., Gawin D.: Effect of titanium dioxide on the self-cleaning properties of paints for etics	205
Koronthályova O., Bágel L., Kullifayová M., Ifka T.: Hygic performance of contemporary and historical ceramic bricks.....	213
Kosiński P.: Air thermal bridges	221
Kovac M., Knizova K., Sedlakova A.: Heat load elimination by using displacement ventilation in a classroom	229
Kovacova K., Kovac M., Kosicanova D.: Evaluating the energy and cost benefits of heat pumps in multi-occupancy dwellings.....	237

Krause P., Steidl T., Orlik-Koźdoń B., Wojewódka D.: Energy analysis of NF40 residential buildings on selected examples	245
Krause P., Wojewódka D., Orlik-Koźdoń B., Steidl T.: Analysis of solutions of lightweight casing made from sandwich panels in the aspect of thermal insulation	253
Kušnir M., Košičanová D., Vranayová Z., Vranay F., Lojkovics J.: Zero energy balance proposal for office buildings.....	259
Lechowska A., Schnotale J.: CFD modelling and analytical calculations of thermal transmittance of multi-layer glazing with ultrathin internal glass partitions	265
Lechowska A., Schnotale J., Fedorczyk-Cisak M., Paszkowski M.: Measurement of thermal transmittance of multi-layer glazing with ultrathin internal glass partitions.....	273
Lis P., Lis A.: The seasonal heat demand for heating, calculated on the basis of peak power values in educational buildings.....	281
Machniewicz A., Borowczyński A., Heim D.: Transparent insulation efficiency determined by different methods.....	291
Malinowski A., Turkowski W., Muzyczak A.: Thermal conditions of buildings: mathematical modeling by power circuit theory.....	299
Markovič G., Ahmidat M.: Parameters of rainwater collection and storage – measurement and evaluation.....	311
Nowak H., Nowak Ł.: The use of active thermography to detect material inclusions in the walls... ..	319
Nowak K., Nowak-Dzieszko K.: Impact of preparation procedures on results of airtightness tests	329
Nowak K., Rojewska-Warchał M.: Thermal comfort of office rooms with a large area of glazing	335
Nowak K., Zastawna-Rumin A.: The possibility of using PCM impregnated gypsum boards of different temperature phase change.....	343
Nowak Ł., Cebat K., Bać A.: Double skin house concept – a study of buffer zone usage in a single family home.....	353
Nowak-Dzieszko K., Dębowski J.: Influence of the thermal modernization of panel buildings on transmission heat losses.....	363
Nowak-Dzieszko K., Rojewska-Warchał M.: Influence of shading systems on the microclimate conditions in large panel buildings.....	371
Nowak-Dzieszko K., Rojewska-Warchał M.: Simulation analysis of microclimate conditions in a multi – family large panel building.....	379
Orlik-Koźdoń B., Szymanowska-Gwiżdż A.: The effect of traditional structural elements of partition walls in residential buildings on the quality of the use of the premises	389
Pawłowski K., Lewandowski F.: Thermal design of exterior walls made of wooden beams.....	397
Radoń J., Wąs K., Flaga-Maryńczyk A., Antretter F.: Thermal performance of slab on grade with floor heating in a passive house.....	405
Sadłowska-Sałęga*, Radoń J.: Experimental and theoretical study of microclimate in historical church in Wiśniowa	415
Sedláková A., Majdlen P., Ťažký L.: Energy efficient buildings – lower structure	425
Sobolewski M.: A study of thick thermal insulation with density foam polystyrene (EPS).....	433
Szczepanik N., Schnotale J.: CFD modelling of air flow and transport of contaminants in a passive house	443
Szymanowska-Gwiżdż A., Steidl T.: Analysis of temperature and humidity processes in existing half-timbered partitions	455
Szymański M., Górzeński R., Szkarłat K.: Automation retrofitting as a first stage of complex renovation of district heating substations in public buildings	465

Trząski A., Panek A., Rucińska J.: Impact of windows parameters on the thermal performance of a multi-family building.....	473
Wesołowska M., Szczepaniak P.: Selected problems of thermal bridges in contemporary multi-occupancy buildings.....	481
Zębala K.: Reactive power compensation and energy saving	489

TREŚĆ

Adamski M., Siergiejuk J., Ojczyk G.: Instalacja pomp ciepła (budynek centrum Jana Pawła II w Krakowie)	3
Bandurski K., Mielczyński T., Koczyk H.: Komfort termiczny i zużycie energii domu ekologicznego – analiza symulacyjna <i>DOMTRZON</i>	11
Belok J., Wilk-Słomka B.: Efektywność energetyczna budynku z systemem ogrzewania płaszczyznowego	23
Bielek B.: Koncepcja nowej fizyko-energetycznej oceny budynków w rozwoju technologicznym architektury dla zrównoważonego społeczeństwa.....	31
Bielek B.: Nowa klasyfikacja odnawialnych źródeł energii w rozwoju technologicznym w architekturze dla zrównoważonego społeczeństwa	41
Byrda A.: Punktowe mostki termiczne w ścianach z okładziną z kamienia naturalnego.....	49
Bzowska D.: Wpływ oporu cieplnego ścian budynku oraz powierzchni przeszklenia na naturalną wymianę powietrza w okresie letnim	57
Chwieduk D. Grzebielec A., Rusowicz A.: Słoneczne chłodzenie w budownictwie	65
Dudzińska A.: Rola osłon przeciwsłonecznych w ograniczeniu zysków solarnych w pasywnej hali sportowej	75
Đurica P., Janiková M., Cangár M., Štaffenová D.: Długofalowe pomiary właściwości termicznych w wybranych oknach	83
Đurica P., Šuštiaková M., Ponechal R., Rybárik J.: Pomiarowe oraz symulacyjne parametry lekkich drewnianych ścian zewnętrznych	91
Fieducik J., Godlewski J.: Dom energooszczędny wykorzystujący słoneczne kolektory powietrzne – studium przypadku.....	99
Firląg S.: Przedwojenne budynki użyteczności publicznej – wyniki badań.....	107
Gałek P.: Optymalizacja pozyskiwania energii z ogniw fotowoltaicznych	117
Gavlik M., Böszörményi L.: Wyznaczenie optymalnej struktury systemu kogeneracji ciepła i elektryczności	125
Gumuła S., Stanisław K.: Eksperymentalna ocena zasobów i możliwości wykorzystania energii kinetycznej wiatru do produkcji energii elektrycznej.....	133
Heim D., Janicki M., Kubacka E.: Model dystrybucji powietrza infiltrującego do budynku przez fasadę dwupowłokową	143
Ickiewicz I.: Białe certyfikaty – uwarunkowania prawne, techniczne i ekonomiczne	153
Jaglarz G., Ciesielski F.: Analiza możliwości przystosowania budynku w starym budownictwie do standardów budynku niskoenergetycznego	163
Kapalo P., Sedláková A., Vilčeková S., Dominta F.: Efektywność energetyczna systemu wentylacji w budynku mieszkalnym	173
Kaposztasova D., Vranayova Z., Purcz P.: Zastosowanie systemu zarządzania ryzykiem przy wykorzystaniu wody opadowej	179
Klemm K.: Ocena komfortu człowieka w strefie niezabudowanej Łodzi	187

Knera D., Szczepańska-Rosiak E., Heim D.: Kształtowanie wewnętrznego środowiska oświetleniowego za pomocą świetlików rurowych	195
Konca P., Kubacka A., Gawin D.: Wpływ dwutlenku tytanu na właściwości samoczyszczące farb do bezspoinowych systemów ociepleń.....	205
Koronthályova O., Bágel L., Kullifayová M., Ifka T.: Higroskopowa analiza współczesnych oraz historycznych cegieł ceramicznych	213
Kosiński P.: Powietrzne mostki cieplne	221
Kovac M., Knizova K., Sedlakova A.: Ograniczenie obciążenia cieplnego w sali lekcyjnej przy zastosowaniu wentylacji wyporowej	229
Kovacova K., Kovac M., Kosicanova D.: Analiza energetycznych oraz kosztowych korzyści stosowania pomp ciepła w budownictwie wielorodzinnym	237
Krause P., Steidl T., Orlik-Koźdoń B., Wojewódka D.: Analiza energetyczna budynków mieszkalnych NF40 na wybranych przykładach	245
Krause P., Wojewódka D., Orlik-Koźdoń B., Steidl T.: Analiza rozwiązań lekkiej obudowy z płyt warstwowych w aspekcie izolacyjności termicznej	253
Kušnir M., Košičanová D., Vranayová Z., Vranay F., Lojkovics J.: Budynek biurowy o zerowym bilansie energetycznym	259
Lechowska A., Schnotale J.: Modelowanie CFD oraz określanie metodami analitycznymi współczynnika przenikania ciepła wielowarstwowego oszklenia z wewnętrznymi ultracienkimi szybami	265
Lechowska A., Schnotale J., Fedorczyk-Cisak M., Paszkowski M.: Pomiar współczynnika przenikania ciepła wielowarstwowego oszklenia z wewnętrznymi ultracienkimi szybami.....	273
Lis P., Lis A.: Sezonowe zapotrzebowanie na ciepło do ogrzewania obliczone na podstawie mocy szczytowej w budynkach edukacyjnych.....	281
Machniewicz A., Borowczyński A., Heim D.: Obliczeniowa efektywność izolacji transparentnych wyznaczana różnymi metodami	291
Malinowski A., Turkowski W., Muzyczak A.: Modelowanie matematyczne stanu cieplnego budynku metodami teorii obwodów energetycznych	299
Markovič G., Ahmidat M.: Parametry związane z gromadzeniem i przechowywaniem wody opadowej – pomiary i ocena.....	311
Nowak H., Nowak Ł.: Zastosowanie termografii aktywnej do detekcji wtrąceń materiałowych w ścianach.....	319
Nowak K., Nowak-Dzieszko K.: Wpływ przygotowania budynku na wyniki badań szczelności	329
Nowak K., Rojewska-Warchał M.: Komfort cieplny pomieszczeń biurowych o dużej powierzchni przeszkleń	335
Nowak K., Zastawna-Rumin A.: Możliwość stosowania płyt gipsowo-kartonowych z dodatkiem PCM o różnej temperaturze przemiany fazowej	343
Nowak Ł., Cebat K., Bać A.: Double skin house – studium wykorzystania strefy buforowej w domu jednorodzinnym	353
Nowak-Dzieszko K., Dębowski J.: Analiza wpływu termomodernizacji budynku wielkopłytkowego na straty ciepła przez przenikanie.....	363
Nowak-Dzieszko K., Rojewska-Warchał M.: Wpływ zacienień na warunki mikroklimatu w budynku wielkopłytkowym	371
Nowak-Dzieszko K., Rojewska-Warchał M.: Analiza symulacyjna warunków mikroklimatu w wielorodzinnym budynku wielopłytkowym.....	379
Orlik-Koźdoń B., Szymanowska-Gwiżdż A.: Wpływ charakterystycznych elementów konstrukcji przegród budynków mieszkalnych na jakość użytkowania pomieszczeń.....	389

Pawłowski K., Lewandowski F.: Projektowanie cieplne przegród zewnętrznych z bali drewnianych	397
Radoń J., Wąs K., Flaga-Maryańczyk A., Antretter F.: Zjawiska cieplne w płycie na gruncie z ogrzewaniem podłogowym w domu pasywnym	405
Sadłowska-Sałęga A., Radoń J.: Eksperymentalne i teoretyczne badanie mikroklimatu w kościele w Wiśniowej	415
Sedláková A., Majdlen P., Ťažký L.: Budynki energooszczędne – strefa kontaktu z gruntem.....	425
Sobolewski M.: Badania cieplne grubych izolacji z polistyrenu spienionego (EPS) o małej gęstości	433
Szczepanik N., Schnotale J.: Modelowanie metodą CFD (komputerowej dynamiki płynów) przepływu powietrza i transportu zanieczyszczeń w domu pasywnym	443
Szymanowska-Gwizdź A., Steidl T.: Analiza procesów cieplno-wilgotnościowych w istniejących przegrodach z muru pruskiego	455
Szymański M., Górzeński R., Szkarłat K.: Rozbudowa układów automatyki jako pierwszy etap kompleksowej modernizacji węzłów ciepła w obiektach użyteczności publicznej	465
Trząski A., Panek A., Rucińska J.: Wpływ parametrów okien na charakterystykę energetyczną budynku wielorodzinnego	473
Wesołowska M., Szczepaniak P.: Wybrane problemy mostków termicznych we współczesnych wielorodzinnych budynkach mieszkalnych.....	481
Zębala K.: Kompensacja mocy biernej a oszczędność energii	489